



International Conference on Research Trends in Engineering & Management

ICRTEM-2021

20th - 21st August 2021

**Virtual
Conference**



ORGANIZED BY

R R INSTITUTE OF TECHNOLOGY, BANGALORE, INDIA

IN ASSOCIATION WITH

INSTITUTE FOR ENGINEERING RESEARCH AND PUBLICATION (IFERP)

ISBN : 978-93-92105-00-5



ICRTEM-21

International Conference on
Research Trends in Engineering & Management

Bangalore, India
20th – 21st August, 2021

Organized by:
R R Institute of Technology, Bangalore, India
In Association with:
Institute For Engineering Research and Publication



Rudra Bhanu Satpathy

Chief Executive Officer

Institute For Engineering Research and Publication.

On behalf of *Institute For Engineering Research and Publications (IFERP)* and in association with *R R Institute of Technology, Bangalore, India*. I am delighted to welcome all the delegates and participants around the globe to *R R Institute of Technology, Bangalore, India* for the “*International Conference on Research Trends in Engineering & Management*” (ICRTEM-2021)” Which will take place from *20th – 21st August 2021*

It will be a great pleasure to join with Engineers, Research Scholars, academicians and students all around the globe. You are invited to be stimulated and enriched by the latest in engineering research and development while delving into presentations surrounding transformative advances provided by a variety of disciplines.

I congratulate the reviewing committee, coordinator (**IFERP & RRIT**) and all the people involved for their efforts in organizing the event and successfully conducting the International Conference and wish all the delegates and participants for their virtual presence.

Sincerely,



Rudra Bhanu Satpathy



(+91) 44 - 4958 9038



info@iferp.in
www.iferp.in



Rais Tower, 2054/B, 2nd Floor, 'L' West Block, 2nd Ave, Anna Nagar, Chennai, Tamil Nadu 600040, India

Preface

The *International Conference on Research Trends in Engineering & Management (ICRTEM -21)* is being organized by *R R Institute of Technology, Bangalore, India* in Association with *IFERP-Institute for Engineering Research and Publications* on the 20th – 21st August, 2021.

The “*International Conference on Research Trends in Engineering & Management*” was a notable event which brings Academia, Researchers, Engineers, Industry experts and Students together.

The purpose of this conference is to discuss applications and development in area of “*Engineering & Management*” which were given International values by *Institute for Engineering Research and Publication (IFERP)*.

The International Conference attracted over 110 submissions. Through rigorous peer reviews 72 high quality papers were recommended by the Committee. The Conference aptly focuses on the tools and techniques for the developments on current technology.

We are indebted to the efforts of all the reviewers who undoubtedly have raised the quality of the proceedings. We are earnestly thankful to all the authors who have contributed their research works to the conference. We thank our Management for their wholehearted support and encouragement. We thank our Principal for his continuous guidance. We are also thankful for the cooperative advice from our advisory Chairs and Co-Chairs. We thank all the members of our local organizing Committee, National and International Advisory Committees.

Message from the Chief Patron



Shri Y RajaReddy

Chairman

PKMET, Bangalore

I am extremely pleased to know that the department of Electronics and Communication Engineering of R R Institute of Technology is organizing an International Conference on Research Trends in Engineering & Management (ICRTEM-2021) on 20th and 21st of August 2021. I understand, a substantial number of researchers have submitted their papers for presentation in the conference and also for publication. The response to this conference from all over India and Foreign countries is most encouraging. I am sure all the participants will be benefitted by their interaction with their fellow scientists and engineers which will help for their research work and subsequently to the society at large.

I wish the conference meets its objective and confident that it will be a grand success.

Welcome message from the Patron



Sri Kiran H R

Secretary

PKMET, Bangalore

I am pleased to state that the Department of Electronics and Communication Engineering of RRIT is organizing a prestigious International Conference on Research Trends in Engineering & Management"- ICRTEM-2021, on 20th and 21st of August 2021. Concept to commissioning is a long route. The conference may strengthen theme of "Innovative India" and may translate the innovations into a workable product. The conference forum will set a path for the academicians, researchers who play a major role in bringing out new products through innovations. Also I am delighted to know that the conference has received innovative ideas for presentation. I wish the participants of the conference to get additional insight into their subjects of interest. I wish the organizers of the conference a great success

Welcome message from the Patron



Sri Arun H R

Director

PKMET, Bangalore

I am delighted to wish Electronics and Communication Engineering department for organizing an International Conference on Research Trends in Engineering & Management"- ICRTEM-2021 on 20th and 21st of August 2021. I have a strong desire that the conference to unfold new domains of research among the Electronics and Communication Engineering fraternity and will boost the knowledge level of many participating budding research scholars by opening a plethora of future developments in the field of Electronics and Communication Engineering and other areas of Engineering.

I appreciate the faculties and department Head of Electronics and Communication Engineering for continuous untiring contribution in making the conference a reality.

I wish the conference a great grand success and motivate other departments to follow the trend, to make RRIT reach higher levels of learning in the next few years.

Welcome message from the Principal



Dr.Mahendra K V

Principal,
RRIT, Bangalore

The International Conference on Research Trends in Engineering & Management (ICRTEM-21) Organized by the department of Electronics & Communication Engineering, R. R. Institute of Technology, Bangalore, India, on 20th - 21st August 2021 in association with IFERP is a great pride and honor for the College. The College has made tremendous progress in all areas of academic, non-academics, capacity building relevant to staff and students. The College has achieved another milestone in getting NAAC accreditation. Conferences are an important way researchers stay connected to others in their field and learn about cutting-edge technologies. It provides a platform for scholars, researchers from industry and academia to demonstrate their findings and studies. The conference brings together the members of research communities to enrich their knowledge in various emerging areas of research. One of the primary aims of all engineers who take part in international conferences is to acquire information and expertise on the latest and most recent advancements that have taken place in their field. Engineering conferences are the right place to learn about new tools that are being used in the field by engineers who are involved in similar streams of research such as yourself. Enrolling yourself into an engineering conference and taking an active part in the event can mean making a considerable and sizable investment of your time, money and resources. My heartfelt encouragement to all staff members and Students for their participation in the Conference and my best wishes for their fruitful effort. I thank all the organizers for their efforts in making the event successful.

Welcome message from the Convenor



Dr.Sunitha HD

Professor & HOD

Department of ECE, RRIT, Bangalore

It gives me immense pleasure to present the proceedings of International Conference on Research trends in Engineering and Management (ICRTEM-21), organized by the department of Electronics and Communication Engineering, R R Institute of Technology, Bangalore in association with IFERP. The main objective of organizing this conference is to share and enhance the knowledge of researchers in engineering & Management domain. This conference aims to bridge the researchers working in academia or industry and other professionals through presentations and keynote sessions on current technology and trends.

My heartfelt thanks to our Management, Principal, IFERP, Keynote speakers, reviewers and organizing committee for their support in organizing this conference and making it a success.

ICRTEM-21

*International Conference on
Research Trends in Engineering &
Management*

Keynote Speakers



Professor Marwan Al-Akaidi

Vice President for Research

The American University in the Emirates, Dubai

Chair SPC, IEEE UK & Republic of Ireland

Biography

An Experienced Vice President for Academic Affairs with a demonstrated history of working in the education management industry. Skilled in Analytical Skills, Lecturing, Leadership, Data Analysis, and Strategic Planning. Strong education professional with a Doctor of Philosophy (PhD) focused in Optical and Communication Engineering from Loughborough University.

Education

Doctor of Philosophy (PhD) Field Of Study Optical and Communication Engineering, Loughborough University, 1985 – 1988

Designation:

- ✓ As Vice president Research & Dean of the College of Computing & Information Technology, The American University in the Emirates (AUE), Dubai, United Arab Emirates
- ✓ As VPR is to encourage research that has practical application for both economy & society in UAE & the region.
- ✓ Working as Vice President for Academic Affairs, Arab Open University, Kuwait

Experience:

- ✓ Started his Career as Lecturer in Software Engineering/ Communication Engineering at Plymouth University
- ✓ Senior Lecturer at De MontFort University and served as Director of External affairs with almost 21 years in De MontFort University



Professor Dr. Hatem Hatem Abdulkadhim Alyasari

Professor of Economics
Cihan University
Kurdistan region, Alsulaymaniya

Biography

- Currently, he is a senior lecturer in Cihan University of Sulaimaniya. Sulaimaniya, KRI, Iraq.
- Chairman of finance and Banking Dept. University of Kalamoon Syria, 2006-2012
- Supervisor of Graduation Project , The Arab Academy for Banki and Financial Sciences, 2006-2012.
- Dean of Administration and Economic College Al-Kufa University, Iraq, 2001-2003
- Dean of Administration and Economic College, Al-Qadisiya University, Iraq, 1993-2001
- Published scores of refereed articles on topics related to banking, finance and economics.
- Editorial board member in five international journals.
- Educated in Iraq, US, and UK universities with a bachelor degree in business and economics from Al-Mustansiriyah University (Iraq) , a master degree in economics from Detroit university and a doctorate degree in econometrics from Bradford University (USA).



Dr. M V Reddy

Institute of Research Hydro-Québec
Centre of Excellence in Transportation
Electrification and Energy Storage (CETEES), Hydro-Québec, J3X 1S1, Canada

Biography

Dr. M.V. Reddy obtained his Ph. D (2003) with the highest honors in the area of Materials Science and engineering from the University of Bordeaux, (ENSCP/ICMCB-CNRS), France. From June 2019 working as a Senior Researcher (level 3) (equivalent to professor) at the Institute of Research Hydro-Québec, Canada. From July 2003 to May 2019, he worked at the National University of Singapore (NUS), Singapore as a Senior Research Fellow. Over the past 20 years, he has conducted leading research on Materials for Energy Storage and Conversion including materials processing and the evaluation of functional properties of materials for electric vehicles, and the development of in situ techniques.

Dr. Reddy has published around 210 papers (1st author; 47, 2nd author 55; * Corresponding author: 92 papers) and one landmark review paper in “Chemical Reviews”, his h-index of 66 with over 16000 citations. These have recently placed him within the top 2% highly cited researchers in Energy (Ranked #1002 out of 186,500 researchers in 2020, Source: Stanford University (USA)).

Dr. Reddy is serving as an editorial advisory board member in Materials Research Bulletin and Journal of Energy Storage (Elsevier) as well as several open access Journals (Materials, Energies and Molecules, MDPI) and the regional editor: Nanoscience & Nanotechnology-ASIA.

Dr Reddy has conducted several workshops related to functional materials and energy storage & conversion and delivered 10 Plenary, 22 Keynote, 78 Invited and 18 Contributory talks at various conferences and conducted a number of workshops on battery materials’ fundamentals, synthesis and characterization techniques. He also delivered Materials Science and Engineering outreach talks to college and high school students all over the world.

Technical Session Chairs

Dr. Manjunath R

Professor & Head

Department of Computer Science & Engineering

R R Institute of Technology, VTU, Bengaluru

Dr. Mangala Gowri S G.

Associate Professor

Electrical and Electronics Engg Department

R R Institute of Technology

Dr. S.M. Subash

Associate Professor & Head

Department of Civil Engineering,

Guru Nanak Institute of Technology, Hyderabad, Telangana

Dr. Ramachandra C. G

Professor

Department of Mechanical Engineering School of Engineering,

Presidency University, Bengaluru, Karnataka

Dr V Sasirekha

Professor - Management

Sri Sairam Engineering College

Chennai

Dr.R.Uma

Professor, CSE Department

Sri Sairam Engineering College

Chennai

Dr. T. Porselvi

Professor, Department of EEE

Sri Sairam Engineering College

Chennai

ICRTEM -2021

International Conference on Research Trends in Engineering & Management

Bangalore, India, 20th – 21st August, 2021

Organizing Committee

CHIEF PATRON

Shri Y Raja Reddy
Chairman, PKMET

PATRON

Sri Kiran H R
Secretary, PKMET

Sri Arun H R
Director, PKMET

CONFERENCE/STEERING COMMITTEE CHAIR

Dr Mahendra K V
Principal, RRIT

CONVENOR

Dr. Sunitha H D
HOD, ECE& EEE, RRIT

STEERING COMMITTEE MEMBERS

Dr. Gullapalli Shankara

HOD – Civil, RRIT

Dr. Channabasavaraju

HOD – Mech, RRIT

Dr. Manjunath

HOD - CSE &ISE, RRIT

Dr Ramachandramurthy

HOD – BS, RRIT

ORGANIZING COMMITTEE MEMBERS

Mrs. G Parimala Gandhi

ECE, RRIT

Dr.Mangala Gowri G

EEE, RRIT

Mrs Anshu Deepa

ECE, RRIT

Mr. Mohan Kumar

ECE, RRIT

Mrs.Sunanda C V

EEE, RRIT

Mr. Chitranjan Das

ECE, RRIT

Mrs Shyamala P

ECE, RRIT

Mrs Divya T M

ECE, RRIT

Mrs. Sungyani Patil

ECE, RRIT

Mr Ashok K N

ECE, RRIT

Mr.Ramachandra

EEE, RRIT

NATIONAL ADVISORY COMMITTEE

Dr. D.K.Sreekantha

Professor, Computer Science & Engineering
NMAM Institute of Technology,
Bangalore, India

Dr CKB NAIR

Director, Mechanical Engineering
Rajiv Gandhi Institute of Technology Bengaluru
Bangalore, India

Dr Rajeshwari Hegde

Professor, Telecommunication Engg
BMS College of Engineering
Bangalore, India

Dr V.Nagaveni

Professor, Computer Science And Engineering
Acharya Institute of Technology
Karnataka, India

Dr. Gurumurthy Hegde

Professor, Nano-Materials And Displays
BMS College of Engineering
BMS College of Engineering, India

Dr. Karabi Sikdar

Professor & Head, Mathematics
BMS Institute of Technology and Management
Karnataka, India

Dr. Keerthiprasad. K.S

Professor & Head, Mechanical Engineering
Vidya Vikas Institute of Engineering & Technology
Bangalore, India

Dr. N. Guruprasad

Professor, Computer Science & Engineering
Global Academy of Technology
Bangalore, India

Dr. Rathnakar.G

Dean, Mechanical Engineering
ATME College of Engineering
Bangalore, India

Dr. Reshma Banu

Professor & Head, Information Science & Engineering
GSSS Institute of Engineering and Technology for Women
Bangalore, India

Dr. Sharanabasava V. Ganachari

Research Scientist, Nanotechnology
Centre for Material Science, Advanced research in Nanoscience & Nanotechnology
Karnataka, India

Dr. Sharmila. K.P,

Professor, Electronics & Communication Engg.
CMR Institute of Technology
Bangalore, India

Dr. Shekhappa G. Ankaliki

Professor & Head, Electrical & Electronics Engineering
SDM College of Engg. & Tech
Bangalore, India

Dr. VPS Naidu

Scientist, Electronics & Communication Engg.
National Aerospace Laboratories
Bangalore, India

Dr. Bharathi Ganesh

Professor & Head, Civil Engineering
Nitte Meenakshi Institute of Technology
Bangalore, India

K.Sujatha

Professor, Electrical & Electronics Engineering
Dr. M.G.R Educational & Research Institute
TamilNadu, India

Dr. Balakrishnan. S

Professor, Computer Science And Engineering
Sri Krishna College of Engg & Technology
TamilNadu, India

Dr. D.K.Sreekantha

Professor, Information Science & Engineering
NMAM Institute of Technology
Karnataka, India

Dr. Geeta R. Bharamagoudar

Professor, Computer Science & Engg
KLE Institute of Technology
TamilNadu, India

Dr. H C Sateesh Kumar

Professor, Electronics And Communication Engg.
Sapthagiri College of Engineering
Bangalore, India

Dr. H S Prasantha

Professor, Electronics & Communication Engineering
Nitte Meenakshi Institute of Technology
Bangalore, India

Dr. S. Sathish Kumar

Professor, Computer Science And Engineering,
RNS Institute of Technology
Karnataka, India

Dr. Suneeth Kumar S M

Professor, Civil Engineering
ATME College of Engineering
Bangalore, India

Dr. Viswanatha B. M.

Professor,
Kalpataru Institute of Technology
Bangalore, India

Dr.M.M Bagali

Director, Management And Human Resources
IREU Group of Educational Institutes
Bangalore, India

Dr.P.Oliver jayaprakash

Professor, CIVIL ENGINEERING
Sethu institute of technology (Autonomous)
TamilNadu, India

Dr.Priya Murugesan

Professor & Head, Physics
Saveetha Engineering College
TamilNadu, India

Dr.R.Shantha Selvakumari

Professor & Head, Electronics & Communication Engineering
Mepco Schlenk Engineering College
TamilNadu, India

Dr.S.Devikala

Professor, Electricals And Electronics Engineering
Varaprasad Reddy Institute of Technology
Karnataka, India

Dr.S.Veena

Professor, Computer Science And Engineering
S.A.Engineering College
TamilNadu, India

Dr. Shakeela Banu C

Professor, Management Studies
CMS-B-School Jain Deemed to be University
Bangalore, India

S.Pathur Nisha

Professor, Professor & Head
Arjun College of Technology
Karnataka, India

Sudhakara A.

Professor, Chemistry
Rajarajeswari College of Engineering
Bangalore, India

CONTENTS

SR.NO	TITLES AND AUTHORS	PAGE NO
1.	Automatic Fire Detecting and Fire Fighting Robot ➤ <i>Abhishek Gowda D</i> ➤ <i>Mohan M</i> ➤ <i>Sai Prashanth S</i> ➤ <i>Tejaswini P</i> ➤ <i>Asst Prof. B N Mohan Kumar</i>	1
2.	Cost-Efficient Arduino-based Automated Washroom Sanitizing System ➤ <i>Aishwarya S</i> ➤ <i>Dr. Sunitha H D</i> ➤ <i>Amrendra Tripathi</i> ➤ <i>Anuradha Lakra</i> ➤ <i>Prabha K</i>	5
3.	Three Phase Power Failure Detector and Voltage Measurement Using Arduino ➤ <i>Akash Kumar Singh</i> ➤ <i>Emborka Syiem</i> ➤ <i>Amit Kumar Singh</i> ➤ <i>Ramachandra C</i>	8
4.	Improved Output from Buck-Boost Converter for Commercial Loads ➤ <i>Akshatha.R.Hegde</i> ➤ <i>Vyshnav B</i> ➤ <i>Pradeesha J</i> ➤ <i>Ramachandra C</i>	12
5.	Design of Single Axis Solar Tracker ➤ <i>Amithkumar Yadav</i> ➤ <i>Saikat Barman</i> ➤ <i>Viresh Hiremath</i> ➤ <i>Rambati N</i> ➤ <i>Asst Prof.Anshu Deepak</i>	15
6.	A Survey Paper on Kidney Cancer and Computer aided methods for their Image Segmentation ➤ <i>Anupkumar Bhatulal Jayaswal</i> ➤ <i>Mahesh Bhimsham Dembrani</i>	20
7.	Application of Lean Six Sigma in cast in-situ construction ➤ <i>Asmita Ghule</i> ➤ <i>Prof.SatishWaysal</i>	24
8.	Image De-noising Using Machine Learning ➤ <i>Charutha M V</i> ➤ <i>Shadakshari</i> ➤ <i>Shyamala P Bhat</i>	32

CONTENTS

SR.NO	TITLES AND AUTHORS	PAGE NO
9.	Behavior of Wear and Corrosion Resistance of thin film coated Titanium alloy substrate <ul style="list-style-type: none"> ➤ <i>K Chandrappa</i> ➤ <i>PC Arunakumara</i> ➤ <i>Sanjay T Setty</i> ➤ <i>Anoop Joshi</i> ➤ <i>K Vineth</i> 	36
10.	Friction Stir Additive manufacturing in Align with Industry 4.0 - A Review <ul style="list-style-type: none"> ➤ <i>S.Deivanai</i> ➤ <i>Dr. Manoj Soni</i> 	41
11.	Review on X2 & S1 handover in LTE Networks <ul style="list-style-type: none"> ➤ <i>Divya T M</i> 	46
12.	Hybrid Optimization Control Algorithm for Grid Connected PV system <ul style="list-style-type: none"> ➤ <i>Gayathri Devi K.S</i> ➤ <i>P.Sujatha Therese</i> 	49
13.	A Short Review on Measuring Impact of Microencapsulated Phase Change Material in Mitigating Urban Heat Island <ul style="list-style-type: none"> ➤ <i>G.R. Gopinath</i> ➤ <i>S. Muthuvel</i> 	55
14.	Roxas City, the Seafood Capital of the Philippines: Myth or Fact? <ul style="list-style-type: none"> ➤ <i>Ian B. Arcega</i> ➤ <i>Pearl Joy G. Mirasol</i> ➤ <i>Angela B. Casios</i> ➤ <i>Sarah Jane D. Malayang</i> 	60
15.	High Speed Data Transmission Using Light Fidelity <ul style="list-style-type: none"> ➤ <i>Bharath Kumar K</i> ➤ <i>Gagan Kumar</i> ➤ <i>Vaibhav S Biradar</i> ➤ <i>Dr. Mangala Gowri S G</i> 	69
16.	Smart Solar Power Management System for Domestic Purpose <ul style="list-style-type: none"> ➤ <i>Pratik Chaudhary</i> ➤ <i>Dr. Mangala Gowri S.G</i> ➤ <i>Sikindra Kumar Thakur</i> ➤ <i>Vikash Kumar Sah</i> ➤ <i>Arun Prasad Yadav</i> 	72
17.	EEG data processing for Emotion detection using DTCWT and FFNN Architecture Design <ul style="list-style-type: none"> ➤ <i>Dr. Mangala Gowri S.G</i> ➤ <i>Priyanka Nagendra Shindogi</i> ➤ <i>Sneha Joesphine</i> 	76

CONTENTS

SR.NO	TITLES AND AUTHORS	PAGE NO
18.	Brain tumor detection in MRI images using MAT lab <ul style="list-style-type: none"> ➤ <i>Kiran C B</i> ➤ <i>Shiva kumar D N</i> ➤ <i>Madhu kumar M</i> ➤ <i>Celeste T</i> ➤ <i>Divya T M</i> 	82
19.	Electricity Theft Detection <ul style="list-style-type: none"> ➤ <i>Lenin Selva M</i> ➤ <i>Monish R</i> ➤ <i>Dharsan S</i> ➤ <i>Sankarnarayanan P</i> 	85
20.	Congruence between Cause Marketing Campaigns and Purchase Intention towards Consumers – An Analysis <ul style="list-style-type: none"> ➤ <i>M.Ancy Raja Nathiya</i> ➤ <i>K.Asha</i> 	88
21.	The influence of Boron Nitride reinforcement on physical and mechanical properties of Polyethylene Tetraphalate (PET) <ul style="list-style-type: none"> ➤ <i>Anand. S. Sonnad</i> ➤ <i>Shravankumar</i> ➤ <i>B. Kerur</i> ➤ <i>Mahesh A. Kori</i> 	92
22.	Fundamental Frequency estimation and analysis of speech signal <ul style="list-style-type: none"> ➤ <i>Mahesh M. Kamble</i> ➤ <i>Tejal S.Bandgar</i> 	98
23.	An Analysis of Deep Learning Models for Dry Land Farming Applications <ul style="list-style-type: none"> ➤ <i>S.Mithra</i> ➤ <i>Dr.T.Y.J.NagaMalleswari</i> 	101
24.	Design and Implementations of Humming Bird Cryptographic Algorithm using FPGA <ul style="list-style-type: none"> ➤ <i>Mohan Kumar BN</i> ➤ <i>N Nandeesh Reddy</i> ➤ <i>Divya KH</i> ➤ <i>Alangir Badsha</i> ➤ <i>Kishore S</i> 	107
25.	Women Empowerment in India: Issues & Challenges <ul style="list-style-type: none"> ➤ <i>Namratha Murthy</i> ➤ <i>Dr.Sunitha H D</i> 	111
26.	Wireless Sensors Network for Radiation Monitoring Using IoT <ul style="list-style-type: none"> ➤ <i>Pallavi M R</i> ➤ <i>Dr. Sunitha H D</i> ➤ <i>Samadrita Roy Chowdhury</i> ➤ <i>Priyanka Nagendra Shindogi</i> ➤ <i>Varsha Biradar</i> 	115

CONTENTS

SR.NO	TITLES AND AUTHORS	PAGE NO
27.	Intelligent Covid-19 Pandemic Bus Service with Safety Measures <ul style="list-style-type: none"> ➤ <i>Parimala Gandhi G</i> ➤ <i>Joy Bhowmik</i> ➤ <i>Adarsha M P</i> ➤ <i>Ajay K S</i> 	118
28.	Smart Indoor Vertical Farming Using IOT <ul style="list-style-type: none"> ➤ <i>Parimala Gandhi G</i> ➤ <i>Sushma V</i> ➤ <i>Monika H</i> ➤ <i>Chithra C</i> ➤ <i>Ullas K S</i> 	122
29.	Investigation of Fluoride Uptake by Chlorine Doped Polyaniline in Continuous Column Mode Operation <ul style="list-style-type: none"> ➤ <i>Sarungbam Pipileima</i> ➤ <i>Potsangbam Albino Kumar</i> 	126
30.	Performance Analysis of Distributed System by the Placement of DG Considering Load Growth <ul style="list-style-type: none"> ➤ <i>Pradeesha J</i> ➤ <i>Vyshnav B</i> ➤ <i>Akshatha R Hegde</i> 	130
31.	Faster RCNN based Automatic Vehicle Detection System <ul style="list-style-type: none"> ➤ <i>T Ragotham Reddy</i> ➤ <i>Taduru Aruna</i> 	133
32.	Identification of adsorption mechanism for Iron uptake by activated carbon derived from Alocasia indica <ul style="list-style-type: none"> ➤ <i>Reenarani Wairokpm</i> ➤ <i>Potsangbam Albino Kumar</i> ➤ <i>Anuj Kumar Purwar</i> 	136
33.	Need For Autonomus System to Revolutionise the Indian Banking Industry – A Study of Blockchain Technology <ul style="list-style-type: none"> ➤ <i>Richa Kashyap</i> ➤ <i>Vivek Saurav</i> 	140
34.	Speed Control of Dc Motor by Using Soft Starter <ul style="list-style-type: none"> ➤ <i>Mohammad Safiullah Musalman</i> ➤ <i>Ashish Yadav</i> ➤ <i>Shovanand Chaudhary</i> ➤ <i>Gowtham G</i> 	144
35.	An Efficient VLSI Implementation of CDF 5/3 Architecture on FPGA for Image Processing Applications <ul style="list-style-type: none"> ➤ <i>Saleema</i> ➤ <i>Dr N.V. Uma Reddy</i> 	146
36.	IoT Based Flood Management and Alerting System <ul style="list-style-type: none"> ➤ <i>Prof. Ramachandra C</i> ➤ <i>Sandeep Pandey</i> ➤ <i>Deepti Thapa</i> 	150

CONTENTS

SR.NO	TITLES AND AUTHORS	PAGE NO
37.	Traffic Congestion Studies and Solutions for Kengeri- Hoysala Junction, Bengaluru <ul style="list-style-type: none"> ➤ <i>G Sankara</i> ➤ <i>Rishikesh Badgujar</i> ➤ <i>Komal</i> 	154
38.	Eye Disease Detection using Machine Learning <ul style="list-style-type: none"> ➤ <i>Sanohi K.C Jatav</i> ➤ <i>Dr. Shikha Nema</i> ➤ <i>Dr. Zia Saquib</i> 	162
39.	Predicting the Quantity of Future Heart Attack Patients Using Random Forest Algorithm <ul style="list-style-type: none"> ➤ <i>B. Sarath Chandra</i> ➤ <i>A. Chandramouli</i> 	168
40.	Forensic Accounting: A paradigm shift of auditing <ul style="list-style-type: none"> ➤ <i>Seema Devi</i> ➤ <i>Prof Ram Rattan Saini</i> 	172
41.	Arduino Based Patient Health Monitoring System using Internet of Things <ul style="list-style-type: none"> ➤ <i>Shadakshari</i> ➤ <i>Charutha M V</i> ➤ <i>Shyamala P Bhat</i> 	181
42.	BLDC Motor Based Solar Photovoltaic Array Fed Water Pumping System Using Interleaved Boost Converter <ul style="list-style-type: none"> ➤ <i>Shailesh Kumar</i> ➤ <i>Shashi Bhushan Singh</i> 	184
43.	Conversion of Waste Heat into Electricity Using TEG <ul style="list-style-type: none"> ➤ <i>Shifanaaz A</i> ➤ <i>Misbah Falak M</i> ➤ <i>Anil Kumar T</i> ➤ <i>Gowtham G</i> 	190
44.	Model Reduction and Optimization of Interval System Using H-infinity Norm and Genetic Algorithm <ul style="list-style-type: none"> ➤ <i>Shubham</i> ➤ <i>A.N. Jha</i> 	194
45.	Cost-Efficient Solar Based Multipurpose Crop Cutting Machine <ul style="list-style-type: none"> ➤ <i>Shyamala P</i> ➤ <i>Amith M Y</i> ➤ <i>Bharath V</i> ➤ <i>Vishwas Gowda H R</i> 	200
46.	Kannada Handwritten Character Recognition (KHCR): A Literature Review <ul style="list-style-type: none"> ➤ <i>Siddanna S R</i> ➤ <i>Dr.Kiran Y C</i> 	203

CONTENTS

SR.NO	TITLES AND AUTHORS	PAGE NO
47.	Assessment of Surface properties of Benincasa hispida and Cucurbita peels for Chromium uptake ➤ <i>Soibam Sangeeta</i> ➤ <i>Thiyam Tamphasana Devi</i> ➤ <i>Potsangbam Albino Kumar</i>	207
48.	Indoor Navigation Using Beacons ➤ <i>Spandana</i> ➤ <i>Veena.S</i>	212
49.	MPPT based Solar PV System Simulation and Analysis using Matlab/Simulink ➤ <i>SriLakshmi R</i> ➤ <i>Dr.Chayapathy V</i> ➤ <i>Dr.Anitha G S</i>	218
50.	Design and Implementation of a Vehicle To Vehicle Communication System Using Li-Fi Technology ➤ <i>Sugnyani Patil</i> ➤ <i>Mr.Mohan Kumar B N</i> ➤ <i>Vani K</i>	222
51.	Radar System Using Arduino and Ultrasonic Sensor ➤ <i>Sunanda C V</i> ➤ <i>Varun K</i> ➤ <i>Bharath KL</i> ➤ <i>Tashi Wangyal B</i> ➤ <i>Prarthan SB</i>	227
52.	Bearing Fault Detection Using Case Western Reserve University Dataset with SVM Approach ➤ <i>Tushar Anand</i> ➤ <i>Bhavnesk Kumar</i>	230
53.	Electronic Voting Machine using Face and Fingerprint Recognition ➤ <i>Vani</i> ➤ <i>Sugnyani Patil</i> ➤ <i>Asha L</i> ➤ <i>Sowmya</i> ➤ <i>Mohit Kumar Singh</i>	238
54.	Case Study on the Effect of Chilling To Reduce Shrinkage Defect on Cast-Iron Castings ➤ <i>Veeresh Gurav</i> ➤ <i>Veeranna</i>	242
55.	Experimental Investigation and Vibration Analysis of Laminated Composite Beam with Multiple Edge Cracks ➤ <i>Vishal Omprakash Jadhav</i> ➤ <i>Prof. Dr. Harshal Ashok Chavan</i>	250

CONTENTS

SR.NO	TITLES AND AUTHORS	PAGE NO
56.	Assessment of Land Suitability for Solid Waste Disposal and Leachate Treatment by waste derived Parkia Speciosa (Petai) pods Activated Carbon ➤ <i>Vivek Laishram</i> ➤ <i>Oinam Bakimchandra</i> ➤ <i>Potsangbam Albino Kumar</i>	259
57.	A New Cascaded Two Level Inverter based Multilevel STATCOM for High Power Applications ➤ <i>Vyshnav B</i> ➤ <i>Akshatha R Hegde</i> ➤ <i>Pradeesha J</i>	264
58.	Comouflage Based Emergency Vehicles Priority with Intelligent Traffic Control Using Movable Road Dividers ➤ <i>Greeshma V</i> ➤ <i>Shruthi A.S</i> ➤ <i>Yashaswini G</i> ➤ <i>Ramya B</i> ➤ <i>Anshu Deepak</i>	270
59.	Design of Hybrid Electric Vehicle with Solar Energy and Wireless Charging ➤ <i>Sunanda C V</i> ➤ <i>Ramachandra C</i> ➤ <i>G Gowtham</i> ➤ <i>Bidhya chhetri</i>	274
60.	Longitudinal Stability Analysis of an Aircraft using RBFANN ➤ <i>G Parimala Gandhi</i> ➤ <i>Dr Nagaraj</i>	278
61.	Disk-Based Real-Time Applications for Power Consumption ➤ <i>B N Mohan Kumar</i> ➤ <i>Divya T M</i> ➤ <i>Sai Prashanth S</i>	281
62.	Cyber Crime ➤ <i>Anshu Deepak</i> ➤ <i>Greeshma V</i>	283
63.	Smart Notice Board Using IoT (Internet of Thing) ➤ <i>Ashok K N</i> ➤ <i>Anil Kumar K</i>	284
64.	Wireless Charging of Electric Vehicle in Smart Cities ➤ <i>Bidhya Chhetri</i> ➤ <i>Hemanjali R</i> ➤ <i>Ruchitha S</i> ➤ <i>Rishi GN</i> ➤ <i>Sunanda C V</i>	285

CONTENTS

SR.NO	TITLES AND AUTHORS	PAGE NO
65.	Image segmentation of White Blood Cells using K-means and Gram-schmidth orthogonalisation algorithm <ul style="list-style-type: none"> ➤ <i>Chitharanjan das V</i> ➤ <i>Dr. Puttamade Gowda J</i> 	286
66.	A wireless sensor networks for early Forest Fire detection and Monitoring <ul style="list-style-type: none"> ➤ <i>Deepti Thapa</i> ➤ <i>Sandeep Pandey</i> ➤ <i>Ramachandra C</i> 	287
67.	Leak Localization on Gas Pipeline using Acoustic Sensors and the MUSIC algorithm <ul style="list-style-type: none"> ➤ <i>Ghassan Alnwaimi</i> ➤ <i>Hatem Boujemaa</i> ➤ <i>Feras Alfosail</i> ➤ <i>Nebras Sobahi</i> 	288
68.	Optimisation of Energy Demand Based on Thermal Comfort Criteria for an Office Building in the Tropical Warm Humid Climate <ul style="list-style-type: none"> ➤ <i>Poornima Kurup</i> 	289
69.	Intelligent Accident Detection and Ambulance Rescue System <ul style="list-style-type: none"> ➤ <i>Rakesh S</i> ➤ <i>Pradeep B M</i> ➤ <i>Shiva Kumar N</i> ➤ <i>Umesh Gouda V Patil</i> ➤ <i>Divya.T.M</i> 	290
70.	Optimization of Physical Parameters for Production of Antimicrobial Compound by Aspergillus Flavus Mtcc 13062 Using Response Surface Methodology <ul style="list-style-type: none"> ➤ <i>Shruti Dudeja</i> ➤ <i>Anil Kumar</i> 	291
71.	Trash Can Monitoring System in the Smart Cities <ul style="list-style-type: none"> ➤ <i>Shyamala P</i> ➤ <i>Charutha .M.V</i> 	292
72.	A Design Pattern Ranking and Optimization Method Based on Intent <ul style="list-style-type: none"> ➤ <i>Marwan Al-Akaidi</i> ➤ <i>Hui Guan</i> ➤ <i>Tianyu Ma</i> ➤ <i>Hongji Yang</i> 	293
73.	Consumer Behaviour in Rural Market of Hanumangarh <ul style="list-style-type: none"> ➤ <i>Dr. Arun Aggarwal</i> ➤ <i>Anjali Chopra</i> 	

ICRTEM -2021

**International Conference on
Research Trends in Engineering &
Management**

**Bangalore, India
20th – 21st August, 2021**

**PAPERS
&
ABSTRACTS**

ICRTEM -2021

Organized by:

R R Institute of Technology, Bangalore, India

In Association with

Institute For Engineering Research and Publication (IFERP)

Automatic Fire Detecting and Fire Fighting Robot

^[1] Abhishek Gowda D , ^[2] Mohan M , ^[3] Sai Prashanth S , ^[4] Tejaswini P , ^[5] Asst Prof. B N Mohan Kumar

Abstract— The safety of humans depends on the safety of where he live, work and travel. The ensurement of security of our home, office and buildings is the utmost priority of human. We develop an security system that contains a fire fighting robot equipped with intelligent sensors. The fire caused by electric may cause huge damages. This is because our present security systems can't detect any small abnormal fires and notify us. In addition, it is difficult for us to detect the small fire caused by electrical circuit / devices. Humans may take a lot of time to find an extinguishing source. Humans may also find it hard to reach the fire, this may be due to small spaces or it ma also lead to dangerous situations where human's may risk their lives due to large fires

I. INTRODUCTION

In present generation robotics is one of the fastest growing engineering field, which has furnished applications in it. The main purpose oof developing a robot is to remove the human factor in any kind of dangerous work and environment. In today's world robots are used widely in almost every field of work. The need of fire fighting robot is that it can detect fire and extinguish it automatically without risking any human lives. Also the objective is to reduce the air pollution ,where the large fire can cause an enormous amount of air pollution, hence with the use of designed robot we can put-off the fire in its early state. The robot is designed ass a wireless controlled and operated box, which runs on battery with no external power source. The robot is designed in such a way that it can detect the fire and extinguish it with a provided extinguishing source. Since robot is a flexible device it can be used in any environment. All these commands, instructions and controlling of the device is done through programming Arduino UNO. And this fire protection robot which can replace the present type of fire fighting units leads to create a high demand in the market. The real life fires occurs without our realization and when it is least expected . Ensuring the safety of living beings a monitoring system is required to look after the surroundings at all moments of time
This design is the basic concept which is easy to understand and learn from beginning to end for freshers as well as masters in the robotics engineering field. The sole purpose of this robot is to detect the fire within its range and extinguish the fire immediately and to ensure that no human lives are endangered by carrying out its job in a perfect and précised manner.

II. RELATED WORK:

The fire fighting robot is an automated system which has flame sensors based on IR technology. The aim is to develop a human free automated device ,which is in working state all the time. Implementation of the fire fighting robot proposed by J.Reinhert.V.Khandwala[1] and Lynette Miller Daniel Rodriguez[2], designed assembly and construction of robot hardware, the processing algorithm based on the sensors response and the navigation algorithm that will enable the robot to find an easy way in and out of the fire prone area. Sahil. S.Shah[3],designed a robot based on embedded system, wherein the robot is capable of fighting a simulated household fire. This robot can even act as path guide for human's to get of the fire prone area. U.Jyostna Sai Prasanna[4] designed a fire detection system using 4 flame sensors, In this design the robot is equipped with 4 thermistor / flame sensors. In this design if the temperature increases beyond the predetermined threshold value, buzzer sounds to intimate the occurrence of fire accident and a warning message will be sent to the respective personnel in industries.

III. HARDWARE REQUIREMENT:

1. Arduino uno



fig 3.1.1 : Arduino uno front



fig 3.1.2 : Arduino uno back

The Arduino uno is a microcontroller board based on the Atmega328. It consists 14 digital input/output pins, 6 analog inputs a 16 MHz ceramic resonator, a usb connection, a

power jack, an ICSP header and a reset button. Its operating voltage is 5V, the recommended input voltage is 7-12V, the maximum input voltage is 6-20V. The DC current per I/O is 40 Ma. The DC current for 3.3V pin is 50mA. It consists of 32 KB of flash memory of which 0.5 KB used by bootloader, 2KB of SRAM, 1KB of EEPROM. It operates at the frequency of 16MHz. it can be powered via usb or an external power supply. This microcontroller can be programmed using Arduino IDE software.

2. L293D Motor Driver



fig 3.2.1 : L293D Motor driver

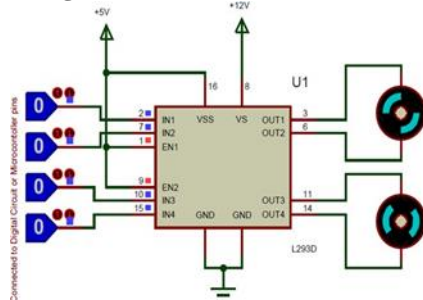


fig 3.2.2 : circuit diagram of L293D IC

A motor driver is an integrated chip, which is usually used to control motors. L293D is a dual H-bridge motor driver integrated circuit (IC). Motor Driver act as a current amplifier since they take low-current control signal and provide a high-current signal. This high current signal is used to drive the motor. The maximum peak motor current is 1.2 A and maximum continuous motor current is 600 mA, with transition time 300ns. This L293D motor drive is available in 16-pin DIP, TSSOP, SOIC packages.

3. Flame Sensor Module



fig 3.3 :Flame Sensor Module

The Flame Sensor is used to detect the flame by detecting the light that is present in the infrared (IR) spectrum produced but an open flame. This Module provides both digital and an analog output with potentiometer to adjust the sensitivity.

This flame sensor is compatible to 3.3V to 5V. This Flame Sensor module is similar to a regular IR sensor, but with a broader detection range, hence it can be used as general IR detector for other applications where wide detection range is required

4. 4-wheel chassis



fig 3.4: 4-wheel chassis

This is a double layered 4-wheel smart car robot base. It consists of four pairs of geared motors and wheels. This kit is transparent so as to create dynamic handling of components mounted on it. This chassis comes with attractive design with huge mounting holes and enough space, hence this makes it easy to install different sensors and other components.

The geared motors operates at the voltage 3V-6V DC at a gear ratio of 1:48. The wheel comes with the diameter of 65mm and width of 27mm with the loading capacity of 2.5Kgs.

5. DC Servo Motor



fig 3.5: DC Servo Motor

This servo motor is a rotary type which can rotate with a great precision. It is made up of a simple motor through a servo mechanism. This type of motor consist of control circuit that provides feedback on the current position of the motor shaft. Since the servo motor comes with a gear arrangement that allows us to get a very high torque. Usually servo motor can rotate from 0-180 degrees but it can go up to 210 degrees, depending upon the manufacturing. The servo motors work directly with +5V supply rails but we have to be careful about the amount of current the motor would consume.

6. 18650 Battery



fig 3.6: 18650 Battery

It is a rechargeable lithium-ion battery. The name 18650 indicates its size 18mm(dia) x 65(height) mm. It works with

the nominal voltage of 3.6V and nominal capacity of 2850 mAh. The minimum discharge voltage is 3V and maximum discharge current of 1 C. The approximate charging time for these batteries is 3 hours. This battery are usually used in power banks, power walls, laptop battery, solar powered devices and electric vehicles.

IV. DESIGN:

This prototype automatically detects the fire and extinguish it. This robot has fire sensors interfaced in it control circuitry, which helps to the presence of fire and to respond accordingly. This robot is designed to operate where the chances of fire to increase is high. Since it is an automatic robot it need not to be operated from any external source.

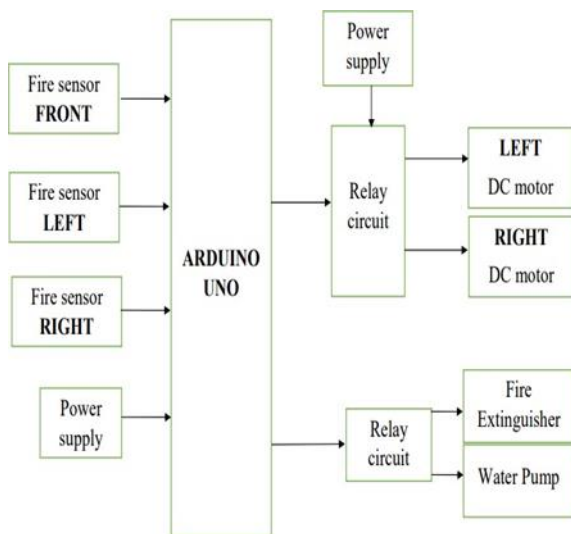


fig 4.1:Block Diagram

circuit explanation: This fire extinguishing robot is a prototype of the actual one. Sensor used in this circuit is flame sensors module.

The flame sensor modules are connected as following

- The VCC pins of flame sensors are connected to pin 5V of Microcontroller ATmega 328.
- The GND pins of flame sensors are connected to pin GND of Microcontroller ATmega 328.
- The DO (Digital Out) pins of flame sensors is connected to pin 8 (front sensor), pin 9 (left sensor), pin 10 (right sensor).

The motors of the wheels are connected as following:

- The left side motors are interconnected and two shorted connections are taken by separate wires.
- The following is done as same to the right side of the motors. The DC servo motor connections are made as following: There are 3 wires connected to the DC servo motor,
- RED colour wire is connected to pin 5V of Microcontroller ATmega 328.
- BLACK colour wire is connected to pin GND of Microcontroller ATmega 328.
- BROWN colour wire is connected to pin 11 of Microcontroller ATmega 328. There are 2 L293D motor drivers used in the circuit connection

L293D motor driver (1):

- The two shorted wires of the left motors are connected to M1 port of L293D motor
- The two shorted wires of the right motors are connected to M2 port of L293D motor driver.
- The pins A1 and A2 of the L293D motor driver is connected to pins 2 and 3 respectively to the Microcontroller ATmega 328.
- The pins B1 and B2 of the L293D motor driver is connected to pins 4 and 5 respectively to the Microcontroller ATmega 328.

L293D motor driver (2):

- The pins B1 and B2 of the L293D motor driver are connected to pins 7 and GND respectively to Microcontroller ATmega 328.
- Two wires of the mini water pump are connected to M1 port of L293D motor driver. The 18650 li-ion battery connections are shown as following:
- From two L293D motor drivers two positive ports are shorted and two negative ports are shorted and these shorted wires are connected as positive to positive and negative to negative of the battery.
- Another two wires from the battery are connected to Vin and negative end is connected to GND to the Microcontroller ATmega 328.

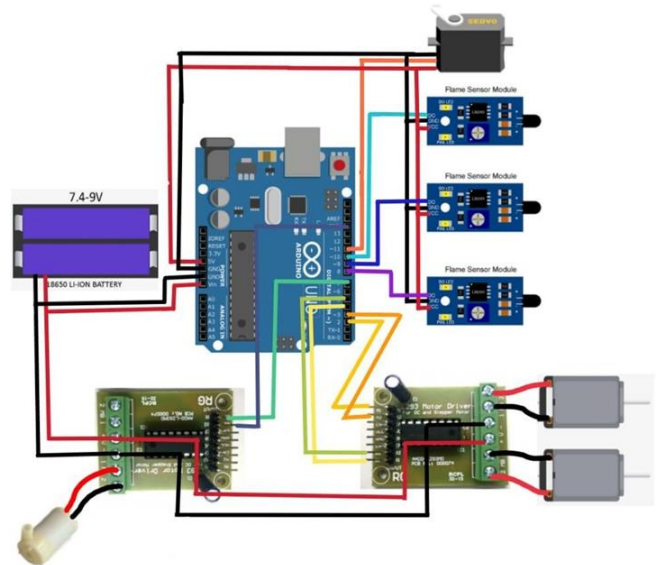


Fig 4.2: Circuit Diagram

V.APPLICATION



fig 5.1: Side View



fig 5.2: Front View

The robot could be maintained in any location where humans cannot go and put off the fire. Also live informs about the fire places are streamed to the user uninterruptedly, if we use the monitoring system

- can be used in record maintaining rooms where fire can cause loss of valuable data.
- can be used in server rooms for instantaneous action in case of fire.
- can be used in extinguishing fire where probability of detonation is high. for e.g.
 - hotel kitchens, lpg/cng gas stores, etc.
- every working location requiring permanent operator's attention.
 - at power plant control rooms.
 - at captain bridges.
 - at flight control centres.

VI. MERITS AND DEMERITS

1. Merits

- Linear detection line.
- Rapid reaction time.
- 24 hours a day ready to use.
- Minimum maintenance
- Reduced human effort.

2. Demerits

- No monitoring system for the vehicle
- No remote control for the robotic movement
- Our system used only for low weight applications
- It is not used to put of large fires
- It cannot be worked beyond the limit

VII. RESULTS AND CONCLUSION

- Here we successfully developed the AUTOMATIC FIRE DETECTING AND FIRE EXTINGUISHING ROBOT.
- In this project we aim to condense the effects of fire accidents which usually start from small flame, therefore people's life and money would be saved.
- The robot can efficaciously find fire and reach it .
 - Robot senses the flame at the place where the robot exists.
- The movement of this robot vehicle is controlled by Microcontroller ATmega 328 as per the program.
- If fire is sensed with the help of flame sensors, Microcontroller ATmega 328 operates the water pump mechanism through L293D motor driver circuit.
- We be able to construct a robot which is user friendly and eco friendly.

VIII. REFERENCES

- [1] LynetteMiller&DanielRodriguez(2003):https://www.google.com/url?sa=t&source=web&rct=j&url=http://www.mil.ufl.edu/publications/fcrar03/Firebot.pdf&ved=2ahUKEwi6je_2juTwAhX64jgGHWtyDSIQFjAAegQIAxAC&usg=AOvVaw0y7-1A2zlt_aPgHcEynLWS
- [2] SahilS.Shah(2013):https://www.google.com/url?sa=t&source=web&rct=j&url=http://ijert.org/papers/IJERT_185446.pdf&ved=2ahUKEWj-06u6j-TwAhVvILcAHbEVCTMQFjAAegQIAxAC&usg=AOvVaw3rxw_gwyuHHyGwrQd4R6mR
- [3] M.V.D.Prasad:https://www.google.com/url?sa=t&source=web&rct=j&url=https://www.ijsr.net/get_absract.php%3Fpaper_id%3DIIJRON2013738&ved=2ahUKEWjxtDdj-TwAhUFzjgGHYDIDlgQFjABegQIJhAC&usg=AOvVaw36UAm-jKwxfyVMUTEWid5o
- [4] Saravanan.P(2015):https://www.google.com/url?sa=t&source=web&rct=j&url=http://ijert.org/papers/IJERT_185446.pdf&ved=2ahUKEWijn8jKkOTwAhWHILcAHaGiAzoQFjADegQICBAC&usg=AOvVaw3rxw_gwyuHHyGwrQd4R6mR
- [5] Abhilash.Dhumatkar,Sumit,Bhigode.(2015):<https://www.google.com/url?sa=t&source=web&rct=j&url=https://acadpubl.eu/hub/2018-119-16/1/184.pdf&ved=2ahUKEWjj5aLskOTwAhXdH7cAHQOWCREQFjAAegQIAxAC&usg=AOvVaw097U6uY6flaIoeQI5uMZt-https://www.pololu.com/product/2191:~:text=The%20Arduino%20no%20is%20a,header%2C%20an d%20a%20reset%20button>
- [7] <https://components101.com/ics/l293d-pinout-features-datasheet>
- [8] <https://protosupplies.com/product/flame-sensor-module/>
- [9] <https://www.electronicshobby.com/4-wheel-smart-car-chassis-kit-india>
- [10] <https://engineering.eckovation.com/servo-motor-types-working-principle-explained/>
- [11] https://en.wikipedia.org/wiki/Lithium-ion_battery

Cost-Efficient Arduino-based Automated Washroom Sanitizing System

^[1] Aishwarya S, ^[2] Dr. Sunitha H D, ^[3] Amrendra Tripathi, ^[4] Anuradha Lakra, ^[5] Prabha k
^{[1][3][4][5]} UG scholar, Dept of ECE, R R Institute of Technology Chikkabanavara, Bangalore
^[2] Professor, Dept of ECE, R R Institute of Technology, Bangalore

Abstract— *The proposed project is based on automated washroom sanitizing system that mainly deals with solving the problem of unhygienic condition of public toilets. Sanitation is one of the largest problems faced by people in our country. Even though 6 percent of the urban people are relying on public toilets for their daily use, they are still not hygienic. This has become one of the most basic issues faced by people everywhere. Providing the best solution to this issue is the aim of our project. The existing method involves manual cleaning done by a human which is not at all an easy task and may not even exist in all areas. Implementing a facility to clean the major units of a washroom after several cycles will maintain a sufficient hygienic environment. The cleaning process is aimed to be automated and simple. Such a provision will ease the job of regular janitors as well as the users. Placing sensor-controlled water flusher attached to the toilet will perform the cleaning task and meanwhile, the number of cycles used is recorded to activate the automated cleaning process. On selecting ESP32 microcontroller as suitable interfaces we aim to provide an easily compatible facility at an economically feasible rate. We aim to ease the brushing technology using a simple belt and DC motor-driven mechanism. Hence, on adopting this methodology, we will be able to increase the standard of public and community toilets and facilitate people to use these effectively.*

Keywords—sanitization, automation, sensors

I. INTRODUCTION

In our country due to unhygienic toilets people suffer from various diseases like typhoid, cholera, hepatitis, etc. This happens because of improper use of given facilities, negligence by maintaining staff, unavailability of resources, etc. Also, the maintenance staff has to be there for maintaining the toilets whole day. This is a pity job to stay in the toilets for whole day even when not paid adequately nor provided safety equipment. A comfort station may be a room or small building with one or more toilets (or urinals) available to be used by the overall public, or by customers or employees of a business. Mostly Public toilets are commonly female facilities although some are unisex, especially for little or single-occupancy public toilets. Increasingly, toilets are also for people with disabilities. Some public toilets are free from charge while others charge a fee. In the latter case they're also called pay toilets and sometimes have a coin-operated turnstile. Local authorities or commercial businesses may provide comfort station facilities. Some toilets are unattended while others are staffed by a janitor or an attendant. Public toilets are typically found in schools, offices, factories, and other places of labor. Similarly,

museums, cinemas, bars, Entertainment venues and many other places usually provide public toilets [1][2][3][5].

We propose a system that ensures the cleanliness of the restroom every time after its use. Even the cleanliness level is monitored keenly and rated so that the travelers who are new to the place can use the restrooms by knowing the cleanliness level.

II. LITERATURE SURVEY

i. Developing smart toilets using IOT [2018]:

This paper is based on IOT and image-processing concepts using different sensors like smell sensor, IR sensor, sonic sensor, RFID reader to create a smart toilet [4]. Model consisted of well-designed brush coupled to the motor which rotates at an appropriate speed. When the motor runs, ultimately the brush rotates. Semi-automatic toilet cleaning brush consists of a tube connected to the container which carries the chemical solution to increase the viscosity between the bowl surface and the toilet stain, thus helping the user to flush away the stain with much less effort. The release of chemical from the tank is by a simple valve mechanism. A telescopic stem with a single plunger pipe is implemented which can be locked at the desirable length. The inner pipe slides through the key way of the outer pipe. It is handy and can be moved anywhere.

ii. Design and Refabrication of Advanced Mechanism for Indian Dome Cleaning [2019]:

This project uses rack and pinion arrangement along with washer to clean complete system. A high torque motor is used to clean the complete floor. This complete system is power saving and takes less time to complete the task. This system is cost effective. This system would be useful at home, schools, colleges, hospitals, companies, factories and anywhere. [9]

iii. Design and development of automatic Indian lavatory Cleaning robot [2019]:

The paper presents design of automatic Indian lavatory cleaning robot. The cleaning system is fully automatic and requires low operational power for cleaning purpose. Furthermore, to thoroughly clean the toilet, robotic arm is used and this arm is part of cleaning module. Microcontroller ARM LPC 2148 is used to control the action of cleaning robot. The real time clock is used to perform particular action at particular time. [6][7][8][10]

III. DESIGN AND DEVELOPMENT

The experimental setup requires ESP32 which is the heart of the system, ultrasonic Sensor, PIR (Passive Infrared) sensor, servo motor, water pump, power supply adaptors, DC motor, relays, and power module (220V to 5V) mainly. Fig 1. shows the block diagram of the automated flushing and floor cleaning unit.

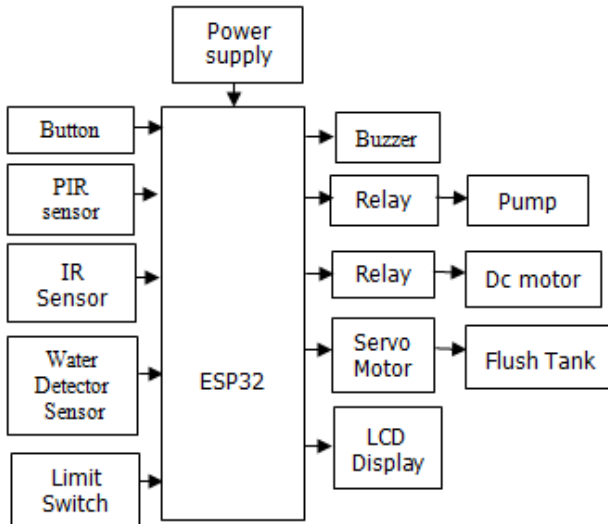


Fig 1: Block Diagram of Proposed system (Flushing and Floor Cleaning Unit)

A. Automated flushing unit:

ESP32 Controller works as the interface to control the components and to act as an output and input detector. PIR sensor is used to detect the presence of the human in the toilet. As well as IR sensor for the detection of range accurately [4]. It is placed top to the seat so that it can easily detect the presence. This sensor will be sensing the presence for a certain amount of time to generate a value and the generated value is sent to the controller. It is placed inside the water container cap. This will measure the distance between the cap and the water level. The sensor records the value and sends it to the controller. The controller is implemented with a program to receive the values from both of these sensors. There are two conditions to be satisfied:

1. First, the presence of the human must be detected. Hence it says that humans had used the toilet for purpose.
2. The state of the water in the container to be checked whether it was flushed by the user or not. Now the controller is connected with the servo motor.

Servo motor is fixed on the flush tank attached to the flush lever [11]. When both the conditions are satisfied, the servo motor is rotated with each step pulling the flush lever down. Hence, automated flushing works. After that, the servo motor steps back to its original position

B. Floor Cleaning Unit:

The purpose of this unit is to spray water from different angles of the bathroom floor. A DC pump is used. It is connected to a relay switch and it turns ON or OFF if the user is provided input [9]. The needful water is taken from the tap valve within the bathroom. The water pump outlet is

connected to different nozzles placed per the shape of the bathroom. When the water is pumped through the nozzle, washable dirt reaches the floor drain trap. It will clean the bathroom roughly for the next user.

C. Brushing Unit:

The third is a portable external unit. The main purpose of this unit is to clean the bowl without any human effort. The only work for the human is to pour the toilet disinfectant liquid solution into the bowl. It can be controlled by an app called Blynk. The controller used for the switch is ESP32 with relay. This is a Wi-Fi module which is acting as wifi switch in this project. This app is downloadable from the play store or apple store. It is used to control the brushing system. ESP8266 can be easily coded using Arduino software and uploaded

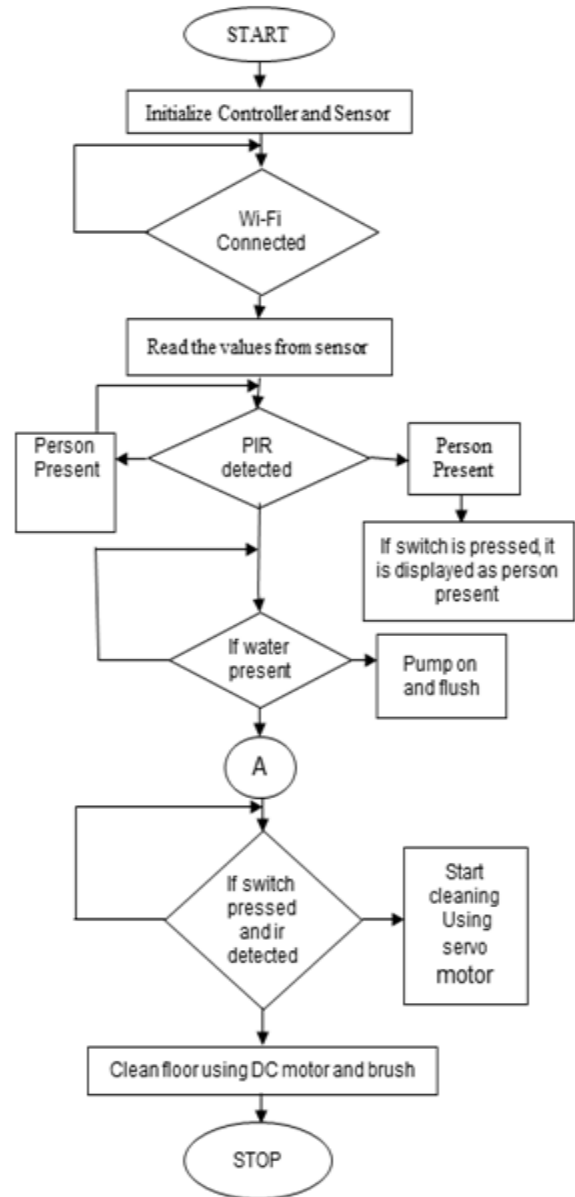


Fig 2 Flow chart of the automated flushing unit

Components used for the Wi-Fi switch are ESP6822, relay switch, a power module. The components used include DC motor to have the rotatory motion we're brushes are connected for cleaning. Figure 2 shows the flow chart of the process.

IV. METHODOLOGY AND EXPERIMENTAL FLOW

Passive sensor and IR sensor were placed at the door to detect the count. A water level sensor is placed in the flushing tank to detect the level of water and a buzzer will turn on/off simultaneously indicating the level of water. The controller which we used here is ESP32 for the ease of programming purposes. The entire project is divided into three units. The first one was automatic flushing, which will flush by detecting whether the user has flushed or not. PIR sensor, servomotor, water level sensor, and ESP32 were used. Fig 3 shows the prototype of the working model. During the implementation of the first phase, several improvements were noted like, the casing of the entire system should be selected which will ease the users and it also depends on the number of users using the toilets. The design of the brushing unit used a dc motor with a metal stand that will be turning and driving the wheels. Semi porous flexible brushes that could squeeze the right amount of cleaning liquid might have been a better option.

V. RESULT AND DISCUSSION

The push button is pressed by the users when he gets inside the washroom, the PIR sensor sends a signal when the user has entered and IR sensor is also used to detect the person as much accurately as possible. Combined with both the inputs, the controller switches the servo motor connected to the brushes. When the person exits the washroom PIR sensor and IR sensor will detect or it will take the count of 5seconds then automatically will flush water in the tank and after cleaning it comes to its original state. The brushing unit is portable so it can be fixed as per the need —, this is controlled by a mobile app known as BLYNK. It can be switched on from outside of the bathroom. It cleans the bowl with plastic synthetic brushes. The proposed system is cost effective compared to the existing systems. When studying the various floor cleaning mechanisms in the existing systems [9][12], we have those systems as extremely complex to be used in washroom cubicles or smaller areas. Such apparatus are seen to take up a large space and they may not be easy to move around to reach every corner of the cubicle areas

VI. CONCLUSION AND FUT URE SCOPE

Because of the unhygienic environment, most individuals avoid using public restrooms. Our project major goal was to improve the sanitary conditions of public restrooms. We choose ESP32 because of its ease of programming and built-in Wi-Fi module. The PIR sensor was chosen because of its increased detection range and precision. We look forward to a world with improved sanitation and fewer diseases. Additionally, with flushing unit we have used

switch and IR for the detection of dirt and to clean inside. For the floor cleaning we have used dc motor and brush. Activated carbon acts as an adsorbent and absorbs the odour particles.

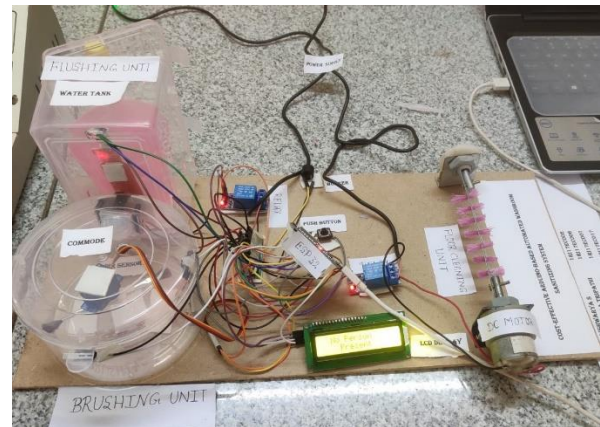


Fig 3 The final prototype of the brushing unit.

REFERENCES

- [1] Surya AV, Vyas A, Krishna M, Abidi N. "Identifying Determinants of Toilet Usage by Poor in Urban India". *Procedia computer science*. 2017 Jan 1; 122:634-41.
- [2] Singavarapu, Praneet & Murray, Emmanuel. "Impact of Inadequate Sanitation on the Marginalised". 2013.
- [3] INDIA IS. "Inadequate Sanitation Costs India Rs. 2.4 Trillion (US \$53.8 Billion)". 2011.
- [4] Elavarasi MK, Suganthi MV, Jayachitra MJ. "DEVELOPING SMART TOILETS USING IOT ". *International Journal of Pure and Applied Mathematics*. 2018;119(14):611 -8.
- [5] Sclar GD, Penakalapati G, Amato HK, Garn JV, Alexander K, Freeman MC, Boisson S, Medlicott KO, Clasen T "Assessing the impact of sanitation on indicators of fecal exposure along principal transmission pathways: a systematic review". *International journal of hygiene and environmental health*. 2016 Nov 1; 219(8):709 -23.
- [6] Kumar A, Bharadwaj A, Balasubramanian R, Gowtham P. "Autonomous lavatory cleaning system". *International Journal of Robotics and Automation (IJRA)*. 2015;6(4):65.
- [7] Deepak B, Brinth Khanna J, Arun Baby M and Robin Raju. "Autonomous Lavatory Cleaning Robot" *International Journal for Scientific Research and Development* 5.8. 2017; 543-545.
- [8] Tokarev D, Allouch D, inventors; Toilet bot Ltd, assignee. "Automatic toilet cleaner". United States patent application US 15/736,640. 2018 Aug 2.
- [9] Gawande AC, Aher S, Barwad S, Bande D, Fatinge S, Dhoble P, Urkude R. "Design and Refabrication of Advanced Mechanism for Indian Toilet Dome Cleaning". 2019.
- [10] Patil A, Awati J. "Design and development of automatic Indian lavatory cleaning robot ". Available at SSRN 3352345. 2019 Mar 14.
- [11] Ben Amram A, inventor; SPINX ROBOTICS LTD., assigned. "TOILET CLEANING SYSTEM". United States patent application US 16/497,453. 2020 Apr 9.
- [12] Khalid U, Baloch MF, Haider H, Sardar MU, Khan MF, Zia AB, Qasuria T A. "Smart floor cleaning robot (clear) ". *IEEE standard*. 2015

Three Phase Power Failure Detector and Voltage Measurement Using Arduino

^[1] Ramachandra C, ^[2] Akash Kumar Singh, ^[3] Embdorka Syiem, ^[4] Amit Kumar Singh

^[1] Asst. Professor, EEE Department, RRIT, Bangalore, India

^[2]^[3]^[4] Student, EEE Department, RRIT, Bangalore, India,

Abstract— Three phase power failure preventor is a device which used in detection of power failure in 3 phase power supply. It is a device where the user would be acknowledged that one of the phase has been failed. This would be known to the user as the circuit trips off the power supply, in other system the detection would be presented with leds or buzzer. Three phase power failure prevention using microcontroller is the device where supply would provide to relays using transformers and rectifier circuit. And the controller we are using in proposed system is arduino nano, the power supply to the controller would be given by using power supply. For displaying fault messages we are making use of 16*2 lcd display. Initially the circuit will be working fine and there would not be any fault messages in the display as there is no failure of any phases. Once any one of these phases fail, the controller detects this failure and with the help of relays the circuit is turned off. Now the failure message displays on lcd display and only particular phase needs to be corrected and circuit will be working fine.

Keywords— WSN, IoT, WI-FI, fire alarm, ESP32, RF module, real-time.

I. INTRODUCTION

The Three phase power failure preventor using microcontroller is protection machine/circuit which prevents dangers taking place, as we all know there will be three phases in a power supply phase, neutral and earthing connections, the normal power phase preventor just trips the phase and user would not know, but in proposed system we would be having a lcd display where we will be getting to know which phase has been failed. Also, in our proposed system as the process is automated by using microcontroller risk is reduced and it becomes easier for the detection and operation processes. In village areas farmers will be using motors for water supply purpose which would be using 3 phase power supply for their operation. This can be overcome by implementing the proposed system in the circuit. Three phase power failure preventor is a device which used in detection of power failure in 3 phase power supply. It is a device where the user would be acknowledged that one of the phases has been failed. Sometimes even if there are some faults in the phase connections the motor still run which in turn results in device get damaged or even failed. This can be overcome by implementing the proposed system. This would be known to the user as the circuit trips off the power supply, in other system the detection would be presented with LEDs or buzzer. Three phase power failure prevention using microcontroller is the device where supply would provide to relays using transformers and rectifier circuit. And the controller we are using in proposed system is Arduino nano,

the power supply to the controller would be given by using power supply. For displaying fault messages, we are making use of 16*2 Iced display. Initially the circuit will be working fine and there would not be any fault messages in the display as there is no failure of any phases. Once any one of these phases fail, the controller detects this failure and with the help of relays the circuit is turned off. Now the failure message displays on Led display and only particular phase needs to be corrected and circuit will be working fine.

II. MICROCONTROLLER

Arduino nano is an open-source firmware and development kit that helps you to prototype or build [OT product. It includes firmware which runs on the where the user would be acknowledged that one of the phases has been failed. Sometimes even if there are some faults in the phase connections the motor still run which in turn results in device get damaged or even failed. This can be overcome by implementing the proposed system. This would be known to the user as the circuit trips off the power supply, in other system the detection would be presented with LEDs or buzzer. Three phase power failure prevention using microcontroller is the device where supply would provide to relays using transformers and rectifier circuit. And the controller we are using in proposed system is Arduino nano, the power supply to the controller would be given by using power supply.

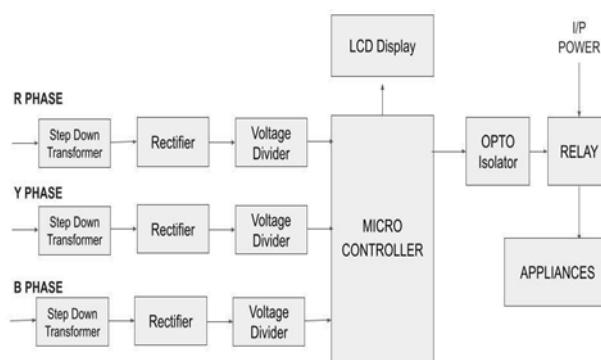


Fig.1: Block diagram

For displaying fault messages, we are making use of 16*2 Iced display. Initially the circuit will be working fine and there would not be any fault messages in the display as there is no failure of any phases. Once any one of these phases fail, the controller detects this failure and with the help of relays the circuit is turned off. Now the failure message displays on

Led display and only particular phase needs to be corrected and circuit will be working fine.

Microcontroller

Arduino prototype Voltage Divider The circuit used to create a voltage equal or less than the input voltage is termed as voltage divider.

Rectifier

It is circuit used to create pulsating DC out of AC input. It is majorly used in power supplies.

Step Down Transformer

As the input voltage is very high, we need to step it down to use it for certain application. The circuit which steps down the input voltage to certain fixed output voltage.

Led Display

A flat panel-display or other electronically modulated optical device that uses the light modulating properties of liquid crystals is called as Liquid Crystal display or LCD display.

Opto-coupler

An electronic component that transfers electronic signals Between two isolated circuit by using lightboat isolators prevent high voltages from affecting the system receiving the signal is called an opto-coupler.

Relay

Here in this block relay is used as an electromechanic switch. It controls the circuit electromechanically.

Power Supply

Here as a source for providing power to the power supply we are using power bank which provides 2.1 volts.

III. HARDWARE DESCRIPTION

Display-LCD 16*2

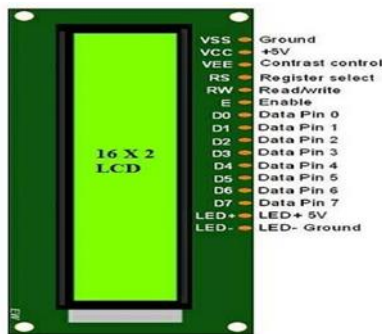


Fig.1: LCD DISPLAY

It is one kind of electronic display module used in an extensive range of applications like various circuits & devices like mobile phones, calculators, computers, TV sets, etc.

These displays are mainly preferred for multi-segment light-emitting diodes and seven segments.

The main benefits of using this module are inexpensive; simply programmable, animations, and there are no limitations for displaying custom characters, special and even animations, etc.

Arduino Nano

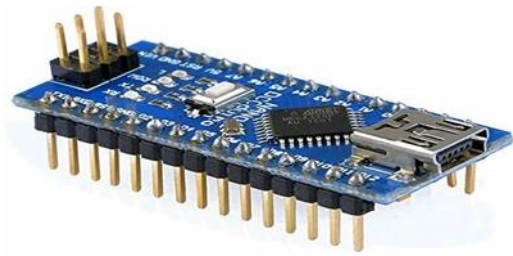


Fig.2: Arduino Nano

The Arduino Nano is a small, complete, and breadboard-friendly board based on the ATmega328 (Arduino Nano 3.0) or ATmega168 (Arduino Nano 2.x).

Features

- It has 22 input/output pins in total.
- 14 of these pins are digital pins.
- Arduino Nano has 8 analog pins.
- It has 6 PWM pins among the digital pins.

IV. SOFTWARE AND TOOLS

Visual Studio code is a source code editor developed by Microsoft for window\ MACOS. It includes support for debugging.

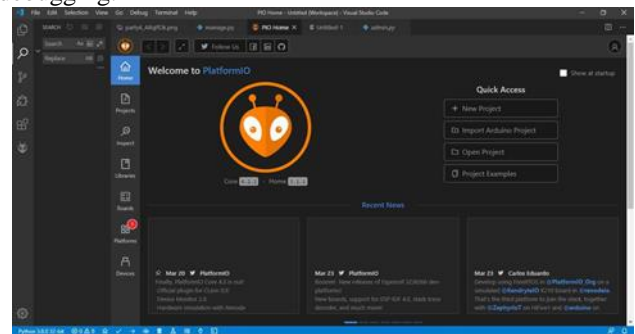
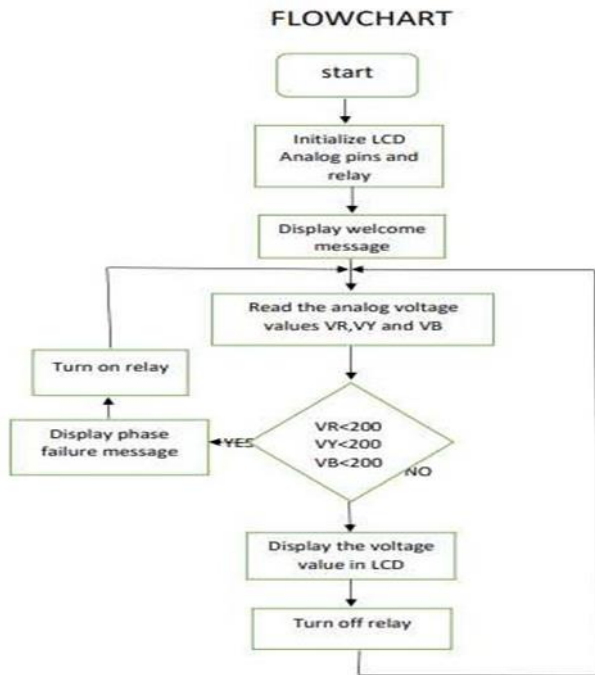


Fig.3: Starting of VS code.

Flow chart

- Initialize
- Display welcome message on display screen
- Read the analog values VR VY VB
- Compare all voltages with 200volts if at least any one is less the LCD displays failure message.
- Now the relay turns on and circuit is tripped.
- If all three condition is satisfied value of voltages are displayed on LCD display,
- Now the relay turns off and procedure repeats.



V. CIRCUIT DIAGRAM

The circuit diagram of Three Phase Power Failure Preventer is shown in figure

Power supply circuit is used for supplying power to the other components except microcontroller. Power bank is used as the source for power supply to the microcontroller. Rectifier circuit is used to provide rectified output by using ac input (ac input is converted to pulse setting dc). Power supply circuit is used for supplying power to the other components except microcontroller. Power bank is used as the source for power supply to the microcontroller.

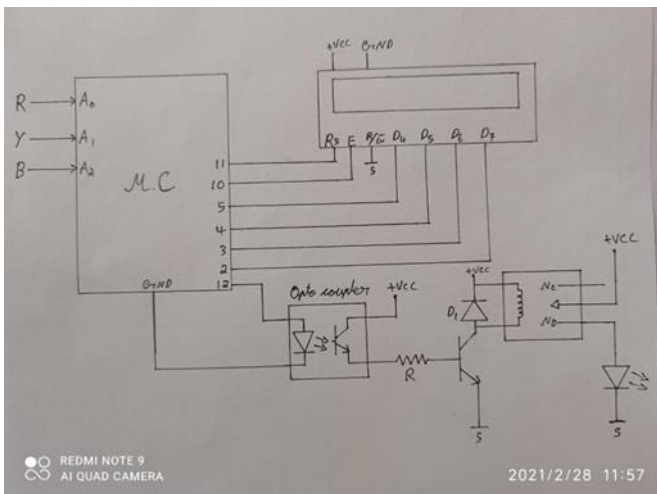


Fig.4: Circuit Diagram

Working

- Initially all the phases are on, and circuit will be functioning properly.
- Rectifiers and transformers pretend to be components of power supply
- LCD display is used in displaying the values so that the user gets the knowledge of what is happening inside the circuit
- When one of the Phase fails to operate, Remains safe. Not only this but proposed trip off the supply so the circuit plays data on LCD display.

VI. ADVANTAGES AND DISADVANTAGES

ADVANTAGES:

- Three phase circuit provides greater power density.
- Makes easier to balance loads in three phases.
- Reduces neutral wiring problems.

DISADVANTAGES:

- Higher cost of standby units.
- Repairing inconvenience are more as the circuit would be complex.

VII. APPLICATIONS AND FUTURE SCOPE

APPLICATIONS:

- It can be used in agricultural sector in water pumping motor sections.
- It can be used in industries where high power motor using 3-phases are used.

FUTURE SCOPE:

This circuit can be further modified by implementing IOT. So, that the device becomes smarter and operation speed can be increased.

VIII. CONCLUSION

This circuit helps in tripping the circuit after letting the user know by displaying phase failure details. It can further be improved by implementing GPS and GSM models and letting user know about the functioning even during his absence.



Fig.5: Working model

REFERENCES

- [1] Sec, D. and Mikulecky, P., 2019, September. Two Phase Failure Detection Using Fuzzy Logic. In International Conference on Computational Collective Intelligence (pp. 271-282). Springer, Cham.
- [2] Waswani, R., Pawar, A., Deore, M. and Patel, R., 2017, March. Induction motor fault detection, protection and speed control using arduino. In 2017 International Conference on Innovations in Information, Embedded and Communication Systems (ICIIECS) (pp. 1-5). IEEE.
- [3] Sase, K.D., 2020. Arduino based Single Phase Fault Detection System using IoT.
- [4] Ali, A.J., Ibraheem, A.M. and Mahmood, O.T., 2020, February. Design of a smart control and protection system for three-phase generator using Arduino. In IOP Conference Series: Materials Science and Engineering (Vol. 745, No. 1, p. 012027). IOP Publishing.
- [5] Waswani, R., Pawar, A., Deore, M. and Patel, R., 2017, March. Induction motor fault detection, protection and speed control using arduino. In 2017 International Conference on Innovations in Information, Embedded and Communication Systems (ICIIECS) (pp. 1-5). IEEE.
- [6] Vadje, R., Kshirsagar, P., Shinde, R., Kamble, A. and Ramteke, A., 3-PHASE FAULT DETECTION WITH GSM MODEM.

Improved Output from Buck-Boost Converter for Commercial Loads

^[1] Akshatha.R.Hegde, ^[2] Vyshnav B, ^[3] Pradeesha J, ^[4] Ramachandra C

^[1] Assistant Professor, R R Institute of Technology

^{[2][3][4]} R R Institute of Technology

Abstract— This paper has improved Multi-output Buck-Boost Converter for commercial purpose which deals with the regulation of the output voltage. Several output voltages can be generated and used in different applications such as multi-level converters with diode-clamped topology or power supplies with several voltage levels employing this topology. . It can be employed for both steady state and transient response Dependency of DC-link voltage balancing and the power factor of the load must be reduced and it is challenging to the suppliers to build such multilevel inverter. Multi-output DC-DC converter has a wide range of applications but it has input voltage disturbance. In this paper, the effect of these disturbances from the output voltages can be reduced.

Keywords— Buck Boost converter, Multi-output converter, PWM

I. INTRODUCTION

The DC - DC Buck-Boost converters are widely used in computer hardware and industrial applications such as computer periphery power supplies, car auxiliary power supplies, aerospace, servo-motor drives and medical equipment and also in agricultural purposes. In recent years, the DC-DC conversion technique has developed greatly. High gain voltage converters are necessary for the above mentioned applications. The Pulse Width Modulation (PWM) technique used to get the variable output voltage from these converters results in high switching losses, high switching stresses, reduced reliability and increased Electromagnetic Interference (EMI) when the converters are operated at high frequencies.

The main objective of this proposed converters is to overcome these drawbacks and to design new converters to achieve high efficiency, high power density and voltage gain. To increase the power density and to reduce the size and weight of the converter with high voltage gain, the proposed Enhanced Multi-Output Buck-Boost Converter is designed with capacitors having individual charging capacities which are greatly used in reducing the imbalance in voltage levels.

The single-inductor multi-output DC-DC converter, named enhanced multi-output buck-boost (MOBB) converter, which is capable of step-up (SU) and step-down (SD) conversions. In this topology, several output voltages can be generated, which may be useful in a variety of applications such as diode-clamped multi-level inverters and multi-voltage DC-networks supplying loads with different requirements.

II. III OPERATION OF THE PROPOSED DOBB CONVERTER

Figure 1 illustrates the newly introduced single input multi-output topology that can carry out both of the step up and step down conversions. DOBB converter offers versatility due to its capabilities in improving the dynamic response during the input voltage and load disturbances. Moreover, for applications where in there is a prior information or predictability regarding the load or input voltage disturbance, DOBB possesses the capability to eliminate the impact of these disturbances from the output voltages. Further, the new topology might act as sign priorities to the output voltages in order to attain a better dynamic performance in which the sensitive loads are provided in addition to loads that frequently vary.

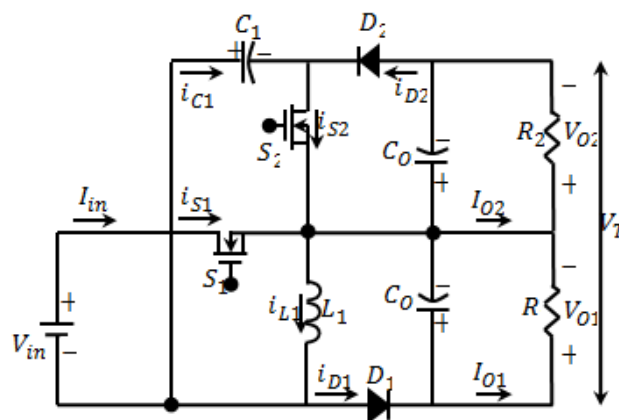


Figure 1 Proposed DOBB converter

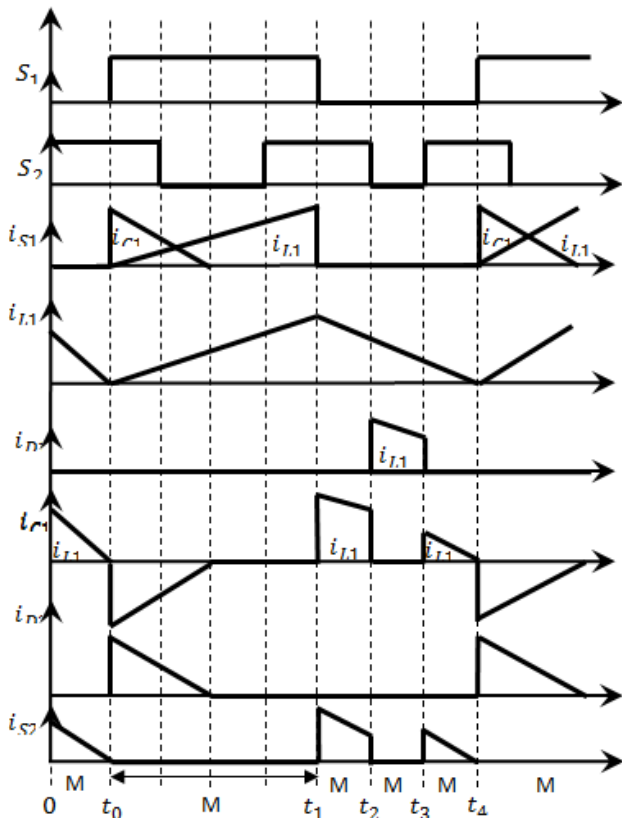


Figure 2 Waveforms of the proposed DOBB converter
 For every switch, a certain responsibility are given. The BB switch (S_1) is active in order to control the inductor (L_1) current to the value desired. Actually, S_1 controls the capacitor (C_{01}) voltage to the necessary value by regulating the inductor (L_1) current. Control of the total output voltage ($V_{out} = V_{01} + V_{02}$) to necessary value is the responsibility of the power sharing switch (S_2). Gate signals of switches and the current waveforms of inductor, switches, diodes and capacitors are illustrated in Figure 2. Based on the states of the switches, there are three various operation modes in the whole switching period as shown below.

III. SIMULATION IMPLEMENTATION AND RESULTS:

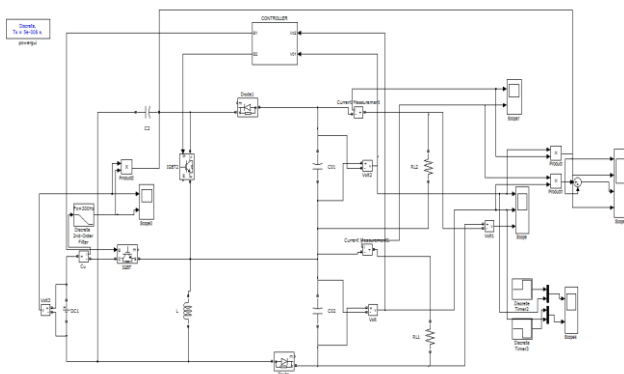
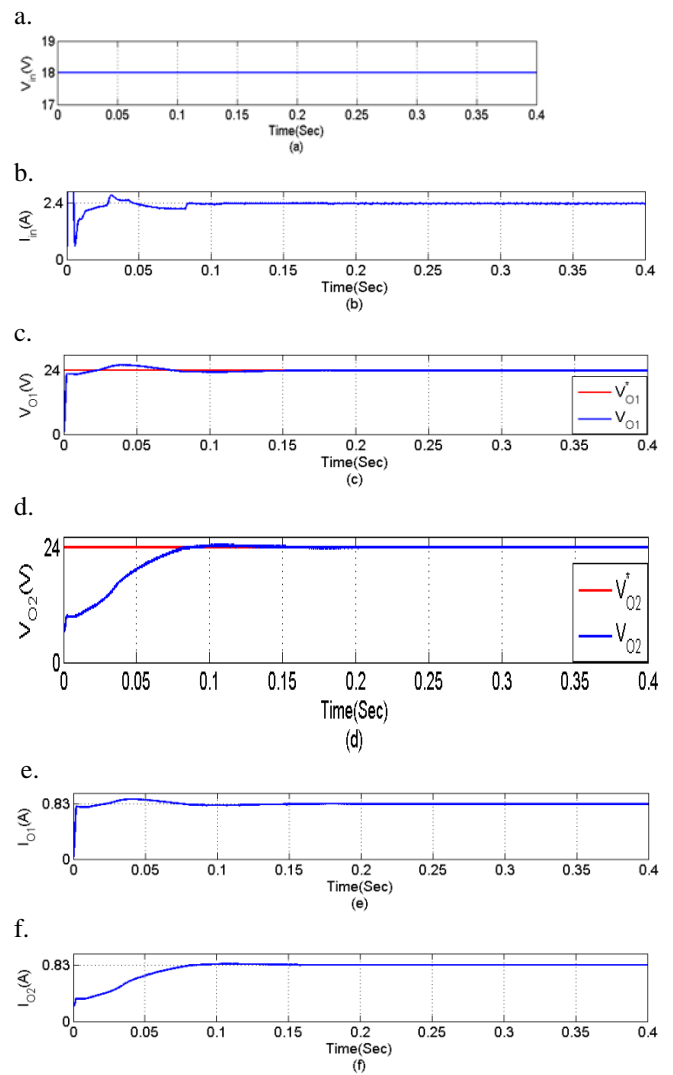


Figure 3 Simulation of Proposed Converter

The simulation parameters such as input voltage (V_{in}), input current (I_{in}), first output voltage, current and power of DOBB converter (V_{01}, I_{01} and P_{01}) respectively, second output voltage, current and power of DOBB converter (V_{02}, I_{02} and P_{02}) respectively and total output voltage (V_T) and total power (P_T) are used to evaluate the performance of the proposed system.

Symmetrical output voltage control of DOBB converter

To verify the symmetrical performance of DOBB converter, input dc voltage source is considered as ($V_{in} = 18 V$) as shown in Figure 4(a). The output voltages of the DOBB converter are desired to be regulated on ($V_{01} = 24 V$ and $V_{02} = 24 V$). Consequently, the total output voltage and total power are desired to be regulated on ($V_T = 48 V$) and ($P_T = 40 W$). Moreover, load resistances ($R_1 = R_2 = 28.8 \Omega$) are considered for symmetrical condition.



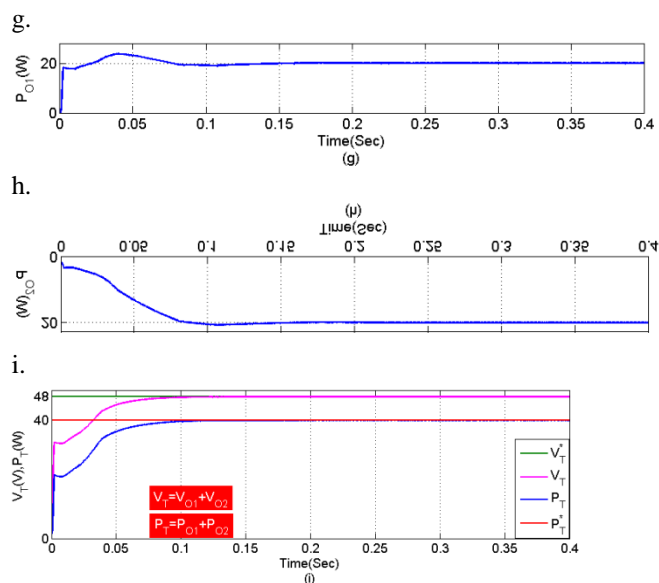


Figure 4 Performance of DOBB converter under symmetrical voltage condition

In Figures 5.11(c) and (d), output voltages (V_{O1} and V_{O2}) are shown. As seen from this figure, the output voltages are tracked with the reference values (V_{O1}^* and $V_{O2}^* = 24 V$) with minimum steady state error. It is obvious that the output voltages are regulated very well. Similarly, the currents (I_{O1} and I_{O2}) drawn from load resistances R_1 and R_2 are shown in Figures 4(e) and (f), both the loads consume 20 W power from input supply individually. Therefore the power drawn from load resistances R_1 and R_2 are shown in Figures 4(g) and (h). In Figure 5.11(i), the total output voltage ($V_T = V_{O1} + V_{O2}$) and total output power ($P_T = P_{O1} + P_{O2}$) are shown. As seen from this figure, voltage and power are tracked with the reference values ($V_T^* = 48 V$ and $P_T^* = 40 W$). It is obvious that the output voltage and power are regulated smoothly. Thus, the 40W loads draw current from input dc source as is revealed in Figure 4(b).

IV. CONCLUSION

The simulation model of Enhanced Multi-Output Buck-Boost Converter has been implemented in MATLAB SIMULINK was presented. The Enhanced multi-output DC-DC converter topology has both step-up and step-down conversion capabilities.

The Enhanced buck-boost converter has been designed and the output parameters have been validated. The complete system has been designed, modeled and simulated in MATLAB/Simulink environment and implemented on a developed hardware prototype. Utilizing all the properties of both the boost and buck converters. The hardware implementation results are verifying the feasibility of the system. The implementation of the proposed work is practically used for Commercial purposes.

REFERENCES

- [1] WING-HUNG K., DONGSHENG M.: ‘Single-inductor multiple output switching converters’. Proc. IEEE PESC’01, 2001, pp. 226–231
- [2] Viswanathan, K., Oruganti, R., Srinivasan, D.: ‘Tri-state boost converter with no right half plane zero’. Proc. Fourth IEEE Int. Conf. on Power Electronics and Drive Systems, 22–25 October 2001, vol. 2, pp. 687–693
- [3] Senanayake, T., Ninomiya, T.: ‘High-current clamp for fast-response load transitions of DC–DC converter’. Proc. 2003 Int. Symp. on Circuits and Systems, ISCAS ’03, 25–28 May 2003, vol. 1, I-653–I-6
- [4] DONGSHENG M., WING-HUNG K., CHI-YING T., MOK P.K.T.: ‘Single inductor multiple-output switching converters with time multiplexing control in discontinuous conduction mode’, IEEE J. Solid-State Circuits, 2003, 38, (1), pp. 89–100
- [5] DONGSHENG M., WING-HUNG K., CHI-YING T.: ‘A pseudo-CCM/ DCM SIMO switching converter with freewheel switching’, IEEE J. Solid-State Circuits, 2003, 38, (6), pp. 1007–1014
- [6] Gezgin, C.: ‘Predicting load transient response of output voltage in DC–DC converters’. Nineteenth Ann. IEEE Applied Power Electronics Conf. and Exposition 2004, APEC-’04, 2004, vol. 2, pp. 1339–1344
- [7] Garcera, G., Figueres, E., Pascual, M., Benavent, J.M.: ‘Analysis and design of a robust average current mode control loop for parallel buck DC–DC converters to reduce line and load disturbance’, IEE Proc. Electr. Power Appl., 2004, 151, (4), pp. 414–424
- [8] TREVISAN D., MATTAVELLI P., TENTI P.: ‘Digital control of single inductor dual-output DC–DC converters in continuous conduction mode’. Proc. IEEE PESC’05, 2005, pp. 2616–2622–5 December 2005, vol. 2, pp. 815–820
- [9] Hsieh, F.-H., Yen, N.-Z., Juang, Y.-T.: ‘Optimal controller of a buck DC–DC converter using the uncertain load as stochastic noise’, IEEE Trans. Circuits Syst. II, Express Briefs, 2005, 52, (2), pp. 77–81
- [10] Amrei, S.R.H., Xu, D.G., Lang, Y.Q.: ‘High power DC–DC converters under large load and input voltage variations: a new approach’. Seventh Int. Power Engineering Conf., IPEC2005, 29 November–5 December 2005, vol. 2, pp. 815–820

Design of Single Axis Solar Tracker

^[1]Amit Kumar Yadav, ^[2]Saikat Barman, ^[3]Viresh Hiremath, ^[4]Rambati Reang,
^[5] Assit.Prof Anshu Deepak

Abstract— This project discusses on the development of horizontal single axis solar tracker using Arduino UNO which is cheaper, less complex and can still achieved the required efficiency. For the development of horizontal single axis solar tracking system, two light dependent resistors (LDR) module has been used for sunlight detection and to capture the maximum light intensity. A 10 RPM gear motor is used to rotate the solar panel to the maximum light source sensing by the light dependent resistor (LDR) module in order to increase the efficiency of the solar panel and generate the maximum energy. The efficiency of the system has been tested and compared with the static solar panel on several time intervals theoretically from a internet source. A small prototype of horizontal single axis solar tracking system will be constructed to implement the design methodology presented here. As a result of solar tracking system, solar panel will generate more power, voltage, current value and higher efficiency.

I. INTRODUCTION

In this globalization era, demand of electricity keeps on increasing year by year. The demanding of electricity gives an impact on the loss of main resources to produce electrical energy. Mankind have explored more ways and technologies for the production of electrical energy using the renewable energy resources. Renewable energy is an energy which generate from natural resources which are naturally replenished. Among all the renewable energy resources that have been discovered, solar energy is the most suitable. The solar energy provides light, heat and energy to all living things. Solar energy is a free energy which does not have any price if using it. Furthermore, solar energy does not produce any pollution, environmental friendly and endless supplies. Solar energy is an energy generated by the sun in the form of solar radiation. Solar radiation from the sun is collected and absorbed by the solar panels and convert into electrical energy. Solar energy shows a great potential for conversion into electrical in entire world because it has very high radiation levels.

Hence a solar tracker is one of the famous devices used that orients a payload toward the sun sunlight and a photovoltaic panel to maximize the amount of energy produced from PV system.

II. OVERVIEW

The proposed tracking system tracks the sunlight by rotating the solar panel on a single axis. The single-axis solar tracker follows the angular height position of the sun in the sky in addition to following the sun's east- west movement. This solution of single-axis solar tracking system based on motion algorithm, which can predict the exact apparent position of the sun, by the latitude's location, thereby avoiding the need

to use guidance systems. To accomplish this, it is used a low-power microcontroller, suitably programmed, to control an electric motor to ensure that the panel supporting structure is always oriented towards the sun. The tracker model consists of Light Dependent Resistor (LDR) Module, Arduino UNO microcontroller,

L239D motor driver, Solar Panel, and 10RPM gear motor in which the motor is basically performing the function of sun tracking.

III. OBJECTIVES

The main Objective of the project is to utilize the maximum solar energy by using the solar panel.

HARDWARE

This section will be focusing on the methods used to develop horizontal single axis solar tracker using Arduino approach. It is divided into sub-section which include the specification of components, software design and hardware design.

ARDUINO UNO

The Arduino UNO is a micro-controller board based on the ATmega328 as shown in Figure 1.

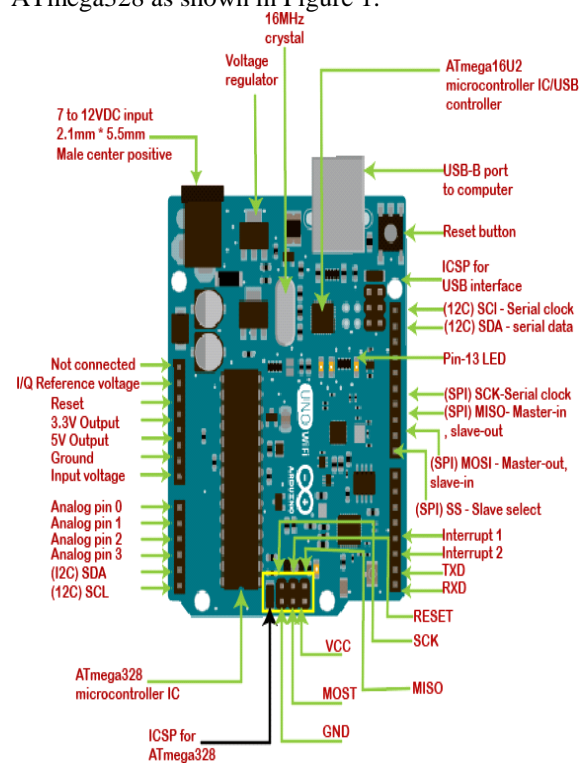


FIGURE 1: Arduino Uno

It has fourteen digital input/output pins (of which six of it can be used as PWM outputs), six analog inputs, a 16 MHz crystal oscillator, a USB connection, a power jack, an ICSP header, and a reset button. It contains everything needed to support the micro- controller; it can simply connect to a computer with a USB cable or power it with AC-to-DC adapter or battery to get started.

Specifications: Microcontroller: ATmega328P Operating Voltage: 5V

Input Voltage (recommended): 7-12V In out Voltage (limit): 6-20V

Digital I/O Pins: 14 (of which 6 provide PWM output)

PWM Digital I/O Pins: 6 Analog Input Pins: 6

DC Current per I/O Pin: 20 mA DC current for 3.3V Pin: 50 mA

Flash Memory: 32 KB (ATmega328P) of which 0.5 KB used by bootloader SRAM: 2 KB (ATmega328P)

EEPROM: 1 KB (ATmega328P)

LED_BUILTIN: 13

Length: 68.6 mm

Width: 58.4 mm

Weight: 25 g

LDR MODULE

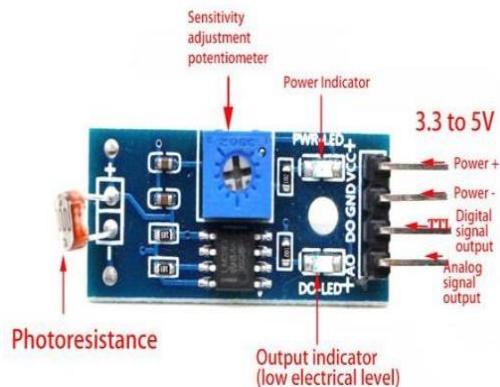


FIGURE 2: LDR Module

LDR sensor module is used to detect the intensity of light. It is associated with both analog output pin and digital output pin labelled as AO and DO respectively on the board. When there is light, the resistance of LDR will become low according to the intensity of light. The greater the intensity of light, the lower the resistance of LDR. The sensor has a potentiometer knob that can be adjusted to change the sensitivity of LDR towards light.

Specifications:

Operating Voltage: 3.3V to 5V DC Operating Current: 15ma Output Digital - 0V to 5V, Adjustable trigger level from pre set.

Output Analog - 0V to 5V based on light falling on the LDR LEDs indicating output and power PCB Size: 3.2cm x 1.4cm

L239D MOTOR DRIVER



FIGURE 3: L239D Motor Driver

The L293D is a dual-channel H-Bridge motor driver capable of driving a pair of DC motors or one stepper motor, that means it can individually drive up to two motors making it ideal for building two- wheel robot platforms, The L293D motor driver IC actually has two power input pins viz. 'Vcc1' and 'Vcc2'. Vcc1 is used for driving the internal logic circuitry which should be 5V. From Vcc2 pin the H-Bridge gets its power for driving the motors which can be 4.5V to 36V. And they both sink to a common ground named GND. The L293D motor driver's output channels for the motor A and B are brought out to pins OUT1, OUT2 and OUT3, OUT4 respectively. Each channel on the IC can deliver up to 600mA to the DC motor. However, the amount of current supplied to the motor depends on system's power supply.

Specifications:

High-Noise-Immunity Inputs

Output Current 600 mA Per Channel Peak Output Current 1.2 A Per Channel

Output Clamp Diodes for Inductive Transient Suppression

GEAR MOTOR (10 RPM)

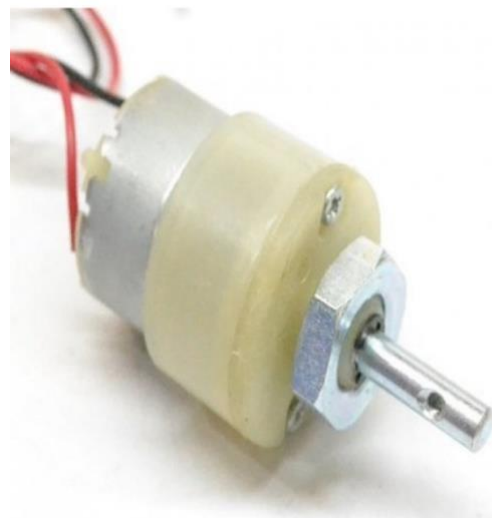


FIGURE 4: Gear Motor 10rpm

Geared motors are complete motor force systems consisting of an electric motor and a reduction gear train integrated into one easy- to-mount and easy to configure package.

Due to the advantage of high torque at relatively low shaft speed or RPM, the use of gear motor greatly reduces the

complexity and cost of designing and constructing power tools, machines and appliances. Geared motors allow the use of economical low-horsepower motors to provide great motive force at close speed such as in lifts, winches, medical tables, jacks and robotics.

Most synchronous AC electric motors have output ranges from 1,200 to 3,600 revolutions per minute.

They also have both normal speed and stall-speed torque specification

The reduction gear trains used in gear motors are designed to reduce the output speed while increasing the torque.

The increase in torque is inversely proportional to the reduction in speed.

Reduction gearing allows small electric motors to move large driven loads, although more slowly than larger electric motors.

Reduction gears consist of a small gear driving a larger gear. There may be several sets of these reduction gear sets in a reduction gear box.

SOLAR PANEL



FIGURE 5: Solar Panel

The 2 watt 6 Volt solar panel is lightweight, waterproof, and designed for long term outdoor use in any environment. The panel uses high-efficiency monocrystalline solar cells, and is UV- and scratch- resistant.

Specifications:

Open Circuit Voltage: 7.7V Peak Voltage: 6.5V

Peak Current: 340mA Peak Power: 2.2W

Power Tolerance: +/-10% Output Cable Length: 26cm

Output Cable Colour: Red PU Coated

Output Cable Plug: Waterproof Male 3.5x1.1mm

Dimensions: 13.6cm x 11.2cm x 0.5cm

Weight: 99g

IV. SOFTWARE REQUIREMENTS ARDUINO IDE

The Arduino Integrated Development Environment (IDE) is a cross platform application

(for Windows, macOS, Linux) that is written in functions from C and C++.] It is used to write and upload programs to Arduino compatible boards, but also, with the help of third-party cores, other vendor development boards.

The source code for the IDE is released under the GNU General Public License, version

2. The Arduino IDE supports the

languages C and C++ using special rules of code structuring.

The Arduino IDE supplies a software library from the Wiring project, which provides many common input and output procedures. User-written code only requires two basic functions, for starting the sketch and the main program loop, that are compiled and linked with a program

stub main() into an executable cyclic executive program with the GNU tool chain, also included with the IDE distribution.

The Arduino IDE employs the program argued to convert the executable code into a text file in hexadecimal encoding that is loaded into the Arduino board by a loader program in the board's firmware. By default, argued is used as the uploading tool to flash the user code onto official Arduino boards.]

Arduino IDE is a derivative of the Processing IDE, however as of version 2.0, the Processing IDE will be replaced with the Visual Studio Code-based Eclipse Their IDE framework.

With the rising popularity of Arduino as a software platform, other vendors started to implement custom open source compilers and tools (cores) that can build and upload sketches to other microcontrollers that are not supported by Arduino's official line of microcontrollers.

Arduino IDE is a derivative of the Processing IDE, however as of version 2.0, the Processing IDE will be replaced with the Visual Studio Code-based Eclipse Their IDE framework.

With the rising popularity of Arduino as a software platform, other vendors started to implement custom open source compilers and tools (cores) that can build and upload sketches to other microcontrollers that are not supported by Arduino's official line of microcontrollers.

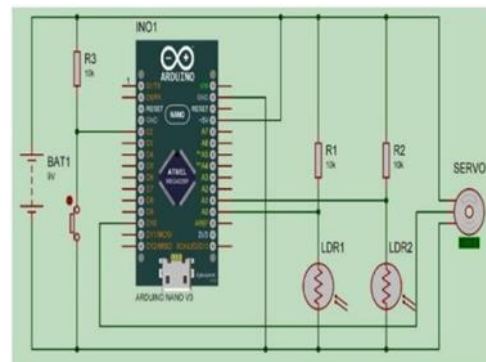
Arduino IDE is a derivative of the Processing IDE, however as of version 2.0, the Processing IDE will be replaced with the Visual Studio Code-based Eclipse Their IDE framework.

With the rising popularity of Arduino as a software platform, other vendors started to implement custom open source compilers and tools (cores) that can build and upload sketches to other microcontrollers that are not supported by Arduino's official line of microcontrollers.

Arduino IDE is a derivative of the Processing IDE, however as of version 2.0, the Processing IDE will be replaced with the Visual Studio Code-based Eclipse Their IDE framework.

DESIGN

CIRCUIT DESIGN



BLOCK DIAGRAM

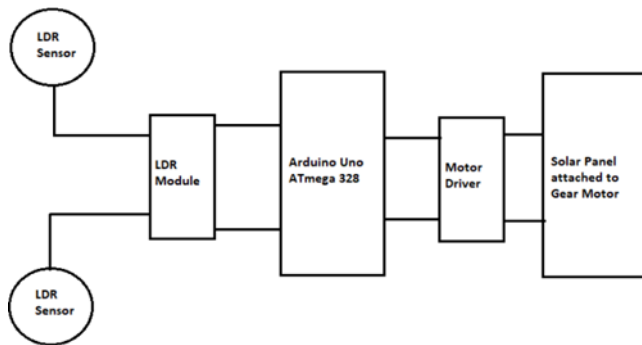


FIGURE 7: Project’s Block Diagram

V.IMPLEMENTATION WORKING OF THE PROJECT

Arduino microcontroller is turned on either by USB (connected to pc / laptop) or battery, The Arduino powers up all the circuits/modules connected, when powered on the LDR modules starts to conduct and if either one of the module amongst two is under the pre-set light intensity the respective LDR module goes to digital HIGH, and the this digital HIGH output is fed as input to the Arduino uno, now according to the given algorithm the Arduino drives the motor drive in turn runs the gear motor to run either clockwise or anti-clockwise depending on the digital HIGH output received from the LDR module to Arduino. If both the LDR doesn’t sense the pre-set light intensity their will be now digital HIGH output going to Arduino as input, therefore the motor will be in off mode, this loop will be there until the Arduino board as power connected to, once the power is turned down the entire circuitry goes down and then the power from the solar panel can be used if stored somewhere.

PROGRAMMING ARDUINO UNO

```

void setup() {
pinMode(2, INPUT); // Initializing pin 2 of Arduino as input pin.
pinMode(3, INPUT); // Initializing pin 3 of Arduino as input pin.
pinMode(4, OUTPUT); // Initializing pin 4 of Arduino as output pin.
pinMode(6, OUTPUT); // Initializing pin 4 of Arduino as output pin.
}
void loop() { if(digitalRead(2)==HIGH && digitalRead(3)==LOW) // Checking condition
{
digitalWrite(4,HIGH); // Turning the motor clockwise
}
else if(digitalRead(3)==HIGH && digitalRead(2)==LOW) // Checking Condition

```

```

{
digitalWrite(6,HIGH); // Turning the motor anti-clock wise
}
else
{
digitalWrite(4,LOW); digitalWrite(6,LOW); // Turning of the motor while the condition is not met.
}
}

```

ADVANTAGES AND APPLICATIONS ADVANTAGES

Generally a lower cost than dual-axis trackers Higher reliability than dual-axis trackers Higher lifespan than dual-axis trackers

VI. APPLICATIONS

Solar energy uses captured sunlight to create photovoltaic power (PV) or concentrated solar power (CSP) for solar heating. This energy conversion allows solar to be used to power auto motives, lights, pools, heaters and gadgets. And by implementing the single axis or the advance dual axis solar panel the energy from the sun can be used effectively.

VII. CONCLUSION

An application of solar tracker using Arduino approach has been presented in this study. As a conclusion, firstly the development of tracking system to control and monitor the movement of solar panel based on the intensity of the light is achieved. The solar panel will face the sun perpendicularly to absorb more solar energy. Secondly, solar tracking systems generate more output during the hours while fixed solar panel installation generates least power. However, shading effect give a slightly impact for solar panel to produce the output value. Thirdly, the percentage efficiency of the system in energy conversion increase when implemented the tracking system. The efficiency gain varies significantly with altitude and the orientation of a fixed solar panel installation in the same location.

VIII. FUTURE WORK

Firstly, the quality of having a solid, almost unyielding structure should be put as one of the main characteristics of a solar tracker. Hard and solid material need to be used as the main material for the solar tracker structure in order to withstand extreme weather condition such as strong windy day. Secondly, build a solar tracker that can be monitored from long range, by adding Global System for Mobile Communication (GSM) or build an application software. Lastly, maximizing the solar-system energy production and produce more energy by upgrading the single axis solar tracker to dual axis solar tracker.

REFERENCES

- [1] Suruhanjaya Tenaga (Energy Commission) Malaysia Energy Statistic Handbook. 2015: 84.
- [2] Aloka Reagan Otieno (2015). Solar Tracker for Solar Panel. Faculty of Engineering Department of Electrical and Information Engineering. University of Nairobi.
- [3] Ayushi Nitin Ingole (2016, May 24-26). Arduino based Solar Tracking System. International Conference on Science and Technology for Sustainable Development, Kuala Lumpur, Malaysia.
- [4] Tiberiu Tudorache, L. K. (2010). Design of a Solar Tracker System for PV Power Plants. *Acta Polytechnica Hungarica.*; 7(1), 17.
- [5] Gagari Deb, Arijit Bardhan Roy. Use of Solar Tracking System for Extracting Solar Energy. *International Journal of Computer and Electrical Engineering*, 4(1), 42–46.
- [6] Muhammad Sami Sabry (2013). Determining the accuracy of solar tracker, 1-88.
- [7] Sohag, H. A., Hasan, M., Khatun, M. M., & Ahmad,
- [8] M. (2015). An Accurate and Efficient Solar Tracking System Using Image Processing and LDR Sensor, (*Eict*), 522–527.
- [9] SA Jumaat, F Mohamad, SA Zulkifli, Development of Portable Case Solar Battery Charger, *Electrical and Electronic Engineering*, Vol. 6 No. 4, 2016, pp. 55-61. doi: 10.5923/j.eee.20160604.01.
- [10] Siti Amely Jumaat, Mohammad Hilmi Othman, Solar Energy Measurement Using Arduino

A Survey Paper on Kidney Cancer and Computer aided methods for their Image Segmentation

^[1] Anupkumar Bhatulal Jayaswal, ^[2] Mahesh Bhimsham Dembrani

^[1] Assistant Professor, ^[2] Assistant Professor

^{[1][2]} R C Patel Institute of Technology

Abstract— *The medical image is segmented. Finding tissue cells or tumors in image data such as CT is among the most challenging tasks in medical image processing, as it provides vital information on their shapes and volumes. Improved imaging predictive validity have emerged from technological breakthroughs in machine vision. Computer aided solutions have contributed significantly for automatic examination of medical images and interpreting the images to provide helpful information for enhancing the medical experts diagnostic procedure. Per year, around 4 million new instances of kidney cancer are diagnosed, the most common treatment to be surgery. To prevent unnecessary surgery is possible only when physicians has proper segmented data from CT. It is of great importance for developing profound learning models to help physicians identify successfully segmented tumors. Hence there is a need to develop or modify algorithm using deep learning approach which will help physicians to classify renal carcinoma and give proper diagnosis.*

Index Terms— *Medical Image, CT, Kidney, Deep learning.*

I. INTRODUCTION

Cancer is a disease that uncontrollably develops and spreads some of the cells of the body to other parts of the body. The human body is made up of cells. cancer begins almost anywhere. Human cells normally become and multiply, as the body needs, to form new cells. They are dying, and cells take their place when they get older or damaged. When this orderly process is disrupted, abnormal or injured cells proliferate and replicate uncontrollably. These cells can combine to produce tumors, which are tissue masses. Cancer or not cancer can occur in tumors (benign). Cancer tumors spread to nearby tissues or invade them It can spread to other parts of the body to produce new tumors. Malignant tumors can be called as well. Tumors that are benign do not spread to nearby tissues or invade them. Usually, benign tumors don't grow back when removed, while cancer tumors do. Sometimes, however, benign tumors may be pretty large. Some may cause severe symptoms or life threats.

1.1 Cancer Cells vs. Normal Cells: What's the Difference?

Cancer cells are distinct from normal cells in a variety of ways. Consider cancer tissue:

- Develop even if there are no outward stimuli to do so. Cells can just respond to so impulses by growing.
- Ignore Apoptosis.

- Infect the entire area and expand to certain other bodily regions. Normal tissues stop growing when they come into contact with other tissue, and the most of normal cells do not move surrounding the body.
- Instruct blood vessels to expand toward tumors. These blood vessels deliver oxygen and nutrients to tumors while also removing waste.
- Instruct blood arteries to expand in the direction of malignancies. These blood vessels provide oxygen and nutrients to tumors while also removing waste products.
- Get the human system to help tumors survive and thrive by tricking it. For instance, certain tumor cells induce immune cells to defend the tumor instead of fight it.
- Repeated chromosomal alterations, including such genomic recombination and losses, aggregate. Most cancer tissues have double the number of genomes as healthy ones.
- Require a different type of nutrient compared to untreated tissues. Furthermore, some cancer cells generate In an unique manner, power is extracted from food. Than most simple tissue. This allows cancer cells to proliferate more quickly.
- Such aberrant activities are sometimes so important to tumor cells how they can live absent it.

1.2 How Does Cancer Grow?

Cancer is a heritable disease, meaning it is caused by mutations in the genes that regulate that our tissues operate especially how they grow. Cancer-causing genetic changes can occur as a result of:

- Throughout meiosis, problems can arise.
- Harmful compounds in the environment, such as cigarette smoke chemicals and UV radiation from the sun, harm the body.
- They were passed down through families

Cells with damaged DNA are normally eliminated by the body before they become malignant. However, as we age, our bodies' ability to do so declines. This is one of the reasons why people are more likely to develop cancer after in life.

Every people's cancer has a distinct set of changes in heredity. Additional changes will occur as the cancer progresses. Different cells within the same tumor may have different genetic changes

1.3 Kidney

The kidneys are two bean-shaped organs that are about the size of a fist. They are attached to the abdomen's upper back wall and are protected by the lower rib cage. One kidney is to the left of the backbone, and the other is to the right. The superior pole and inferior pole of each kidney are terms used to describe the upper and lower portions of each kidney. Each kidney has a small organ called an adrenal gland on top of it. Each kidney and adrenal gland is surrounded by fat and Gerota's fascia, a thin, fibrous layer.

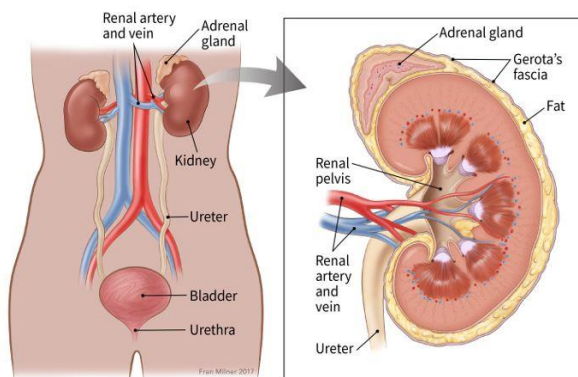


Fig. 1 The Diagram of kidney

The primary function of the kidneys is to remove excess water, salt, and waste products from the blood that enters the renal arteries. These substances degrade into urine. Urine collects in the centre of each kidney, a region known as the renal pelvis, and then exits the kidneys via long, slender tubes known as ureters. The ureters lead to the bladder, which stores urine until you urinate.

The kidneys also perform the following functions:

They help control blood pressure by producing a hormone known as renin.

They contribute to the body's supply of red blood cells by producing a hormone known as erythropoietin. This substance stimulates the production of red blood cells in the bone marrow.

Our kidneys are essential, but we can function with only one. Many people in the United States lead normal, healthy lives despite having only one kidney. Some people do not have functioning kidneys and must rely on a medical procedure known as dialysis to survive. The most common type of dialysis employs a specially designed machine that filters blood in the same way that a real kidney would.

Kidney cancer may strike adults as well as children. The three most prevalent forms of kidney cancer are renal cell cancer, transitional cell cancer, and Wilms tumor. People with certain genetic defects are more prone to develop kidney cancer.

1.4 Kidney statistics

Kidney cancer is one of the top ten cancers in both men and women. In men, the lifetime risk of developing kidney cancer is about 1 in 46. (2.02 percent). For women, the lifetime risk is about 1 in 80. (1.03 percent).

The most recent American Cancer Society estimates for kidney cancer in the United States for 2021 are:

There will be approximately 76,080 new cases of kidney cancer diagnosed (48,780 men and 27,300 women).

This disease will kill approximately 13,780 people (8,790 men and 4,990 women).

All types of kidney and renal pelvic cancer are included in these figures.

The majority of kidney cancer patients are in their forties and fifties. The average age at diagnosis is 64, with the majority of people diagnosed between the ages of 65 and 74. Renal cancer is extremely rare in people under the age of 45.

Men are about twice as likely as women to develop kidney cancer. A risk factor is anything that increases your chances of contracting a disease like cancer. The risk factors for various cancers differ. Some risk factors, such as smoking, can be modified. Others, such as your age or family history, are unchangeable.

1. Risk Factors for Kidney Cancer
2. Smoking
3. Obesity
4. Hypertension
5. A family history of kidney cancer
6. Exposures at work
7. Gender
8. Race

II. RELATED WORK

Ed-Edily Mohd. Azhari et al. proposed [1] a method to segment images and detect edges. The threshold method was used to detect damaged tissue and noise can be removed by filters. They used grey-scale images converted from MRIs, or CT scans through the image segmentation transfer process. The research aims to use a canny edge detector frequently used by the edge detection process in similar areas. Several medical constraints and contributions to future work have also been identified.

A detailed cancer survey has been proposed by Geetha, Selvi in 2015 [2]. The knowledge and experience gained by the expert physicians, it can be used for medical imaging to select the appropriate medical diagnostic optimization technique. This paper shows an impression of cancer and literature surveys by previous researchers on cancer detection.

The research objective of Pawar et al. [3] is to classify the images based on the shape and regional characteristics using Watershed Transform Techniques. Fruits and vegetables are considered in the image categories. The proposed image classification technique uses watershed transformation for segmentation, from which the features of the Haar wavelet are calculated and classified using the SVM, KNN and Naïve Bayes classifier. A voting technique is used to classify images, and the system's overall accuracy is about 90 %.

Attia et al. [4] this paper proposes a computer-aided system for the automatic classification of ultrasound kidney disease. It considered images from five categories: normal, cyst, stone, tumor, and failure. The Region of Interest (ROI) of each image offers a list of quantitative properties and a separate set of parametric feature extraction features, and the great portion was analyzed to minimize the number of

qualities. A human brain classifier was trained using the chosen parameters.

Guanyu Yang et al. [5] suggested a new approach for dividing the renal and kidney tumour in CT angiography pictures with pinpoint accuracy. This technique is based on a pyramid mixing module in a three-dimensional (3D) fully convolutional network (FCN) (PPM). As an end-to-end teaching method, the suggested structure is designed immediately on three dimensional pictures.

On complicated problems as complex, feature extraction, deep learning models such CNN has repeatedly exceeded earlier methods. Furthermore, due to design considerations, the many suggested systems function differently, and training settings having a large influence on behaviour. Konstantinos Kamnitsas et al. [6] investigates EMMA (Ensembles of Multiple Models and Architectures) is a way for combining predictions from a range of approaches to achieve high efficiency. Actual model semantic have less effect, and indeed the possibility of curse of dimensionality the setup to a single database is reduced.

Mredhula et al. [7] presented ideas for techniques for feature extraction, which can be partitioned into different types: image-based, model-based and hybrid. The segmentation of image-based methods is based only on the image information. Image segmentation, area expansion, texture analysis, hough transform sets, watershed, fluid connectivity, and graph cuts are among them (GCS).

Geert Litjens et al. [8] proposed a survey paper on Deep Learning in which he explain different image segmentation using 3D CNN, 2D PATCH based classification, also shows some authors kidneys patches using CNN, Explain pancreas segmentation in CT, also given list of various datasets for different organ segmentation like CT, MRI with different dataset Size.

Mohammad Hesam Hesamian [12] explain in his paper various techniques for image segmentation like CNN, 2DCNN, 2.5DCNN, 3DCNN, FCN, FCN for multi organ segmentation, cascaded FCN, Focal FCN, Multi-Stream FCN, U-Net in which 2D U-NET, 3D U-NET, V-NET, CRNs, RNNs, CLSTM, GRU, CW-RNN, Network Training Techniques likes Deeply Supervised, Weakly Supervised, Network Structure, Organ and Modality, Dataset Size, also explain Achievements and Challenge.

III. CONCLUSION

In this research, we looked at deep learning methods for medical image analysis and analyzed widely used datasets for diverse tissue classifications. We investigate how deep learning is applied to picture classification, object recognition, segmentation, registration, and other applications. For each application area, there are brief abstracts of studies: Breast, cardiac, abdominal, and orthopedic pathology, as well as neuron, retinal, pulmonary, and digital pathology. We wrap up with such a summary of the present latest technology, a structure consisting of outstanding difficulties, and recommendations for future study. We believe that this article will assist researchers in

selecting the appropriate network structure for their problem as well as being aware of potential obstacles and solutions. Deep learning algorithms appear to be playing a key role in medical picture segmentation, according to all considerations.

REFERENCES

- [1] Ed-Edily Mohd. Azhari, Muhd. Mudzakir Mohd. Hatta, Zaw Zaw Htike and Shoon Lei Win. "Tumor Detection In Medical Imaging: A Survey". IJAIT Vol. 4, No. 1, February 2014: pp. 21-29.
- [2] Ms.P.Geetha, Dr.V.Selvi. "An Impression of Cancers and Survey of Techniques in Image Processing for Detecting Various Cancers: A Review". IRJET Volume: 02 Issue: 09 | Dec-2015. e-ISSN: 2395-0056, p-ISSN: 2395-0072 : pp. 236-242.
- [3] M. S. Pawar, L. Perianayagam and N. S. Rani, "Region based image classification using watershed transform techniques," 2017 International Conference on Intelligent Computing and Control (I2C2), Coimbatore, 2017, pp. 1-5, doi: 10.1109/I2C2.2017.8321839.
- [4] Mariam Wagih Attia, F.E.Z. Abou-Chadi, Hossam El-Din Moustafa and Nagham Mekky, "Classification of Ultrasound Kidney Images using PCA and Neural Networks" International Journal of Advanced Computer Science and Applications(IJACSA), 6(4), 2015. <http://dx.doi.org/10.14569/IJACSA.2015.060407>
- [5] G. Yang et al., "Automatic Segmentation of Kidney and Renal Tumor in CT Images Based on 3D Fully Convolutional Neural Network with Pyramid Pooling Module," 2018 24th International Conference on Pattern Recognition (ICPR), Beijing, 2018, pp. 3790-3795, doi: 10.1109/ICPR.2018.8545143.
- [6] Kamnitsas, Konstantinos, Wenjia Bai, Enzo Ferrante, Steven G. McDonagh, Matthew Sinclair, Nick Pawlowski, Martin Rajchl, Minjae Lee, Bernhard Kainz, Daniel Rueckert and Ben Glocker. "Ensembles of Multiple Models and Architectures for Robust Brain Tumour Segmentation." ArXiv abs/1711.01468 (2017): n. pag.
- [7] Mredhula.L., Dr.M.A.Dorairangaswamy, "Detection And Classification Of Tumors In CT Images," Indian Journal of Computer Science and Engineering (IJCSSE), Vol. 6 No.2 Apr-May 2015, ISSN : 0976-5166, pp.52-59
- [8] Litjens, Geert et al. "A Survey on Deep Learning in Medical Image Analysis." Medical Image Analysis 42 (2017): 60–88. Crossref. Web.
- [9] "Kidney Cancer Statistics." World Cancer Research Fund, 12 Sept. 2018, www.wcrf.org/dietandcancer/cancer-trends/kidney-cancer-statistics
- [10] "Cancer Diagnosis and Treatment Statistics." Stages | Mesothelioma | Cancer Research UK, 26 Oct. 2017, www.cancerresearchuk.org/health-professional/cancer-statistics/diagnosis-and-treatment.
- [11] Taha, Ahmed, et al. "Kid-Net: Convolution Networks for Kidney Vessels Segmentation from CT-Volumes." arXiv preprint arXiv:1806.06769 (2018).
- [12] Mohammad Hesam Hesamian et al." Deep Learning Techniques for Medical Image Segmentation: Achievements and Challenges." Journal of Digital Imaging (2019) 32:582–596
- [13] Alakwaa W, Nassef M, Badr A: Lung cancer detection and classification with 3D convolutional neural network (3D-CNN). Lung Cancer 8(8):409, 2017
- [14] Cai J, Lu L, Xie Y, Xing F, Yang L (2017) Improving deep pancreas segmentation in CT and MRI images via recurrent neural contextual learning and direct loss function, arXiv:1707.04912
- [15] Chen H, Dou Q, Yu L, Qin J, Heng PA: Voxresnet: deep voxelwise residual networks for brain segmentation from 3D MR images. NeuroImage 170:446–455, 2017.
- [16] Gibson E, Giganti F, Hu Y, Bonmati E, Bandula S, Gurusamy K, Davidson B, Pereira SP, Clarkson MJ, Barratt DC: Automatic multi-organ segmentation on abdominal CT with dense vnetworks. IEEE Trans Med Imaging 37(8):1822–1834, 2018. <https://doi.org/10.1109/TMI.2018.2806309>.
- [17] Hu P, Wu F, Peng J, Bao Y, Chen F, Kong D: Automatic abdominal multi-organ segmentation using deep convolutional neural network and time-implicit level sets. Int J Comput Assist Radiol Surg 12(3):399–411, 2017.

- [18] Yu L, Chen H, Dou Q, Qin J, Heng PA: Automated melanoma recognition in dermoscopy images via very deep residual networks. *IEEE Trans Med Imaging* 36(4):994–1004, 2017.
- [19] Alakwaa W, Nassef M, Badr A: Lung cancer detection and classification with 3D convolutional neural network (3D-CNN). *Lung Cancer* 8(8):409, 2017
- [20] Armato SG I, McLennan G, Bidaut L, McNitt-Gray MF, Meyer CR, Reeves AP, Zhao B, Aberle DR, Henschke CI, Hoffman EA, et al: The lung image database consortium (LIDC) and image database resource initiative (IDRI): a completed reference database of lung nodules on CT scans. *Med Phys* 38(2):915–931, 2011.
- [21] Baumgartner CF, Koch LM, Pollefeys M, Konukoglu E: An exploration of 2D and 3D deep learning techniques for cardiac mr image segmentation. In: *International Workshop on Statistical Atlases and Computational Models of the Heart*. Springer, 2017, pp 111–119.
- [22] Cai J, Lu L, Xie Y, Xing F, Yang L (2017) Improving deep pancreas segmentation in CT and MRI images via recurrent neural contextual learning and direct loss function, arXiv:1707.04912.
- [23] Chen H, Dou Q, Yu L, Qin J, Heng PA: Voxresnet: deep voxelwise residual networks for brain segmentation from 3D MR images. *NeuroImage* 170:446–455, 2017.
- [24] Chen J, Yang L, Zhang Y, Alber M, Chen DZ: Combining fully convolutional and recurrent neural networks for 3D biomedical image segmentation. In: *Advances in Neural Information Processing Systems*, 2016, pp 3036–3044.
- [25] Cheng JZ, Ni D, Chou YH, Qin J, Tiu CM, Chang YC, Huang CS, Shen D, Chen CM: Computer-aided diagnosis with deep learning architecture: applications to US pictures of breast tumours and CT scans of pulmonary nodules: *Sci Rep* 6:24454, 2016.
- [26] Christ PF, Ettliger F, Grün F, Elshaera MEA, Lipkova J, Schlecht S, Ahmaddy F, Tatavarty S, Bickel M, Bilic P, et al (2017) Automatic liver and tumor segmentation of CT and MRI volumes using cascaded fully convolutional neural networks. arXiv:1702.05970.
- [27] Dhungel N, Carneiro G, Bradley AP: Deep learning and structured prediction for the segmentation of mass in mammograms. In: *International Conference on Medical Image Computing and Computer-Assisted Intervention*. Springer, 2015, pp 605–612.
- [28] Dou Q, Yu L, Chen H, Jin Y, Yang X, Qin J, Heng PA: 3D deeply supervised network for automated segmentation of volumetric medical images. *Med Image Anal* 41:40–54, 2017
- [29] Gordienko Y, Gang P, Hui J, Zeng W, Kochura Y, Alienin O, Rokovyi O, Stirenko S: For chest X-ray analysis of lung cancer, deep learning with lung segmentation and bone shadow exclusion approaches was used. In: *International Conference on Fuzzy Systems and Soft Computing Theory and Applications*. Springer, 2018, pp 638–647.
- [30] Hu P, Wu F, Peng J, Bao Y, Chen F, Kong D: Automatic abdominal multi-organ segmentation using deep convolutional neural network and time-implicit level sets. *Int J Comput Assist Radiol Surg* 12(3):399–411, 2017.
- [31] Lewandowski AJ, Augustine D, Lamata P, Davis EF, Lazdam M, Francis J, McCormick K, Wilkinson AR, Singhal A, Lucas A, et al: Preterm heart in adult life: cardiovascular magnetic resonance reveals distinct differences in left ventricular mass, geometry, and function. *Circulation* 127(2):197–206, 2013.
- [32] Milletari F, Navab N, Ahmadi SA: V-net: fully convolutional neural networks for volumetric medical image segmentation. In: *2016 Fourth International Conference on 3D Vision (3DV)*. IEEE, 2016, pp 565–571.
- [33] Moeskops P, Wolterink JM, van der Velden BH, Gilhuijs KG, Leiner T, Viergever MA, Isgum I: Deep learning for multi-task medical image segmentation in multiple modalities. In: *International Conference on Medical Image Computing and Computer-Assisted Intervention*. Springer, 2016, pp 478–486.
- [34] Moreira IC, Amaral I, Domingues I, Cardoso A, Cardoso MJ, Cardoso JS: Inbreast: toward a full-field digital mammographic database. *Acad Radiol* 19(2):236–248, 2012.
- [35] Nie D, Wang L, Gao Y, Sken D: Fully convolutional networks for multi-modality isointense infant brain image segmentation. In: *2016 IEEE 13th International Symposium on Biomedical Imaging (ISBI)*. IEEE, 2016, pp 1342–1345.
- [36] Poudel RP, Lamata P, Montana G: Recurrent fully convolutional neural networks for multi-slice MRI cardiac segmentation. In: *Reconstruction, Segmentation, and Analysis of Medical Images*. Springer, 2016, pp 83–94.
- [37] Roth HR, Lu L, Farag A, Shin HC, Liu J, Turkbey EB, Summers RM: Deeporgan: multi-level deep convolutional networks for automated pancreas segmentation. In: *International Conference on Medical Image Computing and Computer-Assisted Intervention*. Springer, 2015, pp 556–564.
- [38] Roth HR, Lu L, Farag A, Sohn A, Summers RM: Spatial aggregation of holistically nested networks for automated pancreas segmentation. In: *International Conference on Medical Image Computing and Computer-Assisted Intervention*. Springer, 2016, pp 451–459
- [39] Yu L, Chen H, Dou Q, Qin J, Heng PA: Automated melanoma recognition in dermoscopy images via very deep residual networks. *IEEE Trans Med Imaging* 36(4):994–1004, 2017
- [40] Zhang W, Li R, Deng H, Wang L, Lin W, Ji S, Shen D: Deep convolutional neural networks for multi-modality isointense infant brain image segmentation. *NeuroImage* 108:214–224, 2015
- [41] Zhou X, Takayama R, Wang S, Hara T, Fujita H: Sectional learning at a deep level appearances of 3D CT images for anatomical structure segmentation based on an FCN voting method. *Med Phys* 44(10):5221–5233, 2017
- [42] Codella NC, Gutman D, Celebi ME, Helba B, Marchetti MA, Dusza SW, Kalloo A, Liopyris K, Mishra N, Kittler H, et al: Skin lesion analysis toward melanoma detection: a challenge at the 2017 international symposium on biomedical imaging (ISBI), The international skin imaging cooperative is hosting this event (ISIC). In: *2018 IEEE 15th International Symposium on Biomedical Imaging (ISBI 2018)*. IEEE, 2018, pp 168–172

Application of Lean Six Sigma in cast in-situ construction

^[1] Asmita Ghule, ^[2] Prof. Satish Walsal

^[1] PG Scholar, Construction Management, Karmaveer Adv. Bhaburao Ganpatrao Thakre College of Engineering, Nashik, India;

^[2] Assistant Professor, Department of Civil Engineering, Karmaveer Adv. Bhaburao Ganpatrao Thakre College of Engineering, Nashik, India

Abstract— Construction sector is living in continuous change environment. Rapid growth of construction industry and increasing requirements, demands of customer towards the safety, quality assurance has put pressure on construction companies for implementing advance quality tools. This paper studies the implementation of Lean Six Sigma in construction industry to reduce the deviation and variation in the process of construction activities. The DMAIC (Define, Measure, Analysis, Improve, Control) approach of six sigma and tools of each stage of this methodology is been discussed in this paper. A case study of a residential building has been carried out which demonstrates the application of Lean Six Sigma principles to some construction works: R.C.C work, brickwork and plastering. A defect assessment sheets were prepared for every work and the current sigma level of each has been computed. DMAIC methodology has been applied to improve the quality standards and reduce the wastages and variation in the process by analyzing the defects, their severity and root causes. The study aim at understanding the need of construction industry and customer requirements from quality perspective and fulfill them with the principles of Lean Six Sigma. The results of study suggest that the proper management and minor changes in the work procedure will help to achieve the desire quality standards.

Index Terms— Lean Six Sigma, DMAIC methodology, quality standards, case study.

I. INTRODUCTION

The aim of construction project management is to satisfy the customer requirements and demands, delivering the safe and secure, qualitative and financially feasible project. Now a day's customer requirements towards the quality assurance are increased, as this is one time investment sector. Quality control and quality assurance are very essential parameters to maintain the standards and productivity on site, so it is essential to check the quality of ongoing process of construction activities. The problem is the variation and deviation in the work process, which is censorious to the quality. One popular approach to reduce the variation and for process improvement is Lean Six Sigma. It is a statistical approach, which is combination of two different process improvement methodologies, but there focus is on the different parameters of the process. Lean focuses on waste reduction and six sigma focuses on quality of the product by reducing the defects.

Toyota production is a birthplace of Lean manufacturing. It is based on the theory of continuous improvement of the process by eliminating wastage. Lean focus on the customer viewpoint, customer voice and gives a maximum value during production. Where, six sigma is a derived from the Greek alphabet and was first developed by the Motorola in 1986. The main objective is to analyses the causes of defects and removing it from the process of production. This paper studies the lean six sigma as one combine statistical approach with major aim to reduce the defects and wastage from the process. The paper describes the basic methodology of DMAIC approach, which is a five-stage improvement process. A case study of one residential building has done to which this methodology has been applied to reduce the defects and to ensure the quality of construction.

II. CONCEPT OF LEAN SIX SIGMA

• Lean

Taiichi Ohno, who was an engineer in Toyota production, proposed the theory of lean production and now it has become a fundamental business philosophy. The theory is based on the concept of elimination of waste from the workflow. The three kinds of works were identified form Toyota production system: Waste of time and materials, variations in the workflow and overload of workers etc. In Lean methodology, there is a continuous focus on customer and lowering the cycle time of process by eliminating all the wastage from the process.

• Six sigma

Six sigma has two different meanings- one from quality management and another one is from statistical prospective. In quality management it is a set of tools, used to improve the quality of the product by reducing the defects in the product. It helps to analyses the causes of defects and removing it from the process of production. In mathematical statistic, 'σ' is standard deviation and six sigma means the standard normal distribution, elucidated by the symmetrical bell shaped curve. In six sigma, it considers range from -6σ to $+6\sigma$, which includes 99.9997% of data, therefore it gives close to zero defects in the outcome. It provides a five-stage process improvement methodology- DMAIC. The steps are:

1. Define: This is the first step in which need, requirement, expectation and voice of customer is need to define. More precisely, we have to identify which process, product, or service need

- improvement. The scope of project will decide in this stage.
2. Measure: the selected existing process is measure, evaluated and compare in this step. The current effectiveness of process is evaluated with the help of data collection plan and then the goals are set.
 3. Analyze: in this phase, data collected regarding the process is analyzed to find out the root cause of defect or problems. The factors which are affecting the efficiency of the process is find out in this stage with the help of cause and effect diagram, Pareto chart or control charts, TRIZ, scatter diagrams etc.
 4. Improve: solution to the problems analyzed is found out in this improve stage. It focuses on the use of various experimentation and statistical techniques like brain storming, mind mapping, mistake proofing, value stream mapping etc. to generate possible improvements to reduce defects and variations.
 5. Control: this is the last stage of DMAIC approach in which the control plans are established to ensure that the problems causing variation and defects are eliminated from the process. The new modified process is implemented and the performance of this process is also measure

III. RESEARCH METHODOLOGY

3.1 Applying lean six sigma in construction

Lean Six sigma has been used in manufacturing industry. Now this paper gives detail about how this methodology can be used in construction industry. A case study of one residential building has done to which the DMAIC

methodology is applied to some activities like RCC work, brickwork and plastering work. For the data, collection a quantitative study approach has adopted in which observation method of data collection has used to collect all the data related to site. A defect assessment sheet has prepared for every work from which the sigma level of current work is calculated. From the analysis of data collected the sigma level of each work is:

Table 1: Sigma level

Sr. No	Work name	DPMO	Yield	Sigma level
1	Concreting work	31746.032	96.825	3.356
2	Brick work	25541.126	97.446	3.451
3	Plastering work	38764.266	96.124	3.265

To calculate the sigma level, the Defects per Million Opportunities (DPMO) need to calculate. From the standard six-sigma table, the sigma level of current work has been worked out. The mathematical expression for DPMO is:

$$DPMO = \frac{\text{No. of 'X' in data assessment sheet} \times 100000}{\text{No. of opportunities of defects} \times \text{No. of units}}$$

3.2 DMAIC methodology

After estimating the sigma level, the DMAIC methodology has applied to improve the quality of work as follow:

1. Phase: Define

The factors, which are censorious to quality, are identified to address the problem with the help of project charter

Table 2: Project Charter

6. Project Title: Defects reduction in construction	
7. Purpose for selecting the project:	
8. It is difficult to maintain the quality parameters in cast in situ construction as the site conditions are different than the factory or laboratory environment. It may result in to the poor quality of work and increase in wastage or resources and time overrun. So to avoid these things a site project is selected to improve the process by applying Lean six sigma.	
9. Project Objective:	
10. To reduce the defects and wastages of material by applying Lean Six Sigma in concreting, brickwork and plastering work.	
11. Voice of the Customer (VOC)	12. Quality of structure within the budget and without compromising the safety.
13. Focus of project:	14. Main activities of construction- concreting, brickwork and plastering work.
15. Team members:	16. Contractor, project manager, quality supervisor etc.
17. Expected Benefits:	18. Considerable reduction in waste and defects in the structure.
19. Expected Customer Benefits:	20. Will get quality home with required safety standard.

Furthermore, to understand the process of construction the SIPOC diagram is used as depicted in the following table:

- i. R.C.C. Work:

Table 3: SIPOC for RCC

Supplier	Input	Process	Output	Customers
Builder	<ol style="list-style-type: none"> 1. Cement 2. Aggregate 3. Sand 4. Water 5. Steel 6. Binding wires 7. Batching plant 8. Transit mixer 9. Wheel barrows 10. Shuttering 11. Screeds 12. Vibrator 13. Shovel 14. Measuring tape 15. Float, trowel 16. Spirit Level 	<ol style="list-style-type: none"> 1. Cleaning the surface 2. Setting out position of each structural member according the structural drawing in which dimensions and location of each member is given 3. Place reinforcement as instructed in drawing 4. Fix the formwork of each member 5. Pouring concrete in member 6. After stripping time remove formwork 7. Curing of member 	Finished concrete member	Flat owners

ii. Brick Work

Table 3: SIPOC for Brick Work

Supplier	Input	Process	Output	Customers
Builder	<ol style="list-style-type: none"> 1. Bricks 2. Mortar 3. Mortar pan 4. Wheel barrows 5. Trowel 6. Spirit level 7. Tape measure 8. Plumb bob 9. Line and pins 10. Water level 11. Spades 12. Mason Square 13. Jointer 	<ol style="list-style-type: none"> 1. Line out the area with measuring tape. 2. The bricks 1st laid dry along with a string tightly stretched between cornerstones. 3. Then each brick is removing and lay over a bed of mortar. 4. Check each course for alignment, level and verticality. 5. Mortar with mix ratio of 1:4 is prepared and thickness of mortar joint is 10 mm. 6. Raked out the mortar from the joint with a trowel of each course. 7. Complete the height of wall up to 1 meter in a day. 	Brick walls	Flat owners

iii. Plastering work:

Table 4: SIPOC for Plaster Work

Supplier	Input	Process	Output	Customers
Builder	<ol style="list-style-type: none"> 1. Cement 2. Sand 3. Water 4. Finishing trowel 5. Window trowel 6. Corner trowel 7. Mixing bucket 8. Plasterer float 9. Scarifiers 	<ol style="list-style-type: none"> 1. Roughen the entire masonry wall 2. Clean the joint and surface of wall 3. Fixing dots on the wall to get uniform thickness of plastering 4. Screeds are formed in between the dots 5. Applying the first coat of 12 mm thick plaster by means of trowel 6. Leveling the surface by means of flat floats and straight edges 7. After setting of first coat, roughen it with scratching tool to form a key to the second coat 8. The thickness of finishing coat is 2 to 3 mm and applies it with wooden floats 9. after completing it, keep sprinkling water for 7 days min 	Finished wall surface	Flat owners

2. Phase: Measure

In measure phase the Pareto charts has used which helps to identify the significant factors which need to focus more and allows the better use of resources.

i. R.C.C Work

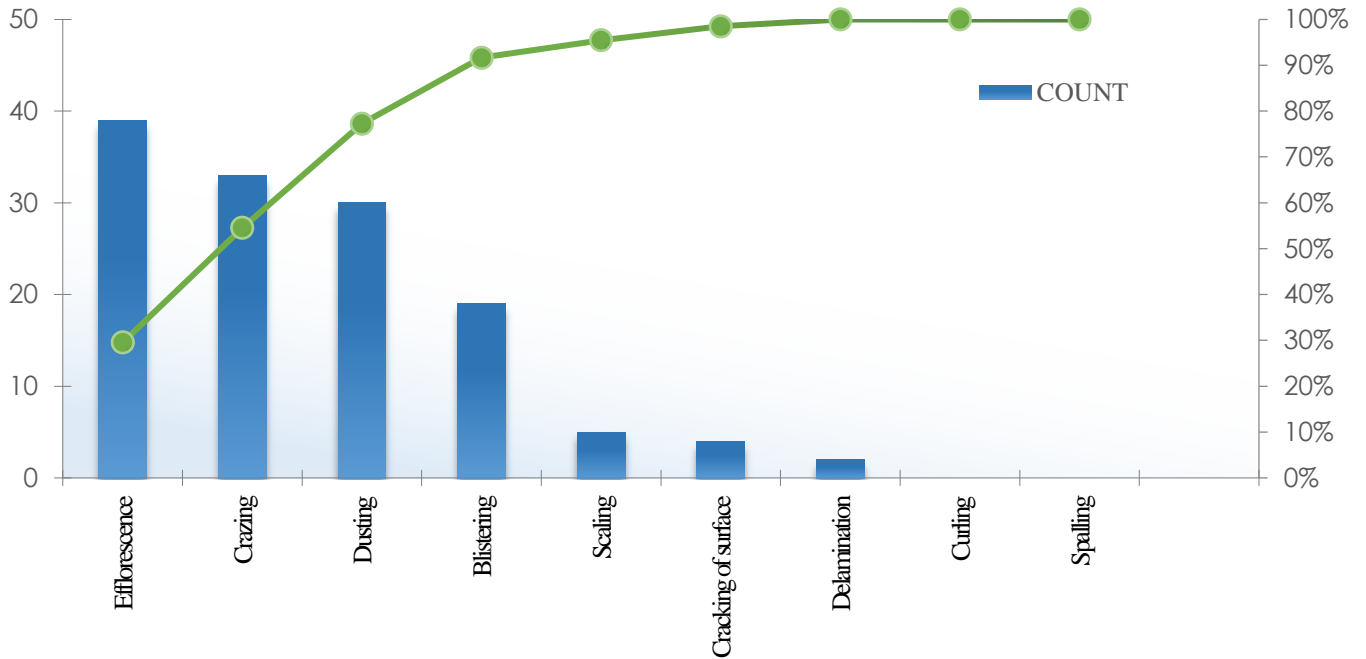


Figure no 1: Pareto chart of R.C.C work

ii. Brick Work

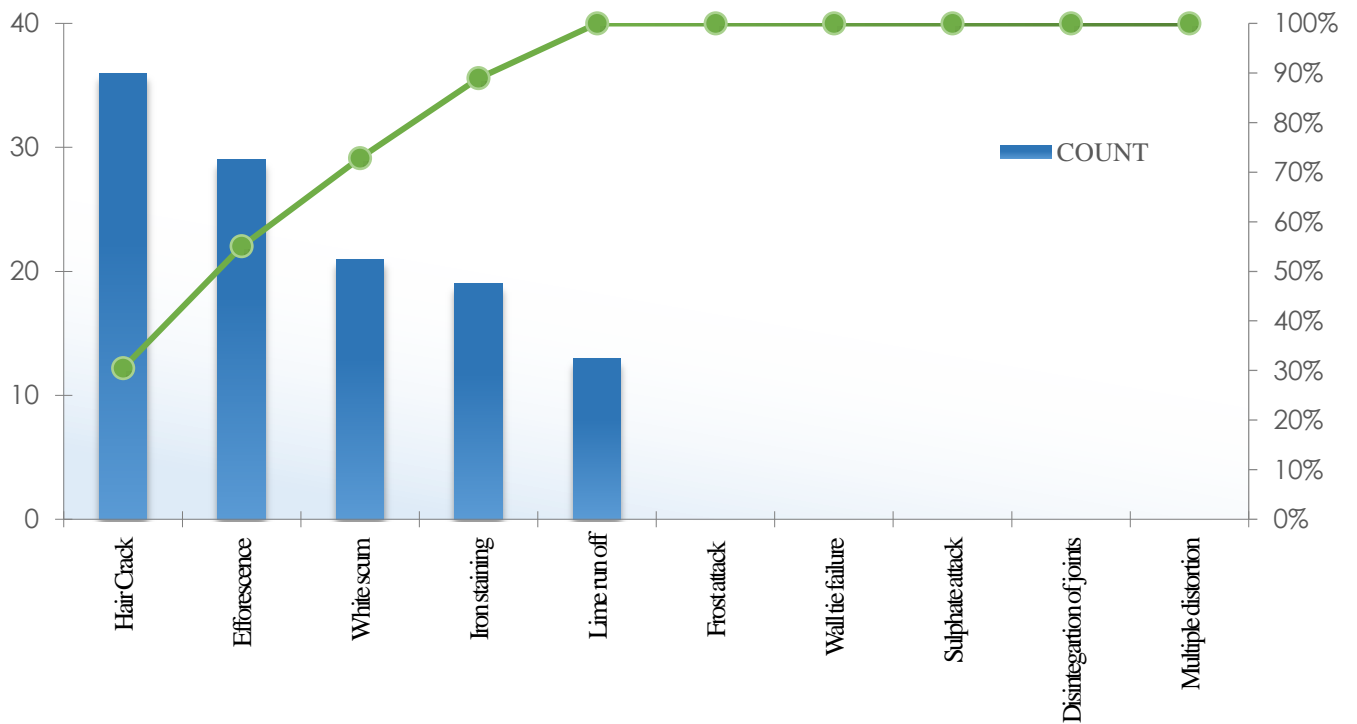


Figure no 2: Pareto chart of Brick Work

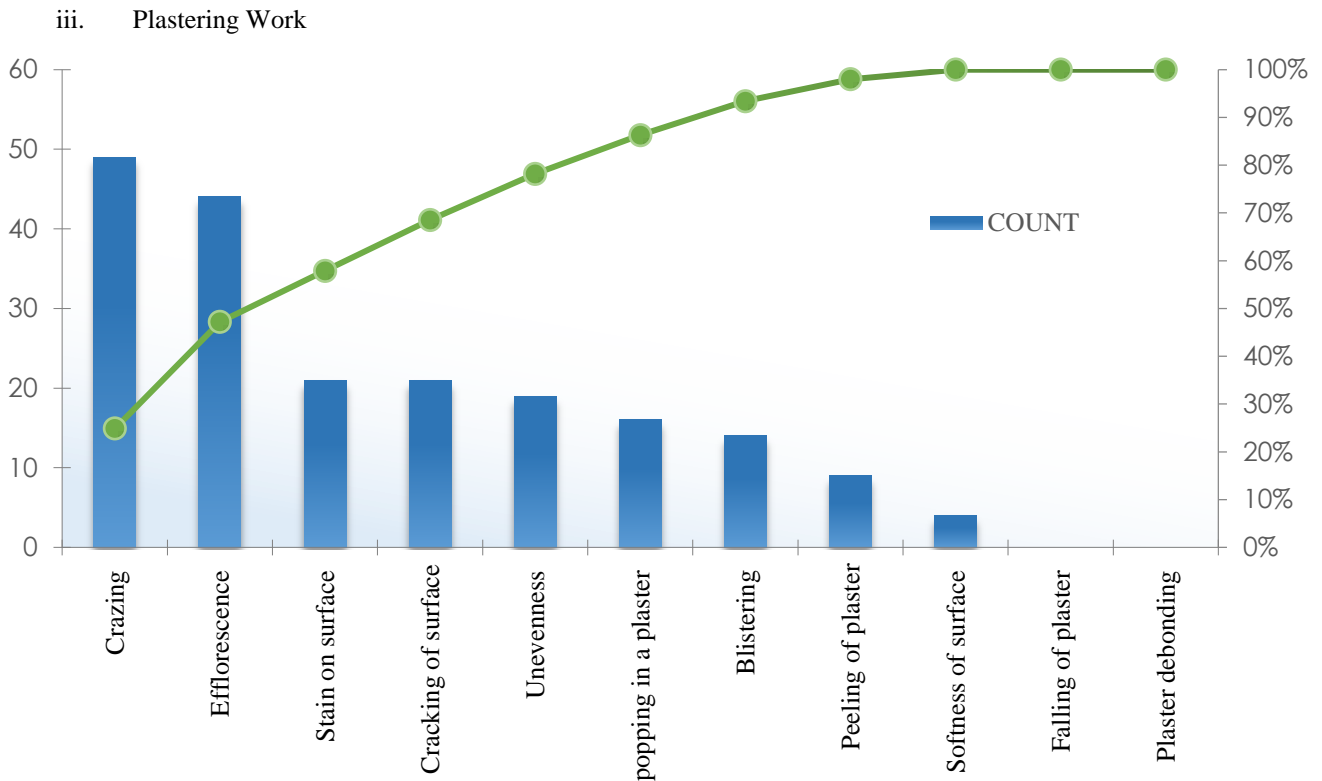


Figure no 3: Pareto chart of plastering work

between the outcome and the influencing factors, helps to understand the causes behind the defects.

3. Phase: Analysis

In analysis phase, Cause and Effect diagram has used to analyse the current outcome and the factors influencing the outcome. The diagram gives a graphical representation

i. R.C.C Work

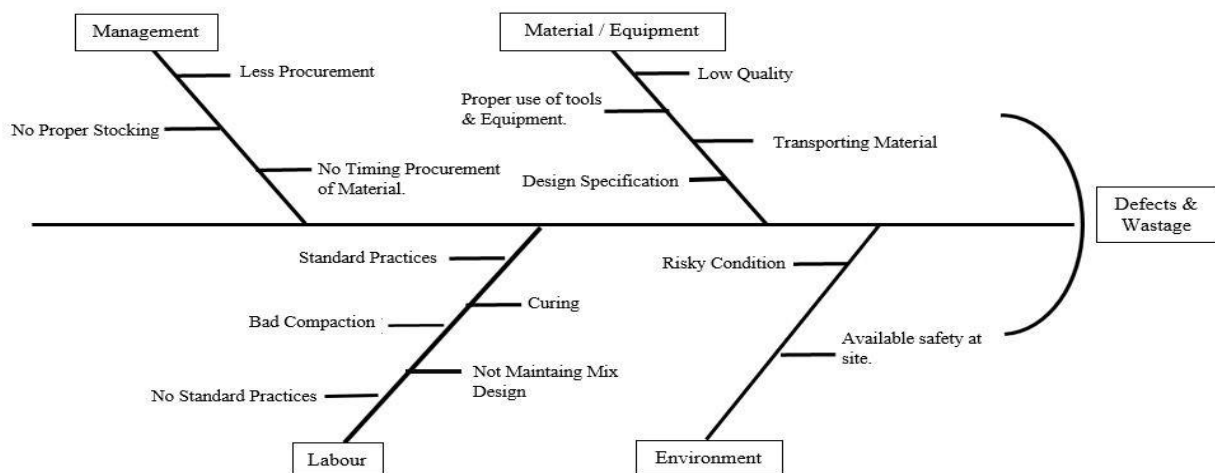


Figure no 4: Ishikawa Diagram for RCC Work

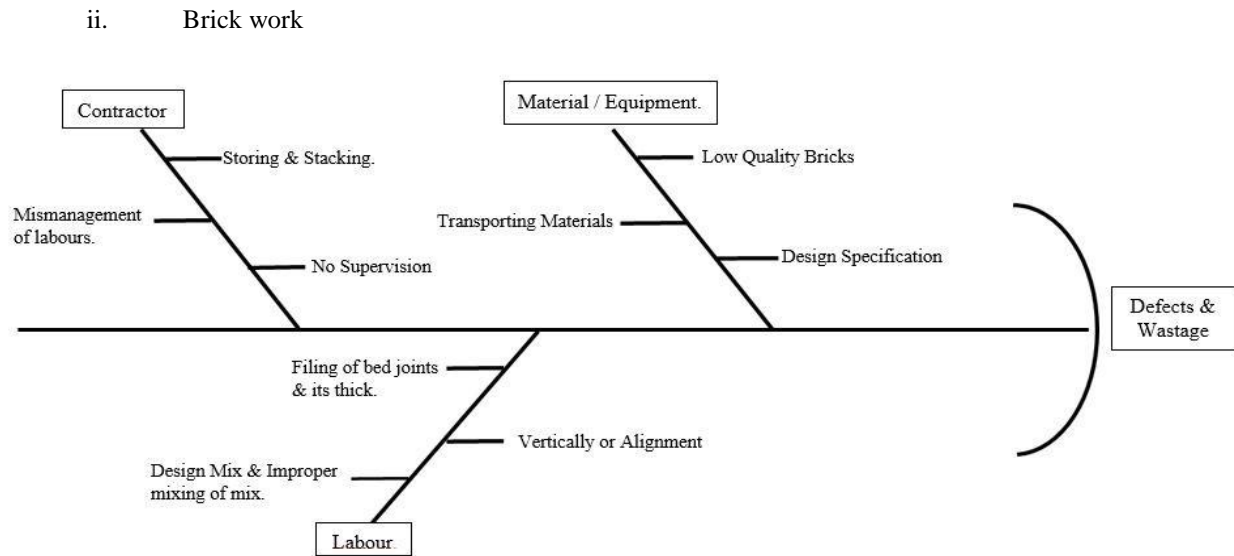


Figure no 5: Ishikawa Diagram for Brick Work

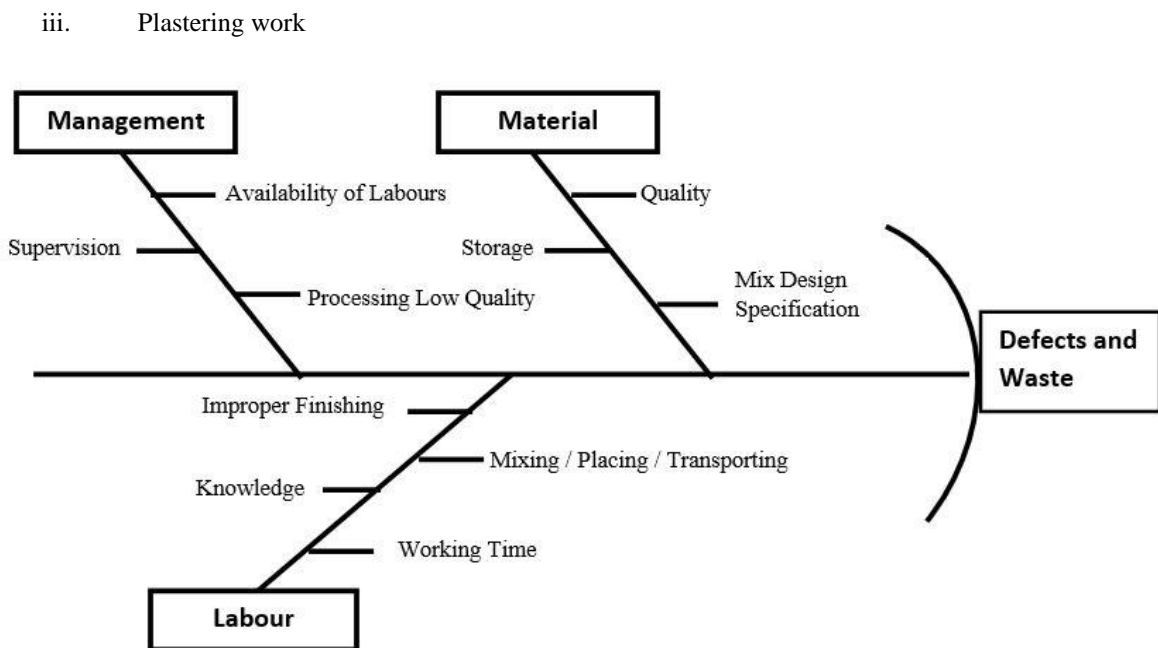


Figure no 6: Ishikawa Diagram for Plastering Work

4. Phase: Improvement- Corrective Actions

i. R.C.C work

- Improve supervision of work
- Execution of work as per given design specification and standards
- Quality and waste control audit
- Co-ordination between contractors and workers
- Making inventory plans
- Attention towards maintaining stock of materials at site
- Improving work safety at site
- Checking availability of equipment and tools prior the start of work
- Checking quality of material while receiving at site
- Allocating skilled workers for important and tedious works

ii. Brick work:

- Use of class 1 bricks
- Proper supervision of brick bonds with maintaining uniformity
- Pressure washing of efflorescence and lime run out
- Sealants can be applied on the surface of wall
- Giving attention to uniform bed thickness throughout the work
- Following a proper mix design mix of mortar and standard practices at site
- Proper care should be taken during transporting bricks and while placing them

iii. Plastering work:

- Curing should be given more attention
- Curing of base coat 1 day before plastering must be done
- Following standard practices of plastering with given mix design.
- Well-graded sand free from bulking and organic impurities should be used
- Surface of plaster should be prepared first before starting of work
- Level marks should be made to avoid uneven surface

5. Phase: Control

Control plan will help us to keep a check on the various preventive measures, which are taken to achieve the desired result. The checklist prepared for defect analysis can be used to check the improvement in work. Establishing a performance measure, monitoring and controlling team to check the improvement in the process.

IV. CONCLUSION

Quality is one of the crucial parameters considered in the construction world. However, completing work within the stipulated time period without compromising the quality is one of the major managerial and challenging tasks faced by construction firms. In maintaining the quality, various factors, which have a high impact on quality, need to be identified so that work can be executed with required quality standards. This paper has studied different construction activities like R.C.C Work, brickwork and plastering work of residential buildings. To find out the root causes of defects occurred, its impact on quality and the measures to reduce them, a systematic framework of DMAIC methodology based on six-sigma principle has been used. The various tools have been used in each step of DMAIC approach which gives a brief and close check on each activity of construction, it increases the quality and at the same time it will be helpful to maintain the time period.

V.5 FUTURE SCOPE OF WORK

The research of study is mainly focused on the conceptual framework for finding out root causes behind defects, lowered quality standards and for applying lean six sigma. It is an advanced quality control tool, which uses many quality management tools in its methodology. In this study, this technique has been applied to three activities of construction i.e. RCC work, Brick work, plastering work. Further, it can be applied to various construction activities where quality plays an important role. However, to apply this paper based research work in actual site practices it needs some standard guidelines to be set and knowledge about the same should be given to the project managers.

REFERENCES

- [1] Abdul-Aziz Banawi, Alia Besné, David Fonseca and Jose Ferrandiz, "A Three Methods Proactive Improvement Model for Buildings Construction Processes", MDPI Journal of Sustainability 25 May 2020, 12, 4335.
- [2] Ahmed Mousa, "Lean, Six Sigma and Lean Six Sigma Overview", International Journal of Scientific & Engineering Research, Volume 4, Issue 5, May-2013.
- [3] Antony, J. and Kaye, M., "Experimental quality: a strategic approach to achieve and improve quality", Kluwer Academic Publishers, Massachusetts, 2000.
- [4] Brahian Román Cabrera and Guillermo Juárez Li, "A lean-TRIZ approach for improving the performance of construction", Waste in Construction, Proceedings IGLC-22, June 2014 Oslo, Norway.
- [5] G. Tiwari and S. Kesavan, "Lean, Green and DMADV tool based approach for an effective execution of residential building project," vol. 5013, no. 5, pp. 383–385, 2016.
- [6] Ivan A. Reneva, Leonid S. Chechurina, "Application of TRIZ in Building Industry: Study of Current Situation", Triz Future 2015.
- [7] Jiju Antony, Ronald Snee, Roger Hoerl, "Lean Six Sigma: Yesterday, Today and Tomorrow", International Journal of Quality & Reliability Management, Vol. 34 Issue: 7, pp.1073-1093.
- [8] Lin, S.Y.; Wu, C.T., "Application of TRIZ Inventive Principles to Innovate Recycling Machine." Adv. Mech.Eng. 2016, 8950, 1–8.
- [9] Mann, D., "Physical Contradictions: Solving or Managing?" Triz Journal. 2019.
- [10] Mir Shariq Jowwad, G. Gangha and B.Indhu, "Lean Six Sigma methodology for the Improvement of the Road construction projects", International Journal of Civil Engineering and Technology, Volume 8, Issue 5, May 2017.
- [11] Mitra Zangeneh, "Identifying the Effect of Inventive Problem Solving Approach (TRIZ) to Reducing Delays in Construction Projects", Mediterranean Journal of Social Sciences MCSER Publishing, Rome-Italy, Vol 7 No 4, July 2016.
- [12] N. V. Fursule and S. N. Fursule, "Understanding the Benefits and Limitations of Six Sigma Methodology," Int. J. Sci. Res. Publ., vol. 2, no. 1, pp. 1–9, 2012.
- [13] R. D. Snee, "Lean Six Sigma – Getting better All the Time," Int. J. Lean Six Sigma, vol. 1, no. 1, pp. 9–29, 2010.
- [14] Shantanu Sathe, Dr. Satish B. Allampallewar, "Application of Six Sigma in Construction", International Journal of Innovative Research in Science, Engineering and Technology, Vol. 6, Issue 11, November 2017.
- [15] Sree Vidhya C, "Quality Management in a Residential building using Six Sigma Construction Techniques", International Journal for Modern Trends in Science and Technology Volume: 05, Issue No: 11, November 2019.
- [16] Sneha P. Sawant and Smitha V. Pataskar, "Applying Six Sigma Principles in Construction Industry for Quality Improvement", Proc. of the Intl. Conf. on Advances In Engineering And Technology - ICAET-2014, PP 407-411, 2014.

- [17] S. P. Sawant and S. V Pataskar, "Applying Six Sigma Principles in Construction Industry for Quality Improvement Basic Framework of Six," *Int. Conf. Adv. Eng. Technol.*, pp. 407–411, 2014.
- [18] S. V Desale and S. V Deodhar, "Identification and Eliminating waste in Construction by using Lean," *Int.J. Innov. Res. Sci.*, vol. 3, no. 4, 2014.
- [19] S. H. Han, M. J. Chae, K. S. Im, and H. D. Ryu, "Six Sigma-Based Approach to Improve Performance in Construction Operations", *J. Manag. Eng.*, vol. 24, no. January, pp. 21–31, 2008.
- [20] V. Raja Sreedharan and R. Raju, "A Systematic Literature Review of Lean Six Sigma in different Industries", *International Journal of Lean Six Sigma* · July 2016.
- [21] Yun-Sheng Lin and Mingchih Chen, "Implementing TRIZ with Supply Chain Management in New Product Development for Small and Medium Enterprises" , *Processes* 2021, 9, 614.MDPI

Image De-noising Using Machine Learning

^[1] Charutha M V, ^[2]Shadakshari, ^[3]Shyamala P Bhat

^[1] Assistant Professor, Raja Reddy Institute of Technology, Bangalore

^[2] Assistant Professor, Raja Reddy Institute of Technology, Bangalore

^[3] Assistant Professor, Raja Reddy Institute of Technology, Bangalore

Abstract— It turns into a great subject to be explored for the better translation of the medical images. Now different de-noising techniques are using but still it is an area of research. Here medical image is de-noised using machine learning technique, is random forest classifier. While diagnosing, some noise cannot be ignored. Therefore it is vital to eliminate the noises from the medical images. To get a fully de-noised image still researches are going on.

Index Terms— image de-noising, image restoration, impulse noise, salt and pepper noise, Speckle noise

I. INTRODUCTION

Digital images has a vital role in daily life applications such as satellite television, magnetic resonance imaging, computer tomography, diagnosing of diseases such as detecting cancer cells, locating tumours, fractures etc as well as in areas of research and technology such as geographical information systems and astronomy. Data sets collected by image sensors are generally contaminated by different types of noises. Noise is a major factor that degrades the quality of images. The images should be free from noises to make accurate decisions. Different noises mainly impulse noises, which is caused by malfunctioning of sensor elements or defects in the transmission of images.

In the imaging process the noise corrupts the images by replacement of few pixels of original image with some of the new pixels, these have luminance which can be within the minimum luminance range or else it can be beyond the luminance range termed as impulse noise. In this paper machine learning technique is used to de-noise this impulse noise in the image. In image analysis image de-noising is an important de-noising step. Diagnostic information must be preserved and noise should be eliminated so the making of de-noising algorithm is a difficult task. So the success of the application is important because it has an impact on the performance of image processing.

II. LITERATURE SURVEY

S. Bhadouria and D. Ghoshal [1] have proposed reduction of noise in SAR images by using discrete wavelet transforms. It is a combination of stationary and discrete wavelet transform technique. The drawback of this method is, it is a hybrid method of two transforms. Suresh Velaga and colleagues [2],[3] have proposed an efficient techniques to de-noise images of corrupted impulse noise by using dual tree complex wavelet transformation. The drawback of this

technique is shift invariance property which is comparably slow when used in filtering. T. Veerakumar and colleagues [4] have proposed a novel technique of modified switching bilateral filter for impulse noise removal. The drawback of this technique is spatial domain bilateral filters are considered and in prior removal of high density noise is not possible. G Panda and colleagues [5] have proposed a novel method of filtering Impulse Noise. This uses ANN [Artificial Neural Networks] and Discrete Wavelet Transform. The drawback of this technique is ANN [Artificial Neural Networks] is having very low training rate and it is difficult to detect pixels using this technique.

Pooja Pandey and colleagues [6] have proposed a Gaussian noise removal. They have used a unique approach using discrete wavelet transform technique. The drawback of this technique is removal of fine structures. Manohar Annappa Koli and colleagues [7] have proposed a novel technique of median filter and a shrinkage technique of adaptive wavelet threshold for de-noising of images. The drawback of this technique is quality of the image is not up to the mark tested against Gaussian noise.

III. METHODOLOGY

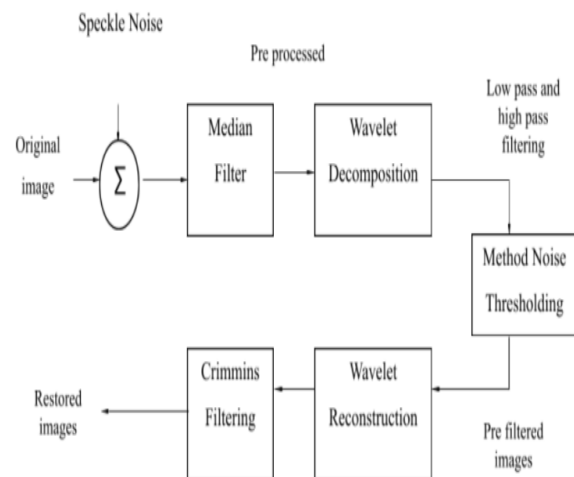


Fig.1 Block diagram

One of the most common noises is salt and pepper (SP) noise, which is a member of the broader category of impulse noises. It consists of two constant values which is distributed randomly on the image. There will be two stages in the algorithm one is detection of noisy pixel and by the help of a proper value it is replaced. The proposed method focused on de-noising the impulse noise in the images using random

forest method. By using this method de-noising ratio is amplified and image resolution will be improved.

In the past technique the image de-noising they tried for isolate the image by endeavor to change the higher recurrence to lower. And it is difficult to obtain the dependable smooth image and huge procedures are followed for the de-noising. Most images seeing as a two-dimensional banner and applying standard banner getting ready procedures to it. The drawback of the method is when clamor proportion extent assembles, it requires unreasonable time, so confused and it is not for proper certifiable applications. The proposed method is having fast computation. In figure 1 the image is gone through the Pre-dealing with based MinMax isolating to starting drive upheaval clearing by then went through Random forest (RF) classifier and to recognize the uproarious pixels by contemplating their enveloping area. The contaminated pixels are capable the Stationary Wavelet Transform (SWT) based pre-channel and the moved pixels are superseded back in the photograph. The pre-disconnected picture is additionally capable the Random woods classifier and to get any additional contamination.

According to the proposed method for de-noising the image

A. Noisy Images

Considering salt and pepper noise and impulse noise, The noisy image is got by including sound the first dark pictures of the given size 512×512. Here 512×512 assigns that a picture is having 512 lines and 512 segments.

B. Min-Max Filter

Max filter is used to find out the brightest points in the images. Because of maximum filter operations can reduce the pepper noise in the image. Min filter is used to find out the darkest points in the image. Therefore salt noise is reduced by the operations of minimum filter. When the medical image with impulse noise is given to min-max filter in the preprocessing step, 20% - 30% of the noise is eliminated.

C. Random Forest

Random forest or random decision forest are ensemble learning method used for classification and regression. The operations are carried out by constructing decision trees during training and output is mode of classes which is for classification and means prediction which is used for regression. It is a supervised learning algorithm, in this method a forest is built randomly. This is by ensemble of decision trees. And the decision trees are trained by bagging method. This method is a learning model, and then overall result is improved. Therefore the pre-processed image endures training and classification of random forest. Parameters of random forest will increase the predictive power so that the model can be fast. Hyper parameter of built-in random forest function is increase of predictive power, increasing the speed of models.

D. Stationary Wavelet De-noising

After classification and training we will get corrupted pixels, next step is to apply SWT and perform de-noising. The steps are 2D wavelet transform is applied and change the noisy picture into orthogonal area. Apply hardly or delicate thresholding to the widely coefficients of the wavelet

transform. And perform backwards discrete wavelet change to get de-noised image. In the de-noising procedure, the edge assumes an imperative part. Finding an ideal limit is an odd procedure.

Averaging filter

Normal channel is windowed channel of direct class, that smoothed flag (picture). The channel fills in as low-pass one. The essential thought behind channel is for any component of the flag (picture) take a normal over its neighbourhood.

Averaging filter algorithm:

1. A window is placed over the element;
2. Average taken — total the elements and sum divided by using number of elements.

The figure 2 shows the design flow of the proposed method. A small limit esteem will hold the uproarious coefficients while the edge esteem supports the loss of coefficients that convey image flag points of interest.

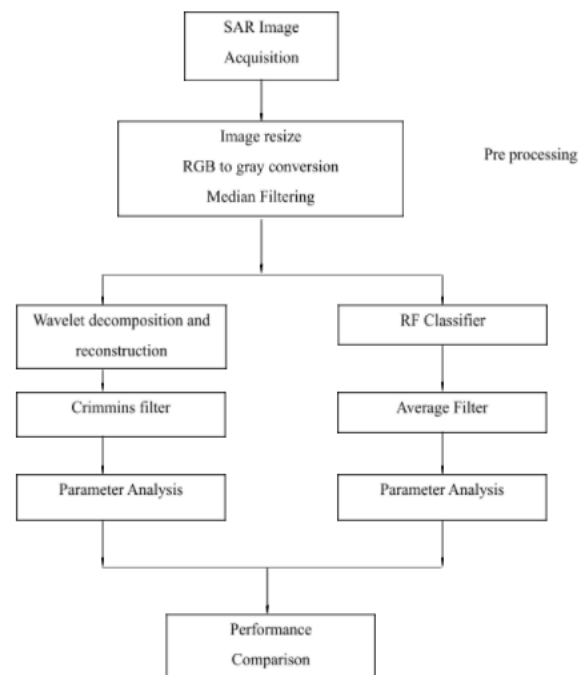


Figure 2. Design flow

Before the starting the process, the data set of sample images is trained and classified. This is done by Machine learning algorithm. This differentiates noisy pixels; easy application of de-noising technique on the image. Steps for de-noising of SAR image is as follows,

Step 1: Input the original noise free SAR image to the summation block.

Step 2: The second input is impulse noise of anticipated noise density.

Step 3: The output of summation is now the SAR image corrupted with impulse noise of certain noise density.

Step 4: SAR image corrupted by impulse noise is now fed to min-max filter for preprocessing of the image. Here around 20% to 30% of the noise is removed.

Step 5: This pre-processed image endures training and classification of Random Forest.

Step 6: Now from the classification and training we are obtaining corrupted pixels, on which we apply SWT and perform de-noising.

Step 7: In final stage Averaging filter is applied on to the image to further reduce the amount of noise in the image.

IV. EXPERIMENTAL RESULTS

Parameters

Different parameters defines the performance of proposed algorithm. The results obtained with the proposed methods have been compared with the existing methodologies. Some of the parameters of evaluation are,

1. Peak Signal to Noise Ratio

The peak signal-to-noise ratio figures, in decibels, between two images. This ratio is frequently utilized as a quality measurement. It is used between the original and a compacted image. The higher the PSNR, the quality of compacted image is better.

PSNR computation using the following equation:

$$PSNR = 10 \left(\frac{R}{MSE} \right)^2$$

R is the maximum fluctuation. For example, if the input image is a double-precision floating-point, then R is 1. If the image is an 8-bit unsigned integer data type, R is 255

2. Mean Square Error [MSE]

The Mean Square Error is one of the metric and the Peak Signal to Noise Ratio (PSNR) is another error metrics. They are used to do comparison of image compression quality. The MSE signifies the cumulative squared error. It occurs between the compressed image and the original image. PSNR signifies a measure of peak error. The error will be reduced as the MSE value is reduced.

To compute PSNR, calculation of the mean-squared error by the following equation:

$$MSE = \frac{\sum_{i=0}^M \sum_{j=0}^N (X_{ij} - R_{ij})^2}{M \times N}$$

M is the total number of rows and N is the total number of columns in the input images.

X is original image, R is restored image

3. Structural Similarity Index Measure [SSIM]

Structural similarity [SSIM] index method computes the similarity between two images. The measure of two windows which has the same size.

$$SSIM = \frac{(2 \mu_p \mu_q + a_1)(2 \sigma_{pq} + a_2)}{(\mu_p^2 + \mu_q^2 + a_1)(\sigma_p^2 + \sigma_q^2 + a_2)}$$

Where μ_p , μ_q is the average of value p and value q.

σ_p^2 , σ_q^2 are variance computed for value p and value q

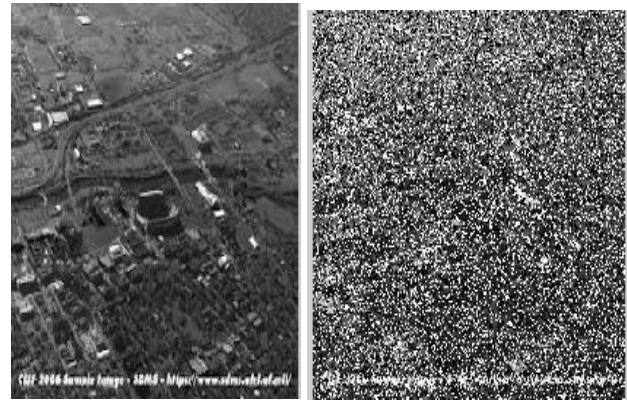
σ_{pq} is covariance of value p and value q

$a_1 = (m_1 N)^2$, $a_2 = (m_2 N)^2$ are the two variables for stabilization

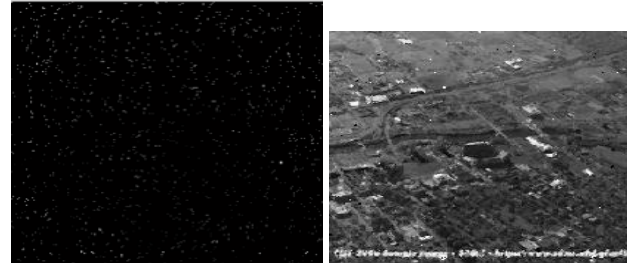
4. Percentage of Spoiled Pixels

It is the measure which gives unaffected original pixels and swapped with different gray value after filtering i.e.

$$PSP = \frac{(\text{No. of original pixels change their grayscale})}{(\text{No. of non-noisy pixels})} \times 100$$



A. Original SAR image B. Image after noise is added



(C) Image after pre-processing (D) Filtered SAR image

Figure 3: The standard SAR images are computed using Random forest classifier.

Parameters	RF
PSNR (db)	49.6234
MSE	214.7376
SSIM	0.84175
PSP	38.62

Table 1. RF for 0.4 noise density on standard SAR image

The figure 3 shows the input SAR image, while added noise, image after pre-processing, filtered SAR image. The table 1 shows the different parameters value in random forest classifier for 0.4 noise density on standard SAR images.

V. CONCLUSION

For de-noising the SAR images involves three stages of filtering. First the preprocessing stage is performed in presence of MinMax filter. The proposed conspire has been simulated utilizing the standard SAR pictures in various impulse noise conditions. Then the preprocessed image is subjected to random forest classifier. The corrupted pixels of the image is again filtered using the stationary wavelet transform de-noiser. As because, by the proposed scheme of filtration, we can achieve improved performance in restored results as compared to the previously reported schemes. Again the malicious pixels hence finally sent through the average filter to obtain the restored image. Then finally parameters PSNR, MSE, SSIM, PSP are obtained. These parameters vary with different SAR images. Apart from de-noising, the future scope could be even focused on getting improved quality of images by employing best synthetic aperture radar.

REFERENCES

- [1] S. Bhadouria and D. Ghoshal, "A study on genetic expressioprogramming-based approach for impulse noise reduction in images," *Signal, Image and Video Processing*, pp. 1-10, 2015
- [2] Suresh Velaga, Sridhar, "Efficient techniques for de-noising of highly corrupted impulse noise images", *International Journal of Soft Computing and Engineering*, Volume 2, Issue 4, September 2012, pp 255-258.
- [3] T. Veerakumar, S. Esakkirajan and IlaVennila, "High Density Impulse Noise Removal Utilizing Switching Bilateral Filter", *International journal of circuits, systems and signal processing*, 2012, Issue 3, Volume 6, pp 189-196.
- [4] Ajeet Singh "Denoising of medical images using wavelet transform" *ISSN 2229-5518*, July-2013.
- [5] G Panda, B Majhi, P K Dash and S K Meher, "A Novel Filtering Scheme for Impulse Noise Cancellation", *IETE journal of research*, March 2015, volume 48, pp 163-170.
- [6] Pooja Pandey, Praveen Chouksey, "Gaussian Noise Removal by a New Approach of Discrete Wavelet Transform", *International Journal of Science, Engineering and Technology Research*, Volume 5, Issue 2, February 2016.
- [7] Manohar Annappa Koli, "Review Of Impulse Noise Reduction Techniques", *International Journal On Computer Science And Engineering*, February 2012, pp 184-196.
- [8] Ami George, S. Logesh Kumar, K. Manikandan, C. Vijayalakshmi and V. Renuga "Medical Image Denoising Using Wavelet Transform, 2016
- [9] Zohreh HosseinKhani, Mohsen Hajabdollahi, Nader Karimi, S.M. Reza Soroushmehr, Shahram Shirani, Kayvan Najarian, Shadrokh Samavi "Adaptive Real-Time Removal of Impulse Noise in Medical Images" October 2018
- [10] S.Deivalakshmi, P.Palanisamy and S.Sarath, "Detection and Removal of Salt and Pepper noise in images by using Improved Median Filter", *IEEE*, 2011, pp 363-368.
- [11] G Panda, B Majhi & P K Dash, "Development of Efficient Filtering Techniques for Image Data Corrupted by Impulse Noise", *The Journal of the Computer Society of India*, March 2000, pp 25-33.
- [12] L. M. Satapathy, P. Das, A. Shatapathy, A. K. Patel, "Bio-medical image denoising using wavelet transform", *ISSN: 2277-3878*, Volume-8, Issue-1, May 2019.
- [13] V N Prudhvi Raj and Dr. T Venkateswarlu "Denoising of medical images using image fusion techniques" Vol.3, No.4, August 2012
- [14] Liming Chen, Bin Xie "A New Signal Denoising Method Based on Wavelet Threshold Algorithm", 2016

Behavior of Wear and Corrosion Resistance of thin film coated Titanium alloy substrate

^[1] K Chandrappa, ^[2] Anoop Joshi, ^[3] Sanjay T Setty, ^[4] K Vineth

^[1] Associate professor, Department of Mechanical Engineering, Siddaganga Institute of Technology, Tumkur, Karnataka, India

^{[2][3][4]} Department of Mechanical Engineering, Siddaganga Institute of Technology, Tumkur, Karnataka, India

Abstract— Thin-film barrier coating on titanium alloy substrate features a vast range of application among which aeronautic and marine application are significant. Talking about 2 very different aspects, whose requirements and application are way apart. Titanium has always been beneficial in both these products applications. The introduction of titanium in aerospace and marine locomotive parts will have significant importance on parameters like pressure withstanding capacity and corrosion resistance. Our immense perseverance is to satisfy the above intent by giving a skinny coating on Titanium alloy substrate. These coated titanium alloy are going to be tested for wear and corrosion resistance and it's hoped are going to be in line with TiN, AlCroNa pro, DLC (diamond-like-carbo) and WCC (Tungsten carbide carbon coating) all the mentioned are coated for about 2 microns to 4 microns over the substrate titanium alloy. TiN is administered in PVD Coating process, AlCroNa pro are administered in arc spray method and DLC, WLC is administered in sputtering process.

Index Terms— Titanium alloy, Arc spray, Sputtering, PVD coating, Neutral Salt spray testing.

I. INTRODUCTION

It has always been Aluminium the primary preference for any aeronautical or submarine application. The inherent property of Al like pressure withstanding capacity, corrosion resistance, and high strength makes the fabric most ideal for its usage. The direct use of uncoated Al might not be suitable to be used within the aeronautic, marine, or automotive industry because it fails to satisfy certain atmospheric threats, hence the coating is preferential. In an attempt to enhance the top requirements fulfilled by coated aluminium, coated Titanium alloy seems to be most ideal because it also has the property of durability.

Having said the above information our immense effort is to prove that Ti alloy provides better quality, efficiency, and sturdiness when it's coated for its applicability within the aerospace and submarine industry or any automotive sector. In reference to this Ti alloy has been subjected to TiN, AlCroNa Pro, DLC, WCC coating, and therefore the end requirements are going to be recorded

II. MATERIALS AND METHODOLOGY

A. PVD coating:

For many applications, PVD has been widely used in films depositing technology with a range of applications already well established, namely improvements in tribological behaviour, optical improvements, look updating and many others [2,4].

Machinery is probably one of the most common uses of this deposition technique, sometimes used in conjunction with chemical vapour deposition (CVD) to extend its life span, reduce friction and improve thermal properties. Variation of the coating characteristics throughout the film are permitted by the use of PVD processes. It also allows alloy compounds, multilayer composition and special structures to be deposited [13]. This versatility has led to the event, improvement and proliferation of techniques for different processes.

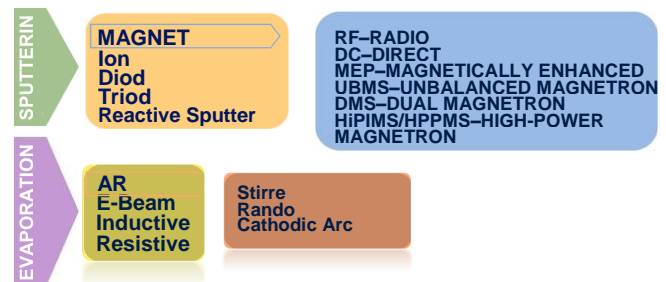


Figure 1. Physical vapour deposition (PVD) approaches for advanced coatings

B. Sputtering

Realize all interaction actions in regards to the gear associated with the reactor, keeping in mind what transpires in the chamber during the testimony cycle, to obtain a more slender film deposition. Prior to deposition, a planned interaction is essential, namely cleaning the substrate to achieve a superior film grip between the covering and the substrate. Cleaning the substrates in an ultrasonic shower outside of the vacuum chamber is also recommended before they are placed on the satellites [3].

A vacuum sputtering chamber has the advantage of being able to be used for both cleaning the substrates and covering

deposition a short time later. However, the length of the cleaning interaction is impressive, and it is a hindrance in terms of industry competition because it increases end-result expenses. The executives of the machine's breakdown times and arrangements are essential for controlling costs [7].

As a result of this reality, improvements to the cycle boundaries are required to cut production times. The deposition rate, in terms of an increase in plasma thickness and energy available at the same time, is an important boundary to be streamlined. In this vein, it is critical to evaluate the full of the cycle's means and constraints when complying with industry standards [13].

Corruption of the films can be avoided by properly caring for the substrate and maintaining the complete vacuum framework, as the pollution sources are either poor professional conditions or framework-related sources. The duration of the interaction process is mostly determined by the vacuum chamber's size and syphoning framework.

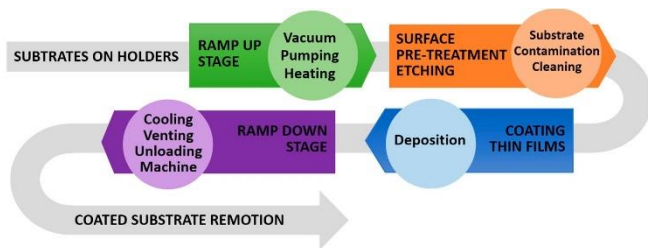


Figure 2. The flow of a traditional PVD sputtering process.

C. Neutral Salt Spray testing (Corrosion Resistance)

Specimens must be cleaned properly. Depending on the nature of the surface and the impurities, the cleaning procedure will be optional. It is important to ensure that specimens are not decontaminated after cleaning due to careless or excessive handling. When determining the progression of corrosion from an abraded spot in a paint or organic coating, a scratch or scribed line through the coating using a sharp instrument must be produced through the coating to expose the underlying metal before testing.

Test solution will be set up by dissolving sodium chloride in refined or de-ionized water to deliver a centralization of 50 ± 5 g/l. The sodium chloride will be white and will give a dull arrangement in water. It will be generously liberated from copper and nickel and will not contain more than 0.1 percent of sodium iodide and not more than 0.4 percent of all out pollutions determined for dry salt. On the off chance that the pH of the arrangements as pre-arranged is outside the scope of 6.0 to 7.0, the presence of bothersome pollutants in the salt or the water or will be explored [1].

The pH of the salt arrangement will be changed so the pH of the splashed solution gathered inside the test bureau will be somewhere in the range of 6.5 and 7.2. Control of the pH will be founded on electromagnetic estimation at 25⁰C yet a short-range pH paper which can be perused in augmentations of 0.3 pH units or less and which had been aligned against electrometric estimations might be utilized in routine checks.

Any essential remedy will be made by the expansion of an answer of hydrochloric corrosive or sodium hydroxide of scientific grade [9,10].

D. Wear resistance (Abrasion Test)

The samples were tested for wear resistance using the IS 11093-1984 standard. The Indian Standards Institution adopted this Indian Standard on July 25, 1984, after the Structural and Metals Division Council approved the proposal finalized by the Methods of Physical Tests Sectional Committee.

The friction and wear behaviour of metallic materials and materials like nylon and resin bonded fabrics, etc., during relative motion in contact with steel surfaces, such as in bearing application is important in selection and development of such materials. Various applications include wear resistant steels for machine slides, non-ferrous materials in journal bearing, balls and rollers in antifriction bearings and nylon slippers and fabric bearings in rolling mills. In the above applications the wear between the mating parts can be under conditions of pure sliding, pure rolling and combined sliding and rolling under constant or repeated loads and with or without lubrication including presence of corrosive Liquids too. Need have therefore arisen to evolve some standard method to evaluate the wear and friction properties of the above materials under various simulate conditions to know their behaviour in actual operating conditions [5,8].

If the final value, observed or computed, is to be rounded off in reporting the result of a test or analysis performed in accordance with this standard, it must be done in accordance with IS: 2-1960.

III. EXPERIMENTS

A. For PVD coating

The fabric to be deposited, namely the target, is converted into atomic particles by a thermal physical collision process and guided to the substrates in a vacuum or gaseous plasma under low-pressure circumstances, where they condense to create a physical coating.

Alloy constituents with similar vapour pressure are often passed into the vapour with little change in composition, particularly when the rod feed beam is employed. Problems are encountered when the alloys contain constituents of widely different vapour pressure [7].

Some chemicals, such as SiO, MgF₂, B₂O₃, and CaF₂, will evaporate as molecules without dissociation. The process of reactive evaporation [10], in which metal atoms are evaporated in the presence of reactive gas pumped into the chamber, is an extension of this process.

B. For Sputtering process

In a conventional e-beam evaporation process, the target has an evaporation source that functions as a cathode and contains the fabric to be evaporated. The particles will be placed on the substrate, producing successively compacted

layers that will allow the film to adhere to the substrate accurately.

There are three distinct ways where the sputtered coating structure differs from the evaporation process. First, the sputtered atoms could also be scattered by working gas in order that they approach substrate at very low oblique angles thus producing a zone 1 type structure. At very low working pressure the atoms will reach the substrate and subject them to bombardment which promotes dense fine-grained, dense zone T structure [4]. Plasma ion bombardment tends to suppress zone 1 structure, even at elevated Ar pressures, and to supply the dense fine-grained structure of zone T type. Ion bombardment on an uncooled substrate also promotes high-temperature structures.

C. For Neutral Salt spray test (Corrosion Resistance)

In light of the major surface being evaluated, the specimens will be held or suspended between 15 and 300 degrees from vertical, preferably matching to the primary bearing of the haze stream across the chamber. The specimens will not come into touch with each other, with any metallic substance, or with any material capable of acting as a wick [1].

Every specimen shall be positioned in such a way that mist may settle freely on all instances. The salt solution from one example will not drop on the salt solution from another example [11,12].

The salt solution will be made by dissolving 5+1 parts sodium chloride by mass in 95 parts water. The salt used will be sodium chloride that has been significantly freed from nickel and copper and contains no more than 0.1 percent sodium iodide and no more than 0.3 percent absolute contaminations on a dry basis. A few salts have additional compounds that may act as erosion inhibitors; the salt's synthetic component should be carefully considered.

D. For Wear resistance (Abrasion resistance)

In general, the test shall be carried out at ambient temperature within limits of 10 to 35°C. The test specimen is fitted on the upper shaft and pressed against the standard disc with the help of the spring loading device. The specimen is cleaned, dried and weighed. Initial readings of revolution counter and energy meter are taken, the machine is run continuously for six hours and the specimen is taken out, cleaned, dried and weighed. Final readings of revolution counter and energy meter are noted. Average torque reading during the test is also noted. Wear loss and co-efficient of friction is evaluated after each run of six hours and a total number of minimum 8 runs will be required to obtain a steady state wear condition [6].

While reporting the results, mention should be made whether testing was conducted with or without lubricant. In case where lubricant is used the characteristics of the lubricant shall be mentioned.

Evaluation of test results:

The symbols used in this standard are as follows:

P = load applied on the specimen, 'N';

p = pressure between test specimen and standard disc, N/mm²;

T = average friction at torque during the test, Joules;

W₁ = the specimen's initial bulk, g;

W₂ = the specimen's final bulk, g;

n = rotating speed, rev/min;

μ = co-efficient of friction;

R = wear factor

\bar{X} = loss in vertical thickness or diameter of the specimen, mm;

Q = total friction energy absorbed during the test, Joules;

v = peripheral velocity of the rotating standard disc, m/mm;

t = time of each run hours;

r = radius of the rotating disc, m; and

a = thickness of the specimen, mm.

Determination of Wear - The wear of the specimen can be represented in terms of mass loss or vertical thickness or diameter loss as determined by the wear factor:

a) Wear loss: $w = w_1 - w_2$

b) Wear factor: $R = \bar{X}/\rho t$

Determination of Co-efficient of Friction - The co-efficient of friction. can be evaluated both from torque as well as energy absorbed. The larger of the two values should be taken.

$\mu = Q/2\pi nPr$

IV. RESULTS AND DISCUSSION

A. Corrosion Resistance

The corrosion experiment was done in a salt spray tester (SST-80S, CMIT, Bangalore). A standard methodology for salt shower testing was applied by ASTM B117-2019. The salt arrangement picked was 5% A.R. NaCl. Four sorts of tests were utilized, to be specific TiN, AlCrNa genius, DLC (Diamond like Carbon), WCC (Tungsten Carbide Carbon). Prior to the actually affidavit, the tests were polished, cleaned, and subjected to argon plasma cleaning. To achieve excellent adhesion, a thin amorphous silicon layer was retained. In contrast to uncoated substrates and testing with base metal OT-41, the examples were exposed to the corrosive environment of the ASTM B117 salt mist test. After 2, 6, 24, 36, 48, 72, and 96 hours, samples were withdrawn to be examined. Optical microscopy, filtering electron microscopy (SEM-EDS), and contact profilometry were used to evaluate the erosion obstruction of the three types of testing.

For the most part, a solitary layer of TiN can't secure the erosion of Titanium created amalgam in salt shower testing. It was found, nonetheless, in this investigation that the overall erosion assault on TiN-covered low-carbon steel substrate can be forestalled through the work of electroless nickel interlayer-altered TiN covering. This presents a potential and promising use of surface change procedures in TiN covering.

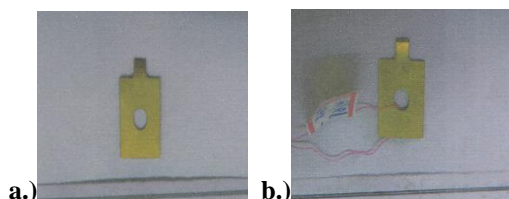


Figure 1. Titanium Nitrate alloy (a) prior to salt spray test (b) following a salt spray test

For all periods, DLC coatings outperform TiN films in terms of corrosion resistance. DLC samples totally protect the substrate for up to 48 hours in a salt fog condition, showing no evidence of corrosion, whereas TiN coatings only protect the substrate for less than 2 hours. Furthermore, even after 96 hours of contact, no deterioration of the DLC coating was seen, suggesting that corrosion occurs at pre-existing surface micropores. Complementary corrosion experiments are being conducted to have a better understanding of the impact of microporosity in coatings.

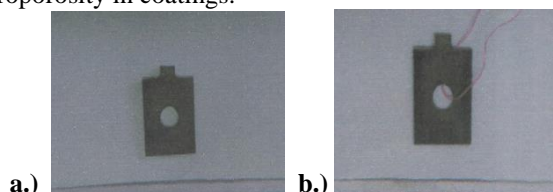


Figure 2. Diamond like Carbon alloy (a) prior to salt spray test (b) following a salt spray test

The salt spray corrosion test did not modify the coating's mean thickness, but it did affect the coating's and substrate's surface morphology. It should be emphasised that salt spray caused significant damage to the substrate. General corrosion was evident on several portions of the substrate; indeed, after a 96-hour salt spray test, a small yellow pin pit appeared on the substrate surface, indicating that pitting corrosion had already occurred at that time. As the duration for the salt spray was extended, the pits grew larger and larger.

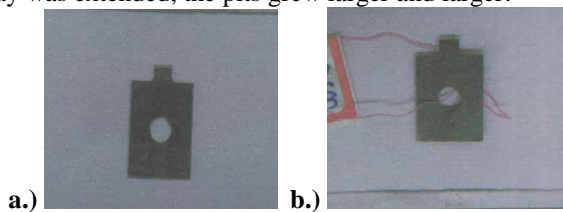


Figure 3. Aluminium Chromium Nitride alloy (a) prior to the salt spray test (b) following a salt spray test

The micrographs show a high amount of porosity that is consistently distributed over the whole coating cross section. Large gaps were more visible on the surface of the WCC coating, while it is clear that the porosity of the coating extends throughout the coating to the substrate. This coating had a porosity of about 15% overall, however it was higher in some regions. This looked to be higher in certain regions. In the WCC coating, a lower value of around 8% was observed. The rough surface topography indicates the presence of an inhomogeneous structure with both granular dispersion and matrix phases separated by regions of significant porosity/voids. On the other coatings, similar topographies were seen.

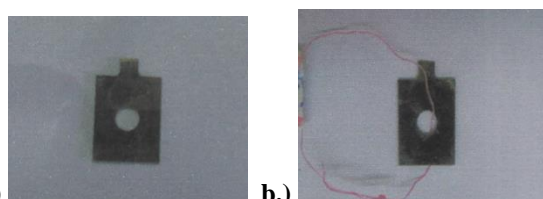


Figure 4. Tungsten Carbide Carbon coating (a) prior to the salt spray test (b) following a salt spray test

B. Wear resistance (Abrasion resistance)

TiN, AlCrONa pro, WCC, and DLC coatings are resistant to wear resistance testing after being tested according to the test method IS:11083-1984. In comparison to other Titanium alloys, AlCrONa was shown to have superior tribological characteristics.

All the samples will be subjected to wear load for about 8 cycles or up to its failure. Sample will be mounted to a circular disc which is run against a standard hardened steel disc at high rpm. These discs are kept intact by spring loaded frame. Results and visual appearance witnesses the better performance of AlCrONa coated sample after 8 cycles of testing. All the other samples have also proven effective when subjected to abrasion, among them AlCrONa coating has provided dominant results.

V. CONCLUSION

With the above discussion We find that testing samples have clearly passed both corrosion resistance test and wear resistance test.

The salt spray test results of each samples are displayed and with the results we can conclude

1. TiN, AlCrONa, WCC and DLC coated samples have clearly passed the salt spray test of 96 hours without any red rust observation.
2. Above point witnesses that there are no defects or cracks in the coated material, any defects would have reflected in failure of salt spray test in early stages of 6-7 hours of test commencement.
3. Generally, PVD coatings are said to show potential salt spray result of 900+ hours. Which makes them suitable for both marine and aerospace application.
4. Titanium and chromium being highly resistant to corrosion help the coating to withstand longer period of salt spray test.

Wear resistance (abrasion resistance test) results were conducted as per IS:11083-1984 standards have passed the test successfully. By this it can be stated that the tested samples work effectively in extreme conditions.

REFERENCES

- [1] Zhiping SUN, Guangyu HE, Qingjie MENG, Yuquin LI, Xiaodong TIAN, “Corrosion Mechanism investigation of TiN/Ti coating and TC4 alloy for aircraft compressor application”, Chinese Journal of Aeronautics, 2020
- [2] A Bapista, J Porerio, F J G Siliva, J L Miguez, G Pinto, L Fernandes “On the Physical Vapour Deposition (PVD): Evolution of Magnetron Sputtering process for Industrial Applications”, 28th International Conference on Flexible Automation and Intelligent Manufacturing, 2018
- [3] W Herr, E Broszeit, “The influence of a heat treatment on the microstructure and mechanical properties of sputtering coatings”.
- [4] Andresa Bapista, Francisco Sliva, Jacobo Portero, Jose Miguez, Guastav Pinto, “Sputtering Physical Vapour Deposition (PVD) Coating: A Critical Review on Process Improvement and Market Trend Demands”, 2018.
- [5] Sivarajan S, Padmanabhan R, “Tribological Evaluation of Wear Resistant PVD Coatings”, Journal of Manufacturing Engineering, Vol 12, Issue 2, June 2017.
- [6] Piotr Lacki, Wojciech Wieckowski, Grzegorz Luty, Pawel Wieczorek, Maciej Motyka, “Evaluation of Usefulness and AlCrN Coating for Increased Life of Tools Used in Friction Stir Welding (FSW) of Sheet Aluminium Alloy, 2020
- [7] M Polok-Rubiniec, L A Dobrzanski, M Adamiak, “Comparison of the PVD coating”, International Scientific Journal, Vol 38, Issue 2, 2009.
- [8] El-Tayeb, N. S. M., Yap, T. C., & Brevern, P. V. “Wear characteristics of titanium alloy Ti54 for cryogenic sliding applications”. Tribology International, 2010.
- [9] Kuphasuk, C., Oshida, Y., Andres, C. J., Hovijitra, S. T., Barco, M. T., & Brown, D. T. “Electrochemical corrosion of titanium and titanium-based alloys”. The Journal of Prosthetic Dentistry, 2010.
- [10] Sharif, S., & Rahim, E. A. “Performance of coated- and uncoated-carbide tools when drilling titanium alloy—Ti-6Al4V”. Journal of Materials Processing Technology 2007
- [11] Tomashov, N. D., Altovsky, R. M., & Chernova, G. P. “Passivity and Corrosion Resistance of Titanium and Its Alloys”. Journal of The Electrochemical Society 1961
- [12] Bloyce, A., Qi, P.-Y., Dong, H., & Bell, T. “Surface modification of titanium alloys for combined improvements in corrosion and wear resistance”. Surface and Coatings Technology, 1998.
- [13] Andresa Bapista, Francisco Silva, Jacobo Portero, Jose Miguez and Gustavo Pinto, “Sputtering Physical Vapour Deposition (PVD) Coatings: A Critical Review on Process improvements and Market Trend Demands”, 2018.

Friction Stir Additive manufacturing in Align with Industry 4.0 - A Review

^[1] S.Deivanai, ^[2] Dr. Manoj Soni

^[1] Department of Mechanical & Automation Engineering, Indira Gandhi Delhi Technological University for Women, Kashmere Gate, New Delhi, India.

^[2] Department of Mechanical & Automation Engineering, Indira Gandhi Delhi Technological University for Women, Kashmere Gate, New Delhi, India.

Abstract— Additive Manufacturing, also referred to as 3D Printing, is a technology that produces three-dimensional parts layer by layer from a material, be it polymer or metal based. The method relies on a digital data file being transmitted to a machine that then builds the component. Typical applications of metal AM are production of models and prototypes during a product's development phase, parts for pilot series production in medical, automotive and aerospace industry, short series production where tooling costs for casting or injection molding would be too high and Parts of high geometrical complexity which cannot be produced by means of conventional manufacturing (molding, grinding, milling, casting, etc.). Magnesium, aluminum, aluminum silicon carbide, copper, copper matrix materials and steels have been successfully made with FSAM. Additive friction stir deposition is solid-state additive manufacturing technique that can be used to process metals and metal matrix composites. It consists of a hollow shoulder through which the feed material (solid rod or powder) is delivered. The shoulder rapidly rotates and generates heat through dynamic contact friction at the shoulder-material interface and at the material substrate interface. The heat generation, dissipation, and transfer mechanisms in the deposited material are similar to the stirred material in friction stir welding. In both cases, heat is generated by dynamic contact friction between material and tool, dissipated by severe plastic deformation of the material, and transferred inside the material by thermal conduction and thermal convection via material flow. Heated and softened, the filler material is fed through the tool and bonds with the substrate through plastic deformation at the interface. The transverse motion of the shoulder results in deposition of a single track of material. 3D parts are made selectively adding subsequent layers upon layers. In this study various parameters defining the quality and strength are explored. The present work aims to highlight the working principle and the past research work carried out by the various authors that utilize FSAM as a fabrication process. Based on the available experimental data, the summary of additive based friction stir processes, type of machine for fabrication, materials, process parameters taken for the study is also discussed in detail. Mechanical properties such as grain refinement, microhardness variation, and tensile strength are also summarized, in comparison with their base materials. In addition, the current scenario and future scope of the FSAM process are also discussed in detail in terms of its utilization in various sectors of engineering along with estimated future trends.

Index Terms— Friction stir additive manufacturing; Metal additive manufacturing; Friction stir processing; Microstructure

Grain refinement; Tensile strength

I. INTRODUCTION

High strength aluminum alloy components are widely used in aircraft, sporting equipment, and other safety-critical application. With corrosion, wear, or impact damages, these components need to either be replaced—which is expensive, time consuming, and inefficient—or repaired. For repair, fusion welding has proved highly successful for a broad range of metals. However, using fusion welding to repair aluminum alloy (AA) 7075 components is extremely challenging owing to the material's poor weldability, which is characterized by hot cracking and void formation during solidification and susceptibility to stress corrosion cracking after welding. The high failure probability and unpredictable failure time from fusion welding have incited numerous studies on solid-state repair for AA 7075 [1-2].

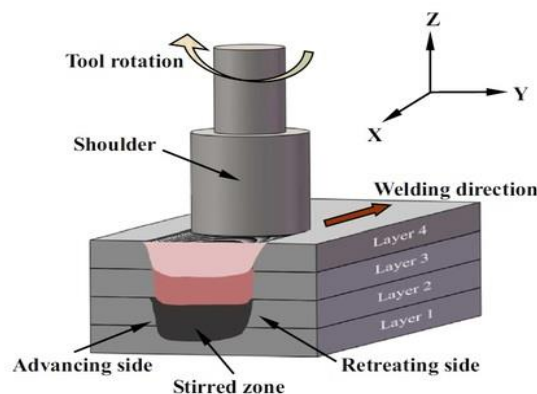


Figure 1 Schematic diagram of FSAM

Friction stir welding and friction stir processing can heal surface cracks along the tool path, courtesy of the plastic material flow around the cracks driven by the shoulder rotation and traverse motion [3]. One drawback of these techniques is that they only reallocate the existing material. Without material addition, these friction stir-related processes are unable to heal wide cracks or repair volume defects [4-5]. Another drawback is the keyhole formed as the rotating tool retracts from the welded plate, which leaves an additional volume defect to be repaired. These drawbacks can be addressed by equipping the friction stir-related processes

with filler materials. For example, in friction taper plug welding, a tapered plug is co-axially forced into a keyhole with a similar taper. This method has proved successful at sealing through-holes left by the friction stir welding of 10 mm-thick AA 2219-T87 plates [6]. Here, the taper angles of the hole and plug should be compatible, otherwise defects are likely to form at the lower part of the weld. As a result, this technique performs better for tapered holes than standard cylindrical through-holes [7-8]. Derived from friction taper plug welding, filling friction stir welding enables better repairs of volume defects, by adding a shoulder portion on the tapered plug to avoid stress concentration at the plug-hole interface. This technique has proven effective at sealing the exit holes in similar Al alloy repair (e.g., with an Al-Cu-Mg plug and an Al-Cu-Mg plate) [9], as well as in dissimilar Al alloy repair (e.g., with an AA 7075 plug and an AA 2219 plate) [10]. Other applications of a similar approach include vertical compensation friction stir welding, friction bit joining, and stationary shoulder friction stir welding [11-12]. Recently, refill friction stir spot welding has been demonstrated to

be effective at filling keyholes in AA 6061-T6 [13] as well as AA 7075-T651 with the welded samples showing ultimate tensile strength as high as 74% of the base material. While the 'friction stir-filler' solutions have been effective at filling volume defects like keyholes, they are stationary and require an additional step to place the filler plug of desired geometry in to the hole before repair. Moreover, without the capacity to continuously add material, these processes are limited to certain defect geometries defined by the size and shape of the hole.

In order to repair various types of volume damages in AA 7075—including keyholes, long grooves, large-scale corrosion or wear damages—it is vital to develop a versatile solid-state technique that can continuously supply filler material, while also allowing for digital control of the material addition and repair paths. Such a technique remained elusive until the recent emergence of a solid-state metal additive manufacturing technique—additive friction stir deposition. Additive friction stir deposition integrates the friction stir principle with a robust material feeding mechanism to enable site-specific deposition. It leverages the benefits of friction stir—e.g., in the prevention of hot cracking, high residual stresses, and void formation—while providing the additional capability of adding material for a more robust repair of volume damages. The current tool size in additive friction stir deposition enables a high build rate, ~103 cm³/h for Al alloys, which is uniquely suitable for the large-scale repair of AA 7075.



Figure 2 (a) A product being manufactured in a lab(EWI)

Despite the great potential for repair of AA 7075, the research in additive friction stir deposition is still at an initial stage and there is a lack of feasibility studies on this topic. The aim of the present work is to bridge this gap. As a first attempt to use additive friction stir deposition for repairing volume damages in AA 7075, this work investigates the filling of both cylindrical through-holes and long, wide square grooves. Such repair geometries are critically important for a wide variety of aerospace and defense applications [14]. For each of these defects, an elaborate repair strategy, examine the repair quality, discuss the benefits and limitations of additive friction stir deposition-enabled repair, and provide comparisons to other repair approaches.

The article[15], the objectives are (I) to describe FSAM as an additive technique and (II) to demonstrate higher strength in builds fabricated by FSAM. Since the drive for incorporating lightweight alloys in structural applications is increasing with time, Mg-4Y-3Nd (WE43, precipitation strengthened) and AA5083 (solid-solution strengthened) alloys are illustrated as two specific examples. The results of the Mg alloy build are restated from a previous published work by the authors. The tool features and dimensions used for fabricating are given in Figure 2(b) and (c). A 5.6-mm build of WE43 (sheet thickness: 1.7 mm) was fabricated using a right-handed stepped spiral tool. On the other hand, for AA5083 (sheet thickness: 3.17 mm), a triple flat left-handed stepped spiral tool was used for fabricating an 11.2-mm build. In both cases, a concave-shaped featureless shoulder was used with a 1.5° tilt to contain the material

Mg-4Y-3Nd—MECHANICAL PROPERTY

Figure 3a shows the macrograph of an Mg-4Y-3Nd alloy. A sound build with 100% consolidation can be noted. To fabricate the four-layered lap welded stack, a tool rotational speed of 800 revolutions per minute (rpm) and a traverse speed of 102 mm/min were used. Hardness testing along the center-line of the build direction showed

scatter on the either sides with respect to the base line. However, irrespective of the location, the hardness of build was higher than the base material (T5 temper, 97 HV) after post process aging. Another significant observation was that the hardness was highest (135 HV) at the interfacial locations. These proper-ties have been previously correlated to the favorable precipitate descriptors and grain size obtained by FSAM using microscopic studies.

experiments, 6.35 mm thick commercial AA 7075-T651 plates were used as the substrate, with the cylindrical holes and long wide grooves machined. The feed material for additive friction stir deposition was also cut from the commercial Al 7075-T651 plates, with a cross-section of 9.535 _9.535 mm². After the repair experiments, cross-sections of the filled holes and grooves were cut and polished using standard metallographic techniques. For electron

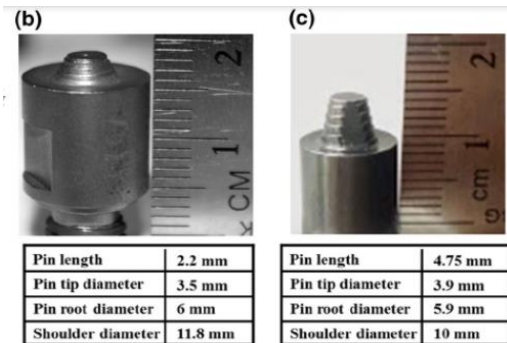


Figure 2(b) and (c) tool dimensions [2]

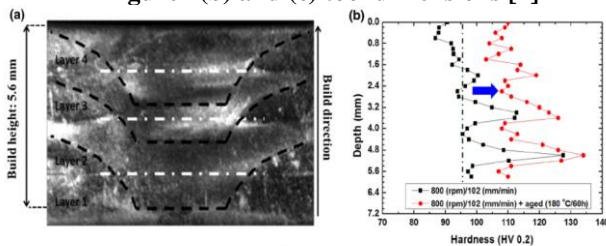


Fig. 3 (a) Macrograph of an Mg-4Y-3Nd alloy fabricated using FSAM at 800 rpm and 102 mm/min. The horizontal dashed lines represent the original interface positions between the individual layers. (b) Hardness profile along the build direction in the as-built and post-aged conditions. The vertical dashed line represents the hardness in the base material that was rolled and aged (T5 temper—97 HV). Note that the hardness profile shifts to the right compared with the base material after post-aging. [2]

II. MATERIALS AND METHODS

All additive friction stir depositions were performed using a rotation rate of 400 RPM. Three types of experiments were performed. Experiment 1 involved double hole filling, in which two cylindrical through-holes with the diameters of 6.35 mm (i.e., 1/4”) and 3.125 mm (i.e., 1/8”) were drilled in series into an AA 7075 plate. In this work, double hole filling using additive friction stir deposition was implemented by (i) traveling of the tool (i.e., the print head); (ii) dwelling (i.e., zero traverse speed); and (iii) traveling again. Experiment 2 involved single hole filling, in which one cylindrical through-hole with the diameter of 6.35 mm (i.e., 1/4”) was drilled into the plate. In this work, single hole filling using additive friction stir deposition was implemented by (i) traveling; (ii) dwelling; and (iii) the lift of the tool. In Experiment 1 and Experiment 2, the traverse speed during tool traveling was 0.32 mm/s and the linear feed rate was 0.1 mm/s. Experiment 3 involved the filling of long, wide grooves, which were 12.7 mm (i.e., 1/2”) wide, 3.175 mm (i.e., 1/8”) deep, and 304.8 mm (i.e., 12”) long. In this work, such groove filling was implemented by the slow traveling of the tool without dwelling, wherein the traverse speed was 0.42 mm/s and the linear feed rate was 0.06 mm/s. Figure 1 shows an image of the additive friction stir deposition. In all

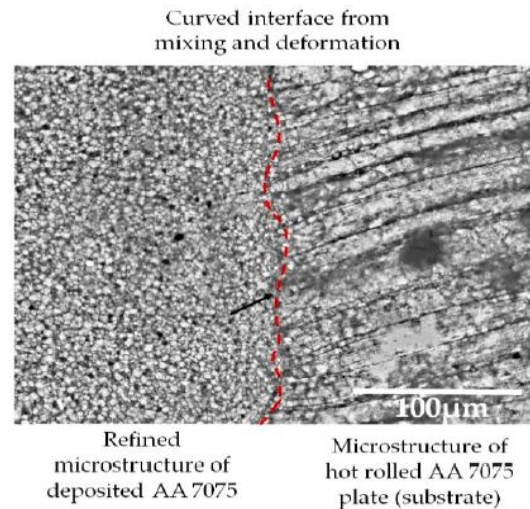


Figure.4 zoomed in image of interface [4]

microscopy, the samples were first etched with a caustic mixture, consisting of 1 g of NaOH and 100 mL of water, in order to reveal the grain boundaries. For optical microscopy, samples were electro-etched using 50 mL of Barker’s reagent etching solution—comprised of 1.9 mL of 48 wt.% HBF₄ solution and 48.7 mL of H₂O—with an etching voltage of 30 V for 1 min. Polarized optical microscopy and scanning electron microscopy were used to characterize the microstructures after repair. For optical microscopy, multiple images were taken and stitched together using ImageJ, an open-source image processing software, to allow for a holistic view of the entire cross-section. Micro hardness testing was performed using micro hardness tester at 300 N load and with 10 s dwell time.

Hardness for the single hole filled sample was measured using 20 points along the width of the repair cross-section with a spacing of 0.5 mm and 14 points along the height of the repair with a spacing of 0.4 mm. The groove sample was tested at 20 points along the width of the repair with a spacing of 1.0 mm and 9 points along the height of the repair with a spacing of 0.6 mm.



Figure 5(a) Bracket for an Airbus A380, with conventional bracket behind (Courtesy EADS)



Figure 5(b) AM fuel nozzle in LEAP passenger jet engine (Courtesy GE Aviation)

Some potential applications of FSAM in the aviation sector pertains to the integrated fabrication of stiffeners/stringers. Figure 6(a) illustrates a few high performance stiffener/stringer configurations for different aircraft components. The first among these is a general schematic showing the assembly of sheets to create transverse stiffeners on an I-beam. Essentially, such a structure can be fabricated by a combination of FSW for tee joint and FSAM for stiffener. In Figure 6(b), integrated stringer assemblies on a skin panel fabricated by FSAM for aircraft fuselage are shown. FSAM can also be extended for designing and manufacturing longerons in skin panels that are long in circumferential direction. Furthermore, Figure 6(c) shows the use of FSAM in wing spars

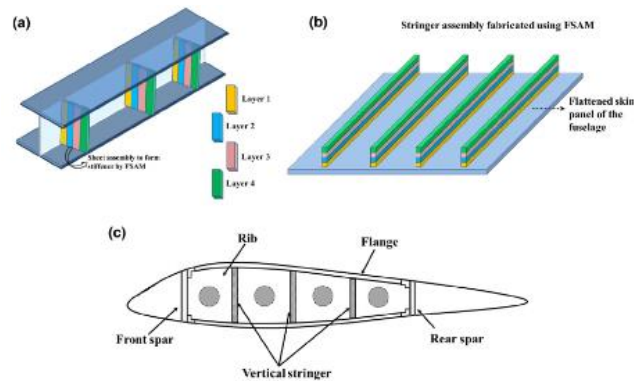


Figure 6(a) stiffeners on an I-beam (b) stringer assemblies on a skin panel (c) wing spars

III. CONCLUSIONS

Additive friction stir deposition always enables sufficient mixing between the deposited material and the side wall of the hole or groove in the upper portions of the repair. This is indicated by a gradual transition from the elongated grains of the AA 7075 plate to the fine, equi axed grains of the deposited AA 7075, showing no distinct interface. The thermo mechanical history in additive friction stir deposition generally leads to a slight decrease (<15%) in the hardness of the repaired volume as compared to the original feed material, although the peak hardness in the repaired volume can be comparable to the feed material. Overall, this work presents an initial investigation on the solid-state additive repair of AA 7075 using additive friction stir deposition, which shows promising results despite imperfect repair quality. With systematic optimization work on process control and repair strategies developing in the future, high-quality and highly flexible repairs are expected to be achieved using additive friction stir deposition. The ability to fabricate structures with variable properties using FSAM might open avenues for niche applications. Such an approach is promising from the perspective of high-performance structures mainly due to its principle that is sheet building rather than plate machining. These preliminary results are encouraging. Further research efforts focused on the technology with modifications to the current machine design could possibly be the answer to the one most important challenge in the tetrahedron structural performance. The FSAM can be an effective technique for production of high-performance components. It certainly seems promising for simpler and complex geometries.

REFERENCES

- [1] S.PalanivelP.NelaturuB.GlassR.S.Mishra/Friction stir additive manufacturing for high structural performance through microstructural control in an Mg based WE43 alloy/Materials & Design (1980-2015)Volume 65, January 2015, Pages 934-952
- [2] Sivanesh Palanivel, Harpreet Sidhar, Rajiv S. Mishra/Friction Stir Additive Manufacturing: Route to High Structural Performance, March 2015,JOM: the journal of the Minerals, Metals & Materials Society 67(3)DOI:10.1007/s11837-014-1271-x
- [3] AshishKumar SrivastavaaNileshKumaraAmitRai Dixitb/Friction stir additive manufacturing – An innovative tool to enhance mechanical and microstructural properties/Materials Science and Engineering: BVolume 263, January 2021, 114832
- [4] Kumar, P.V.; Reddy, G.M.; Rao, K.S. Microstructure, mechanical and corrosion behavior of high strength AA7075 aluminium alloy friction stir welds—Effect of post weld heat treatment. Def. Technol. 2015, 11,362–369.
- [5] Huang, Y.X.; Han, B.; Tian, Y.; Liu, H.J.; Lv, S.X.; Feng, J.C.; Leng, J.S.; Li, Y. New technique of filling friction stir welding. Sci. Technol. Weld. Join. 2011, 16, 497–501
- [6] Han, B.; Huang, Y.; Lv, S.;Wan, L.; Feng, J.; Fu, G. AA7075 bit for repairing AA2219 keyhole by filling friction stir welding. Mater. Des. 2013, 51, 25–33.
- [7] Yin, Y.; Yang, X.; Cui, L.; Cao, J.; Xu, W. Investigation on welding parameters and bonding characteristics of Under water wet friction taper plug welding for pipeline steel. Int. J. Adv. Manuf. Technol. 2015, 81, 851–861.
- [8] Yu, H.Z.; Jones, M.E.; Brady, G.W.; Gri_ths, R.J.; Garcia, D.; Rauch, H.A.; Cox, C.D.; Hardwick, N.Non-beam-based metal additive manufacturing enabled by additive friction stir deposition. Scr. Mater. 2018,153, 122–130
- [9] Gri_ths, R.J.; Perry, M.E.J.; Sietins, J.M.; Zhu, Y.; Hardwick, N.; Cox, C.D.; Rauch, H.A.; Yu, H.Z. A Perspective on Solid-State Additive Manufacturing of Aluminum Matrix Composites Using MELD. J. Mater. Eng. Perform 2019, 28, 648–656.
- [10] Rivera, O.G.; Allison, P.G.; Jordon, J.B.; Rodriguez, O.L.; Brewer, L.N.; McClelland, Z.; Whittington,W.R.; Francis, D.; Su, J.; Martens, R.L.; et al. Microstructures and mechanical behavior of Inconel 625 fabricated by solid-state additive manufacturing. Mater. Sci. Eng. A 2017, 694, 1–9.
- [11] Hashimoto, S. Hot Working of Aluminum Alloy 7075; Massachusetts Institute of Technology: Cambridge, MA,USA, 1986; p. 91.
- [12] Sakai, T.; Belyakov, A.; Kaibyshev, R.; Miura, H.; Jonas, J.J. Dynamic and post-dynamic recrystallization under hot, cold and severe plastic deformation conditions. Prog. Mater. Sci. 2014, 60, 130–207.
- [13] Huang, K.; Logé, R.E. A review of dynamic recrystallization phenomena in metallic materials. Mater. Des.2016, 111, 548–574.
- [14] Phillips, B.J.; Avery, D.Z.; Liu, T.; Rodriguez, O.L.; Mason, C.J.T.; Jordon, J.B.; Brewer, L.N.; Allison, P.G.Microstructure-deformation relationship of additive friction stir-deposition Al–Mg–Si. Materialia 2019, 7,100387
- [15] Rivera, O.G.; Allison, P.G.; Brewer, L.N.; Rodriguez, O.L.; Jordon, J.B.; Liu, T.; Whittington,W.R.; Martens, R.L.;
- [16] McClelland, Z.; Mason, C.J.T.; et al. Influence of texture and grain refinement on the mechanical behavior of AA2219 fabricated by high shear solid state material deposition. Mater. Sci. Eng. A 2018, 724, 547–558.
- [17] Ivano_, T.A.; Carter, J.T.; Hector, L.G.; Tale_, E.M. Retrogression and Reaging Applied to Warm Forming of High-Strength Aluminum Alloy AA7075-T6 Sheet. Metall. Mater. Trans. A 2019, 50, 1545–1561.
- [18] Wang, P.; Li, H.C.; Prashanth, K.G.; Eckert, J.; Scudino, S. Selective laser melting of Al-Zn-Mg-Cu: Heattreatment, microstructure and mechanical properties. J. Alloy Compd. 2017, 707, 287–290.
- [19] Taheri, H.; Kilpatrick, M.; Norvalls, M.; Harper,W.J.; Koester, L.W.; Bigelow, T.; Bond, L.J. Investigation of Nondestructive Testing Methods for Friction Stir Welding. Metals 2019, 9, 624.
- [20] Mishra, R.S.; Ma, Z.Y. Friction stir welding and processing. Mater. Sci. Eng. R Rep. 2005, 50, 1–78.
- [21] Sinhmar, S.; Dwivedi, D.K. A study on corrosion behavior of friction stir welded and tungsten inert gas welded AA2014 aluminium alloy. Corros. Sci. 2018, 133, 25–35.
- [22] Kuryntsev, S.V. Structure and Properties of Welded Joints of the Aluminum Alloy 1550 Produced by Double-Side Friction Welding with Mixing. Met. Sci. Heat Treat. 2014, 56, 310–314.
- [23] Qin, H.-l.; Zhang, H.; Sun, D.-T.; Zhuang, Q.-Y. Corrosion behavior of the friction-stir-welded joints of 2A14-T6 aluminum alloy. Int. J. Miner. Metall. Mater. 2015, 22, 627–638

Review on X2 & S1 Handover in LTE Networks

[1] Divya T M

[1] Assistant professor, Department of ECE, Raja Reddy Institute of Technology, Bangalore

Abstract— Handover is the greatest advantage of wireless device over wired. Handover allows transfer of an ongoing call, data or services conveniently, when UE switches from one base station to another base station. Handover allows transfer of data or calls without losing any data and being interrupted. UE has an antenna which can search for multiple frequency channels. When UE is travelling from serving cell to another cell, it receives weak signals from current serving cell whereas receives stronger strength from neighboring cell to which it is moving. A decision has to be made for handover from eNodeB. A handover report configuration will be initiated from eNodeB. Then UE initiates Measurement report to eNodeB. Later Handover decision will be made and then handover preparation followed by handover completion phase. This paper describes the purpose of Handover, types of Handover and different phases of X2 handover.

Index Terms— eNodeB, Handover, LTE

I. INTRODUCTION

Handover is a procedure initiated when a UE moves from one network coverage area to another. One eNodeB can usually serve three geographical cells. Each cell has a frequency band and associated signal strength. Handover is categorized as category I and category II. Category I- A handover can be whether EPC entities are changed or not after Handover. Category II handover is categorized under whether EPC entities are involved or not. Category I has Intra LTE Handover (MME and S-GW remains same after handover), Inter LTE handover has Inter MME (MME is different but S-GW is same after handover), Inter S-GW (S-GW is different but MME remains same after handover) and Inter MME/S-GW handover (MME and S-GW are changed after handover) lastly Inter RAT (handover is between different radio access technology networks. For example, UTRAN to E-UTRAN, E-UTRAN to UTRAN etc.).

Category II has X2 handover and S1 handover. The interface between eNodeB is X2. When UE is travelling, a source eNodeB has to decide whether X2 handover or S1 handover is to be initiated. If there is X2 connection between source eNodeB and target eNodeB (eNodeB to where UE is travelling), X2 handover will be initiated. These two eNodeBs are connected over X2 interface. They can communicate to handle handover without the help of MME. S1 is the interface between eNodeB and EPC (MME-control messages and S-GW-user/data packets). This will be initiated when two eNodeBs (source and target) are connected over S1 interface. After this handover, source eNodeB communicates with target eNodeB with the help of MME.

In the figure, we have three eNodeB. eNB1, eNB2 and eNB3. We have eight geographical cells (cell1 – cell 8). Cell 1,2 &3

are covered by eNB1, cell 4,5 & 6 are covered by eNB2 and cells 7,8 &9 are covered by eNB3. eNB1 and 2 are connected over X2 interface whereas eNB2 and eNB3 are not connected over X2 interface. UE in cell1 moves to cell 5. Since there is X2 interface over these two eNBs. X2 handover is initiated between these two when UE moves from cell 1 to cell 5. Later UE moves to cell 9. There is no X2 interface over these two eNBs hence S1 handover has to be initiated upon decision taken by eNodeB.

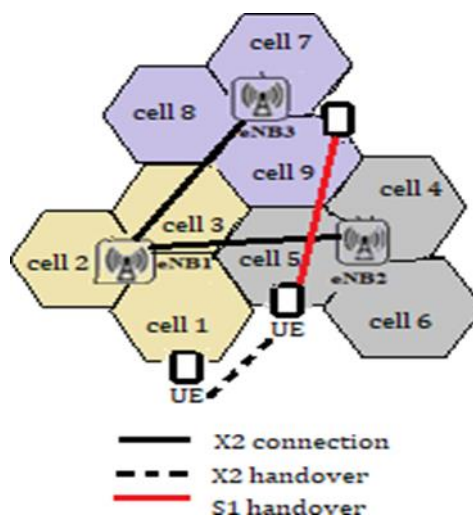


Fig 1: X2 & S1 connection over eNodeB

II. MEASUREMENT CONFIGURATION & HANDOVER DECISION

UE establishes a RRC connection with eNodeB. eNodeB provides measurement configuration message called RRC connection reconfiguration which provides details of triggering event, report interval, neighbor cell list, information about E-UTRAN cells including frequency channel number, physical cell ID of the cell. The strength of the signal can be measured as reference signal received power. Neighbor cells use different carrier frequencies. UE should synchronize to this new cell carrier frequency and then measure the strength of the signal using measurement gaps. All this information will be provided in reconfiguration message. UE reports eNodeB periodically with measurement report message.

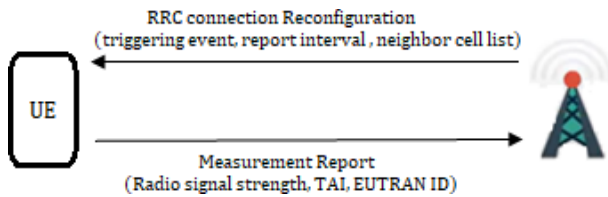
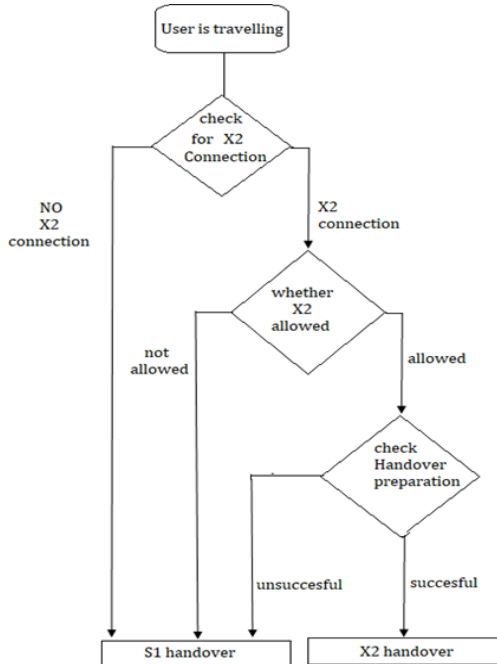


Fig 2: Measurement Report

Handover decision is made by eNodeB depending on the type of event reported. eNodeB decides whether X2 handover should be initiated or S1 handover.

Flow chart of handover decision



source eNodeB. Then it establishes a direct tunnel between two eNodeBs. Figure 3 shows X2 handover preparation phase.

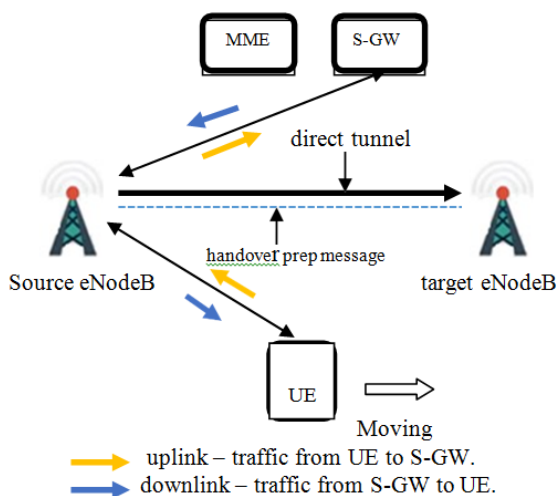


Fig 3: X2 Handover preparation phase

In case of S1 handover, when UE is moving from source eNodeB towards target eNodeB but source eNodeB and target eNodeB are not connected over X2 interface. So source eNodeB sends handover request to MME (also sends information about the target eNodeB to which UE is moving). Then an indirect tunneling is established which connects source eNodeB, S-GW and target eNodeB. Figure 4 shows S1 handover.

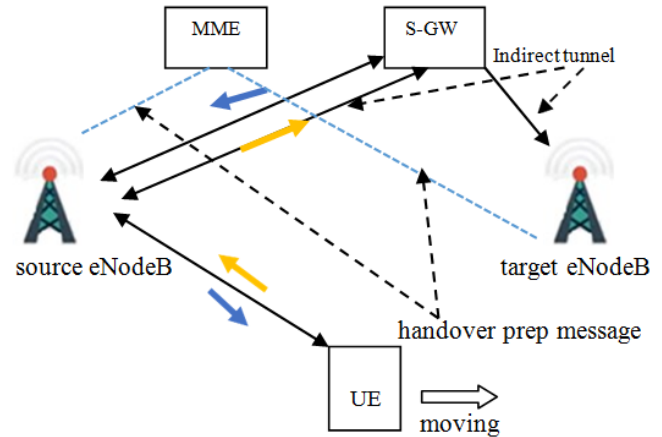


Fig 4: S1 handover preparation phase

Uplink/Downlink bearer traffic path (solid line–two way), control message path (dotted line) and Downlink packet path (solid line)

III. PROCEDURE FOR HANDOVER

UE receives measurement configuration report from eNodeB. then UE reports measurement results to eNodeB. eNodeB will make decision about handover. The handover procedure consists of three phases: Handover preparation, Handover execution and completion.

Handover Preparation phase

eNodeB decides X2 handover as source and target eNodeB are directly connected over X2 interface. They can directly communicate with each other without the help of MME. The source eNodeB sends the UEs security and QOS context to the target eNodeB. It checks whether target eNodeB can provide service to this UE. If target eNodeB can satisfy the service to UE, the target eNodeB establishes a downlink packet forwarding transport bearer in order to forward packets. Then the target eNodeB allocates C-RNTI value that is required by UE to access eNodeB and forwards the same to Handover execution phase

In this phase, UE disconnects from source eNodeB and connects with target eNodeB. Once the bearer and C-RNTI and the required resources are allocated to UE at the target side in the preparation phase, the two eNodeB s are ready for handover. The source eNodeB sends handover command message to UE. In this phase UE uses C-RNTI to access target eNodeB. Downlink packets are forwarded to target eNodeB through the bearer and they are buffered until UE can completely access target eNodeB. Once this is successful, Uplink packets can also be forwarded.

Figure shows X2 handover and S1 handover uplink/downlink delivery path

A new bearer path is established in this completion phase. An indirect tunnel is released. A new bearer path is established. Figure 8 shows S1 handover completion phase.

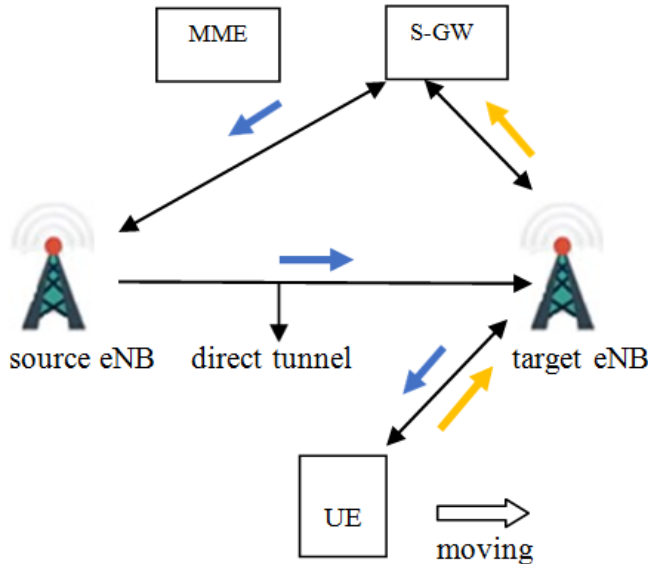


Fig 5: X2 Handover Execution Phase

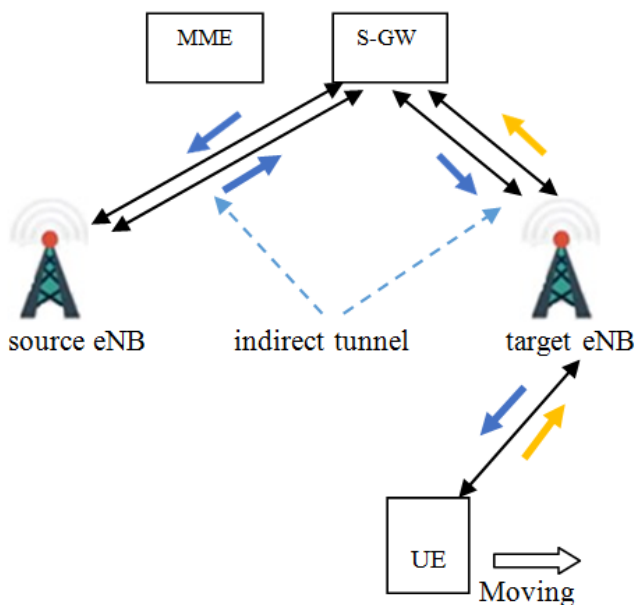


Fig 6 : S1 Handover Execution Phase

Handover completion phase

In this phase, UE bearer path is connected to target eNodeB successfully. The forwarding bearer established in handover execution phase is released. A direct tunnel is released.

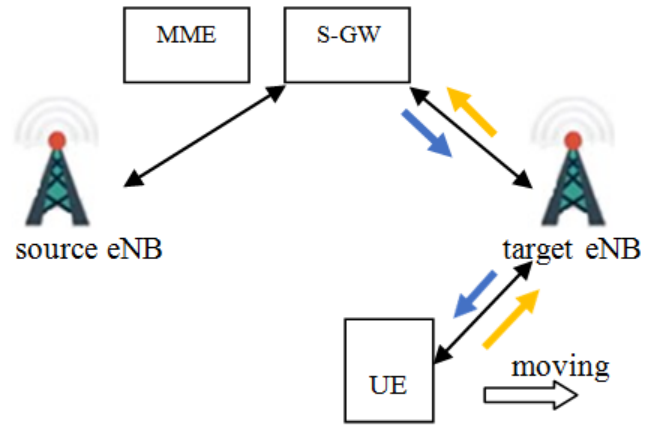


Fig 8: S1 Handover Completion Phase

Abbreviations

- C-RNTI – Cell Radio Network Temporary Identifier
- eNB – eNodeB
- EUTRAN – Evolved Universal Mobile Telecommunications System Terrestrial Radio Access Network
- EPC – Evolved Packet Core
- LTE – Long term Evolution
- MME – Mobility Management Entity
- QoS – Quality of Service
- S-GW – Serving gateway
- UE – User Equipment

REFERENCES

- [1] Khin May Yee, Be Nue “Study of LTE X2 Handover algorithm”, IJCIRAS 2020.
- [2] Yun Li, Bin cao, chonggong wang. “Handover schemes in heterogeneous LTE networks: challenges and opportunities”, IEEE wireless communications, April 2016
- [3] Ulvan A, Bestak R, “The study of handover procedure in LTE based femtocell network” IEEE book ISBN: 978-1-4244 – 8431 -7.
- [4] Magri Hicham, Noredine Abghour, Mohammed Ouzzif, RITM research lab , Casablanca , Morocco “ 4G system : Network Architecture and performance” IJIRAE , 2015.

Hybrid Optimization Control Algorithm for Grid Connected PV system

^[1] Gayathri Devi K.S, ^[2]P. Sujatha Therese, ^[3]Dr. M. Eugene Prince

^[1] Scholar, EEE Department, NI Center for Higher education, Nagercoil, India

^[2] EEE Department, NI Center for Higher Education, Nagercoil, India

^[3] Professor, Department of Physics, St.Hindu college, Nagercoil, India

Abstract— In the field of power sector Renewable Energy Sources (RES) plays an important role. They are abundant in nature and clean sources of energy. At the present condition it is very important to reduce the carbon emission and pollution to the environment. Hence the integration of RES with the utility grid is increased. The main problems of the RES are; they are dynamic in nature and their efficiency is also very less. Researches are going on to increase the efficiency of the system and also manage the dynamics in the system. There are so many optimization techniques in the literature to reduce the dynamics in the system. In this work the performance of Dragonfly Algorithm (DA), Grey wolf Algorithm (GWO), Firefly Algorithm (FF) and Sea lion combined with Firefly (SL-FF) Algorithm were analysed by applying those to a grid connected PV system. The model is simulated using MAT Lab Simulink software.

Index Terms— Grey wolf, levy update, seven level inverter

I. INTRODUCTION

The fossil fuel power plants causing pollution to the environment. Hence nowadays the use of renewable energy is increasing. The solar energy is abundant in nature and available at almost all places. Extraction of energy from wind and other RES are only possible at certain places and in limited quantity. So solar energy is widely integrated to utility. The renewable energy is not stable. The PV system generates a variable output due to the variation in the irradiation. There are different control techniques to make them stable. Maximum power point tracking (MPPT) method is used to extract maximum power from the PV system. The power obtained from the PV system is DC and has very low value. Inverters are required to convert this DC to AC. Two level inverters have a lot of harmonics and the waveform is also not sinusoidal. As the number of levels increases the harmonics are reduced and the waveform approach near sinusoidal waveform. Inverters with more than two levels are called multilevel inverters. Boost converter system increases the outcome of PV to higher value which when converted to AC by means of inverter matches with the grid voltage. Maximum Power Point Tracking (MPPT) mechanism is used to extract maximum power. PI controllers are one of the simplest method for closed loop control of MPPT, Boost converter and inverter integrated to RES [1][18][19]. But their results are less accurate if there is dynamics in the RES. While using Perturbation and Observation Algorithms [2][3] a reduction in power extracted is occur due to the oscillation

of the system around the maximum power point at steady state. Genetic Algorithm based approach [4] is expensive and the losses are high. The computational time is high and large number of parameters are required for Particle Swarm Optimization (PSO) [5] [6][7]. Dragonfly Algorithm [8] [20] gives poor voltage regulation at higher loads and the output signal amplitude has distortions. GWO algorithm converges slowly and its ability for local searching is not so good [9][10][11]. To improve the performance of the system with the dynamics of the parameters a new tuning method by combining the Dragonfly and Grey wolf optimization techniques is proposed. Firefly Algorithm [12][13][14][15] has good exploration phase but the processing time is more. Sea lion Algorithm [16][17] has best exploitation phase but its exploration phase is not so good.

Fine tuning of the PI controller gains are achieved by this proposed methodology SL-FF (combined FF and Sea lion). As a result the active and reactive power compensation, the steady state response, three phase current and voltage profile etc. are improved. The inverter is controlled after d q transformation. The simulation is done in MAT Lab using a model having a PV system with MPPT controller, boost converter and a seven level inverter integrated with a utility grid. The results are compared with the results Obtained from the simulation using Dragonfly, Grey wolf and Firefly optimization algorithms

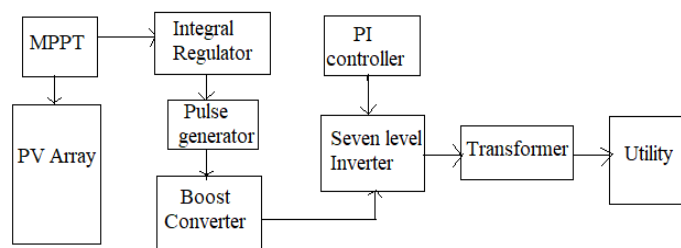


Fig.1 Block Diagram of Grid Connected PV System

II. GRID CONNECTED PV SYSTEM

Fig.1 shows the block diagram of Grid connected PV system. Its capacity is 100KW and consists of a PV array of 66 parallel strings with each string having 5 modules. MPPT controller is using to track maximum power. It also controls the boost converter whose output is connected to a seven level inverter. Each leg of the three phase inverter consists of

three full bridges cascaded together and are controlled by PI controller. The inverter output is connected to the utility grid via transformer in order to satisfy the grid voltage requirement.

A. MPPT Controller

Maximum power point tracking is achieved by incremental conductance method and integral regulator minimizes the error ($dI/dV + I/V$). The Integral controller gives the duty correction for the pulse generator of boost converter also.

B. PI Controller

The PI controller [20] controls the output of seven level inverter. The inverter voltage is converted to $\alpha\beta 0$ reference frame and then it is converted to $dq0$ reference frame and this decoupled voltage is controlled by PI controller. The gains of PI controller k_p and k_i are tuned by SL-FF Algorithm. The signals from the controllers are pulse width modulated to generate switching pulses for the inverters.

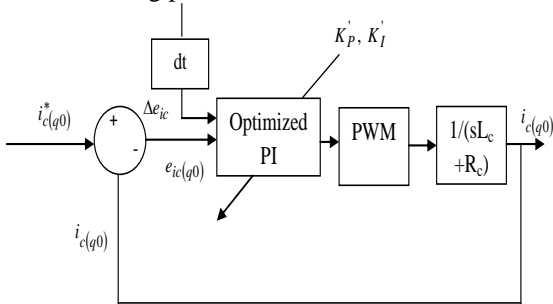


Fig.2 qo Axis Control of Inverter

The optimization algorithm minimizes the error between the reference voltage and the inverter output voltage.

III. OPTIMIZATION CONTROL TECHNIQUE

A. Objective Function

The error between the reference voltage and the inverter voltage is minimized by the optimization algorithm. Fig. 3 shows the input gain solution for the optimization algorithm. The objective function (OF) of the minimization algorithm is given by the equation

$$OF = \text{Min} (r + Q + 1/P) \tag{1}$$

Where r is the error voltage, Q is the reactive power and P is the active power.

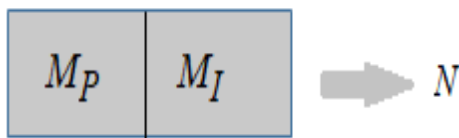


Fig.3 Solution encoding

B. SS-LF Optimization Algorithm and Flow Chart

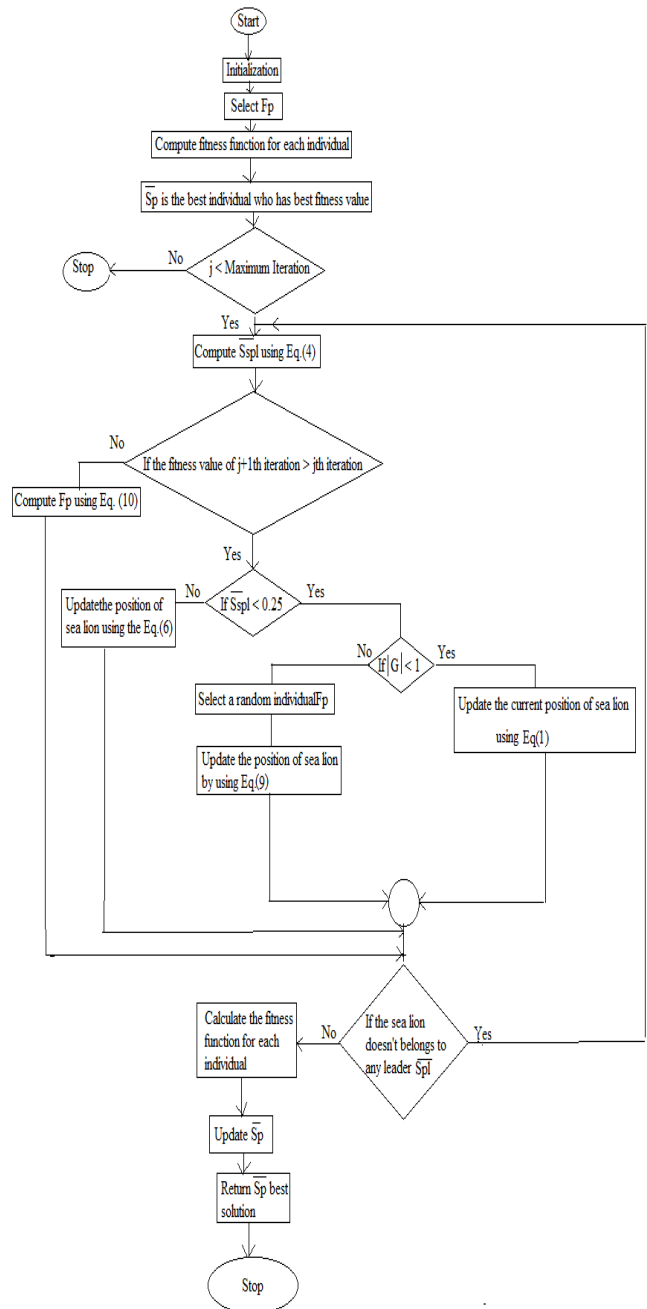


Fig.4 flow chart of SL-FF Algorithm

The Sea lions live together by forming huge colonies []. Sea lions hunt their prey through various phases such as “spotting and tracking phase, vocalization or communication phase, attacking phase (exploitation phase) and searching for prey (exploration phase)”.

1. Spotting and tracking stage: Sea lions detect and find the position of their prey with their whiskers. The sea lion which identify the position of the prey communicate with others and they group together to encircle the prey. Eqn. (2) represents this behaviour.

$$\bar{D}_i = |2\bar{C}\bar{F}_p - \bar{S}_p| \quad (2)$$

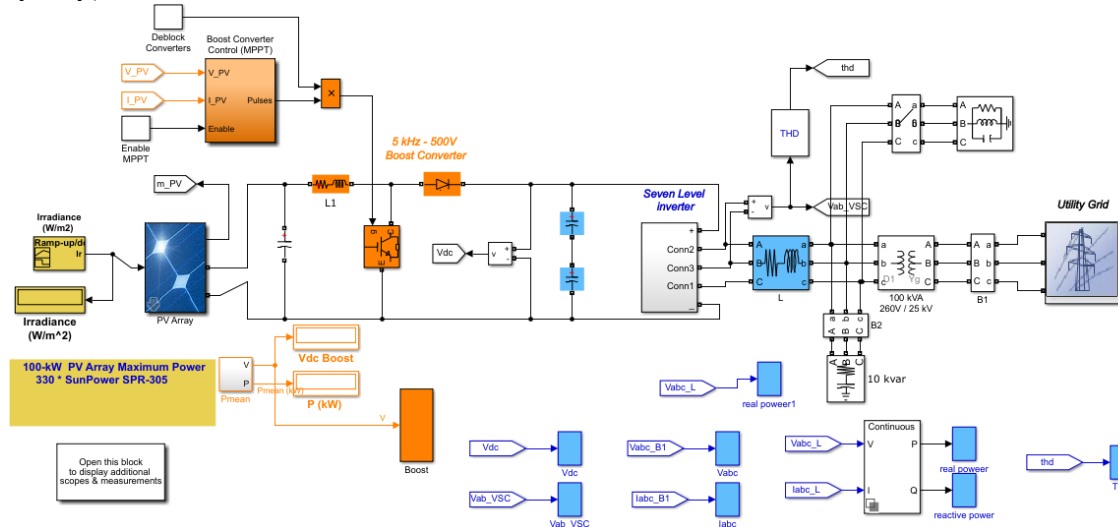


Fig.5 Simulink Diagram of Grid connected PV System

the distance between the prey and the sea lion is represented by \bar{D}_i and the position of prey and position of sea lion is represented by \bar{F}_p and \bar{S}_p respectively. \bar{C} is a random vector and p corresponds to the current iteration.

The sea lion reaches the nearby prey in the next iteration. This is expressed in Eq. (3)

$$S_{p+1} = \bar{F}_p - \bar{D}_i \bar{G} \quad (3)$$

Here S_{p+1} express the upcoming iteration and \bar{G} is a random number.

2. Vocalisation phase: While hunting together as a group sea lions produce various vocals to communicate with each other. This nature of sea lions expressed by Eq, (4), (5) and (6).

$$\bar{S}_{spl} = \left| \frac{\bar{W}_1(1 + \bar{W}_2)}{\bar{W}_2} \right| \quad (4)$$

Here \bar{S}_{spl} indicate the velocity of sound of sea lion leader and \bar{W}_1 and \bar{W}_2 are the velocity of sound in air and water.

$$\bar{W}_1 = \sin\alpha \quad (5)$$

$$\bar{W}_2 = \sin\beta \quad (6)$$

3. Exploiting phase: This phase has two sub phases
 - a. Dwindling encircling technique: The Random number \bar{G} is reduced from 2 to 0 gradually till the iteration ends. This enables the sea lion to reach close to the prey and encircle them.
 - b. Circle Updating Position: The bait ball of fishes are followed and hunted by the sea lion in this phase. The Eq. 7 shows this algebraically.

$$S_{p+1} = |\bar{F}_p - \bar{S}_p| \cdot \cos(2\pi t) + \bar{F}_p \quad (7)$$

Here $|\bar{F}_p - \bar{S}_p|$ gives the distance between prey and the sea lion. The sea lions chase the prey in a circular path. This is represented by the term $\cos(2\pi t)$.

4. Exploitation phase: In this phase the sea lions updates their position by randomly selected sea lions position. SL algorithm gives global optimum solution using Eq. (8) and (9).

$$\bar{D}_i = |2\bar{C}\bar{S}_{rp} - \bar{S}_p| \quad (8)$$

$$\bar{S}_{p+1} = \bar{S}_{rp} - 2\bar{G} \bar{D}_i \quad (9)$$

According to SL-FF if the current fitness value is greater than the preceding fitness value then \bar{F}_p is computed using SL algorithm.

If current fitness is less than the previous fitness value then \bar{F}_p is calculated using Firefly (FF) Algorithm [] as shown in Eq. (10).

$$\bar{F}_p = \phi_p k l \gamma_e \quad (10)$$

kl is length of scale, γ_e is an arbitrary value.

$\phi \in [0, 1]$ is the step factor

The Flow chart of the SL-FF Algorithm is shown in Fig.4

IV. SIMULATION AND RESULT

Simulation model of Grid connected PV system is developed in MAT Lab Simulink and the control of the inverter using SL-FF optimization algorithm is achieved by generating MAT Lab codes. The Simulink diagram consists of the Solar PV array, MPPT controller, pulse generator circuit for DC Boost converter, DC Boost converter, Inverter, Pulse Width Modulated (PWM) circuit for generating switching pulses for inverter, transformer, different types of loads and utility.

The control voltage for the PWM technique is the output of a PI controller whose gains k_p and k_i are tuned by the SL-FF optimization algorithm. A fault voltage is applied at 0.08 sec. and the outputs are observed. The active and reactive power compensation and reduction in error voltage are attained by setting objective function of the optimization algorithm such that minimize the error voltage and reactive power and maximize the active power. The steady state analysis and statistical analysis also conducted to analyse the performance of the system.

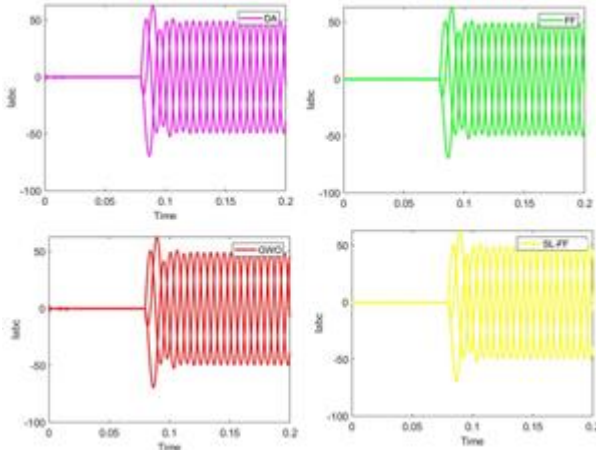


Fig. 6 Current Waveforms of DA, GWO, FF, and SL-FF During and After Fault

A. Analysis of Current

Analysis of current is done using Fig.6. The current waveforms of DA, GWO, FF and SL-FF are analyzed after applying a fault at 0.08sec. The wave form of SL-FF shows a perfect sine wave whereas wave form of DA shows slight disturbance after fault.

B. Analysis of Voltage

Three phase voltage of the system before and after applying fault with the algorithms DA, GWO, FF and SL-FF are given in Fig. 7. The wave form obtained with SL-FF method is perfect sine wave than the others. From Fig. 8 it can be observed that only the waveform with DA shows a large disturbance and SL-FF gives the best result. The others have very low disturbance. The voltage waveforms across phases AB and the waveforms of DC link voltage during and after the fault can be noticed from Fig.9. In all the cases DA performs poorer than others and SL-FF performs the best. The others have very small distortions

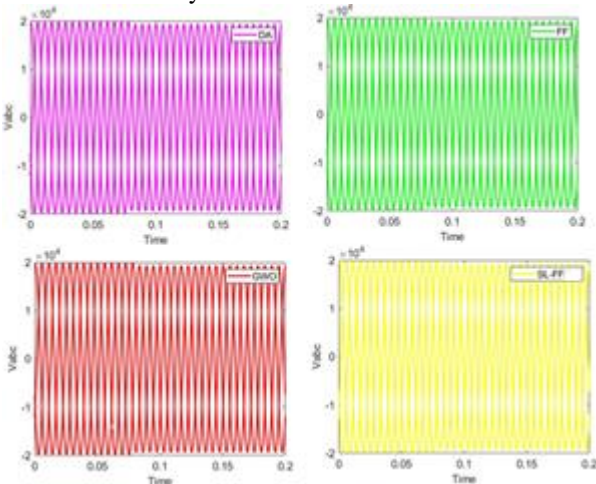


Fig.7 Three Phase Voltage Waveforms of DA, GWO, FF, SL- FF During and After Fault

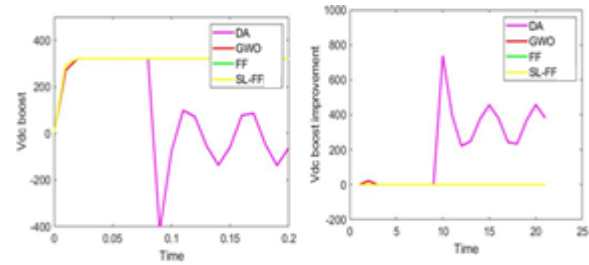


Fig.8 Voltage Waveform of Vdc Boost Converter During and After Fault

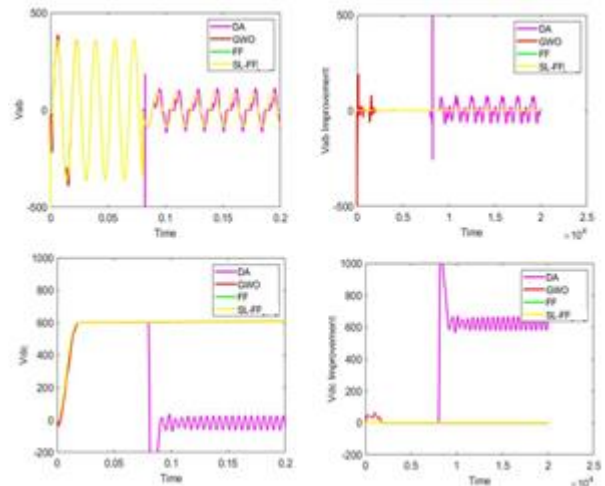


Fig.9 Voltage Waveform between A and B Phases and voltage at the DC Link during and After Fault

C. Active Power and Reactive Power Analysis

Real and reactive power during and after fault are given in Fig.10. Here also the SL-FF method gives best result and the others have low performance. GWO shows more distortion in both real and reactive power. It can be viewed that DA and FF also have small distortions

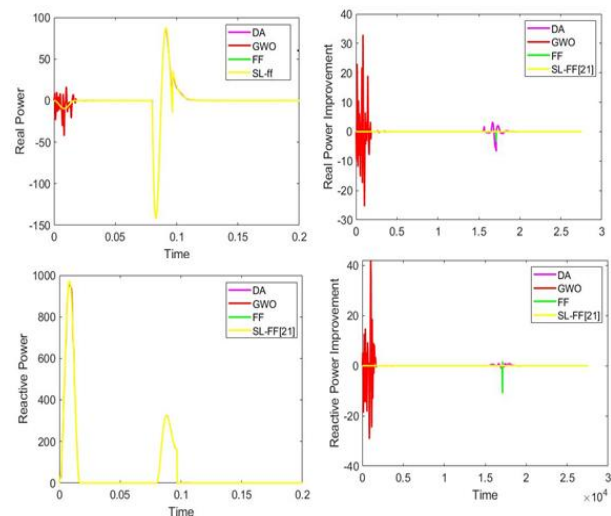


Fig.10. Real and Reactive Power During and After Fault

Steady State Analysis

The steady state analysis in terms of rise time, settling time, settling min, settling max, overshoot, undershoot, peak and peak time are given in Table 1. From the analysis the steady state conditions of the DA are not in a level of satisfaction, the GWO have almost same values of FF and SL-FF except rise time, settling time and overshoot.

Table 1 STEADYSTATE ANALYSIS

	DA	GWO	FF	SL-FF
Rise time	0.0006 842	0.0123 44	0.0087 363	0.008736 2
Settling time	0.1990	0.0187 0	0.0176 26973	0.017626 971
Settling Min	-416.8 3	321.00	294.11 20	294.1121
Settling Max	99.30	321.0	321.0	321.0
Overshoot	581.7	7.1	7.75	7.72
Undershoot	525.04	0	0	0
Peak	416.8	321.0	321.0	321.0
Peak time	0.09	0.02	0.02	0.02

D. Standard Deviation

Standard deviation of all the above discussed methods are given in Table2. Standard deviation of all the methods except DA have almost same values for best, worst, mean, median and standard.

Table II STANDARD DEVIATION

	DA	GWO	FF	SL-FF
Best	1.49e-08	1.49e-08	1.49e-08	1.49e-08
Worst	1.0013	1.30294	1.30290	1.30291
Mean	0.364	0.621	0.051	0.504
Median	0.0822	0.00058	0.0001196	0.0001194
STD	0.4099	0.224	0.217	0.216

V.CONCLUSION

The simulation of Grid interconnected PV system was performed with various optimization algorithms DA, GWO, FF and SL-FF. The three phase voltage and current analysis during fault and after fault shows that almost all the methods perform in a similar way. While considering DC link voltage and DC Boost voltage, the DA exhibits worst performance. In the case of real and reactive power GWO causes more distortion than all other methods. Steady state and statistical analysis were also conducted. From the analysis it is clear that the DA perform poorer than other algorithms. GWO is better than DA and FF and SL-FF has almost same but SL-FF is best of all.

REFERENCES

- [1] Ayman Alhejji, Mohamed I. Mosaad, "Performance enhancement of grid-connected PV systems using adaptive reference PI controller", Ain Shams Engineering Journal, vol.12, pp 541-554, September 2020.
- [2] Muhammad Ibrahim Munir, Tasneim Aldhanhani, Khalifa Hasan Al Hosani, "Control of Grid Connected PV Array using P&O MPPT Algorithm", Ninth Annual IEEE Green Technologies Conference, 2166-5478/17, DOI 10.1109/GreenTech.2017.14
- [3] Murari Lal Azad, Soumya Das, Pradip Kumar Sadhu, Biplab Satpati, Anagh Gupta, P. Arvind, "P&O algorithm based MPPT technique for solar PV System under different weather conditions", International Conference on circuits Power and Computing Technologies, 978-1-5090-4967, July2017
- [4] Anis Ammous, Abdulrahman Alahdal, and Kaiçar Ammous, "Optimization of an On-Grid Inverter for PV Applications Using Genetic Algorithms", Hindawi Journal of Engineering, Volume 2020, Article ID 7063243, 12 pages.
- [5] S.Kamalsakthi, J.Baskaran, S.A.Elankurisil, "Optimization of Grid Connected PV System by Partial Shading Mppt Using Modified PSO Algorithm", International Conference on Computation of Power, Energy, Information and Communication, 978-1-7281-0837-7/19
- [6] M. F. Roslan, Ali Q. Al-Shetwi, M. A. Hannan, P. J. Ker, A. W. M. Zuhdi, "Particle swarm optimization algorithm-based PI inverter controller for a grid-connected PV system", PLoS one journal, 15(12): e0243581.
- [7] Klemen Deželak, Peter Bracinik, Klemen Sredenšek, Sebastijan Seme, "Proportional-Integral Controllers Performance of a Grid-Connected Solar PV System with Particle Swarm Optimization and Ziegler-Nichols Tuning Method", Energies 2021, 14, 2516
- [8] Thomas Thangam, Dr.K.Muthuvel, "Parametric Analysis on Optimized PFOPID control design of a Grid-connected PV inverter for MPPT", Proceedings of the Fourth International Conference on Trends in Electronics and Informatics (ICOEI 2020), IEEE Xplore Part Number: CFP20J32-ART; ISBN: 978-1-7281-5518-0
- [9] Seyedali Mirjalili, Seyed Mohammad Mirjalili, Andrew Lewis, "Grey Wolf Optimizer", Journal of Advances in Engineering Software ,vol.69,pp-46-61,January 2014
- [10] Koray Atici, Ibrahim Sefa, Necmi Altin, "Grey Wolf Optimization Based MPPT Algorithm for Solar PV System with SEPIC Converter", The 4th International Conference on Power Electronics and their Applications (ICPEA), 25-27 September 2019
- [11] M. H. Qais, H. M. Hasanien and S. Alghuwainem, "A Grey Wolf Optimizer for Optimum Parameters of Multiple PI Controllers of a Grid-Connected PMSG Driven by Variable Speed Wind Turbine," in IEEE Access, vol. 6, pp. 44120-44128, 2018, doi: 10.1109/ACCESS.2018.2864303.
- [12] Nur Farahlina Johari, Azlan Mohd Zain, Noorfa Haszlinna Mustafa, "Firefly Algorithm for Optimization Problem", Journal of Applied Mechanics and Materials, Vol. 421 (2013) pp 512-517,19 April 2014
- [13] Shahril Irwan Sulaiman, Ismail Musirin, Zulkifli Othman, Nor Syakila Mohd Zainol Abidin, "Optimization of an Artificial Neural Network using Firefly Algorithm for Modeling AC Power from a Photovoltaic System", SAI Intelligent Systems Conference 2015, November 10-11, 2015
- [14] Giraja Shankar Chaurasia, Amresh Kumar Singh, Sanjay Agrawal, N.K. Sharma, "A meta-heuristic firefly algorithm based smart control strategy and analysis of a grid connected hybrid photovoltaic/wind distributed generation system", International Journal of Solar Energy, vol.150, pp265-274, May 2017
- [15] Mingrui Zhang, Zheyang Chen Li Wei, "An Immune Firefly Algorithm for Tracking the Maximum Power Point of PV Array under Partial Shading Conditions", Energies 2019, 12, 3083; doi:10.3390/en12163083
- [16] Raja Masadeh, Basel A. Mahafzah, Ahmad Sharieh, "Sea Lion Optimization Algorithm", International Journal of Advanced Computer Science and Applications, Vol. 10, No. 5, 2019
- [17] Dr. Nidhal Kamel Taha El-Omari, "Sea Lion Optimization Algorithm for Solving the Maximum Flow Problem", International Journal of Computer Science and Network Security, VOL.20 No.8, August 2020
- [18] Sujatha Therese, P, N. Kesavan Nair, "A Unique Novel Approach for Design and Analysis of A Robust Decentralized Self-Tuning Fuzzy PI

Controller for a Multi Input Multi Output Process” American Journal of Applied Sciences, 9 (3): 331-336, 2012

- [19] P. Josephin shermila, P. Sujatha Therese, M. Ugrine Prince, “Design of Fuzzy PI Controller for Room Temperature control loop of HVAC System by using an Analytical approach for selecting the scaling factors”, International Journal of Applied Engineering Research, vol.10, Issue3, PP-9581-9600, January 2015
- [20] Gayathri Devi K S, Sujatha Therese P.,” Optimized PI controller for 7-level inverter to aid grid interactive RES controller [J]”, Journal of Central South University, 2021, 28(1): 153–167. DOI: <https://doi.org/10.1007/s11771-021-4593-1>.

A Short Review on Measuring Impact of Microencapsulated Phase Change Material in Mitigating Urban Heat Island

^[1] G. R. Gopinath, ^[2] S. Muthuvel

^[1] Research Scholar, Department of Mechanical Engineering, Kalasalingam Academy of Research and Education, Krishnankoil, Tamilnadu, India.

^[2] Associate Professor, Department of Mechanical Engineering, Kalasalingam Academy of Research and Education, Krishnankoil, Tamilnadu, India.

Abstract— *The mitigating urban heat island (UHI) has been extensively studied by many researchers because of its favorable Micro Encapsulated Phase Change Material (MEPCM) property. This helps to reduce the indoor temperature and this article reviews the major effects of reducing the indoor temperature by using MEPCM. The study wants to illustrate that the Phase Change Material (PCM) application is helpful for surface temperature supervision and enhancing indoor thermal performance by passive cooling. Suitable PCMs will maintain the comfort room temperature in the summer by dropping the inner temperature and increasing the temperature in winter. Basic methods of PCM incorporation are macro encapsulation and micro encapsulate by PCM implantation in the buildings. Encapsulation of PCM is essential to increase fusion of heat in the material. The several manufacturing companies on the commercial - scale produced a variety of PCMs, fatty acids, Paraffin, and Fatty acid esters as (MEPCM). PCM application in the Inter Building Environment (IBM), which is a PCM embedded building envelope, reduces the negative impact on energy usage and reasonable progress of yearly Heating Ventilation and Air Conditioning (HVAC) energy consumption. A basic understanding of UHI under various PCM is used to analyze the thermal effect in a better.*

Index Terms— *Urban Heat Island (UHI), Phase Change Material (PCM), paraffin wax, cool roof, thermal comfort.*

I. INTRODUCTION

The increase in temperature plays a major role in UHI and due to the reduction of temperature; there is a need huge amount of energy as well as money. In the UHI the temperature, in the metropolitan is very warmer than the nearby suburban and country [1]. There is a cause of global warming due to the higher temperature in the UHI. It compromises the lifespan happening earth, the dangerous emission such as carbon dioxide, nitrous oxide, methane, etc. It also impacts the negative climatic condition and causes some diseases to human beings [2].

In recent years, the buildings' energy performance is increasing due to the implement of new material and the development of technology in constructing buildings [3]. Particularly in areas like exciting climatic environments; the building is consumed a huge amount of energy. By enhance

the indoor thermal comfort and falling the building temperature by using of Vacuum Insulation Panel (VIPS), PCM, window glazing, and polymer skin. The materials are preferred for installation of thermal energy storing system in industries by latent heat [4]. In UHI, temperature ascend can be reduced by using PCM to progress the thermal performance of the rooftops and walls to cumulative thermal storage capacity [5]. The thermal energy in various physical processes can be stored like sensible heat or by latent heat storage. These thermal energy storage technologies are an eco-friendly and to reduce energy consumption and high-power absorption for air conditioning [6]. The effective energy storage and recovery devices particularly in solar thermal applications is useful for latent heat thermal energy system [7]. Though, the presentation of heating energy structures is due to the limited by the poor thermal conductivity of embedded PCMs. The study on heating energy system utilizing for presentation improvement methods takes primarily studied in detail. The study mainly focuses on valuation of heat transfer rate, amount of energy stored/retrieved and melting/solidification period in contrast by those of system without development techniques and acquired an improved output [8]. The study also has illustrated that the PCM application is helpful for surface temperature supervision. PCM usage helps to enhance indoor thermal performance by maintaining comfort room temperature in the summer by the inner temperature is dropping and the temperature is rising in winter. Results anchored in the studies on PCM applied heating and cooling were analyzed and exercised in research with the exploitation of prototype models and practical rooms [9]. The PCM application in the Inter Building Environment (IBE), which is a PCM-embedded building envelope, reduces the negative impact on energy usage and reasonable progress of annual energy consumption by HVAC. PCM implantation in the buildings has been achieved by their basic methods of PCM incorporation which are macro encapsulation, incorporation of microencapsulation. The PCMs fatty acids, Paraffin, and Fatty acid esters are produced as the (MEPCM) by several manufacturing companies on the commercial scale [10, 11]. The concrete/MEPCM at different proportions explored compressive strength, flexural strength, thermal conductivity and diffusivity, volumetric heat capacity, and microstructural

characterization for better understanding of suitable MEPCM proportion with concrete [12].

PCM Cool roof system used in mitigating UHI

Suffering from severe negative UHI effects in various countries, the usage of PCM cool roof is widely discussed by many authors because of it increasing the temperature in mitigating UHI. The cooling energy demand in construction by cool roofs, reflecting coatings is reduced by the emerging technology like passive cooling [13]. The Wood Polymer Composite (WPC) was effectively applied in the PCM to the roof surface in the sub urban areas and urban areas to promote the building energy saving [14]. The PCM doped tiles are used to create a cool roof structure with PCM, in summer condition the chamber temperature is low and when the surface temperature is decrease and while in the winter condition the chamber temperature higher than the cool paint when the surface temperature is low [15]. In the outer layer the PCM must be installed in a high mass fraction, also combined in a water proofing film otherwise as a board, located under the casing or otherwise under an external metallic sheet, the effective result was only found from a PCM board with the thickness of about 10mm and PCM content about 60% [16]. The compatibility among the hydrophobic coat then MEPCM containing RT31 remained very low, it is used towards decrease the highest temperature in a construction sector due toward higher PCM loading it has higher latent heat capacities [17]. The PCM is encapsulated in Poly Ethylene- Raised Temperature (PE-RT) pipe the PCM containing tetradecenoyl and myristate have relatively higher latent heat storage it is mostly used in the building envelope and the roof was covered with cool materials composed of glass-fiber cement polystyrene core[18]. The PCM is implanted with an asphalt concrete coating it reduces the temperature and the thermal belongings remain independent to phase of each layer and the properties of PCM are dependent to phase [19]. The two passive cooling techniques like ASV system and PCM tiled roof was combined to reduce the temperature in the building envelope [20]. Compared to the other general insulation the PCM cool roof system has higher thermal insulation performance, in the solid PCM thermal conductivity is almost eight times higher than the general insulation [21].

Impact of PCM with cool material roofs are used in UHI

Author	Results	Location
Min Hee Chung et al., (2016) [15]	The PCM doped tiles can reduced the temperature upto 7.2 ^o C.	South Korea
Mohammad Saffari et al., (2018) [13]	The melting temperature of PCM reaching from 10 to 20 ^o C.	Pacific Northwest National Laboratory
Young Kwon Yang et al., (2019) [14]	when the PCM cool roof system is implanted. The maximum temperature	South korea

	difference is achieved in winter season is 2.5 °C, in spring and autumn season is 4.7 °C, and in summer season is 5.7 °C	
Su-GwangJeonget et al., (2016) [17]	A small amount of hydrophilic paint is added to the PCM to reduce the peak temperature	South Korea
Hyo Eun Lee, et al., (2017) [21]	PCM is applied to cooling energy consumption and used for energy saving.	United States
Anna Laura Pisello, et al., (2015) [25]	PCM integrated into the cool membrane saves 10.4% of cooling energy	Engineering Campus at University of Perugia, Italy
Yilong Han, et al., (2016) [22]	When the PCM layer is implanted in the indoor side of the building and the 17% of energy conversation is achieved	United States
Christopher Gunasingh et al., (2017) [32]	In the cement concrete block, it reduces the temperature upto 3 to 6 degree Celsius by the use of paraffin wax	-
C. Tzivanidis et al., (2012) [28]	The PCM layer is used to maintain the indoor air temperature is 28°C during a day	-

Table 1.1 Impact of PCM with cool material roofs are used in UHI



Figure 1: Flat roof with cool white waterproofing film [16].

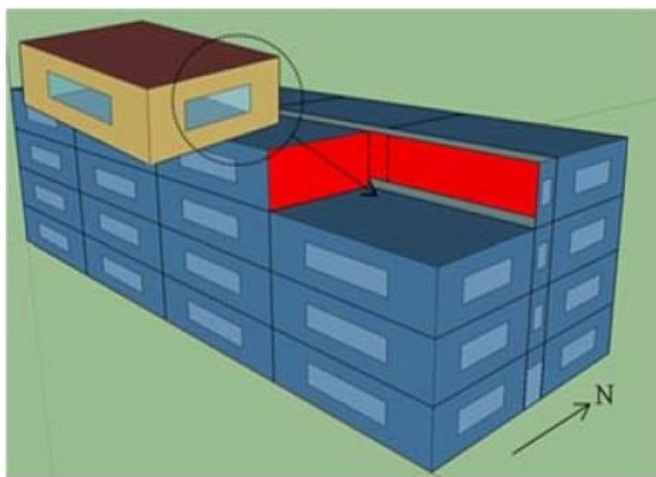


Figure 2: Construction model [13]

Organic PCM used in mitigating UHI

Organic PCMs are useful for latent heat storage in certain building elements. The PCM is divided into different types are organic compounds, inorganic compounds and eutectic compounds each type has different melting temperature [22,23]. The energy saving for the cooling period found higher than total cooling and heating consumption [24]. Due to increase in heat capacity the PCM having the melting temperature from 20°C to 25°C [25]. The organic paraffin based PCM is used to melting and solidification of PCMs, by usage of circulated water baths the desired temperature is kept.[26]. The PCM remain to store heat throughout the diurnal through the melting process and to release it at nocturnal time over solidification progression [27,28]. The PCM higher melting point is incorporated in a building envelope, the PCM is installed in an exterior wall on outer surface to dissipate the stored heat at night time [29]. Select the PCM material and then the PCM can be encapsulated to reduce the mitigating UHI to estimate the thermal conductivity, thermal diffusivity specific heat and characterize the optical finishing of the concrete surfaces [30]. During encapsulation process the energy storage

capacity can change by different speed, the lesser speed during encapsulation having better thermal energy storage than the higher speed during encapsulation [31]. The paraffin wax is selected as PCM in different weight percentage of 0.5, 0.75, 1.0, 1.25 of cement, the addition of paraffin to concrete cubes is not affected by the concrete strength cubes, the 1.0 percentage weight of PCM will enhance the cooling effect on side walls [32]. The Micro Encapsulated Eicosane capsules content 71%wt PCM modified AC pavement shows in reducing high temperature, during crystallization process of PCM heat is released [33].

In Organic PCM used in mitigating UHI

The inorganic PCM are hydrated salt, molten salt, metal, etc. [34]. The inorganic PCM have the high volumetric latent heat storage capacity, it takes high thermal conductivity and has sharp melting point. The hydrated salt PCM are used in the building envelope to reduce the mitigating UHI. The inorganic PCM have high melting enthalpy, high density with corrosive properties [35]. Ion phase separation is due to the crystallization of hydrates, degradation of durability melting and solidification [36]. The solar reflectance can be increased by using the inorganic pigments are composed of metal oxides, and have the capabilities like good water retention, simple spraying, high durability, dirt resistance, heat insulation, high reflectivity [37]. The thickness of the PCM layer was calculated based on assumption need to solidify and melt during a single day [38]. The PCM temperature range can be identified by three different states 1. PCM is not melted below 25°C. 2. PCM is fully melted when it reaches above 34°C. 3. PCM temperature is between 25°C and 34°C it is partially melted state [39]. The sodium silicate pentahydrate as PCM admixture of different proportion as 0.5, 0.75, 1.0, 1.25 on quantity of cement to prepare a concrete cube, the 1% weight of sodium silicate pentahydrate concrete cube will store maximum latent heat and reduce temperature on cross sides upto 3 to 6°C [40].

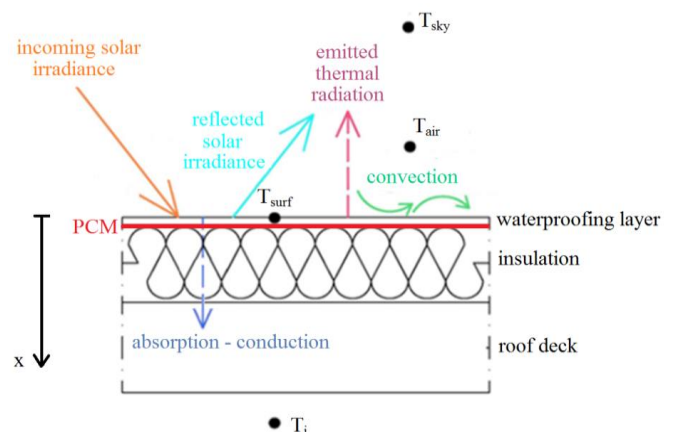


Figure 3: Surface heat transfer process and rooftop construction [16]

II. CONCLUSION

The mitigating urban heat island have very extreme hot climate. To overcome by using Micro Encapsulated Phase Change Material (MEPCM) property. This benefits to decrease the inside building temperature. The effect of reducing the inside building temperature by using of MEPCM. The study wants to illustrate that the PCM application is helpful for surface temperature supervision and enhancing indoor thermal performance by passive cooling. variety of PCMs, fatty acids, Paraffin and Fatty acid esters are produced as Micro Encapsulated PCM (MEPCM) by several manufacturing companies on the commercial - scale. The organic paraffin wax PCM will suitable to maintain comfort room temperature at the summer by decreasing the inner temperature and in the winter increasing the temperature, because organic PCM are thermally and chemically stable, it is corrosive resistance. PCM implantation in the buildings will be achieved by basic methods of PCM incorporation which are macro encapsulation and micro encapsulation. Encapsulation of PCM is essential to increase fusion of latent heat of the material. Amongst PCM application in the Inter Building Environment, which is a PCM embedded building envelope, reduces the negative impact on energy usage and reasonable progress of yearly (HVAC) energy consumption. A basic understanding of urban heat island under various PCM is needed to analyze the thermal effect in a better way.

REFERENCE

- [1] Pratiwi, S. N. (2018). a Review of Material Cover Features for Mitigating Urban Heat Island. *International Journal on Livable Space*, 3(2), 71-80.
- [2] Lassandro, P., & Di Turi, S. (2017). Façade retrofitting: from energy efficiency to climate change mitigation. *Energy Procedia*, 140, 182-193.
- [3] Yoon, S. G., Yang, Y. K., Kim, T. W., Chung, M. H., & Park, J. C. (2018). Thermal Performance Test of a Phase-Change-Material Cool Roof System by a Scaled Model. *Advances in Civil Engineering*, 2018.
- [4] Latha, P. K., Darshana, Y., & Venugopal, V. (2015). Role of building material in thermal comfort in tropical climates—A review. *Journal of Building Engineering*, 3, 104-113.
- [5] Kolokotsa, D., Santamouris, M., & Zerefos, S. C. (2013). Green and cool roofs' urban heat island mitigation potential in European climates for office buildings under free floating conditions. *Solar Energy*, 95, 118-130.
- [6] Gao, C., Kuklane, K., Wang, F., & Holmér, I. (2012). Personal cooling with phase change materials to improve thermal comfort from a heat wave perspective. *Indoor air*, 22(6), 523-530.
- [7] Piselli, C., Castaldo, V. L., & Pisello, A. L. (2019). How to enhance thermal energy storage effect of PCM in roofs with varying solar reflectance: Experimental and numerical assessment of a new roof system for passive cooling in different climate conditions. *Solar Energy*, 192, 106-119.
- [8] Jegadheeswaran, S., Pohekar, S.D., Energy and Exergy analysis of particle dispersed latent heat storage system, *International Journal of Energy Conservation and Management*, 1(3) (2010), 445-458.
- [9] Han, Y., & Taylor, J. E. (2016). Simulating the Inter-Building Effect on energy consumption from embedding phase change materials in building envelopes. *Sustainable cities and society*, 27, 287-295.
- [10] Kenisarin, M., & Mahkamov, K. (2016). Passive thermal control in residential buildings using phase change materials. *Renewable and sustainable energy reviews*, 55, 371-398.
- [11] Papadaki, D., Foteinis, S., Binas, V., Assimakopoulos, M. N., Tsoutsos, T., & Kiriakidis, G. (2019). A life cycle assessment of PCM and VIP in warm Mediterranean climates and their introduction as a strategy to promote energy savings and mitigate carbon emissions. *AIMS Materials Science*, 6(6), 944.
- [12] Dehdezi, P. K., Hall, M. R., Dawson, A. R., & Casey, S. P. (2013). Thermal, mechanical and microstructural analysis of concrete containing microencapsulated phase change materials. *International Journal of Pavement Engineering*, 14(5), 449-462.
- [13] Saffari, M., Piselli, C., de Gracia, A., Pisello, A. L., Cotana, F., & Cabeza, L. F. (2018). Thermal stress reduction in cool roof membranes using phase change materials (PCM). *Energy and Buildings*, 158, 1097-1105.
- [14] Yang, Y. K., Kim, M. Y., Chung, M. H., & Park, J. C. (2019). PCM cool roof systems for mitigating urban heat island-an experimental and numerical analysis. *Energy and Buildings*, 205, 109537.
- [15] Chung, M. H., & Park, J. C. (2016). Development of PCM cool roof system to control urban heat island considering temperate climatic conditions. *Energy and Buildings*, 116, 341-348.
- [16] Muscio, A. (2016). Coupling of solar reflective cool roofing solutions with sub-surface phase change materials (PCM) to avoid condensation and biological growth. *International Journal of Environmental Science & Sustainable Development*, 1(1).
- [17] Jeong, S. G., Chang, S. J., Wi, S., Kang, Y., & Kim, S. (2016). Development and performance evaluation of heat storage paint with MPCM for applying roof materials as basic research. *Energy and Buildings*, 112, 62-68.
- [18] Lu, S., Chen, Y., Liu, S., & Kong, X. (2016). Experimental research on a novel energy efficiency roof coupled with PCM and cool materials. *Energy and Buildings*, 127, 159-169.
- [19] Athukorallage, B., Dissanayaka, T., Senadheera, S., & James, D. (2018). Performance analysis of incorporating phase change materials in asphalt concrete pavements. *Construction and building materials*, 164, 419-432.
- [20] Bottarelli, M., Gallero, F. J. G., Maestre, I. R., Pei, G., & Su, Y. (2020). Solar gain mitigation in ventilated tiled roofs by using phase change materials. *International Journal of Low-Carbon Technologies*.
- [21] Lee, H. E., Yang, Y. K., Chung, M. H., & Park, J. C. (2017). Simulation Analysis of Thermal Insulation Performance of PCM for Mitigating Urban Heat Island Effect. *Journal of the Architectural Institute of Korea Structure & Construction*, 33(6), 79-86.
- [22] Han, Y., & Taylor, J. E. (2016). Simulating the Inter-Building Effect on energy consumption from embedding phase change materials in building envelopes. *Sustainable cities and society*, 27, 287-295.
- [23] Ma, T., Yang, H., Zhang, Y., Lu, L., & Wang, X. (2015). Using phase change materials in photovoltaic systems for thermal regulation and electrical efficiency improvement: a review and outlook. *Renewable and Sustainable Energy Reviews*, 43, 1273-1284.
- [24] Saffari, M., de Gracia, A., Ushak, S., & Cabeza, L. F. (2017). Passive cooling of buildings with phase change materials using whole-building energy simulation tools: A review. *Renewable and Sustainable Energy Reviews*, 80, 1239-1255.
- [25] Pisello, A. L., Castaldo, V. L., & Cotana, F. (2015). Dynamic thermal-energy performance analysis of a prototype building with integrated phase change materials. *Energy Procedia*, 81, 82-88.
- [26] Tokuç, A., Başaran, T., & Yeşüey, S. C. (2015). An experimental and numerical investigation on the use of phase change materials in building elements: The case of a flat roof in Istanbul. *Energy and Buildings*, 102, 91-104.
- [27] Pisello, A. L., D'Alessandro, A., Fabiani, C., Fiorelli, A. P., Ubertini, F., Cabeza, L. F., ... & Cotana, F. (2017). Multifunctional analysis of innovative PCM-filled concretes. *Energy Procedia*, 111, 81-90.
- [28] Tzivanidis, C., Antonopoulos, K. A., & Kravvaritis, E. D. (2012). Parametric analysis of space cooling systems based on night ceiling cooling with PCM- embedded piping. *International journal of energy research*, 36(1), 18-35.
- [29] Saffari, M., De Gracia, A., Fernández, C., & Cabeza, L. F. (2017). Simulation-based optimization of PCM melting temperature to improve the energy performance in buildings. *Applied Energy*, 202, 420-434.

- [30] Pisello, A. L., Castaldo, V. L., Piselli, C., Pigliautile, I., Cabeza, L. F., Pérez, G., & Cotana, F. (2016). Microclimate Mitigation by means of Thermal-energy Storage: A case study in Central Italy.
- [31] Dom, M., Bakar, A., Tulos, N., Ahmad, W., Yunus, W., Mohd, A. F., & Yahya, M. F. (2016). Thermal Conductivity of Paraffin Wax as Microencapsulated Phase Change Material (PCM) Coated on Polyester Fabric. In *Advanced Materials Research* (Vol. 1134, pp. 160-164). Trans Tech Publications Ltd.
- [32] Gunasingh, K. C., & Hemalatha, G. (2006). IMPACT OF PARAFFIN AS PHASE CHANGE MATERIAL IN CONCRETE CUBES FOR ENHANCING THE THERMAL ENERGY STORAGE.
- [33] Refaa, Z., Kakar, M. R., Stamatou, A., Worlitschek, J., Partl, M. N., & Bueno, M. (2018). Numerical study on the effect of phase change materials on heat transfer in asphalt concrete. *International Journal of Thermal Sciences*, 133, 140-150.
- [34] Lassandro, P., & Di Turi, S. (2017). Energy efficiency and resilience against increasing temperatures in summer: the use of PCM and cool materials in buildings. *International Journal of Heat and Technology*, 35(S1), S307-15.
- [35] Rodriguez-Ubinas, E., Ruiz-Valero, L., Vega, S., & Neila, J. (2012). Applications of phase change material in highly energy-efficient houses. *Energy and Buildings*, 50, 49-62.
- [36] Nagano, K., Ogawa, K., Mochida, T., Hayashi, K., & Ogoshi, H. (2004). Thermal characteristics of magnesium nitrate hexahydrate and magnesium chloride hexahydrate mixture as a phase change material for effective utilization of urban waste heat. *Applied Thermal Engineering*, 24(2-3), 221-232.
- [37] Pisello, A. L., Paolini, R., Diamanti, M. V., Fortunati, E., Castaldo, V. L., & Torre, L. (2016). Nanotech-based cool materials for building energy efficiency. In *Nano and Biotech Based Materials for Energy Building Efficiency* (pp. 245-278). Springer, Cham.
- [38] Roman, K. K., O'Brien, T., Alvey, J. B., & Woo, O. (2016). Simulating the effects of cool roof and PCM (phase change materials) based roof to mitigate UHI (urban heat island) in prominent US cities. *Energy*, 96, 103-117.
- [39] Jin, X., Zhang, S., Xu, X., & Zhang, X. (2014). Effects of PCM state on its phase change performance and the thermal performance of building walls. *Building and Environment*, 81, 334-339.
- [40] Gunasingh, K. C., & Hemalatha, G. (2017). Impact of Sodium Silicate Pentahydrate as Phase Change Material in Concrete Cubes for Enhancing the Thermal Comfort. *International Journal of Civil Engineering and Technology*, 8(1).

Roxas City, the Seafood Capital of the Philippines: Myth or Fact?

^[1] Ian B. Arcega, ^[2] Pearl Joy G. Mirasol, ^[3] Angela B. Casios, ^[4] Sarah Jane D. Malayang
^{[1][2][3][4]} Capiz State University, Faculty Members of the College of Management

Abstract— *The purpose of this study attempts to prove the branding of Roxas City, which is part of the Province of Capiz, as the Seafood Capital of the Philippines. The researchers utilized secondary data from the Fisheries Statistics of the Philippines from 2007 to 2017. The study was on the determination of the performance of the Province of Capiz in the type of production on Commercial, Marine Municipal, Inland Municipal, and Aquaculture its volume and value at the same time knowing the performance on various species and determine who are the top fisheries producing Provinces by sector from 2007 to 2017.*

Results of the study revealed that the volume and value in the fishing industry in commercial, marine municipal, inland municipal in the Province of Capiz was decreasing. It was observed that the Capiz is not part of the top producing province in the Philippines. However, the volume and value in the aquaculture industry were increasingly focused on different species such as milkfish, mud crab, mussel, oyster, tiger prawn, white shrimp, and endeavor prawn. If the basis of the City of Roxas to become the Seafood Capital of the Philippines is in volume and value across industry types, the claim is a myth

Index Terms— *Province of Capiz, Time-Series Analysis, Fisheries, Commercial, Municipal, Inland Municipal and Aquaculture*

I. INTRODUCTION

In 2016, the Philippines ranked 8th among the top fish-producing countries globally, with 4.2 million metric tons of fish, crustaceans, mollusks, and aquatic plants (including seaweeds). The production constitutes 2.1% of the total world production of 202. 2 million metric tons (FAO Statistics).

The Philippines' 0.796 million metric tons aquaculture production of fish, crustaceans, and mollusks in 2016 ranked 11th in the world and a 1.0% share of the total global aquaculture production of 80.03 million metric tons. In terms of value, the country's aquaculture production of fish, crustaceans, and mollusks has amounted to over 1.79 billion dollars (FAO Statistics).

Similarly, the Philippines is the world's 3rd largest producer of aquatic plants (including seaweeds), having produced a total of 1.4 million metric tons or nearly 4.7% of the total world production of 30.14 million metric tons (FAO Statistics).

The fishing industry's contribution to the country's Gross Domestic Products (GDP) was 1.2 % and 1.4% at current and constant 2000 prices. It translates to P197.23 billion and

P122.25 billion for current and constant prices of the country's GDP of P15,806 billion (current prices) and P8,666 billion (constant prices).

Roxas City is the self-proclaimed seafood capital of the Philippines. The city serves as the entry point for a fertile agricultural area, exporting the surplus to nearby islands. The town is economically booming because of various industries such as agriculture and aquaculture products. Roxas City was heavily damaged when Super Typhoon Haiyan, a powerful tropical cyclone that swept the Region in early November 2013 (Pletcher, Kenneth, 2020).

The study investigates if Roxas City is still the Seafood Capital of the Philippines through a time-series analysis on volume and value. Also, the researchers want to prove if this branding can bring a competitive advantage over other Provinces in the country and cascade this to the community.

Specifically, it sought to answer the following (1) What is the performance (volume and value) of the production in the Province of Capiz in terms of fisheries, commercial, municipal, inland municipal, and aquaculture for the period covered 2007 to 2017 in volume (in metric tons) and value (in Pesos); (2) What is the performance (volume and value) of the various species in the Province of Capiz for the period covered 2007 to 2017; (3) What is the performance (volume and value) of the production by type of Aquafarm in the Province of Capiz for the year 2007 to 2017 and; (4) What are the top fisheries producing provinces by sector from 2007 to 2017.

The study results would benefit the Provincial Government and Roxas City Government, entrepreneurs, people of Capiz, BFAR, higher education institutions, DTI, and future researchers. The results will be the basis for policy formulation, revisiting the strategic plan and direction of the City Council, and development of valuable strategies to maintain the volume and value of the fishing industry in the Province of Capiz.

II. THEORETICAL FRAMEWORK

The study anchored on the BFAR laws and other related laws. System theory and Motivation-Opportunity-Ability (MOA) model, proposed by MacInnis and Jaworski (1989) and MacInnis et al. (1991), who theorized the degree to which people process information by using various combinations of MOA when taking action. According to the MOA model, motivation incorporates readiness, willingness, interest, and the desire to engage in information processing. The opportunity has been conceptualized as to the extent of the situation is conducive to achieving the desired outcome.

Ability refers to consumer skills or proficiencies in interpreting brand information from an advertisement (MacInnis et al., 1991). Mainly, opportunity represents the environmental or contextual factors that enable action (Rothschild 1999).

III. THE FRAMEWORK OF THE STUDY

The framework of the study will map the performance, volume, and production in terms of volume and value of fisheries, commercial, inland municipal and aquaculture, various species available in the Province of Capiz.

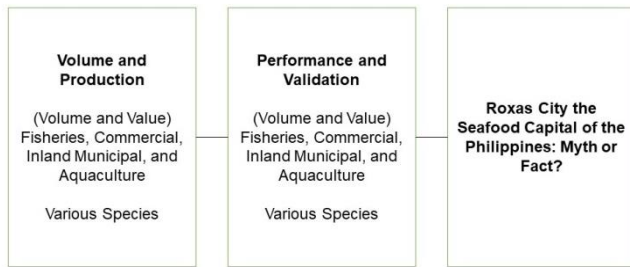


Fig. 1. Showing the constructs of the study.

IV. SCOPE AND LIMITATION OF THE STUDY

This study focused on exploring the fishing industry data and tourism of the Province of Capiz. And to know whether Roxas City is the Seafood Capital of the Philippines. The data used is the consolidation of a Fisheries Statistics report of the Philippines from 2007 to 2017. Data of Roxas City is part of the total number of the Province of Capiz. The analysis of whether Roxas City branding as the Seafood Capital of the Philippines is through the volume and species of the fishing industry produced in the province and validated with various vital informants.

V.METHODOLOGY

This is a descriptive research design utilizing the quantitative and qualitative methods of gathering the data—using secondary data for analysis. Data used are the Fisheries Statistics of the Philippines from 2007 to 2017 from Luzon to Mindanao. A time series of research was also used in processing and analyzing the data. They compared the performance of the Province of Capiz to other Provinces in the country. In validating the results, key informants are selected for an interview. The informants are the BFAR Officers, Fisherfolks, Roxas City Officials, Roxas City Community, Officers from the Department of Trade and Industry, Business Owners their business is in fishing and restaurant, tourists, and Head of the Higher Education Institutions.

VI. RESULTS AND DISCUSSIONS

This section presented the results and findings of the study.

Fisheries, Commercial, Inland Municipal, and Aquaculture Production

The researchers are comparing based on 2007 to 2017, but also analyzed data for future analyses.

Fig. 2 shows that Capiz was ranked fourth (4th) in the fisheries production among five (5) Provinces in the Western Visayas. In the 2017 volume of fisheries production, there were 87,582.82 metric tons. For the last ten years, the year 2010 reached the highest volume, 104,881.45 metric tons. It implies an increase and decreases in production for eleven (11) years of operation. It might cause an immediate cause of weather, climate change, and marine diseases. It was supported by growers, which they encountered water-borne conditions such as red tide that affect aquaculture production that impacted the industry due to climate change.

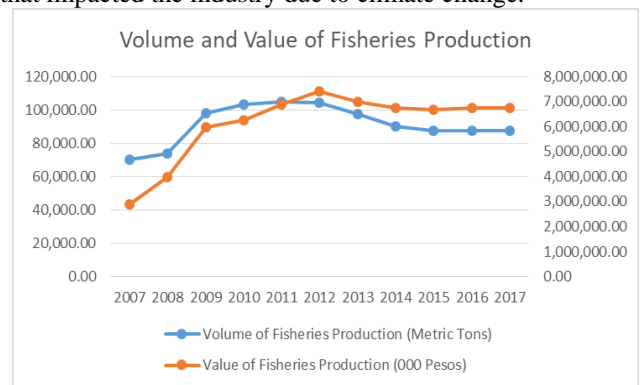


Fig. 2. Shows the volume and value of Fisheries Production.

Commercial Fisheries

Fig. 3 shows the commercial production of Capiz for the last 11 years. Capiz was ranked third (3rd) among six Province in Western Visayas. In 2011, 24,604.65 metric tons produced and its value of 1,530,827.22. It implies that the production volume was decreasing, but other Provinces maintained their production volume in commercial fisheries.

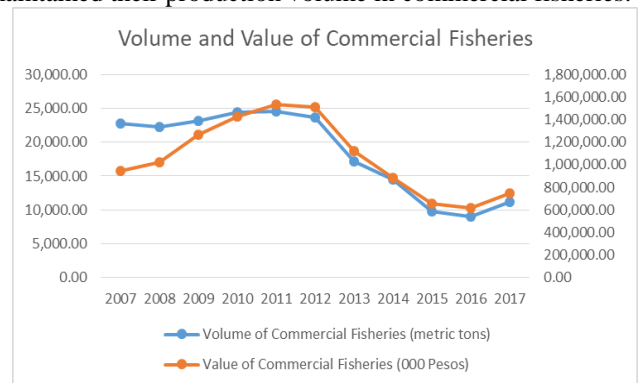


Fig. 3. Shows the volume and value of Commercial Fisheries.

Fig. 4 shows the volume of production and its value of Municipal Fisheries from 2007 to 2017. In 2010, it was the highest production in the Province of Capiz, which has 38,931.72 metric tons, and 2012 has the highest value of

2,451,745.85. And Capiz was ranked third (3rd) among five Provinces in Western Visayas.

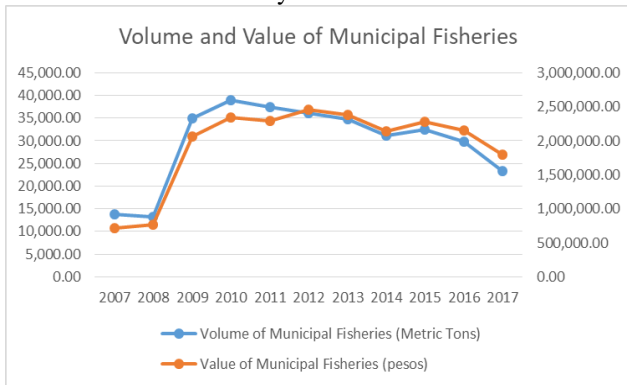


Fig. 4. Shows the volume and value of Municipal Fisheries.

Inland Municipal Fisheries

Fig. 5 shows the volume of production and its value of Municipal Fisheries from 2007 to 2017. In 2013, it was the highest production in the Province of Capiz, which has 256.76 metric tons, and 2012 has the highest value of 18,947.10. And Capiz was ranked fifth (5th) among five Provinces in Western Visayas.

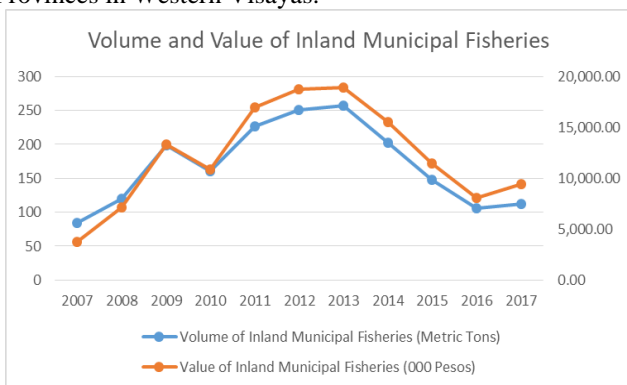


Fig. 5. Shows the volume and value of Inland Municipal Fisheries.

Aquaculture

Fig. 6 shows the volume of production and its value of Municipal Fisheries from 2007 to 2017. In 2017, it was the highest production in the Province of Capiz, which has 52,957.76 metric tons, and 2017 has the highest value of 4,200,456.92. And Capiz was ranked second (2nd) among five Provinces in Western Visayas. Based on the data presented, the findings are formulated: (1) the Province of Capiz was not part of the top producing Provinces in the Philippines based on the data analyzed from 2007 to 2017 in Commercial, Marine Municipal, Inland Municipal, and Aquaculture; (2) through the years the Province of Capiz has a declining volume of production based on the fishing industry cited above; (3) the value of the produced was also erratic due to the inflation and deflation experienced by the country; (4) however, on Western Visayas, the Province of Capiz was ranked lower compared to other provinces in the Region. The informants postulate that the Province of Capiz has no

organized group related to this kind of industry, which they can adopt best practices to other growers. And it is noted that the province was affected by various typhoons and other calamities that destroy the business and its production.

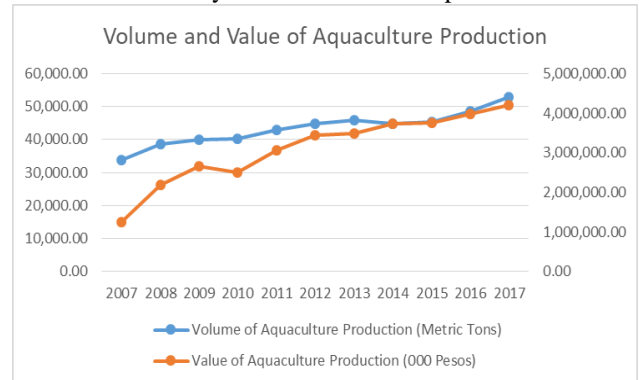


Fig. 6. Shows the volume and value of Aquaculture Production.

Performance of Different Species Produced in Volume and Value

Fig. 7 shows the volume and value of anchovies (*dilis*). Capiz was ranked first (1st) in the total produced 2010 has 5,463.76 metric tons and P 237,996.57. It implies that in Capiz, this species is abundant, but the volume is decreasing through the years.

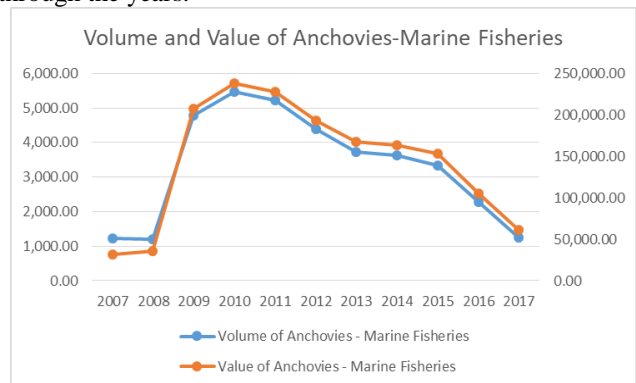


Fig. 7. Shows the volume and value of Anchovies-Marine Fisheries.

Fig. 8 shows the volume and value of the big-eyed scad (*matang-baka*). Capiz was ranked first (1st) in total produced; in 2015, it has 2,030.63 metric tons and 152,842.37. It implies that in Capiz, this species is abundant, but the volume is decreasing through the years.

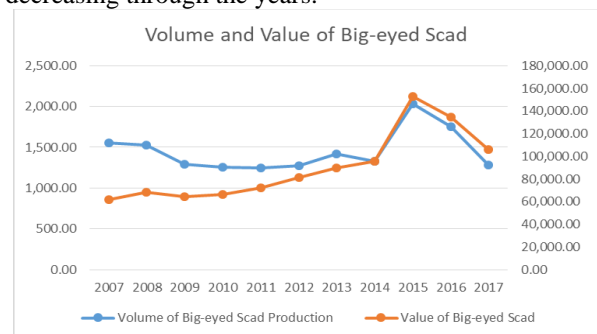


Fig. 8. Show the volume and value of Big-eyed Scad.

Fig. 9 shows the volume and value of big-eyed tuna (*tambakol/bariles*). This species is not abundant present in the Province of Capiz. But in 2007, 2008 and 2009 there is volume produced, but it's very minimal.

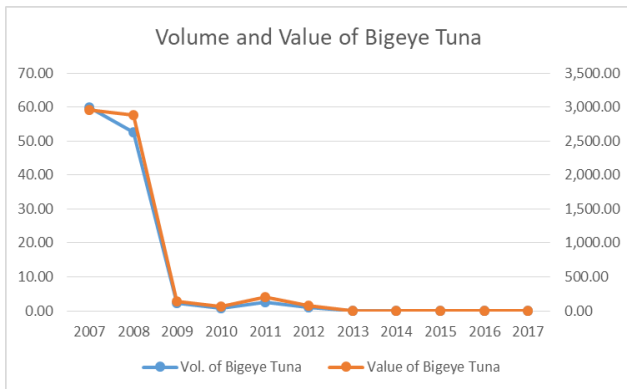


Fig. 9. Shows the volume and value of Bigeye Tuna.

Fig. 10 shows the volume and value of the blue crab (*alimasag*). Capiz was ranked third (3rd) in this kind of species produced. In 2011, the total produced was 2,064.17, and in 2017, the highest value was 129,215.21.

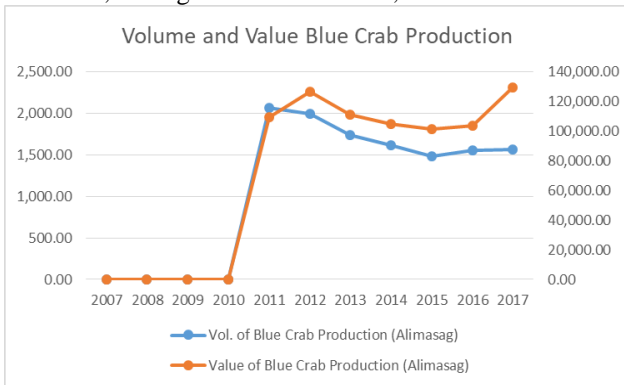


Fig. 10. Shows the volume and value of Blue Crab Production.

Fig. 11 shows the volume and value of cavalla (*talakitok*). Capiz was ranked sixth (6th) in this kind of species produced. In 2013, the total grew 50.79 metric tons, and in 2011 highest value was 7,522.52.

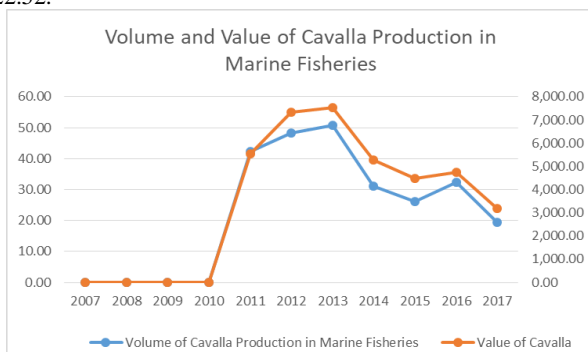


Fig. 11. Shows the volume and value of Cavalla Production in Marine Fisheries.

Fig. 12 shows the volume and value of the crevalle (*salay-salay*). Capiz was ranked third (3rd) in this kind of species produced. In 2016, the total produced was 1,359.21 metric tons, and in 2011, the highest value was 72,533.25.

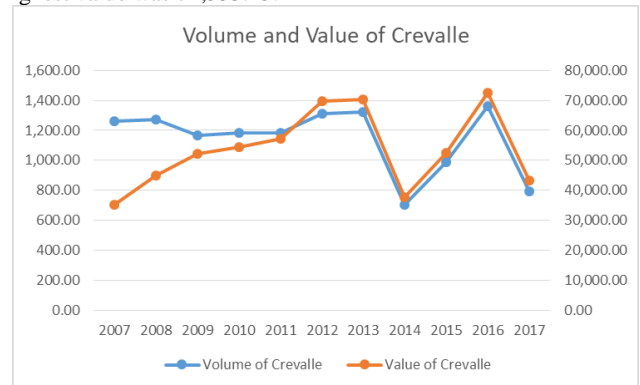


Fig. 12. Shows the volume and value of the Crevalle.

Fig. 13 shows the volume and value of frimbriated sardines (*tunsoy*). Capiz was ranked second (2nd) in this kind of species produced. In 2014, the total produced was 9,014.64 metric tons, and in 2014 the highest value was 494,471.70.

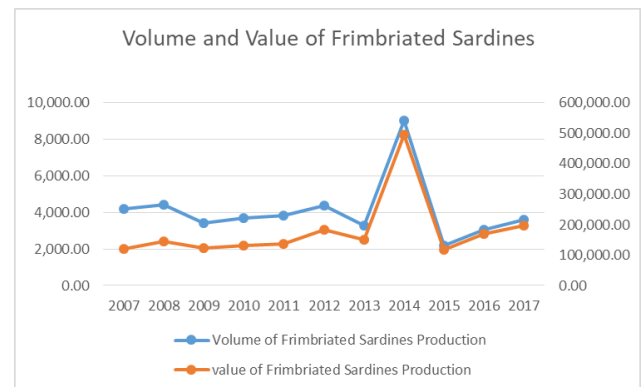


Fig. 13. Shows the volume and value of Frimbriated Sardines.

Fig. 14 shows the volume and value of frigate tuna (*tulingan*). Capiz was ranked fifth (5th) in this kind of species produced. In 2017, the volume made was 451.91 metric tons, and in 2009, the highest value was 34,680.12.

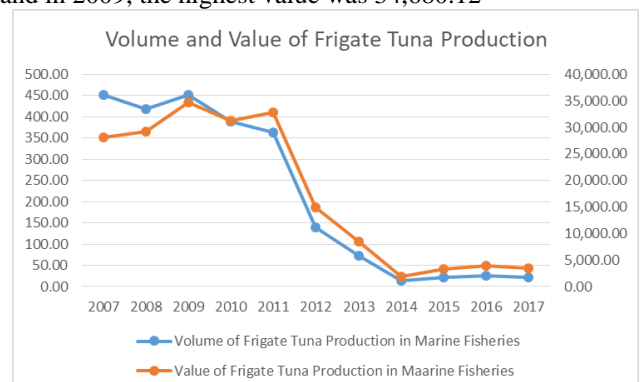


Fig. 14. Shows the volume and value of Frigated Tuna production.

Fig. 15 shows the volume and value of grouper (*lapu-lapu*) and Indian mackerel (*alumahan*). For grouper, Capiz was ranked first (1st) in this kind of species produced. In 2015, the volume grew 1,047.77 metric tons, and in 2009 the highest value was 168,660.74.

For Indian mackerel, Capiz was ranked third (3rd) with the volume produced of 1,881.83 metric tons in 2007, and the highest value was in 2011 that is 103,417.25.

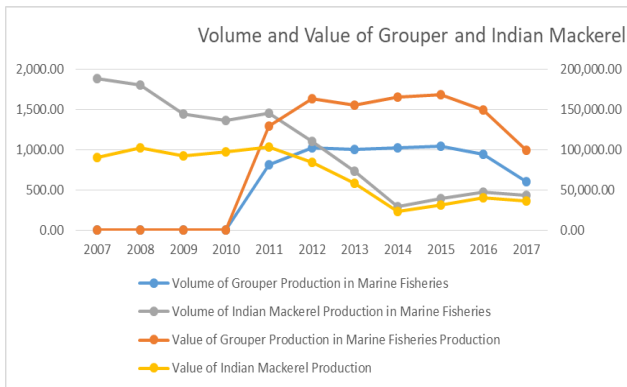


Fig. 15. Shows the volume and value of Grouper and Indian Mackerel.

Fig. 16 shows the volume and value of Indian sardines (*tamban*) and indo-pacific mackerel (*hasa-hasa*). For Indian sardines, Capiz was ranked second (2nd) in this kind of species produced. In 2017, the volume grew by 2,643.98 metric tons, and the highest value was 149,253.24.

For indo-pacific mackerel, Capiz was ranked second (2nd) with the volume produced of 4,478.36 metric tons in 2011, and the highest value was in 2012 that is 259,335.68.

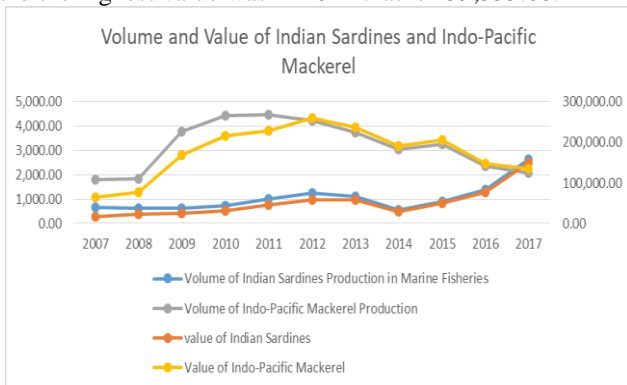


Fig. 16. Shows the volume and value of Indian Sardines and Indo-Pacific Mackerel.

Fig. 17 shows the volume and value of round scad (*galunggong*) and skipjack (*gulyasan*). For round scad, Capiz was ranked fourth (4th) in this kind of species produced. In 2013, the volume grew by 2,505.19 metric tons, and the highest value was 151,646.74. For skipjack, Capiz made this with minimal volume.

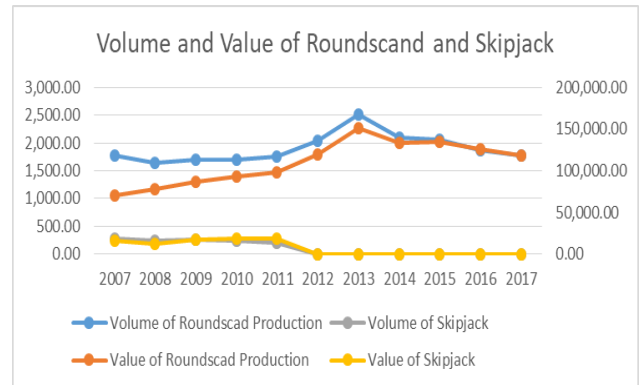


Fig. 17. Shows the volume and value of Roundscad and Skipjack.

Fig. 18 shows the volume and value of slipmouth (*sapsap*) and snapper (*maya-maya*). For slipmouth, Capiz was ranked third (3rd) in this kind of species produced. In 2009, the volume grew 6,872.04 metric tons, and the highest value was 350,986.06 in 2012. For snapper, Capiz was ranked first (1st), the highest volume produced was in 2012, which has 1,206.57 metric tons with a value of 191,878.33.

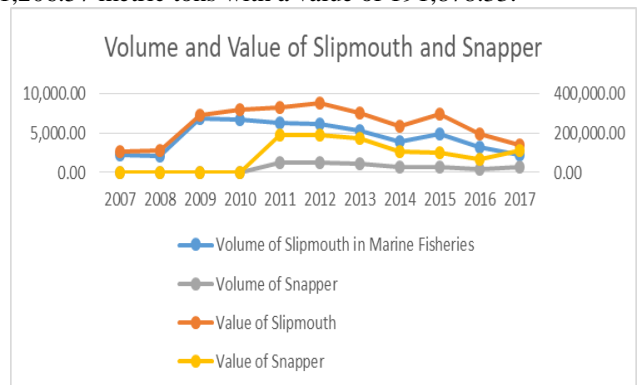


Fig. 18. Shows the volume and value of Slipmouth and Snapper.

Fig. 19 shows the volume and value of Spanish mackerel (*tanigue*) and squid (*pusit*). For Spanish mackerel, Capiz was ranked third (3rd) in this kind of species produced. In 2011 the volume made was 516.15 metric tons, and the highest value was 69,481.36 in 2012. For squid, Capiz was ranked third (3rd), the highest volume produced was in 2011, which has 2,572.83 metric tons with 219,868.89.

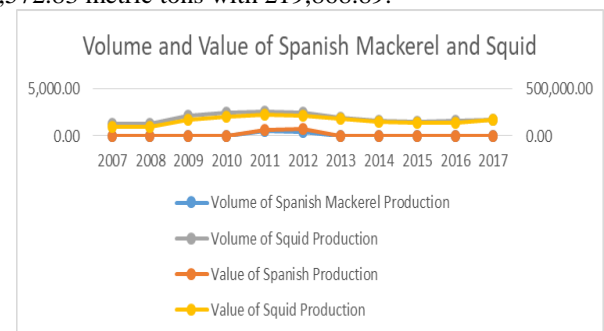


Fig. 19. Shows the volume and value of Spanish Mackerel and Squid.

Fig. 20 shows the volume and value of threadfin bream (*bisugo*) and yellowfin tuna (*tambakol*). For Spanish mackerel, Capiz was ranked third (3rd) in this kind of species produced. In 2012 the volume made was 3,519.81 metric tons, and the highest value was 298,335.77 in 2012. For yellowfin tuna, Capiz was ranked fifth (5th) due to a decline in volume. In 2009, there were 474.69 metric tons produced.

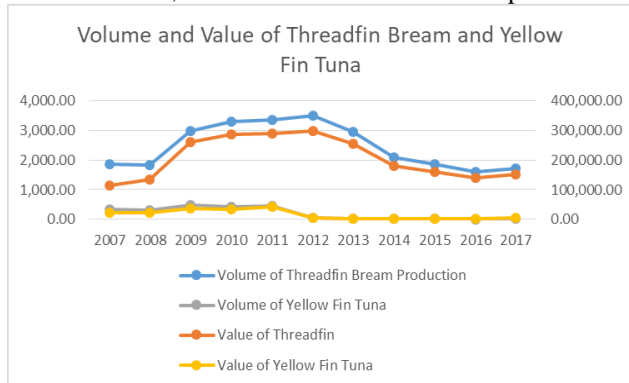


Fig. 20. Shows the volume and value of Threadfin Bream and Yellow Fin Tuna.

Species in Inland Fisheries

Fig. 21 shows the volume and value of milkfish (*bangus*) and carp (*carpa*). For milkfish, Capiz was ranked fourth (4th) in this kind of species produced. In 2012 the volume grew 12.65 metric tons, and the highest value was 1,114.64 in 2012. For carp, Capiz was ranked second (2nd). In 2013, produced 24.97 metric tons, and the value was 1,961.

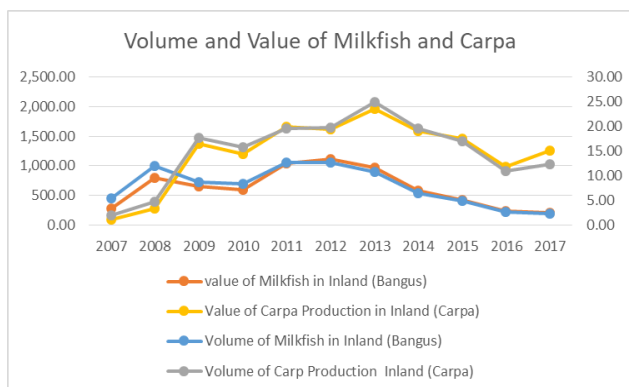


Fig. 21. Shows the volume and value of Milkfish and Carpa.

Fig. 22 shows the volume and value of mudfish (*dalag*) and gourami. For mudfish, Capiz was ranked second (2nd) in this kind of species produced. In 2013 the volume made was 25.88 metric tons, and the highest value was 2,352.14 in 2012. For gourami, Capiz was ranked second (2nd). In 2015, it produced 3.70 metric tons, and the value was 152.81.

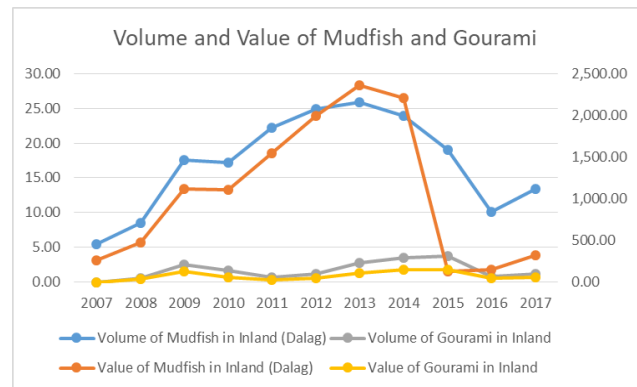


Fig. 22. Shows the volume and value of Mudfish and Gourami.

Fig. 23 shows the volume and value of freshwater catfish (*kanduli*) and freshwater eel (*igat*). For freshwater catfish, Capiz was ranked fifth (5th) in this kind of species produced. In 2015 the volume grew 13.77 metric tons, and the highest value was 1,300.43 in 2015. For freshwater eel, Capiz has no made with this species.

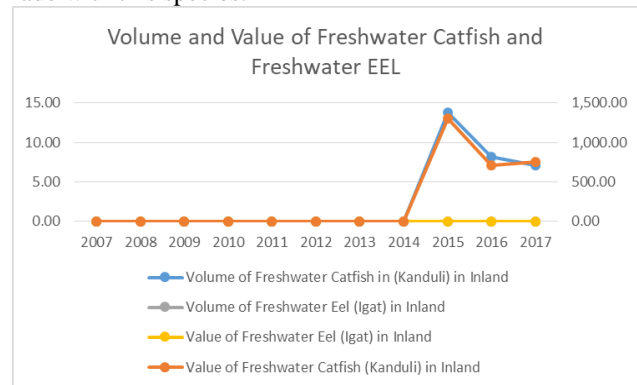


Fig. 23. Shows the volume and value Freshwater Catfish and Freshwater Eel.

Fig. 24 shows the volume and value of tilapia and freshwater catfish (*hito*). For tilapia, Capiz was ranked third (3rd) in this kind of species produced. In 2013, the volume grew 44.66 metric tons, and the highest value was 3,062.52 in 2013. For catfish (*hito*), Capiz was ranked second (2nd) and the highest volume produced was 26.22 metric tons in 2017, and the value was 2,552.24.

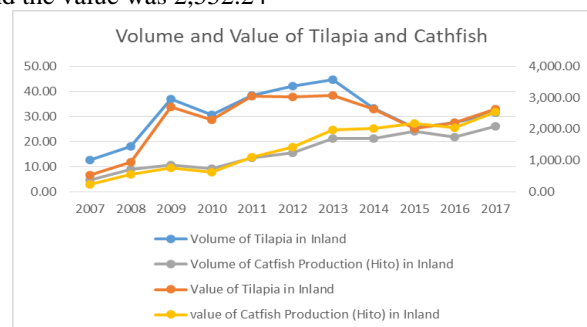


Fig. 24. Shows the volume and value of Tilapia and Cathfish.

Species in Aquaculture Fisheries

Fig. 25 shows the volume and value of grouper and carp. For grouper, Capiz was ranked first (1st) in this kind of species produced. In 2017, the volume grew 32.69 metric tons, and the highest value was 11,870.80.

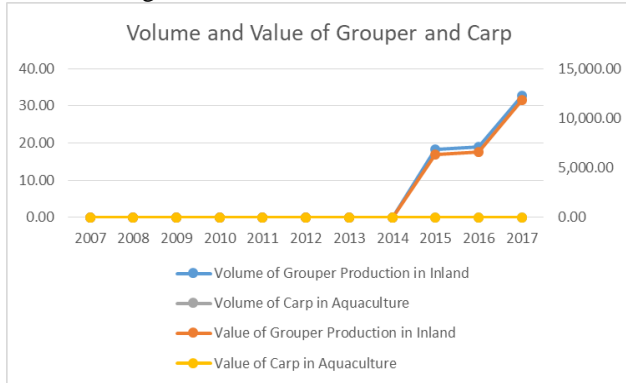


Fig. 25. Shows the volume and value of Grouper and Carp.

Fig. 26 shows the volume and value of catfish and grouper. For catfish, Capiz was ranked second (2nd) in this kind of species produced. In 2009, is the highest volume made and was 29.02 metric tons, and the highest value was 2,552.24 in 2017. For grouper, Capiz was ranked second (2nd). The highest volume produced was 32.69 metric tons in 2017, and the value was 11,870.80.

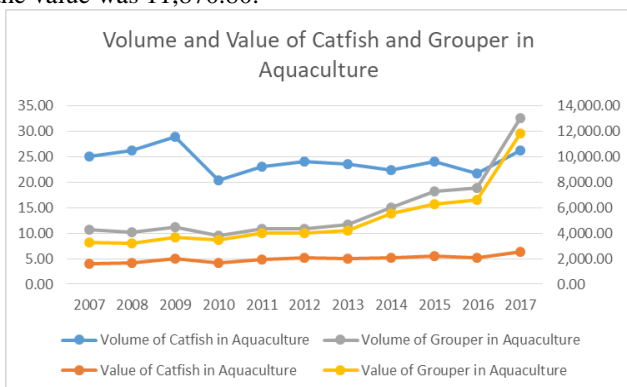


Fig. 26. Shows the volume and value of Catfish and Grouper in Aquaculture.

Fig. 27 shows the volume and value of milkfish and mud crab (*alimango*). For milkfish, Capiz was ranked first (1st) in this kind of species produced. In 2017, is the highest volume made and was 33,242.74 metric tons, and the highest value was 2,793,311.62.

For mud crab, Capiz was ranked first (1st). The highest volume produced was 2,048.37 metric tons in 2017, and the value was 853,046.57.

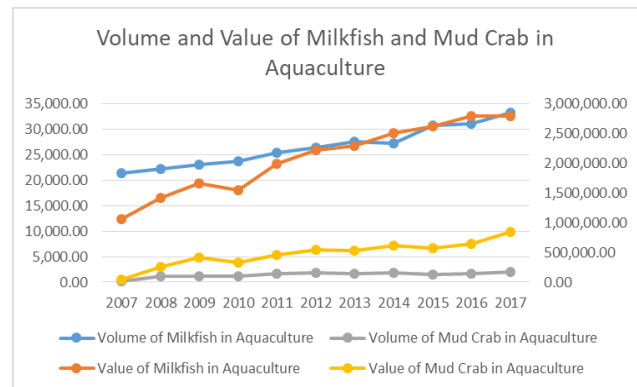


Fig. 27. Shows the volume and value of Milkfish and Mud Crab in Aquaculture.

Fig. 28 shows the volume and value of mussel (*tahong*) and oyster (*talaba*). For mussels, Capiz was ranked first (1st) in this kind of species produced. In 2017, is the highest volume made and was 9,032.38 metric tons. For the oyster, Capiz was ranked first (1st). The highest volume produced was 7,343.17 metric tons in 2017, and the value was 59,921.50.

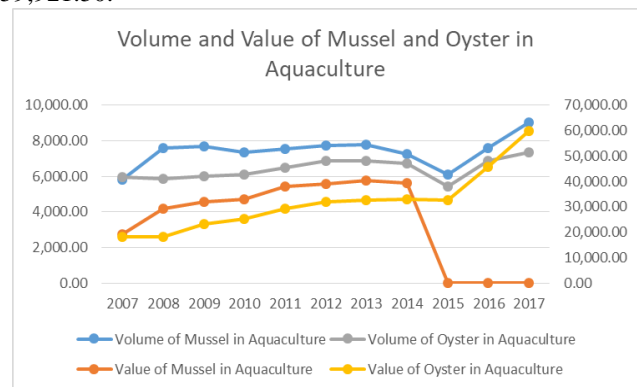


Fig. 28. Shows the volume and value of Mussel and Oyster in Aquaculture.

Fig. 29 shows the volume and value of tiger prawn (*sugpo*) and tilapia. For tiger prawns, Capiz was ranked first (1st) in this kind of species produced. In 2009, is the highest volume made and was 1,525.53 metric tons, and the value was 495,364.40. For tilapia, Capiz was ranked third (3rd). The highest volume produced was 283.69 metric tons in 2013, and the highest value was 18,376.05 in 2017.

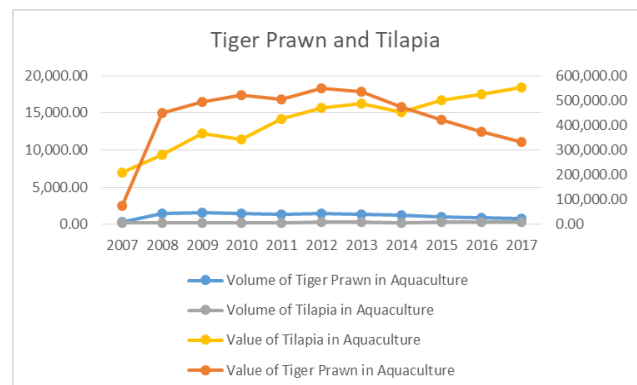


Fig. 29. Shows and value of Tiger Prawn and Tilapia.

Fig. 30 shows the volume and value of white shrimp (*hipong puti*) and endeavor prawn (*suahe*). For white shrimp, Capiz was ranked first (1st) in this kind of species produced. In 2017, is the highest volume made and was 11.39 metric tons, and the value was 1,977.34. For endeavor prawn, Capiz was ranked first (1st), and the highest volume produced was 99.45 metric tons, and the value was 15,962.21. The results highlight that the province, including Roxas City, made less on various industries and species to other areas in the Western Visayas; second, the production of Aquaculture species such as milkfish, mud crab, mussels, oyster, tiger, white, and endeavor prawn Capiz producing well.

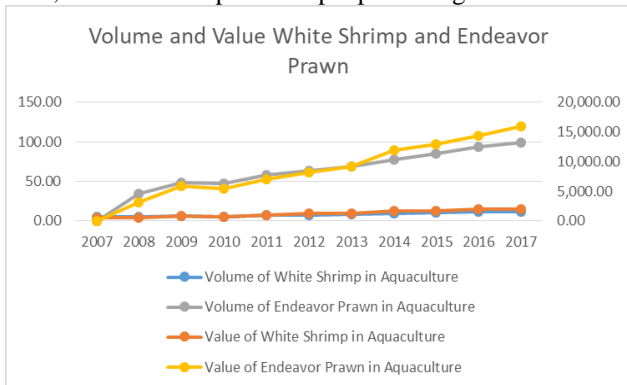


Fig. 30. Shows the volume and value of White Shrimp and Endeavor Prawn.

Production by type of Aquafarm

Fig. 31 shows the volume and value of production by type of aquafarm in the Province of Capiz. In brackishwater fishpond, Capiz was ranked first (1st) with the highest volume produced of 36,466.96 in 2017 with a value of 4,015,889.89.

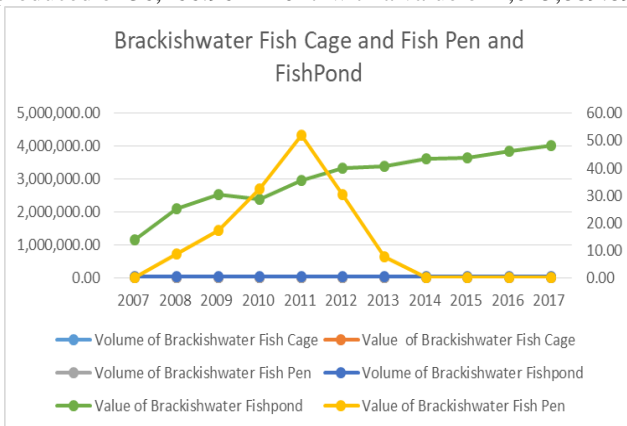


Fig. 31. Shows the volume and value of Fish Cage and Fish Pen and Fishpond.

Fig. 32 shows the volume and value of production by type of aquafarm in the Province of Capiz. The data shows that the Capiz had a minimal volume produced in freshwater fishpond production. BFAR also validates that the provincial government-mandated fish cage owners to stop their operation because it causes perennial floods in the province. After all, the Panay River level becomes low.

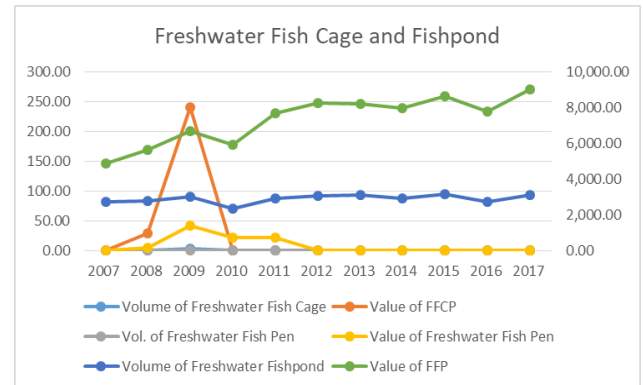


Fig. 32. Shows the volume and value Freshwater Fish Cage and Fishpond.

Fig. 33 shows the volume and value of production by type of aquafarm in the Province of Capiz. In the marine fish cage, Capiz was ranked third (3rd); the highest volume produced was 42.77 metric tons, with a value of 17,819.34.

On marine fish pen, the highest volume produced was 878.65, with a value of 70,396.17. But at present, there was no volume produced starting in 2014.

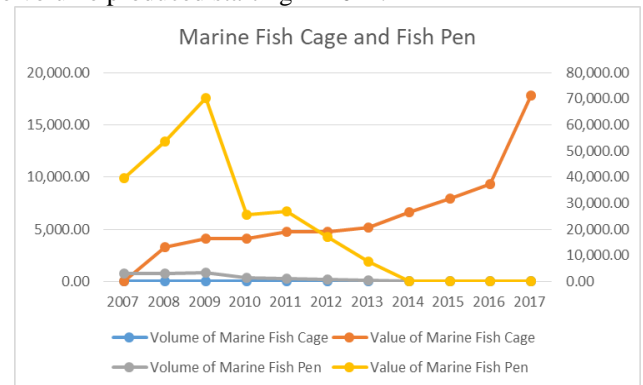


Fig. 33. Shows the volume and value of Marine Fish Cage and Fish Pen.

Fig. 34 shows the volume and value of production by type of aquafarm in the Province of Capiz. In oyster production, Capiz was ranked first (1st) with the highest volume produced of 7,343.17 and with a value of 59,921.50 in 2017.

On mussel production, Capiz was also ranked first (1st) with the highest volume produced of 9,032.38 with a value of 97,814.62 in 2017.

Based on the data presented, the following findings are: (1) on the volume and value of production by type of aquafarm the Province of Capiz is producing high on the brackishwater fishpond; (2) in marine fish pen starting 2014 to 2017, there was no production; (3) in Oyster and Mussel, the province is commendable due to its volume produced because it was ranked first in the Western Visayas.

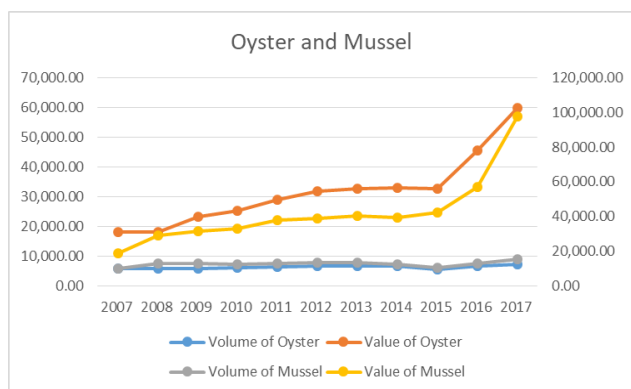


Fig. 34. Shows the volume and value of Oyster and Mussel.

Top Fisheries Producing Provinces by Sector

This section presented the data on the top fisheries producing provinces by sector. From the year 2005 to 2010, the Province of Capiz was not part of the list.

2010-2012-Marine Municipal

The province ranked seventh (7th) among nine (9) provinces in the Philippines on the average annual production of 37,258.03 with a percent share of 3.28 and a cumulative share of 38.26.

On the other hand, the province ranked eighth (8th) among nine (9) areas in the Philippines in terms of the average annual production of 35,840.58 metric tons with a percent share of 3.27 and a cumulative share of 40.65.

2015-2017-Marine Municipal

The Province of Capiz was ranked ninth (9th) among nine provinces in the Philippines in terms of the average annual production of 28,468.93 metric tons with a percent share of 2.89 and cumulative share of 41.70.

VII. CONCLUSIONS AND RECOMMENDATION

Among fishing industries where the Capiz involved with Commercial, Marine Municipal, Inland Municipal produced poorly. On the other hand, the province is doing well in aquaculture species production like milkfish, mud crab, mussel, oyster, white shrimp, tiger, and endeavor prawn produced by an identified municipality Ivisan, Pontevedra, Pilar, Panay, President Roxas, and Roxas City.

Brackishwater fishpond production based on volume and value, the Province of Capiz is doing well due to the increasing volume produced for the last eleven (11) years.

The claim of the Roxas City government as the Seafood Capital of the Philippines has no basis on various sources like policy passed by the Provincial and City government.

The baseline data used by the researchers quantify and prove that Roxas City is not producing seafood abundantly.

The branding of Roxas City as the Seafood Capital of the Philippines is a myth based on the researchers' investigation through various analyses such as on the trends of volume and

value, types of production, and species. Hence, the production stage is not from Roxas City, but it is only a gateway of logistics from neighboring municipalities and provinces. Roxas City, specifically the Libas Fishing Port, delivered and distributed to other parts of the country and local businesses.

With the above conclusions, the following recommendations are: first, the policymakers in the Province of Capiz may formulate a policy or revised any provisions to support the claim that Roxas City is the Seafood Capital of the Philippines; second, the growers and entrepreneurs may look into sustainable fishing basically in the aquaculture side to improve its production and value; third, the higher education institutions may study the supply chain management of aquaculture products for value-adding; fourth, may the BFAR of the Province of Capiz may look into consideration for sustaining and developing the competitive edge of the province with regards to aquaculture products and improving its value proposition and studying and producing other species also available in the area; and lastly, improve the fishing tourism industry of the Province of Capiz through a social marketing plan, and inclusivity of the claims.

REFERENCES

- [1] BFAR National Program for Municipal Fishing
- [2] Fisheries Statistics Division, PSA (www.psa.gov.ph)
- [3] Fisheries Statistics of the Philippines, 2007-2017
- [4] Food and Nutrition Research Institute Website, (<http://www.fnri.dost.gov.ph>)
- [5] FAO Yearbook, Fishery, and Aquaculture Statistics (<http://www.fao.org>)
- [6] Directory of Philippine Wetlands, Volume II, AWBPFI
- [7] National Accounts of the Philippines, Philippine Statistics Authority (PSA)
- [8] 1992 Fishery Statistics, Bureau of Agricultural Statistics (BAS)
- [9] 2002 Census of Fisheries Trade Statistics Division, PSA Regulatory and Licensing Division (FRLD), BFAR
- [10] Vessels and Gears Registration (BoatR)
- [11] Price Statistics Division, PSA
- [12] MacInnis, D.J. and Jaworski, B.J. (1989) 'Information Processing from Advertisements: Toward an Integrative Framework', *Journal of Marketing* 53 (October): 1–23.
- [13] MacInnis, D.J., Moorman, C. and Jaworski, B.J. (1991) 'Enhancing and Measuring Consumers' Motivation, Opportunity, and Ability to Process Brand Information from Ads', *Journal of Marketing* 55 (October): 32–53.

High Speed Data Transmission Using Light Fidelity

^[1] Bharath Kumar K, ^[2] Gagan Kumar, ^[3] Vaibhav S Biradar, ^[4] Dr. Mangala Gowri S G

^{[1][2][3]} Student, Dept. of EEE, R. R. Institute of Technology, Bengaluru, VTU, Karnataka, India

^[4] Associate Professor, Dept. of EEE, R. R. Institute of Technology, Bengaluru, VTU, Karnataka, India

Abstract— *Current era many people are using internet to accomplish their task through wired or wireless network. As no of users get increased in wireless speed decreases proportionally. Though Wi-Fi gives us speed up to 150Mbps as per IEEE 802.11n, it is still insufficient to accommodate no of users. To remedy this limitation of Wireless Fidelity, we are introducing concept of Li-Fi. As per german physicist Harald Haas data through illumination taking the fiber out of fiber optic by sending data through an LED light bulb that varies in intensity faster than the human eye can follow. It's the same idea behind infrared remote controls but far more powerful. Haas says his invention, which he calls D-LIGHT, can produce data rates faster than 10 megabits per second, which is speedier than your average broadband connection.*

Index Terms— *Wi-Fi, Light-emitting diode (LED), Video LAN Client (VLC), Technology, Entertainment and Design (TED), Visible Light, Data utilization, server, lamp driver.*

I. INTRODUCTION

Li-Fi, as coined by Prof. Harald Haas during his TED Global talk,^[1] is bidirectional, high speed and fully networked wireless communications similar to Wi-Fi. Li-Fi is a subset of optical wireless communications (OWC) and can be a complement to RF communication (Wi-Fi or Cellular network), or are placed in contexts of data broadcasting. It is wireless and uses visible light communication or infra-red and near ultraviolet (instead of radio frequency waves) spectrum, part of Optical wireless communications technology, which carries much more information, and has been proposed as a solution to the RF-bandwidth limitations. A complete solution includes an industry led standardization process. Light Fidelity is a wireless communication technology which enables a wireless data transmission through LED light. Light Fidelity is based on a unique ability of solid state lighting systems to create a binary code of 1s and 0s with a LED flickering that is invisible for human eyes. Data can be received by electronic devices with photodiode^[3] within area of light visibility. This means that everywhere where LEDs are used, lighting bulbs can bring not only the light but wireless connection at the same time. With increasing demand for wireless data, lack of radio spectrum and issues with hazardous electromagnetic pollution, Light

Fidelity appears as a new greener, healthier and cheaper alternative to WiFi. The term was first used in this context by Harald Haas in his TED ^[4] Global talk on Visible Light Communication. The technology was demonstrated at the 2012 Consumer Electronics Show in Las Vegas using a pair

of Casio smart phones to exchange data using light of varying intensity given off from their screens, detectable at a distance of up to ten meters. In October 2011 a number of companies and industry groups formed the Light Fidelity Consortium, to promote high-speed optical Wireless systems and to overcome the limited amount of radio based wireless spectrum available by exploiting a completely different part of the electromagnetic spectrum. The consortium believes it is possible to achieve more than 10 Gbps, theoretically allowing a high-definition film to be downloaded in 30 seconds. Li-Fi has the advantage of being able to be used in sensitive areas such as in aircraft without causing interference. However, the light waves used cannot penetrate walls ^[5]. Later in 2012, Pure VLC, a firm set up to commercialize Li-Fi, will bring out Li-Fi products for firms installing LED-lighting systems. Moreover Li-Fi makes possible to have a wireless Internet in specific environments (hospitals, Airplanes etc.) where Wi-Fi is not allowed due to interferences or security considerations. gives nice opportunities for transmitted data. —It is possible to encode data in the Light by varying the rate at which the LEDs flicker on and off to give different strings of 1s and 0s. The LED intensity is modulated so rapidly that human eye cannot notice, so the output appears constant. More sophisticated techniques could dramatically increase VLC data rate. Terms at the University of Oxford and the University of Edinburgh are focusing on parallel data transmission using array of LEDs, where each LED transmits a different data stream. Fig2: Harald Haas Other groups are using mixtures of red, green and blue LEDs to alter the light frequency encoding a different data channel. The Li-Fi Consortium is an international platform focusing on optical wireless Technologies. It was founded by four Technology based organizations in October 2011. In technical terms, LI-FI is a light communication system that is capable of transmitting data at high speed over the visible, ultraviolet infrared spectrums. In its present states only LED lamps can be used for the transmission of data in visible light. In terms of its end use, the technology is similar to WI-FI, the key technical difference being that WI-FI uses radio frequency to induce a voltage in an antenna to transmit data, whereas LI-FI uses the modulation of light intensity to transmit data. LI-FI can theoretically transmit at speed of up to 100Gbits/s.

II. LITERATURE

The most of the people are using Wi-Fi Internet devices, which will be useful for 2.4-5GHz RF to deliver wireless Internet access surrounded our home, offices, schools, and

some public places also. We are quite dependent upon these nearly ubiquitous services [7-15]. While Wi-Fi can cover an entire house, school, the bandwidth is limited to 50-100 megabits per seconds (Mbps). It is a most current Internet services, but insufficient for moving large data files like HDTV movies, music libraries and video games. The most of the dependent upon 'the cloud' or our own 'media services' to store all of our files, including movies, photos, audio and video devices, games, the more and most bandwidth and speed should be needed to access this data. Therefore RF-based technologies such as today's Wi-Fi are not the optimal way. In addition, Wi-Fi may not be the most efficient way to provide new desired capabilities such as precision indoor positioning and gesture recognition. The optical wireless technologies, sometimes called visible light communication (VLC), and more recently referred to as Li-Fi. On the other hand, offer an entirely new paradigm in wireless technologies in the terms of communication speed, usability and flexibility, reliability.

III. DESIGN AND IMPLEMENTATION

On this system, light emitter on one end, for example, an LED, and a photo detector on the other. The photo detector registers a binary one when the LED is on; and a binary zero if the LED is off. To build up a message, flash the LED numerous times or use an array of LEDs of perhaps a few different colors, to obtain data rates in the range of hundreds of megabits per second. Light-emitting diodes can be switched on and off faster than the human eye can detect, causing the light source to appear to be on continuously, even though it is in fact 'flickering'. The on-off activity of the bulb which seems to be invisible enables data transmission using binary codes: switching on an LED is a logical '1', switching it off is a logical '0'. By varying the rate at which the LEDs flicker on and off, information can be encoded in the light to different combinations of 1's and 0's. The data can be encoded in the light by varying the flickering rate at which the LEDs flicker on and off to generate different strings of 1s and 0s. The LED intensity is modulated so rapidly that human eye cannot notice, so the light of the LED appears constant to humans. Block Diagram of Li-Fi System The method of using transmit information wirelessly is technically referred to as Visible Light Communication (VLC), though it is popular called as Li-Fi because it can compete with its radio based rival Wi-Fi connection devices within room. Many other sophisticated techniques can be used to dramatically increase VLC data rate. The LED data rate is directly transmits a different data streams.

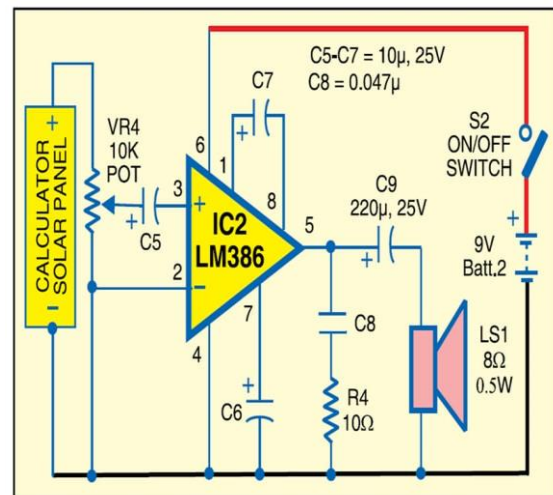


Fig:1 Circuit diagram of LI-FI

IV. RESULTS AND DISCUSSION

The concept of Li-Fi is used in our project to transfer an audio signal into a speaker through visible light. The audio signal is given through both a smartphone and a mic. The LED used as the medium to provide the visible light, because it is the fastest method to turn on and off the light. The receiver section consists of a photodetector which absorbs the audio signals through visible light and gives it to the speaker. The speed needed to transfer the audio is less than 0.5 seconds. The data transfer speed is 1 gigabit. Thus we successfully transmitted the audio signal into a speaker with the help of light at a very high speed rate.

V. CONCLUSION

There are a plethora of possibilities to be explored in this field of technology. If this technology becomes justifiably marketed then every bulb can be used analogous to a Wi-Fi hotspot to transmit data wirelessly. The possibilities are numerous and can be explored further. If this technology can be put into practical use, every bulb can be used something like a Wi-Fi hotspot to transmit wireless data and we will proceed toward the cleaner, greener, safer and brighter future. The concept of Li-Fi is currently attracting a great deal of interest, not least because it may offer a genuine and very efficient alternative to radio-based wireless. As a growing number of people and their many devices access wireless internet, the airwaves are becoming increasingly clogged, making it more and more difficult to get a reliable, high-speed signal. This may solve issues such as the shortage of radio-frequency bandwidth and also allow internet where traditional radio-based wireless isn't allowed such as aircraft or hospitals. One of the shortcomings however is that it only works in direct line of sight.

REFERENCES

- [1] Ravi Prakash, Prachi Agarwal —The New Era of Transmission and Communication Technology : Li-Fi (Light Fidelity) LED & TED Based Approachl, International Journal of Advanced Research in Computer Engineering & Technology (IJARCET) Volume 3, Issue 2, February 2014
- [2] Jitender Singh, Vikash —A New Era in Wireless Technology using Light-Fidelityl International Journal of Recent Development in Engineering and Technology ISSN 2347- 6435(Online) Volume 2, Issue 6, June 2014.
- [3] R.Karthika, S.Balakrishnan —Wireless Communication using Li-Fi Technologyl SSRG International Journal of Electronics and Communication Engineering (SSRG-IJECE) volume 2, Issue 3 March 2015
- [4] Dinesh Khandal, Sakshi Jain —Li-Fi (Light Fidelity): The Future Technology in Wireless Communicationl International Journal of Information & Computation Technology. ISSN 0974- 2239 Volume 4, Number 16 (2014)

Smart Solar Power Management System for Domestic Purpose

^[1] Pratik Chaudhary, ^[2] Dr. Mangala Gowri S.G, ^[3] Vikash Kumar Sah, ^[4] Sikindra Kumar Thakur, ^[5] Arun Prasad Yadav
^{[1][3][4][5]} Student, Dept. of EEE, R. R. Institute of Technology, Bengaluru, VTU, Karnataka, India
^[2] Associate Professor, Dept. of EEE, R. R. Institute of Technology, Bengaluru, VTU, Karnataka, India

Abstract— *The integration of small sized standalone solar systems to the grid is technically complicated resulting into expensive operation which is not affordable to all. As such, this paper will presents a smart controller based design using digital signal processing for cost effective operation of solar-grid tied system. The hybrid system is able to size the connected system and deploy the operation strategy so as to get the effective utilization of solar output. The synchronization is not necessary as this method can be effectively altered by the use of load discretization. This gives cheap, efficient, reliable and cost effective operation. The system has been tested for the 50Watt solar panel with the battery backup storage and its effectiveness will be observed. The battery backup is made to operate during the cut off of Grid or Grid and Solar supply. The performance of the system over the wide range of operation and transient states are assured by practical observation and modification. This system is defined to fill the necessity of regions where solar power is used only as back up purposes to charge the battery and is actively dumped during the presence of active grid. These regions include many parts of the world where grid cut off is common due to the shortage of energy.*

Index Terms— *Solar Systems, load discretization, Solar panel, SPWM inverter, Dump Power utilization*

I. INTRODUCTION

conversion of energy from sunlight into electricity, either directly using photovoltaics (PV), indirectly using concentrated solar power, or a combination. Concentrated solar power systems use lenses or mirrors and solar tracking systems to focus a large area of sunlight into a small beam. Photovoltaic cells convert light into an electric current using the photovoltaic effect. Photovoltaics were initially solely used as a source of electricity for small and medium-sized applications, from the calculator powered by a single solar cell to remote homes powered by an off-grid rooftop PV system.. As the cost of solar electricity has fallen, the number of grid-connected solar PV systems has grown into the millions and utility-scale photovoltaic power stations with hundreds of megawatts are being built. Solar PV is rapidly becoming an inexpensive, low-carbon

technology to harness renewable energy from the Sun. The overwhelming majority of electricity produced worldwide is used immediately since storage is usually more expensive and because traditional generators can adapt to demand. Both solar power and wind power are variable renewable energy, meaning that all available output must be taken whenever it is available by moving through transmission lines to where it can be used now. Since solar energy is not available at night, storing its energy is potentially an important issue particularly in off-grid and for future 100% renewable energy scenarios to have continuous electricity availability. The alternative energy is definitely the choice of future energy as the cost of conventional energy and its availability continues to reduce.

II. LITERATURE

1. Krishna Neupane, Amit Rouniyar paper published reviews the existing methods and techniques used for distributing the load across the grid and solar power with the real time operation
2. Christopher B Barth, Thomas Foulkes, Intae Moony, Yutian Leiz, Shibin, Qin Robert C.N. Pilawa-Podgurski had published paper the energy density and quality factor of ceramic capacitors is compared to polyester and polypropylene film capacitors
3. P. Nagalaxmi, M. Veda Chary has proposed a system to distribute the power generated from renewable source efficiently.
4. G. Saravanan, Prakash, K.Dhanapal, M. Gowtham ,P. ArunKumar, KPR had published paper

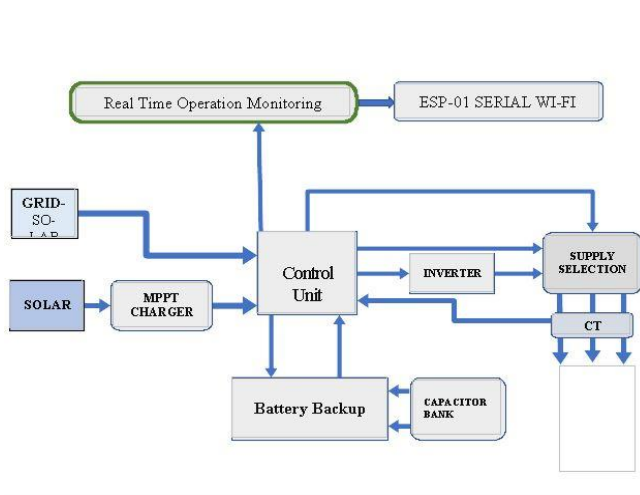


Fig : 1 Current Practice with Solar Energy at Houses

5. which explains lead acid battery charging process from Solar system by using the buck ,buck-boost, boost modes of operation.
6. Parimita Mohanty, K. Rahul Sharma, Mukesh Gujar, Mohan Kolhe and Aimie Nazmin Azmihad published paper with emphasized with Solar Energy

III. DESIGN AND IMPLEMENTATION

Various methods have been purposed to synchronize the grid and PV to supply of the load however this is not feasible for places where grid cut-off is a common problem. Also, voltage and frequency fluctuation in these regions are well beyond the ability that can be designed for the inverter to accept for synchronization and provisions for feeding energy from the households to the grid are not defined properly. With the current scenario grid, which is extremely unreliable, is used as the main source of energy which feeds general loads at household including lightings, televisions, computers etc, and battery backup and solar energy is utilized with the separate circuit for separate critical loads that have to be utilized during the grid cut-off. Thus, the energy source and the load systems are independent of the grid and solar systems are underutilized during the active grid with fully charged battery as the energy received from the solar during this phase is dumped. This introduces the waste of energy. Even if the amount of the energy thus dumped is lower in the range of few watts to sometimes up to few kW depending upon its location, these energy if utilized in many houses including the houses from towns and remote areas can add up a huge amount of energy. This consequently helps to both grid load reduction as well as reduction in the energy metering in the household. The method of reverse energy metering is mentioned in; however this is not possible in the developing countries where they don't have provisions for such. Further, the load scheduling, fluctuating voltage and frequency makes this option obsolete. A method to supply the load with synchronization with grid is purposed; however this is also not feasible during the period

of grid cut-off. This paper here gives an overview of an alternative economical and technical feasible smart controller based discretized method for the utilization of the dumped power. Further it explains in details how this is achieved technically and its practical implementation observation and stability. The approaches are further discussed and evaluated in order to recognize its integration with the existing technology.

A simple method with discrete control algorithm is developed and implemented to overcome the effects of neglecting the solar energy during the case where battery is fully charged and grid is active. Microcontroller based system is developed to govern the above requirement with the pre-defined algorithm to utilize the full energy from the PV panel and add the remaining requirement from either grid or battery. This makes solar energy effectively operate even during the presence of the grid supply. For the period where the grid and PV both operating, two methods can be applied. Either the energy from the PV is synchronized with the grid and supplied to the load or discrete switching can be implemented with cheap and effective operation without having to use complicated and expensive phase locked loop control and synchronization algorithm. The discretized method is prioritized and implemented in the lab. This proposed technology can also be utilized in the developed countries as well for cheap and reliable alternative to grid synchronization as it promises to not only reduce the

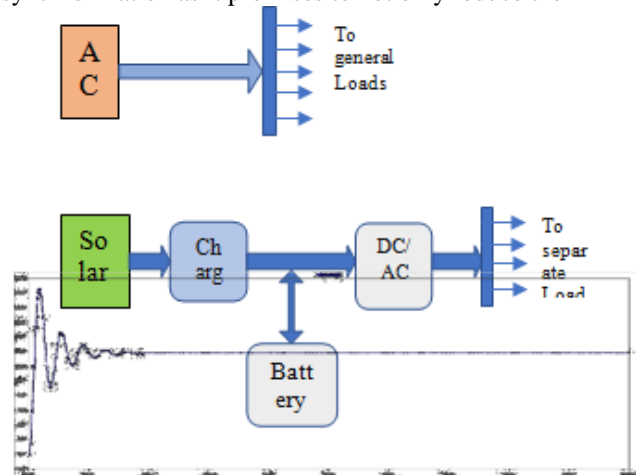


Fig : 2 Switching Load Feed between Grid and Solar/PV Battery

electricity consumption from the Grid and thus the bill of electricity but also make the reliable supply to the load in the home. Fig 3 . Controller Algorithm The sizing of the system is done according to the load profile. Load profile is a combination of regular house load. The discretization method is applied to distribute the available power resource to various loads in the system. This Algorithm has been designed with an increase in the capability of the system by modifying the design constraints

IV. RESULTS AND DISCUSSION

An LT-spice as the stimulation tool where synchronous buck converter has been stimulated it is based on the Ir2104 half bridge driver. After the stimulation we had performed this with Real hardware and we got this result in order to get proper pure DC we had connected 2 Capacitor of 50v ,1000uf and we got almost pure DC in order to Charge the battery or supply to the Inverter. By using this filter we had connected electrolytic capacitor to get stable Dc output.

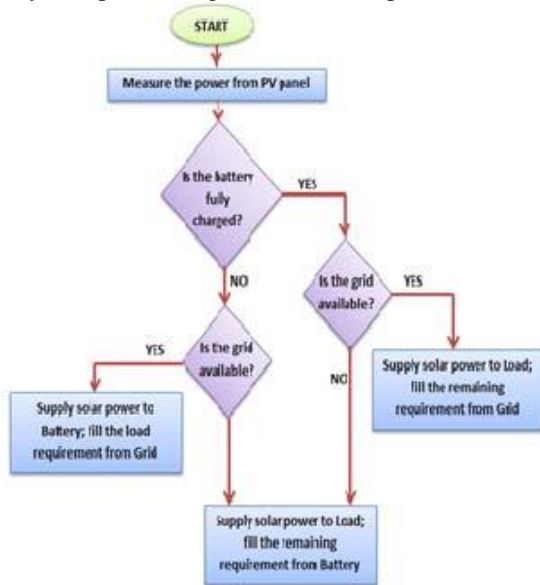


Fig: 3 Flow Chart of Smart Solar System

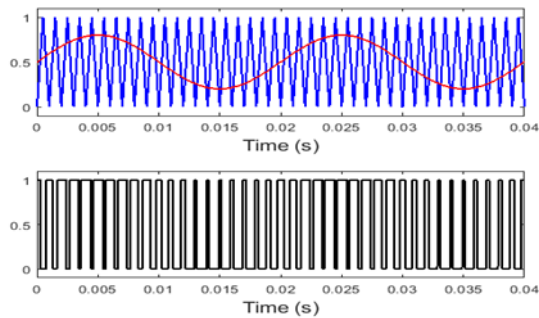


Fig : 4 Switching wave of SPWM

In this work the output through code so we programmed

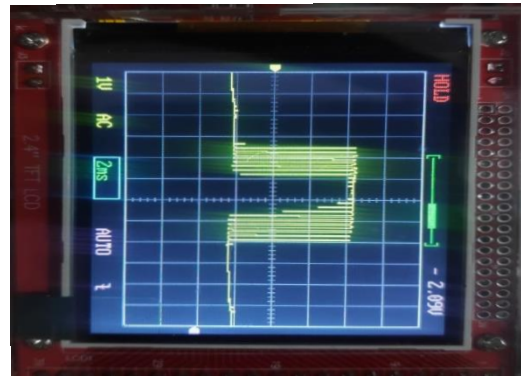


Fig: 5 Spwm wave received from Micro controller

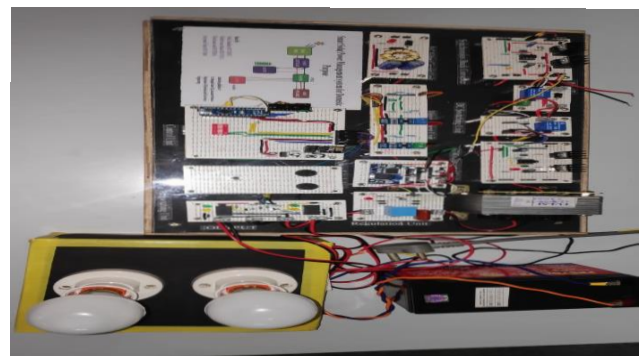


Fig: 6 Complete Project setup

microcontroller by plotting the data we get the result. By using this Spwm Code we were able to get the Spwm wave as shown in the DSO. The complete project consists of two Led Bulb as the Loads and there is switching either load should be Operated from the Solar Power or Ac Grid.

IV. CONCLUSION

The method and algorithm is presented for smart Solar power management system for Domestic purpose controller, specifically for the utilization of usually dumped power from the Solar PV. All methods rely on the ability to make effective co-operation of the different units in the hybrid system, and mainly the programming algorithm and interface used with smart controller. The described algorithm is demonstrated with practical observation from the lab. Even in case where government has policies for Grid-tied system this method can be used for cheap alternative to save energy. Research along this direction will expand the scope and applicability of reducing the current scenario of energy crisis.

REFERENCES

- [1] Krishna Neupane, Amit Rouniyar“Smart Controller Design for Solar-Grid Hybrid System, Microcontroller based automatic adjustable discretized solar-grid integration system” IEEE, 2013
- [2] M.Subashini, M. Ramaswamy “A Novel Design Of Charge Controller For A Standalone Solar Photovoltaic System”IEEE 978-1-4673-8262-5/16,2016

- [3] Christopher B Barth, Thomas Foulkes, Intae Moony, YutianLeiz, Shubin Qin, Robert C.N. Pilawa-Podgurski “Experimental Evaluation of Capacitors for Power Buffering in Single-Phase Power Converter” IEEE transaction of Power electronics,2018
- [4] G.Saravanan ,P.Prakash ,K.Dhanapal ,M.Gowtham ,P.Arun Kumar “Lead-acid Battery Charging with a Buck-Boost Power Converter for a Solar Powered Battery Management System” IJERP Vol 1,Issue 9,2015
- [5] Parimita Mohanty, K.RahulSharma,Mukesh Gujar, Mohan Kolhe and AimieNazminAzm “PV System Design for Off-Grid Applications”IEEE10.1007/978-3-319-14663-8_3 ,2015
- [6] Jeng-Nan Juang and R. Radharamanan “Design of a Solar Tracking System for Renewable Energy” IEEE, 2014
- [7] Yash Ajgaonkar,Mayuri Bhirud ,Poornima Rao “Design of Standalone Solar PV System Using MPPT Controller and Self-Cleaning Dual Axis Tracker” IEEE 2019
- [8] P. Nagalaxmi, M. Veda Chary “Efficient Energy Management System with Solar Energy”IJMER Vol3,Issue 5, 2013
- [9] Layate Zakaria, Bahi Tahar, Abadiallssam, LekhchineSalima, Bouzeria Hamza “Static variable load for grid-connected photovoltaic system”Energy Procedia 74 ,2015
- [10] Parimita Mohanty, Karnamadakala Rahul Sharma, Mukesh Gujar,Mohan Kolhe “PV System Design for Off-Grid Applications” sept 2015

EEG data processing for Emotion detection using DTCWT and FFNN Architecture Design

^[1]Dr. Mangala Gowri S.G, ^[2]Priyanka Nagendra Shindogi, ^[3]Sneha Joesphine

^[1]Associate Professor, Dept. of EEE, R. R. Institute of Technology, Bengaluru, VTU, Karnataka, India

^{[2][3]} Student, Dept. of EEE, R. R. Institute of Technology, Bengaluru, VTU, Karnataka, India

Abstract— Emotion detection and classification algorithms developed are based on wavelet features and neural network approaches which have limited to software implementation only. Very little literature is reported on hardware implementation of EEG detection and classification approaches. One of the major challenges in hardware implementation is the computation complexity of DWT processor and FFNN architecture. In this paper, architectures for data path operation of both DWT and FFNN structures are designed and are implemented on FPGA platform. A low power and high speed architectures for DTCWT and neural network are designed based on customized systolic array logic and reusable data path circuitry respectively. The nine-stage DTCWT architecture designed is designed to work at maximum frequency of 322 MHz consuming less than 0.71 W of power. The FFNN structure is designed to operate at maximum frequency of 321 MHz consuming less than 2.2 W of power. Both of the architectures are suitable for real time EEG data processing.

Index Terms— DTCWT, Emotion detection, FFNN architecture, FPGA platform

I. INTRODUCTION

With complex wavelet transforms demonstrating shift invariance property, EEG signal analysis using Dual Tree Complex Wavelets (DTCWT) has recently gained much importance. In EEG data processing, artifacts that get integrated with EEG recording cause disturbances in accurately extracting features. Due to the complex interconnections between billions of neurons, the recorded EEG signals are complex, non-linear, non-stationary and random in nature, **U.R. Acharya** [1]. Feature based classification algorithm based on neural network approaches rely on input data vector and the intensity levels of feature vectors for accurate classification. The trained network weights and biases that process the input data performs classification of emotions and any deviations in input patterns may lead to unsuccessful in classification. In addition to artifacts, any movement electrode due to head movement also introduces artifacts. Further to artifacts, recording of EEG data at different time intervals also lead to variations in event occurrence in EEG. In order to design reliable and invariant system for feature detection and classification, DTCWT is used in place of DWT. In this paper, a detailed discussion on EEG feature detection and classification based on DTCWT and Feed Forward Neural Network (FFNN) is presented. DTCWT is

an enhancement to the discrete wavelet transform (DWT). It is a shift invariant and directionally selects two and higher dimensions, **Selesnick Ivan W** [2]. It achieves a redundancy factor of 2^d for d-dimensional signals, which is lower than the undecimated DWT. The multidimensional (M-D) DTCWT Transform is non separable but is based on a computationally efficient, separable filter bank (FB). The DTCWT of a sign, $x(n)$ is executed utilizing two fundamentally inspected DWT's as a part of parallel on the same information. DTCWT coefficients are non-swaying with an almost move invariant greatness and altogether lessened associating with more directionalities when contrasted with the DWT. Thus is it more efficient in time frequency localization of EEG signal. Similar to the positive or negative post-filtering of real subband signals, the idea behind dual tree approach is quite simple. **Kingsbury N** [3] according to the author, DWT is very sensitive in the translation, it is very less effective in the domain of statistical signal processing. To address the, shift-variance problem a new method is employed by considering two DWT's, one of DWT gives the real part of the transformed co-efficients and the other one gives the imaginary part. By combining the co-efficients of two DWT's into complex-valued co-efficients, a new transform is obtained by the name Dual Tree Complex Wavelet Transform (DTCWT). This new transform has some, characteristic properties including near shift-invariance, better directional selectivity, which is very important in signal processing. **Musa et. al** [4], in this study first the features of EEG data are extracted using a dual-tree complex wavelet transformation at different levels of granularity to obtain size reduction and statistical features are extracted. Five statistical features are extracted from new dataset with reduced size and are classified with the help of Complex valued neural networks (CVANNs) using DTCWT in the classification of EEG data. The proposed method is tested using a benchmark of EEG dataset, and high accuracy rates are obtained. The stated results show that the proposed method can be used to design an accurate classification system for epilepsy diagnosis. **R.Y.Yu** [5] proposed that DWT is not able to cancel the aliasing, thus resulting in unclearly separated sub-bands. The dual-tree complex wavelet transform (DTCWT) was first introduced by Kingsbury, and he proposed to extract the signal component related to sensory motor rhythms. There are several 1D-DWT architectures the most popular ones are, Direct Mapped Architecture, Folded Architecture, MAC Based Programmable Architecture, Flipping Architecture,

Generalized Architecture, Recursive Architecture, Dual Scan Architecture and DSP Type Architecture. In this paper architectures for data path operation of both DWT and FFNN structures are designed and are implemented on FPGA platform. The literature survey of the previous works are summarised here .

Po-Cheng Wu and Liang-Gee Chen [6] propose DWT architectures which are based on linear convolution property of the wavelet filters. The architecture proposed uses multipliers, adders and memory elements in computing wavelet coefficients. The mathematical analysis in this architecture is presented, for hardware implementation thus becomes the basic design.

Wim Sweldens [7] proposes the lifting scheme computation of DWT, however, it is more popular over the convolution-based scheme for its lower computational complexity. Compared to the convolution-based algorithm, the lifting-based computation involves much less number of multipliers, adders and storage elements. The above attributes make the lifting scheme more suitable for low-complexity hardware implementation of DWT. For an efficient implementation of DWT computation, different architectures have been proposed. The polyphase matrix of a wavelet filter is decomposed into a sequence of alternating upper and lower triangular matrices and a diagonal matrix to obtain the so-called lifting-based architectures with low hardware complexity. However, such architectures have a long critical path, which results in reducing the processing rate of input samples.

A. S. Lewis and G. Knowles [8] proposed single-stage architectures in which the DWT computation is performed using a recursive pyramid algorithm (RPA). The computation complexity is reduced, however, the latency of the design and design of intermediate memory structure for recursive architecture are the limitations.

C. Chakrabarti and M. Vishwanath [9] have proposed a single-stage SIMD architecture that is aimed at reducing the computation time. The control logic in this design is very complex and data synchronization is one of the most challenging aspects in this design.

A. Grzeszczak et. al [10] have proposed single-stage systolic array architecture with a reduced hardware resource. The throughput and latency are found to be higher than the other architectures compared in the paper, as the systolic cell requires more number of multipliers and adders the area requirement is huge in this structure.

Chao Cheng and Keshab K. Parhi [11] have proposed a high-speed single-stage architecture based on hardware-efficient parallel finite-impulse response (FIR) filter structures for the DWT computation. These structures differ in terms of size of arithmetic-unit, on-chip memory, cycle period and average computation time (ACT). The architecture proposed is based on mathematical analysis, for practical implementation on FPGA or VLSI platforms. Use of appropriate number system would complicate the proposed architecture.

S. Masud and J. V. McCanny [12] have proposed a technique for the design of efficient, modular, and scalable pipeline architecture by using reusable silicon intellectual property (IP) cores for the DWT computation. The pipeline architectures have the advantages of requiring a small memory space and a short computing time and are suitable for real-time computations. The computational performance of such architectures could be further improved, provided that the design of the pipeline makes use of inter and intrastate parallelisms to the maximum extent possible, synchronizes the operations of the stages optimally, and utilizes the available hardware resources judiciously.

II. DESIGN OF DTCWT ALGORITHM

The DTCWT uses analytic filters to perform the wavelet analysis. DTCWT has a more complex structure compared to standard DWT, the dual tree CWT employs two real DWT's the first DWT gives the real part of the transform and is called the real tree while the second DWT gives the imaginary part called the imaginary tree that work parallel to each other, as shown in Fig. 1. One of these trees is called the real tree, whereas the other is called the imaginary tree. DTCWT uses a pair of filters for mother wavelet function $\psi(t)$ and scaling function $\phi(t)$. Let the filters $h_0(n)$, $h_1(n)$ denote the low-pass and high-pass filter pair for the upper FB, and let $g_0(n)$, $g_1(n)$ denote the low-pass/high-pass filter pair for the lower FB [12][2]. Wavelet function and scaling functions are represented by Eq. (1) and Eq. (2),

$$\psi_h(t) = \sqrt{2} \sum_n h_n \phi_h(2t - n) \quad (1)$$

$$\phi_h(t) = \sqrt{2} \sum_n h_0(n) \phi_h(2t - n) \quad (2)$$

The two real wavelet transforms uses two different sets of filters, with each satisfying the PR conditions. The two sets of filters are jointly designed so that the overall transform is approximately analytic. The two real wavelets are associated with each of the two real wavelet transforms are denoted as $\psi_h(t)$ and $\psi_g(t)$. The PR conditions, the filters are designed so that the complex wavelet $\psi(t) = \psi_h(t) + j\psi_g(t)$ is approximately analytic [2]. $\psi_g(t)$ is designed approximately as the Hilbert transform of $\psi_h(t)$ where $\psi_g(t) \approx H\{\psi_h(t)\}$. The DTCWT is not a critically sampled transform as it is two times extensive in one-dimensional because the total output data rate is exactly twice the input data rate. The inverse of the dual-tree CWT is as simple as the forward transform. To invert the transform, the real part and the imaginary part are each inverted and the inverse of each of the two real DWTs are used to obtain two real signals. These two real signals are then averaged to obtain the final output. The original signal $x(n)$ can be recovered from either the real part or the imaginary part. The inverse dual-tree Complex wavelet transform do not capture all the advantages as an analytic wavelet transform offers. If the two real DWTs are represented by the square matrices F_h and F_g , then the

dual-tree CWT can be represented by the rectangular matrix [10] as in Eq. (3),

$$F = \begin{bmatrix} F_h \\ F_g \end{bmatrix} \quad (3)$$

If the vector x represents a real signal, then $w_h = F_h x$ represents the real part and $w_g = F_g x$ represents the imaginary part of the dual-tree CWT. The complex coefficients are given by Eq. (4),

$$w_h + jw_g \quad (4)$$

The dual-tree complex DWT of a signal $x(n)$ is implemented using two critically-sampled DWTs in parallel on the same data as shown in Fig. 1. The input signal $x(n)$ is decomposed to four sub bands at level-1 by the tree-a and tree-b filter banks that consists of low pass and high pass filters. The low pass filtered output of tree-a and tree-b are further decomposed into level-2 sub bands by the second stage filter banks. The first stage filter coefficients represented by $\{H_{0a}, H_{1a}, H_{0b}$ and $H_{1b}\}$ are different from second stage filter coefficients represented by $\{H_{00a}, H_{01a}, H_{00b}, H_{01b}\}$.

Table I presents the DTCWT filter coefficients as presented by author Nick Kingsbury that represents 10-tap filter. Table II presents the DTCWT filter coefficients for higher levels of decomposition.

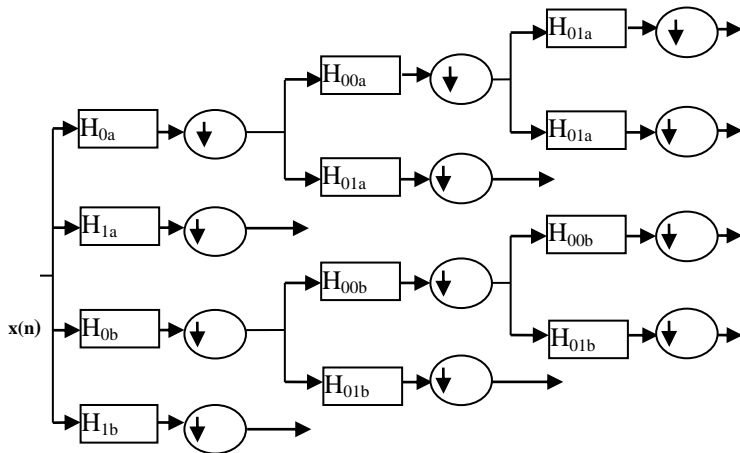


Fig. 1 Three level DTCWT decomposition structure

Table I. DTCWT Filter Co-efficients for Level-1 Decomposition

Tree a		Tree b	
H_{00a}	H_{01a}	H_{00b}	H_{01b}
0.03516384	0	0	-0.03516384
0	0	0	0
-0.08832942	-0.11430184	-0.11430184	0.08832942
0.23389032	0	0	0.23389032
0.76027237	0.58751830	0.58751830	-0.76027237

0.58751830	-0.76027237	0.76027237	0.58751830
0	0.23389032	0.23389032	0
-0.11430184	0.08832942	-0.08832942	-0.11430184
	0	0	0
	-0.03516384	0.03516384	0

Table II. DTCWT Filter Co-efficients for Level-2 Decomposition

Tree a		Tree b	
H_{0a}	H_{1a}	H_{0b}	H_{1b}
0	0	0.1122679	0
-0.08838834	-0.1122679	0.1122679	0
0.08838834	0.1122679	-0.08838834	-0.08838834
0.69587998	0.08838834	0.08838834	-0.08838834
0.69587998	0.08838834	0.69587998	0.69587998
0.08838834	-0.69587998	0.69587998	-0.69587998
-0.08838834	0.69587998	0.08838834	0.08838834
0.01122679	-0.08838834	-0.08838834	0.08838834
0.01122679	-0.08838834	0	0.1122679
0		0	-0.1122679

The EEG electrodes capture real time data which is in the format of .xls format is loaded to the MATLAB workspace which is converted to .csv format. From all the electrodes stored in .xls data format represents the voltage levels in micro volts. From the EEG data available, only the most suitable electrodes that are selected for emotion analysis are considered for wavelet decomposition. Selection of electrodes are presented in previous chapter. The electrodes for which DTCWT is computed are $\{FP2-F4, F4-C4, P4-O2, FP1-F3, F3-C3, P3-O1\}$. For the EEG data acquired from six electrodes is transformed into wavelet domain by performing DTCWT that generates both real and imaginary bands. From the DTCWT bands, energy levels are computed and from the energy levels obtained are the most distinct energy levels are considered for further classification into normal and abnormal EEG data.

III. DESIGN OF FFNN ARCHITECTURE

The neural network structure proposed in for DWT energy classification is designed to process 15 features and to classify the features as either normal or abnormal. The network structure proposed consists of 25-1-1 neurons for structure 1 and 20-6-6 neurons in structure 2. In this section design of both these neural network structures are presented in detail. The 15-25-1-1 network shown in Figure 2, comprises of 15 DTCWT features that are processed by 25 hidden layer neurons in first stage and further 1 neuron in second stage and 1 neuron in output stage. The functionality of the designed FFNN structure that generates two intermediate outputs and one final output is represented as $a^1_i = f(n^1_i)$, $i = 1 \dots 25$ (hidden layer output), $a^2_i = f(n^2_i)$, $i = 1$ (second layer output) and $a^3_i = f(n^3_i)$, $i = 1$ final output layer

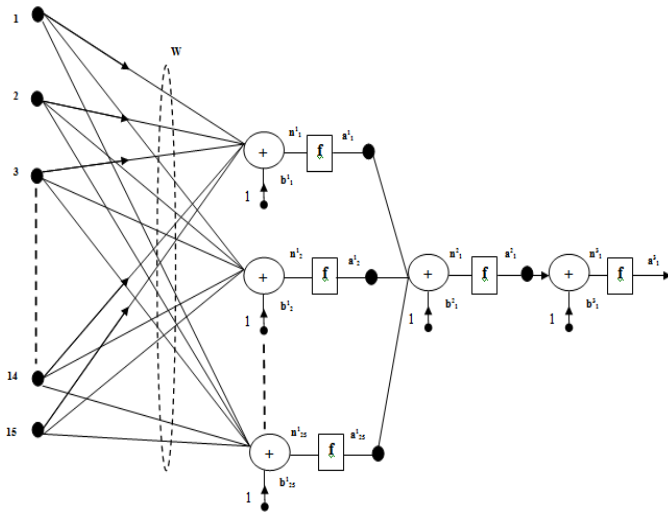


Fig. 2 Coarse classifier 15-25-1-1 structure

Based on the discussions presented the reduced structure design of 15-25-1-1 and 15-20-6-6 FFNN architecture is designed with reduced number of arithmetic units and Table III, compares the arithmetic unit requirement of proposed design with generic implementation. The proposed FFNN structure is modeled using Verilog HDL and is verified for its functionality considering various test vectors the functionally correct HDL model is synthesized using Xilinx ISE targeting Virtex-5 FPGA.

Table III. Comparison of arithmetic unit complexity

Parameters	Generic 15-25-1-1	Proposed 15-25-1-1	Generic 15-20-6-6	Proposed 15-20-6-6
Multipliers HL1	375	15	300	15
Multipliers HL2	25	25	120	20
Multipliers OL3	1	1	36	36
Total	401	41	456	71
Adders HL1	375	15	300	16
Adders HL2	25	26	120	21
Adders OL3	1	2	36	6
Total	401	43	456	43

Next section discusses FPGA implementation results.

IV. RESULTS AND DISCUSSION

Verilog HDL code is developed to model the proposed DTCWT computation unit. FSM is designed to model control logic that synchronizes the forward transform operation. The input stage consists of serial to parallel converter realized using de-multiplexer and multiplexer that is designed to work as parallel to serial converter at the output stage. The DTCWT module is modelled using Xilinx IP cores and glue logic. A test bench is developed that uses known test vectors to verify logic correctness of the developed Verilog HDL model. Figure and Figure presents the simulation results of

DTCWT filters. EEG data sets that are represented using 8 bit signed representation are stored in test bench and are forced into the HDL model for DTCWT computation. The DTCWT coefficients computed by HDL model are observed for its numerical values and compared with theoretical values. From the comparison of practical and theoretical values, the logic correctness of HDL code is verified. In addition to processing EEG data, the filter is verified for its impulse response and the output of filter is observed to produce filter coefficients.

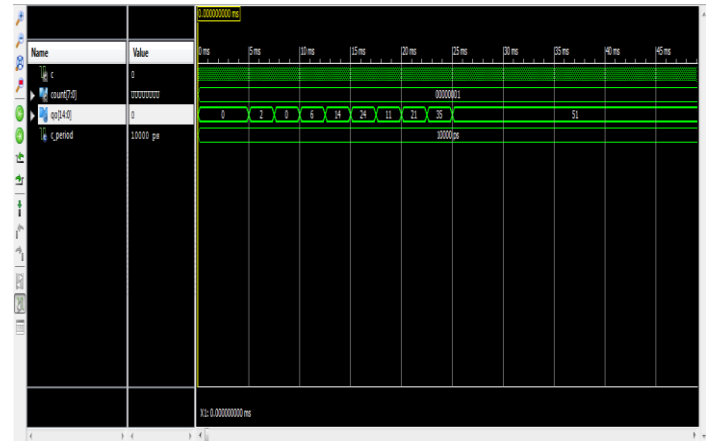


Fig.3 Filter bank simulation

The first stage four filter bank structure results shown in Figure 4, is verified for impulse response and the output is observed to be the filter coefficients demonstrating logic correctness of Verilog HDL and architecture design

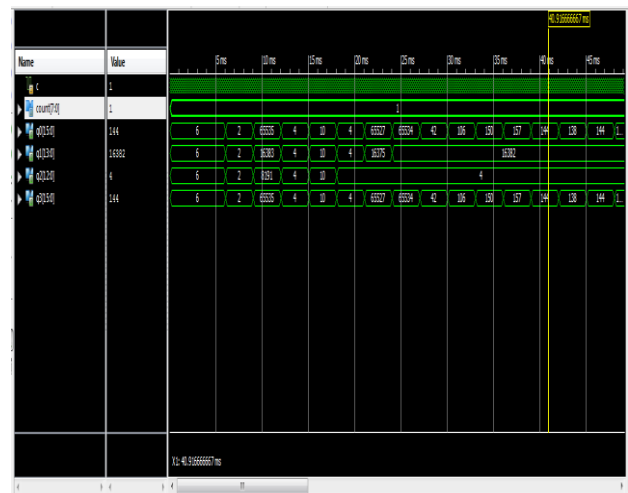


Fig. 4 First stage four filter bank simulation

The functionally verified HDL code is synthesized and RTL schematic is obtained and is shown in Figure 5 and Figure 6, for one filter and four filter structure.

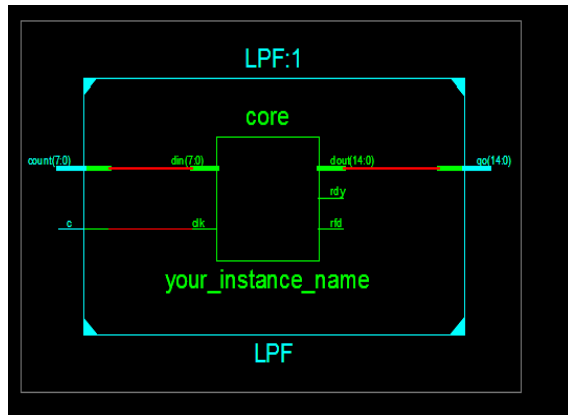


Fig. 5 RTL schematic of single filter

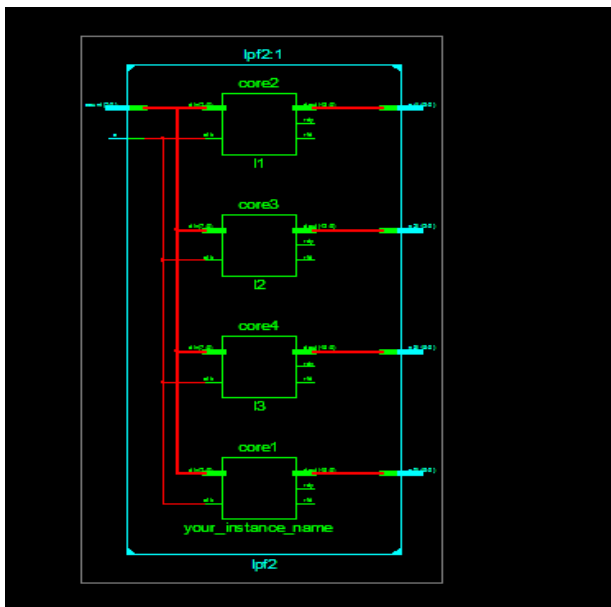


Fig. 6 RTL schematic of four filter

Table IV Summary of Synthesis Report

Parameter	One filter	Two filter	Four filter	Nine stage filter
Number of Slice Registers	87	168	376	1288
Number of Slice LUTs	88	170	373	1268
Number of fully used LUT-FF pairs	81	156	353	1236
Number of bonded IOBs	24	37	68	266
Number of BUFG-BUFGCTRLs	1	1	1	9
Number of DSP48A1s	1	2	4	36
Minimum Period	4.028ns	4.028ns	2.041ns	3.098ns
Maximum Frequency	248.262MHz	248.262MHz	489.896MHz	322.78MHz
Dynamic Power	0.000	0.000	0.000	0.00
Quiescent Power	0.036	0.036	0.082	0.71
Total Supply Power (Watts)	0.037	0.037	0.082	0.71

Table IV, presents the summary of synthesis report of DTCWT implementation on Spartan-6 FPGA. The nine stage DTCWT filter operates at maximum. frequency of 322 MHz

consuming power dissipation of less than 0.71 W occupying 1268 LUTs and 9 DSP arithmetic resources. The design is synthesized in the Xilinx tool, post place, map and route simulation also have been carried out. The synthesized netlist of FFNN is shown in the Figure below. The design is optimized for power, area and timing. RTL synthesized block diagram of FFNN is obtained using Xilinx ISE and the synthesis report is analyzed for estimation the performances of the proposed design in terms of area, speed and power. Table V, shows the power report of coarse classifier and fine classifier which is shown in the below Table

Table V Power report of coarse and fine classifier results

Name	15-25-1-1	15-20-6-6
Total quiescent power	1.10120(W)	2.10133(W)
Total dynamic power	1.12090(W)	1.10004(W)
Total power	2.22210(W)	3.20137(W)

The maximum operating frequency of the proposed design on Spartan-6 FPGA is found to be 312 MHz for coarse classifier and 278 MHz for fine classifier. The operating frequency can be further improved by utilizing the internal resources such as multipliers and adders on Virtex-5 platform.

V.CONCLUSION

In this paper the design of high speed architecture for DTCWT architecture design and neural network architecture design. For DTCWT implementation systolic array based architecture is proposed for FPGA implementation. The processing element design for systolic array structure plays a vital role. The processing element is designed with optimum number of arithmetic units and is further reused in computation of 1D and 2D DTCWT. The proposed FFNN structure for feature classification is designed considering reduced logic approach. The maximum operating frequency of the proposed design on Spartan-6 FPGA is found to be 312 MHz for coarse classifier and 278 MHz for fine classifier. The operating frequency can be further improved by utilizing the internal resources such as multipliers and adders on Virtex-5 platform.

REFERENCES

- [1] U.R. Acharya, F. Molinari, S.V. Sree, S. Chattopadhyay, K.H. Ng, J.S. Suri, "Automated diagnosis of epileptic EEG using Entropies", Biomedical Signal Processing Control, vol.7, no. 4, pp.401-408,2012
- [2] Selesnick Ivan W, Richard G. Baraniuk, and Nick C. Kingsbury, "The dual-tree complex wavelet transforms" Signal Processing Magazine, IEEE 22, vol. 6, pp. 123-151, 2005
- [3] Kingsbury N, "Complex Wavelets for Shift Invariant Analysis and Filtering of Signals, Applied and Computational Harmonic Analysis", vol.10, no. 3, pp.234-253, 2001.
- [4] Musa Peker, BahaSen, and Dursun Delen, "A Novel Method for Automated Diagnosis of Epilepsy Using Complex-Valued Classifiers", IEEE Journal of Biomedical and Health Informatics, Vol. 20, no. 1, 2016
- [5] R. Y. Yu, "Theory of dual-tree complex wavelets", IEEE Transactions on Signal Processing, vol. 56, no. 9, pp. 4263-4273, Sep 2008.

- [6] Po-Cheng Wu and Liang-Gee Chen, “An efficient architecture for two-dimensional discrete wavelet transform”, IEEE Transactions on Circuits and Systems for Video Technology, Vol. 11, No. 4, pp. 536–545, 2001
- [7] Wim Sweldens, “The lifting scheme: A custom-design construction of biorthogonal wavelets” Applied and Computational Harmonics Analysis, Vol. 3, No. 2, pp. 186-200, 1996
- [8] A.S. Lewis and G. Knowles, “VLSI architecture for 2-D Daubechies wavelet transform without multipliers”, Electronics Letters, Vol. 27, No. 2, pp. 171–173, 1991
- [9] C. Chakrabarti and M. Vishwanath, “Efficient realizations of the discrete and continuous wavelet transform: from single chip implementations to mapping on SIMD array computers”, IEEE Transactions on Signal Processing, Vol. 43, No. 3, pp.759–771, 1995
- [10] A. Grzeszczak, M. K. Mandal and S. Panchanathan, “VLSI implementation of discrete wavelet transform”, IEEE Transactions on VLSI Systems, Vol. 4, No. 4, 1996
- [11] Chao Cheng and Keshab K. Parhi, “High-Speed VLSI Implementation of 2-D Discrete Wavelet Transform”, IEEE Transactions on Signal Processing, Vol. 56, No.1, pp. 393-403, 2008
- [12] S. Masud and J. V. McCanny, “Reusable Silicon IP Cores for Discrete Wavelet Transform Applications”, IEEE Transactions on Circuits and Systems I: Regular Papers”, Vol. 51, No. 6, pp. 1114-1124, 2004

Brain tumor detection in MRI images using MATLAB

^[1]Kiran C B, ^[2]Shiva kumar D N, ^[3]Madhu kumar M, ^[4]Celeste T, ^[5]Divya T M

^{[1][2][3][4]} Student, department of ECE, RRIT

^[5] Assistant professor, Department of ECE, RRIT

Abstract— Image segmentation is one of the most challenging techniques in the area of medical image processing. The brain tumor detection is emerging in this field. This paper refers to the detection of brain tumor from MRI images using the interface of GUI in matlab.

I. INTRODUCTION

Due to irregular development of cells inside the brain, people are influenced by brain tumors severely. This bug can be dangerous because it can disturb legitimate mind work. Two types of cerebrum tumors have been distinguished as benign tumors and malignant tumors. Benign tumors are more secure than threatening tumors. This is explained by the fact that dangerous tumors are quick creating and destructive while favorable are moderate developing and less harmful. Medical imaging system is used to make visual portrayal of inside of the human body for restorative purposes and noninvasive potential outcomes can be analyzed by this innovation. Magnetic Resonance Image (MRI) is significantly utilized and it gives more prominent differentiation pictures of the mind and dangerous tissues. On the other hand, image processing is a process where the image gets analyzed and processed intensively. Image processing is one of the branches of computer sciences. It is interested in performing operations on images in order to improve them according to specific criteria or extract some information from them. There are some steps that need to be taken into account to assure image processing. The idea developed in this work can make MRI image processing and

II. RELATED WORK:

Praveen Amritpal Singh proposed algorithm is a combination of SVM and fuzzy c means a hybrid technique for prediction of brain tumour. Fuzzy c means clustering is used for image segmentation. Grey level run length matrix is used for extraction of the feature. Linear, Quadratic, SVM technique is applied to classify the brain MRI images. Real data set of 120 patients MRI images have been used to detect 'tumour' and 'non tumour' MRI images. The SVM classifier is trained using 96 brain MRI images, after that 24 brain MRI images we used for testing the trained SVM. SVM

tumor detection process faster and cheaper presenting an optimal solution of the tumor detection. To avoid the different kinds of noises presenting in the first part, we will compare between some types of filter and then select the best to continue using the morphological operators to extract tumor.

classifier with Linear, Quadratic kernel function give 91.66% 83.33% accuracy respectively.

Atsina mina, Prof. Chandrakant Mahobiya in 2017 proposed an effective automatic classification method for brain MRI on the dataset of 50 MRI images is projected using Ad boost machine learning algorithm. The proposed system consists of 3 parts Preprocessing Feature extraction and classification. Preprocessing has removed noise in the raw data, it transform RGB image into gray scale, median filter and thresholding segmentation is applied. For classification boosting technique is used. It gives 89.90% accuracy and result in normal brain or in malignant or benign type of tumor.

III. METHODOLOGY

These are the steps performed on MRI image of brain tumor using MATLAB Algorithms.

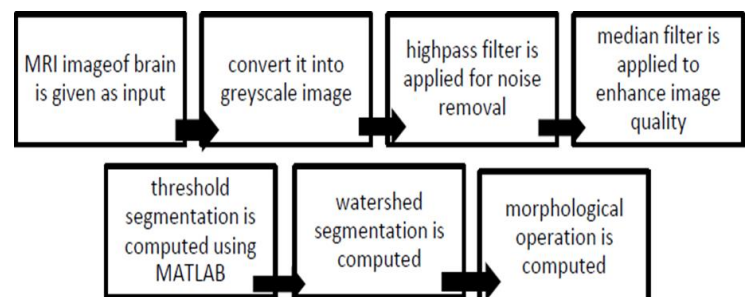
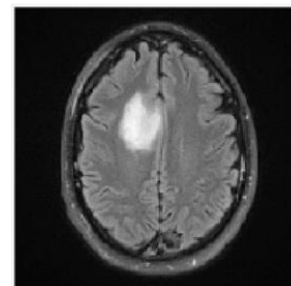


Figure 1. System Level Block Diagram

INPUT MRI IMAGE:



The first stage i.e. the image acquisition stage which starts with taking a collection of images from the database.

Images are stored in MATLAB will be displayed as a Gray scale image. As our MRI DICOM dataset was in .mat file, we have extracted the images using MATLAB code.

We have collected our MRI image dataset from: Brain MRI Dataset (BRATS 2015)

<https://in.mathworks.com/matlabcentral/answer/343191-brain-mri-dataset-brats-2015>

The Brain MRI dataset (BRATS 2015) consists of 2000 images of resolution 200*200 mm Of both tumor and non tumor MRI images in DICOM format.

6. GRAYSCALE IMAGE:

Gray scale image is better format for the image processing because it is low complex and it can take in detail contrast, brightness and edges without considering color. The color is complexes to process the image. So it is better to convert to gray scale before further processing.

7. THRESHOLDING:

Thresholding is a major process in image processing which threshold the each pixel to a certain value and it will give the some quality to the each pixel.

Formula:

$$THz=t0+ ((\max (\text{input} (:)) +\min (\text{input} (:)) /2)$$

8. MORPHOLOGICAL OPERATION:

After the filtering process the image is removed from the noise and the image is threshold to certain value, whatever the image is in the form of matrix so the matrix is compared with the density. If the density of the cell is more than the value it will confirm and extract the tumor from the MRI image of patients. In the above process it doesn't have the clear image, but in the process we can get the enhanced image of tumor

Formula:

$$\text{Area}=\sum_{i,j=0}^{m,n} b(i-j)$$

Solidity=Area/covers Area.

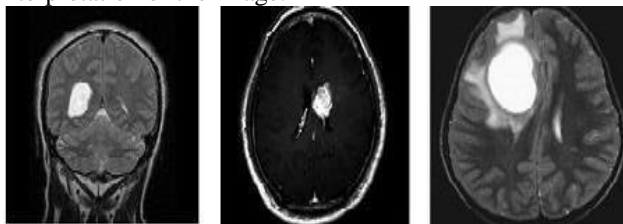
WATERSHEDING SEGMENTATION:

The watershed image is the superimposed over the image after Filtering has been applied it is done to the segment of the cells in the image.it is applied on the grey scale image using mat lab algorithms.

The tumor intensity is more than the background that's why it is easy to locate the tumor from image.

ANISOTROPIC FILTER:

It is a technique aiming to reducing image noise without removing significant parts of the image content, typically edges, lines or other details that are important for the interpretation of the image.



Anisotropic diffusion is a generalization of this diffusion process: it produces a family of parameterized images, but

each resulting image is a combination between the original image and a filter that depends on the local content of the original image. As a consequence, anisotropic diffusion is a non-linear and space variant transformation of the original image.

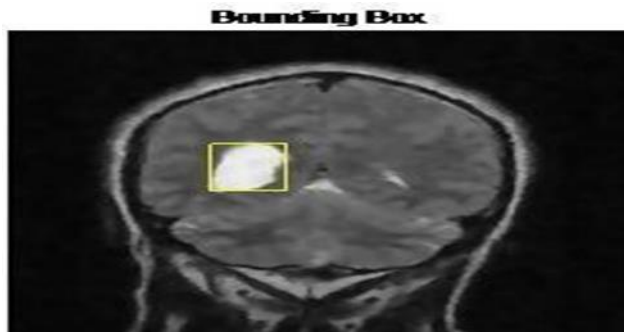
In the rest of work, we will use the anisotropic diffusion filter because it is the best in terms of filtering the image and remove noise from them. Also anisotropic diffusion preserves the sharpness of edges better than Gaussian blurring. So we dilation and erosion. We used the Erosion which replaces each pixel with the local minimum of the neighborhood around the pixel. The object operates on a stream of binary intensity values. This object uses a streaming pixel interface with a structure for frame control signals. In contrary, the dilation is block that replaces each pixel with the local maximum of the neighborhood around the pixel. The block operates on a stream of binary intensity values. This block uses a streaming pixel interface with a bus for frame control signals. This interface enables the block to operate independently of image size and format. In case of

tumor, we must follow the steps cited next or display a message "no tumor" else. First, we will measure properties of image region using the function "region props" which has as output Stats. This contains area, Bounding Box, solidity. Second, we will appear separately the tumor alone in Figure 10 We will detect the tumor using "Bounding box" knowing that Bounding boxes are imaginary boxes that are around objects as shown in above fig.



Tumor alone

Third, after determining the position, density and area of tumor, there is a function called "rectangle" which surround the tumor as shown in the next figure:



Bounding Box

Bounding box

Then, to complete the steps of morphological operation we obtain these figures: erosion and dilation:



eroded image

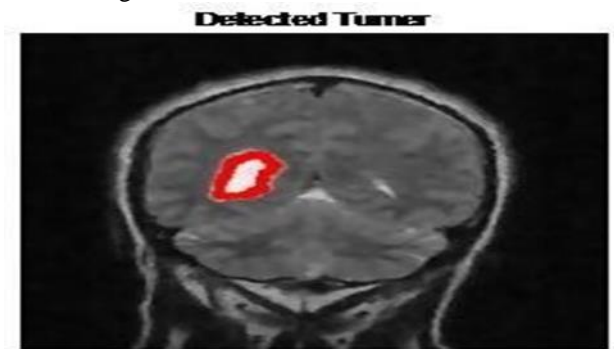
Erosion step



Tumor Outline

Dilation step

As last part, to confirm the detection we insert the outline in filtered image in red color:

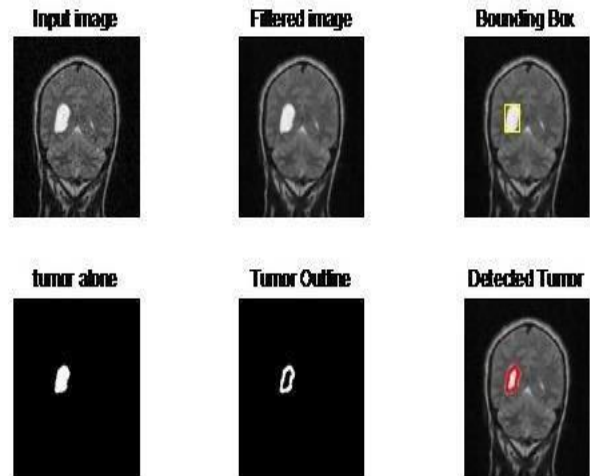


Detected Tumor

Tumor detected

Finally, the goal is achieved. To conclude, we try to enumerate all

stages followed from the beginning after selecting the right filter and continue the work with it. The Figure 15 showed this succession of steps



Stages of tumor detection

IV. CONCLUSION

This work has written an algorithm for the brain tumor detection from MRI using MATLAB software. A selection of the best filter and methods improves our algorithm compared to the standard algorithms. Image processing in the other hand is a process where the image gets analyzed and processed intensively and is a one of the main points in the paper. This work can make MRI

REFERENCE:

- [1] <https://www.google.com/url?sa=t&source=web&rct=j&url=https://www.mathworks.com/matlabcentral/fileexchange/55107-brain-tumor-detection-and-classification&ved=2ahUKEwiFwp2LnfHwAhXIIbcAHYK8Bdcw1GcQ82NbO4HcFZ9Pgstf9b>
- [2] <https://www.google.com/url?sa=t&source=web&rct=j&url=https://ieeexplore.ieee.org/document/8390202%23~:~:text=3DThis%2520paper%252C%2520mainly%2520focuses%2520on,processing%252C%2520edge%2520detecti%2520on%2520and%2520segmentation.&ved=2ahUKEwiFwp2LnfHwAhXIIbcAHYK8Bdcw1GcQ82NbO4HcFZ9Pgstf9b>
- [3] https://www.google.com/url?sa=t&source=web&rct=j&url=http://www.hep.upatras.gr/class/download/psi_epe_iko/5-Brain-Tumor-Extraction-from-MRI-Images-Using-MATLAB.PDF&ved=2ahUKEwiFwp2LnfHwAhXIIbcAHYK8Bdcw1GcQ82NbO4HcFZ9Pgstf9b
- [4] Fergus Davnall, Connie S. P. Yip, Gunnar Ljungqvist, Mariyah Selmi, Francesca NgBal, Sanghera Balaji, Ganeshan, Kenneth A. Miles, Gary J. Cook, Vicky Goh, Assessment of tumor heterogeneity: an emerging imaging tool for clinical practice?, *Insights into Imaging*, 3, 573-589 (2012)
- [5] MT Vlaardingerbroek, JA Boer, *Magnetic Resonance Imaging: Theory and Practice*, 454. Springer, Netherlands (2013) 6. Jan J.W. Lagendijk and Bas W. Raaymakers and Marco van Vulpen, *The Magnetic Resonance Imaging–Linac System*, *Seminars in Radiation Oncology*, 24, 207-209 (2014)

Electricity Theft Detection

^[1] Lenin Selva M, ^[2] Monish R, ^[3] Dharsan S, ^[4] Sankarnarayanan P

^{[1][2][3][4]} Department of Electrical and Electronics Engineering, Bannari amman institute of technology
Sathyamangalam, Erode T

Abstract— During these days the number of electricity thieves are increasing, so that the electricity boards are facing problems in providing electricity to their consumers in an efficient way. In order to encounter this issue, we need an accurate Electricity Theft Detection (ETD) which is quite challenging due to the inaccurate classification on the imbalance electricity consumption data, the overfitting issues and the High False Positive Rate (FPR) of the previous techniques. To overcome mainly the above given limitations, this paper presents a new model, which is mainly based on the supervised machine learning techniques and real electricity consumption data. At the beginning, electricity data are pre-processed using interpolation, three sigma rule and normalization methods. Since the electricity consumption data is imbalanced, an Adasyn algorithm is utilized to overcome this class imbalance problem. It has two objectives. At first, it intelligently increases the minority class samples in the data. At second, it prevents the model from being biased towards the majority class samples. After all these process, the balanced electricity consumption data are fed into the Visual Geometry Group (VGG-16) module to detect abnormal patterns in electricity consumption. Finally, a Firefly Algorithm based Extreme Gradient Boosting (FA-XGBoost) module is exploited for classification. The simulations are done to show the performance of our proposed model.

Index Terms – ETD - Electricity Theft Detection, FPR - False Positive Rate, VGG16 -Visual Geometry Group, FA-XGBoost-Firefly Algorithm based Extreme Gradient , Boosting.

I. LITERATURE REVIEW

This invention mainly detects the electricity thieves using supervised machine learning and real electricity consumption data. During these days the number of electricity thieves are increasing, so that the electricity boards are facing crisis in providing electricity to their consumers in an efficient way. Hasan et al. proposed a hybrid model which consist of CNN and Long Short-Term Memory (LSTM). The CNN is used over here for feature extraction while LSTM used the refined features for the purpose of classification of the data into honest consumers and electricity thieves. To encounter the problem of an imbalanced dataset, the Synthetic Minority Over Sampling Technique (SMOTE) is used. It has achieved effective results. i.e., precision 90% and recall 87%. However, the overfitting problem is not considered by this module, which is caused by the addition of duplicate information through SMOTE.

II. INTRODUCTION

In this paper, the proposed methodology is implemented for the electricity theft detection using the real smart meter data which is currently used. ETD is based on the supervised machine learning techniques and real time electricity consumption data over the period of time. Initially, the power consumption data are pre-processed using interpolation, three-sigma rule and then normalization methods are followed. Since the electricity consumption data is imbalanced, an Adasyn algorithm is used effectively to overcome this imbalance problem. It has two objectives. Firstly, it gradually increases the minority class samples which are provided in the data. Secondly, it prevents the model from being biased towards the side of the majority class samples which are given. After, all these process the balanced power consumption data are fed into a Visual Geometry Group (VGG-16) module. The work of this module is to detect abnormal patterns in electricity consumption. Finally, a Firefly Algorithm based Extreme Gradient Boosting (FA-XGBoost) technique which is exploited for the further classification. The simulations were done to show the performance given by us proposed model. We conduct extensive simulations on real electricity consumption data set which is collected exclusively from the consumers and for comparative analysis, precision, recall, F1-score.

The proposed model mainly consists of five points:

- »Data pre-processing.
- »Data balancing.
- »Feature extraction.
- »Classifications.
- »Validation.

III. DESCRIPTION

The flowchart of the proposed method for electricity theft detection is also given in Fig 1. In the proposed methodology, the power consumption data are pre-processed using the process of interpolation of the missing data's, three sigma rule and normalization methods are also used to compute the missing values and remove the outliers present in the collected data. An Adasyn algorithm is proposed for balancing the imbalance present in the dataset. After completing this process, the balanced data are sent to the Visual Geometry Group (VGG-16) module for further features extraction. A VGG-16 is perfect Module which is used to detect the abnormal patterns in electricity

consumption data. Finally, the extracted features are provided to the Firefly Algorithm based Extreme Gradient Boosting (FA-XGBoost) module for further classification.

The main applications of this paper are listed below.

- The proposed approach provides the best solution for the problem which is present in the power sector, such as to wastage of electrical power due to electricity theft.
- This model can efficiently be used by the companies using the real electricity consumption data to identify the electricity thieves and reduce the non-technical energy wastage.
- The proposed approach can be used against the all types of consumers who consume the electricity in unauthorized ways.

The key contributions of this paper are:

- A comprehensive data pre-processing is performed using the method of interpolation, three sigma rule, and normalization methods to deal with missing values and outliers present in the dataset. These data pre-processing step gives the refined input, which improves the performance of the classifier used in this model.
- A class balancing technique, Adasyn, is mainly proposed to address the problem of imbalance data. The benefit of using Adasyn is twin-fold. Firstly, it improves the learning performance of classifier to be more concerned on theft cases that are really harder to learn. Secondly, it prevents the model from being biased.
- We have introduced a new module VGG-16 to solve the problem of overfitting of the power consumption data to improve the classification performance. This technique is never being used before in ETD models, and it has great improvement in the accuracy of the classification model. The VGG-16 effectively extracts useful information from data to truly represent electricity theft cases.
- XGBoost is applied to predict further and final classification, which improves the performance by combining group of multiple weak learners to make a strong learner.
- Along with XGBoost, an optimization module, the Firefly Algorithm (FA) is utilized for efficient parameter optimization of the given classifier.
- We conduct extensive simulations on real time electricity consumption data set and for comparative analysis, precision, recall, F1-score.

Figures

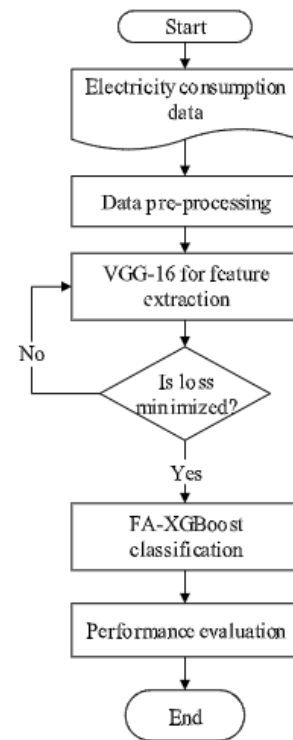


Fig1. Flowchart of the module

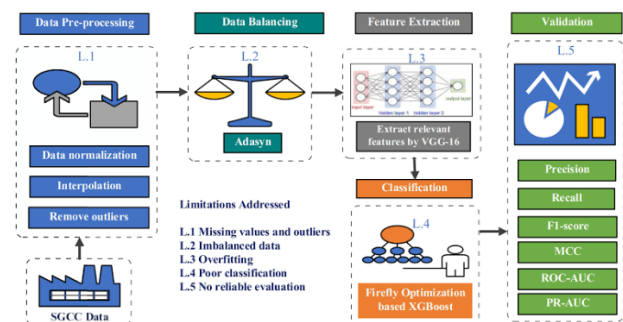


Fig2. Proposed system model

B. Abbreviations and Acronyms

- ETD - Electricity Theft Detection.
- FPR - False Positive Rate.
- VGG16 - Visual Geometry Group.
- FA-XGBoost- Firefly Algorithm based Extreme Gradient Boosting.

C. Equations

For more accurate prediction, the proposed model aims to reduce the loss function. The widely used logarithmic loss function is cross entropy. As we are doing binary classification, the loss function we are using the binary cross entropy. It is calculated by using the following equation

$$Nf(x) = \frac{1}{N} \sum_{i=1}^N -(y_i \log(p(y_i)) + (1 - y_i) \log(1 - p(y_i)))$$

In above Equation N is the total number of consumers samples, $p(y_i)$ is the probability of electricity theft, and y_i is the ground truth label.

IV. RESULTS AND CONCLUSIONS

In this paper, the proposed methodology is implemented for ETD using the real smart meter data. The different limitations in literature are addressed in this work. The conclusions were drawn and are summarised as follows. Initially, the real smart meter data, which is collected from SGCC, have a number of missing values and outliers. For this reason, we performed a comprehensive data pre-processing which consists of interpolation, the three sigma rule, and normalization methods. In addition, the dataset has a small number of instances for electricity thieves, which makes the classification model biased due to its training on majority honest instances. We employed the Adaboost algorithm to address this problem. This technique has improved the performance of the FA-XGboost classifier, which has achieved F1-score, precision, and recall of 93.7%, 92.6%, and 97%, respectively. Afterwards, the model has overfitting issues due to training the model on a large time series data, a VGG-16 module is introduced in ETD, which extracts relevant features from the data. It achieved a higher generalized performance by securing accuracy of 87.2% and 83.5% on training and testing data, respectively. Finally, the XGBoost method is applied to classify data into honest and dishonest consumers. To enhance the performance of XGBoost method, an FA is used for parameters' optimization. This method improved the performance of XGBoost and achieved 95.9% ROC-AUC and outperforming the benchmarks: SVM, LR, and CNN. However, as the dataset increases, the execution time of our proposed model also increases. In the future, we will improve its performance by reducing the delay in detecting the electricity theft.

REFERENCES

- [1] Pattern Recognition and Machine Learning by Christopher M. Bishop.
- [2] Applied Predictive Modelling by Max Kuhn and Kjell Johnson
- [3] https://en.wikipedia.org/wiki/Machine_learning

Congruence between Cause Marketing Campaigns and Purchase Intention towards Consumers – An Analysis

^[1]M.Ancy Raja Nathiya, ^[2]K.Asha

^[1]Research Scholar, ^[2]Assistant Professor

^[1]Department of Management Studies, Noorul Islam Centre for Higher Education,

^[2]Faculty of Management Studies, Noorul Islam Centre for Higher Education

Abstract— Cause marketing is a type of marketing activity which involves both the 'for profit' business and a non-profit organization together for a mutual benefit. Cause marketing is considered to be a tactical philanthropic instrument which commercialize the charity into a new orbit. Nowadays, many firms are actively participating in the Cause related marketing programs to fulfil their corporate social responsibility. Cause marketing also helps to combine the social responsibility and the marketing strategy of a firm to attain the social and economic goals. This article gives brief note about the term Cause marketing and its benefits. The main aim of the study is to explore the opinion of the consumers regarding the Cause marketing campaigns and to interrogate whether it influence the purchase decisions of consumers. As a result, it is found out that consumers were having positive response towards Cause marketing campaigns and are tend to be more prone to support the brand which engage themselves towards societal activities.

Index Terms – Cause marketing, Cause marketing campaigns, Consumers, Purchase intention.

I. INTRODUCTION

Cause marketing can also be termed as Cause related marketing where they align the businesses with social affairs (or) beliefs which are highly important for them to execute a campaign. Companies use this method to create awareness towards the cause and create social responsibility. For instance, it makes the customers to actively participate in the Cause marketing campaign with a donation towards charities. Often companies will commit themselves with a non-profit organization for the campaign purpose, which highly help both the parties to be benefited by the reach of a campaign. On other hand, the companies better create a cause and support it. Cause marketing is mandatory for the companies who are required to create a positive perception towards their brand. For a consumer, brands which are visually responsible towards society will easily catch their eyes. If they found a company working towards a cause, automatically they used to follow it and give support for it financially. Additional to this, the customers become more loyal towards the company. When the awareness regarding this are raised more among society, it leads way for many improvement. On behalf of the campaign and the support it helps to make a forwards step in a massive way.

A. Benefits of Cause marketing

- The major benefits of Cause marketing campaign is portrayed to be a situation of a win-win-win, which involves the company, the public and non-profit organization.
- Cause marketing campaigns creates positive impact and positive purchase intentions.
- Cause marketing campaigns generates an in-depth emotional engagement with the customers and stakeholders to have a cordial relationship with them.
- Cause marketing campaign improves the brand and corporate image by enhancing the brand awareness towards a good corporate reputation.
- Cause marketing campaign enhances it activity more to reach new geographic markets, to get prevent from negative phase of publicity, improves the customer base and create exposure with low cost by breaking the advertisement clutter.
- Beyond all the external benefits, few of the internal benefits of Cause marketing campaign are increasing the employee commitment, loyalty and morale.
- On the other hand, where the non-profit company gets benefits through Cause marketing campaigns are obtaining high public awareness, better image and high publicity.

II. REVIEW OF LITERATURE

Varadarajan and Menon (1988), defines as, it is a process of implementing and formulating the marketing activities which are characterized by the firm towards contributing a specific amount for a designated cause. Cause marketing also creates the relationship between the businesses and consumers.

Ptacek and Salazar (1997), expresses that, Cause marketing's goal is to create more sales and high corporate image while at the same time providing contribution towards non-profit organization. It clearly states that Cause marketing is not about philanthropy but about sales.

Lucke and Heine (2015), portrays that, Cause marketing campaigns positively enhance the purchase intentions of consumer. Every choice of cause creates more

purchase decisions towards that particular brand. The product and cause sequentially mediate together.

Liu (2013), reveals that, there is no particular type of Cause marketing. It relays on the hand of the manager to choose the specific type of cause. In detail, it explains that when a sports committee is in need of a volunteers social Cause marketing kind of approach is most reliable for the situation.

A. Few Most Popular Cause Marketing Campaigns:

In the new era, everyone are knowledgeable about the hidden practices of business. It is revealed as, 80% of the consumers are more prone towards the brands which involves them towards societal affairs. Let us see some of the India's best Cause marketing campaigns which created high impact among society:-

a. Fly the new feeling – 'Vistara'

A joint venture of Vistara airline belongs to 'Tata Group' and 'Singapore airlines' performed a activity with the partnership of 'Salaam Baalak's Trust', a non-profit organization offered a support for 12 homeless children aged 7 to 8 to fly the first flight ever accompanied with the passengers to create happiness among them. It is also filmed under the name as "when the little feet founds their little wings with vistara#Fly the new feeling".

b. Johnson Tiles – Project of Red Ramp

'Johnson Tiles', a manufacturer of bath tile maker wishes to create a sensation among Indian society by creating the public places a disable-friendly one. Over 10 million people who are differently abled arose a voice to have space for them to move everywhere. A ramp on Kiri beach, Goa were raised by Johnson Tiles titled as, 'Red Ramp Project'. Where it open doors for the differently abled people to visit the beach and lap their feet on water.

c. Dark Is Beautiful

'Women of worth' conducted a campaign called 'Dark is Beautiful' in India to recreate the sentence dark skinned girls are not beautiful compared to fair skinned girls. So, this campaign is conducted to create a revolution on this statement and recreate it as dark is too beautiful. The campaign directly discourages all the dusky girls on using fairness products and encourages them to hold their true colors.

d. Jaago Re – Tata Tea

A largest tea brands in India named 'Tata Tea' conducted a campaign named 'Jaago Re', to spread awareness and importance of right to vote, an estimation of 6.5 lakhs new voters were registered. This campaign is conducted a month before the time of election.

e. NGO's – Save Our Tiger

A campaign titled as "Save our tiger" aims to throw light facts about the decrease in population of the tiger. It creates interest among citizens to know more about tigers and make them to stay updated about the tiger's facts. It also enforces the people to donate money for NGO's who is working towards that cause.

f. Project Saraswathi – Fair & Lovely

'Fair & Lovely' foundation conducted a campaign called 'Project Saraswathi' to empower India's young women economically. In this project, an amount of Rs.1 lakh were awarded to many young deserved girls to do their under graduate and post graduate degrees.

g. CARE – Horlicks Ahaar Abhiyam

A campaign named 'Horlicks Ahaar Abhiyam' initiated by 'CARE' India (West Bengal) with 'Save the children' (Tamil Nadu) to enlighten all the mothers, communities and families about the awareness of malnutrition among children. Horlicks, raise funds from consumers to spread awareness about malnutrition for children by creating a Child Development Program. As a result, on the sale of every single Horlicks bottle which priced above Rs.100, an amount of Re.1 will be initiated towards the fund contribution.

h. Nestle – Educate the girl child

In late 2016, a famous company called Nestle, tied up with a non-profit firm 'Nanhi – Kali' to educate every girl child for a long term project. It helps the low income Indian girls to upgrade their career.

i. India's Mom Touch – Nivea

A Top leading cosmetic brand called 'Nivea' partnered with a charitable Trust named as 'Aseema' to give quality education to all the marginalized community children. A film named "Mom's touch" should be shared by consumers in social media and for every single share, the consumers gets pay for it and at the same time a 100 grams of rice is contributed by Nivea to the charity.

j. Plate of Hope – KFC

To fight against hunger from 2016 in India, KFC created an offer in online orders. On every order, who makes contribution towards the option 'Virtual Plate of Food' on KFC website, it leads to offer a plate of food for hungry mouths across India. Through this program among 20 million people hunger were served.

III. METHODOLOGY

A. Objectives:

This study was carried out to explore the opinion on consumers regarding the Cause marketing campaigns by seeking the answer for below questions to understand what makes the consumers to choose a preferred brand at the time of purchase and give insights to marketers about the effect on Cause marketing campaigns.

The following questions were specially designed for the purpose of study:-

- i. Does the consumers feel supporting a cause is a good idea for helping the charity?
- ii. How about the remembrance of Cause marketing campaigns they came across?
- iii. Does the consumers switch from their favourite brand to others if it is not synced with a cause?
- iv. What are the causes consumers wish the marketers to tie up and support?
- v. Suggestion based on the study

B. Sample and Methods:

The sample which consists of 100 respondents around Kanyakumari District were taken for the study. A Convenience Sampling Method is used for the study. Questionnaire method is followed for collecting the data. Few questionnaire were sent through e-mails and few are done manually. A description about cause marketing is given above in all the questionnaire. The collected sample expresses that, among 100 respondents 83 are from urban area and 17 are from rural, 59 respondents are male and 41 are female, 53 are married and 47 are unmarried, 34 have completed their post-graduation, 40 were under graduates and 26 respondents are done with their schooling. The respondents are mostly with the income category of Rs.25,000 to Rs.40,000 and less in number are with above Rs.1,00,000.

IV. RESEARCH FINDINGS

- i. The study reveals as, about 79% of the consumers feel it as a good idea and more prone towards supporting a cause. On the other hand, 13% of the people are not sure about this and the rest of 8% didn't accept this as a good concept.

I. Table (i) Consumer's idea towards Cause marketing

Particulars	Percentage
Cause Marketing is a good idea	79
Not sure	13
Bad idea	8

- ii. It explores as, about 75% of the consumers could be able to remember the Cause marketing campaigns, and most of them were tend to mention it as Lifebuoy, Ariel, etc. Among all, about 25% of the people were unable to know about the campaign.

II. Table (ii) Consumer's recall on Cause marketing campaigns

Particulars	Percentage
Yes	75
No	25

- iii. The study reveals that, 61% of the consumers respond as, they would try a different brand if the particular brand support for a worthy cause, instead 30% of the respondents stick to their favourite brand and remaining 9% were not sure about the point

III. Table (iii) Consumer's option on Purchase Decision

Particulars	Percentage
Will switch from preferred brand to other brand which support cause	61
No, Stick to the preferred brand	30
Not sure	9

- iv. It opines that, consumers are likely to support various cause and they pretend the marketers to get involve with those causes. Such causes are, providing child labours good education (17%), donating food for homeless (16%), education for the poor (19%), relief funds for disaster affected causes (3%), for cancer foundation (12%), pollution free environment (2%), about covid-19 vaccination (20%), help people who lost their family members by corona virus (11%).

IV. Table (iv) Preferred Causes of Consumers to support

Causes	Percentage of Support
Providing Child labours with good education	17
Donating food for the needy and homeless	16
Education for the poor	19
Relief funds for Naturally affected causes	3
Cancer & Disease Foundation	12
Pollution Free Environment	2
Awareness about Covid-19 Vaccinations	20
Help for people who lost their family by Corona Virus	11

V.CONCLUSION, SUGGESTION & DISSCUSION

In today's world Cause marketing are considered to be a buzz word. Even though few Indian companies did this, their extent of commitment towards this is unimpressive. Thus, when the level of awareness grows more and more, the managers of every firm has to fulfil their corporate social responsibility to meet the company's betterment and societal needs.

A. Discussion & Suggestions based on the study:

The study reveals that, Cause marketing campaigns do create an impact among consumers at the time of making purchase. People get a kind of satisfaction on making purchase with the brand which supports the cause. People

also feels like the marketers help the consumers to get involve in good activities towards a monetary contribution by them. Many people are more prone towards the brands which are related towards a cause than the brand which are not. The study also suggests as, people wish every marketers to involve in cause marketing practices. They are satisfied with the brand which support a cause. Thus, it is concluded as, there is a congruence between Cause marketing campaigns and purchase intention.

B. Limitations & Suggestions for future research:

This study was an attempt to investigate about the influence of congruence between Cause marketing campaigns and purchase intention towards consumers. For this purpose, data was collected only around few places in Kanyakumari district. Further study can be carried out in other region to increase the results generality. The target respondents for the study were consumers and further study can be carried out among professionals (or) any particular group of people.

REFERENCES

- [1] D.C. Moosmayer and A. Fulijahn, "Consumer Perceptions of Cause Related Marketing Campaigns," *Journal of Consumer Marketing*, vol. 27, no. 6, pp. 543-549, 2010.
- [2] K. Westberg and N. Pope, "An examination of Cause-related marketing in the context of brand attitude, purchase intention, perceived fit and personal values," *Conference: Social, Not-for-profit and Political Marketing*, pp.222-230, 2005.
- [3] G. Zasuwa, "The Role of Company-Cause Fit and Company Involvement in Consumer Responses to CSR Initiatives: A Meta-Analytic Review," *Sustainability*, June 2017.
- [4] E. Cheron, F. Kohlbacher and K. Kusuma, "The Effects of Brand-Cause Fit and Campaign Duration on Consumer Perception of Cause-Related Marketing in Japan," *Journal of Consumer Marketing*, vol. 29, no. 5, pp. 357-368, 2012.
- [5] K. Adiwijaya and R. Fauan, "Cause-related Marketing: The Influence of Cause-Brand Fit, Firm Motives and Attribute Altruistic to Consumer Inferences and Loyalty and Moderation Effect of Consumer Values," *International Conference on Economics Marketing and Management*, vol. 28, 2012.
- [6] I. Melero and T. Montaner, "Cause-related Marketing: An Experimental Study about How the Product Type and the Perceived Fit may Influence the Consumer Response," *European Journal of Management and Business Economics*, vol. 25, pp. 161-167, 2016.
- [7] X. Nan and K. Heo, "Consumer Responses to Corporate Social Responsibility (CSR) Initiatives," *Journal of Advertising*, vol. 36, no. 2, pp. 63-74, 2007.
- [8] R. E. Goldsmith and Z. Yimin, "The Influence of Brand-Consumer Responses to Cause Related Marketing," *Journal of Applied Marketing Theory*, vol. 5, no. 2, pp. 74-95, December 2014.
- [9] S. Gupta and J. Pirsch, "The Company-cause-customer fit in Decision in Cause-related Marketing," *Journal of Consumer Marketing*, vol. 23, no. 6, pp. 314-326, 2006.
- [10] A. Zhang, A. Scodellaro, B. Pang, H. Lo and Z. Xu, "Attribution and Effectiveness of Cause-related Marketing: The Interplay between Cause-brand fit and Corporate Reputation," *Sustainability*, October 2020.

The influence of Boron Nitride reinforcement on physical and mechanical properties of Polyethylene Terephthalate (PET)

^[1]Anand. S. Sonnad, ^[2]Shravankumar. ^[3]B. Kerur, ^[4]Mahesh A. Kori

^{[1][2][3][4]}Mechanical Engineering Department, Basaveshwar Engineering College, Bagalkot, Karnataka, India

Abstract— Polymers are economical, easy to fabricate, low weight, decent strength, good thermal and electrical insulating properties, and many more advantages made polymers reach the highest magnitude and replace all traditional materials with various types of reinforcing elements as desired. In many capacities, they have significantly suppressed traditional materials. There are numerous advantages that make polymers very promising contenders for domestic, commercial, and engineering applications. In the present research, Polyethylene terephthalate (PET) polymer as a matrix and hexagonal boron nitride (h-BN) as reinforcement were used, and are fabricated using ball milling and injection molding process. The properties of h-BN addition to (0 – 40 wt. %) were studied, recorded, and analyzed the physical and mechanical properties. Optical microscopy images showed good distribution of BN particles in the PET matrix. The Vickers microhardness, impact strength, were found to increase by 28% and 70%. Tensile strength and flexural bending test results of composites were found to increase approximately 54% and 52%, and percent elongation has reduced by almost 46% by an increase in the BN particles compared to pure PET matrix.

Index Terms – Boron nitride, Injection molding, Mechanical properties, Polymer composite, Optical Microscopy.

I. INTRODUCTION

Polymer composite materials are a combination of matrix and reinforcement which have different physical and chemical properties. The need of adding materials in the pure polymer is to take advantage of the better properties of both materials without compromising on the properties of either. The reinforced particle composites absorb the major load and the matrix assists as the mediocre for transfer of the load. The addition of reinforcing materials further increases the purposeful properties of the composites. These composite materials find applications in aerospace components, industrial, automotive, naval, defense, electric insulation, transportation, etc. Particle reinforced polymers have to function efficiently and effectively in the corrosive environment as all traditional cannot function for a longer period and this leads to functional failure as a result it leads to larger economical damage. Harder reinforcement particles usually high strength metals, oxides, and ceramics particles are getting used these days to enhance the surface damage resistance, even up to a few orders of magnitude [1]. Many researchers have carried out extensive research on Polymer

matrix composites and investigated and determined polymer composites play a vital role in decreasing the applications of corrosion resistance and wear-resistant properties by the addition of reinforcement materials [2, 3], [4, 5,6]. Therefore polymers have become an issue of extended interest. The reinforcement materials generally added are metallic, organic, and inorganic particulate materials in numerous shapes (fibers, particles, particulates) and sizes (micro and nano). Polymer composites with thermal durability at high temperatures are most desirable for industrial applications [6]. Polymer composites are most desired due to their flexibility in manufacturing design, low cost of fabrication, corrosion resistance, and majorly its low density, [3, 4, 5]. For almost the last decade ceramic reinforced particles in a polymer matrix have the potential substance of extensive research. The mainly intended ceramic reinforced polymers have properties of stiffness improvement, cost reduction, simplicity of fabrication, and sustainable applications [6, 7]. Polymers have been widely used owing to their advantages such as low cost, low weight, endurance, hygiene, and design adaptability. The specified properties of polymer composite are achieved by numerous reinforcing materials of chemical compounds to achieve the physical, mechanical, electrical, thermal, and tribological applications [8]. For many engineering applications of polymer composites, the tribological behavior is important for understanding the mechanical properties [9].

PET material is the most common polymer used in day-to-day life. It's one of a leading polymer having applications starting from domestic to aerospace, and extensively used for electronics as PCB's, automotive as decorative interiors, aerospace as ergonomic structures, marine as corrosion-resistant materials, food packaging, lightweight fabrics, domestic usage molded parts, and plenty of applications in numerous fields [10]. Even in domestic applications, PET polymer is prominently used as a general pure plastic bottle container. Due to the versatility of PET polymer, many researchers have studied extensively to increase the properties of PET polymer as matrix material. Various materials are reinforced in PET polymer, like commonly used reinforcement are oxides such as ZrO₂, Al₂O₃, SiO₂, TiO₂, Cu, CuO, CuS, CuF₂, PBS, CaS, and boron nitride [1-12] for prerequisite applications, however, very limited research is done with PET polymer reinforced with BN ceramic particles processed by an injection molding

process. Hence an attempt is made to enhance the physical properties and mechanical properties of PET polymer by BN particles of average 50 microns size as reinforcement was used.

II. MATERIALS AND METHODS OF EXPERIMENTAL WORK

2.1 Materials

Commercial purity of 99% PET powder Accucomp PET008L grade of 1.38 g/cm³ density is used as matrix material and h-BN (purity: > 99%) powder of 2.1 g/cm³ density received from Intelligent Materials Pvt. Ltd, India, and M/s Nanoshell LLC were used as reinforcement material.

2.2 Preparation of PET/BN composites

The powdered PET polymer and BN particles were mixed and ball milled at room temperature together in correct proportions as per calculated wt. % (0 – 40%) by using eqn. 1 in an lab developed ball milling setup. The zirconia balls were used for mixing in the ball mill PET to BN powder at a 10:1 ratio. The ball mill was rotated at a speed of 60 rpm for 4 hours under dry conditions, BN micro size powder was added in 0, 5, 10, 15, 20, 30, and 40 wt. % in the PET matrix. During the ball milling process, the temperature of the mixture is maintained at room temperature by turning off the machine for 15 minutes every hour. The mixed powders from the mill were taken out and dried at 180 °C in the oven (INLAB Equipment (Madras) Pvt. Ltd. Chennai, India) to ensure complete moisture is removed from the composite mixture if any. The composite powder after drying was taken for processing in the molding machine. The injection molding machine barrel has 3 heating zones of temperature 200, 250, and 290 °C, and a pressure of 200 bar pressure is applied. The samples are cooled in the die only are ejected from the machine. All the test specimens are fabricated as per ASTM standards. The schematic of the injection molding machine process is as shown in Fig. 1. Commercially injection molding machines are used widely for polymer processing for several applications by varying the die molds. The benefits of the Injection molding process are process automation, low cost, permitting better-quality contours details, and cost of manufacturing is also economical, produce larger volume components and mass production in contrast to compression or hot compacting molding processes [13-18].

The composite powder is taken in the machine hopper and the barrel is preheated to 200, 250, and 290 °C. The melting temperature of PET polymer is 280 °C and is achieved in three phases in the barrel heaters, in the barrel at 200 °C and 250 °C the composite material becomes softer by the heat transfer from the barrel wall heaters, as the lead screw rotates it applies the high-shear forces on the powder and transfers the material to the die cavity. The powder turns completely into the molten state at 290 °C and is injected through runner and gates into mold die with high pressure. Later the die mold is allowed to cool for solidification at room temperature. The

specimens are prepared as showed in Table 1 for different weight percent, by using Equation 1. The specimens were fabricated as per ASTM standards, Impact test-ASTM D256, tensile test-ASTM D628, and flexural test-ASTM D790 [19, 20].

Table 1. Specimen codes and compositions.

Specimen code	PET -0	PET -5	PET -10	PET -15	PET -20	PET -30	PET -40
Wt. % BN	0	5	10	15	20	30	40
Vol. % BN	0.0	3.34	6.8	10.4	14.1	22.0	30.5

The equivalence vol. fraction (V_f) of wt. fraction (W_f) of BN was calculated by using equation:

$$V_f = \frac{W_f}{W_f + \left[(1-W_f) \left(\frac{\rho_f}{\rho_m} \right) \right]} \quad (1)$$

Where, W_f = wt. fraction of reinforcement, ρ_f = density BN (2.1 g/cm³), ρ_m = density PET (1.38 g/cm³). Table 1 shows the W_f Composition and equivalent V_f in percent. Theoretical density ρ_c (th), of PET/BN composite and weight of matrix and filler required for sample preparation of PET/BN composite are calculated by “Rule of Mixture (ROM)” [11] by using Archimedes principle experimental density was calculated [11,12]. The average of 3 readings were considered for calculations, specimen is weighed in air and later when immersed in medium and its weight is recorded.

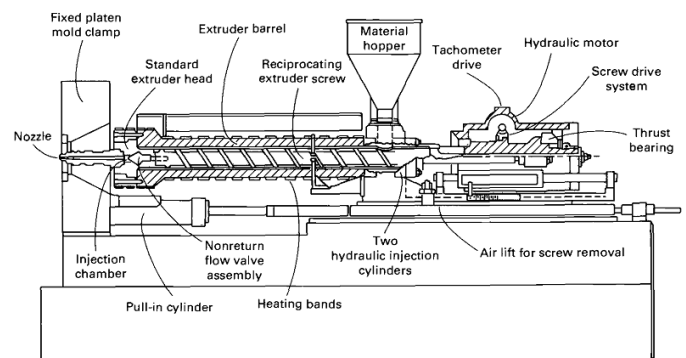


Fig. 1. Schematic diagram of molding machine

2.3 Characterization

PET/BN composite theoretical densities were calculated by using rule of mixtures (ROM) [11]. Densities of PET matrix 1.38 g/cm³ and BN reinforcement 2.1 g/cm³ were used. It was presumed that no loss and no cavities were formed in the processing of specimen fabrication. A high precision electronic balance AFCOSET model: ER200A is used to weigh the specimen. XRD peaks of BN powder (pure PET-100), PET powder (PET-0), and its composite comprising 5, 10, 15, 20, 30, and 40 wt% BN were carried out at room temperature by Philips X'Pert X-ray diffraction system with Cu K α radiation ($\lambda = 1.54$) for 2 θ . Microhardness

of PET/BN composite were calculated using (Model-MVH-S-AUTO-Z, Metatech Industries, Pune, India,) at 100 g load and 10 s dwell time. Average of five readings were used for calculations of microhardness of PET/BN composites. Tensile tests and flexural tests are carried out by using a UTM machine (Model-UNITEK-16100-STS) until specimens breaks. 5 mm/min were speed rate was used for applying a load, and Percent elongation and applied forces were recorded and results obtained from the tests generally suggest or predict the material behaviors and responses under other different loadings, this helps to select composite for a suitable applications. In tensile test, some of properties can be directly measured are tensile strength, elongation, and % reduction in area. Some properties can be determined indirectly are Young's modulus, yield strength, Poisson's ratio, and strain hardening characteristics, similarly flexural load, maximum deflection are studied from flexural testing and flexural strength, flexural modulus are determined. The impact test of PET/BN composite results was obtained using a Fine testing Machine (FTM), Model FIT-14, Miraj, India, the average of three specimens was considered for the impact test. The energy (J) absorbed by the specimen before fracture determines the impact toughness of a material to its cross sectional area. The weight and height at which the pendulum is released (potential energy) and swing of pendulum after it has struck the specimen start and end of energy pointer determines the energy absorbed (J). The PET/BN material impact strength is determined by energy absorbed before fracture to the cross-sectional area of the specimen. Optical microscopy images were observed by model SuXma-Met III, Metallurgical inverted microscope, Conation Technologies, Pune, India.

III. RESULTS AND DISCUSSIONS

3.1 Density

The theoretical and experimental densities of PET/BN composites are shown in Fig. 2. The increase in BN percent linearly increases the composite densities. The higher density of BN particles increases the pure PET matrix. The results shows good samples of defect free specimens during injection molding process and proper ball mill blending. Therotical and experimental densities of PET/BN are nearer to therotical densities at lower vol.% (PET-0, PET-5, PET-10 and PET-15) and at upper vol.% (PET-20, PET-30 and PET-40) differs from linearity as some porosity was observed, and higher concentration (PET-30 and PET- 40) more porosity was observed by addition of BN percent. The porosity confirms by addition of BN wt.% the interparticle space reduces and in turn resulting in bigger agglomerations of BN elements. The controlling of uniform distribution of BN particles in molten polymer at machine barrel becomes more challenging as a result agglomeration is observed as cnfirmed in optical microscopy, which leads to porosity. The maixmum 4.21 % porosity was observed at PET- 40 composite compared with therotical density. The results obtained are inline with other researchers [11,12].

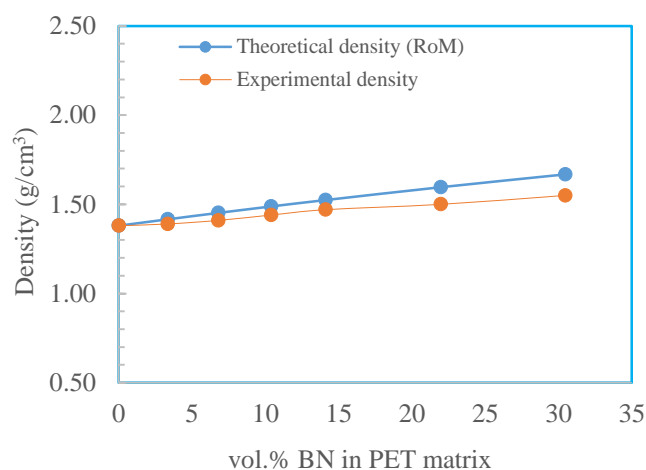


Fig. 2, Density - vol. % BN of composites

3.2 Microhardness Hardness

Fig. 3, shows theoretical and experimental microhardness of PET/BN composites, by using rule of mixtures (ROM), theoretical values were calculated. The microhardness of pure PET is 7.9 kg/mm² and BN microhardness is 76 kg/mm² the microhardness of composites increases with addition of BN percent in the virgin PET matrix. The experiemntal hardness ic calculated from the machine readings as shown in Fig. 3 and average of 5 readings were considered.

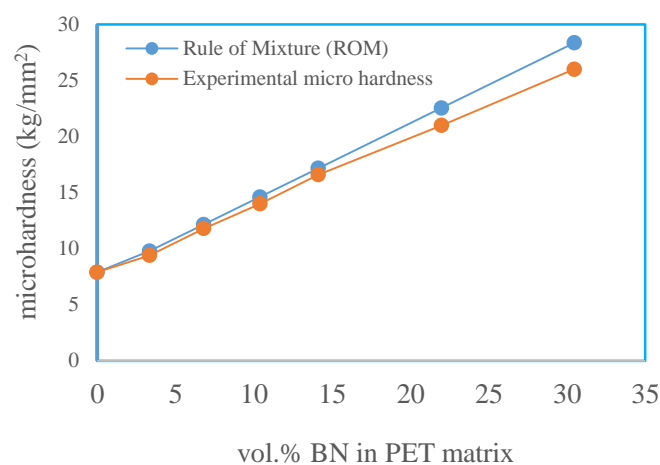


Fig. 3, Microhardness - vol. % BN of composites

The vickers micro hardness tester uses micro indentation technique and extensivly for polymer composites to get micromechanical properties of polymers and polymer composites. The microhardness of PET/BN composite progressively increases with addition of BN reinforcement. The maximum microhardness values of the PET-40 composite increased to 21 kg/mm², approximately 35% increase compared to pure PET matrix. By addition and uniform dispersion of BN particles increase the microhardness and attributing to the higher hardness. The BN particles uniform dispersion resists the deformation to externally applied load. However, increasing BN percent in the PET matrix reduces the inter-particles spaces of BN thus,

resulting in increased resistance to indentation as observed presence of agglomeration and voids in optical microscopy. At higher vol. % (PET-40) the maximum porosity was around 4.21%. The theoretical microhardness were calculated by using rule of mixture [11] and were compared with experimental microhardness values. The presence of voids in the matrix offers least resistance to indenter and resulting lower microhardness values related to void free specimens.

3.3 Impact strength

Impact test results at room temperature of PET/BN composite are shown in Fig. 4. Fracture energy and impact strength increases and absorbs more energy for higher concentration BN powder compared to pure PET matrix before failure. As BN particles in per unit volume increase with wt. % obstructs the crack propagation, (i.e. absorbed energy increases). The fracture energy and Impact strength are increasing as the contact surface area of PET are decreasing for increased wt. % as wettability of BN particles increases resulting in increasing in transmitting energies from matrix to BN reinforcement. The grain boundaries are increasing as an agglomeration of BN reinforcement addition at higher wt. % resulting in the better impact strength of PET/BN composite.

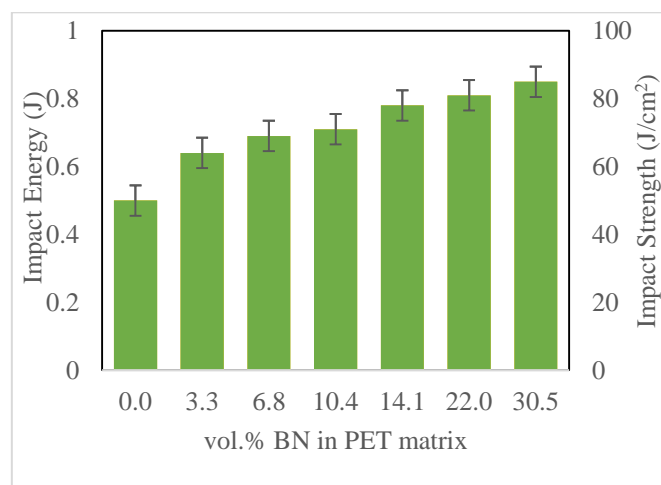


Fig. 4, Impact energy and impact strength versus vol. % BN of the PET/BN composites

3.4 Tensile strength

Mechanical properties - The most basic characteristics of semi crystalline polymers are tensile behavior. Generally, the predictable that microscopic properties depend closely on the strain rate, hence the dependence of strain rate behavior is necessary to promote the wide engineering applications. The necking of the polymeric material generally signifies softening and reduces the elastic module [13], the morphology changes of a particle structure with increase in elastic modulus known as strain hardening, as the neck grows and reaches a limiting region. Similar trend was reported by other researchers [13, 14].

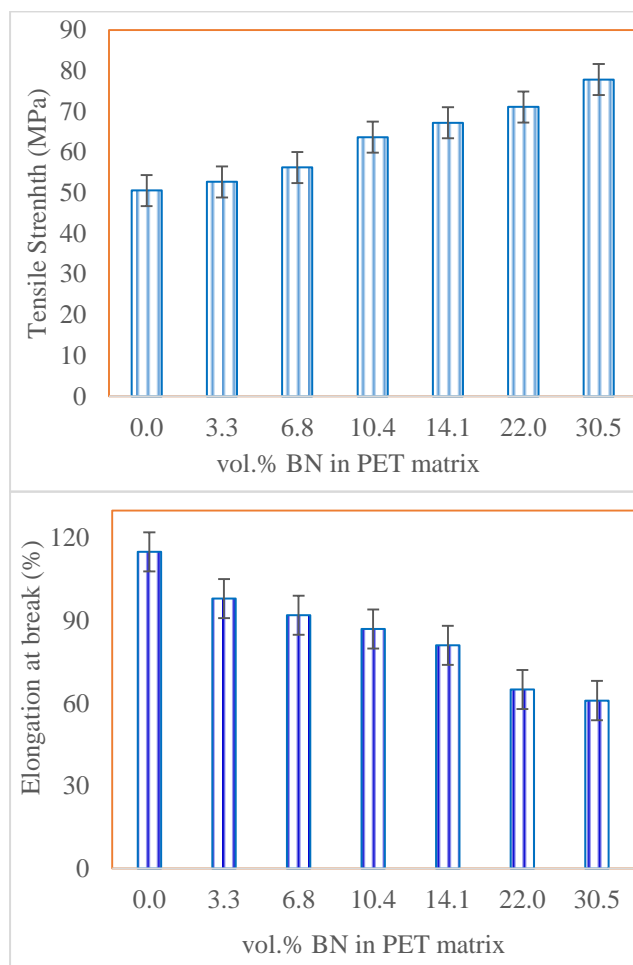


Fig. 5 (a, b), Tensile strength and % elongation versus vol. % BN of the PET/BN composites

Fig. 5 (a, b) shows, tensile strength and % elongation of the PET/BN composites, this shows the tensile strength of composite has increased by almost 54%, and percent elongation reduced by almost 39%, this attributes the behavior is brittleness by addition of BN particles resulting into agglomeration resulting in insufficient transfer of stress to PET matrix and the lack of proper load distribution between the matrix and the BN. Moreover, BN particle reinforcement has shown to contribute to an enhancement of Young's modulus.

3.5 Flexural bending

The addition of BN reinforcement increases the flexural modulus or stiffness of pure PET polymer as shown in Fig. 6. The properties of reinforcement majorly depends on its particle size and aspect ratio. Higher the aspect ratio, higher the stiffness for improving flexural strength and flexural modulus [14].

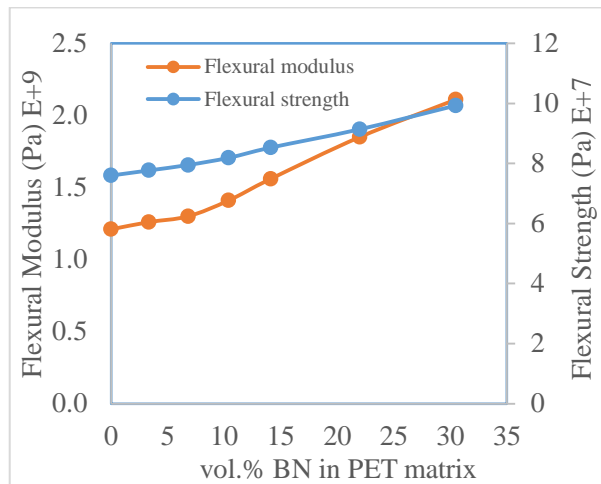


Fig. 6, Flexural modulus and flexural strength - vol. % BN of the PET/BN composites

Pure PET samples are ductile and yielding higher deformation compared to BN reinforcement composites. By the addition of BN particles yielding is reduced and flexural strength and flexural modulus are increased, it's observed from results due to BN addition tensile strength and flexural strength, microhardness, impact strength are increasing and resulting in a decrease in elongation at break and deformation this is due to ductile to the brittle transition of composite specimens.

3.6 XRD analysis

The (2θ) diffraction peaks (JCPDS: 34-0421[15]) are predominant crystallographic reflections for virgin PET polymer (PET-0), and virgin BN (PET-100), and compositions containing 10, 20, and 30 wt. % (PET-10, PET-20 and PET-30 respectively). Fig. 7, shows 2θ values of XRD patterns for pure PET and BN reinforced composites. The patterns of XRD test shows a superimposition of crystalline peaks. This suggests that the PET is a semi-crystalline polymer [16]. This PET/BN powder mixture no longer shows any peaks of elements present in the system as impurity. All compositions shows diffraction peaks of PET and BN elements only. This confirms the BN morphology is unchanged in the fabrication process. It is likewise determined that the peak intensity of BN vol. % increase in the PET matrix.

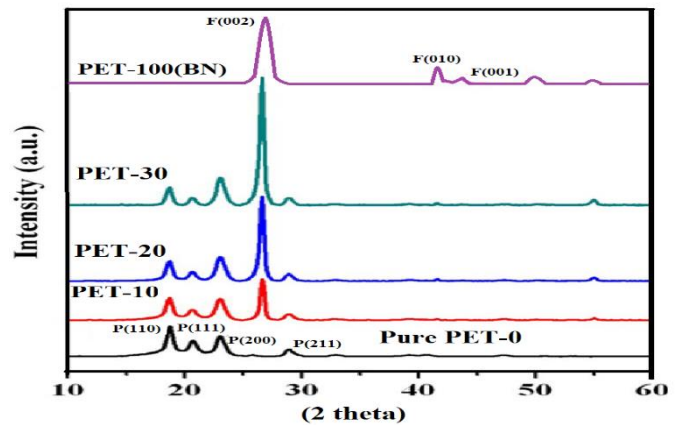


Fig. 7, XRD (2θ) peaks of PET and BN powder PET/BN composites

3.7 Optical microscopy.

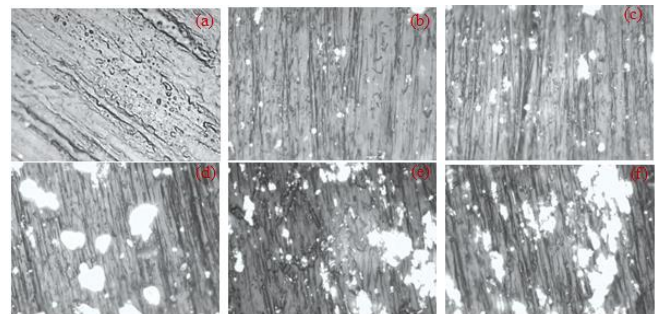


Fig. 8, Optical micrographs of (a) PET-0, (b) PET-5 (c) PET-10 (d) PET-20 (e) PET-30 (f) PET-40 vol. % BN of the PET/BN composites (Scale bar 100 μm, at 100 X magnification)

Fig. 8 (a-f), shows the distribution of BN in PET matrix prepared by ball milling. BN is homogeneously dispersed throughout the PET matrix to lower concentration (a-d) and at higher concentration agglomeration is observed, BN particles tend to form a fine 3^D network and causing in increasing impact strength, hardness, and tensile strength of the PET/BN composite [17]. The porosity present in BN vicinity, leads to agglomeration affecting decreased density, and lower elongation of composite results in brittleness and higher vol. % decreases particle distances between the BN particles.

IV. CONCLUSIONS

The PET/BN composites added up to 40 wt.% (30.5 vol.%) BN particles were successfully fabricated by injection molding process are almost defect-free samples, theoretical and experimental densities are identical at lower vol.% and 4% porosity was observed at higher vol. % due to agglomeration of BN particles forming a three-dimensional network structure, as observed by the optical microscopy. Optical microscopy photographs shows uniform dispersion of BN particles at lower vol. % and agglomeration in higher vol. %. XRD confirms the absence of new materials in the composites. i.e., the BN particle presence didn't affect PET

morphology. Microhardness was increased by 28% and are close to theoretical hardness. Impact energy and impact strength were increased nearly 70% compared to virgin PET, tensile strength (50 to 77MPa) and flexural strength increased by 22%. Ductility/Elongation of the composite is decreased (115 to 61%) and brittle fracture nature was observed at a higher vol. % of the polymer.

REFERENCES

- [1] A.M. Al-Sabagh, F.Z. Yehia, Gh. Eshaq, A.M. Rabie, A.E. ElMetwally (2016) "Greener routes for recycling of polyethylene terephthalate" *Egyptian Journal of Petroleum* 25, 53–64
- [2] F. Khoffi, N. Khenoussi, O. Harzallah, J-Y. Drean, (2011), "Mechanical behavior of polyethylene terephthalate/copper composite filament" *Physics Procedia*, 21 240 – 245
- [3] Antonio F. A vila, Marcos V. Duarte (2003) "A mechanical analysis on recycled PET/HDPE composites" *Polymer Degradation and Stability*, 80, 373–382
- [4] Young-Ho Seo, Chung-Gil Kang (1995) "The effect of applied pressure on particle-dispersion characteristics and mechanical properties in melt-stirring squeeze-cast SiCp/Al composites", *Journal of Materials Processing Technology*, 55, 370-379.
- [5] Muzamil Hussain, Rizwan Ali Naqvi, Naseem Abbas, Shahzad Masood Khan, saad Nawaz, Arif Hussain, Nida Zahra, Muhammad Waqas Khalid (2020), "Ultra- High-Molecular Weight polyethylene (UHMWPE) as a Promising Polymer material for Biomedical Applications: A Concise Review" *polymers* 12, 323, DOI:10.3390/polym12020323
- [6] Javeriya Siddiqui and Govind Pandey (2013) "A Review of Plastic Waste Management Strategies" *International Research Journal of Environment Sciences* Vol. 2(12), 84-88,
- [7] B. Aldousiri, A. Shalwan, and C. W. Chin (2013), "A Review on Tribological Behaviour of Polymeric Composites and Future reinforcements" *Hindawi Publishing Corporation, Advances in Materials Science and Engineering*, Volume DOI:10.1155/2013/645923
- [8] Watthanaphon Cheewawuttipong, Daisuke Fuoka, Shuichi Tanoue, Hideyuki Uematsu, and Yoshiyuki Iemoto (2013) "Thermal and Mechanical Properties of Polypropylene/Boron Nitride Composites" *Energy Procedia*, 34, 808 – 817
- [9] F. Khoffi, N. Khenoussi, O. Harzallah, J.Y. Drean (2011) "Mechanical behavior of polyethylene terephthalate/copper composite filament" *Physics Procedia*, 21, 240 – 245
- [10] Courtney Harrison, Sean Weaver, Craig Bertelsen, Eric Burgett, Nolan Hertel, Eric Grulke (2008) "Polyethylene/Boron Nitride Composites for Space Radiation Shielding" *Journal of Applied Polymer Science*, Vol. 109, 2529–2538 VVC Wiley Periodicals, Inc.
- [11] M. A. Kori, M. G. Kulthe, R. K. Goyal, (2014) "Influence of Cu Micro Particles on Mechanical Properties of Injection Molded Polypropylene/Cu Composites" *International Journal of Innovative Research in Science, Engineering and Technology (An ISO 3297: 2007 Certified Organization)* Vol. 3, Issue 6, ISSN: 2319-8753
- [12] M. G. Kulthe and R. K. Goyal, (2012) "Microhardness and electrical properties of PVC/Cu composites prepared by ball mill", *Adv. Mat. Lett.* 3(3), 246-249, , DOI: 10.5185/amlett.2012.3326
- [13] Zishou Zhang, Chunguang Wang, Kancheng Mai, (2019) "Reinforcement of recycled PET for mechanical properties of isotactic polypropylene", *Advanced Industrial and Engineering Polymer Research*, 2, 69-76
- [14] Muhammad Akmal Ahmad Saidi, Azman Hassan, Mat Uzir Wahit, and Lai Jau Choy (2018) "mechanical and thermal properties of polyethylene terephthalate/polybutylene terephthalate blends" *University Technology Malaysia, Johor Bahru, Malaysia, IGESH2018*,
- [15] Liang Huang, Pengli Zhu, Gang Li, Fengrui Zhou, Daoqiang Lu, Rong Sun, Chingping Wong, "Spherical and flake-like BN filled epoxy composites morphological effect on the thermal conductivity, thermo-mechanical and dielectric properties", *J Mater Sci: Mater Electron*, DOI:10.1007/s10854-015-2870-1
- [16] Ding Chen, Feng Wei, Santosh K. Tiwari, Zhiyuan Ma, Jiahao Wen, Song Liu, Jiewei Li, Kunyapat Thummavichai, Zhuxian Yang, Yanqiu Zhu and Nannan Wang (2020) "Phase Behavior and Thermo-Mechanical Properties of IF-WS2 Reinforced PP-PET Blend-Based Nanocomposites" *Polymers* 2020, 12, 2342; DOI:10.3390/polym12102342
- [17] Liu Liu, Linghan Xiao, Ming Li, Xiuping Zhang, Yanjie Chang, Lei Shang, Yuhui Ao, "Effect of hexagonal boron nitride on high-performance polyether ether ketone composites", *Colloid Polym Sci*, DOI:10.1007/s00396-015-3733-2
- [18] K.K. Chawla, *Composite Materials: science and Engineering*, (Springer, New York, London, 2012)
- [19] R.T. Rao, J.R. Eugene, G.K. Alan, *Microelectronics Packaging Handbook, Technology Drivers, Part I*, 2nd edn. (Chapman and Hall, London, 1997)
- [20] *Electronic Materials Handbook, Packaging*, vol. 1 (ASM International Handbook Committee, Materials Park, 1998)

Fundamental Frequency estimation and analysis of speech signal

^[1] Mahesh M. Kamble, ^[2] Tejal S. Bandgar

^[1] PG Student, ^[2] Assistant Professor

^{[1][2]} Electrical Department, PVPIT Budhgaon Sangli, Dr. Babasaheb Ambedkar Technological University, Lonere Maharashtra India

Abstract— Fundamental frequency is a critical component in speech signal processing analysis. The fundamental frequency (f_0) is the rate at which the vocal cords vibrate, and the fundamental frequency range for a person is 120 to 400 Hz. This basic frequency varies depending on the size and form of the vocal cords, and it might differ for males, females, and children. Different domain of time and frequency pitch estimation techniques are utilised. The time domain methods include autocorrelation and AMDF (Average Magnitude Difference Function), whereas the frequency domain algorithm is Cepstrum. The fundamental frequency may be determined by pitch preprocessing and extraction.

Index Terms – Autocorrelation function, Center-clipping, Pitch Detection Algorithm, Pitch

I. INTRODUCTION

Signals that are audible to humans are referred to as audio signals. Audio signals are generated by a sound source that vibrates at audible frequencies. The vibrations cause pressure waves to develop in the air, which travel at a speed of roughly 340 metres per second. These pressure signals are received by our inner ears, which then convey them to our brain for further analysis. Pitch, also known as fundamental frequency, is a key characteristic of audio transmissions. It represents the sound source's frequency of vibration. Pitch can be term as requite of the rudimentary period, or the rudimentary frequency of audio signals. The time discipline or domain and the frequency discipline are used to estimate pitch or fundamental frequency. In time discipline Autocorrelation process and AMDF(Average Magnitude Difference Function) process can used whereas in frequency discipline Cepstrum process is used. The human voice production system involves following steps as open and close of vocal cords which is also called as glottis which create a vibration in the air flow, a resonance is provided by Oral cavity, pharyngeal cavity, and nose cavity; there is a approach of a voiced signal or unvoiced signal .Due to the glottis pressure and the pushed air.The vocal chords get air from the lungs, open and close rapidly and further modulated by the resonances of pharyngeal, oral and nasal cavities. Pitch is determined by the vibration frequency by the vocal cords. The fundamental frequency is different for male, female and children category.

II. BACKGROUND

A. Autocorrelation Method and AMDF

Pitch tracking using the auto-correlation function (ACF) is a simple approach. This method is a time domain method which is used to determine the similarity between a frame and a shifted or delayed version of the frame.

$$R_x(m) = \lim_{N \rightarrow \infty} \frac{1}{2N+1} \sum_{n=-N}^N x(n)x(n+m)$$

N is the breadth of the frame, n is the index of time in a frame, m is the shifted version in the signal, $x(n)$ is the signal which can be called as sampled. To acquire n values of ACF, shift the delayed version m times and compute the inner product of the overlapping portions.

AMDF is quite similar to ACF, except that it uses the following formula to determine the distance between a frame and its delayed version, rather than similarity.

$$D_m = \frac{1}{L} \sum_{n=1}^L |X(n) - X(n-m)|$$

I. Where the input voice samples are $x(n)$, and the samples time shifted by m seconds are $x(n-m)$.

II.

B. Cepstrum

The Cepstral method gives analyzer which is designed primarily for use in speech analysis. The logarithm of each successive amplitude spectrum so produced can be fed into a second spectrum analyzer of the same type. The cepstrum, or power spectrum, of the logarithm spectrum is then produced by this analyzer. A voice example, with X referring to the speech signal's spectrum, F referring to excitation components such as the glottal pulse train, and V referring to the excitation spectrum's vocal tract shaping.

C. Feature Extraction

The process of turning a stream of audio signals into a sequence of frames is known as frame blocking. To extract a single segment at a time, the signal $s(n)$ is multiplied by a specified length analysis window $w(n)$. This is alluded to as windowing. Speech signal includes very rich harmonic components. The f_0 varies in the range about 80 Hz to 500 Hz as per the age and gender of person. Pitch detection is ineffective over 500 Hz. Pitch detection is implemented using a low pass filter with a pass band of up to 900 Hz. One specific shape nonlinear processing is commonly employed

center-clipping of speech to decrease the influence of formant structure. Energy is a characteristic that may be utilised to distinguish between voiced and unvoiced communication. It takes into account the limited time energy. Short time means the energy of analysis period.

$$E = \sum_{k=-\infty}^{\infty} s(n)^2$$

PDA's	Formulae
Autocorrelation function	$R_x(m) = \lim_{N \rightarrow \infty} \frac{1}{2N+1} \sum_{n=-N}^N x(n)x(n+m)$
AMDF function	$D_m = \frac{1}{L} \sum_{n=1}^L X(n) - X(n-m) $
Cepstrum function	$c(n) = \frac{1}{2\pi} \int_{-\pi}^{\pi} \log x(\omega) e^{j\omega n} d\omega$

III. IMPLEMENTATIONS

According to the discourse above, the approach desire that the speech signal be low-passed filtered to 900 Hz. The filtered signal is digitised at a 10-kHz sampling rate and split into overlapping 30-ms (300 samples) chunks for refining. Because all pitch detectors estimate the pitch period 100 times per second, or every 10 milliseconds, adjacent sections of the waveform overlay by 20 milliseconds, or 200 samples. The second stage of refining involves identifying a clipping threshold CL for the 30-ms segment of speech. In the first and last 10-ms of the segment, the clipping threshold is set to 68 percent of the smaller of the peak absolute sample values. After determining the clipping level, the 30-ms speech segment is centre clipped, followed by indefinite peak clipping.. Then the energy of the signal is calculated. After computing the ACF/AMDF according to peak values the fundamental frequency is estimated.

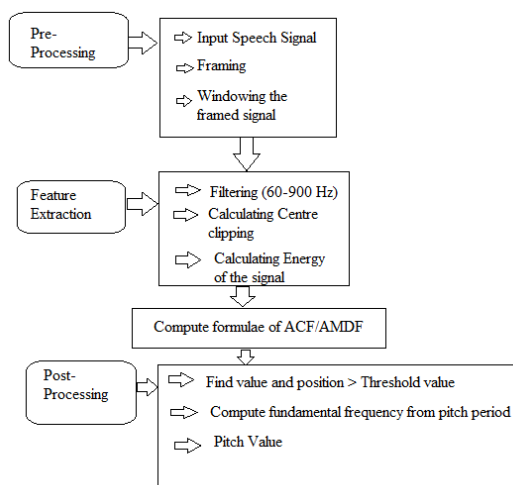


Fig. 1 ACF/AMDF technique for fundamental frequency estimate (fo) on the blockchain

IV. RESULTS

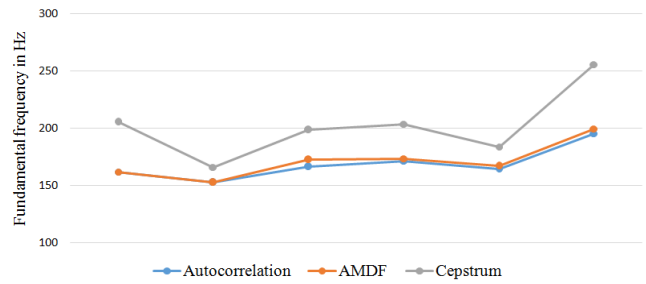


Fig. 2 Comparison chart of three pitch detection algorithm for adult male samples

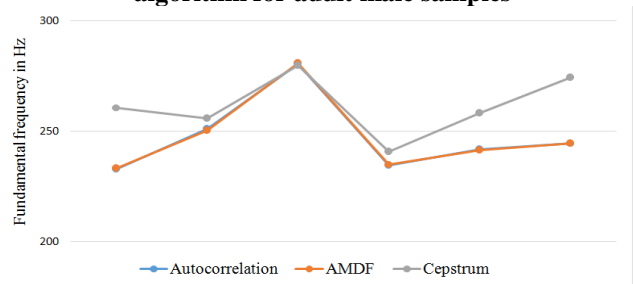


Fig. 3 Comparison chart of three pitch detection algorithm for adult female samples

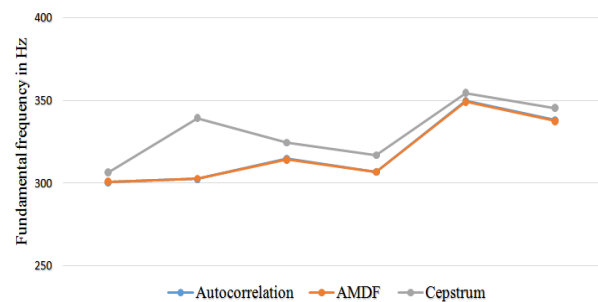


Fig. 4 Comparison chart of three pitch detection algorithm for children samples

V. CONCLUSIONS

The tone of human and pitch are influenced by the fundamental frequency of a sound wave. The method to ascertain the pitch period of voice signal is important not only in speech signal processing, but also in diagnosing vocal cord symptoms.

Pitch is the most distinctive difference between male and female speakers. The autocorrelation function, the average magnitude difference function, and cepstrum analysis are three PDAs that have been introduced. The results show that children has a fundamental frequency near or above 300 Hz whereas female has fundamental frequency in the range 210-280 Hz whereas male fundamental frequency lies in between 150-220 Hz.

REFERENCES

- [1] Smt.SanjivaniS.Bhabad, G.K.Kharate, Smita C. Shinde, 'Pitch detection in time,frequency and cepstral domain for articulatory handicapped people',978-1-4799-1626-9/\$31.00 2013 IEEE.
- [2] Savitha S Upadhya, 'Pitch Detection in Time and Frequency Domain', 2012 International Conference on Communication, Information & Computing Technology (ICCICT), Oct. 19-20, Mumbai, India, 978-1-4577-2078-9/12/\$26.00©2011 IEEE.
- [3] zhijun Cui, 'Pitch Extraction Based on Weighted Autocorrelation Function in Speech Signal Processing', 2012 2nd International Conference on Computer Science and Network Technology, 978-1-4673-2964-4/12/\$31.00 ©2012 IEEE.
- [4] Jeiran Choupan, SeyedGhorshi, Mohammad Mortazavi, FarshidSepheband, 'PITCH EXTRACTION USING DYADIC WAVELET TRANSFORM AND MODIFIED HIGHER ORDER MOMENT', 978-1-4244-6871-3/10/\$26.00 ©2010 IEEE.
- [5] YANG Fan, LIU Ming-hui, XU Sun-hua, PAN Guo-feng, 'Research on aNew Method of Preprocessing and Speech Synthesis Pitch Detection', 2010 International Conference On Computer Design And Appliations (ICCCA 2010), 978-1-4244-7164-5/\$26.00 © 2010 IEEE
- [6] Li Tan and MontriKarnjanadecha, 'PITCH DETECTION ALGORITHM: AUTOCORRELATION METHOD AND AMDF.
- [7] Geliang Zhang, Simon Godsill, 'TRACKING PITCH PERIOD USING PARTICLE FILTERS', 2013 IEEE Workshop on Applications of Signal Processing to Audio and Acoustics, 978-1-4799-0972-8/13/\$31.00 ©2013IEEE.
- [8] S. S. Nimbhore, G. D. Ramteke, R. J. Ramteke, 'Pitch Estimation of Marathi Spoken Numbers in Various Speech Signals', International conference on Communication and Signal Processing, April 3-5, 2013, India, 978-1-4673-1622-4/12/\$31.00 ©2013 IEEE.
- [9] Yuan Zong, Yumin Zeng, Mengchao Li, RuiZheng, 'Pitch Detection Using EMD-Based AMDF', 2013 Fourth International Conference on Intelligent Control and Information Processing (ICICIP) June 9 – 11, 2013, Beijing, China, 978-1-4673-6249-8/13/\$31.00 ©2013 IEEE.
- [10] NutthachaPrukkanon, KosinChamnonngthai, Y oshikazuMiyanaga, 'VT -AMDF Pitch Detection Algorithm and Thai Tone Recognition System', Signal ProcessingAudio, Speech and Language ProcessingPaper 10 1177, The 8th Electrical Engineering/Electronics, Computer,Telecommunications and Information Technology (ECTI) Association of Thailand - Conference 2011, 2009 International Symposium on Intelligent Signal Processing and Communication Systems (ISPACS 2009) December 7-9, 2009, 978-1-4244-5016-9/09/\$25.00_c 2009 IEEE
- [11] Jongmin Lee, Pingping Zhu, and Jose C. Principe, 'A Parameter-free Kernel Design Based on Cumulative Distribution Function for Correntropy'.
- [12] Roshapokharel and Jos'e. C. Principe, 'Kernel Classifier with Correntropy Loss', WCCI 2012 IEEE World Congress on Computational Intelligence June, 10-15, 2012 - Brisbane, Australia.

An Analysis of Deep Learning Models for Dry Land Farming Applications

^[1] S.Mithra, ^[2] Dr.T.Y.J.NagaMalleswari

^[1] Ph.D Full Time Scholar, Department of CSE, SRMIST, Chennai

^[2] Assistant Professor, Department of CSE, SRMIST, Chennai

Abstract— Smart farming is a farming system that integrates information technology (IT) to ensure that plants, animals and soil receive what they have for optimum health and production. The goal of Smart Farming is to provide the profitability, viability and security of the ecosystem. Agriculture is indeed a challenge in drought-prone areas with limited water supplies. Using remote sensing data such as UAV images is exceptionally sufficient to detect the in-field variability of soil and plant properties in dry soil. UAV images produce faster and more accurate NDVI with higher resolution. New technologies such as IoT, Artificial Intelligence, Global Positioning Systems (GPS) and Big Data Analysis are promising tools to optimise farmed operations and inputs to enhance productivity and reduce losses and returns of information. Finally, the fundamental Dry Land Agricultural issues under study, their applications, specific models and sources were examined. Besides, the study compares standard deep learning algorithms with the results of classification or regression accuracy.

Index Terms – Smart Farming, Dry Land, UAV Images, Deep Learning, Soil Management, Crop Prediction.

I. INTRODUCTION

Precision Agriculture first appeared in tractors with GPS facilities in the 1990s. Therefore, this adoption of technology is now so increasingly rapid that it is undoubtedly the most widely used instance of Ag precision today. Access to real-time data on the conditions of crops, plants, livestock, soil and ambient air is included in the Precision Farming method, alongside other related details such as labour costs, hyper-local weather forecasts and availability of equipment [1]. Satellites and Robotics Drones offer real-time images of individual plants to farmers. For immediate guidance and future agricultural land decisions, satellite and drone data are beneficial, resulting in data such as what fields to water and when and where to plant a specific crop. In agricultural areas, the sensors measure the moisture content of the soil and the temperature of the soil and surrounding air. Agricultural Control Centres incorporate additional data from sensor data and imagery input, providing farmers with the facility to classify areas for treatment and to determine the optimal amount of water, fertilisers and pesticides to be used. It helps the farmer prevent water wastage and stop run-off, ensuring that the soil has the correct amount of optimal health additives, while reducing costs and controlling the farm's environmental effects. The use of data technology (IT) and a good range of items, such as GPS guidance, sensors, control

systems, robots, drones, autonomous vehicles, automated hardware, variable rate technology, soil sampling based on GPS, telematics and software, are a vital component of this farm management approach.

In the case of dry lands, agriculture may be challenging due to water scarcity and invasive trees. Dry Land Agriculture is a particular farming case that is hooked into rain conditions and without secure irrigation facilities. However, some injurious plants or trees reduce the quantity of water and quality of the fodder [2]. One among those plants is Prosopis Julifora which is native to West Africa. It had been delivered to India in the 1960s to satisfy the agricultural poor's fuel wood requirement and to revive degraded lands. It results in the absorption of water from the soil and moisture from the atmosphere, and it forms a more significant impression on the environment. It also affects the expansion of nearby plants and absorbs the water content in those lands. Eventually, the Madras Supreme Court orders the Tamil Nadu government as introduced an Act to eradicate invasive shrubs within a period.

In smart farming, UAV technologies can hit each and every nook of the earth. There are enormous prospects of using UAVs for intelligent agriculture. For more timely evaluation, UAVs may obtain more reliable and faster NDVI data than satellite imagery. High-resolution UAV-based NDVI imaging allows for much earlier diagnosis, identification, corrective action and continuous monitoring than low-resolution satellite imaging [3]. UAV-based NDVI imagery can also support variable-rate broadcasters operating at a resolution level of 1 square metre.

Land Sat satellite-based NDVI imagery, on the other hand, can only support variable speed spreaders operating at a resolution level of 900 square metres, 30 metres by 30 metres. The frequency of UAV images is the maximum amount required by the farmer per day, while the satellite may provide an average of 4 images per month. In motivating farmers, however, the importance and ease of controlling UAVs for smart farming may play an important role [4].

II. SMART FARMING APPLICATIONS USING UAV IMAGERY

The UAV industry has grown from a niche market to widespread availability, lowering the cost of taking images and opening up a range of exciting applications. The advantages of UAV technology include small sizes, low cost, environmental protection of operation and, most of all, fast and on-demand acquisition of photographs. The development

of UAV technology has reached the stage of being able to provide remote sensing images that provide a lot of spatial and contextual information that is too high-resolution [5]. Revolutionizing precision agriculture is the spatial resolution that UAVs offer. Workflows for crop condition assessment, identification of plant density, growing season yields, fruit counting, weed identification and tracking, vegetation and crop monitoring and disease detection, irrigation and pest infestation control and classification of crop types [6].

2.1 Weed Detection:

In agriculture, the major yield losses are due to weed growth. The farmers spray a large amount of herbicides uniformly on the field to kill weed. This approach is harmful for the environment and humans. The techniques of Precision Farming allow farmers to spray herbicides in the correct portion and at the right time [7].

Techniques Used:

- Transformation of UAVs to an aerial image acquisition device for localizing and controlling weeds.
- Acquisition systems for specialized UAVs automate cannabis segmentation.
- Complex classification to distinguish weeds is generalized and context segmentation is combined with line detection to classify weeds from the actual crop [8]. The architecture for this type-type approach is ResNet.
- Thresholding technique for weed identification and measurement of plant/weed density/weed species from far above the field and near the canopy. CNN for the description and probability assessment of weed species [9].

2.2 *Crop Mapping:* Plant and vegetation mapping is an important planning strategy for the long term and broader management of crops and agricultural products. [10].

Techniques Used:

- A new hybrid CNN platform model for deep learning, consisting of four different CNNs combined to map vegetation crops [11]. The proposed CLA is based on the pre-trained Alex-net architecture which has been updated slightly to handle data.
- A deep model, a mixture of convoluted neural networks is provided with multiple ConvNet models, which obtain feedback from various context windows around labelled pixels and a training-specific pixel strategy [12].

2.3 *Crop Counting and Predictions for Yield:* The invention of the UAV industry greatly reduced the cost of aerial imaging and paved the way for too many exciting applications, such as grain counting and yield forecasting.

Techniques Used:

- A new approach to the deep-sharp Google model involves four steps: image acquisition, pre-processing, model classification, sampling, and adaptation of the identification and mapping of scale techniques of existing coffee crops.

2.4 *Identification, Segmentation and Classification of vegetation:* Automatic segmentation and classification of crops and vegetation by UAVs is becoming a key technology for the identification and classification of vegetation. Classic artificial neural network machine learning methods and deep learning approaches for identification and segmentation of aerial vegetation images [14].

Techniques Used:

- 3D convolutionary neural networks are used for crop classification with multi-temporal UAV images [15].
- The input layer, two pooling layers, three convolutionary layers, two top link layers, two local contrast adjustment layers and one output layer are the traditional CNN 11 layers with spatio-temporal characteristics. This process has a higher accuracy rate in the classification.
- The HistNN model uses the per-window histogram to improve the efficiency of crop classification.
- Morphology, Segmentation and CNN: a new 3-stage deep neural network based algorithm for the detection of tobacco plants [17].
- Terrestrial data and faster R-CNN deep network and individual maize segmentation regional growth algorithms.

2.5 *Ailment and Nutrient Detection:* A big problem for agriculturalists who regularly deal with crop diseases. Early diagnosis and identification of crop diseases are important for reducing production yields and increasing disease infestation containment [18].

Techniques Used:

- NDVI map for the detection of leaf stripe disease with the aid of multispectral images.
- In order to predict the magnitude of late blight in potato crops, the CNN model implemented machine learning algorithms including multilayer perceptron, random forests and support vector regression.
- Multilayer Perceptron (MLP) neural networks are applied from the images to some different spectral bands to define the best association among the model of the neural network and the status of water [19].
- Local binary models and VGG-A network for the identification of Fusarium wilt contaminated radish captured by UAV mounted high-resolution RGB cameras.

- LeNet-5 for Helminthosporium Leaf Blotch (HLB) disease detection and classification in Wheat Harvest.

III. DRY LAND SMART FARMING APPROACHES USING DEEP LEARNING METHODS

Agriculture is dependent on it as the single largest source of livelihood in India with almost two-thirds of individuals. Growing of crops is understood as land cultivation entirely under rain fed conditions. Approximately 70% of rural people live in dry farming areas and their livelihood depends on crop success or failure [20].

Limitations for Crop Production in Dry Farming Regions:

- Insufficient and unequal distribution of precipitation.
- Late-onset of early rain interruption.
- Prolonged periods of dryness during the crop season.
- Low ability for maintaining moisture.
- Poor soil fertility.
- Danger from invasive trees and weeds.

Weed detection, field tracking, crop counting and yield predictions, vegetation recognition, classification and segmentation, disease and nutrient deficiency detection [21] are the most popular applications that use deep learning models in agriculture.

3.1 Plant/Shrubs Identification Methods in Dry Land:

Various machine learning algorithms have been published for an increasing conventional distribution maps of invasive alien plant species (IAPS). In two other implementations, a deep neural learning network, a random forest, a vector support machine and a generalized linear model, this analysis compares the performance of five MLAs: a gradient booster machine; thus defining the most efficient ones for the fractional cover and distribution of IPAS [22].

TABLE I: SHRUBS IDENTIFICATION METHODS

S. No	Algorithm	Description	Data set	Parameter	Accuracy
1	Artificial Neural Network (ANN)	Using leaf picture features, identification of particular plant leaves	Flavia Dataset	Shape, Color, Texture, Leaf Vein	94.4%
2	Convolutional Neural Network (CNN)	Leaf Classification based on the sense of	Flavia Dataset	Shape-context, Shape-texture	94%

		marginalised form, texture of shape using deep CNN			
3	Probabilistic Neural Network (PNN)	The loaded function vector with a higher speed rate is trained by the PNN classifier	Flavia and Swedish Dataset	Centroid gap and least inertia axis	82.1% and 80.1%
4	Support Vector Machine (SVM)	Combined classifier for classification of plants and leaf image recognition.	Flavia Dataset	Shape, color, texture, vein pattern	91.85%
5	K-Nearest Neighbor (KNN)	Based on form and edge characteristics, leaf classification	Flavia Dataset	Shape, Edge	94.4%

The results of five algorithms in invasive tree distribution and fractional cover abundance plotting. Of the five algorithms tested in Table I, the Artificial Neural Network performed the best with 94.4 percent accuracy and >0.89 sensitivity and specificity. With an accuracy of 94.4 percent, the next best-performing algorithm is k-Nearest Neighbour. Comparably poor outputs were obtained by the other algorithms tested [23].

3.2 Seed Degradation

By feeding on large quantities of water, increasing soil acidity, CO₂ pollution, taking over land from native flora, and so on, invasive dry land plants or shrubs affect insufficient, underground water supplies. Some researchers estimate that in order to grow to weigh one kilogram, the weed consumes as much as 1000 liters of water, while other plants consume less than 50 liters. Actually, weed removal is performed using manual tools in many agricultural and rural communities in Asia. More affordable and advanced technologies are required that can be built by indigenous

communities using skills to combat the invasion of shrubs [24]. This method is important because unless the deep roots are extracted, Deep Learning techniques used in seed/weed identification tend to regrow the species.

TABLE II: SEED DEGRADATION METHODS

S. No	Algorithm	Description	Dataset	Parameter	Accuracy
1	Artificial Neural Network (ANN)	Detection and mapping of invasive shrubs	https://github.com/inkyusa/weedNet	Red, green and NIR and Texture layer spectral bands	98.8 %
2	Convolutional Neural Network (CNN)	Root and shoot feature identification and localization	https://www.ipb.uni-bonn.de/people/lottes/	Root, Leaf bases, ear tips and ear bases	94%
3	Support Vector Machine (SVM)	Root and soil segmentation, Identify roots from soils	https://github.com/AlexOlsein/DeepWeeds	Root or Soil	97.9 %

The classification of weeds and crops is used to classify the weed and automate the process of weed removal. The root characteristics provide distinct attributes for weed and crop categorization [25]. The performance of classifiers based on SVM, ANN and CNN is evaluated. It is noted that, compared to SVM and CNN, ANN offers better understanding because of its deep learning ability to learn relevant characteristics from the picture in Table II.

2.3 Soil Management:

Soil Management is the applications of operations, practices and treatments to protect soil and enhance its performance. It includes Soil Conservation, Soil Amendments and optimal soil health such as Condition, Moisture and Temperature in Table III. The Prediction-Identification of agricultural soil properties consists of estimating soil drying, condition, temperature and moisture content [26]. The accurate estimation of soil condition can lead to improved soil management [27].

TABLE III: SOIL MANAGEMENT METHODS

S. No	Application	Algorithm Used	Parameter	Dataset	Accuracy
1	Soil Dryness: Evaluation of Soil Dryness	KN N/A NN	Evapotranspiration Data	https://esdac.jrc.ec.europa.eu/ESDB_Archive/Soil_Data/Global.htm	91 – 94%
2	Soil Condition : Prediction of Soil organic carbon(OC), moisture content(MC) and total nitrogen(TN)	SV M/L S-S VM	OC, MC and TN	https://opendata.syngenta.com/dataset/soil-data	Measured OC, MC and TN with 90% accuracy
3	Soil Temperature: Estimation of Soil for Different Depths in two different climate	AN N/ SaE -EL M	Air Temperature, Radiation and atmospheric Pressure at 5, 10,20, 30, 50, 100 cm depth	https://www.arcgis.com/home/item.html?id=37c15c747f84478888d8d80131b59b11	87% to 98% depending on Depth
4	Soil Moisture: Estimation of Soil Moisture	AN N/M LP	Chisel and Speed	https://esdac.jrc.ec.europa.eu/ESDB_Archive/Soil_Data/Global.htm	87%

2.4 Crop Prediction: The production of crops can be a dynamic development that is affected by input parameters for soil and environmental conditions. Development in agriculture also depends on various parameters of the soil, such as nitrogen, phosphorus, potassium, crop rotation, soil humidity, surface temperature and even weather, including temperature, precipitation, etc. [28]. India is now moving swiftly towards technological growth. When an unfavorable condition occurs, crop managers might use predictions to reduce losses. This section presents some of the

important work carried out in the crop prediction area of agriculture [29] in Table IV.

TABLE IV: CROP PREDICTION METHODS

S. No	Algorithm	Description	Dataset	Parameter	Accuracy
1	Support Vector Machine	Detection and mapping of soil	https://www.kaggle.com/c/fyp	Soil Moisture, Water Content, Crop History	98.5%
2	Artificial Neural Network	Soil and crop feature identification and prediction	https://data.world/thatzprem/agriculture-india	Soil Type, Crop List, Production and Climate Condition	92%
3	K-Nearest Neighbor	Segmentation of soil and Identify soil type	https://www.kaggle.com/tag/agriculture	Soil pH value, moisture, temperature, condition	89.4%
4	Naïve Bayes	Classification and regression with Climatic Changes	https://data.world/datasets/wether	Humidity, Temperature, wind and Rainfall	74%

IV. DISCUSSION

This work reviewed recent UAVs applications for precision agriculture and identified a research gap in dry land agriculture [30]. We presented the most critical application for dry land farming and focused on machine learning and deep learning algorithms for managing soil and processing methods exploiting UAV Imagery [31]. In the Figure 1, the following graph compares the most accurate machine learning and deep learning algorithms in the literature for controlling the application.

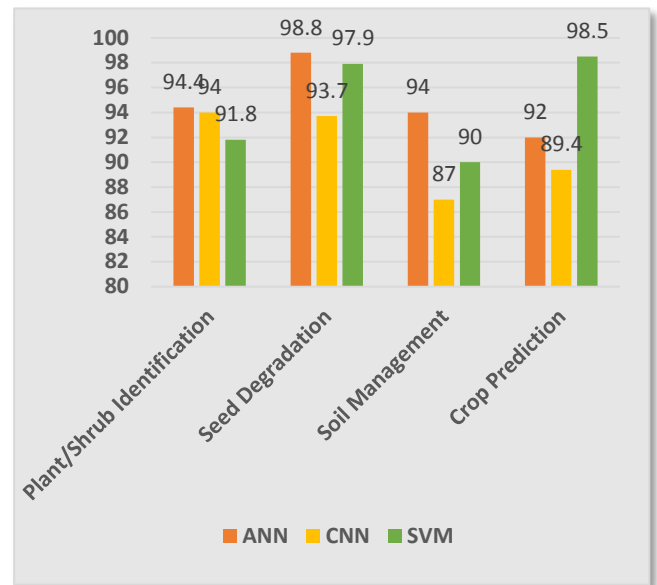


Figure 1: Comparison Chart

V. CONCLUSION:

Dry farming using Smart Agriculture Techniques is the primary focus of this article. Agriculture in drought-prone areas with limited water supplies can be difficult and UAV Dry Farming Methods can resolve these issues. The significance of smallholder agriculture UAVs will be to provide high-resolution images at user-defined temporal resolution and to automate low-cost data collection, processing, and analysis. By using deep learning models, UAV remote sensing will better transform smallholder agriculture. Scientific analysis of various significant methods will ensure that farmers with improved crop yields and sound field management use deep learning models. In dry land smart agriculture, we identified problems by identifying weeds/shrubs in small croplands, depleting seeds, evaluating soil management, improving crop predictions and estimating very accurate crop yields.

This technical survey findings from various deep learning models explored with datasets and parameters implemented in different smart farming applications. The findings' overall benefits are promising to find a better hybrid model for more stylish and more sustainable dryland farming.

REFERENCES

- [1] Danbaki, C. & Onyemachi, N. & Gado, D. & Mohammed, G. & Agbenu, D. & Ikegwuro, P.. (2020). Precision Agriculture Technology: A Literature Review. Asian Journal of Advanced Research and Reports. 30-34. 10.9734/ajarr/2020/v14i330335.
- [2] Bana, R S. (2019). 1. Dryland farming An Introduction. 10.13140/RG.2.2.15075.09766.
- [3] Bansod, Babankumar & Singh, R. & Thakur, Ritula & Singhal, Gaurav. (2017). A comparison between satellite based and drone based remote sensing technology to achieve sustainable development: A review. Journal of Agriculture and Environment for International Development. 111. 383-407. 10.12895/jaeid.20172.690.

- [4] Panagiotis Radoglou-Grammatikis, Panagiotis Sarigiannidis, Thomas Lagkas, Ioannis Moscholios. A compilation of UAV applications for precision agriculture. *Computer Networks*, Volume 172, 2020.
- [5] Reddy, Praveen & Hakak, Saqib & Alazab, Mamoun & Bhattacharya, Sweta & Gadekallu, Thippa & Khan, Wazir & Pham, Quoc-Viet. (2020). Unmanned Aerial Vehicles in Smart Agriculture: Applications, Requirements and Challenges.
- [6] Tsouros, Dimosthenis & Bibi, Stamatia & Sarigiannidis, Panagiotis. (2019). A Review on UAV-Based Applications for Precision Agriculture. *Information*. 10. 349. 10.3390/info10110349.
- [7] Sadiku, Matthew & Kotteti, Chandra & Musa, Sarhan. (2018). Machine Learning in Agriculture. *International Journal of Advanced Research in Computer Science and Software Engineering*. 8. 26. 10.23956/ijarcesse.v8i6.713.
- [8] Bah, Mamadou & Hafiane, Adel & Canals, R.. (2018). Deep Learning with Unsupervised Data Labeling for Weed Detection in Line Crops in UAV Images. *Remote Sensing*. 10. 10.3390/rs10111690.
- [9] Huang, Huasheng & Lan, Yubin & Deng, Jizhong & Yang, Aqing & Deng, Xiaoling & Zhang, Lei & Wen, Sheng. (2018). A Semantic Labeling Approach for Accurate Weed Mapping of High Resolution UAV Imagery. *Sensors*. 18. 2113. 10.3390/s18072113.
- [10] Garg, Pradeep & Garg, Rahul & Shukla, Gaurav & Srivastava, Hari. (2020). Prediction Models for Crop Mapping. 10.1007/978-981-15-3238-2_5.
- [11] Nijhawan, Rahul & Sharma, Himanshu & Sahni, Harshita & Batra, Ashita. (2017). A Deep Learning Hybrid CNN Framework Approach for Vegetation Cover Mapping Using Deep Features. 192-196. 10.1109/SITIS.2017.41.
- [12] Belgiu, Mariana & Zhou, Y. & Marshall, M. & Stein, Alfred. (2020). DYNAMIC TIME WARPING FOR CROPS MAPPING. *ISPRS - International Archives of the Photogrammetry, Remote Sensing and Spatial Information Sciences*. XLIII-B3-2020. 947-951. 10.5194/isprs-archives-XLIII-B3-2020-947-2020.
- [13] Valente, João & Sari, Bilal & Kooistra, Lammert & Kramer, H. & Mûcher, Sander. (2020). Automated crop plant counting from very high-resolution aerial imagery. *Precision Agriculture*. 21. 10.1007/s11119-020-09725-3.
- [14] Faria Pinto, Milena & Melo, Aurelio & Honorio, L.M. & Marcato, André & Conceição, André & Timotheo, Amanda. (2020). Deep Learning Applied to Vegetation Identification and Removal Using Multidimensional Aerial Data. *Sensors*. 20. 6187. 10.3390/s20216187.
- [15] Ustuner, Mustafa & Abdikan, Saygin & Bilgin, Gökhan & Balik Sanli, Fusun. (2020). Crop Classification Using Light Gradient Boosting Machines.
- [16] Dyson, J. & Mancini, Adriano & Frontoni, Emanuele & Zingaretti, Primo. (2019). Deep Learning for Soil and Crop Segmentation from Remotely Sensed Data. *Remote Sensing*. 11. 1859. 10.3390/rs11161859.
- [17] Kulkarni, Ms. (2020). Rice Plant Disease Detection. *International Journal for Research in Applied Science and Engineering Technology*. 8. 237-241. 10.22214/ijraset.2020.6033.
- [18] Iswarya, P. & Maheswari, D.. (2019). Paddy Leaf Disease Identification and Classification System A Review. *International Journal of Computer Sciences and Engineering*. 7. 976-979. 10.26438/ijcse/v7i5.976979.
- [19] Poblete, Tomas & Ortega-Farias, Samuel & Moreno, Miguel & Bardeen, Matthew. (2017). Artificial Neural Network to Predict Vine Water Status Spatial Variability Using Multispectral Information Obtained from an Unmanned Aerial Vehicle (UAV). *Sensors*. 17. 2488. 10.3390/s17112488.
- [20] Div, Land. (2020). Problems of dryland farming.. XF2006101178.
- [21] Kamilaris, Andreas & Prenafeta Boldú, Francesc. (2018). Deep Learning in Agriculture: A Survey. *Computers and Electronics in Agriculture*. 147. 10.1016/j.compag.2018.02.016.
- [22] Vogt, Michael. (2018). An overview of deep learning techniques. at - Automatisierungstechnik. 66. 690-703. 10.1515/auto-2018-0076.
- [23] Bonnet, Pierre & Goëau, Hervé & Hang, Siang & Lasseck, Mario & Sulc, Milan & Malécot, Valéry & Jauzein, Philippe & Melet, Jean-Claude & You, Christian & Joly, Alexis. (2018). Plant Identification: Experts vs. Machines in the Era of Deep Learning Deep learning techniques challenge flora experts.
- [24] Hiremath, Swathi & Suresh, Suhas & Kale, Sanjana & Ranjana, R & Suma, K & Nethra, N. (2019). Seed Segregation using Deep Learning. 1-4. 10.1109/GHCI47972.2019.9071810.
- [25] Jaeger, Paul & Isensee, Fabian & Petersen, Jens & Zimmerer, David & Wasserthal, Jakob & Maier-Hein, Klaus. (2018). Advanced Deep Learning Methods. 10.1007/978-3-662-56537-7_6.
- [26] kavoosi, Zahra & Raoufat, Mohammad & Dehghaani, Maryam & Jafari, Abdolabbaas & Kazemini, Seyed Abdolreza & Naazemossadat, Mohammad. (2018). Feasibility of satellite and drone images for monitoring soil residue cover. *Journal of the Saudi Society of Agricultural Sciences*. 19. 10.1016/j.jssas.2018.06.001.
- [27] Bhattacharyya, Pratap & Pathak, Himanshu & Pal, Sharmistha. (2020). Soil Management for Climate-Smart Agriculture. 10.1007/978-981-15-9132-7_4.
- [28] Prabhu, Shubham & Revandekar, Prem & Shirdhankar, Swami & Paygude, Sandip. (2020). Soil Analysis and Crop Prediction. *International Journal of Scientific Research in Science and Technology*. 117-123. 10.32628/IJSRST207433.
- [29] Panchamurthi.S (2019). Soil Analysis and Prediction of Suitable Crop for Agriculture using Machine Learning. *International Journal for Research in Applied Science and Engineering Technology*. 7. 2328-2335. 10.22214/ijraset.2019.3427.
- [30] Shafi, Uferah & Mumtaz, Rafia & García-Nieto, José & Hassan, Syed & Zaidi, Syed Ali Raza & Iqbal, Naveed. (2019). Precision Agriculture Techniques and Practices: From Considerations to Applications. *Sensors*. 19. 3796. 10.3390/s19173796.
- [31] Koul, Sumit. (2020). Machine learning and deep learning in agriculture. 10.1201/b22627-1.

Design and Implementations of Humming Bird Cryptographic Algorithm using FPGA

^[1] Mohan Kumar BN, ^[2] N Nandeesh Reddy, ^[3] Divya KH, ^[4] Alangir Badsha, ^[5] Kishore S

^{[1][2][3][4][5]} Department of Electronics and Communication Engineering R R Institute of Technology, Bengaluru, Karnataka

Abstract— Hummingbird is a new ultra-lightweight cryptographic algorithm targeted for resource-constrained devices like RFID tags, smart cards, and wireless sensor nodes. In this project, we describe efficient hardware implementations of a stand-alone Hummingbird component in field-programmable gate array (FPGA) devices. We implement an encryption only core and an encryption/decryption core on the low-cost Xilinx FPGA series Spartan-6 and compare our results with other reported lightweight block cipher implementations on the same series. Our experimental results highlight that in the context of low-cost FPGA implementation Hummingbird has favorable efficiency and low area requirements. Hummingbird algorithm is one of the recently proposed light weight cryptographic algorithms targeted for resource constrained devices like RFID (radio frequency identification), smart cards and majority of wireless sensor nodes. The main advantage of this algorithm is that it provides adequate security with smaller block size

I. INTRODUCTION

Cryptography, the art and science of keeping messages ancient Egypt some 4000 year ago. Undoubtedly, cryptanalysis, the art and science of revealing messages secure, has a long history which can be traced back to hidden by means of cryptography, has an equally long history. Together cryptography and cryptanalysis are called cryptology. When history of cryptology is discussed, it must be emphasized that historical cryptology has little common with modern cryptology which started in the 20th century, and which is the topic of this is First, some fundamental terminology is introduced. The message, which is to be kept in secret, is referred to as plain text. The process of hiding its content is called encryption and the encrypted message is referred to as cipher text. Hummingbird is a recently proposed ultra-lightweight cryptographic algorithm targeted for low-cost smart devices like RFID tags, smart cards, and wireless sensor nodes. It has a hybrid structure of block cipher and stream cipher and was developed with both lightweight software and lightweight hardware implementations for constrained devices in mind. Moreover, Hummingbird has been shown to be resistant to the most common attacks to block ciphers and stream ciphers including birthday attack, differential and linear cryptanalysis, structure attacks, algebraic attacks, cube attacks, etc. In practice, Hummingbird has been implemented across a wide range of different target platforms. Those implementations demonstrate that Hummingbird provides efficient and flexible software solutions for various embedded applications. However, the

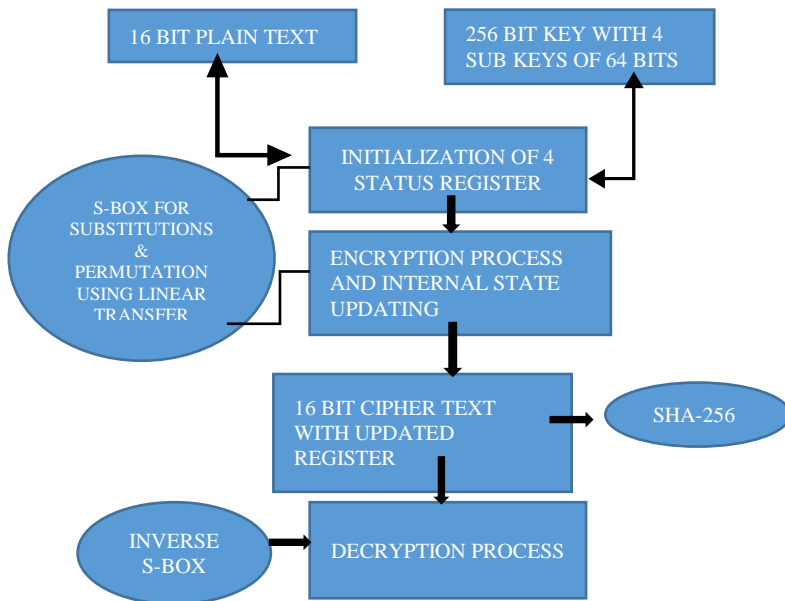
hardware performance of Hummingbird has not yet been investigated in detail. As a result, our main contribution in this paper is to close this gap and provide the first efficient hardware implementations of Hummingbird encryption/decryption cores on low-cost FPGAs.

II. LITERATURE SURVEY

It was introduced in 1998. It has different key size 128,192,256 bits. It is hard to implement with software. It is complex to implement in software taking both performance and security into considerations.

Ramadhan J. Mustafa et. al(2016) —Over the past few decades, the art of secretly embedding and communicating digital data has gained enormous attention because of the technological development in both digital contents and communication. The imperceptibility, hiding capacity, and toughness next to attacks are 3 main necessities that some video steganography way should get into thought. In this, a tough and protected video steganographic algo inside the DWT and DCT domain names is to be based on Multiple Object Tracking known as MOT algo and Error Correcting Codes this is called (ECC) is being proposed. Primarily, motion-based MOT algorithm be implemented resting on host videos to differentiate the regions of attention in moving objects. After that, the process of data hiding is being performed by concealing top secret message into DWT and DCT coefficients of each and every motion regions in video depending on center masks. Our experimental outcome exemplify that suggested algo not only improves capacity of embedding and imperceptibility although it also enhances its safety and robustness by encoding the secret message and withstanding against various attacks. Alavi Kunhu et.al (2016) they recommend a new blind color video watermarking way for copyright safety of multimedia color films through the use of index mapping concept. The inventiveness in obtainable approach consists in crafty a hybrid Discrete Wavelet Transform (DWT) and Discrete Cosine Transform also recognized as (DCT) based distortion caused all the way through watermarking be assess by way of peak signal to sound ratio (PSNR) along with correspondence structure index measure (SSIM) and robustness within antagonism to different types of attacks have been assessed using StirMark. The proposed video watermarking algo provide improved imperceptibility within harmony by way of human visual system and offers advanced tough

III. BLOCK DIAGRAM EXPLANATION



3.2. Flow Diagram

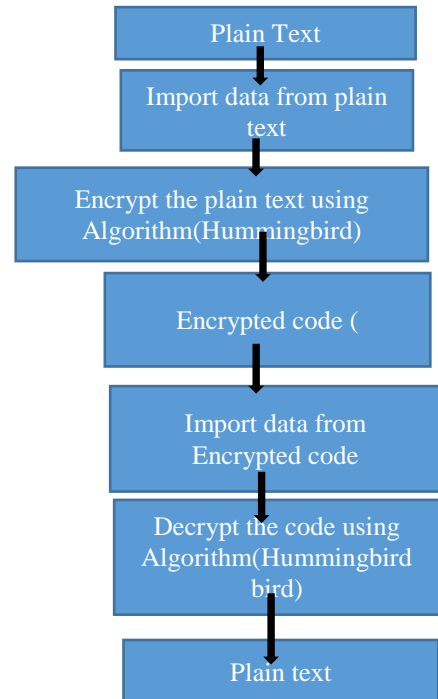


Fig 1 Block diagram of Hummingbird Cryptographic

This architecture works on the encryption only and decryption only processor. The initialization block consists of four status registers and a ready pin. A 5-bit counter is used to count the number of clock cycles. When the data ready pin goes high, the counter starts counting and the status registers are initialized with some random values. The registers are then updated by undergoing encryption round of block cipher in next 16 clock cycles.

The Encryption block uses the initialized status registers to encrypt the plain text into cipher text. Encryption undergoes the modulo 216 addition of register RS1 and plain text and undergoes through the block encryption using the secret key. This is repeated four times and the resulting cipher text is given to the decryption module making the enc_ complete signal high. The decryption is just reverse of encryption. The input is cipher text and output is plain text. Modulo 216 subtraction is used in decryption. Thus when both dec_ complete and Enc_ complete signals are high the output is given in one clock cycle. The registers are updated for the next process.

3.1.Algorithm use

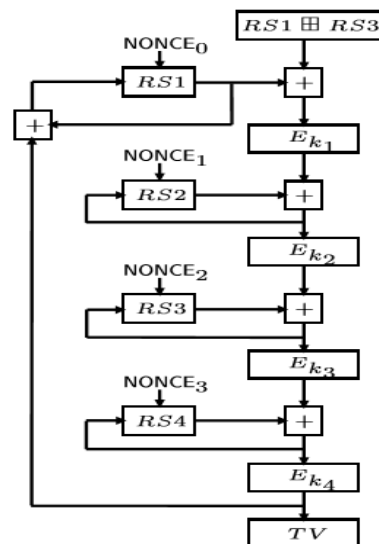
Humming Bird Algorithm: is a new ultra-light cryptographic algorithm targeted for resource constrained devices. This cryptographic algorithm is designed to deal with the trade off among security, cost and performance. Humming bird is used to meet the requirements of constrained devices.

Hash Algorithm: is a function that converts a variable size data into fixed size data. The use of Hash algorithm make system more secure.

3.1.Fig Flow diagram of Hummingbird

Plain text refers to any message that is not encrypted. The data from plain text will be imported and the imported data will be given as input to the Encryption algorithm (Hummingbird and Hash function). The encrypted code contains Cipher and Hash code.

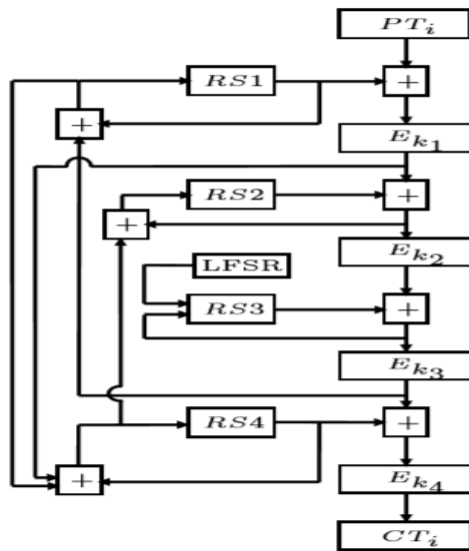
IV. 4.INITIALIZATION PROCESS



The overall structure of the Hummingbird initialization algorithm is shown in Figure 1(a). When using Hummingbird in practice, four 16-bit random NONCE_i are first chosen to initialize the four internal state registers RS_i (i = 1; 2; 3; 4),

respectively, followed by four consecutive encryptions on the message RS1 RS3 by Hummingbird running in initialization mode . The final 16-bit cipher text TV is used to initialize the LFSR. Moreover, the 13th bit of the LFSR is always set to prevent a zero register. The LFSR is also stepped once before it is used to update the internal state register RS3.

4.1 Encryption Process

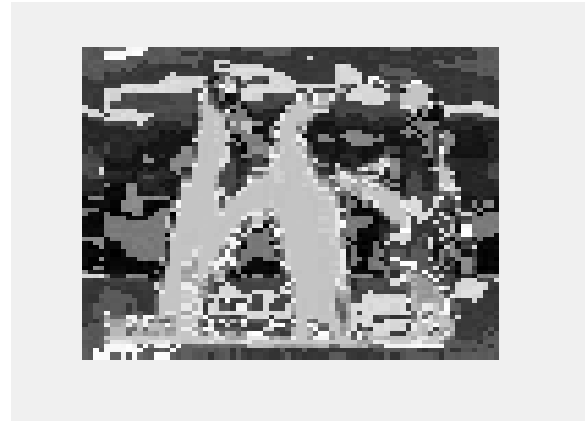
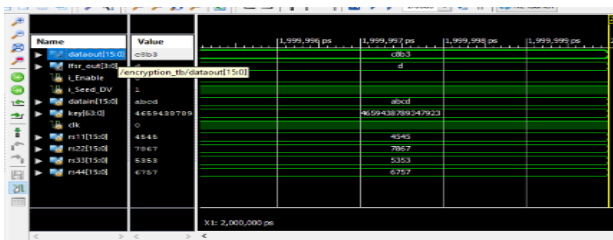


4.1.1 Working of Encryption Process

The overall structure of the Hummingbird encryption algorithm consists of four 16-bit block ciphers Ek1,Ek2,Ek3 and Ek4, four 16-bit internal state registers RS1,RS2,RS3 and RS4, and a 16-stage LFSR. The 256-bit secret key K is divided into four 64-bit sub keys k1,k2,k3 and k4 which are used in the four block ciphers, respectively.

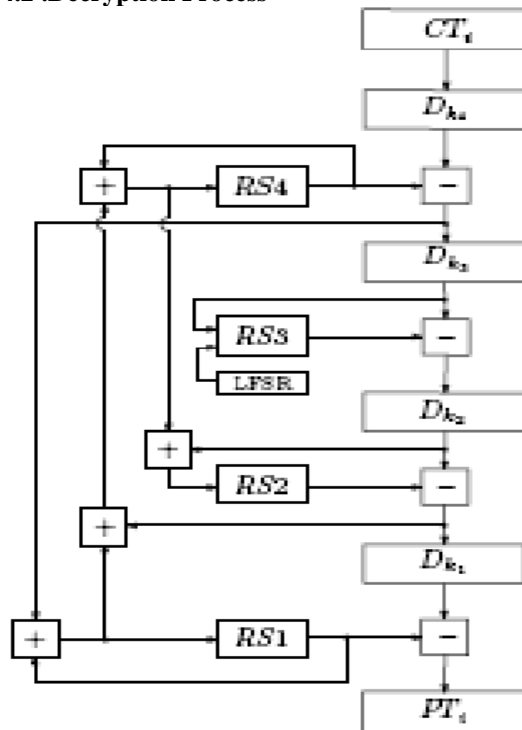
A 16-bit plaintext block PTi is encrypted by first executing a modulo 216 addition of PTi and the content of the first internal state register RS1. The result of the addition is then encrypted by the first block cipher Ek1 by the loop unrolled process. The out put of the loop unrolled condition of Ek1 is executing a modulo 216 addition and connect to the 2nd internal state register RS2. The result of the addition is then encrypted by the second block cipher Ek2 by the loop unrolled process.

Output of Encryption for text



4.2 Encrypted Image Output

4.2 .Decryption Process

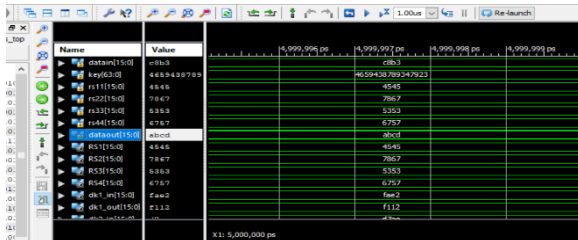


The conversion of encrypted data into its original form is called Decryption. It is generally a reverse process of encryption. It decodes the encrypted information so that an authorized user can only decrypt the data because decryption requires a secret key or password.

One of the reasons for implementing an encryption-decryption system is privacy. As information travels over the Internet, it is necessary to scrutinise the access from unauthorized organisations or individuals. Due to this, the data is encrypted to reduce data loss and theft. Few common items that are encrypted include text files, images, e-mail messages, user data and directories. The recipient of decryption receives a prompt or window in which a password can be entered to access the encrypted data. For decryption, the system extracts and converts the garbled data and transforms it into words and images that are easily

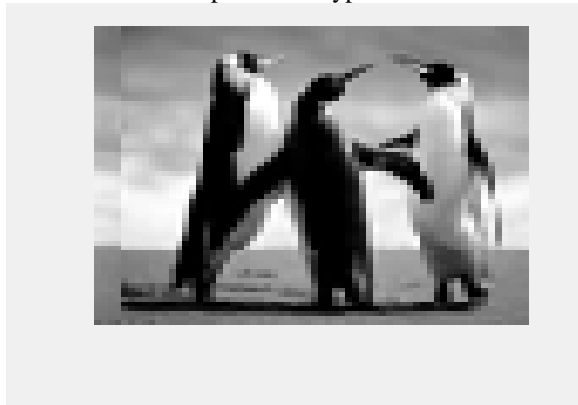
understandable not only by a reader but also by a system. Decryption can be done manually or automatically. It may also be performed with a set of keys or passwords.

Output of Decryption for Text and image



Name	Value	5,999,996 pc	5,999,997 pc	5,999,998 pc	5,999,999 pc
dataIn[15:0]	cibb3		cibb3		
key[63:0]	444444447777		444444447777		
ri1[15:0]	4545		4545		
ri2[15:0]	7867		7867		
ri3[15:0]	5353		5353		
ri4[15:0]	8282		8282		
dataOut[15:0]	abcde		abcde		
ki1[15:0]	4545		4545		
ki2[15:0]	7867		7867		
ki3[15:0]	5353		5353		
ki4[15:0]	8282		8282		
dk1_in[15:0]	7ae2		7ae2		
dk1_out[15:0]	2112		2112		

4.3. Simulation output of Decryption for Text



4.4: Simulation output of Decryption for Image

Future Scope

That we believed to be resistant to most of the standard attacks on block ciphers and stream ciphers.

Password based authentication. However, password guessing can make the application vulnerable expose to damage with the sensitive information.

Therefore, in our future work, we will focus on hybrid techniques for generation of the encryption key to make the application more secure.

We can also make use of the biometrics, which is used to generate key for the encryption with the help of random number generator to make the key complex.

V.CONCLUSION

The algorithm due to its prominent internal structure very precisely achieves the security and performance factor. Compared to other lightweight FPGA implementations of block ciphers SEA, AES, Hummingbird can achieve larger throughput with the smaller area requirement. Consequently, Hummingbird can be considered as an ideal cryptographic primitive for resource constrained environment. The efficient FPGA implementation of Hummingbird is possible using the given software algorithms so that it can achieve larger throughput with smaller area requirement. Hummingbird can

be used in high-security required devices as it is resistant to most cryptographic attacks.

The Hummingbird encryption algorithm has been implemented with area optimization. The hardware implementation has been done on FPGA. The synthesis and simulation results have been compared and improvement has been observed. Compared to other lightweight FPGA implementations of block ciphers PRESENT, XTEA and AES, Hummingbird can be implemented with smaller area requirement. Consequently, Hummingbird can be considered as an ideal cryptographic primitive for resource-constrained environments. As the future research, we intend to conduct Encryption/Decryption core of Hummingbird cipher as well as propose low power ASIC implementations for low-cost RFID tags.

REFERENCES

- [1] Bose, R. C.; Ray-Chaudhuri, D. K. (March 1960), "On A Class of Error Correcting Binary Group Codes" (PDF), *Information and Control*, 3 (1): 68–79, doi:10.1016/s0019-9958(60)90287-4, ISSN 0890-5401
- [2] Gill, John (n.d.), EE387 Notes #7, Handout #28 (PDF), Stanford University. And Welch, L. R. (1997), *The Original View of Reed–Solomon Codes* (PDF).
- [3] Taher ElGamal (1985). "A Public-Key Cryptosystem and a Signature Scheme Based on Discrete Logarithms" (PDF). *IEEE Transactions on Information Theory*.
- [4] Commercial National Security Algorithm Suite and Quantum Computing FAQ U.S. National Security Agency, January 2016.
- [5] IEEE Communications Magazine paper on G.hn Archived 2009-12-13 at the Wayback Machine
- [6] Daemen, Joan; Rijmen, Vincent (March 9, 2003). "AES Proposal: Rijndael" (PDF). National Institute of Standards and Technology.

Women Empowerment in India: Issues & Challenges

^[1]Namratha Murthy, ^[2]Dr.Sunitha H D

^[1] 2nd Sem Law student, Kristu Jayanti College of Law, Bengaluru,

^[2]Professor, Dept of ECE, R R Institute of Technology, Bangalore

Abstract— Empowering a woman has been one of the main concerns in 21st century. Women are becoming victims of various social evils. Women empowerment can be used as a vital instrument in supporting a woman to access resources and to make strategic life choices. The main objective of this paper is to assess the need for women empowerment in India, analyze the factors that influence empowerment of women in India, discuss various government schemes for women empowerment-implementation and hindrances. The data used here are from secondary sources.

Index Terms— Empowerment, crimes against women, government schemes, IPC, SLL

I. INTRODUCTION

Empowerment and autonomy of a women plays a very important role politically, socially and economically to achieve sustainable development of the society. Participation of both women and men is essential in the development of the society, maintenance of household, reproductive life and nurturing children. In almost all parts of the world, women are not treated at par with men in respect to wages, power and influence. In many regions across the world women are not allowed to pursue their education, or receive less formal education compared to men. To overcome the disparity, we need policy and programs that will support women and create an awareness regarding their rights and duties. Education plays a very important role of empowering women with knowledge and skills to participate in the development process. Indian constitution in its preamble, Fundamental duties ,rights and directive principles has ensured protection of gender equality. The constitution grants equality to women and also has authorized the states to take measures in favour of women against discrimination. From the 5th five year plan onwards there was a significant shift in the way women's issue were approached from welfare to development. A girl may be a victim of crime, or target of crime from the time of her birth. As they grow, nature of crimes vary. The table below lists various types of crimes a women may suffer from her birth time.

Many women suffer quietly and do not dare to report it. If she tries to do so, she will be suppressed or silenced.

Table1: Various crimes on women during their life stages

Life stages	Crimes
Foeticide & Infanticide	Preferences for son both economically and culturally, diagnostic tools leading to female foeticide
School going age	denied access for primary education compared to boys and discrimination
Adolescence	Rape, acid attack, early marriage, sexual abuse, exploitation
marriage	Harassment- both physical and mental, dowry deaths
Motherhood	Lack of proper medical care, hygiene, healthy food, compelled to abort a female foeticide
Workplace	Unequal pay and promotions, exploitation, physical, economic and emotional abuse

➤ Crimes against women in India:

Crimes against women in India have a large negative impact on women empowerment in India. The statistics released by NCRB (National crime records Bureau) has revealed a shocking fact about the number of crimes on women during the year. As per the NCBR (National Crime records Bureau) report, a crime rate of 46 per 100,000 has only been reported. Table 2 lists the NCBR statistics of crime against women for the year 2018 & 2019.

Table2: NCBR statistics of crime against women in India for the year 2018 & 2019[1]

Sl no	Crime Head(IPC+SLL)	Year	
		2018	2019
1	Murder with rape/gang rape	294	283
2	Dowry deaths(sec 304B IPC)	7166	7115
3	Abetment to suicide(sec 305/306 IPC)	5037	5009
4	Acid attack(sec 326A IPC)	131	150
5	Cruelty by husband or his relatives(sec 498A IPC)	103272	125298
6	Kidnapping and abduction of omen	72751	72780
7	Human trafficking(sec 370 & 370A IPC)	854	1991
8	Selling of minor girls	40	22
9	Assault on women ith intent	89097	88367

	to outrage her modesty		
10	Cyber crimes(publishing explicit material, morphing, fake profile etc.,	1268	1621
Total crimes		278642	301015

The data above shows an **alarming rise of 8% increase in crime against women from 2018 to 2019**. When women are fulfilled and are leading a safe and productive life, they will be able to reach their full potential by contributing towards happier and healthier family and society. Healthy, educated and empowered women contribute at large towards the development of the society. Women and girls should be supported such that they gain opportunity to speak for their rights. Organisations, policies and charities towards women empowerment should gain momentum.

II. EMPOWERMENT OF WOMEN

Women empowerment can be categorized into 5 categories:

1. Social
2. Economic
3. Education
4. Political
5. Psychological

i. **Social empowerment of women can be ensured in many ways:**

- Provide equal access for women and girls to education
- Equal opportunity and freedom to develop herself [2]
- Recognition and enforcement to women's human rights are the keys to women empowerment [3]
- Ensure special measures to eliminate discrimination, eradicate illiteracy, have a gender sensitive education system, improve enrolment and retention rates of girls in education.
- Special focus in existing policies should be provided for girls and women belonging to weaker sections.
- Measures to be taken to ensure women have access to affordable health care.
- Policies should ensure special attention towards safe drinking water, toilet facilities, sewage disposal and sanitation to be easily accessible to all households. Women participation in delivery of this system would be beneficial.
- Women should be involved in policy making.

Women participation must be ensured in the conservation of the environment

ii. **Economic empowerment of women:**

Employed women contribute to the family with a strong sense of economic independence. Economic empowerment can be brought about by implementing the following:

- Poverty eradication schemes should address the social discrimination and harsh realities of intra house hold.

- Earning women will feel secured, will have assets in her name, feels economically strong, independent and autonomous.[4]
- Strengthen micro credit and micro finance institution, ensure all women below poverty line have access to credit.
- Growing global economy has led to uneven distribution leading to wider economic disparities, increased gender inequality through unsafe working environment and conditions. Strategies must be designed to empower women to meet negative social and economic impacts.
- Training programmes in occupations allied to agriculture should be expanded to benefit women in agriculture sector.
- Women are playing a major role in the development of electronics, information technology, food processing, agro and textile sectors. Suitable measures have to be taken to ensure for the safety of women working in night shifts in factories.
- Availability of child care facilities, crèches and homes for old and disabled should be expanded and improved to create a healthy and safe environment to ensure for their cooperation in social, political and economic life.

iii. **Role of education in women empowerment**

- Education plays a very important role in empowering women.
- Educated women and girls will be aware of their rights, will be more confident and handle their family in a better way.
- In rural areas many women die during pregnancy due to lack of awareness of complications. Education will make them understand better and would take necessary precautions.
- Education helps in personality development

iv. **Political empowerment:**

5 factors that deter women from entering politics:

- Lack of confidence
- Lack of money
- Lack of support from family
- Domestic responsibilities
- Prevailing cultural attitudes

➤ **Political empowerment of women:**

Women account for only 26% of all parliamentarians in the world. Women who are really talented to be public leaders will not get a chance due to social, legal and financial barriers. When women hold a public office, they are sure to prioritize facilities like water, infrastructure, sanitation, roads, education and health. According to Pam Rajput (2001), empowerment of women particularly in political sphere is crucial for their advancements and foundation of gender equal society. Lack of political participation would

make it difficult for women to improve capacity, increase effectiveness and challenge the patriarchal ideology.

Empowerment means “bringing women into main stream as national activity as equal partners along with men”[5]

Awareness should be brought about in women to actively participate in government, politics and decision making. Global statistics indicates that most of the women are under-represented as leaders, elected representatives and voters due to cultural and social norms, that hinders their participation in the political process. These challenges can be addresses by the following:

1. Gender quota- reservations for female elected representatives will make communities to associate with women leadership and the trend would be carried forward. Reservation in political seats for women will increase the women participation in the electoral process.
2. Women in leadership roles inspire the young girls to aspire for leadership.
3. Training programs or political campaign education can be implemented to improve the participation of women in decision making despite hurdles.

v. Psychological empowerment of women:

- It is important to empower women psychologically so that it helps them to deal with the changes in the work place effectively. This improves the employees sense of personal control and motivates them to deal with changes at work and improves their performance. Psychological hindrances like insecurity, fear, lack of self confidence and self esteem, lack of information, lack of autonomy in work place acts as barriers in empowerment of women.
- Psychological empowerment can be brought about by organizing training programs to build their confidence, communication and self esteem. Higher the psychological empowerment of women, lower will be the work related stress.

III. GOVERNMENT SCHEMES FOR EMPOWERMENT OF WOMEN

Within the structure of a democratic policy, our laws, development policies, Plans and programmes have aimed at women’s advancement in different fields. From the Fifth Five Year Plan (1974-78) onwards stress was laid on women’s issues from welfare to development. The National Commission for Women was set up by an Act of Parliament in 1990 to safeguard the rights and legal entitlements of women. Reservation of seats for women in the local bodies of

Panchayats and Municipalities was provided in the 73rd and 74th amendments of the constitution that laid a strong foundation for women participation in decision making at the local levels.

➤ **CENTRAL GOVERNMENT SCHEMES FOR EMPOWERMENT OF WOMEN [6]**

- 1) **Mahila E-Haat** - It is an online marketing platform launched by Ministry of Women and Child Development on 7th March 2016. It supports women entrepreneurs, self help groups (SHG’s) and non- governmental organizations (NGO’s) to showcase their products and services .
- 2) **Beti Bachao , Beti Padhao** – This social campaign aims at eradicating female foeticide and to raise awareness about the welfare services intended for young girls, was launched on 22nd January 2015 . “Save the girl movement” was a joint initiative launched by the Ministry of Women and Child Development and the Ministry of Human Resource Development and the Ministry of Health and Family Welfare. Sex selective abortion or female foeticide in India has led to a sharp decline in the ratio of girls in contrast to boys especially in few states of India. The gap in the gender ratio was first noticed in the year 1991, when the national census data was released. To bridge the gap between the birth of the girl and boy infants, the Government of India took up several measures such as “Beti Bachao Beti Padhao”, “Save Girl Child” , and “ Educate Girl Child” since 2015.
- 3) **One Stop Centre Scheme** – This scheme was popularly known as “Sakhi ”, was launched on 1st April, 2015. They are established across India. They provide shelter, legal, medical counselling services for victims of violence under one roof . These centres can be contacted for the following reasons –
 - ⋈ Medical Assistance.
 - ⋈ Legal aid counselling.
 - ⋈ Shelter.
 - ⋈ Assisting in lodging FIR/NCR/DIR.
 - ⋈ Facilities to record statement for courts and police.
- 4) **Working Women Hostels** – This scheme was introduced in the year 1972- 1973. The main aim of this scheme is to provide a safe and conveniently located accommodation for working women with the facilities of day-care for their children.
- 5) **Swadhar Greh** – This scheme was launched in 2002 by the Union Ministry of Women and Child Development for rehabilitation of women in difficult circumstances. According to these schemes

they provide shelter, clothing and care to marginalized widows / girls who are in need. The implementing agencies are mainly NGO's.

- [5] Batliwala, S. (1995). Meaning of women's empowerment. *Women's World*, 23-34
[6] web reference- <https://wcd.nic.in>

- 6) **STEP** – The Support To Training And Employment Programme for Women Scheme aims to provide employability skills for women and enable them to become self employed or entrepreneurs. The sectors included in this schemes are as follows

- Agriculture
- Handloom
- Tailoring
- Stitching
- Embroidery
- Handicrafts
- Computer and IT enable services
- Soft skills
- Skills for the workplace such as spoken English , gems and jewellery, hospitality etc.

- 7) **Nari Shakti Puraskars** – These are the national level awards which recognizes the efforts of women and the institutions which particularly work towards the development of women especially marginalized and vulnerable women. This award is presented on 8th of March every year by the President of India on the event of International Women's Day at the Rashtrapati Bhavan in New Delhi.

IV. CONCLUSION

In conclusion I would like to underline about the importance of women empowerment. Women empowerment can only be achieved when there is a change in the attitude of the society in regards to equality and fairness. Women empowerment means empower or enable them to make their own decisions. Women can be empowered only when they are given equal rights as men in the society. They need to be strong, alert and aware every time for their development and growth. Women should be respected and given a chance to move forward. It is true that in the present times, women are enjoying freedom more than ever but even today various kinds of social evils such as dowry harassment , physical abuse etc are still prevalent in the society. When women are made socially , economically, politically and psychological empowered the dream to make women empowered becomes a reality.

REFERENCES

- [1] Web reference: <https://nvbr.gov.pl>
[2] Gangrade, K.D. (2001). Gandhi and empowerment of women: Miles to go" in Promilla Kapur (ed.), *Empowering the Indian Women*, New Delhi: Ministry of Information and Broadcasting,
[3] Manohar, S. (2001). Human rights for women's empowerment. In Promilla Kapur (ed.), *Empowering the Indian Women*, Publications Division, Ministry of Information and Broadcasting, Government of India, New Delhi.
[4] Prasad, R.R. (2002). Participation and empowerment – rhetoric and realities. *Kurukshetra, a Journal on Rural Development*, New Delhi.

Wireless Sensors Network for Radiation Monitoring Using IoT

^[1] Pallavi M R, ^[2] Dr. Sunitha H D, ^[3] Samadrita Roy Chowdhury, ^[4] Priyanka Nagendra Shindogi, ^[5] Varsha Biradar

^{[1][3][4][5]} Student RRIT, ^[2] HOD/Professor ECE Dept. RRIT

Abstract— The changes in climate led to the increased importance of environmental monitoring. In order to determine the quality of the environment, continuous tracking of the environmental parameter is needed. As the IoT is the most emerging technology, it plays an important role in collecting the information from the sensing unit. Generally sensing unit is composed of different sensors like temperature, humidity, moisture etc. The project uses a Node MCU Wi-Fi module that helps in processing and transferring the sensed data to the Thingspeak cloud. Thus the parameters received are stored in the cloud platform (Thingspeak). The changes in the environment are updated in the form of database through the cloud computing method. This paper presents the development of a flexible environmental monitoring system that allows the monitoring of parameters in the workplace, required for optimal performance. Several sensors and three modules, with different functionalities, are used to complete the system.

I. INTRODUCTION

The advancement and innovations in technology triggers the needs for controlling and monitoring of different environmental parameters such as temperature, humidity and CO₂. The system hardware platforms are basically low-power embedded micro-controller systems with onboard sensors and analog I/O ports for connecting the sensors. Prediction and estimation with Node MCU has two components, Hardware components and Software components. Hardware components detect and organize the environmental parameters

e.g. Node MCU board, bread board, sensors, jumper wires, USB cable for connecting Node MCU board with computer. Then second component is Node MCU software which tells the hardware components of Node MCU what to do. Initially, the hardware connection is made and deployed, the connection in environment surfaces to detect the parameters (e.g. temperature, humidity, sound, pressure and CO₂ and etc.) while the program codes extract and organize data from the sensors which are placed at different locations, manage it and display variations in the environmental parameters. The output of each sensor is then loaded and displayed in a serial monitor (LCD). The program in Arduino IDE uses looping i.e. a particular program will keep on iterating until it has been terminated.

II. LITERATURE REVIEW

Vax, E.etal [1] grew Fast arrangement, constant Environment Radiation Monitor Systems (E R M S), this meets before and after radiation occasion necessity. This complete framework empowers online ecological and radiation information exchange on different customers of an assortment in sensor composes, e.g., radiation gamma rays, wind heading and fast, gathered in quick arrangement observing stations. This entire framework empowers fleeting spatial investigation in radiation well-being and post occasion hazard examination. Sean M. Brennan, et al[4], in their work have described discovery points of confinement in sensor systems in move the radiation source utilizing Bayesian techniques in conjunction along PC reproduction. This investigation includes point source moved in consistent speed, imitating vehicle transport in a Narrow Street. Reenactments are appeared to be valuable for positioning hopeful hub layouts. Seen M. Brennan, Et al[4], in their work have portrayed location breaking points of sensor systems in transporting radiological source utilizing Bayesian techniques on conjunction along PC reproduction. This examinations include point source moving at steady speed, imitating vehicle transport in a narrow street. Reproductions are appeared to be helpful for positioning competitor hub designs.

R. Lubis and A. Sagala[5], proposed another strategy Redis, an in memory database innovation which is another development in elective No SQL and huge information which empowers minimal effort ware equipment. Rather than plate, memory utilize as a part of Redis is for the most part to evade inertness amid I/O forms. They endeavor to uncover dormancy and enhance execution by testing multi-string approach amid short message (SMS) conveyance in single string Redis condition in mix with Rapid pro, a mass SMS administration stage.

G. Venkatesh and P. Chandramouli[6], explains complete design and integration of WSN, used for monitoring of remote places and about various applications of IOT. Parameters such as long lifetime, low maintenance, high QOS etc., for wide range monitoring applications are discussed.

III. BLOCK DIAGRAM

The equipment design of the sensor organize hub comprises of three primary segments: (i) Sensor and sensors interface, (ii) Node MCU, (iii) power control circuit. The five sensors as shown in Figure 1 are used to monitor the environment for humidity and temperature, pressure, sound, carbon monoxide levels. Atmospheric pressure sensor, Temperature and humidity sensor, Gas sensor MQ-5 and Sound sensor are used in the sensor module. The data collected from the sensor is sent to the interface where it controls and manipulates the sensor

output data. The data is sent to Node Microcontroller Unit (MCU). The microcontroller board deals with the communication with the local network communication and processes the measures provided by the interface sensor. The user can access local network to get the sensors data through things speak web server.

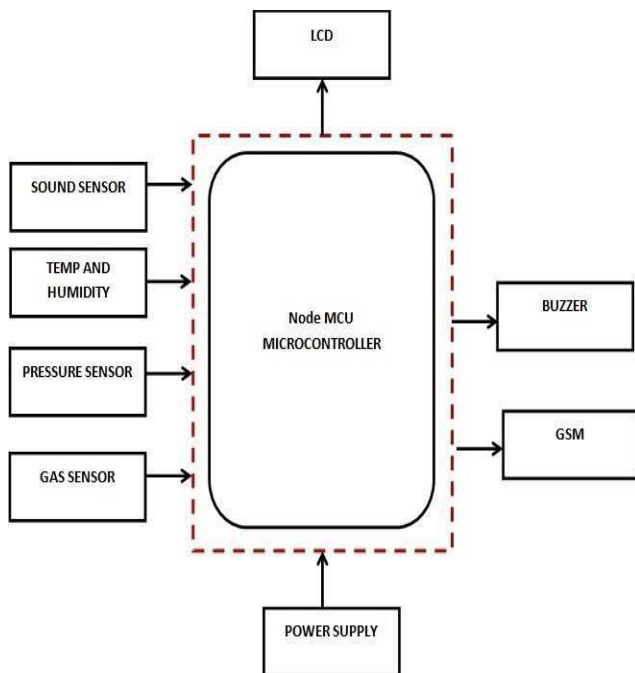


Figure 1: Block diagram of wireless sensor of radiation monitoring

IV. FLOWCHART

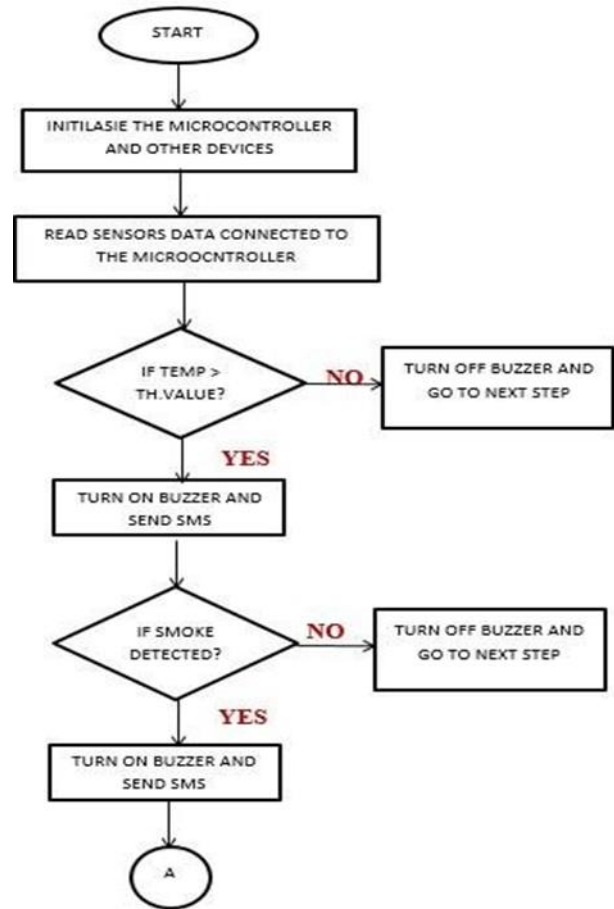


Figure 2: Flowchart of working process

V.WORKING PRINCIPLE

In this project we are using Node MCU microcontroller which is the heart of the system. This system is used to monitor the environment, based on the different parameters. Here we are using four sensors as shown in Figure 1 i.e. DHT11, pressure sensor, sound sensor and sensor as an actuator buzzer and GSM is used. To display the data we are using LCD. To turn on the module we need power supply. All the sensors are connected to the microcontroller which will work accordingly as per program and the user requirement. DHT11 sensor is the digital humidity and temperature sensor which is used to monitor temperature and the humidity of the environment, the sensor reads the data and sends that data to the microcontroller. Sound sensor is the one which gives output both in analog as well as digital form. Here we are using digital sensor for reading the data. Pressure sensor is used to detect the pressure in the environment, if unknowingly more pressure is detected this sensor helps to detect it and sends the data to microcontroller. Gas sensor is used to detect the hazardous gases present in the environment. Once all the sensor data is monitored, it will be

sent to the microcontroller. The microcontroller will read the data from the sensor and display it on the Liquid Crystal Display unit and sends data to the cloud, where cloud platform (IoT) stores the data, only the authorized person can login to the account and if any of the sensor crosses the threshold value [Figure 2], buzzer acts as an alert system and GSM will send the SMS to the authorized person.

V.RESULTS

The microcontroller will read the data from the sensors and display them on the Liquid Crystal Display (LCD) unit as shown in Figure 4 and sends the data to only the authorized person who can login into the account and view the data. If any of the sensor crosses the threshold values as given in the program, the buzzer acts as an alert system and GSM will send the message to the authorized person.

The proposed technology involves physical interaction with the devices which are capable of detecting hazardous gases in power plants by monitoring environment parameters which changes during radiation leakage. Those changes are indicated by Thingspeak web server, so that anyone can access the data and know about the radiation leakages without any expose to the radiation leakages. The final prototype is shown below in Figure 3.

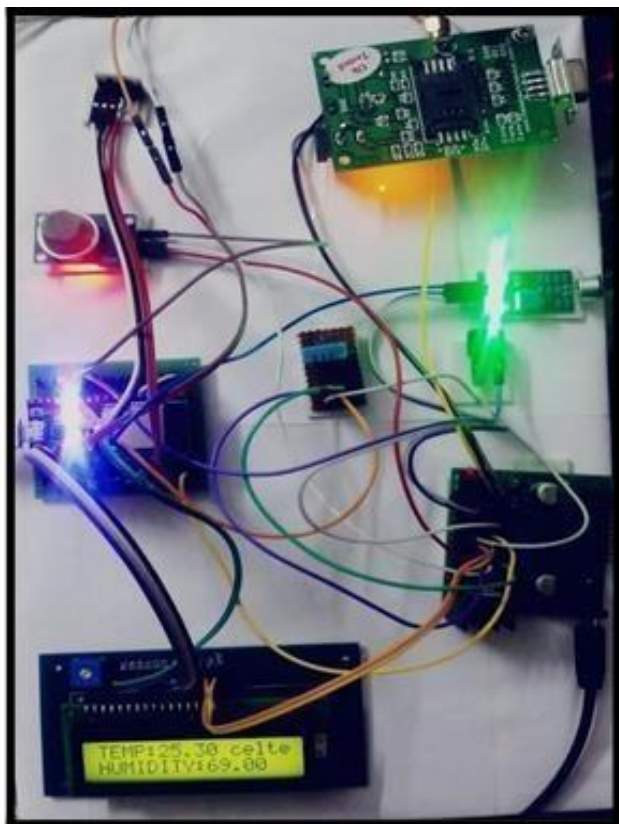


Figure 3: Execution of Prototype



Figure 4: LCD Display for monitored results

VI. COMPARISION WITH EXISTING AND PROPOSED WORK

The existing systems which are used to detect radiation are: Geiger counter with Geiger-Mueller: In this method, a gas filled tube is used when a high voltage is passed through it creates an electrical pulse when radiation interacts.

Micro R Meter with sodium iodide detector: In this process sodium iodide crystal is used which gives a pulse of light when interacted with radiation, this pulse of light when converted on an instrument gives the reading.

All above mentioned existing systems have the following disadvantages such as, employees or field workers working in the nuclear plants are exposed to radioactive materials and there are no proper alerting systems to notify about the radiation leakage.

Advantages:

IoT mechanism will greatly improve in reducing the costs and enhancing the flexibility of the sensor node, in order to increase the range of possible measures, authors are working on a revised hardware version.

Less cost.
More flexible.
Detectors can be extended without much problem.
Easily scalable.

Applications:

In the surrounding areas of Nuclear reactors.
In the Nuclear submarines.

VII. CONCLUSION

The outlining and executing a modest wide territory sensors arrange for natural radiological checking around atomic reactors is proposed in this project. This device acts as an early warning system against nuclear radiation leakages.

This gadget utilizes new source programming instrument, this is pushed towards a system arranged vision of IoT. Thus the data in regards to the sensor information can be observed continuously by individuals who approach the site and can trigger if there is a caution. The proposed method monitors the environment continuously and each employee or technical operator in the power plant can access the data without any expose to the radiation in radiation leakage areas.

REFERENCE

- [1] Vax. E Sarusi B., Shinfeld, M., Levison. S.,Bradys L, Marcus E and Cohn Y, “ An Integrated approach for Multipurpose Fast Deployment of Environmental Radiation Monitor Systems”, Nuclear Science Symposium Conference Record(N S S/ M I C), 2009 IEEE(pp.912-913).
- [2] Goma, R I Shiddy, I A Shashar KA, Alkabbani, A S and Raai, H.F. “ Realtime Radiation Monitor of Nuclear Facilities using ZigBee Technologies”. IEEE Sensor Journal, 14 (11), 4007-4013(2014).
- [3] S. Brennan, A. Mielke, D. C. Torney, & B Macabe, “Radiation Detection with Sensors Detectors” Complete Vol. 37, pp. 57-59, 2014.
- [4] S. M. Brennan, A. M. Mielke, and D. C. Torney, “Radioactive source detection by sensor networks,” IEEE Transactions on Nuclear Science, vol. 52, no. 3, pp. 813– 819, 2005.
- [5] R Lubis & A Sagala, “Multi Thread Performance in single thread in-memory database”, 2015 7th
- [6] International Conference in Information Technology & Electrical Engineering (I C I T E E), ChingMai, 2015, pp. 571--575.doi: 10.1109/ICI TE ED.2015.740 9012
- [7] G. Venkatesh and G. Chandramouli, “An IOT based Environmental Radiation Monitoring through Wireless Sensors Network”, Published 31st December 2017, DOI 10.29042/2018-2753-2756.

Intelligent Covid-19 Pandemic Bus Service with Safety Measures

^[1] Parimala Gandhi, ^[2] Joy Bhowmik, ^[3] Adarsha M P, ^[4] Ajay K S

^[1] Associate Professor, Department of ECE, R.R Institute of Technology, Bengaluru, India

^[2]^[3]^[4] BE Students, Department of ECE, R.R Institute of Technology, Bengaluru, India

Abstract— This paper depicts the intelligent covid-19 pandemic bus service with safety measures. Many will travel from one place to other for their work by the means of public transportation. In this case, the government needs to take more precautions by finding out the infected people along with that they need to avoid the spreading of the virus. This paper will make a good impact on finding out the people who are having the primary symptoms and follows the WHO rules. In this paper, the main focus is to find the people who are close to the infection by checking their temperature automatically, along with this the counter will be there to keep a count of people who is boarding and de-boarding the bus. so that the passengers get to know that whether there are empty seats on the bus or not. In addition to this, the sanitization process will be carried out for each passenger automatically before entering the bus.

Keyword: temperature, sanitization, counter

I. INTRODUCTION

The COVID-19, an acronym for "Coronavirus Disease-2019", is a respiratory illness caused by the severe acute respiratory syndrome coronavirus (SARS-CoV-2), a contagious virus belonging to a family of single-stranded, positive-sense RNA viruses known as coronaviridae. Much like the influenza virus, SARS-CoV-2 attacks the respiratory system and causes ailments such as cough, fever, fatigue, and breathlessness. While the exact source of the virus is unknown, scientists have mapped the genome sequence of the SARS-CoV-2 and determined it to be a member of the β -CoV genera of the coronavirus family, which typically derives its gene sources from bats and rodents. The COVID-19 was first reported to affect human life in Wuhan City, in the Hubei province of China in December 2019. Since then, the COVID-19 has spread like wildfire throughout the rest of the world, marking its presence in 213 countries and independent territories. COVID-19 statistics for the worst affected countries and regions of the world have been presented in Fig1. According to the WHO, the current global tally of confirmed coronavirus cases stands at 65.2M while the death toll has reached 1.51M. The rapid rise in the number of COVID-19 incidents worldwide has prompted the need for immediate countermeasures to curb the catastrophic effects of the COVID-19 outbreak.

The Government authorities and stakeholders need to work out a Module so that the public transport bus can go on to continually serve and be a sustainable part of the city life. What it needs at this juncture is for organizations promoting sustainable mobility to hold its back. Otherwise, the

consequences of a fall in revenue due to limited service and ridership can seriously hinder meeting the mobility and connectivity needs of the people residing in the Metropolitan Area – having a deep impact on the lives of people and the state economy.

As the whole world is suffering from covid-19, the scientists are busy finding out the vaccines. It's time for us to take precautionary measures, our project aims at providing safety measures for passengers riding on a bus has instilled confidence among riders.



Figure 1: Covid-19 Statistics

II. LITERATURE SURVEY

Wellsprings of measurements for the writing overview had been many, anyway the significant assets are reports, diaries, net, magazines and records. As the set of experiences for executing the mission required a skill of installed gadget, it likewise includes the investigate Arduino IDE for programming the product program to unique sensors utilized and Arduino Nano board.

Non-Contact Temperature Reader with Sanitizer Dispenser (NCTRSD) A research paper, Non-Contact Temperature Reader with Sanitizer Dispenser (NCTRSD) [1], via Marlon Gan Rojo, Jolan Baccay Eunelfa Regie Calibara, Alain Vincent Comendador, Wubishet Degife, Assefa Sisay helped us to realize more about Temperature studying without a bodily contact and automated sanitizer dispenser.

This device is supposed to assist prevent the unfold of SARS-CoV-2 infection and help in preserving and/or enhancing community health and reducing the negative impact of the contamination on the economy and society.

The hardware components used are:

Arduino Uno, Temperature Sensor (MLX90614), Ultrasonic sensor, Submersible Motor Pump, Liquid Crystal Display (LCD)

The very last end result from this undertaking specially makes a speciality of non-touch temperature analysing and it almost fits to the hand held temperature analysing.

Automatic Room Monitoring with Visitor Counter (ARM – VC) A research paper, Automatic Room Monitoring with Visitor Counter (ARM – VC)[2], through Jothibas M, Aakash B, Shanju Ebanesh K, Gokul Vinayak L, helped us to understand more approximately implementation of Bi-directional counter.

Hardware Requirements:

Arduino–UNO, LCD Display, 5V Relay Module, Infrared Sensors, Potentiometer, Bread Board, Jumpers, Led lighting, 5V DC motor (as fan), Power Source, Resistors and a Laptop. The IR sensors placed at the doorway of the door will understand the movement of someone and increment the overall quantity of men and women count. If the individual crosses the sensor positioned faraway from the door and then sensor close to the door, then it is going to be decremented. This project gave an accurate count of number of persons entering and leaving a room.

Summary-This chapter explained the literature survey made for this chapter. The explanation is given to prompt how the devices will works.

III. SYSTEM REQUIREMENTS

Hardware

1. Non-contact Thermometer
2. Arduino NANO
3. Infrared Temperature Sensor (MLX-9061)
4. Proximity Sensor (APDS-9960)
5. OLED Display
6. Piezo Buzzer
7. Charging Module (TP4056)
8. Lithium Ion Cell

IR based Hand sanitizer dispenser

1. IR Sensor
2. BD140
3. Mini Water Pump
4. Potentiometer

Passenger Counter

1. Arduino UNO
2. LCD Display
3. IR Sensor
4. LED

Software

1. Arduino IDE tool
2. Embedded C

IV. METHODOLOGY

The fundamental point of view of this paper is to give a protected transportation to individuals who ventures day by day through the public vehicle.

Non-Contact Thermometer [1] the accompanying shows the proposed block graph of non-contact Thermometer, IR based Hand sanitizer allocator and Bidirectional counter.

The fundamental part of this Non-Contact Thermometer is a MLX90614 Non-contact temperature sensor which is associated corresponding to the Proximity sensor and I2C LCD which all are associated with the Arduino Nano (associated with the simple pin A4 and A5 where SDA associated with the A5 and SCL associated with the A4 in equal). I2C LCD, piezo Buzzer, LED are associated. The figure 2 shows the circuit outline of the noncontact thermometer. The principle moto of this model is to identify the temperature of the individual at whatever point he/she place their hand closer to the noncontact Thermometer. The functioning guideline of infrared sensor MLX90614 is to change the infrared radiation signal gathered from articles and Bodies into electrical signs. Then, at that point the temperature will be ship off the I2C LCD where it show the Ambient and Body temperature of the Object With the assistance of a vicinity sensor for an exactness. At whatever point the individual spot the hand close to the non-Contact thermometer of reach 0.5cm to 1cm the mirrored light from the article will showed on the showcase screen. In the event that the temperature of the individual is over 36 degree Celsius the signal will be high demonstrating basic in the showcase showing the internal heat level with squinting of LED then we can say that the individual is contaminated or having an essential indication of covid (Asymptomatic).

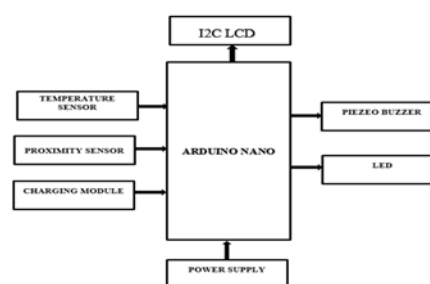


Figure: 2 Noncontact thermometer block diagram

IR BASED HAND SANITIZER [5]-The fig 3 shows the block diagram of the ir based hand sanitizer when the person need to have the sanitizer or wash their hands, the user's hands are placed under the nozzle and before the sensor. The activated sensor will further activate a pump that dispenses a specific amount of sanitizer (or soap) from the nozzle. Modern sensors used in electronic faucets, electronic flush valves and electronic soap dispenser's use Infrared light with wavelength in the range of 850 nm. The sensor employs an emitter and a collector.

The emitter emits pulses of infrared light while the collector, which is positioned to face in the same direction as the emitter, "sits" dormant waiting to sense the emitted pulses.

When no hands are present in front of the device, no reflection of light takes place, and therefore, no pulse is sensed. When hands

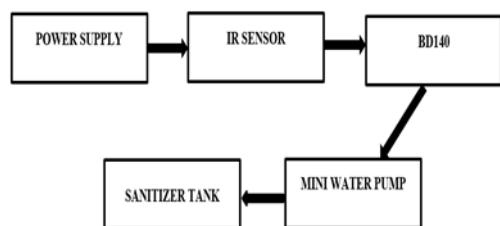


Fig 3: IR based Hand Sanitizer Block diagram

are present in the path of the emitted light, a portions of the emitted infrared light is bounced back in the direction of the collector which then becomes excited by the light (in the event a photodiode is used) and generates voltage to switch the pump on. If a photo transistor is utilized, then the photo transistor, upon sensing the infrared pulse, will simply switch the pump on and dispense the sanitizer or liquid soap. Infrared sensors detect infrared energy that is emitted by one's body heat. When hands are placed in the proximity of the sensor, the infrared energy quickly fluctuates. This fluctuation triggers the pump to activate and dispense the designated amount of liquid soap.

Passenger Counter [3]The main components of this model are IR sensor, Arduino UNO, LCD, Piezo Buzzer, LEDs. The fig 4 shows the block diagram of the passenger counter. The IR sensor continuously senses the presence of any obstacles (a person in our case). If sensor 1 senses a person, it informs the controller that a person has boarded so that controller can increment the count. At the same time it gives a delay of 1sec so that the person can cross the sensor 2 and the count is maintained correctly. When a person De-boarded, the sensor 2 informs the controller to decrement the count. Similarly it also provides a delay of 1 sec to maintain count properly. The count is displayed on LCD by the controller. Whenever the count reaches the maximum that has defined already it will shows stop Boarding No seat. If the count is less than zero it will shows No passengers to Exit.



Fig 4: Passenger Counter block diagram

V.RESULTS

Through this paper we have used intelligent covid-19 pandemic Bus has been designed for providing a safe transportation for the people who travels daily through the public transport.



Fig 5 intelligent covid-19 pandemic Bus

VI. CONCLUSION

Even with the pandemic posing travel restrictions our project will overcome this restriction by providing certain safety measures for the people those who are travelling in the public transport which is also helpful to hold back the revenue. In future this can be implemented in Schools, collages, offices, banks, Conventional Halls, Party halls and etc. Because of everywhere we need counters, Non-contact thermometer, and Automatic hand sanitizer for this present situation.

REFERENCES

- [1] Rojo, Marlon Gan, Jolan Baccay Sy, Eunelfa Regie Calibara, Alain Vincent Comendador, Wubishet Degife, and Assefa Sisay. "Non-Contact Temperature Reader with Sanitizer Dispenser (NCTRSDD)".
- [2] Jothibasu, M., B. Aakash, K. S. Ebanesh, and G. L. Vinayak. "Automatic room monitoring with visitor counter (ARM-VC)." Int. J. Innov. Technol. Explor. Eng.(IJITEE) 8, no. 7 (2019).
- [3] BidirectionalCounter: <https://forum.arduino.cc/index.php?topic=440765.0>
- [4] Non-contactThermometer: [https://www.journalofhospitalinfection.com/article/S0195-6701\(20\)30058-X/fulltext](https://www.journalofhospitalinfection.com/article/S0195-6701(20)30058-X/fulltext)
- [5] SanitizerDispenser https://www.researchgate.net/publication/224924900_Hand_Sanitizerr_Dispensers_and_Associated_Hospital-Acquired_Infections_Friend_or_Fomite

Smart Indoor Vertical Farming Using IoT

[¹] Parimala Gandhi G, [²] Sushma V, [³] Monika H, [⁴] Chithra C, [⁵] Ullas K S

[¹] Electronics And Communication Engineering, R.R Institute of Technology, Bangalore

Abstract— Vertical farming is the practice of producing food in vertically stacked layers or in vertically inclined surfaces in which plants are grown in a controlled environment. The proposed system uses the concept of IOT (Internet of Things) and is much more efficient. The indoor vertical farming environmental parameters are continuously sensed using various sensors and the collected data is displayed on a customized website. Thus, the indoor vertical farming can be monitored from anywhere and at any time. Basic functions like detecting the soil moisture, temperature, humidity are performed. Artificial photosynthesis for the plants using grow-lamps and also drip irrigation is implemented to maintain the urban gardens. GSM provides systematic alerts regarding the status of garden to the user at regular intervals of time. An android app interface is used to remotely control the garden functioning encouraging the smart way of agriculture.

I. INTRODUCTION

Agriculture has been one of the primary occupations of man since early civilizations and even today manual interventions in farming are inevitable. The world's population is expected to reach around 9.7 billion by the year 2050. The overall food production will need to increase by 50% of the current rate. A indoor vertical farming is mainly used to grow more plants in less space because mass urbanization and land degradation has resulted in diminishing of agricultural land. The issue is that there is a lack of space in the Urban areas. At present most of the indoor vertical farming are manually controlled and monitored. This paper proposes a system to monitor and automatically as well as manually control the system in indoor vertical farming using temperature sensor, humidity sensor, light intensity sensor and soil moisture sensor.

If the sensed data crosses a predefined threshold range an alarm will be triggered which will alert the user. This method of indoor vertical farming monitoring is labour intensive and time consuming. Urban gardens are needed to be turned into intelligent, independent and productive spaces. The technology proposed will not only benefit the urban agriculture, but also will help the rural agriculture to enhance the efficiency in a smart manner.

II. PROPOSED SYSTEM

This proposed system aims at reducing the human interference thus also reducing the error and the wastage of resources. In this all the required actions are automated because of which the farmer can take the required action from a remote location itself. The existing systems though they

had numerous features had failed to bring certain new implementations. Hence to overcome the drawbacks of the existing system, collaboration of new technologies is undertaken. The proposed model analyses the home gardening, collecting data through sensors & respected outputs are obtained. This model is also automated using IoT model & controlled through an app in the mobile phone.

Following are the main objectives of the proposed system:

Design and develop a microcontroller based sensor interfacing for reading a soil parameters.

Build a interface between LCD and microcontroller to show the sensor readings.

Converting the sensor value using ADC port of microcontroller.

• Sending all reading to mobile serial port using Wi-Fi module and microcontroller UART port.

Use of android mobile application for displaying real time soil status.

• Establishing the cloud server connectivity in order to store all soil test records over server with time.

The outline of proposed block diagram is shown in Fig:1 and brief explanation about each hardware components used is discussed. This chapter also lists the hardware components and software tools required.

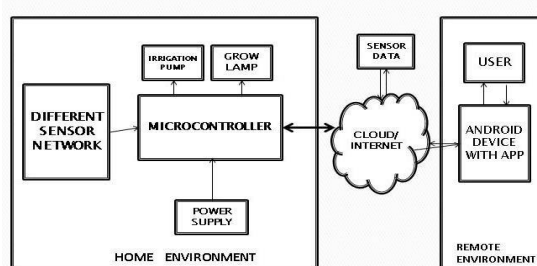


Fig:1. Block Diagram of the Proposed System

III. HARDWARE AND SOFTWARE REQUIREMENTS

Hardware:

- Microcontroller
- Vertical Garden frame
- Soil moisture sensor
- Humidity sensor
- LCD
- Grow lamps
- Pump with drip irrigation
- Wi-Fi module

Software

- Arduino IDE
- Flash Magic

- Embedded C

Blynk app interface

Blynk app is a digital dashboard where one can build a graphical interface for their project. It is done by dragging and dropping the pre-available widgets. It is used to satisfy the requirement to reach the information to the cultivator. The sensor's data are stored in the cloud which can be utilized for the further future analysis whenever it is required. Fig 2.11 illustrates the Blynk app interface.

Steps:

First, go to Blynk App and sign in with your credentials. open a project (or create a new one -- use Project > Start New Project and give your project a name). You can build your interface by working with

Widgets

- Adding buttons and assigning functions.
- Terminal interface.

IV. IMPLEMENTATION

In this chapter we discuss about the methodology and working of our project. This chapter also includes the outcome of proposed project. Pictures of the result are presented.

Methodology

The Internet of things (IoT) is the extension of Internet connectivity into physical devices and everyday objects. Embedded with electronics, Internet connectivity, and other forms of hardware (such as sensors), these devices can communicate and interact with others over the Internet, and they can be remotely monitored and controlled. Objects that have been assigned an IP address, they have the ability to transfer data over a network without requiring human-to-human or human-to-computer interaction. The embedded technology in the objects helps them to interact with internal states or the external environment, which in turn affects the decisions taken. A system is an arrangement in which all its unit assemble work together according to a set of rules. It can also be defined as a way of working, organizing or doing one or many tasks according to a fixed plan. Computer hardware system having software embedded in it. An embedded system is a microcontroller or microprocessor based system which is designed to perform a specific task. Industrial machines, agricultural and process industry devices, automobiles, medical equipment, cameras, household appliances, airplanes, vending machines and toys, as well as mobile devices, are possible locations for an embedded system.

Two designs have been proposed in this project first the microcontroller operation and second is the mobile app development. All the operations related to the microcontroller are written in embedded C and these programs obtain the required results. The entire device is functioning on microcontroller and is controlled using a mobile application. Home environment consists of the hardware equipment embedded with the frame container where plant or crop is grown. Here, ARM controller is the

microcontroller used and it is used for taking the data from different sensors and for taking the necessary actions effectively. The hardware implementation can be seen in the figure 5. Temperature sensor used here is LM35. It is used to measure temperature and it provides the output in in °C format (degree Celsius). The LM35 sensor doesn't need any amplifier unlike the regular thermistor. A soil moisture sensor is used. It collects the amount of water level present in the soil. If it is low then it sends a notification to the user in the remote environment. By receiving the notification data from the soil sensor, the automated action can be executed. The output is obtained in three ways. The digital data, the analog data and the serial data. The Light dependent resistor (LDR) is made up of a highly resistant semiconductor. When the light falls on the LDR, it doesn't conduct, but when the light intensity falling on it is low, it conducts and is made use of lighting certain LED's. Humidity sensors are used to measure the amount of humidity level in the Home environment. They are used to measure both temperature and the moisture level in the air. Relative humidity is expressed as a percentage of the ratio of moisture in the air to the maximum amount that can be held in the air at the current temperature.

The humidity constantly varies with the temperature. If the temperature increases the humidity level increases, if temperature decreases, humidity level decreases. Watering of plants based on the results collected by different sensors in the top layer and in return appropriate pump is switched on, as required. A mobile application (Smart Garden) using IoT concept is developed in order to automatically control this device using Blynk interface. Grow lights are used for indoor gardening and food production. They can be used for horticulture, indoor hydroponics which includes aquatic plants. Grow lights are usually used in an industrial level that is, on a large scale. They can also be used in small scale for indoor cultivation. They consist of combination Red and Blue LEDs and give output as a pink light. The combined lights of a unique wavelengths give the plants only the wavelengths of light they require. The photosynthesis machinery of plants is tuned in such a way to absorb the pink (red and blue light) most effectively. User will be able to control the watering of plants

In this an android application is developed using Blynk interface. This app accesses the data through a web server. The sensor data can be remotely monitored by this manner. The water irrigation pump and light intensity present Home environment can be controlled remotely with the help of the developed android app. The information of the home environment to the cultivator is also provided through the email. The farmer or the cultivator now can access the data even with poor network access. The data stored in the cloud can also be accessed for certain range of days. The cultivator therefore can know how much amount of water is required and is used by the crop in the certain period of time.

Overview of the project

All the hardware components including microcontroller, sensors, grow lamp are connected in the home environment are connected to the vertical frame as shown in the figure.

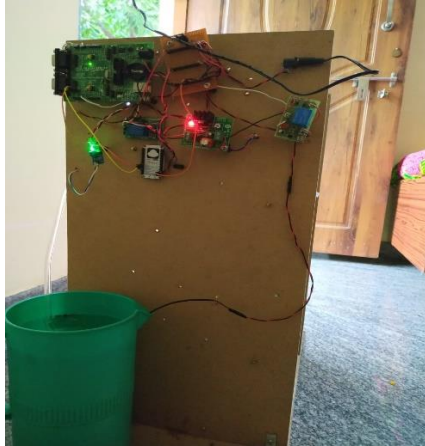


Fig:2.Hardware connections



Fig:3.overview of the project



Fig:4.plants growth in soil and hydroponics method

V. EXPERIMENTAL RESULTS

The experimental setup of a vertical garden is arranged with two different stacks containing two different plants for purely experimental purposes. As this project aims at vertical watering of plants the two plants chosen are such that one requires water and the other one requires nutrient medium. To access to the garden like setup in a easy manner, an user friendly application is created using Blynk app interface. The sensors are deployed in the soil for recording information like soil moisture, humidity and temperature data. The results are observed for invoking alarm to the user when required. These monitored real time sensed data is stored on the cloud server for decision making and controlling actions through Blynk platform. The user can monitor the controlling actions taken at the garden as well as control the supply of water via android app on user’s mobile phone. Wi-Fi connection is a must for the system above operations. In a moist soil resistance is less therefore it has good conductivity of current as compared with dry soil. Therefore, it helps to detect the moisture contained in the soil. A plot of soil moisture data received through the microcontroller and a similar variations in the humidity and temperature can be seen with the help of Blynk.

Sensor type	Threshold range	Output Effect
Humidity	55% - 70%	Notification
Temperature	25 degrees C (optimum)	Notification
Soil moisture	650 (5% - 30%)	Pump for Drip Irrigation will be Switched On.

Fig:5.Threshold range is discussed in the above table

The line-graph of output voltage v/s temperature is shown in figure 4.2 . The lightbulb temperature under ON/OFF conditions is shown in figure 4.3.

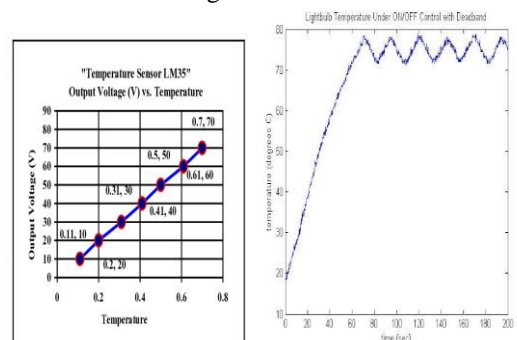


Fig:6.voltage v/s temperature

Fig:7.temperature under on and off conditions

According to the threshold level set up in the code, when the soil moisture value reduces below or goes above the threshold level, it notifies the user in the form of texts indicating the condition of the garden. Fig 4.4 is the mobile application interface and terminal output respectively.

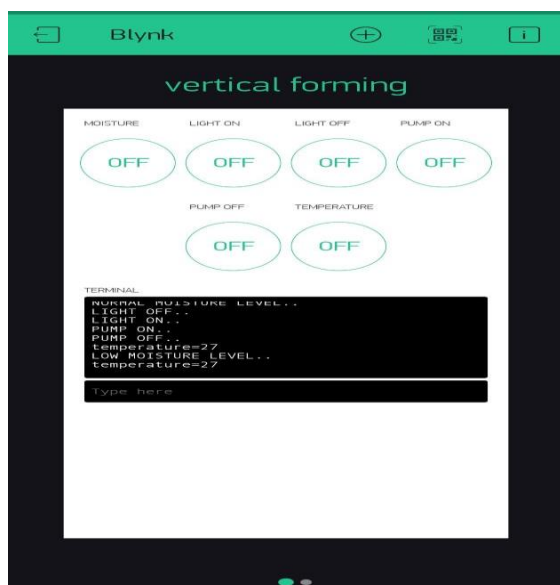


Fig:8.Sensor values retrieved in Terminal output

VI. ADVANTAGES

1. Good monitoring of water regulation can be achieved by saving space with vertical stacked layers.
2. Low-cost and energy efficient.
3. Affordable for a small group of people.
4. Easily implementable in urban gardens.
5. Better control and more eco-friendly.
6. Accurate values of temperature and humidity can be known.
7. Environmental friendly spraying method.
8. Reduced work, time saving.
9. More Green Earth
10. Provides easy access by providing alerts through the App.
11. Good monitoring of water regulation can be achieved by saving space with vertical stacked layers.
12. Low-cost and energy efficient.
13. Affordable for a small group of people.
14. Easily implementable in urban gardens.
15. Better control and more eco-friendly.
16. Accurate values of temperature and humidity can be known.
17. Environmental friendly spraying method.
18. Reduced work, time saving.
19. More Green Earth
20. Provides easy access by providing alerts through the App.
21. This promotes the fast development of a modernization.
22. Better breathable air.
23. Saves space available for agriculture.
24. Smart watering network,
25. Usage of Grow lamps helps encourages artificial photosynthesis

VII. APPLICATIONS

1. Vertical zones will always be watered according to a specific schedule
2. Evaluate the real quantity of water required depending on the crop and type of soil
3. It is not only confined to home gardening, these can also be implemented in agriculture fields.
4. Used in many multinational companies
5. For case studies, research and development of particular plants like medicinal plants, mineral plants.
6. It can be used by any people who are passionate about gardening.
7. Easily implementable in Urban gardens.

VIII. CONCLUSION AND FUTURE SCOPE

This project is not only confined to home gardening, this can also be implemented in agriculture fields, which in turn is helpful for farmers .

Our project has multiple applications in research laboratories like for case studies, research and development of particular plants like medicinal plants, mineral plants.

This can also be implemented in vertical skyscrapers which are going to be one of the future agricultural means.

Our project also demonstrates more efficient method for agriculture when compared to traditional techniques.

The conventional methods of supplying water to the plants include disadvantages such as increase in dependence on place, overall high costs, dependence on weather.

Our system overcomes these disadvantages by providing an effective supply of water to the plants.

REFERENCES

- [1] Thenmozhi, S., Sudharsan R, Dhivya M.M., and Nirmalakumari K., "Greenhouse Management Using Embedded System and Zigbee Technology." International Journal of Advanced Research in Electrical, Electronics and Instrumentation Engineering, India, Vol. 3, Issue 2, pp. 2320-3760, February 2014.
- [2] Shah, AFM Shahan, and M. Shariful Islam. "Solar Powered Automatic Drip Irrigation System (SPADIS) using Wireless Sensor Network Technology " International Research Journal of Engineering and Technology (IRJET) Bangalore, India, pp. 66-78, July 2017.
- [3] Patel, Nidhi, Hiren Kathiriya, and Arjav Bavarva. "Wireless Ensor Network using
- [4] Rashmi Maria Royston1, Pavithra M.P "VERTICAL FARMING: A CONCEPT", International Journal of Engineering and Techniques , May 2018.

Investigation of Fluoride Uptake by Chlorine Doped Polyaniline in Continuous Column Mode Operation

^[1] Sarungbam Pipileima, ^[2] Potsangbam Albino Kumar

^[1] Department of Civil Engineering, National Institute of Technology Manipur

Abstract— This study focuses on optimisation of pH for fluoride uptake by adsorbent polymer polyaniline doped with chloride and synthesised on surface of jute fiber (PANI-Cl-Jute) in continuous column mode operation. At reactor bed depth of 1.5 m, flowrate of 1.2 mL/min and initial fluoride concentration of 5 mg/L, the breakthrough time at pH 1, 2, 4 and 6 were 11, 7, 5 and 1 hour respectively suggesting favourable adsorption at acidic pH. On characterized with Scanning Electron Microscope (SEM) and Energy Dispersive X-ray Measurements (EDAX), F- uptake by PANI-Cl-jute was confirmed. Total amount of ions adsorbed at different bed depth of 1.5, 2 and 3 m yields and F- uptake of 11.87, 15.85 and 26.53 mg respectively thus amounting an average uptake of 0.07 mg F-/g PANI-Cl-jute against a higher uptake of 12.99 mg/g in batch mode studies. The formation of mass transfer zone in continuous mode unlike adsorption equilibrium in batch mode is the main reason for lower uptake in continuous column mode operation. However a throughput volume of 620 mL was able to achieve under the study condition with F- below the permissible limit suggesting the effective adsorption of F- by PANI-Cl-jute.

Keywords: Polyaniline, fluoride, adsorption, BDST, throughput volume.

I. INTRODUCTION

Fluoride is an essential element for our health and permissible its limit in drinking water as per WHO is 1.5 mg/L [1]. Excess fluoride in drinking water has harmful effects on human causing spotting and decolouration of teeth or skeletal fluorosis [2]. Various techniques of defluoridation include precipitation-coagulation [3], membrane separation process, ion exchange, electrodialysis, chemical precipitation [4], ion-exchange [5], reverse osmosis [6], nano-filtration [7], and adsorption [8]. Among these methods, adsorption is widely used method for the effective removal of Fluoride for its cost effective, no sludge regeneration, flexibility and simplicity of design and operation. In the last decades, several adsorbent have been employed like activated alumina, synthetic resin, red mud, tea leaves, rice husk, chitosan, etc and lately functional group based adsorbent has been used for its effective removal of fluoride. Amines are reported to get protonated with H⁺ in acidic medium and have strong affinity to bind highly electronegative fluoride ion [9,10,11]. To further increase the adsorption of fluoride, chloride doped amine based polymer will be synthesized on surface of jute fibre (PANI-Cl jute) as supporting materials employed for defluoridation. The doped chloride are postulated to be replaced by fluoride ions. Adsorption studies are generally carried out in batch mode operation but

preferred continuous column mode operation in practical situation. This study emphasises on investigation of fluoride uptake in continuous mode. Optimisation of doped chloride amount, pH, different bed depth of the reactor are considered for this study.

II. MATERIALS AND METHODS

A. Chemicals and reagents

The adsorbent PANI-Cl-jute was prepared as per our previous studies [12]. All chemicals and reagents used are purchased from Merck (AR Grade) and used as received. Only, aniline for the preparation of polymer was distilled using KOH yielding only 65-70% volume and remaining discarded as impurities. All the samples were prepared using double distilled water and Fluoride stock solution of 100 mg/L were prepared daily. Further lower concentration for experiments were prepared by series dilution of the stock solution.

B Experimental methodology

Fixed bed column for the adsorption study was set up using a PVC reactor of 4 cm diameter with various outlets at bed depths of 1.5, 2 & 3 m from the top. The column is fed with known quantity of PANI-Cl-jute and is well supported at bottom with cotton and PVC cover to prevent wash out and leakage. The reactors were fed with desire concentration of F- solution using peristaltic pump (Model: Miclins PP 60 Ex, India) controlling the required flow rate. Acidic and basic pH of solution is maintained by addition of HCl and NaOH of varied strength and maintained the added acid/base volume to be less than 1% of the total solution. At varied time, the effluents were collected from the various outlets for analysis of F-. All experiments were conducted till the concentration of effluent becomes 95% of the initial F⁻ concentration which is called the exhaustion. Fluorides concentrations were estimated using Ion selectivity electrode (Cole Parmer, USA) using TISAB buffer. Collection of effluents and estimation were all done in plastic ware avoiding glass ware to minimize the adsorption of fluoride in glass.

III. RESULTS AND DISCUSSION

A. Characterization

The SEM images of PANI-Cl-jute before and after F⁻ adsorption are shown in Fig.1 and 2 respectively where smooth and even surface disappears after F⁻ adsorption. The EDX spectra of PANI-Cl-jute before adsorption (Fig. 3)

contains no F⁻ peak whereas the emerged after adsorption (Fig. 4).

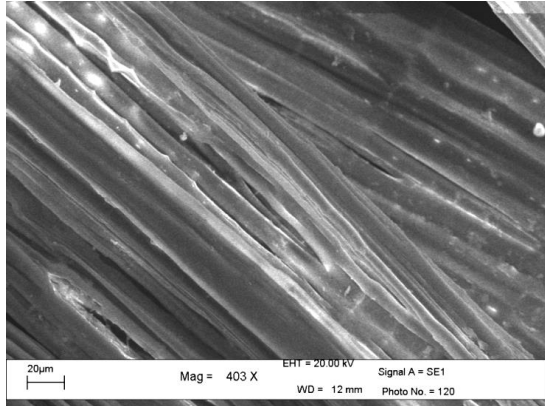


Fig. 1: SEM image of PANI-jute-Cl before F⁻ adsorption

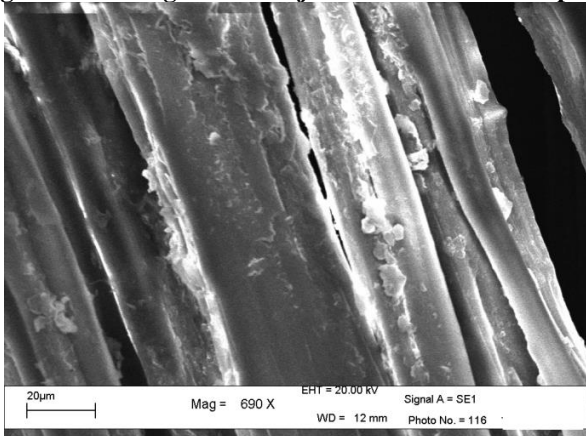


Fig. 2: SEM image of PANI-jute-Cl after F⁻ adsorption

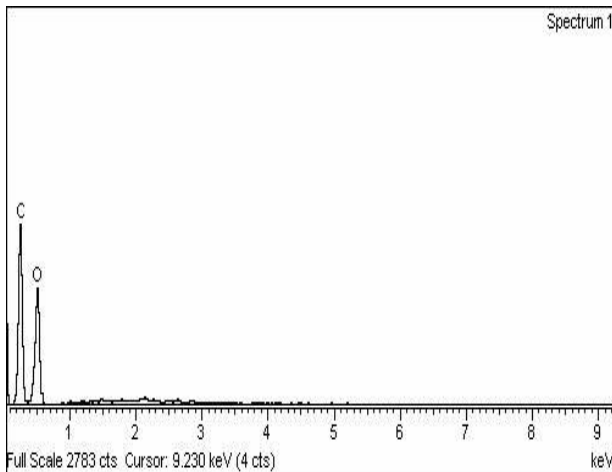


Fig. 3: EDAX image of PANI-jute-Cl before F⁻ adsorption

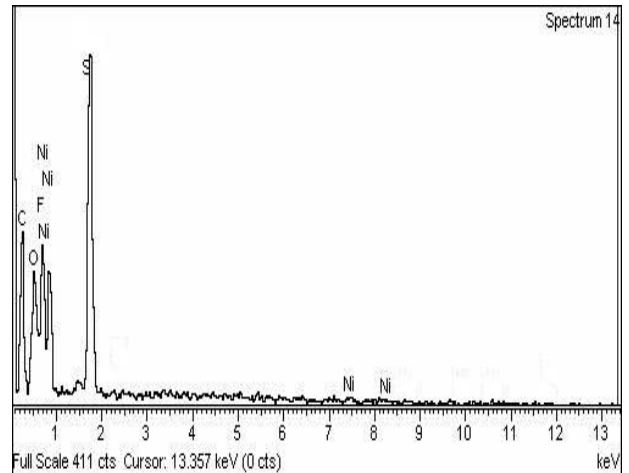


Fig. 4: EDAX image of PANI-jute-Cl after F⁻ adsorption

B. Chloride doping

During the synthesis of the adsorbent, the polymer polyaniline was doped by chloride introducing various chloride of 0.5, 1, 1.5 and 2 M. The obtained adsorbents PANI-Cl-jute were employed in column reactor with 1.5 m depth reactor, initial F⁻ 5 mg/L and 1.2 mL/min flow rate. The result obtained is plotted in Fig. 5, obtaining a S-curve. From the figure, it can be seen that PANI-Cl-jute with 0.5 M and 1 M doped chloride started leaking at the beginning of the experiment itself at C/C₀ of 0.04 and 0.03 respectively. At chloride amount of 1.5 and 2 M, a throughput volume of 1150 and 1100 mL were achieved respectively. The optimum chloride doping was thus attained at 1.5 M chloride. With increased in chloride, more ion exchange with fluoride results higher uptake. However with higher doped chloride amount, excess chloride are leaked into the solution due to saturated doping of chloride on chain of PANI-Cl-jute. Thus all further works were carried out with PANI-Cl-Jute doped with 1.5 M.

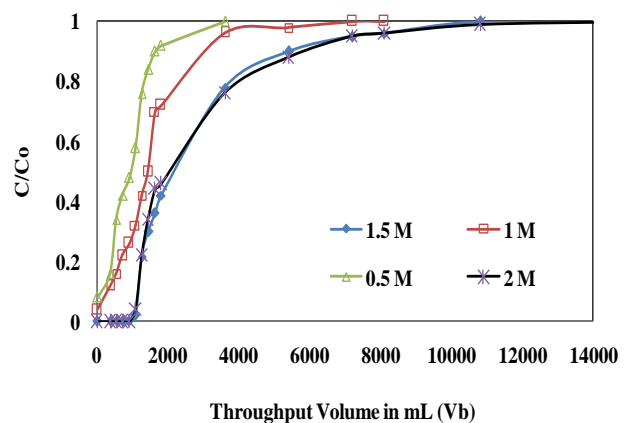


Fig. 5: Breakthrough curve for fluoride adsorption at various chloride doped PANI-Cl-jute

C. Optimisation of pH

In order to optimise the pH of the adsorption, experiments were conducted by maintaining influent pH from 1-6, bed depth of the reactor as 1.5 m, flowrate 1.2 mL/min and initial concentration of F⁻ as 5 mg/L. The results obtained is represented at Fig. 6. From influent pH 3 - 4, the effluent leaks F⁻ at the beginning itself. pH 2 experiment makes breakthrough at 7.5 hours whereas that of acidic pH 1 have a breakthrough time of 12 hours. The finding clearly indicated that the optimum pH is acidic pH 1 for the adsorption of F⁻ by PANI-Cl-jute. At acidic pH, the protonated amines of PANI-Cl-jute electro statically attract the anionic F⁻ and adsorbs more fluoride ions.

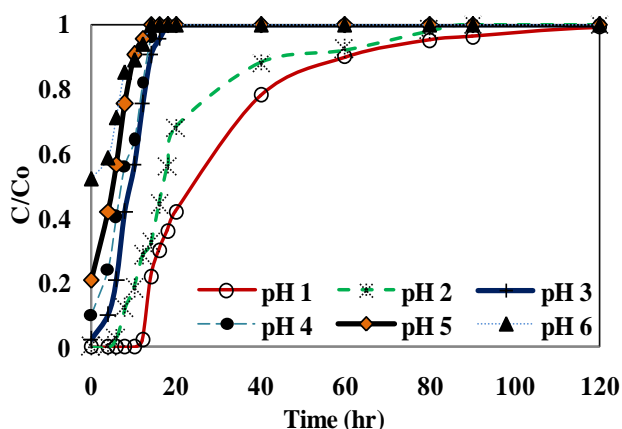


Fig. 6: Breakthrough curve at different pH for fluoride adsorption

D. Effect of bed depth

Effect on bed depth was studied at varied bed depth of 1.5 m, 2 m and 3.5 m which were filled with PANI-Cl-jute of 165g, 220 g and 330 g respectively. The experiment was conducted at flow rate of 1.2 mL/min and initial F⁻ concentration of 5 mg/L. The breakthrough curve of the column reactor is shown in Fig. 7. The evaluated parameters for the continuous column experiment for F⁻ adsorption by PANI-Cl-jute are shown in Table 1. The obtained curve is called S-curve or Breakthrough Curve. The area above the breakthrough curve denotes the total amount of F⁻ ions adsorbed (mg).

With the increase in bed depth from 1.5 - 3 m, both the breakthrough time (considered at 5% effluent) and exhaust time (considered at 95% effluent) increased from 8.6 - 17.5 h and 88 - 200 h respectively. Subsequently, the corresponding throughput volume and exhaust volume were also increased from 0.62 L to 1.26 L and 6.33 L to 14.4 L respectively. Thus amount of F⁻ ions adsorbed (M_R) were 11.87, 15.85 and 26.53 mgF for bed depth of 1.5, 2 and 3 m respectively. As bed depth increase, the amount of active sites of adsorbent increase and adsorb higher F⁻, thus treating more volume. Also, increasing the bed depth should lead to decrease in axial dispersion and encourage higher F⁻ diffusion on PANI-jute. Similar cases are observed in almost all fixed bed studies [13, 14]. However despite more contact time between adsorbate and adsorbent with increase in bed depth, the q_e

value are almost same with 0.7-0.8 mg/g without much significant change.

This finding was compared with batch adsorption studies by conducting experiment with F⁻ 10 mg/L contacting with 1 g/L PANI-Cl-jute. The amount of ions adsorbed, q_e was observed to be 12.99 mg/g which is higher than that of continuous results with 0.7 mg/g. Very insignificant or minimum adsorption of F⁻ occurs beyond the Mass Transfer Zone in continuous column process and this may be due to strict chemical adsorption of F⁻ on PANI-jute with minimum or insignificant physical diffusion. However equilibrium is achieved in batch process unlike the concept of mass transfer zone in column process resulting higher uptake. In practical application of fixed bed column either for water or waste water treatment, the fixed bed will be employed till the effluent is within permissible limit or breakthrough time. The running of fix bed after the occurrence of the breakthrough till the exhaust point is not necessary as ions will start leaking above the permissible limit. The purpose of running till the exhausting point is for study purpose to understand the column profiles and gain the inside mechanism.

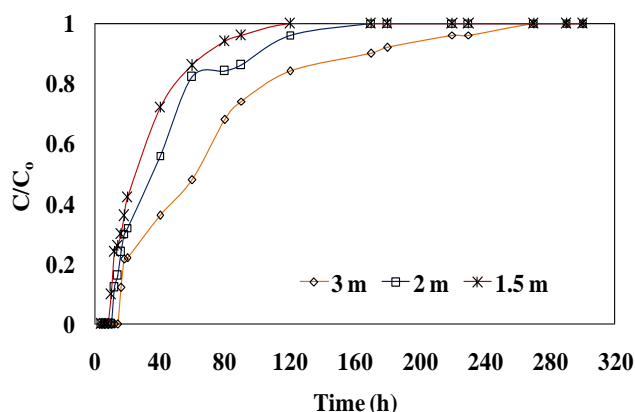


Fig. 7: Breakthrough curve at different bed depth of the reactor

E. Comparison of performance between synthetic and actual fluoride contaminated ground water

A comparative study between the synthetic fluoride contaminated ground water and actual ground water was carried out to evaluate the practical feasibility of employing PANI-Cl-jute. The actual ground water F⁻ contamination was observed to be 3 mg/L, therefore synthetic F⁻ contaminated water with 3 mg/L was also prepared. The S-curve for both the experiments are illustrated in Fig. 8. The actual ground water sample yields a breakthrough time of 6.5 hour against 9.5 hour for synthetic F⁻ contaminated water yielding a respective throughput volume of 468 mL and 684 mL. Better efficiency of PANI-Cl-jute is obtained for synthetic since the presence of other co-ions in actual ground water probably hindered the adsorption process. Again, the S-curve of actual ground water is more steeper than that of synthetic water can be explained by the fact that adsorption is immediate in

ground water and got exhausted sooner than the synthetic. The absence of co-ions in synthetic allows more F⁻ ions to adsorb probably through diffusion also leading to flatter curve and finally achieve the exhaust at 150 hours of adsorption.

higher uptake of 12.99

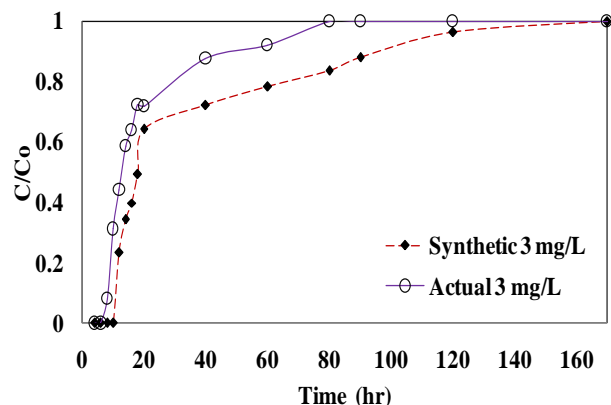


Fig. 8: Comparison between adsorption from synthetic F- contaminated water and actual ground water

IV. CONCLUSION

The study of fluoride adsorption by chloride doped polyaniline polymer, PANI-Cl-jute was investigated for the F⁻ uptake at various conditions. The chloride concentration of 1.5 M was observed to be the optimum for doping with maximum F⁻ uptake with throughput volume of 1150 mL. Optimum pH was observed at acidic pH 1 with maximum breakthrough time of 12 hours. At various bed depth of 1.5, 2 and 3 m, amount of F⁻ ions adsorbed (M_R) were 11.87, 15.85 and 26.53 mgF⁻ respectively with average uptake of 0.7-0.8 mg/g. The adsorbent PANI-Cl-jute proved to be an effective adsorbent for the defluoridization from ground water.

Table 1: Parameters of F- adsorption at continuous bed at different bed depth of reactors.

Depth (m)	Breakthrough time (T _b)	Exhaust time (T _e)	Breakthrough volume (V _b) (L)	Exhaust Volume (V _e) (L)	Mass of adsorbent, m (gm)	Total amount of F- uptake (mg)	Total amount of F- uptake per unit gram of adsorbent (q _e)
1.5	8.6	88	0.619	6.33	165	11.865	0.072
2	11.7	112	0.842	8.06	220	15.852	0.072
3	17.5	200	1.260	14.40	330	26.531	0.080

REFERENCE:

- [1] WHO Report, "Fluoride and Fluorides: Environmental Health Criteria", World Health Organisation, Geneva, 1984.
- [2] Amor, Z., Bariou, B., Mameri, N., Taky, M., Nicolas, S., Elmidaoui, A., 2001. Fluoride removal from brackish water by electrodialysis. *Desalination* 133, 215–223.
- [3] K. Sarala, P. R. Rao, "Endemic Fluorosis in the village Ralla, Anantapuram in Andhra Pradesh-an epidemiology study", *Fluoride*, 26, 1993, pp. 177-180.
- [4] S. Maurice, O.Y. Kojima, O. Aoyi, C. Eileen, B.H. Matsuda, "Adsorption equilibrium modeling and solution chemistry dependence of fluoride removal from water by trivalent-cation-exchanged zeolite", *F-9, J. Colloid Interface Sci.*, 2004, pp. 341–350.
- [5] Renuka Piddennavar, Pushpanjali Krishnappa, "Review on defluoridation techniques of water", *International Journal of engineering and Science*, vol.2, No.3, 2013, pp. 86-94.
- [6] S.V. Joshi, S.H. Mehta, A.P. Rao, A.V. Rao, "Estimation of sodium fluoride using HPLC in reverse osmosis experiments", *Water Treatment*, 7, 1992, pp. 207-211.
- [7] R. Simons, "Trace element removal from ash dam waters by nanofiltration and diffusion dialysis", *Desalination*, 89, 1993, pp. 325-341
- [8] Meenakshi, S., Viswanathan, N., 2007. Identification of selective ion-exchange resin for fluoride sorption. *J. Colloid Interf. Sci.* 308, 438–450.
- [9] M. Karthikeyan, K.K. Satheshkumar, K.P. Elango, "Defluoridation of water via doping of polyanilines", *Journal Hazardous Material*, 163, 2009, pp. 1026–1032.
- [10] M. Mucha, K. Wankowicz, J. Balcerzak, "Analysis of water adsorption on chitosan and its blends with hydroxypropylcellulose", *e-Polymers*, 16, 2007, pp. 1–10.
- [11] G. Crini, "Non-conventional low-cost adsorbents for dye removal: a review", *Bioresour. Tech.*, 9 (9), 2007, pp. 1061–1085.
- [12] S. Pipileima, P. A. Kumar, "Kinetics study of fluoride uptake by functionalised polymer polyaniline synthesized on jute fibre", *Journal of Basic and Applied Engineering Research*, Vol.3 (12), 2016, pp 1136-1137
- [13] Roy S, Das P, Sengupta S, Manna S "Calcium impregnated activated charcoal: Optimization and efficiency for the treatment of fluoride containing solution in batch and fixed bed reactor", *Process Safe and Env Protect* 109, 2017, pp. 18–29
- [14] Mohan S. , Singh D K, Kumar V, Hasan S S, "Modelling of fixed bed column containing graphene oxide decorated by MgO nanocubes as adsorbent for Lead(II) removal from water", *Journal of Water Process Engineering* 17, 2017, pp. 216–228

Performance Analysis of Distributed System by the Placement of DG considering Load Growth

^[1]Pradeesha J, ^[2]Vyshnav B, ^[3]Akshatha R Hegde
^{[1][2][3]} Assistant Professor, Dept of EEE, RRIT

Abstract— Load growth in a system is a natural phenomenon and analysis of load growth is very important to evaluate the future performance of the system. With the increase in load demand, system power loss and voltage drop increases. Placement of Distributed generators (DGs) are one of the best solutions to cope up with the load growth if they are allocated appropriately in the distribution system. In the work planned, the optimal size and location of multiple DGs will be able to satisfy the incremental load on the system and minimization of energy loss without violating system constraints. It is planned that with the penetration of DG in distribution system, there will be a great improvement in several distribution system parameters. Moreover, the loading capacity of distribution system will be enhanced through DG and capacitor placement considering load growth by undergoing detailed analysis. Two test system 33bus and 69bus RDS will be considered to evaluate the result.

Index Terms: Placement of Distributed generators (DGs), Load growth, Minimization of energy loss, Energy demand.

I. INTRODUCTION

Distributed Generator or Decentralized Generation is a small power generator ranging from few Kilowatts to few Megawatts. It can operate stand-alone or in correlation with distribution network but is not dispatchable by a central operator. To maximize DG benefits, DG must be of appropriate size, to be placed at the appropriate location and in appropriate number. Inappropriate capacity of DG may cause higher system power loss. This is because the reverse power flows from larger DG units to the source which results into instability of the system.

Steady increase in energy demand on distribution system due to natural growth of a service territory or through stimulation of energy market is a big challenge to planning engineers so that the system is adaptable without violating service quality. Load growth on system results into either extra expenditure made towards the addition of new substation or expanding the existing substation capacity. Due to Power System Deregulation and environmental concerns as well as technological advancements, the Disco (Distribution Company) planners are forced to investigate expansion planning through alternatives such as Distributed Generation (DG). In this work, a Simple Algorithm is used to find out the DG size and site for catering the load on the feeders without violating the voltage limits of the feeder. Here the objective function is to minimize the Active Power Loss and to reduce Cost of Electricity considering Load Growth. The main

contribution of the work deals with the Impacts of following issues with load growth. They are:

1. Increase in load capacity of the distribution system.
2. Multiple number of DG in a distribution network on active power losses.
3. Multiple number of DG on reactive power losses.
4. Cost of Feeder Energy Loss from the transmission network.
5. Total cost of DG.
6. Voltage profile.

II. LITERATURE REVIEW

A rapid rise in load demand, due to the industrial and commercial loads results in voltage problem, draws excessive power and energy loss in the distribution system[1]. The literature on distribution system is very much diversified; the brief review is presented on the subject of DG placement and optimal size and location of multiple DGs are found to cater the incremental load on the system[2] and minimization of power loss without violating system constraints.[3]

III. OBJECTIVE OF THE WORK

The Objective of DG placement is either Active Power Loss minimization or minimization of Cost of Electricity. Moreover, Integration of DG with Active Power Loss minimization with Load Growth is not reported. In this work, Optimal Size and Location for DG/s are computed to solve the problems that arise due to load growth on several power system parameters. Main objective is:

1. To minimize Active Power loss considering load growth with different kinds of DG/s.
2. To minimize Cost of Electricity considering Load Growth.

IV. DISTRIBUTION NETWORK CONFIGURATIONS

Distribution networks are divided into two types, radial or network. A radial system is arranged like a tree where each customer has one source of supply. A network system has multiple sources of supply operating in parallel. The secondary network is commonly found in big cities and is the most reliable system. Spot networks are used for concentrated loads. Radial systems are commonly used in rural or suburban areas.

Radial systems usually include emergency connections where the system can be reconfigured in case of problems, such as a fault or required replacement. This can be done by

opening and closing switches. It may be acceptable to close a loop for a short time.

Within these networks there may be a mix of overhead line construction utilizing traditional utility poles and wires and, increasingly, underground construction with cables and indoor or cabinet substations. However, underground distribution is significantly more expensive than overhead construction. In part to reduce this cost, underground power lines are sometimes co-located with other utility lines in what are called common utility ducts.

Distribution feeders emanating from a substation are generally controlled by a circuit breaker which will open when a fault is detected. Automatic circuit reclosures may be installed to further segregate the feeder thus minimizing the impact of faults. Long feeders experience voltage drop requiring capacitors or voltage regulators to be installed.

Characteristics of the supply given to customers are generally mandated by contract between the supplier and customer. Variables of the supply include:

AC or DC - Virtually all public electricity supplies are AC today. Users of large amounts of DC power such as some electric railways, telephone exchanges and industrial processes such as aluminium smelting usually either operate their own or have adjacent dedicated generating equipment, or use rectifiers to derive DC from the public AC supply

Nominal voltage, and tolerance (for example, +/- 5 per cent)
Frequency, commonly 50 or 60 Hz, 16.7 Hz and 25 Hz for some railways and, in a few older industrial and mining locations, 25 Hz.

Phase configuration (single-phase, polyphase including two-phase and three-phase)

Maximum demand (some energy providers measure as the largest mean power delivered within a 15 or 30 minute period during a billing period)

Load factor, expressed as a ratio of average load to peak load over a period of time. Load factor indicates the degree of effective utilization of equipment (and capital investment) of distribution line or system.

V. LOAD GROWTH

Increase in energy demand. Load growth occurs either through natural growth of a service territory resulting from increased prosperity, productivity or population growth, or through stimulation of the energy market. While the latter is usually frowned upon today based on current knowledge of actual energy costs and externalities, it was once a common practice of utility companies to encourage increased energy consumption and reliance. The load on a feeder is increasing due to the addition of new load. A feeder can take additional load on the basis of its capacity or the thermal limit. Feeder capacity is calculated based on current carrying capacity, i.e., thermal constraint or voltage regulation. Once the feeder capacity exceeds, new substation or existing substation through addition of new feeder needs to be created.

I) INTEGRATION of DG WITH THE GRID

Distributed energy resource (DER) systems are small-scale power generation or storage technologies (typically in the range of 1 kW to 10,000 kW) used to provide an alternative to or an enhancement of the traditional electric power system. DER systems typically are characterized by high initial capital costs per kilowatt. DER systems also serve as storage device and are often called Distributed energy storage systems

For reasons of reliability, distributed generation resources would be interconnected to the same transmission grid as central stations. Various technical and economic issues occur in the integration of these resources into a grid. Technical problems arise in the areas of power quality, voltage stability, harmonics, reliability, protection, and control. Behaviour of protective devices on the grid must be examined for all combinations of distributed and central station generation. A large-scale deployment of distributed generation may affect grid-wide functions such as frequency control and allocation of reserves.

II) TYPES OF DISTRIBUTED GENERATORS

Based on the ability of delivering active and reactive powers, DGs are classified as follows:

Type 1: Active power producers like photovoltaic arrays and fuel cells which are connected to the grid by means of inverters. This type can only produce active power.

Type 2: Reactive power producers like synchronous condensers which can only produce reactive power.

Type 3: Active power producers and reactive power consumers. This type of DGs produces active power and absorbs reactive power from the grid.

Type 4: Active and reactive power producers. This type of DG produces reactive power to maintain the voltage of the bus in which they are connected.

III) Load flow analysis: Power flow or load flow studies are performed for the determination of the steady state operating condition of a power system. This is the most frequently carried out study by power utilities and is required to be performed for power flow planning, operation, optimization and control. At the design stage, load flow analysis is used to check whether the voltage profiles are expected to be within limits throughout network. At the operation stage, it is run to explore different arrangement to maintain the required voltage profile and to minimize system losses. The main objective of load flow study is to determine the bus voltage magnitude with its phase angle, real and reactive power flow in different lines and the transmission power losses. Some of the basic power flow algorithms were developed and applied such as Newton Raphson (NR), Gauss Seidel (GS) to the transmission network. These methods may become inefficient for the distribution network because of its special features like radial structure, high R/X ratio, unbalanced load etc. These features make the distribution systems power flow computation different and somewhat difficult to analyse as compared to the transmission systems.

IV) TO CALCULATE POWER LOSS IN TERMS OF LOAD GROWTH

The real power loss at any year k is given by,

$P_{Loss}(k)$:

$$P_{Loss}(k) = P_{Loss}(0) (1 + \text{growth})^{\alpha k}$$

where

g = annual load growth rate

$P_{Loss}(0)$ = real power loss in the base years (0th year)

$P_{Loss}(k)$ = real power loss in the kth year ($k = 1, 2, \dots, M$)

α = constant which is equal to 2.15

VI. RESULTS AND DISCUSSION

Two test system have been used to test and validate the proposed algorithm, the 33-bus Radial Distribution System, 69-bus Radial Distribution System. The 33-bus RDS has the total real power load of 3715 kW and the total reactive power load of 2300 kVAR. The 69-bus RDS has the total real power load of 3801 kW and the total reactive power load of 2694 kVAR. Table 6.1 gives the details about the effect of load growth on 33-bus RDS.

Table 6.1 Effect of load growth on 33-bus RDS

Parameters	0th Year	1st Year	2nd Year	3rd Year
P load (MW)	3.715	3.9936	4.02931	4.6151
Q load (MVAR)	2.3	2.4725	0.276	2.8573
P loss (kW)	0.201	0.236	0.276	0.323
Q loss (kVAR)	0.134	0.157	0.184	0.216
Minimum Voltage (p.u)	0.9134	0.9063	0.8986	0.8901
Maximum Current(A)	363.651	392.6618	424.1698	458.4279

Table 6.2 Effect of placement of Type I DG on load growth- 33 bus RDS

Parameters	0th Year	1st Year	2nd Year	3rd Year	4th Year	5th Year	6th Year	7th Year	8th Year	9th Year
P load (MW)	1.251	1.32	1.42	1.53	1.591	1.7	1.798	2.15	2	2.09
Q load (MVAR)	2.3	2.47	2.66	2.86	3.072	3.3	3.55	3.82	4.1	4.41
P loss (kW)	104.3	121	141	164	190.2	221	257.5	305	349	407
Q loss (kVAR)	74.71	86.8	101	117	136.3	159	184.7	217	251	292
Minimum Voltage (p.u)	0.951	0.95	0.94	0.94	0.934	0.9	0.924	0.91	0.9	0.91
Maximum Current(A)	211.3	227	244	263	281.1	302	324.7	358	373	401
Location	26	26	26	26	26	26	26	26	26	26
Size(MW)	2.5	2.5	2.5	2.5	2.5	2.5	2.5	2.5	2.5	2.5

Table 6.3 Effect of load growth on 69-bus RDS

Parameters	0th Year	1st Year
P load (MW)	3.8019	4.087
Q load (MVAR)	2.6942	2.8962
P loss (kW)	224.3448	263.0797
Q loss (kVAR)	101.9722	119.3784
Minimum Voltage (p.u)	0.9102	0.9028
Maximum Current(A)	387.0268	417.8608

Table 6.4 Effect of placement of Type I DG on load growth- 69 bus RDS

Parameters	0th Year	1st Year	2nd Year	3rd Year	4th Year	5th Year	6th Year
P load (MW)	1.9	2.05	2.176	2.35	2.53	2.71	2.9
Q load (MVAR)	2.6	2.89	3.1134	3.34	3.59	3.86	4.15
P loss (kW)	81.5	94.34	109.218	126.41	146.34	169.4	199.38
Q loss (kVAR)	39.64	45.88	53.0498	61.42	71.09	82.25	96.86
Minimum Voltage (p.u)	0.9694	0.9671	0.9648	0.962	0.9591	0.9561	0.9529
Maximum Current (A)	260.69	280.56	300.12	323.5	347.9	373.44	400.61
Location	61	61	61	61	61	61	61
Size (MW)	1.9	1.9	1.9	1.9	1.9	1.9	1.9

Also it is clear that the analysis is stopped at the end of second year due to the violation in current limit. In third year, the current was 424 A which violated the maximum current carrying capacity i.e., 400A. In order to resist the additional load, an additional feeder or substation must be added to the existing system. Installation of DG extends the life of the existing system.

VII. CONCLUSION

The system parameters of distribution system has been studied by the placement of DG/s. Similar way the performance with capacitor placement considering load growth by undergoing detailed analysis such as checking for the maximum current carrying capacity, studying the active power losses, calculating cost of feeder energy losses and cost of DG for various systems under several cases will also be done. Load flow analysis has been done for 33, 69 bus system.

REFERENCES

- [1] Khyati D. Mistry, Ranjit Roy. "Enhancement of loading capacity of distribution system through distributed generator placement considering techno-economic benefits with load growth". Electrical Power and Energy Systems 54 (2014) 505–515
- [2] D.Das . "Maximum loading and cost of energy loss of radial distribution feeders". Electrical Power and Energy Systems 26 (2004) 307-314
- [3] Gopiya Naik, D.K.Khatod, M.P.Sharma, "Optimal allocation of combined DG capacitor for real power loss minimization in distribution networks". Electrical and energy systems 53; pp.967-973, 2013.
- [4] Rajesh Kumar, R.A. Gupta, Ajay Kumar Bansal, "Economic analysis and power management of a stand-alone wind/photovoltaic hybrid energy system using biogeography based optimization algorithm". Swarm and Evolutionary Computation- Accepted 16 August 2012. Article in Press
- [5] Y. Mohamed Shuaib, M. Surya Kalavathi, C. Christofer Asir Rajan. "Optimal capacitor placement in radial distribution system using Gravitational Search Algorithm". Electrical Power and Energy Systems 64 (2015) 384-397

Faster RCNN based automatic vehicle detection system

^[1]T Ragotham Reddy, ^[2]Taduru Aruna

^[1]Lecturer in Computer Applications, Kakatiya Government College, Warangal, Telangana, India.

^[2]Lecturer in Computer Science and Applications, Pingle Govt. College for Women, Waddepally, Warangal, Telangana, India.

Abstract— The aim of this study is to propose a pre-processed faster Regional convolution neural network (faster RCNN) for on-street vehicle identification. The framework includes a faster RCNN preprocessing pipeline. The preprocessing method is used to improve the Faster RCNN's preparation and detection time. To identify pathways, a preprocessing path identification pipeline based on the Sobel edge administrator and Hough Transform is used. A rectangular area is then eliminated from the gallery's organisation, resulting in a less intriguing location (ROI). When compared to faster RCNN without preprocessing, the suggested approach enhances the preparation time of faster RCNN.

Index Terms: RPN, ROI, Hough Transform, Convolution Neural Network, Sobel edge detection

I. INTRODUCTION

Vehicle identification is critical to a variety of applications, including free wellness and security, surveillance, intelligent traffic lights, and self-driving. Because of the vast differences in look and camera viewpoint, as well as significant occlusions, it's a difficult problem to solve[1]. Weather and lighting conditions exacerbate the problem. Previous research on vehicle location has focused on specific reason structures such hand-created highlights and component and impediment showing [2]. Despite the fact that these suggested methods function admirably, today's top approaches are completely based on deep neural networks. Deep learning methods to object identification have exploded in popularity in recent years. These methods have used larger datasets than ever before, and they consistently provide unique results on datasets with many arrangements or jobs. When compared to other methods for a comparable class, the region convolution neural network (RCNN) has obtained substantial identification results. The RCNN operates by using a CNN network to execute region suggestions generated by proposition methods. The disadvantage of RCNN is that it has a high computational cost since each area is treated separately. By using area suggestions as consideration indicators for a mutual element map, the fast region convolution neural network (quick RCNN) improves on the disadvantage of RCNN. The standard element map eliminates the need to prepare each area separately, lowering the RCNN computation cost. The proposal generation method is a disadvantage for fast RCNN, which is modest in comparison to the CNN network. As a result, it has a detrimental impact on the by and significant speed of fast

RCNN. Faster RCNN works well for general item recognition, but not so well for vehicle detection. Boundary adjustment and algorithmic change may help with this. The algorithmic modification of Faster RCNN is the focus of this work. To enhance preparation and location speed, a preprocessing method is combined with a faster RCNN[3]. The preprocessing method reduces the interest region, resulting in fewer pixels to be measured by the faster RCNN. The Sobel edge discovery and Hough change are used in the preprocessing channel, and the final result is an extricated rectangular area. This speeds up the Faster RCNN's preparation time. Because we're focusing on cars near the conscious vehicle and their behaviour, we're overlooking the next technique of route finding.

II. OVERVIEW OF FASTER R-CNN

In a window-based search, a two-class object classifier was fully conveyed, resulting in verifiable object finding. All windows were trimmed using non-maximal hiding across all feasible scale and perspective dimensions to restore a happy item arrangement. This approach was subsequently enhanced with the use of object proposition computations, which are a kind of pre-channel. Limiting pursuit regions using Branch and Bound and item size cutoff points from alignment information, collecting super-pixels counting Selective Search, and pre-choosing windows based on an objectness standard, for example, are all features of models like Spatial Pyramid Pooling and Edge Boxes[4]. Although pre-separating has increased efficiency by sharing convolutions across suggestions, it remains a significant barrier in runtime discovery computational cost. Quicker R-CNN builds on this concept by combining the highlights of an entirely convolutional network to accomplish both region and item identification. RCNN system that is more responsive. The region proposition network and the item classifier both have layers that are fully convolutional. Together, these layers may be successfully produced. The region proposal network serves as a consideration chief, determining the optimal bounce boxes for object arrangement over a wide variety of sizes and perspective proportions.

A. Vehicle detection

In-depth learning methods, such as CNN, outperform best-in-class object localization approaches, such as RCNN, which has achieved substantial discovery outcomes. The requests highlighted are eliminated using CNN, and each

region is subsequently described using an area vector machine (SVM). RCNN figures 2000 base up suggestions from an information picture. RCNN runs a special search for proposal age, creating a 4096-include vector from each area proposal. The image is then twisted into 227×227 pixels so that highlights may be calculated. Five convolution neural networks and two fully associated layers are then used to deal with the distorted image[5]. The recorded features are subsequently scored using a segment vector machine that has been pre-programmed. Figure 1 shows how the Fast RCNN approach creates a convolutional include map for the whole data image and then organises each item proposition using a component vector extracted from the mutual component map. The handling speed is improved as a result of this. The proposal creation method, which is modest in comparison to the discovery network, is the bottleneck of Fast RCNN[6]. Quicker RCNN solves this problem by providing a Region Proposal Network (RPN) that combines full-picture convolutional highlights with the location network, resulting in region suggestions that are virtually free of charge. RPN serves as a consideration chief, guiding the assembled system on where to search. An RPN is a completely convolutional network that predicts object boundaries and objectness scores at each location at the same time. The RPN is ready to generate substantial region suggestions from start to end, which Fast R-CNN uses for recognition[7].

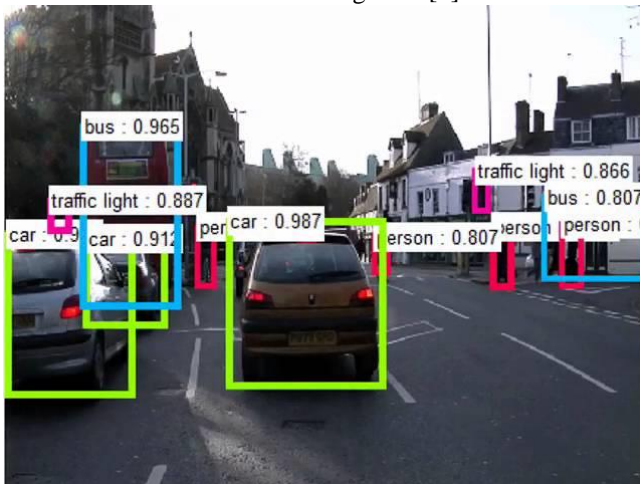


Figure 1: Vehicle detection using CNN

B. Lane detection

The following improvements are included in lane detecting and following:

1. Recognizing lane markers in relation to the personality vehicle when out & about
2. Using such lane markings to identify the direction of the markings on a model.

To identify roadway markers based on pixel changes in an image, edged detection methods are used.

The angle-based edge detection method is often employed, in which an edge is identified if the slope exceeds a certain threshold. The angled edge detection family includes Sobel, Roberts cross administrator, Prewitt administrator, and

Canny edge. The Laplacian put-together edge detection method is based on locating zeros in the second component of an image, which distinguishes areas of rapid power fluctuations as edges. Steerable channels, which swivel to different advantages and then combine those channels of discretionary direction from straight blends of foundation channels for lane following and flexible edges, are also included in lane stamping confinement. This method uses a greyscale or shading image as input and produces a two-dimensional image that represents the division. A limit is established for each pixel in the picture[8]. Hough change is a technique for detecting straight lines in a vision by connecting focuses that are arranged in a logical sequence. It has been used to identify lane markings in the field following edge detection[9]. As a last step, another following-based method, such as bend fitting or a lane position tracker, may be used.

III. EXPERIMENTAL RESULTS

To consider their preparation time, a comparison preparing measure for faster RCNN and the suggested method are used. For planning, the same asset and information calculations are utilised. The preparation is carried done in a faster RCNN pipeline, using the following methodologies:

1. The regional proposal network (RPN) is created initially.
 2. The RPN is then utilised to quickly prepare RCNN.
 3. RPN is retrained and now offers Fast RCNN loading.
 4. The updated RPN is used to retrain the Quick RCNN.
- Preparation is carried out on a single Intel Celeron CPU with 2GB of RAM[10]. The finder's learning rate is 0.000001. For the suggested method and faster RCNN, a piece of comparable data is used.

Table:1 RESULTS in EXISTING METHODS

Method	Iteration	Time elapsed (s)	Mini batch accuracy
Faster RCNN	70	189.13	100%
Proposed	72	92.32	96.8%
Faster RCNN	56	59.34	73.5%
Proposed	52	39.32	72.3

The previous method's effects are compared to those of a faster RCNN and the suggested approach. Table I shows the impacts of preparation time, number of emphases, and tiny clump exactness.

IV. CONCLUSION

A vehicle identification method is proposed that preprocesses an image before it is generated by a faster RCNN, reducing an area of excitement. Preprocessing an image into a reduced rectangular chunk of the initial image increases training time, according to the findings. Because of the rectangular trimmed image that is reliant on lane recognition, the idea is handled

quicker. This is because there are less pixels to measure in the reduced area, resulting in a faster preparation time.

REFERENCES

- [1] R Alugubelli. (2016). Exploratory Study of Artificial Intelligence in Healthcare. *International Journal of Innovations in Engineering Research and Technology*, 3(1), 1–10
- [2] N.Bhaskar, S.Ramana, & M.V.Ramana Murthy. (2017). Security Tool for Mining Sensor Networks. *International Journal of Advanced Research in Science and Engineering*, BVC NS CS 2017, 06(01), 16–19. ISSN Number: 2319-8346
- [3] G. Ollman, „Securing WLAN Technologies: Secure Configuration Advice on Wireless Network Setup“, *Technicalinfo* retrieved 18 April2008.
- [4] N.Bhaskar, S.Ramana, & M.V.Ramana Murthy. (2017). Security Tool for Mining Sensor Networks . *International Journal of Advanced Research in Science and Engineering*, BVC NS CS 2017, 06(01), 16–19. ISSN Number: 2319-8346
- [5] S.Ramana, M.V.Ramana Murthy, & N.Bhaskar. (2017). Ensuring data integrity in cloud storage using ECC technique, *International Journal of Advanced Research in Science and Engineering*, BVC NS CS 2017, 06(01), 170–174. ISSN Number: 2319-8346
- [6] R Alugubelli, (2018) "DATA MINING AND ANALYTICS FRAMEWORK FOR HEALTHCARE", *International Journal of Creative Research Thoughts (IJCRT)*, ISSN:2320-2882, Volume.6, Issue 1, pp.534-546, February 2018, Available at :<http://www.ijcrt.org/papers/IJCRT1134096.pdf>
- [7] Network Protocol Challenges of Internet of Things (IoT) Features-Review, *International Journal of Innovative Research in Science, Engineering and Technology*, Volume 10, Issue 3, March 2021,page 2305-2309.
- [8] I. Ahmad and K. Pothuganti, "Smart Field Monitoring using ToxTrac: A Cyber-PhysicalSystem Approach in Agriculture," 2020 *International Conference on Smart Electronics and Communication (ICOSEC)*, 2020, pp. 723-727.
- [9] sridevi Balne, Anupriya Elumalai, Machine learning and deep learning algorithms used to diagnosis of Alzheimer's: Review, *Materials Today: Proceedings*, 2021, <https://doi.org/10.1016/j.matpr.2021.05.499>.
- [10] Kuo, W., B. Hariharan, and J. Malik, DeepBox: Learning Objectness with Convolutional Networks. *CoRR*, 2015. abs/1505.02146.

Identification of adsorption mechanism for Iron uptake by activated carbon derived from *Alocasia indica*

^[1]Reenarani Wairokpm, ^[2]Potsangbam Albino Kumar, ^[3]Anuj Kumar Purwar
^{[1][2]}Department of Civil Engineering, National Institute of Technology Manipur
^[3]School of Engineering and Technology, IGNOU, Delhi

Abstract— The present study assess the potential of activated carbon derived from *Alocasia indica*, Taro, (ACT) for the removal of Fe(II) from the groundwater of Yaingangpokpi, Imphal East District, Manipur, India. The ground water was observed to be having Fe (II) concentration of 4.34 mg/L which is very much above the permissible limit of 1 mg/L. The adsorbent was activated using phosphoric acid and characterized by scanning electron microscopy (SEM) and energy dispersive X-ray measurements (EDAX). Adsorption kinetics study reveals that the kinetic data were better obeyed the Elovich kinetic model with correlation coefficient (R²) of 0.992 as compared to that of diffusion model with 0.93. Though, activated carbon are predominately physical adsorption due to the presence of large surface area, the study reveals a major chemical based adsorption due to the presence of functional groups in *Alocasia indica* (Taro). Adsorption isotherm studies reveals the adsorption was able to explained by both the non-linear Langmuir and Freundlich isotherm with insignificant error Chi square value of 0.05 and 0.003 respectively. The maximum adsorption capacity obtained was 4.03 mg Fe (II)/g ACT. These results proved that the adsorbent ACT is effective for the removal of Fe (II) from ground water.

Keywords: *Alocasia indica*, Elovich model, Fe(II), intraparticle diffusion.

I. INTRODUCTION

Heavy metal causes enormous threat to environment and public health, being a pollutant in source and treated water. The iron content in groundwater depends on weathering of rocks and minerals and man-made activities [1]. Most iron contamination occurs mainly due to these man-made activities. Iron is important for the human health, especially for proper functioning of body cells. Iron deficiency causes Anaemia and excess consumption leads to cirrhosis of liver, hearth diseases, liver cancer, and infertility etc. [2]. The presence of higher concentrations of iron changes color, taste, odour of water, staining of clothes and utensils and corrosion of water pipes [3]. Fe (II) in the dissolved form is colorless, but on oxidation Fe(II) oxidizes to Fe(III) forming precipitates which is reddish in color causing unpleasant odour in groundwater. According to Bureau of Indian Standard (BIS) as well as World Health Organisation (WHO), the desirable limit for iron content is 0.3 mg/L and the permissible limit is 1 mg/L, whereas, the desirable limit is 0.1mg/L according to Indian Council of Medical Research

(ICMR) [4]. As stated by the Central Groundwater Board, the extent of iron contamination was found maximum in the Northeast. Therefore, it is necessary to remove excess iron in order to procure safe drinking water.

Many treatment techniques were employed by different researchers in the past few decades for iron removal from contaminated groundwater namely, precipitation and filtration, membrane technique, manganese greensand filter, oxidation, ion exchange and biological iron removal [5]. All the mechanism depends on the groundwater quality and the process conditions. And, most of these techniques are either extremely expensive or too ineffective to reduce metal ions from water. Among these techniques, adsorption process is widely used in recent years due to its cost effectiveness, easy operation and ample availability of adsorbents.

This study aims to investigate the removal of Fe (II) ions from groundwater samples using *Alocasia indica*(Taro). It is a tropical plant which is also a traditional food and is widely cultivated throughout the year and is easily available at low cost all over Manipur. The samples for the estimation of iron were collected from the groundwater of Yaingngpokpi area, Imphal East, Manipur. For this study, the non-linear regression form was used to analyse the kinetic and isotherm models.

II. METHODOLOGY

A. Preparation of Adsorbent

Alocasia Indica (Taro) was collected from local market, washed thoroughly with distilled water to remove dirt and other impurities. It is then peeled and dried in an oven at 150⁰ C for 15 hours. Dried Taro were powdered, sieved (Indian Standard Sieve) and treated with phosphoric acid for 24 hrs. The activated carbon was then washed thoroughly and dried in an oven at 100⁰ C till it reached constant density and humidity. The activated carbon derived from Taro (ACT) was then stored in desiccators for further use.

B. Adsorbent characterization

The Scanning Electron Microscope (SEM) and Energy Dispersive X-Ray Analysis (EDAX) were used for the determination of the adsorbent characteristics. The surface morphology of the adsorbent before and after the adsorption process was obtained from SEM (Sigma - 300) operated at 5.00 KV, magnification 300X along with EDAX (Zeiss Gemini). EDAX determines the elemental analysis and composition evaluation of the sample. BET technique was

also used to analyse the surface area, pore volume and pore size of the adsorbent.

C. Batch experiment and Analysis

The batch study determines the capacity of adsorption of Fe (II) on activated Taro and were conducted in Jar-test apparatus (Phipps and Bird Model PB-600). The tests were conducted by mixing certain amount of ACT adsorbent with 500 ml of sample in a beaker and stirred at 300 rpm at room temperature until equilibrium is reached. The effect of pH was found out by varying the pH (2 – 10) and a dose ACT (1 – 8g). The desired pH of the solutions were adjusted using 0.1N NaOH and 0.1N HCl by pH meter (ESICO-1013). Thereafter, the supernatant were separated and absorbance of the solutions were determined for Fe(II) by UV-Visible Spectrophotometer (Thermo Scientific-Evolution 201) at a fixed wavelength of 510 nm. All the chemicals used were of analytical grade without purification. The sample concentrations were determined by calibration curve. The amount of Fe (II) ion adsorbed by adsorbent can be calculated based on the difference of Fe(II) ion concentration in the groundwater sample before and after adsorption according to the following equation:

$$q_t = \frac{C_o - C_t}{m} V \quad (1)$$

where, q_t (mg/g) is the amount of Fe(II) ions adsorbed at time t , C_o and C_t are the concentrations of Fe (II) ions (mg/L) at initial time and at time t respectively, V (L) is the volume of Fe(II) ions sample and m (in gram) is the mass of the adsorbent.

D. Error Analysis

It is extensively used for the minimization and maximization of error distributions based on the convergence criteria of the experimental and predicted values. Also, the error analysis presents the fitting of diffusional and adsorption models. The chi square value is measured by the difference between the experimental and the calculated equilibrium data of the different models used.

$$\chi^2 = \sum_{i=0}^n \frac{(q_e - q_{pred})^2}{q_{pred}} \quad (2)$$

where q_e (mg/g) and q_{pred} (mg/g) are iron adsorbed at equilibrium evaluated from experiment and predicted isotherm models respectively.

III. III. RESULTS AND DISCUSSION

A. Characterization

The ACT adsorbent has the BET surface area of 4.125 m²/g , pore volume of 0.009cm³/g and pore size of 3.311nm. The SEM images of ACT adsorbent before and after adsorption are shown in Fig.1 and Fig.2 respectively. The micrograph of the adsorbent shows fractured and rough surface morphology indicating the presence of good adsorbent sites. The EDAX spectra of the same are also shown in Fig. 3 and 4 respectively. The peak on the EDAX image of ACT after adsorption (Fig. 4) confirms the iron uptake on the surface of the adsorbent.

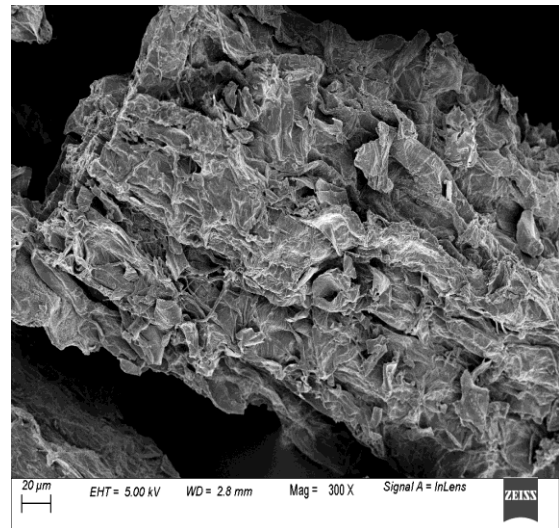


Fig.1: SEM images of ACT before adsorption for the removal of Fe(II) ion.

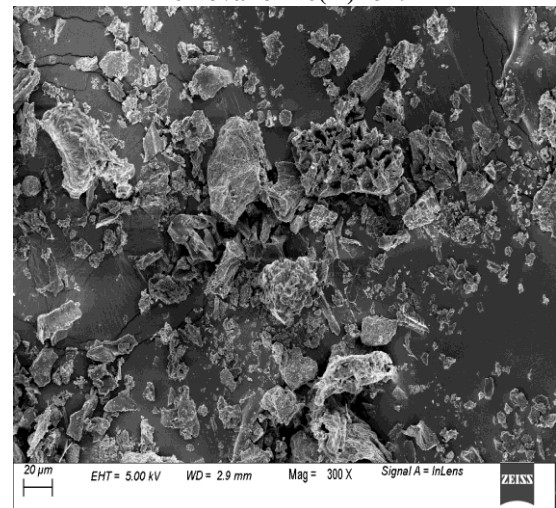


Fig.2: SEM images of ACT after adsorption for the removal of Fe(II) ion.

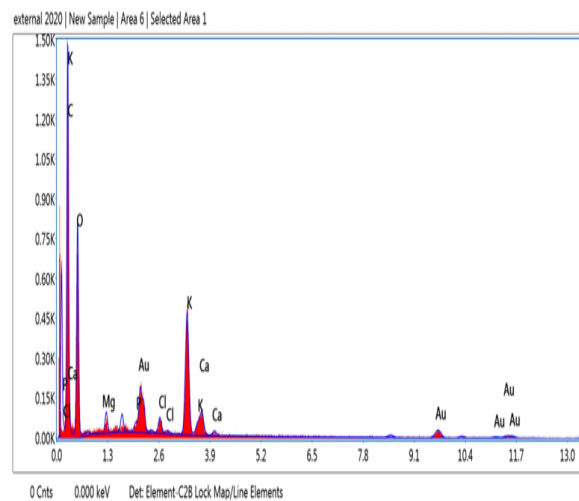


Fig.3: EDAX images of ACT before adsorption for the removal of Fe(II) ion .

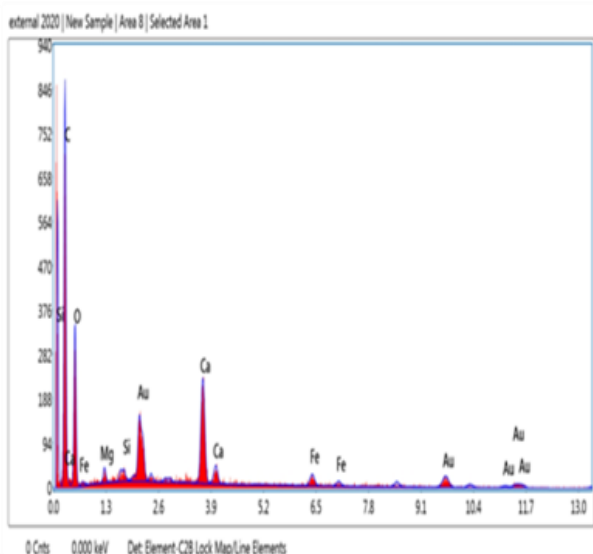


Fig.4: EDAX images of ACT after adsorption for removal of Fe(II) ion .

B. Adsorption kinetics

The adsorption kinetic models generally determines the potential rate of the process and the mechanism of adsorption [6]. The adsorption kinetics of Fe (II) onto ACT evaluates the experimental data which were analysed using non-linear regression kinetic models, Pseudo-1st-order, Pseudo-2nd-order, intraparticle diffusion model and Elovich model. The intra – particle diffusion determines the rate of the reaction. The Elovich kinetic model describes the chemisorption kinetics of adsorption of adsorbates in aqueous phase onto adsorbents. The expressions of the kinetic models are as follows:

$$q_t = q_e (1 - e^{-k_1 t}) \tag{3}$$

$$q_t = \frac{q_e^2 k_2 t}{q_e k_2 t + 1} \tag{4}$$

$$q_t = k_d t^{0.5} \tag{5}$$

$$q_t = \frac{1}{\beta} \ln(1 + \alpha \beta t) \tag{6}$$

where q_t (mg/g) and q_e (mg/g) are the amount of Fe(II) ions adsorbed at time t (min) and at equilibrium time respectively, k_1 (min^{-1}) and k_2 (g/mg min) are the Pseudo-1st-order and Pseudo-2nd-order constants respectively, k_d [$\text{mg}/(\text{g min}^{1/2})$] is the intraparticle diffusion rate constant, α [$\text{mg}/(\text{g min})$] and β (g/mg) are the Elovich rate constant.

Parameters of the kinetic model for adsorption of Fe(II) onto ACT are shown in Table 1. From the table, it is found that Elovich kinetic model has higher value of correlation coefficient ($R^2=0.99$) with lower chi square ($\chi^2= 0.001$) as compared to the other kinetic models.. Thus, it can be concluded that Fe (II) ion adsorption onto ACT obeyed the Elovich kinetic model, suggesting that chemical adsorption is predominant. The plot of intra-particle diffusion model for adsorption of Fe (II) ion on ACT is presented in Fig.5. The experimental values were compared with predicted values for Pseudo-1st-order, Pseudo-2nd-order and Elovich kinetic model as shown in Fig.6.

Table 1. Parameters of Kinetic Model for Fe(II) ions removal.

Kinetic Model	Calculated Parameters	R ²	χ ²
Pseudo-1 st -order	$k_1=0.0133$ $q_e(\text{cal}) =2.461$ mg/g	0.96	0.26
Pseudo-2 nd -order	$k_2=0.0074$ $q_e(\text{cal}) =2.389$ mg/g	0.97	0.15
Intra-particle Diffusion	$k_d=0.1123$	0.93	0.65
Elovich	$\alpha=2.446$ $\beta=3.15$	0.99	0.001

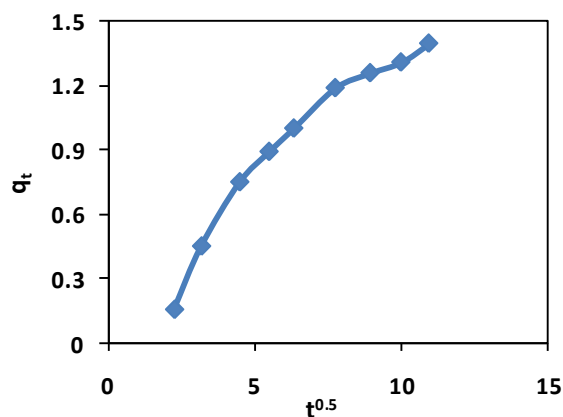


Fig.5: Intraparticle diffusion model for Fe (II) ion adsorption by ACT.

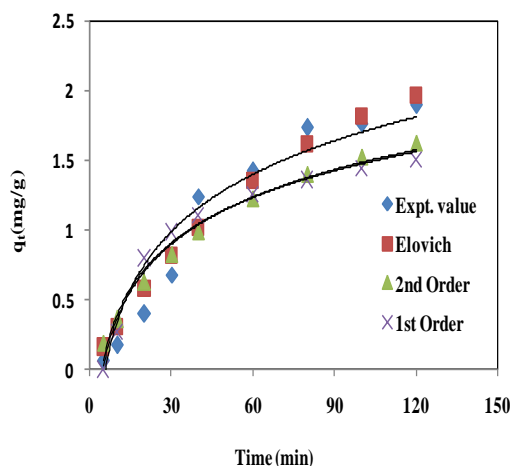


Fig.6: Comparison plot of Experimental and Predicted value of kinetic models for Fe (II) ion removal by ACT.

C. Adsorption Isotherms

In this study, two mostly applied isotherm models, Langmuir and Freundlich isotherms, were used for non-linear regression analysis. Langmuir isotherm assumes the adsorption of both monolayer and homogenous surface, while Freundlich isotherm describes the exponential

adsorption and formation of heterogenous surface and does not assume monolayer adsorption[7]. The non-linear expression of Langmuir isotherm model (Eqn.7) and Freundlich isotherm model (Eqn.8) equations are expressed as follows:

$$q_e = \frac{q_m b C_e}{(1 + b C_e)} \quad (7)$$

$$q_e = K_f C_e^{1/n} \quad (8)$$

where, q_e (mg/g) is the amount of Fe(II) ions adsorbed at equilibrium, q_m (mg /g) is the maximum adsorption required, C_e (mg/L) is the equilibrium concentration of Fe(II), b (L/mg) is enthalpy constant, and K_f and n are Freundlich constants.

Table 2 listed the parameters of the isotherm models along with Chi-square (χ^2) test between the experimental and predicted q_e value to identify the best fit isotherm. Fig.7 shows the comparison plot between Experimental and predicted value for adsorption of Fe(II) ion onto ACT for both Langmuir and Freundlich isotherms. The maximum adsorption capacity was found to be 4.03 mg/g. The experimental data for the removal of Fe (II) ion by ACT fits adequately to both Langmuir and Freundlich isotherm, giving correlation coefficient (R^2) values of 0.97 and 0.96 respectively, thus suggesting the better fit of Fe (II) adsorption onto ACT by both the isotherm models [8].

Table 2 : Non - linearized Isotherm coefficients for the adsorption of Fe(II)ion onto ACT.

Langmuir Isotherm	q_m (mg/g)	b	R^2	χ^2
	4.03	0.97	0.96	0.05
Freundlich Isotherm	K_f	$1/n$	R^2	χ^2
	0.7556	0.3229	0.97	0.003

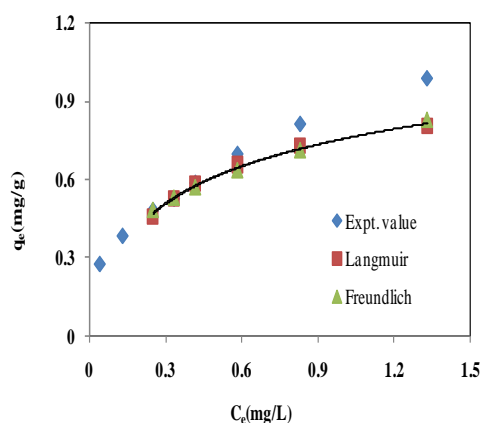


Fig.7: Comparision plot of Experimental and Predicted value of Isotherm models for Fe (II) ion removal by ACT.

IV. CONCLUSION

The experimental data were evaluated with the existing kinetic models and isotherms. The finding reveals that the experimental data agrees well with the Elovich kinetic model

with the correlation coefficient (R^2) of 0.99 and chi square of 0.001 thus ,confirming chemical adsorption behaviour of Fe (II) ion onto ACT. The isotherm data fitted best with both the Langmuir and Freundlich isotherms with R^2 values of 0.96 and 0.97 respectively through the formation of both homogenous and heterogenous surface. The maximum adsorption capacity obtained was 4.03 mg Fe(II)/g ACT.

REFERENCES

- [1] Y. Zevi , S. Dewita , A. Aghasa and D. Dwinandha, "Removal of Iron and Manganese from Natural Groundwater by Continuous Reactor Using Activated and Natural Mordenite Mineral Adsorption," Earth and Environmental Science, vol. 111 pp. 1-6, Dec.2017.
- [2] S. L. Shrestha, "A Comparative Study of Fe (II) Ion Adsorption onto Chemically Activated Banana Peel and Sawdust Bio-adsorbent," International Journal of Applied Sciences and Biotechnology, vol. 6(2), pp.137-141, June. 2018.
- [3] M. Oktrianty, N. R. Palapa, R. Mohadi and A. Lesbani," Effective Removal of Iron (II) from Aqueous Solution by Adsorption using Zn/Cr Layered Double Hydroxides Intercalated with Keggin Ion," Journal of Ecological Engineering, vol.21(5), pp.63-71, July 2020.
- [4] United States Environmental Protection Agency.
- [5] M. Shafiq, A. A. Alazba and M.T. Amin, "Kinetic and Isotherm Studies of Ni²⁺ and Pb²⁺ Adsorption from Synthetic Wastewater Using Eucalyptus camdulensis—Derived Biochar," Sustainability, vol. 13(7), pp.1-16, March 2021.
- [6] A. D. Zand and M.R. Abyaneh , "Adsorption of Lead, manganese, and copper onto biochar in landfill leachate: implication of non-linear regression analysis," Sustainable Environment Research, vol.18, pp. 1-16, Sept. 2020.
- [7] E. E. Jasper, V. O. Ajibola and J. C. Onwuka," Nonlinear regression analysis of the sorption of crystal violet and methylene blue from aqueous solution onto an agro-waste derived activated carbon," Applied Water Science, vol.10, pp.1-11, May 2020.
- [8] T. S. Osmari, R. Gallon, M. Schwaab and E. B. Coutinho," Statistical Analysis Of Linear and Non-Linear Regression for the Estimation of Adsorption Isotherm Parameters," Adsorption Science and Technology, vol. 31(5), pp.433-458, May 2013.

Need for Autonomous System to Revolutionize the Indian Banking Industry – A Study of Blockchain Technology

^[1] Richa Kashyap, ^[2] Vivek Saurav

^[1] Assistant Professor of Law, Kirit P. Mehta School of Law, NMIMS University, Mumbai

^[2] Assistant Professor of Law, Anil Surendra Modi School of Commerce, NMIMS University, Mumbai

Abstract— *Organisational effectiveness and internal governance framework is imperative for the real success of our financial sector. The paper discusses the need for digital transformation through technology driven mechanism for effective governance. Further, the paper highlights the need for robust and transparent technology with less human intervention to mitigate the risk in the internal regulation of the banks. Blockchain Technology has gained a lot of importance globally due to its dependable feature and high level of protection to data. Today, it is conceptually acknowledged that blockchain technology will secure the financial services and improve governance in banking sector. The paper studies the legal application of blockchain technology, regulatory responses and recommend the prospect for implementation of the technology for future governance in the banking sector.*

Keywords: Governance, Reforms, Financial Sector, Blockchain.

I. INTRODUCTION

In the era of digital transformation banks have to depend a lot on technologies to perform day to day operations. Today, banks are connected with the technological networks such as SWIFT for information flow. But with advancement older technologies become obsolete and vulnerable to corruption. Fintech and neo-banks are growing and competing with traditional banks. Banks are often criticized as disorganised, costly, and opaque. Blockchain proposes solution for these criticism as well as provides competitive advantage over the Fintech industry. Thus, blockchain could be the significant catalyst to help banking industry. All around the world many banks have explored the potential of blockchain technology for mitigating internal risks in the banking system, lately central government in India also started exploring the usage of the same but there is no legal regulation for the same in the Indian banking sector. "A Blockchain is an ordered, decentralized, immutable ledger that allows a recording of transactions in a network. The transactions are recorded in a block that is unchangeable and contains all the information of the transaction. Any transaction or information of value can be recorded and shared within the network."

II. BLOCKCHAIN WORKING MECHANISM

The name blockchain comes from the way it works, which is by connecting blocks to form a chain. A hash (digital

signature), the hash of the previous block, and the ledger of all valid transactions are all included in each transaction recorded in a block. The hash binds the blocks together and boosts the previous block's verification. As a result, an unchangeable blockchain is created. To understand how blockchain works, you must first comprehend five concepts: a network of nodes, tokens, a structure, a consensus method, and rules. To begin, each participant (computer) in a network is referred to as a node in the network. The nodes are linked together, and there are checks in place. The transaction's legitimacy. The stronger the network, the higher the nodes' connectivity. Second, tokens, often known as digital currency or cryptocurrencies, offer a form of value ownership. It can be used to trade value and can represent money or any other type of asset. Following that, the blockchain's structure is an ordered succession of transactions. A blockchain is formed by connecting each block.

The consensus method thus functions as a communal decision-making process in which each node in a network contributes to determining the correct ledger version. The nodes prevent transaction manipulation and double payment. 'Proof-of-Work' and 'Proof-of-Stake' are the two types of mechanisms. To add new blocks to the blockchain, the proof-of-work process requires a network of nodes to solve complicated challenges. This is the reason; changing the transactions is impossible since the third party must outperform the entire network. Bitcoin makes advantage of it. Proof-of-stake functions based on token ownership. More blocks can be created by the network with the highest token. Finally, rules are a set of communication protocols between the parties. It is what gives ledger systems their personality. A blockchain is formed by combining all five concepts.



Fig. 1. Illustration of Centralized ledger and Distributed ledger

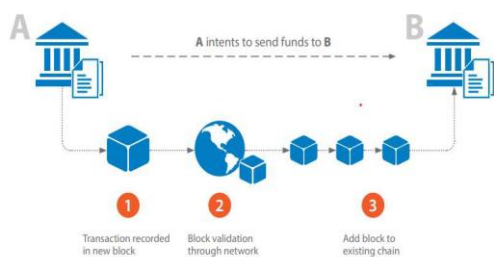


Fig. 2. Illustration of the process of a blockchain

III. NEED FOR BLOCKCHAIN TECHNOLOGY AND ITS USES

Today, banking industry is reliant on the technology and therefore, blockchain could prove to be the game-changer in the industry. In the last decade the technology sector has seen rapid advancement and innovation. It was challenging to disrupt the banking sector due to strong regulation but with advancement of fintech sector the regulation and system requires revamping. Many companies like Apple are providing customer’s virtual wallet which can be used for payment and credits. Facebook has also launched facility of digital currency in the year 2021 to facilitate payment.

Recently, blockchain has earned lot of attention from various financial institutions, banks, private equity firms and start-ups. The big banks such as “J.P Morgan, The Bank of America, Merrill Lynch, HSBC, and many others have already executed a transaction with blockchain and are looking forward to implement the technology in their business model as they believe that the decentralized, and immutability ledger could bring the revolution in the record keeping system”. Blockchain technology promises to transform the backend of banking system and cut operational cost to a great extent. Record keeping and management can be automated and accomplished more quickly than with human labour. Second, it reduces the cost of transactions and operations. Payment and settlement can be completed without the involvement of a third party or the payment of expensive service fees. Cryptography is used in blockchain to offer third-party trust. Finally, because blockchains are distributed, they provide both parties with real-time transaction information, resulting in transparency. The blockchain technology has immense potential in reshaping the whole financial industry. The most prominent contribution of this technology in the Indian banking sector has been analysed below:

I. Cross-Border Payments-

Banks have been playing a key role in cross-border payment since the establishment of monetary transactions. Presently the Indian Banks are using SWIFT (Society for Worldwide Interbank Financial Telecommunications) network to send and receive international payments through secured codes.

Though SWIFT is reliable way for International Payments, it is a lengthy and costly process. The average transfer time is 1-5 business day and the average cost is \$40- \$50 (Transfer-Wise). Additionally, we have witnessed the failure

of the system during the PNB Fraud - Nirav Modi Scam wherein the officials benefited from the glitch in the system. Let’s see how blockchain technology can play an important role here- “Blockchain technology can facilitate banks to make direct international payments economical and efficient. First, banks need to have blockchain networks of their own allowing them to transfer funds directly to another bank’s network. All the trans-actions are recorded in the block and are unchangeable. The ledger will be available to the parties involved and no middleman is required. This way blockchain technology has the potential to reduce the time and cost associated which is required with SWIFT”.

The below diagram helps us in understanding how blockchain technology can solve issues related to global payment and bring ease and transparency for customers.

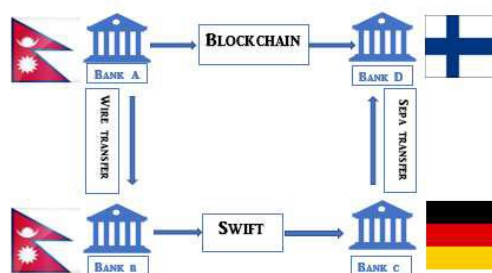


Fig. 3. Illustration of cross-border payment using blockchain technology.

The figure shows the process involved in cross-border payment from Nepal to Finland. For a SWIFT Transaction normally third party and sometimes fourth party is needed, e.g. here Bank B and C depending on banks connection. On the other hand blockchain network connects two parties directly and expedites direct transaction. While SWIFT blockchain can complete the same in few hours.

II. Know Your Customer -

It is the fiduciary duty of the bank to record the details of its customers and also ensure that the verification has been done before allowing any financial transactions. Thus, KYC (Know your customer) is considered to be an important process for banks and blockchain technology can play role in governing the same. It is important to govern KYC and provide a legal framework for it to prevent money-laundering and terrorism financing. Presently, when a customer opens an account with the bank he is required to submit KYC details to each of the bank. With the use of blockchain technology the customer’s data can be stored in a block and then the block can be shared amongst them. It increases the efficiency of operation and removes the repetitive works. As data stored in block is immutable it ensures that right information is used by every bank.

III. Financial Reporting and Compliance -

The banks are mandated by the regulator under various directives of RBI to submit various financial reports like tax reports, audit, and other financial reports on a regular basis. It is pertinent for banks to submit the reports effectively to keep track and control of anti-money laundering activities. Blockchain technology can ease the work for banks as well as the regulator. The technology will help in recording the

transaction and gives an easy track to auditors and regulators. The systematic recording, automatic updation and monitoring increases transparency in the process and help in reducing frauds. Many banks and regulators are testing the ways to implement blockchain.

IV. CURRENT PROGRESS AND DEVELOPMENT IN BANKS

Cross-Border payments and transactions are one of the most used and crucial functions of banks. Ripple created by US based technology company is currently being experimented and used in more than 250 financial institutions across over 40 countries. Bank of America, Barclays PLC, Royal Bank of Canada, J.P Morgan, Mitsubishi UFJ Financial Group etc. have already partnered with ripple for global transactions. Ripple provides banks and financial institutions with its online service called RippleNet, which allows participants to transfer the message. The Ripple functions similar to SWIFT but the payment made through ripple can be settled within minutes as compared to SWIFT which usually takes 1-5 days for settlement. The technology used by Ripple is non-distributed, private blockchain technology using its own Ripple-XRP currency.

Many banks all over the world are testing blockchain technology to maintain KYC and other data of customers. A start up named Bluzelle which was providing database for decentralised application collaborated with 3 banks- HSBC, Mitsubishi and OCB in 2017 to test the platform of KYC. The outcome showed reduction of cost by 25-45% and strict monitoring of fraud. Master-Card is testing blockchain to record, identify, and verify the ownership of transaction. Spring Labs, Cambridge Blockchain, Norbloc and Block-stack are also experimenting KYC platform. The report published by Bank for International Settlements states that more than 40 Central Banks around the world will soon be exploring blockchain technology. The first Central Bank to explore Distributed Ledger Technology in 2014 was Bank of England. Similarly “Bank of Canada, the Monetary Authority of Singapore, Bank of Japan, the Swedish Central Bank, the German Central Bank, and more others joined and are actively testing different blockchain and distributed ledger technology”. The Bank of France started testing from 2016 and now is using blockchain to process the SEPA (single euro payment area) Credit Identifiers (SCIs). With the help of smart contract information sharing becomes faster, automated and easier. One of the first bank which is implementing blockchain technology for payments within the country is the National Bank of Cambodia.

V. CHALLENGES IN IMPLEMENTATION

According to the World Economic Forum blockchain can solve the problem faced by people and bank regarding payments and transactions. But the technology comes with its own challenges and hindrance and without addressing these challenges, the technology cannot be used or implemented.

VI. LEGAL REGULATION -

One of the most important discussion amongst the regulator is how to regulate the blockchain technology. The blockchain is mainly a decentralised system which makes the issue of regulating it more complicated. The author analyses that to regulate internal functioning of the banking sector in India we cannot have a fully decentralised system and there must be an authority to control the financial institutions. This is not impossible at all, the government need to look for ways to control the blockchain and have governance mechanism for the same.

Global Finance Execs' View Of Blockchain Challenges

Q: Which of the following will be the biggest barriers to blockchain adoption in your industry in the next three to five years

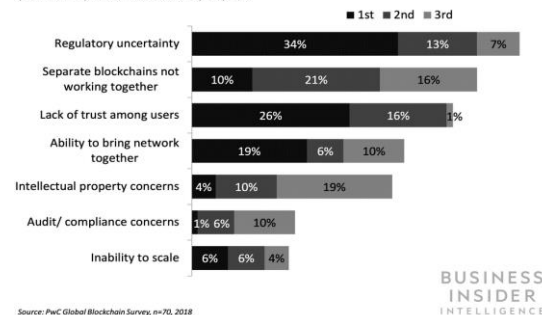


Fig. 4. Global Blockchain Survey

The above figure clearly depicts the major barriers to blockchain adoption and regulatory uncertainty being one of the main reasons. There is no formal law in India that oversees and regulates blockchain technology and its applications. The benefits of implementing blockchain technology in the banking sector are being examined by the Reserve Bank of India discussion paper and expert committee comments.

VII. SMART CONTRACTS AND LEGAL ENFORCEABILITY -

Smart contracts, according to the RBI, are “essentially lines of code or logic using distributed ledger technology that execute automatically whenever preset circumstances are met.” These are digitally encrypted agreements in which the smart contract validates the contents of the agreement and transfers the tokens according to the conditions. Its ability to execute pre-determined orders while conforming to regulatory standards is what makes it smart. Because every step and procedure is documented and approved by all systems at the same time, there are no human errors. As a result, the parties may assess where the agreement is in its life cycle and if it has been properly implemented. Smart contracts, such as franchise agreements, are a lucrative choice for organisations dealing in and sharing sensitive information. The data in smart contracts is encrypted using cryptography, and the distributed ledger system’s functionality ensures data security. In order for smart contracts to be legitimate and enforceable, these must conform to the terms of the Indian Contract Act, 1872 (ICA). Section 10 outlines the characteristics of a legal contract, which must be met by a smart contract in order for it to be considered legal and binding in India. This obligation is in

addition to any sector-specific rules that the government may establish to support smart contracting (such as those that may apply to insurance contracts). While the ICA only covers tangible contracts, the Information Technology Act of 2000's Section 10-A (Validity of Contracts Formed through Electronic Means) covers electronic contracting and execution (IT Act).

VIII. DATA PRIVACY AND CYBER-SECURITY -

The IT Act of 2000 allows for the use of digital signatures to authenticate documents. For authentication and limited access, smart contracts use digital signatures. Though the IT Act does not directly prohibit the use of self-generated digital signatures using blockchain technology, the lack of clear recognition of the same will render any blockchain-based contract needing signature for authentication illegal. It is critical to follow the rules and regulations governing cyber security and data privacy in India in order to ensure that Blockchain technology is used effectively. The impossibility of enforcing the same is hampered by the decentralized system of blockchain.

IX. CONCLUSION

While blockchain technology has a bright future in the realm of technology development, some of the technology's unique properties may make it a grey area for legal enforcement purposes. The difficulties that a decentralised digital system with no territorial boundaries presents may be incalculable. While this may be true in terms of legal enforcement, it must not be overlooked that blockchain technology has introduced a simple, yet powerful system based on anonymous users' trust and cryptography. This makes it ideal for use in a variety of sectors across national borders. Maker's Ripple, R3's Corda, and Hyperledger Fabric are among the leading producers of digital platforms based on their respective versions of blockchain technologies. These are permissioned systems that, in the case of Corda and Hyperledger, limit access to transaction data to the people engaged in the transaction rather than making the data publicly available in a public ledger like Bitcoin. This means that a bank or organization may create their own blockchain and choose which transactions to include in it. The bank can implement blockchain technology to mitigate their internal and operational risk. The code of ethics and governance is dependent on the human conduct and there is always a risk of corruption. On the contrary blockchain technology is based on peer-to-peer secured network and tampering of the blocks are near to impossible which can help in better risk management.

REFERENCES

- [1] Sharma, S., Kothari V., RBI Proposes to Strengthen Governance in Bank, (June 15, 2020) <http://vinodkothari.com/2020/06/rbi-proposes-to-strengthen-governance-in-banks/>
- [2] Attaran, M., Gunasekaran, A. The Evolution of Blockchain. In: Applications of Blockchain Technology in Business. Springer Briefs in Operations Management, p. 13. Springer (2019).
- [3] Gupta, A., Gupta, S., Blockchain Technology: Application in Indian Banking Sector, issue 2 vol. 19, pp. 75-84. Delhi Business Review (2018)
- [4] Thakor, A.V., Fintech and Banking: What do we know?, vol. 41 Journal of Financial Intermediation. Elsevier (2020) <http://www.sciencedirect.com/science/article/pii/S104295731930049X>.
- [5] Fenghua Song, Anjan V. Thakor, Financial System Architecture and the Co- evolution of Banks and Capital Markets, vol. 120, issue 547, pp. 1021-1055. The Economic Journal (2010).
- [6] Chari, A., Jain, L., Kulkarni, N., The Origins of India's NPA Crisis, Working Paper No. 2019-04, Columbia SIPA (2019)
- [7] <https://indianeconomy.columbia.edu/sites/default/files/content/2019-04-Chari%20et%20al-NPA%20Crisis.pdf>
- [8] Guo, Y., Liang, C., Blockchain application and outlook in the banking industry, vol. 2, p. 24. Financial Innovation (2016) <https://doi.org/10.1186/s40854-016-0034-9>.
- [9] Mark, B., Understanding and applying Blockchain technology in banking: Evolution or revolution?, vol. 1, pp. 111-119. Journal of Digital Banking, Henry Stewart Publications (2016)
- [10] Citation Yeoh, P., Regulatory issues in blockchain technology, vol. 25 No. 2, pp. 196-208. Journal of Financial Regulation and Compliance (2017), <https://doi.org/10.1108/JFRC-08-2016-0068>
- [11] Cocco, L., Pinna, A., Marchesi, M., Banking on Blockchain: Costs Savings Thanks to the Blockchain Technology, vol. 9, p. 25. Future Internet (2017), <https://doi.org/10.3390/fi9030025>
- [12] Bhargava, R., Blockchain Technology and Its Application: A Review, vol. 15, pp. 7-15. IUP Journal of Information Technology (2019)
- [13] Mao, D., Wang, F., Wang, Y., Hao, Z., Visual and User-Defined Smart Contract Designing System Based on Automatic Coding, vol. 7, pp. 73131-73143. Access IEEE (2019).

Speed Control of DC Motor by Using Soft Starter

^[1] Mohammad safiullah musalman, ^[2] Ashish Yadav, ^[3] Shovanand Chaudhary, ^[4] Gowtham. G

^{[1][2][3]} Student, EEE Department, RRIT, Bangalore, VTU University

^[4] Guide, Assistant professor, EEE Department, RRIT, Bangalore, VTU University.

Abstract— Different methods of speed control, pulse width modulation, firing angle method, speed control using chopper and speed control using PID method control are discussed in this paper. For soft start. In PWM technique the relationship between duty cycle, output voltage shows that when the pulse width is wider, more average voltage is applied to the motor. Due to this there is stronger magnetic force in the armature windings. The motor rotates at maximum speed. The application of microcontroller provides flexible and smooth control of the duty cycle of the PWM pulse. Also in firing angle scheme there was linear relationship between the speed and the firing angle of the converter thus PWM and firing angle scheme are efficient methods for speed control of DC motor. In our project using microcontroller (Arduino Nano) and power electronic components to reduce the initial voltage such that starting high current is reduced and also we can control the speed of dc motor using PWM technique

Keywords: PID, PWM, Arduino Nano, soft start, duty cycle.

I. INTRODUCTION

Motion plays an important role in industries. The production process of industries varies differently and require different speed profiles. Also, the speed control of DC motor is simpler & less costly compare to other drive. DC machine is highly versatile & flexible machine. They also employ in many cutting applications such as actuators & speed sensors that is DC motors are very versatile for the purpose of speed control. Motors use different types of control in industry. Due to this there is increased machine wear as increasingly fast acceleration causes high torque transients and high peak currents. Soft starters solve this problem through controlling the application of current during acceleration production and deceleration. Armature voltage variable speed control was first used in the early 1930s using a system involving a constant speed ac motor driving a DC generator. DC output of generator was varied using a rheostat to vary the field excitation and resulting dc voltage was used to power the armature circuit of the ac motor. This system was properly known as Ward-Leonard system. This system was used until late 1960s when the Electric Regulator Company introduced a general purpose, static, solid state controller which converted the line ac directly to dc using MOSFET devices. The paper will focus on the speed control of DC motor using soft starter. Pulse width Modulation, firing angle method, PID control, Fuzzy Logic control method of speed control will be discussed.

II. BLOCK DIAGRAM

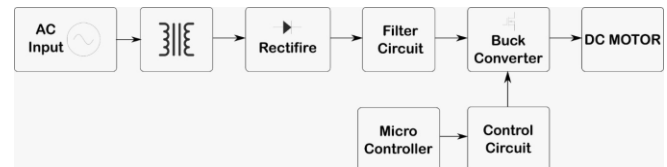


Figure .1: Block diagram

III. PWM

Concept of PWM Pulse width modulation is a simple method of speed control of DC motor by controlling the driving voltage, when the voltage is high speed is high. There are many applications where voltage control would cause a lot of power loss in the system, so PWM method is mostly used in DC motor. In PWM method high frequency is avoided as we know that large motor is highly inductive. We know that on and off time is referred as duty cycle. If we consider an example, Figure 1 shows waveforms for different duty cycles, 75%, 50% and 25%. For 50% waveform 50% duty cycle signal is on and 50% off while a for 25% waveform 25% duty cycle signal is on and 75% off. The result of the PWM is that power is send to the motor and it can adjust from 0% to 100% duty cycle with stable control and high efficiency. When a specific voltage is supplied to the motor, it rotates the motor shaft at some speed. The motor's power can be controlled by varying applied PWM pulses by changing there width and thereby varying the average DC voltage applied to the motors terminals. by changing or adjusting the timing of the pulses speed of the motor can be controlled. The longer time the pulse is "ON", the faster the motor will rotate and whereas, the shorter time pulse is (ON). The slower the motor will rotate.

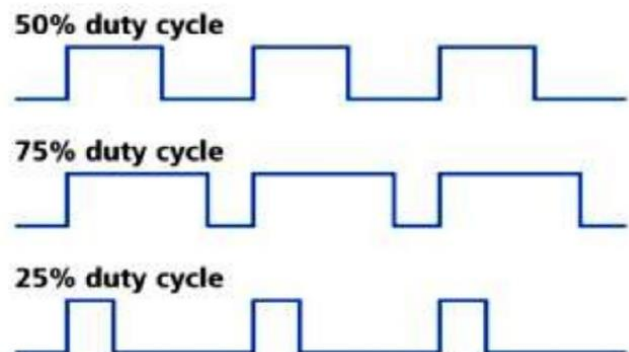


Figure .2: Duty cycle waveforms.

IV. SOFTWARE & HARDWARE EQUIPMENT

Arduino Uno: Arduino is open source microcontroller, board based on the microchip ATmega328P microcontroller. Consist of 8 bit memory, 14 digital I/O pins in which 6 pins are PWM pins 6 Analog pins and is programmable using Arduino IDE with embedded C language, 32KB of flash memory, 2KB SRAM and 1KB EEPROM. The Arduino Nano is a small, complete, and breadboard-friendly board based on the ATmega328. It has the same functionality of the Arduino Duemilanove, but in a different package.

A microcontroller (MCU for microcontroller unit) is a small computer on a single metal-oxidesemiconductor (MOS) integrated circuit chip. In modern terminology, it is similar to, but less sophisticated than, a system on a chip (SoC); a SoC may include a microcontroller as one of its components. A microcontroller contains one or more CPUs (processor cores) along with memory and programmable input/output peripherals. Program memory in the form of ferroelectric RAM, NOR flash or OTP ROM is also often included on chip, as well as a small amount of RAM. Microcontrollers are designed for embedded applications, in contrast to the microprocessors used in personal computers or other general purpose applications consisting of various discrete chips.

A microcontroller is a highly integrated single chip, which consists of on chip CPU (central process unit) RAM (random Access Memory), EPROM /PROM /RON (Erasable Programmable Read only memory),I/O(input/out)-serial and parallel ,timer, interrupt controller.

In this proposed system we are using both discrete component control circuit along with microcontroller to generate the PWM pulses. A toggle switch which helps with selection of automatic and manual control will helps in deciding whether the buck convertor control pulse is through discreet component or through microcontroller



Microcontroller	Atmega328p
Operating Voltage	5v
Input voltage	7-12v
Input voltage(limit)	6-20v
PWM digital i/o pins	6
Clock speed	16MHZ
Flash memory	32kb(Atmega328p)
DC current for 3.3v pin	50 milli amps

V.CONCLUSION

Different methods of speed control, pulse width modulation, firing angle method, speed control using chopper and speed control using PID control are discussed in this paper. In PWM technique the relationship between duty cycle and output voltage shows that when the pulse width is wider more average voltage is applied to the motor. Due to this there is stronger magnetic force in the armature windings. The motor rotates at maximum speed. The application of microcontroller provides flexible and smooth control of duty cycle of the PWM pulse. Also, in Firing Angle Scheme there was linear relationship between the speed and the firing angle of the converter. Thus, PWM and Firing Angle Scheme are efficient methods for speed control of DC motor.

REFERENCES

- [1] [1] Jeetender Singh Chauhan, Sunil Semwal, International Journal of Engineering Research and Applications (IJERA), Vol. 3, Issue 1, January- February 2013, ISSN: 2248-9622.
- [2] [2] Cosmas TatendaKatsambe, VinukumarLuckose and NurulShahrizanShahabuddin, Effect of pulse width modulation on motor speed, International Journal of Students' research In technology & Management, Vol 5, No 2, June 2017, pp42-45, ISSN 2321-2543.
- [3] [3] Arvind, S.K., Arun, T.A., Madhukar, T.S., and Deka, J., Speed control of DC motor using PIC16F877A microcontroller, Multidisciplinary Journal of Research In Engineering and Technology, 1(2), 223-234.
- [4] [4] Bakibillah, A.S.M., Rehman, N. and Zaman, U.A., Microcontroller based closed loop speed control of DC motor using PWM technique, International Journal of Computer Applications, 3(1), 778-783.
- [5] [5] SaritaShastri, Pawan Pandey, A Comparative analysis of firing Angle based speed control, International Journal of Reasearch and Applications, Vol. 3, Issue 4, Jul-Aug 2013, pp.232-235, ISSN 2248-9622.
- [6] [6] M. Rehman, M.A. Chaudhary, Tafayel Ahmed Zulfikar, An AT89C51 microcontroller based control circuit for dual three phase controlled rectifier, Third International Conference on Electrical and Computer Engineering, pp 347-350 IEEE 2008.

An Efficient VLSI Implementation of CDF 5/3 Architecture on FPGA for Image Processing Applications

[¹] Saleema, [²] Dr N.V. Uma Reddy

[¹] M Tech Student, AMC Engineering College, Bangalore

[²] HOD of ECE, AMC Engineering College, Bangalore

Abstract— The wavelet transform has emerged as a innovative technology, in the field of image compression. There are different kinds of wavelets exists. In that wavelet transforms most of the wavelets are lossy in nature. Only CDF-5/3 wavelet is lossless in nature. The proposed architecture uses lifting based scheme of wavelet and it is lossless in nature. Number of multipliers are reduced by using add and shift operation due to this the proposed architecture complexity reduced. To keep up with low region and high recurrence we use multiplier-less engineering for CDF-5/3 DWT for our execution. The VHDL code for multiplier-less construction is taken care of to framework generator instrument utilizing standard strategy and union the design to get the region and recurrence. The spartan6LX45 board tool will used to work on this project, it has the operating speed of 70MHZ on board, and it also has soft processor Micro Blaze. The tools like Xilinx ISE 14.5 and MATLAB 2012a are used with system generator.

Keywords: Discrete Wavelet Transform (DWT), Lifting Schemes, CDF- Cohen–Daubechies–Feauveau wavelets, 1D-DWT, 2D-DWT.

I. INTRODUCTION

The discrete wavelet transform (DWT) has become one among the foremost used technologies for signal analysis and image processing applications. The discrete wavelet transform performs a multi-resolution signal analysis which has adjustable locality in both time domain and frequency domains [1]. Due to its well time and frequency characteristics, one of the most significant uses for DWT has been for image compression as within the (JPEG 2000). The available DWT architecture can be divided into two schemes, and them named as convolution scheme and lifting scheme. The convolution scheme is normally used to implement DWT filters. But convolution scheme uses the huge number of multipliers which is very difficult to implement, and it will take a large amount of resources in hardware. To eliminate those problems lifting schemes is used. Lifting scheme uses the basic convolution equations in such a way that the number of multipliers is drastically reduced. Because of this reason lifting scheme is widely used to build a chip than convolution scheme.

II. METHODOLOGY

1 DWT

In this paper we use a lifting scheme to produce D-DWT architecture. The lifting scheme consists of three phases named as split, predict and update. Initially the color image is converted into gray image. The image is 2-dimensional, initially it will be converted in to 1-dimensional data values. This original 1-d signal are splitting in to odd and even signals, and then these signals are predicted as low pass and high pass signals.

The lifting scheme equation for LPF coefficients

$$Y[2n] = x[2n] + [y[2n-1] + y[2n+1]] \quad \dots (1)$$

$$YLPF(n) = \{ -x[n] + (\ll 1)x[n-1] + ((\ll 2) + (\ll 1))x[n-2] + (\ll 1)x[n3] - x[n-4] \} \quad \dots (2)$$

For HPF coefficients

$$Y[2n+1] = x[2n+1] - \left[\frac{x[2n] + x[2n+2]}{2} \right] \quad \dots (3)$$

$$YHPF(n) = \{ -x[n-1] + (\ll 1)x[n-2] - x[n3] \} \quad \dots (4)$$

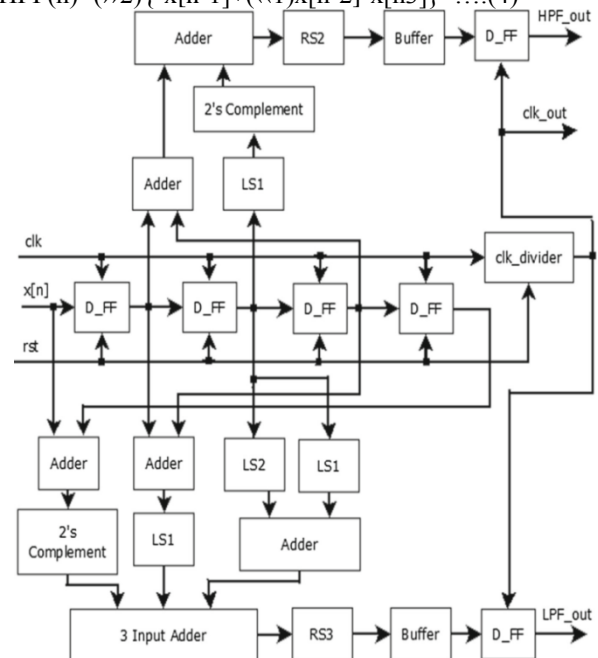


Fig 2: 1D-DWT block diagram

The basic block diagram of proposed 1D-DWT is shown in Fig. 1. The 1D-DWT block is built by six shifters, six adders, 2's complement blocks, one FIFO and one clock divider. The clock divider mainly used to make decimation block. The

latency of 1D-DWT block is 4-clock cycle. To indicate that the device is ready there is an extra signal *rst_out* is taken as output port. Here we use one counter which counts up to four and when it reaches four then it maintain constant four values. When this counter reaches four then *rst_out* signal will be high which indicate next block is that 1D-DWT block is ready to give output.

2D-DWT

➤ **MEMORY UNIT**

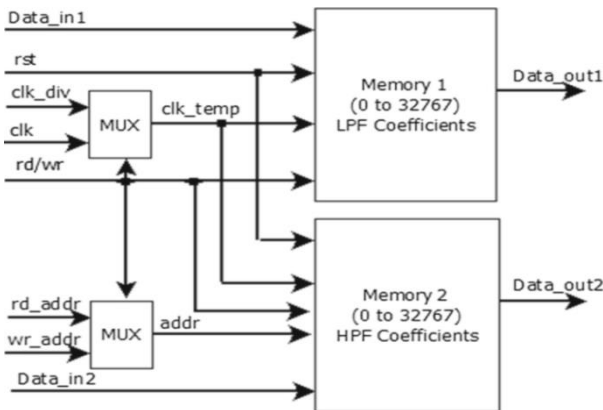
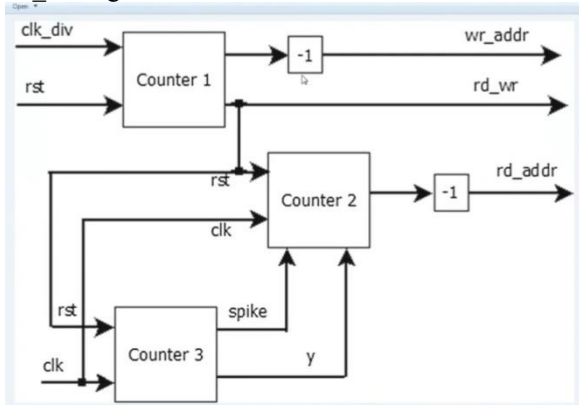


Fig.2. Memory unit

The above figure shows the memory unit. The memory unit is required to store the image pixels read from the 1D-DWT output. There are two memory blocks named as memory 1 and memory 2. The memory-1 has *data_out1* as output port contains LPF coefficients. The memory-2 has output port named as *data_out2* contains HPF coefficients. The output of the memory unit is fed to controller unit to get transpose of 1D-DWT.

➤ **CONTROLLER UNIT**

The controller unit consists of three counters. To generate the address we need the three inter related counters which is shown in fig.4. Counter-1 use *clk_div* signal as clock and it count upto 32767. When it reaches 32768 then the *wr_address* remains at 32768. Counter-2 uses main 'clk' signal and its *rst* terminal of this block is connected to *rd_wrt* of the counter-1. Counter-3 uses main 'clk' signal and it uses 'rd_wrt' signal as 'rst'.



This module is consists of three 1D-DWT and one *dwt_memory* block, controller, mux and demux blocks.

Initially all signals are '0'. The mux and demux are designed in such a way that when select line is '0' then it select 0 terminal. So, when *rst*='1' then 1st 1D-DWT block is active and it starts processing image data serially. The DWT0 (1D-DWT block) provides one level compression for input image which means it convert 256x256 image into either 128x256 or 256x128 image based on the input reading method of image data. This compressed image pixel data is stored in the *dwt_memory*. This stored image pixel data will be taken as transpose for further process. This transposed image pixels is given to DWT1 and DWT2 block to produce LL, LH, HL and HH bands.

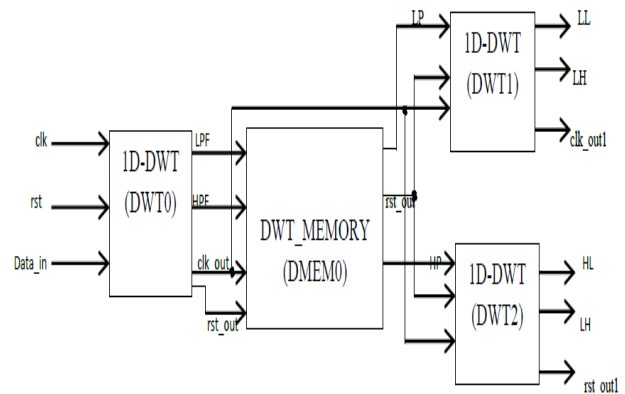


Fig. 3: Proposed 2D-DWT Architecture

III. SIMULATION OUTPUTS

The fig 4 Shows the RTL schematic of the 1D-DWT and fig.5 shows an output waveform of 1D-DWT.

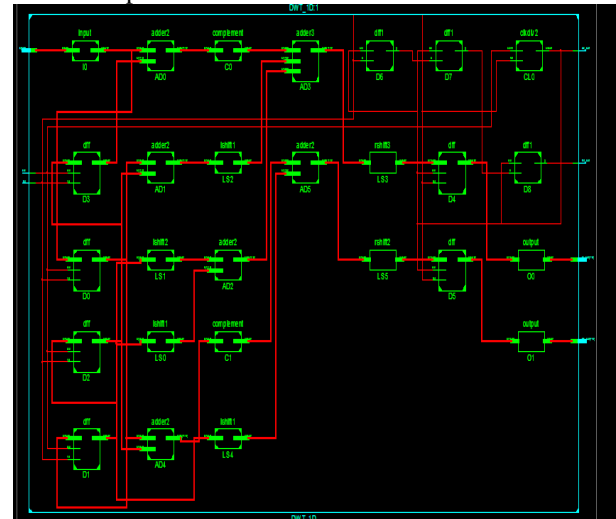


Fig 4. 1D-DWT schematic

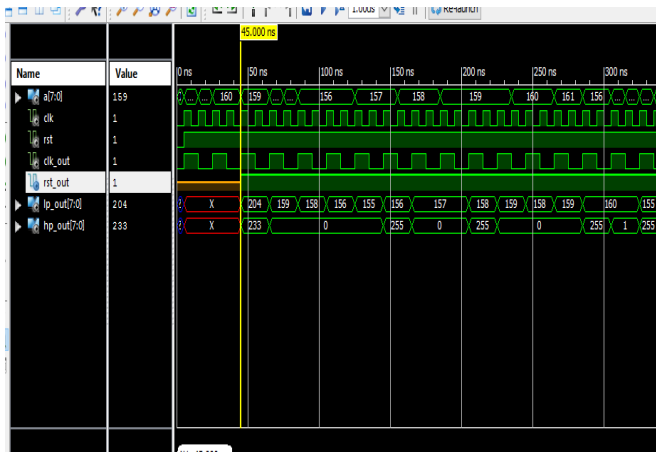


Fig 5. 1D-DWT Output Waveform

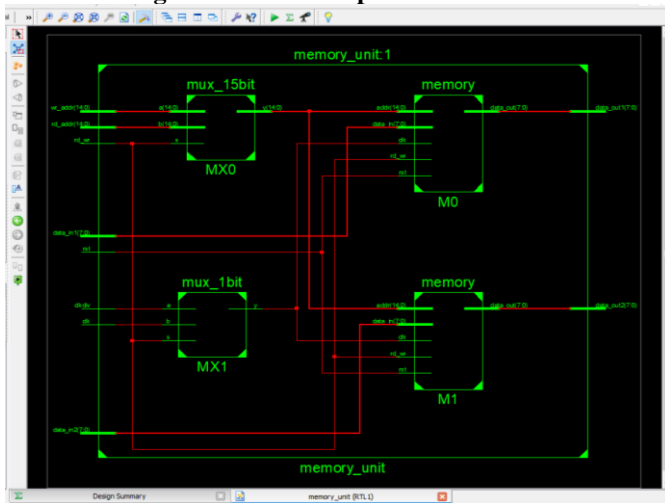


Fig 6. Schematic of Memory Unit

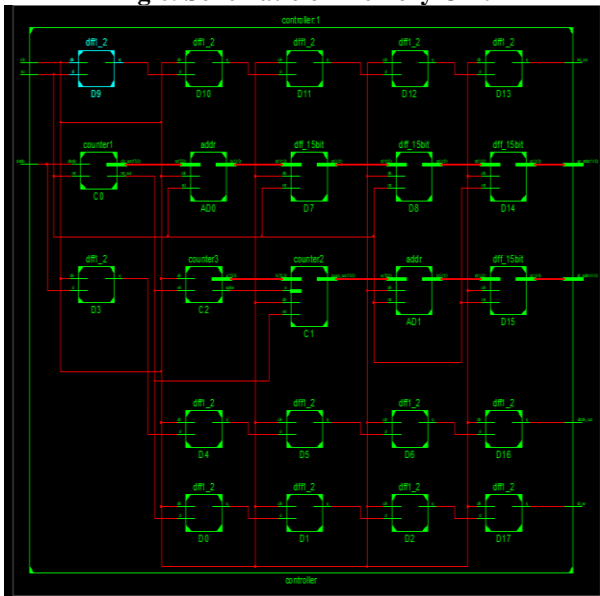


Fig 7. Schematic of controller unit

IV. SYSTEM GENERATOR OUTPUT

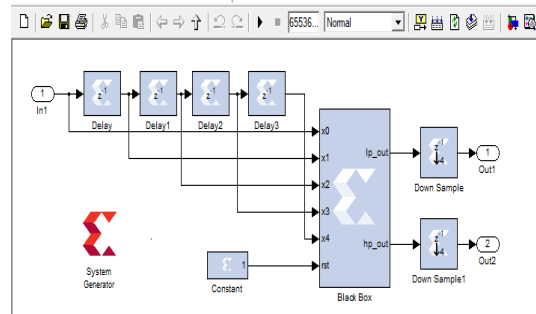


Fig 8. System generator implementation of 1D-DWT

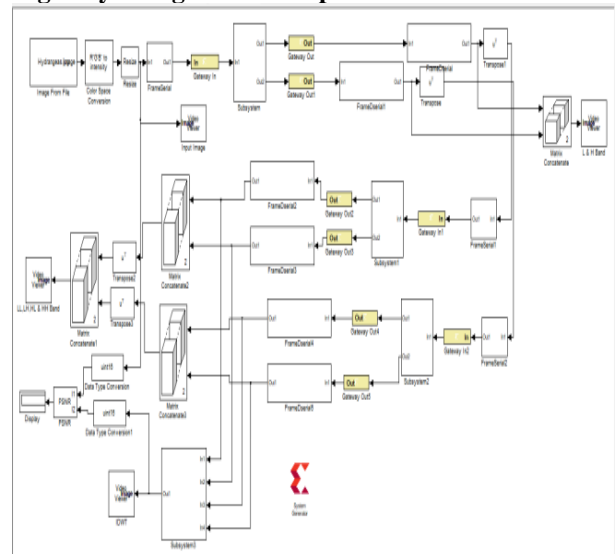


Fig 9. System-Generator Implementation of 2D-DWT

1D-DWT:

The output image of 1D-DWT which has a size of 128x256 of two bands (L and H).



Fig. 10: Output of 1D-DWT Block

2D-DWT:

The output image of 2D-DWT is shown in below fig. 11 which has a size of 128x128 of four bands (LL, LH, HL and HH).



Fig. 10: Output of 2D-DWT Block

V.CONCLUSION

In this paper, we propose FPGA execution of multiplier-less CDF-5/3 wavelet change for picture preparing application utilizing System-Generator tool. To keep up with low region and high recurrence we use multiplier-less engineering for CDF-5/3 DWT for our execution. The VHDL code for multiplier-less construction is taken care of to framework generator instrument utilizing standard strategy and union the design to get the region and recurrence. Number of multipliers are reduced by using add and shift operation due to this the proposed architecture complexity reduced.

REFERENCES

- [1] S. Mallat, "A Theory for Multiresolution Signal Decomposition: The Wavelet Representation", IEEE Transaction on Pattern Analysis and Machine Intelligence, Vol. 11, No. 7, pp. 674-693, 1989.6.
- [2] Durgasowjanya, K.N.H. Srinivas and P. VenkataGanapathi, "FPGA Implementation of efficient VLSI Architecture for fixed point 1-D DWT using Lifting Scheme", International Journal of VLSI Design and Communication Systems, Vol. 3, No. 4, 2012.
- [3] Nagabushanam M and Ramachandran S., "Fast implementation of Lifting Based 1D/2D/3D DWT-IDWT Architecture for Image Compression", International journal of computer Applications, Vol. 12, Issue. 11, pp. 23-29, 2012.
- [4] K. Andra, C. Chakrabarti and T. Acharya, "A VLSI Architecture for Lifting-Based Forward and Inverse Wavelet Transform," IEEE Transaction on Signal Processing, Vol.50, No. 4, pp. 966-977, 2002.
- [5] Husain K. Bhaladar, V.K. Bairagi and R.B. Kakkeri, "Hardware Design of 2-D High Speed DWT by Using Multiplierless 5/3 Wavelet Filters", International Journal of Computer Applications, Vol. 59, No. 17, pp. 42-46, 2012.
- [6] Sowmya KB, SavitaSonali and M Nagabushanam, "Optimized DA Based DWT-IDWT for Image Compression", International Journal of Electrical and Electronics Engineering, Vol. 1, Issue. 1, 2013.
- [7] Naseer M. Basheer, Mustafa Mushtak Mohammed, "Design and FPGA Implementation of a Lifting Scheme of 2D-DWT Architecture", International Journal of Recent Technology and Engineering, Vol. 2, Issue. 1, pp. 34-38, 2013.

IoT Based Flood Management and Alerting System

^[1]Sandeep Pandey, ^[2]Ramachandra C, ^[3]Deepti Thapa

^[1] Student, EEE Department, RRIT, Bangalore 2, India

^[2] Asst. Professor, EEE Department, RRIT, Bangalore, India

^[3] Student, EEE Department, RRIT, Bangalore 1, India

Abstract— Flooding is one of the major disasters occurring in various parts of the world. In any water system, when there is an increased quantity of water, it causes flooding, like a river or lake overflowing. Flooding is a natural disaster that occurs in many countries. Many occasions are responsible for flooding such as heavy rainfall or dam fractures. In case of flooding or dam fractures, it rapidly releases a huge quantity of water and floods the riverbanks and surrounding areas. It causes loss of life and property also. Flood monitoring and alerting systems are helpful for monitoring and to reduce the losses faced by the society. This paper gives an overall survey on the various flood monitoring and alerting systems in the different flood prone areas around the world.

Keywords: Raspberry PI, Ultrasonic sensor, IoT, GSM (Global system for Mobile communication), WLAN.

I. INTRODUCTION

Flood monitoring is a particularly challenging application for Internet of Things (IoT). In fact, it offers a complex scenario for the variety and number of sensors involved, their location and relative communication problems. The type of sensors involved in the process and the corresponding type of installation depend on the kind of collected data and on their geo-localization (i.e., urban areas, where powering and communication are relatively simple, or in remote and difficult to access mountainous or country locations). The kind of data collected ranges from rain monitoring to river gauging with several parameters to be monitored and compared. In the case of rivers, the problem depends on their size and dimension and geography of the region where they flow, if they are small creeks or wide rivers, if they flow in a steep or fiat area, in open air or are channeled underground, etc.

From this point of view, we already activated different collaborations and definitions of common goals with public administrations involved in the management of the experimental areas. To this aim, we designed a general hardware and software IoT infrastructure and architecture applicable to the environmental problem mentioned above, but extensible to the more general problem of monitoring the environment in densely inhabited areas.

II. RESEARCH METHODOLOGY

Our research will be an element of great importance to train specific risk management and to deliver elements of innovation and encouragement for the definition of land management strategies both on the local and regional scale.

Moreover, this research will help to provide knowledge and tools for effective decision making and public engagement. In particular, we detail the sensor classes (their design for the new ones), their communication mechanisms and associated software services as components of a general IoT infrastructure. The aim is to monitor either rainfalls, river discharge or their temporal correlation in order to obtain early alarming information. In our IoT approach, all collected data will be continuously transmitted, through the Internet communication infrastructure, to software components designed to compute the stream-flow and to quantify the spatial distribution of flood risk for each controlled watershed. The computed risks, together with data coming from other sources (barometric and river discharge sensors, cameras operators of public organizations, emergency agencies, private citizens), will be examined by a diagnostic decision system implementing a risk-alert scheduling strategy, able to diagnose the health state of the controlled environment and to define specialized alarm levels for each potentially interested area. Finally, the computed risks will be used for specializing alerting messages, to be sent to all citizens (ubiquity) present in each selected area only (alerting locality).

III. LITERATURE SURVEY

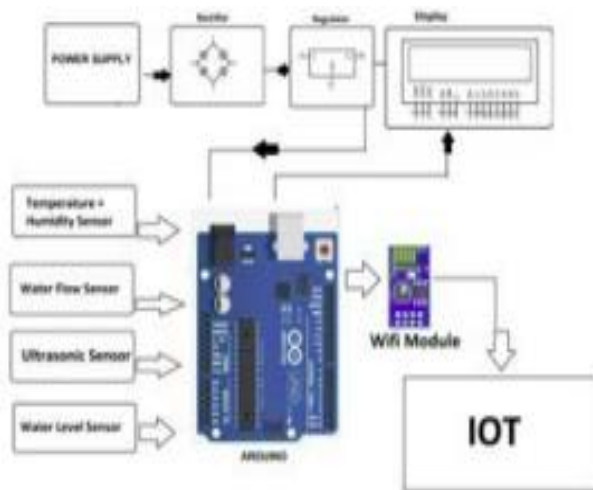
1. To decrease the challenges that the cities face such as scarcity of energy sources, flooding prevention, healthcare, housing water and deteriorating infrastructure, making a city 'Smart' is emerging. The Internet of Things or IOT provides the ability for human and machines to interact from billions of things that include sensors, services, or other Internet connected things. This paper aims to realize the security requirement and security architecture of Internet of things technology for urban flooding prevention management system and discussed the demand and overall design of urban flooding prevention management system. Finally, the application process of the Internet of things technology in Chongqing flooding prevention management system is summarized. For emergency command and dispatch there is visual management, and at the same time, network assessment management for the drainage pipe can be conducted correctly. The flood control and drainage function of Chongqing will gradually improve with smooth drainage facilities also the inspection and maintenance management will be standardized.

2. Floods, extreme weather events, have occurred with frequent regularity over last two decades causing severe urban flood related inundations. India is primarily an

agricultural country and rural infrastructure was adequate to sustain country population. Expansion of urban sector increased due to migration of population towards mega cities. Such migrations are due to industrial growth. Every year floods affect nearly 400 million hectares of land in India. Now a day's weather information is used for monitoring and warning on urban flooding. The citizens get notification when of people check, people on vehicles check or camera check, which has the defects of poor continuity, little data, slow speed, and time lag. The people living in apartment do not get waterlog information exactly and quickly and thus they are not able to take corresponding measures and unemployment and other reasons. The population count is increasing day by day and due to that cities are facing many new challenges. Flooding condition is one of the big challenges increased due to uncontrolled growth of mega cities.

IV. PROPOSED MODEL

1. SYSTEM OVERVIEW



We have introduced an engineering that give early warnings to the citizens and to the government agencies. With the help of the android application, real time data will be available to the individuals instead of depending on the government for analyzing the situation.

With the help of the proposed hardware module, alert will be provided when values reach a pre-defined threshold depending on the region. The idea is to develop a device which is going to save economy, society, lives and their habitat. Using various gadgets and sensors will increase the precision. Keeping that factor in mind, we are developing a device which a user needs to install in the smartphone, rest all the analysis work is done by the system and alert is provided in the form of notifications.

2. EQUIPMENT REQUIRED

2.1 Hardware requirements:

In this project, some hardware devices are used such as power supply, ultrasonic sensors, temperature and humidity sensors and electronic platform Arduino. The hardware is connected with Wi-Fi module which enable the system to connect and share the information through internet.

A. Raspberry Pi - The Raspberry Pi 3 Model B+ is the latest product in the Raspberry Pi 3 range, boasting a 64-bit quad core processor running at 1.4GHz, dual-band 2.4GHz and 5GHz wireless LAN, Bluetooth 4.2/BLE, faster Ethernet, and PoE capability via a separate PoE HAT. The dual-band wireless LAN comes with modular compliance certification, allowing the board to be designed into end products with significantly reduced wireless LAN compliance testing, improving both cost and time to market.



Fig 2. Raspberry PI model B+

B. Water level measurement sensor- For water level measurement, we have used ultrasonic sensors. This sensor will work on sound navigation and ranging. It will work by transmitting the wave of short and high frequencies and echo will get reverted back, depending on these the level will be measured. The distance between sensor and water level will be calculated as –

$$\text{Distance } L = \frac{1}{2} \times T \times C$$

Where L=Distance

C=Sonic speed

T=Time between transmission and reception



Fig 3. Ultrasonic sensor

2.2 Software requirements:

- a) **Open Weather API**- This is the simplest, fast as well as free to fetch the real time data like weather forecasts, clouds, winds, maps with precipitations.
- b) **XML**- Layout xml files are used to define the user interfaces of the application and holds all the tools that user wants to use.
- c) **C-compiler**

V.METHODOLOGY

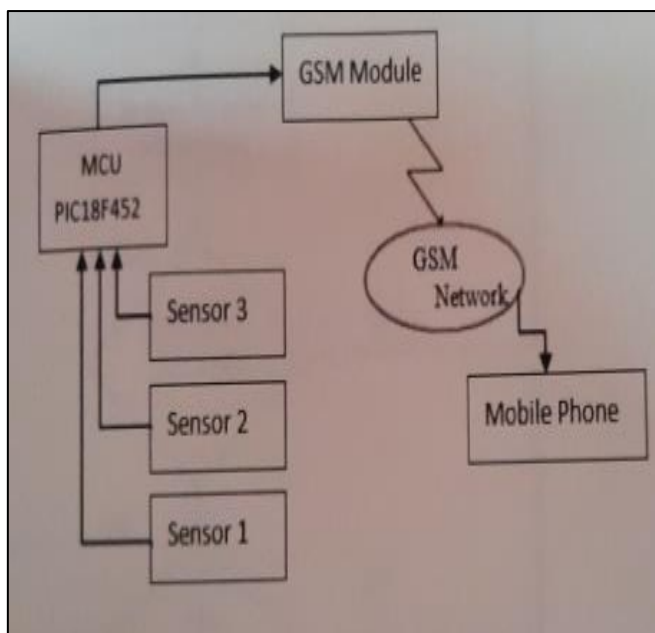


Figure.1.1: Working Module.

System structure is illustrated in Fig. 1.1 System composed of three sensors, one microprocessor based Raspberry model, a GSM module, and a mobile phone. Sensors used are retro reflective, NPN type. It uses system of blocking interruption where the system will give 5V signal to the amplifier. Liquid sensors been used for this project due to its unique ability of detection for liquid substance. MPU used is PIC18F452 from Microchip. Raspberry model was chosen because it is C

compiler optimized architecture. Since this project runs on C compiler program, it's the best option to use this MPU.

Other special features include 32K byte flash memory that could be used to write high capacity of programming language. GSM Module is a device used to transmit SMS signal to the intended user. By using GSM module, GSM network can be used since it is much more accountable during flood season.

VI. SCOPE OF FUTURE WORK

The future work in this project will be a deeper testing phase of the network of low-cost sensors both in simulated and real-life scenarios, and an implementation of the software behaviour in Things speak or other platforms. According to definitions of IoT, if we consider a sensor as an element of IoT which enables to communicate its current status and be published on Internet, then our proposal is very close to what we are intending to achieve within the concept of Internet of things. Nevertheless, the real intent of the proposal is to achieve a flood early warning system.

VII. CONCLUSION

Flash flood alarming systems require a dense network of rain gauges for monitoring intense local rainstorms both to ensure its survival in case of extreme weather and to have a more accurate collection of data. Those data have to be interpreted by means of empirical and formal models by correlating in real time the river level and the flow intensity for early flood forecasting and consequent anticipated alarming. The number of required sensors, their communication mechanisms and reliability requirements show that a IoT/M2M approach is able to resolve the problem, even if today commercially available gauges are not designed with the specific objective of flash floods control.

REFERENCES

- [1] D. Giusto, A. Iera, G. Morabito, and L. Atzori, The Internet of Things. Springer-Verlag, 2010.
- [2] L. Atzori, A. Iera, and G. Morabito, "The internet of things: A survey," Computer Networks, vol. 54, no. 15, pp. 2787 – 2805, 2010.
- [3] D. Miorandi, S. Sicari, F. D. Pellegrini, and I. Chlamtac, "Internet of things: Vision, applications and research challenges," Ad Hoc Networks, vol. 10, no. 7, pp. 1497 - 1516, 2012.
- [4] J. Gubbi, R. Buyya, S. Marusic, and M. Palaniswami, "Internet of things (iot): A vision, architectural elements, and future directions," Future Generation Computer Systems, vol. 29, no. 7, pp. 1645 – 1660, 2013.
- [5] W. Kang and Y. Shibata, "Performance Evaluation of Disaster Information System Based on P2P network," in Advanced Information Networking and Applications Workshops (WAINA)
- [6] J. Kim, D. Kim, S. Jung, M. Lee, K. Kim, C. Lee, J. Nah, S. Lee, J. Kim, W. Choi, and S. Yoo, "Implementation and Performance Evaluation of Mobile Ad Hoc network for

- Emergency Telemedicine System in Disaster Areas,” in Engineering in Medicine and Biology Society, 2009. EMBC 2009. Annual International Conference of the IEEE, 3-6 2009, pp. 1663 - 1666.
- [7] S. Saha and M. Matsumoto, “A Framework for Data Collection and Wireless Sensor Network Protocol for Disaster Management,” in Proceedings of the Second International Conference on Communication System software and Middleware (COMSWARE 2007) Bangalore, India. IEEE, January 2007, pp. 7-12.
- [8] Y. Shibata, Y. Sato, N. Ogasawara, and G. Chiba, “A Disaster Information System by Ballooned Wireless Adhoc Network,” Complex, Intelligent and Software Intensive Systems, International Conference, vol. O, pp. 299–304, 2009.

Traffic Congestion Studies and Solutions for Kengeri- Hoysala Junction, Bengaluru

^[1]G Sankara, ^[2]Rishikesh Badguja, ^[3]Komal

^[1] Professor, R.R. Institute of Technology, Visvesvaraya Technological University, Bengaluru, India

^{[2][3]} U.G. Student, R.R. Institute of Technology, Visvesvaraya Technological University, Bengaluru, India

Abstract— Bengaluru occupied top place in the list of top most traffic-congested cities in India and the world in 2019. Kengeri is a prime location situated in south-west Bengaluru and surrounded by several public offices, educational institutions, commercial zones, stone crushing mills, hospitals and IT hubs. Bengaluru's upcoming and well settled IT hub 'Kengeri global village' faces congestion through nearby educational institutions non-functioning traffic signals, insufficient road width to carry current traffic conditions are attributed to the problem. Further increase in population and number of vehicles can further aggravate the situation. Traffic volume is heaviest on bangalore university road and mysore road. It is highest for 2 hours in the morning and 2 hours in the evening. Road widening, relocating parking areas, providing traffic signals, sufficient turning radius, etc., can control the traffic. Constructing a flyover on Bangalore-mysore stretch can ease the traffic flow. The signal-less solution mentioned in this study provides an innovative approach to mitigate traffic congestion.

Keywords: Traffic congestion, Junction, traffic signals, signal less solution, median stretch

I. INTRODUCTION

Traffic congestion has become a significant problem that need the attention of city planners, municipal authorities, road engineers, and traffic controlling personnel in many cities. Many cities in across globe are facing this problem due to reasons such as rapid growth in of vehicular traffic, heterogeneous traffic flow, unplanned or ill-planned Roads, indiscplined road users, etc. According to [1] TomTom survey index 2019 published by a location technology firm based in the Netherlands, five major cities of India ranked in the world's most congested cities, with Bengaluru topping the list shown in Table 1. This index indicates that compared to Bengaluru's baseline uncongested conditions, travel time during rush hours in Bengaluru will take 71% more time. All other top 10 ranking cities are from developing countries.

Table 1. Highly traffic-congested cities in the world as per TomTom Traffic Index – 2019

Rank	City	Country	Congestion level
1	Bengaluru	India	71%
2	Manila	Philippines	71%
3	Bogota	Columbia	68%
4	Mumbai	India	65%
5	Pune	India	59%
6	Moscow	Russia	59%

	Region (Oblast)		
7	Lima	Peru	57%
8	New Delhi	India	56%
9	Istanbul	Turkey	55%
10	Jakarta	Indonesia	53%

Table 2. Heavy traffic-congested cities in the world as per TomTom Traffic Index – 2018 and 2017

Rank	City	Country	Congestion level	
			2018	2017
1	Mumbai	India	65%	66%
2	Bogota	Columbia	63%	62%
3	Lima	Peru	58%	50%
4	New Delhi	India	58%	62%
5	Moscow	Russia	56%	57%
6	Istanbul	Turkey	53%	59%
7	Jakarta	Indonesia	53%	61%
8	Bangkok	Thailand	53%	55%
9	Mexico City	Mexico	52%	52%
10	Recife	Brazil	49%	47%

Bengaluru is not in the top ten rankings in [2] 2017 nor in [3] 2018. It appeared in 2019 in the top ten list that too at number one position. It establishes the alarming rise in the traffic congestion in Bengaluru in the recent period an urgent need to find solutions to this issue.

When we compare Table 1 and Table 2, Bengaluru city, which took the top spot in the 2019 study, was nowhere in the top ten during the traffic index of 2018 & 2017, resulting in an exponential rise in traffic congestion in Bengaluru city

Table 3. Vehicles registered in Bengaluru according to TomTom traffic index

TomTom Traffic Index Data	
Year	Vehicles registered in Bengaluru
JULY 2019	82,53,218
DECEMBER 2018	78,84,998
DECEMBER 2017	72,58,889

Table 3 gives a better overview of the traffic congestion on the rise. It shows that in just 6 months from December 2018-July 2019, the number of vehicles has increased from 78,84,998 to 82,53,218, increasing 3,68,220 registered vehicles, a five per cent increase in only six months.

Continuous research is going on worldwide to find out solutions for persisting traffic problems. Sunil Kumar and Rajitha (2013), who conducted a traffic volume study at Bikenalli signalized Junction Bengaluru, suggested road widening, improved level of service (LOS), and other alternatives at the Junction [5]; Yun Zhu et al. (2016) proposed a modern approach to identify the traffic flow pattern by fuzzy C-means clustering algorithm [6]; Patil and Vishwanath (2017) conducted traffic volume study at Whitefield Mahadevapura, Bengaluru to improve the planning and design of junctions at the location [7]. Hetal et al. (2018) conducted a Road Junction redesign study to solve Surat's traffic congestion problem and suggested improvements in Junction planning and design [8]. Stephen et al. (2015) performed an analysis of 3 roundabouts in Sunyani and suggested a signalized roundabout to improve the vehicular movement by conducting traffic volume data [9].

Among various methods to reduce traffic congestion at Junctions, "Michigan left turn/U-turn" a popular way used in Michigan, USA, as described by Pline LJ (1996) [10]. It is being used for left-turning traffic in Michigan as left turns create interlocking at Junctions without traffic signals. In this practice, as shown in figure 1, drivers drive either straight or turn right and then complete a U-turn through a median instead of just turning left near the junction. In India, traffic moves on the left side on Roads, and right turning traffic leads to interlocking, and this concept can resolve with suitable modifications.

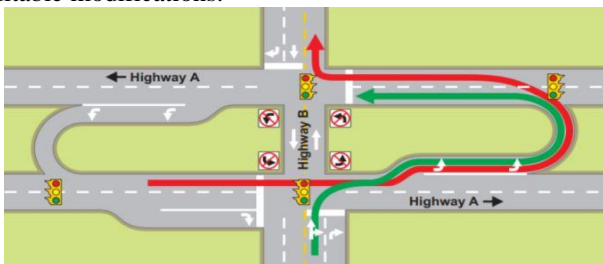


Figure 1. A Michigan left traffic solution [10]

Data collection and analysis

Collection of data such as i) Location details of the study area, collection of ii) Road inventory details at the Junction understudy, such as pavement widths and footpaths, pavement material types, Road dividers, shops, and other commercial establishments, street vendors, bus stops, parking lots, street lighting facilities, etc., iii) Existing traffic control measures like traffic signals, one-way Roads, and traffic signs boards, etc., iv) Traffic data such as the composition of vehicle types, peak volume, peak timings, etc., are essential for the safe, efficient and economical design of Junctions. The authors collected all these particulars through site visits. Manual counting methods are used to calculate traffic volume data.

Location Details



Figure 2. Google map location of Kengeri-Hoysala Junction (12.92481, 77.48508)

Kengeri is a suburb in Bangalore city. It is located on the western corridor along Mysore Road, bordered by Nagarbhavi to the north and Rajarajeshwari Nagar to the east. It is located in the south-western part of Bengaluru and about 14 Km from the city central railway station. The road links some important towns like Electronic city, Kengeri, Uttarahalli, Banashankari and Rajarajeshwari nagar.

Road inventory

The Road inventory data for Kengeri-Hoysala Junction provides the existing design configuration of the Junction. Four Roads are joining at the Junction, as shown in figure 3. All Roads are bi-directional. That two Roads, Road 1 and 2, are part of old ring road. Road is directed towards bangalore university. Road 2 is directed towards mysore road. Road 3 is directed towards kengeri and road 4 is directed towards kumbalgodu.

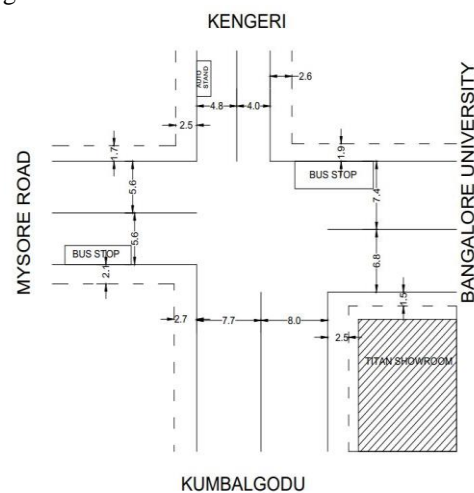


Figure 3. Road details at Kengeri-Hoysala Junction

From Table 4, we observed that Roads 1 and 2 have a carriage width of 14.2 m and 11.2 respectively. There are Road dividers for bifurcating the traffic on these Roads. Frequently traffic crisscrosses over into opposite lanes during peak hours, leading to obstructions to smooth traffic flow. Restaurants and many commercial shops present on these two Roads. Public transport buses ply on these two Roads. Bus stops and parking lots are also situated here. Road 3 has a carriage width of 8.8 m and has concrete dividers to separate

the traffic in opposite directions. Road 4 is having a carriage width of 15.4 m and without shoulders. Compared to the recommended Road widths mentioned in Geometric design

standards for urban Roads in plains IRC86-1983 clause 6.2.4 page 7, Table 5 carriageway widths. This width are sufficient

Table 4. Road inventory data of Kengeri-Hoysala Junction.

Sr.no	Description	Carriage width	Shoulder		Right of way	Drainage
			LHS	RHS		
1	Road 1-from Junction towards Jalahalli cross	7.4+6.8=14.2m (without kerb)	1.9	1.5	17.6	2.1
2	Road 2- from Junction towards air force area	5.6+5.6=11.2m (without kerb)	1.7	2.1	15	1.9
3	Road 3-from Junction towards Peenya 2nd stage	4.8+4=8.8 (without kerb)	2.5	2.6	13.9	2.4
4	Road 4- from Junction towards Hesarghatta	7.7+8=15.7 (without kerb)	2.7	2.5	20.9	2.5

Traffic volume data

The manual count of traffic volume employed in this study helped segregate the type of vehicles and their numbers in each lane and direction on each road. The data was collected during a working day and weekend (dt05/06/2020 Friday & 06/06/2020 Saturday), respectively. Data was collected from 8 am to 11 am and 5 pm to 8 pm, which are usually considered peak traffic hours. The type of vehicles moving at this Junction can broadly be classified into two-wheeler motor vehicles, auto-rickshaws (three-wheeler motor public carriers), cars, government and private buses and trucks. The collected traffic volume data is presented below in bar charts (Figures 4 to 7) and Tables 5 and 6. In bar charts, the types of

vehicles are plotted on X-axis, and the number of vehicles -volume per hour/ passenger car units, PCU /hr- is plotted on the y-axis. Further, different types of vehicles are shown in different colours and segregated hour-wise.

Figure 4 shows the traffic volume data of different vehicle types in passenger car units (PCU) on Road 1 towards the Kengeri-Hoysala Junction during peak hours on a working day. It can be noted that the total traffic flow from 9 am to 10 am is 2206 PCU/hr. Two-wheeler motor vehicles are the major component of the traffic, followed by cars and three-wheeled auto-rickshaws, respectively. Time-wise, 9 am to 10 am is the next peak hour, followed by 6 pm to 7 pm in the order.

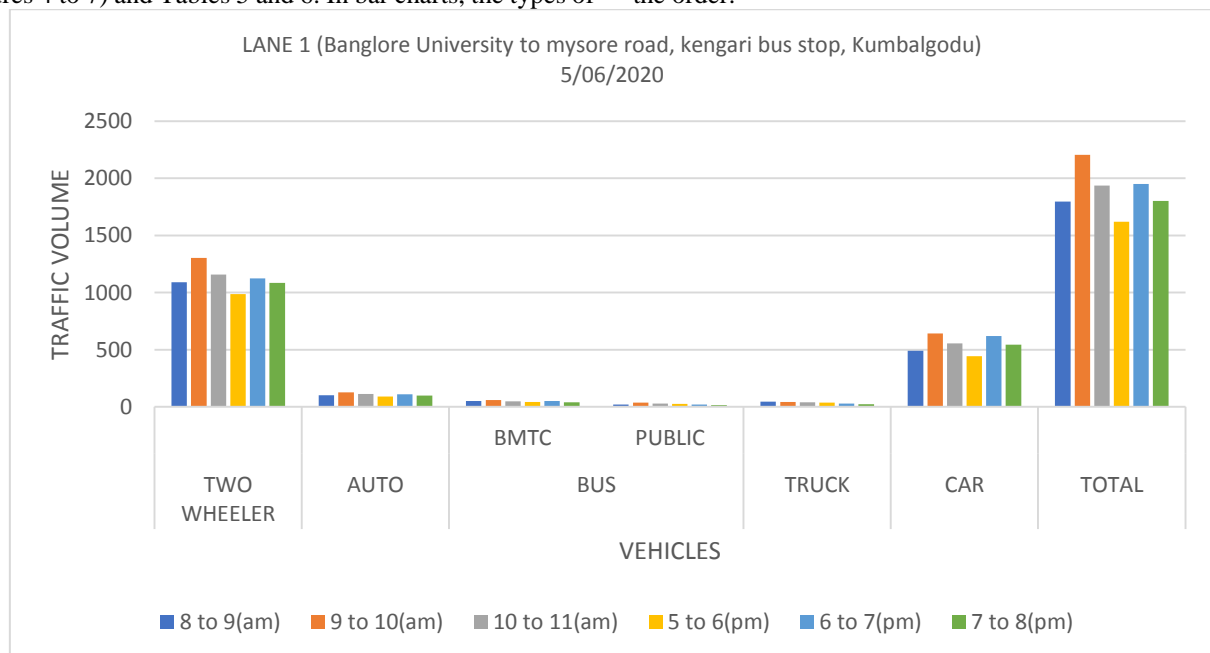


Figure 4. Traffic volume on Road 1 towards the Kengeri-Hoysala Junction on a working day (05/06/2020)

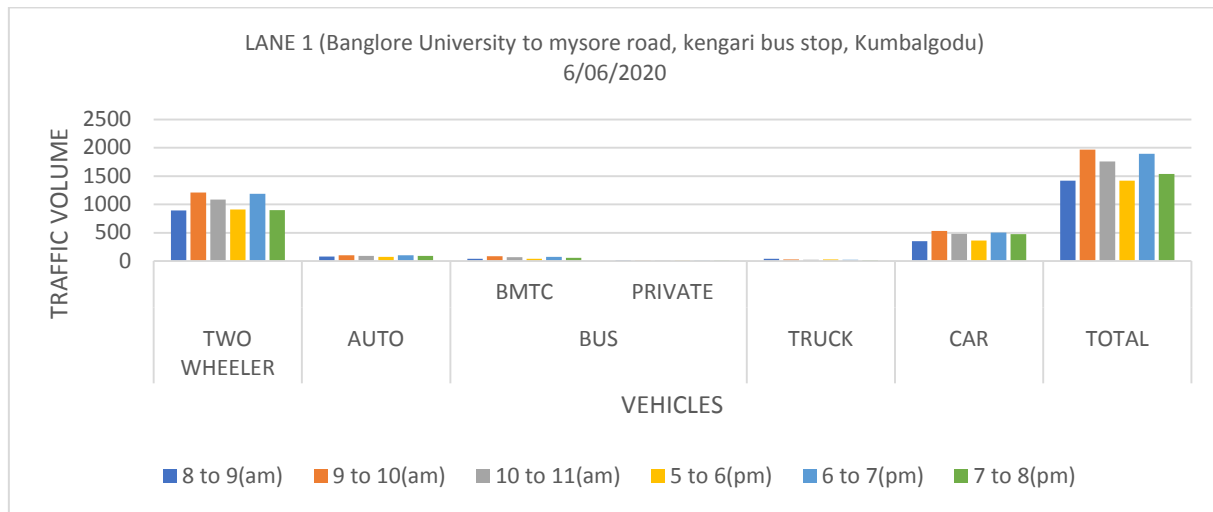


Figure 5. Traffic volume on Road 1 towards the Kengeri-Hoysala Junction on a weekend (06/06/2020)

Figure 5 shows the traffic volume data of different vehicle types in passenger car units (PCU) on Road 1 towards the Kengeri-Hoysala Junction during peak hours on the weekend. It can be noted that the traffic volume from 9 to 10 am is 1970 PCU/hr. Two-wheeler motor vehicles are the primary traffic driver, followed by cars, Auto rickshaws, buses, and trucks, respectively. The peak hour again is observed from 6 pm to 7 pm.

10 am is 1970 PCU/hr. Two-wheeler motor vehicles are the primary traffic driver, followed by cars, Auto rickshaws, buses, and trucks, respectively. The peak hour again is observed from 6 pm to 7 pm.

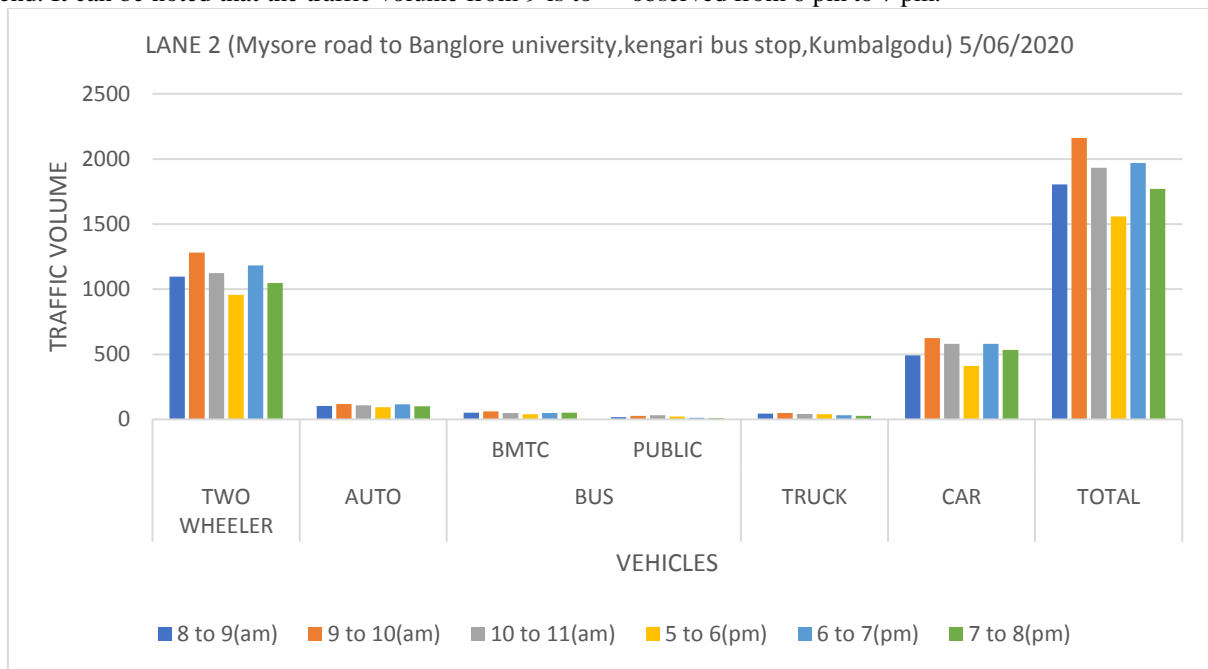


Figure 6. Traffic volume on Road 2 towards the Kengeri-Hoysala Junction on a working day (05/06/2020)

Figure 6 shows the traffic volume data of different vehicle types in passenger car units (PCU) on Road 2 towards the Kengeri-Hoysala Junction during peak hours on a working day. It can be noticed that the total traffic flow from 9 am to 10 am is 2162 PCU/hr. Among various vehicle types, two-wheeler, motor vehicles are the primary traffic component, followed by cars, Three-wheeler auto-rickshaw, buses, and trucks, respectively. The peak hour on this road was observed again from 6 pm to 7 pm.

Figure 7 shows the traffic volume data of different vehicle types in passenger car units (PCU) on Road 2 towards the Kengeri-Hoysala Junction during peak hours on the weekend. It can be noticed that the total traffic flow from 9 am to 10 am is 1971 PCU/hr. It can be noted that two-wheeler motor vehicles are the primary component of traffic, followed by cars, three-wheeled auto-rickshaws, buses, and trucks, respectively. The peak hour on this road was observed again from 6 pm to 7 pm.

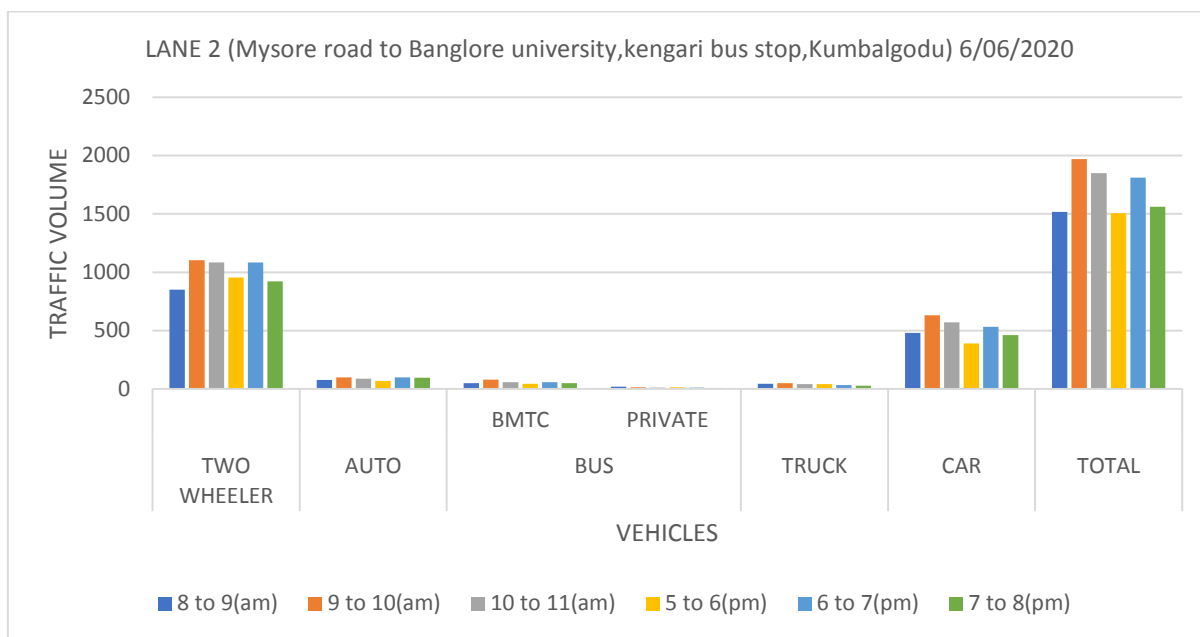


Figure 7. Traffic volume on Road 2 towards the Kengeri-Hoysala Junction on a weekend (06/06/2020)

Table 5. Traffic volume on Road 3 towards the Kengeri-Hoysala Junction on a working day (05/06/2020) and weekend (06/06/2020)

LANE 3 (Kengari bus stop to Kumbalgodu, mysore, Bangalore university)							
WEEK DAYS			DATE -5/06/2020				
TIME	TWO WHEELER	AUTO	BUS		TRUCK	CAR	TOTAL
			BMTC	PRIVATE			
8 to 9(am)	331	35	7	4		89	466
9 to 10(am)	345	22	4	2		69	442
10 to 11(am)	321	15	5	3		65	409
5 to 6(pm)	326	25	4	5		68	428
6 to 7(pm)	310	21	7	2		72	412
7 to 8(pm)	301	7	2	3		68	381
WEEKEND			DATE-6/06/2020				
TIME	TWO WHEELER	AUTO	BUS		TRUCK	CAR	TOTAL
			BMTC	PRIVATE			
8 to 9(am)	239	26	4	1		57	327
9 to 10(am)	284	11	2	0		71	368
10 to 11(am)	253	19	3	2		61	338
5 to 6(pm)	241	22	2	2		52	319
6 to 7(pm)	249	14	5	1		68	337
7 to 8(pm)	257	17	1	2		59	336

Table 5 shows the traffic volume data of different vehicle types in passenger car units (PCU) on Road 3 towards the Kengeri-Hoysala Junction during peak hours on working and weekend days, respectively. We can observe that the peak traffic flow during the morning at 8 am to 9 am with 466 PCU/hr on working days and peak traffic condition at 5 pm to 6 pm with 428 PCU/hr on working days. Various types of

vehicles which have the highest PCU count from 8 am to 8 pm are highlighted in Table 5.

From the above data, we can observe that peak hours during the weekend are from 9 am to 10 am with 368 PCU/hr and again from 6 pm to 7 pm with 337 PCU/hr. It can also be observed that PCU/hr is affected due to weekend days as people travelling during weekends are considerably less.

Table 6. Traffic volume on Road 4 towards the Kengeri-Hoysala Junction on a working day (05/06/2020) and weekend (06/06/2020).

LANE 4 (Kumbalgodu to kengeri bus stop , Banglore universiry,mysore road)							
TIME	WEEK DAYS			DATE -5/06/2020		CAR	TOTAL
	TWO WHEELER	AUTO	BUS		TRUCK		
			BMTC	PUBLIC			
8 to 9(am)	301	52	6	5	9	128	501
9 to 10(am)	390	62	8	11	12	133	638
10 to 11(am)	32	47	7	8	7	142	243
5 to 6(pm)	320	45	5	6	6	103	485
6 to 7(pm)	370	59	9	10	10	145	603
7 to 8(pm)	356	36	4	5	5	99	505
WEEKEND							
TIME	WEEKEND			DATE-6/06/2020		CAR	TOTAL
	TWO WHEELER	AUTO	BUS		TRUCK		
			BMTC	PRIVATE			
8 to 9(am)	286	36	3	4	7	80	416
9 to 10(am)	301	41	4	7	9	95	461
10 to 11(am)	273	28	2	5	4	76	388
5 to 6(pm)	279	25	2	3	3	68	380
6 to 7(pm)	310	35	4	7	5	83	444
7 to 8(pm)	290	21	3	4	4	61	383

Table 6 shows the traffic volume data of different vehicle types in passenger car units (PCU) on Road 4 towards the Kengeri-Hoysala Junction during peak hours on working and weekend days. We can observe the peak traffic flow during the morning from 9 am to 10 am with 636 PCU/hr. The peak hour was followed again from 6 pm to 7 pm with 603 PCU/hr. Different types of vehicles with the highest PCU count from 8 am to 8 pm are highlighted in Table 6.

Similarly, we can observe peak hours during the weekend from 9 am to 10 am with 461 PCU/hr and again from 6 pm to 7 pm with 444 PCU/hr. We can find that PCU/hr is affected due to weekend holidays as people travelling during weekends are considerably less.

Proposed solutions

From the above Road inventory and traffic flow data, primary causes for the traffic congestion at this Junction are lack of traffic signals, traffic signs, a large volume of traffic on Roads 1 & 2 during peak hours, insufficient Road width of Road 4, short turning radius at corners, parking lots, bus stops, etc. Congestion can further be aggravated in future by the population growth and rise in the number of vehicles. Hence there is a need to find out suitable mitigation measures to address the problem. Broad conceptual solutions were identified and discussed below. Exact working details can be developed when the BBMP wishes to take up the project.

The solutions to facilitate smooth traffic flow can be classified into i) With traffic signals at the Junction and ii) Without traffic signals. Both the solutions are explained below. Widening of the Roads as per IRC norms, providing sufficient turning radius at corners, relocating and staggering the auto-rickshaw parking stand, parking lots, bus stops, and street vendors to a suitable distance away from the Junction, constructing Road dividers, providing traffic signboards,

pedestrian markings are some essential measures common to both solutions with traffic signals and without traffic signals.

Solution with Traffic Signals

Installing and operating traffic signals at all the corners of the Junction provides an economical solution. The duration of signal timings in various directions can be varied according to the traffic volume in that direction. At the Junction under study, the green signal duration, which allows the traffic flow from Roads 1 & 2 on kengeri-hoysala junction needs to be increased compared to other Roads.

Signal less solution

An Junction without traffic signals has certain advantages, particularly on busy roads. The Road users need not stop, wait and restart their travel at the Junctions. It can save time and fuel. It reduces carbon emissions and pollution levels. Frequent stoppages at many signals in their route can cause fatigue to drivers. Though construction costs and land requirements are more for providing such signal-less solutions, in the long run, they are highly beneficial, as discussed above, particularly in cities like Bengaluru, where the traffic is consistently on the rise.

The fundamental requirement for designing a signal less Junction is that there shall not be any crisscrossing of traffic with each other. In India, vehicles move on the left-hand side of the road, compared to the USA, where vehicles drive on the right-hand side. Hence in India, Crisscrossing can occur when right-turning traffic and straight-moving traffic intersect each other. It can be avoided by relocating the right turns at a certain distance away from the Junctions, something similar to the Michigan left Junction design explained earlier. Initially, the vehicle takes a left turn, travels a certain distance, and then takes a right turn. It merges with straight moving traffic up to that right turning point, and at the right turning point, it diverges from the

straight moving traffic. These principles of a delayed right turn and merging and demerging of traffic can be employed to avoid traffic crisscrossing at Junctions up to a specific limit. Though these measures may slow down the movement, they can help eliminate sudden stoppages and wait at the signals. In the case of Junctions where traffic is heavy on a particular Road, then a flyover or underpass can be provided on that road near the Junction to segregate and free traffic flow in that road. All these options are employed in the solutions suggested for this signal less Junction. IRC: S.P.: 90:2010 [12] provides the design guidelines for grade separator and elevated structure as per Indian standards.

At Kengeri-Hoysala junction, according to the data furnished above, more traffic flow is observed on Road in both straight directions. Hence a bidirectional flyover spanning over the Junction with separate single lanes for each movement is proposed on Road, as shown in figure 8. This facilitates the uninterrupted traffic flow on this road and a significant reduction in traffic at the Junction. Construction of a median strip below the flyover in the flyover's direction, as shown in figure 9, is suggested. Traffic movements from all the roads are

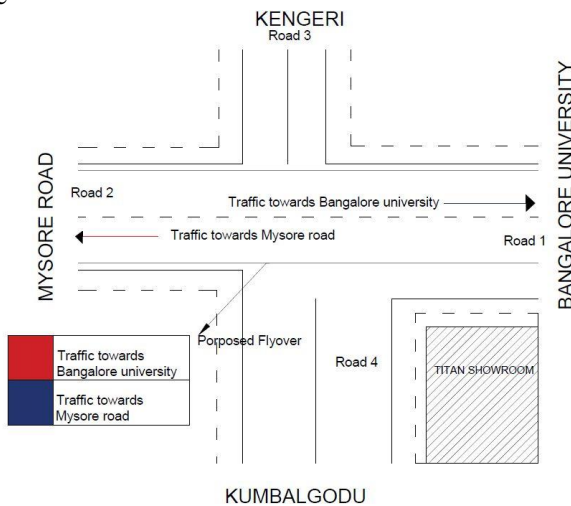


Figure 8: Proposed flyover at Kengeri-Hoysala Junction (not to scale)

described below and can be visualized from figure 9. It shows a typical traffic movements from Road 4 to all other three roads. Traffic movements from other three roads follows similar pattern.

Traffic from Road 1

Straight traffic towards Road 2 will run on the flyover. Traffic movement into Road 3 consists of going straight on the left side lane of flyover and taking a U-turn at the end of the median stretch, and entering Road 3 by taking a left turn. Traffic movement into Road 4 will run on the left side lane of flyover without entering the flyover and take a left turn at the Junction.

Traffic from Road 2

Straight traffic towards Road 1 will run on the flyover. Traffic movement into Road 3 will run on the left side lane of flyover without entering the flyover and take a left turn at the Junction.

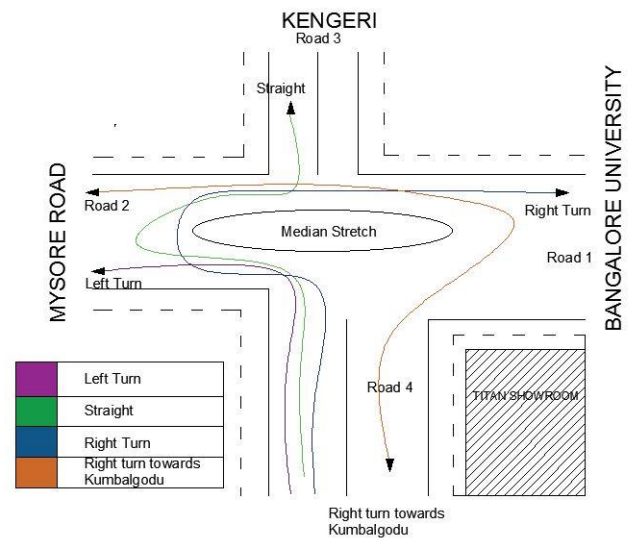


Figure 9: Typical left, right and straight traffic movements from Road 4 around the median stretch

Traffic movement into Road 4 consists of going straight on the left side lane of flyover and taking a U-turn at the end of the median stretch, and entering Road 4 by taking a left turn.

Traffic from Road 3

Traffic from Road 3 towards Road 1 will move straight by taking a left turn and proceeding directly on the flyover's left side lane. Traffic movement for Road 2 will follow a left turn at the Junction, then a U-turn at the end of the median stretch below the flyover and proceeding straight towards Road 2. The traffic towards Road 4 will take a left turn at the Junction and a U-turn at the median stretch, followed by a left turn and enters Road 4.

Traffic from Road 4

Traffic movement towards Road 1 will follow a left turn at the Junction, then a U-turn at the end of the median stretch below the flyover and will proceed straight towards Road 1. The traffic towards Road 2 will move straight by taking a left turn and proceeding directly on the flyover's left side. The traffic towards Road 3 will take a left turn at the Junction and a U-turn at the median stretch, followed by a left turn and enters Road 3.

During the above traffic movements, merging and demerging of traffic flow occurs. The merging and demerging measures along the median stretch below the flyover help to prevent traffic crisscrossing and establish a signal less Junction at Kengeri-Hoysala Junction.

II. CONCLUSIONS:

1. Kengeri-Hoysala Junction is a prime four Road Junction located in Kengeri, situated in a bustling industrial and commercial area of Bengaluru.
2. Insufficient Road widths, lack of turning radius, lack of traffic signals, signs and Road dividers, existing auto-rickshaw parking stand, restaurant, temple, parking lots, Bus stop, etc. very close to the Junction are the reasons for the traffic congestion at this Junction. An

increase in the number of vehicles can further aggravate the congestion

3. Traffic volume is highest for 2 hours in the morning and 2 hours in the evening.
4. Vehicle type wise, two-wheelers followed by cars are most in numbers.
5. Roads' Widening, providing traffic signs, turning radius, relocating the parking lots, bus stop, auto-rickshaw stand, etc., are primary steps in any decongestion solution.
6. Providing traffic signals at corners and adjusting their timings according to the traffic volume in a particular direction can provide an economical solution.
7. Signal less solutions can eliminate the waiting time, stopping and restarting vehicles at signals.

REFERENCES

- [1] TomTom Traffic index rankings 2019 https://www.tomtom.com/en_gb/traffic-index/ranking/ (accessed on 2020/08/08)
- [2] TomTom Traffic index rankings 2017 https://www.tomtom.com/en_gb/traffic-index/ranking/ (accessed on 2020/08/08)
- [3] TomTom Traffic index rankings 2018 <https://www.tomtom.com/company/press-releases/news/25601/> (accessed on 2020/08/08)
- [4] Indian Road Congress, IRC: 86:1983-IRC86-1983 page 7.
- [5] Sunil Kumar V, J. Rajitha "Improvement of Traffic Operations in Congested Signalized Junctions- A Case Study in Bengaluru City" International Journal of Engineering Research & Technology (IJERT) Vol.2 Issue 7, July - 2013
- [6] Yun Zhu, Ningbo Gao, Jianhua Wang, Chen Liu. "Study on Traffic Flow Patterns Identification of Single Junction Intelligent Signal Control" Procedia Engineering 137 (2016) 452 – 460.
- [7] Aravind B. Patil, Vishwanath B.B "Junction Improvement Planning and Design A Case Study for Whitefield in Mahadevapura Traffic Zone-Bengaluru" International Journal of Advance Engineering and Research Development Volume 4, Issue 2, February -2017.
- [8] Hetal b. Patel, Bhasker Vijaykumar Bhatt "a critical study of Road Junctions in the southeast part of Surat city" etic April 2018, volume 5, issue 4
- [9] Stephen Agyeman, Herbert Abeka, Samuel Boamah Asiedu, "Capacity and Performance Analysis of 3 Roundabouts in Sunyani" International Journal of Science and Research (IJSR) Volume 4 Issue 10, October 2015
- [10] Pline, L.J., NCHRP Synthesis 225. "Left-Turn Treatments at Junctions." Transportation Research Board, National Research Council, Washington D.C., 1996.
- [11] Indian Road Congress, IRC: 86:1983-IRC86-1983 page 7.
- [12] IRC: S.P.: 90:2010 Manual for grade separator and elevated structures

Eye Disease Detection using Machine Learning

^[1]Sanohi K.C Jatav, ^[2]Dr. Shikha Nema, ^[3]Dr. Zia Saquib

^[1] Department of Electronics and Communication Engineering, Usha Mittal Institute of Technology, SNDT University Mumbai, India

^[2] U. Head of Department of Electronics and Communication Engineering, Usha Mittal Institute of Technology, SNDT University, Mumbai, India

^[3] Jio Platforms Ltd, Mumbai, India

Abstract— Diabetic Retinopathy (DR) is an ocular condition that causes damage to the retinal blood vessels. Diabetic retinopathy is the most visible symptom of diabetic microangiopathy and one of the most prevalent problems in diabetics. At the moment, the diagnosis of diabetic retinal problems is primarily based on images. For decades, predicting the existence of microaneurysms in fundus pictures and detecting diabetic retinopathy in its early stages has been a serious difficulty. If not detected early, DR causes visual impairment and, in severe cases, blindness. To identify this deadly illness, highly educated professionals often analyze colored fundus pictures. Clinicals' manual diagnosis of this disease is time-consuming and error-prone. As a result, numerous computer vision-based approaches for automatically detecting DR and its various phases from retina pictures have been presented. These approaches, however, are unable to encapsulate the underlying complex characteristics and can only categorize DR's many stages with extremely poor accuracy, particularly in the early stages. In recent years, deep neural has led to several advancements in a variety of domains. The purpose of this paper is to utilize convolutional neural networks to classify data.

Keywords: Diabetic Retinopathy, VGG 19, Convolutional Neural Networks (CNN), Diabetes, Machine learning

I. INTRODUCTION

The retina is a sphere-shaped structure in the rear of the eye that is made up of a thin layer. The retina's role is to convert light into neural impulses and communicate with the brain so that visual information may be processed. The macula is a black circular region of the retina that is positioned in the centre of the retina, next to the optic nerve. The fovea is a key component of the macula that allows for clear vision. Diabetes is a condition that affects people all over the world.

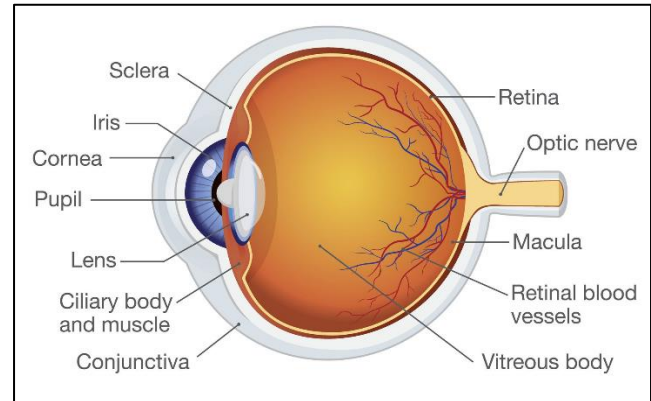


Fig. 1. Retina structure

Diabetic Retinopathy (DR) is a leading cause of blindness. Diabetic individuals aged 20 to 74 years old can become blind as a result of hysterical diabetes, which is known as diabetic retinopathy. A diabetic patient's retinal blood vessels are damaged by DR. Floating and flashing lights, hazy vision, and abrupt vision loss are all frequent signs of diabetic retinopathy.

Non-Proliferative Diabetic Retinopathy (NPDR) and Proliferative Diabetic Retinopathy (PDR) are the two main forms of DR. Patients with DR remain undiagnosed in the early stages, but as the disease progresses, it causes floaters, blurred vision, distortions, and gradual visual loss. As a result, detecting the DR in its early stages is challenging yet critical in order to avoid the harsher effects of later phases. No DR, Mild DR, Moderate DR, Severe DR, and Proliferative DR are the five distinct types of DR. Through the inspection of their retinal fundus pictures, an automatic identification of DR assigns each patient into one of these groups.

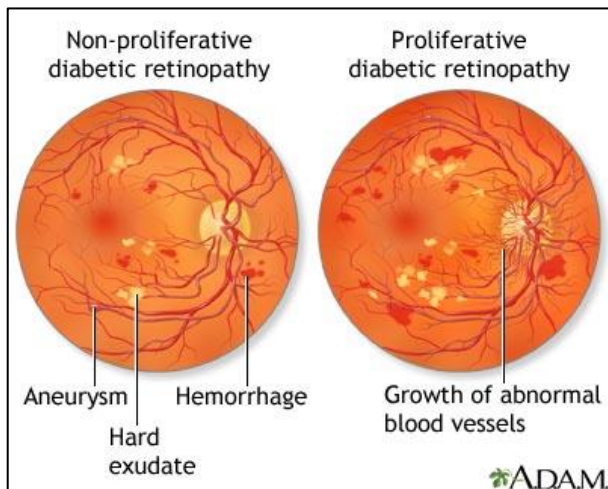


Fig. 2. (a) Non Proliferative DR (b) Proliferative DR

Early versions of such technologies were restricted to computer-assisted methods that segmented fundus pictures into vessels. There are also several computer vision DR detection methods proposed, however their accuracy rates are poor. Deep learning and convolutional neural networks (CNNs) bring a new level to this challenge. They assist researchers in the development of a dependable end-to-end diabetic retinopathy detection system. Although most of these programs perform as well as human specialists, they are focused on diagnosing a specific retinal condition. Many of these systems use the retinal picture to identify, extract, and evaluate disease-specific characteristics. This necessitates a thorough understanding of the illness as well as time spent developing characteristics for the classifiers.

Early detection of DR may aid the affected individual in receiving prompt and appropriate therapy. The identification of DR can be done manually by ophthalmologists or automatically by a computerized method. Both manual and automated diabetic retinopathy diagnostic methods have advantages and limitations. The sole benefit of the manual DR detection approach is that it does not require computer help, but it is more crucial that the ophthalmologist be an expert in the field of DR identification. Occasionally, the early signs of diabetic retinopathy are so small that they are overlooked by ophthalmologists. In the field of ophthalmology, on the other hand, artificial intelligence (AI) is playing a critical role in diagnosing severe illnesses such as diabetic retinopathy (DR). The advantages and utility of an automated system much outweigh those of a manual method. An automated approach for detecting diabetic retinopathy is considerably more authentic, reliable, quicker, efficient, and simple than a manual system. As a result, automated identification of DR is critical.

II. LITERATURE SURVEY

This study offers a comprehensive review of automated methods for detecting diabetic eye disease. The study gives a thorough overview of diabetic eye disease detection techniques, including cutting-edge field approaches, with the

goal of providing important information into research communities, healthcare professionals, and diabetic patients.[1]

This study examines machine learning techniques introduced in the previous four years for detecting ocular disorders. Each section summarizes the public datasets and problems associated with each disease, as well as the current approaches that have been applied to the problem. Furthermore, current machine learning approaches for retinal vascular segmentation, methods for retinal layers and fluid segmentation, and Machine learning approaches for glaucoma diagnosis using eye measurements and visual field data are discussed. [2]

In this paper, electronic medical record information of 301 hospitalized patients with diabetes from 2009 to 2013 has been used. A CNN technique is applied to unconnected one-dimensional data sets. In addition, the CNN model is coupled with the BN layer to avoid gradient dispersion, increase training speed, and enhance model accuracy. According to the results of the tests, this technique can obtain a training accuracy of 99.85 percent and a testing accuracy of 97.56 percent, which is more than 2% higher than logistic regression.[3]

This study proposes a method for retinal image categorization based on the integration of multi-scale shallow CNNs. Experiments on public datasets demonstrate that the suggested technique can increase classification accuracy by 3% when compared to current representative integrated CNN learning algorithms on short datasets. When applied to a larger dataset, the suggested technique can enhance classification accuracy by 3% to 9% when compared to other representative approaches such as conventional CNN.[4]

The author of this work proposes an improved automated method for detecting the severity of diabetic retinopathy using a dictionary-based approach that does not involve pre- and post-processing stages. The method incorporates an explicit picture representation into a learning framework and creates a dictionary of visual characteristics, places of interest that are recognized to calculate descriptive features from retinal images using a fast robust features algorithm and histogram of directed gradients. In comparison to the stated state-of-the-art techniques, the suggested system achieves 95.92 percent sensitivity and 98.90 percent specificity.[5]

This study emphasizes the need of appropriate strategies/models with accessible cost-effective early screening tools. Models must have a well-developed mechanism for screening, diagnosis, and referral at each hierarchical level, beginning with basic health facilities and progressing to specialist eye care institutes. Also included in the entire approach should be the creation of knowledge and behavior modification among diabetes. Community engagement and improving health seeking behavior among

diabetics can play a significant role in reaching a broader population and promoting compliance for continuing care.[6]

A deep learning architecture is proposed to predict if a person has diabetes or not from a photograph of his/her retina. multi-stage convolutional neural network (CNN)-based model named DiaNet is developed using a relatively small dataset and can achieve an accuracy level of over 84 percent on this task, successfully identifying the regions on the retina images that contribute to its decision-making process, as confirmed by medical experts in the field.[7]

The performance of three convolutional neural network (CNN) models with different learning strategies is compared to that of ophthalmologists in an autonomous glaucoma diagnostic framework in this paper. On both labelled and unlabeled data, transfer and semi-supervised learning approaches were utilized. The findings of the experiments, which used two datasets, RIM-ONE and RIGA, show that deep learning models are effective when applied to glaucoma, which is a potential step toward automated screening for identifying people with early-stage glaucoma.[8]

III. III. PROPOSED WORK

Deep learning techniques are built on convolutional neural networks. They're made up of node levels, each of which has an input layer, one or more hidden layers, and an output layer. Each node is connected to the others and has a weight and threshold assigned to it. If a node's output exceeds a certain threshold value, the node is activated, and data is sent to the next tier of the network. Otherwise, no data is sent on to the network's next tier.

Convolutional Neural Networks are the heart of deep learning algorithms. They are comprised of node layers, containing an input layer, one or more hidden layers, and an output layer. Each node connects to another and has an associated weight and threshold. If the output of any individual node is above the specified threshold value, that node is activated, sending data to the next layer of the network. Otherwise, no data is passed along to the next layer of the network.

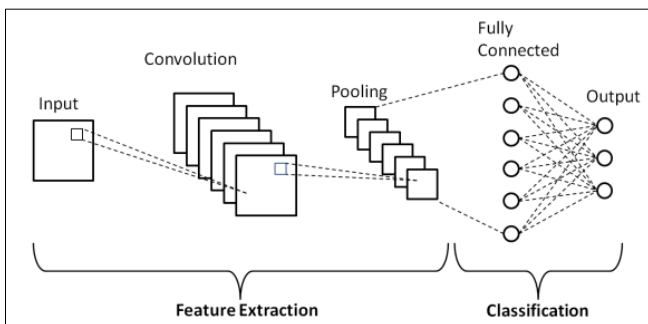


Fig. 3. CNN Network

Convolutional neural networks are used to drive image recognition and computer vision tasks. Computer vision is a branch of artificial intelligence (AI) that allows computers and systems to extract meaningful information from digital pictures, videos, and other visual inputs and then act on that information. This capacity to provide suggestions sets it apart from picture recognition jobs. Today, some popular applications of computer vision may be found in:

- Healthcare: Machine learning has been integrated into radiological equipment, allowing doctors to detect malignant tumours in healthy anatomy.
- Marketing: Social networking sites indicate who could be in a photo submitted on a profile, making it easy to tag people in photo albums.
- Automotive: While the age of autonomous cars has not yet arrived, the underlying technology is making its way into autos, increasing driver and passenger safety through features such as lane line detection.

A. VGG 19

It is a trained Convolutional Neural Network, from Visual Geometry Group, Department of Engineering Science, University of Oxford. The number 19 stands for the number of layers with trainable weights. 16 Convolutional layers and 3 Fully Connected layers. Figure. 6 shows the VGG 19 model.

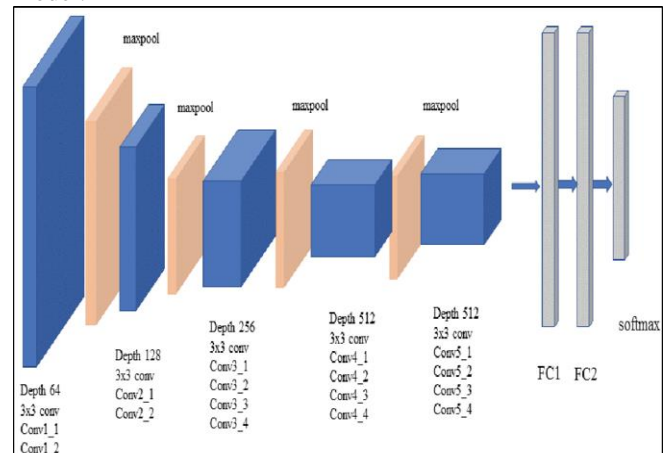


Fig. 4. VGG 19 Model

B. DENSENET 201

We designed our model architecture using the Dense Net 201. The problem of vanishing gradients is the major obstacle with very deep neural networks. The output of one layer is transmitted to all the layers in front of it in the Dense Net. Any layer in the network has direct access to the characteristics created by all previous levels. As a result, if any picture characteristics are lost during forward propagation, they are recreated at the input of subsequent layers via dense connections. As a result, this design is well suited to identifying minute statistical characteristics such as those linked to the image's source camera-model.

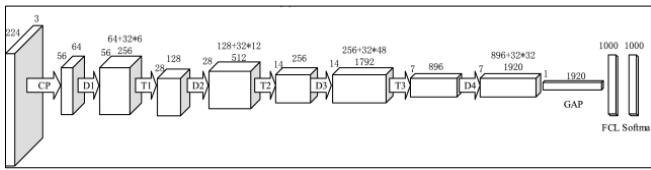


Fig. 5. Dense Net 201 Model

C. Ocular Disease Intelligent Recognition (ODIR) Dataset
 ODIR is a structured ophthalmic data collection containing 5,000 patients' ages, colored fundus images from the right and left eyes, and specialized diagnostic keywords from doctors. Shang gong Medical Technology Co., Ltd. collected the data from many hospitals/medical institutions in China. This dataset provides a "significant" set of medical information. Fundus pictures are collected in these institutions using various cameras such as Canon, Zeiss, etc. resulting in varying picture quality and resolution. Annotations were annotated by qualified human workers under the supervision of a quality control manager. They have categorized patients into eight categories which are as follows: Normal (N), Cataract (C), Glaucoma (G), Age related Macular Degeneration (A), Diabetes (D), Hypertension (H), Pathological Myopia (M), Other diseases (O).

IV. RESULT AND DISCUSSION

A. Simulation Results

The outcomes of the experiments are depicted in the picture below. The results are described in the following format: Accuracy/loss/specificity/sensitivity. We selected a combination of three categories of pictures in the first section which are normal, glaucoma, and cataract. Also, we chose a combination of four types of pictures in the second section which are normal, cataract, glaucoma, and diabetes. We evaluated 5, 10, and 15 epochs but were restricted by system resources. For three label classifications, VGG16 fared the best across both designs, with a specificity of 93 percent and a sensitivity of 75 percent. From the results it appears that 15 epochs gave the most optimum results and as the number of epochs increased to 15 the accuracy increased. When compared to label four categorization, label three performed the best.

**TABLE I. THREE LABEL CLASSIFICATION:
 NORMAL V/S GLAUCOMA V/S CATARACT**

model/ epochs	Vgg 19	Dense net 201
Epochs: 5	0.7685/0.3526/0.868 9/0.7349	0.785/0.0860/0.8009/ 0.8433
Epochs: 10	0.8013/0.3183/0.932 0/0.7469	0.6115/0.1161/0.5788 /0.6931
Epochs: 15	0.8151/0.3210/0.902 9/0.7590	0.85/0.0719/0.7378/0. 8554

**TABLE II. FOUR LABEL CLASSIFICATION:
 NORMAL V/S GLAUCOMA V/S CATARACT V/S
 DIABETES**

model/ epochs	Vgg 19	Dense net 201
Epochs: 5	0.5817/0.4001/0.702 3/0.7386	0.5879/0.1420/0.6674 /0.625
Epochs: 10	0.5889/0.3945/0.574 4/0.7272	0.6135/0.1159/0.7093 /0.75
Epochs: 15	0.5899/0.3978/0.439 5/0.6818	0.61/0.1258/0.6255/0. 7727

B. Graphical Illustration

The outcomes are visualized in two sections. The first section compares the performance parameters of the VGG 19 Model for three and four labels. The performance parameters for the Resnet 50 model for three and four labels are illustrated in the second section.

• VGG 19 Model

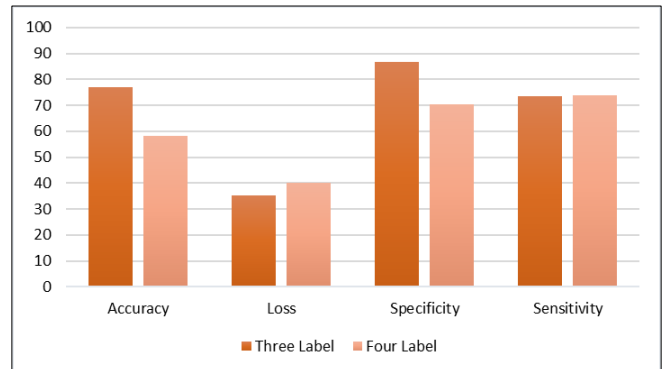


Fig. 6. For Epochs = 5

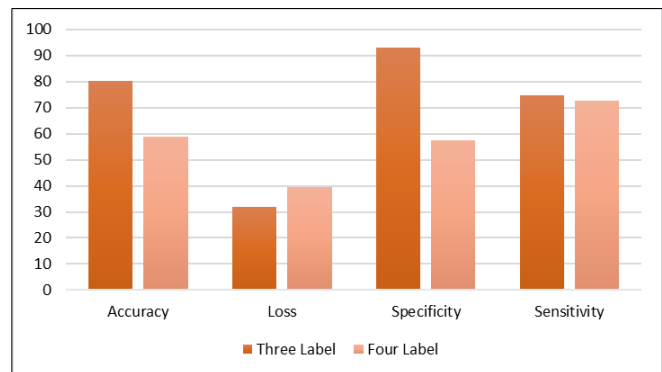


Fig. 7. For Epochs = 10

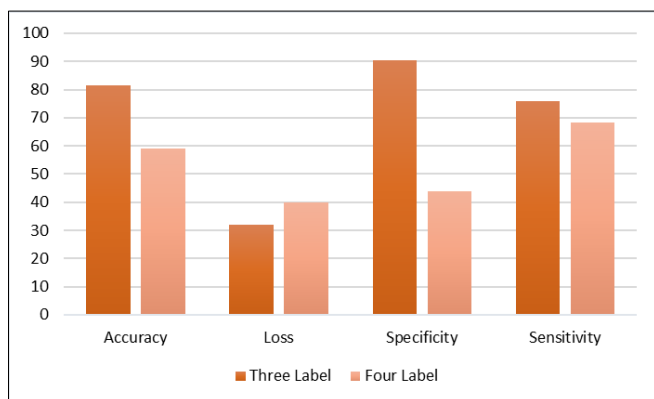


Fig. 8. For Epochs = 15

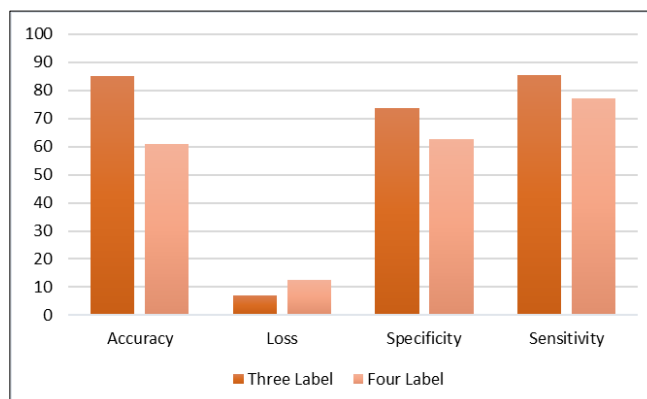


Fig. 11. For Epochs = 15

•Dense Net 201 Model

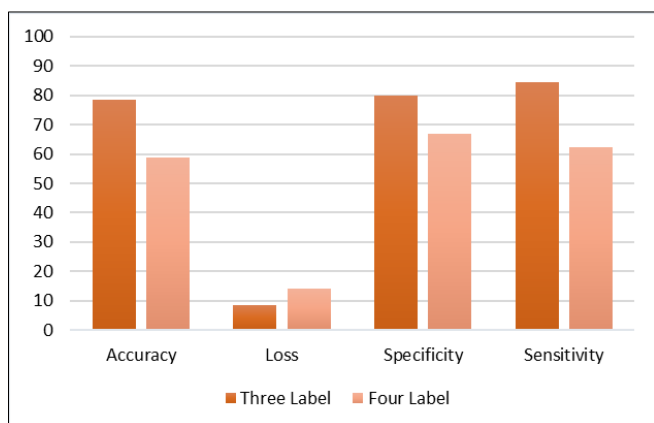


Fig. 9. For Epochs = 5

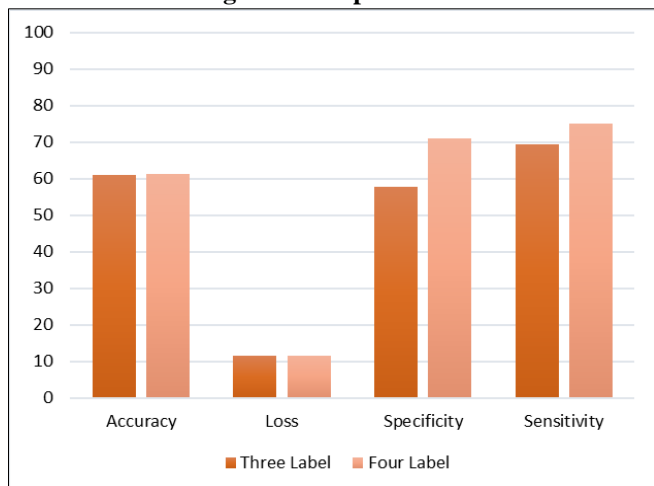


Fig. 10. For Epochs = 10

V. CONCLUSION AND FUTURE WORK

Diabetes has developed as a significant public health issue. Diabetes occurrence is rising as a result of increased urbanization, industrialization, and lifestyle changes. Diabetic retinopathy is a leading cause of preventable blindness. Treatment measures in the early stages of diabetic retinopathy can minimize the burden of blindness caused by the disease. Appropriate strategies/models must be created using the current cost-effective means of early screening. Such models must include a well-developed mechanism for screening, diagnosis, and referral at each hierarchical level, from basic health clinics to specialist eye care institutes. We presented CNN models to identify and categorize the various stages of the DR in fundus pictures. To train and test our model, we used the Kaggle dataset, which has the largest publicly available collection of fundus images. Our tests demonstrate that CNN architectures do a good job of assessing DR severity in diabetic individuals. Some well-known architectures were tested, and VGG 19 worked excellently. In the future, we want to combine several architectures to achieve multiple benefits. Furthermore, in order to improve the accuracy of initial phases, one might arrange to train distinct models for various phases and then combine the results.

REFERENCES

- [1] Rubina Sarki; Khandakar Ahmed; Hua Wang; Yanchun Zhang, "Automatic Detection of Diabetic Eye Disease Through Deep Learning Using Fundus Images: A Survey", IEEE Access, Vol. 8, pp. 151133 – 151149, ISSN: 2169-3536, 10 August 2020.
- [2] Mhd Hasan Sarhan; M. Ali Nasser; Daniel Zapp; Mathias Maier; Chris P. Lohmann; Nassir Navab; Abouzar Eslami, "Machine Learning Techniques for Ophthalmic Data Processing: A Review", IEEE Journal of Biomedical and Health Informatics, Vol. 24, pp. 3338 – 3350, Issue: 12, Dec. 2020, 28 July 2020.
- [3] Yunlei Sun, "The Neural Network of One-Dimensional Convolution-An Example of the Diagnosis of Diabetic Retinopathy", IEEE Access, Vol. 7, pp. 69657 - 69666, ISSN: 2169-3536, 15 May 2019.
- [4] Wanghu Chen; Bo Yang; Jing Li; Jianwu Wang, "An Approach to Detecting Diabetic Retinopathy Based on Integrated Shallow Convolutional Neural Networks", IEEE Access, Vol. 8, pp. 178552 - 178562, ISSN: 2169-3536, 29 September 2020.

- [5] Mona Leeza; Humera Farooq, "Detection of severity level of diabetic retinopathy using Bag of features model", IET Computer Vision, Volume: 13, Issue: 5, pp. 523 – 530, ISSN: 1751-9640, 12 August 2019.
- [6] P. Vashist, N. Gupta, S. Singh and R. Saxena, "Role of Early Screening for Diabetic Retinopathy in Patients with Diabetes Mellitus: An overview", Indian J. Community Med. Off. Publication Indian Assoc. Preventive Social Med., vol. 36, no. 4, pp. 247, 2011.
- [7] Mohammad Tariqul Islam; Hamada R. H. Al-Absi; Essam A. Ruagh; Tanvir Alam, "DiaNet: A Deep Learning Based Architecture to Diagnose Diabetes Using Retinal Images Only", IEEE Access, Vol. 9, pp. 15686 - 15695, ISSN: 2169-3536, 18 January 2021.
- [8] Manal Alghamdi; Mohamed Abdel-Mottaleb, "A Comparative Study of Deep Learning Models for Diagnosing Glaucoma From Fundus Images", IEEE Access, Vol. 9, pp. 23894 - 23906, ISSN: 2169-3536, 02 February 2021.

Predicting the Quantity of Future Heart Attack Patients Using Random Forest Algorithm

^[1] B. Sarath Chandra, ^[2] A. Chandramouli

^{[1][2]} Assistant Professor PSCMR CET

Abstract— These days, heart disease is the original source of death, and that's all. It's a complex and difficult job to predict a doctor's heart attack and it requires a little more experience and know-how. On the other hand, the heart rate monitor is the most convincing at this scale, because it is one aspect of management, myocardial infarction, other health and fitness indicators like blood pressure, serum cholesterol and blood sugar. In this period, characterized by a rapid revolution, the Internet of Things, sensors for monitoring heart rate is becoming increasingly close to the patient. This work offers a range around heart rate and other data, monitoring technologies and use a machine learning method, a random forest classification algorithm, use to calculate the heart of tutmasndan in the sense that it consists of heart rate and the health status of each rib

Keywords: Internet of Things, heart attract, machine learning, Random Forest.

I. INTRODUCTION

The Internet of Things represents a common understanding of the ability of networks, devices to receive and collect information from the world around us, and then share this data

Online, they can be managed and used for various interesting purposes. Forecasts for the impact of the Internet of Things (IoT) Internet and economy are important, with some expecting that already 100 billion IoT-related devices will show a global economic impact. The Internet of Things of Healthcare plays an important role in monitoring certain types of healthcare activities and diagnosing any problems in the course of these activities. The device they are connected to the Internet has been owned by patients in a wide variety of ways and forms. If it's revenue from related blood pressure monitoring instrumentation, ECG, temperature monitoring or blood sugar monitoring and regular sharing of health information is vital for some people. Many of these activities require follow-up interaction with a healthcare professional. Information always comes from the clouds, and many views, analyses, and reports are created by the cloud and sends you the most relevant results for patients or healthcare professionals using your mobile phone or other enabled devices.

It is considered that a large amount of medical data created online, that is a high cost. Mining algorithms can be applied to the Internet of Things to detect unknown information about this information. With the help of intelligent analysis, knowledge, technology and software, including

classification, clustering, association analysis, time series analysis and waste analysis, it can also provide a projected indicator of the patient's future illness report, is. Governments or authorities will be able to use this analysis can also add a step to cure, prevent or any disease. In this article, I explain the process of collecting data, tools, and techniques using this data to analyze information. From this point of view, a number of analyses of the information contained in this report will be presented here. A well-known data mining algorithm, the random forest algorithm, is used for future prediction of patients with cardiovascular diseases using relevant heart-related information.

II. RELATED WORKS

Heart rate variability has significant potential to evaluate the role of autonomic nervous system changes, both in normal, healthy subjects and patients with various cardiovascular and cardiovascular diseases. Machine learning is now the main date in the "Internet of things". Different natures, results of data mining, like prediction or other IoT, data, can be evaluated using machine learning tools, which is implemented through monitoring vital health indicators and the healthcare system. Banai, Ahmed and Loutfi went through the latest techniques and algorithms that are being used to analyze the future of wearable device sensors . They used some of the widespread methods of data mining, anomaly detection, estimation and decision-making about when and, in particular, in terms of sustained when in a series of measurements. Finally, based on a review of the literature, a number of important issues were identified, such as the importance and methods of data mining in health monitoring systems. Allen Parker & Ersoy we have covered some of the issues related to wireless sensor network health services. Developed several state-of-the-art models, along with a draft documentation on the idea, so: "unobtrusiveness, expansion, energy security, and provide a comprehensive analysis of the benefits and challenges of these systems. Security and privacy of the Internet of Things in healthcare is the most important thing. There is a strong social concern that may arise from the fear that these devices are being used for spying and tracking individuals by the government and other private organizations.

III. THE REASON OF HEART ATTACK

Cardiovascular disease is the leading global cause of death. The National Institutes of Health and other government sources accounting for 17.3 million deaths per year, a number that is expected to grow to more than

23.6 million by 2030. Canto & Iskandrian, 2003 analysed some risk factor of heart diseases. Some traditional myths relating with heart rate and heart attack are published in health related website (<http://www.webmd.com>) are as follows: A normal heart rate is 60-100 beats per minute. However, heart rate higher than 76 beats per minute when in resting may be linked to a higher risk of heart attack. Having an irregular heartbeat doesn't mean having a heart attack. But if it's a new symptom, or if you have chest pains or problems breathing, may be the preliminary symptom for heart attack.

Slow rates are only a problem if also pass out, feel dizzy, are short of breath, or have chest pain.

In this paper different health related data with heart rate used for the prediction of heart attack and reveal these myths.

IV. METHOD OF DATA COLLECTION

I was able to separate the breeds, data types of three different levels to predict a heart attack. First, it's the company's personal profile, like age and gender. The second level is the periodic table, information entered on a single day or during a week that determines your blood sugar and serum cholesterol levels. The third indicator is the level of blood pressure and heart rate.

- Portable, devices and structures, home, health monitoring IoT can be used for monitoring, data collection of the second and third levels. Note: Some devices may monitor the patient's blood pressure and heart rate in real time. Some devices are equipped with a trigger system that outputs results after a certain time, or using a manual trigger. Wi-Fi connection, digital glucose meters and blood cholesterol tests, activate the system, use for this purpose.



Fig a: Conceptual diagram for prediction

V. DATA MINING ALGORITHM

Random forest is a type, control, algorithm, machine learning based on ensemble learning. Ensemble learning is a type of learning that you can combine what to do, when to do different kinds of algorithms, or the same algorithm multiple times to create more powerful prediction models. A random forest algorithm is an algorithm that combines several of the same type, i.e. simultaneously in multiple decision trees, results in a very large number of trees, thus the name

"Random Forest". The random forest algorithm can be used for both regression and classification problems.

Working model of Random Forest Algorithm

The following are the basic steps involved in performing the random forest algorithm

1. Pick N random records from the dataset.
2. Build a decision tree based on these N records.
3. Choose the number of trees you want in your algorithm and repeat steps 1 and 2.
4. In case of a regression problem, for a new record, each tree in the forest predicts a value for Y (output). The final value can be calculated by taking the average of all the values predicted by all the trees in forest. Or, in case of a classification problem, each tree in the forest predicts the category to which the new record belongs. Finally, the new record is assigned to the category that wins the majority vote.

Advantages of using Random Forest

As with any algorithm, there are advantages and disadvantages to using it. In the next two sections we'll take a look at the pros and cons of using random forest for classification and regression.

1. The random forest algorithm is not biased, since, there are multiple trees and each tree is trained on a subset of data. Basically, the random forest algorithm relies on the power of "the crowd"; therefore the overall biasedness of the algorithm is reduced.
2. This algorithm is very stable. Even if a new data point is introduced in the dataset the overall algorithm is not affected much since new data may impact one tree, but it is very hard for it to impact all the trees.
3. The random forest algorithm works well when you have both categorical and numerical features.
4. The random forest algorithm also works well when data has missing values or it has not been scaled well (although we have performed feature scaling in this article just for the purpose of demonstration).

VI. EXAMPLE DATA SOURCE

Samples of data sets from the UCI Machine Learning Repository of the Learning and Intelligent Systems Center were used here. One out of 303 patients to have information collection re-structured in this way, keep in mind that results are usually achieved in the cloud of the health cloud platform.

The information consists of 303 observations and 8 variables as follows: patient ID, gender, Age, resting blood pressure, serum cholesterol, fasting blood sugar, 120 mg/dl, ca, trestbps, thalach, exang, oldpeak, slope, thal, maximum heart rate for 24 hours and cardiovascular disease (prognosis)

In real life, more important parameters that may be required to measure a patient during the period of stroke risk. I classify these data areas based on the data collection procedure. These are three ways. Two of them-real-time data, blood pressure

and pulse-will be achieved using the device's wearable sensors. This information is stored on a separate temporary storage device and, perhaps, the highest heart rate, average blood pressure for a certain time will be recalculated from the temporary content and, ultimately, stored in the master data. The national database will consist of patients with static data like age, gender and any other tasks, as well as such as blood glucose and serum cholesterol. This data set in binary values is used to measure blood glucose levels on an empty stomach. If the blood sugar level is more than 120 mg / dl, then this result should look like this, if it is 120-mg / dl) or less, then this is defined as normal or even low. The class value of real, heart disease, and is also measured in terms of doubles and for reference, this and the lack of a single for. Here's the data set looks like:

A	B	C	D	E	F	G	H	I	J	K	L	M	N	O
1	Age	Sex	ChestPain	RestBP	Chol	Fbs	RestECG	MaxHR	ExAng	Oldpeak	Slope	Ca	Thal	AI
2	1	63	1 typical	145	233	1	2	150	0	2.3	3	0	fixed	N
3	2	67	1 asymptot	160	286	0	2	108	1	1.5	2	3	normal	Ye
4	3	67	1 asymptot	120	229	0	2	129	1	2.6	2	2	reversabi	Ye
5	4	37	1 nonangini	130	250	0	0	187	0	3.5	3	0	normal	N
6	5	41	0 nontypica	130	204	0	2	172	0	1.4	1	0	normal	N
7	6	56	1 nontypica	130	236	0	2	178	0	0.8	1	0	normal	N
8	7	62	0 asymptot	140	268	0	2	160	0	3.6	3	2	normal	Ye
9	8	57	0 asymptot	120	354	0	0	163	1	0.6	1	0	normal	N
10	9	63	1 asymptot	130	254	0	2	147	0	1.4	2	1	reversabi	Ye
11	10	53	1 asymptot	140	203	1	2	155	1	3.1	3	0	reversabi	Ye
12	11	57	1 asymptot	140	192	0	0	148	0	0.4	2	0	fixed	N
13	12	56	0 nontypica	140	294	0	2	153	0	1.3	2	0	normal	N
14	13	56	1 nontypica	130	256	1	2	142	1	0.6	2	1	fixed	Ye
15	14	44	1 nontypica	120	263	0	0	173	0	0	1	0	reversabi	N
16	15	52	1 nonangini	172	199	1	0	162	0	0.5	1	0	reversabi	N
17	16	57	1 nonangini	150	168	0	0	174	0	1.6	1	0	normal	N
18	17	48	1 nontypica	110	229	0	0	168	0	1	3	0	reversabi	Ye
19	18	54	1 asymptot	140	239	0	0	160	0	1.2	1	0	normal	N
20	19	48	0 nonangini	130	275	0	0	139	0	0.2	1	0	normal	N
21	20	49	1 nontypica	130	266	0	0	171	0	0.6	1	0	normal	N
22	21	64	1 typical	110	211	0	2	144	1	1.8	2	0	normal	N
23	22	58	0 typical	150	283	1	2	162	0	1	1	0	normal	N
24	23	58	1 nontypica	120	284	0	2	160	0	1.8	2	0	normal	Ye
25	24	58	1 nonangini	132	224	0	2	173	0	3.2	1	2	reversabi	Ye
26	25	60	1 asymptot	130	206	0	2	133	1	2.4	1	2	reversabi	Ye

Fig b: Sample Data Set of Patients

VII. RESULT AND ANALYSIS

The random forest algorithm is used to train the data, and the results are verified by the test dataset. To do this, I divide the collection of information into 2 units in the ratio of 70: 30 for training and testing data, respectively. The y value is, in general, the square root of the number of observations. I know the accuracy of the predicted y_pred values is checked to see if they correspond to the known values of prc_test_labels.

The test data consisted of 303 observations. Out of which 160 cases have been accurately predicted (TN->True Negatives) as Absence (A) in nature which constitutes 58%. Also, 143 out of 303 observations were accurately predicted (TP-> True Positives) as Present (P) in nature which constitutes 44%. Thus a total of 160 out of 303 predictions where TP i.e, True Positive in nature.

There were 48 cases of False Negatives (FN) meaning 48 cases were recorded which actually are present in nature but got predicted as benign. The FN's if any poses a potential threat for the same reason and the main focus to increase the accuracy of the model is to reduce FN's.

There were 19 cases of False Positives (FP) meaning 19 cases were actually absent in nature but got predicted as present.

The total accuracy of the model is 84 % ((TN+TP)/303), that means model performance is better.

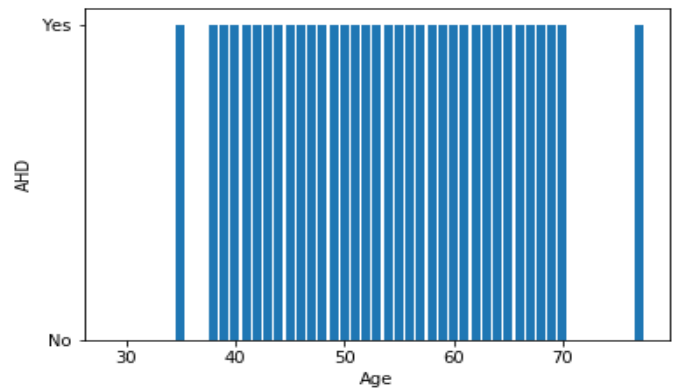


Fig c: Bar Graph Based on Age

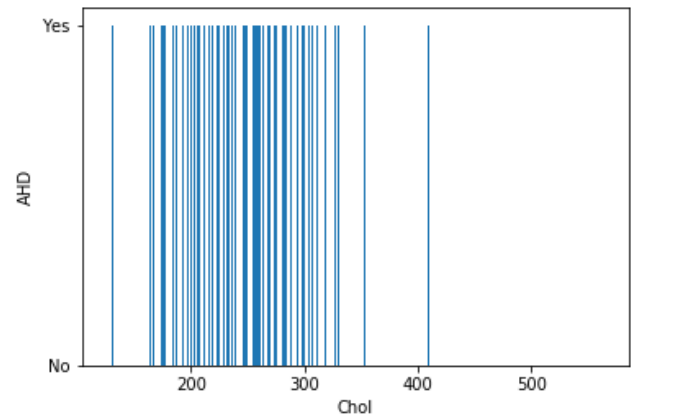


Fig d: Bar Graph Based On Cholestrol

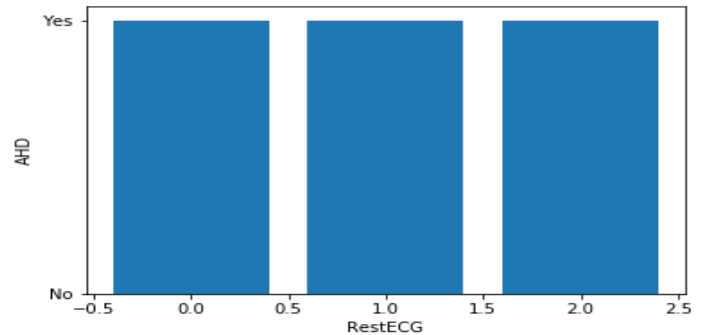


Fig e: Bar Graph Based On RestECG

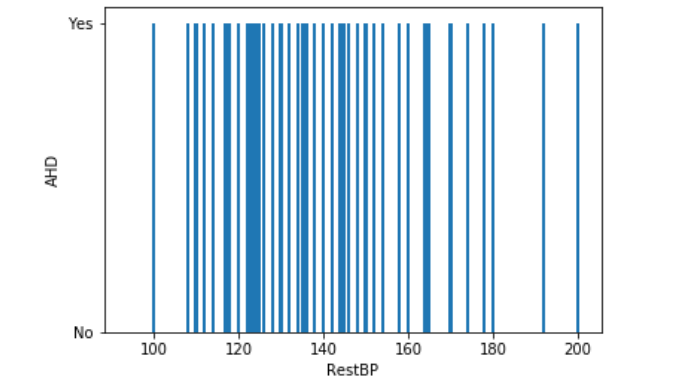


Fig e: Bar Graph Based On RestBP

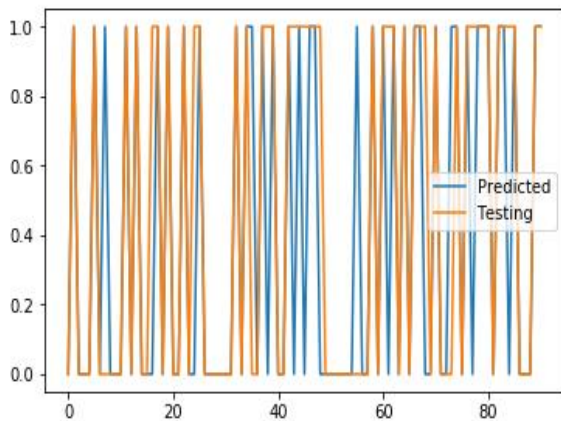


Fig g: Graph Based On Prediction and Testing precision recall f1-score support

0	0.81	0.92	0.86	48
1	0.89	0.77	0.82	43
micro avg	0.85	0.85	0.85	91
macro avg	0.85	0.84	0.84	91
weighted avg	0.85	0.85	0.84	91

Accuracy:0.8461538461538

VIII. CONCLUSIONS

A portable device buy is quite sensitive to the needs of the patient, in view of these devices, and, despite the fact that an allergic disease, it must be borne in mind that at this time of wear. - Due to this problem, such as battery, error or other problems, maybe eliminate the cause of devices that may be bad or termination results. This may also be the reason for the correct analysis. After that, in the long-term infrastructure to get it all finished, to try for a proper calculation should be the first priority for every job.

REFERENCES

- [1] Salih A., Abraham, A.: Review of Ambient Intelligence Assisted Healthcare Monitoring. International Journal of Computer Information Systems and Industrial Management (IJCSIM)5,741-750 (2013) ISSN2150-7988Google Scholar.
- [2] Fizar Ahmed ,Business Information Department, Corvinus University of Budapest, Hungary, Volume 164, April 2017 [36-40].
- [3] Task Force of the European Society of Cardiology. (1996). Heart rate variability standards of measurement, physiological interpretation, and clinical use. Eur Heart J, 17, 354-381.
- [4] Jothi, N., & Husain, W. (2015). Data Mining in Healthcare-A Review. Procedia Computer Science, 72,306-313. Banaee, H., Ahmed, M. U., & Loutfi, A. (2013) 13(12), 17472-17500.
- [5] Alemdar, H., & Ersoy, C. (2010). Wireless sensor networks for healthcare: A survey. Computer Networks, 54(15), 2688-2710.
- [6] Al Ameen, M., Liu, J., & Kwak, K. (2012). Issues realted to security and privacy of health care applications in wireless sensors networks, Journal of medical systems, 36(1), 93-101. Issues realted to security and privacy of health care applications in wireless sensors networks.

- [7] Rose, K., Eldridge, S., & Chapin, L. (2015). The internet of things: An overview. The Internet Society (ISOC), 1-50.
- [8] Mozaffarian, D., Benjamin, E. J., Go, A. S., Arnett, D.K., Blaha, M. J., Cushman, M., ... & Huffman, M. D. (2015). Executive summary: heart disease and stroke statistics—2015 update. Circulation, 131(4), 434-441.
- [9] Canto, J. G., & Iskandrian, A. E. (2003). Cardio Vacular Diseases having major risk factors : debunking the only 50% myth. Jama, 290(7), 947-949.

Forensic Accounting: A Paradigm Shift of Auditing

^[1] Seema Devi, ^[2] Prof Ram Ratan Saini

^[1] Research Scholar, Dept. of Commerce, Maharshi Dayanand University, Rohatk, Haryana, India

^[2] Dept. of Commerce, Maharshi Dayanand University, Rohatk, Haryana, India

Abstract— Organizations need to have forensic accounting as important as profit. Fraud became an accepted part of big business houses' culture. Auditors should be able to detect it and prevent it from becoming a problem but the auditors have their own limitations. In today's world auditors are not enough to deal with fraudulent activities. The forensic accountant is tasked with this difficult job. The data was collected from both internal and external auditors. SPSS 20 software is used to analyze data and the chi square test is applied. The study revealed that fraud is more common in companies with higher turnover. Frauds are more common in the public and govt. sectors. Private companies are more likely to commit financial statement frauds than corruption or asset misappropriation. The study suggested that the forensic accounting should be accepted and applied in organizations to prevent and detect frauds at its early stage.

Keywords: Culture, fraudulent activities, turnover, financial statement frauds.

I. INTRODUCTION

The proverb "Auditors are watch dog, not the bloodhound", outlines the prerequisite skills that auditors must have to deal with the changing business environment. In normal business life, extortion and deceit are common. Every day, newspapers and news channels show a multitude of economic frauds and irregularities. It is important to ask the question: Should we invest in public, private, govt or nonprofit organizations; whom to trust- employees, managers, or owners/executives? Are auditors able to spot fraudulent activities in the organization? An investor who is rational seeks a high return with minimal risk. As a result, expectations from auditors increase. However, there is a gap in expectations between what auditors are expected to do and what they actually do. As investors begin to believe that auditors are only there to provide financial information, the auditor's tagline of "Trust Me" has become less trustable. (Olojede et al., 2020). Forensic accounting is a new branch of accounting that grew out of financial failures in businesses and the failure of auditors meet expectations. Although it is a branch of accounting, forensic accounting seems to be more important than auditing. Failure of auditors spot frauds, resulting in huge losses for investors and companies. Harshat Mehta scam, Vijay Mallya fraud, 2G scam, Coalgate scam and Commonwealth games are just a few examples. The loss to the nation from these scams is numerous. It is imperative that multinational companies, whether they are PriceWaterHouse Copper, Deloitte, or KPMG, appoint auditors who have forensic accounting knowledge. This is why forensic accounting has

become more important in the education sector as well (Akhidime & Uagbale-Ekatah, 2014) (Rezaee et al., 2014). Global study on occupational Fraud and Abuse: A report to nation (2020) shows that frauds are responsible for more than \$3.6 billion in annual losses around the world. It is also suggested that frauds can be detected earlier and will result in a decrease in loss. The loss will increase the longer it takes. Auditors who are familiar with forensic accounting can detect frauds early. An increase in the awareness of frauds by auditors can reduce financial crime court cases. (Evaz & Ramazani, 2012).

An auditor is someone who verifies and confirms the accuracy of financial statements. They also submit a report to management. Auditors review all supporting documents and have face-to-face interaction with employees or managers in the event of any doubts. After verifying and verifying the information, they will be able to determine if there is a shell company, ghost employees or other fraudulent activities. To detect and prevent fraud, an auditor must also be able to perform investigative tasks. Sometimes auditors didn't have enough documents to verify accuracy of financial statements. For financial statements to be accurate, an auditor must have legal and investigative knowledge. Auditors are able to identify fraudulent activity by closely studying documents within organizations. This study examines the auditor's awareness of frauds and fraudulent activity occurring in an organization. The auditors can inspect the managers, employees, owners/ executives, and any other areas that are most closely related to fraudulent activities. When fraud is committed within an organization that auditors cannot identify, the forensic accountant is called. Organizations are most vulnerable to fraud due to misrepresentations of financial statements and misappropriation of resources. (Enofe et al., 2015). In the past, forensic accounting was not in existence. It was auditors that identified fraudulent activities and prevented them from happening again. Although auditors and forensic accountants have similar skills but the roles of these professionals are quite different. While auditors are bound by generally accepted accounting standards and principles, the power of a forensic accountant is unlimited. They are not responsible at all stages of an investigation. It assists companies in reaching their goals by using a systematic and disciplined approach to assess and improve the effectiveness and efficiency of their risk management, control, governance processes. (Shaheen et al., 2014). The reality is that accountants focus on the numbers, while forensic accountants are more interested in the facts. (Okoye, E.I. & Gbegi, 2013). Forensic accountants can see beyond the numbers and deal directly with the business realities. It is a prominent profession that specializes

in analysis, interpretation, summarization and presentation. (Bhasin, 2007) Auditors aren't mentally equipped to spot frauds. Mind-set, rather than methodology, will probably be the best method of detecting frauds. (Singleton et al., 2006).

II. REVIEW OF LITERATURE

Forensic accounting can be described as old wine in a new bottle. Although its origin is not new, its increasing importance is attracting the attention of all parties. Auditors shouldn't limit themselves to verifying accuracy and completeness of documents. This is where their proficiency and capacity are more. Although they are not often in command, forensic auditors work with organizations continuously. (Dibia, 2017) (Konar & Aiyar, n.d.). Auditors are objective and subjective in their opinions. Their ability to resolve 30-40% of frauds within an organization cannot be doubted. The auditor needs to learn investigative skills to meet the expectations of investors and the company. 39% of organizations today accept the need for forensic accounting. (Mishra & Singh, 2017) (Chakrabarti, 2014). An auditor's ability to detect fraudulent activity can help reduce mismanagement and frauds. Beyond the basics of auditing, the forensic accountant can use special techniques to detect and prevent frauds such as Benford's Law and Theory of relative size factor. As they handle all aspects of financial audits, chartered accountants are the best suited for forensic auditors. An auditor can acquire expertise by completing a rigorous and thorough training program, a post-qualification degree, or obtaining a diploma in investigation. (Dutta, 2018) (Moid, 2016) (Biswas et al., 2013) (Asllani & Naco, 2014). India's white collar crime boom is due to the delusion of unlimited profit and failure of law enforcement. These financial crimes crash the economy and entrepreneurial spirit. While auditors evaluate the risk and provide reports, forensic auditors (also known as investigator) use investigative techniques to examine human behavior and present evidence in legal proceedings. Auditing failures can be caused by frauds such as improper management, rotation of auditors according to their needs, verification and bias in the appointment of auditors. These are the reasons for a new area of accounting, forensic accounting. (Lama & Chaudhuri, n.d.) (Mcgurrian et al., 2013) (Silverstone & Sheetz, 2007) (Sharma, 2014). India is the most corrupted country in BRICS, with 40% of frauds significantly higher than 32% of the global average. As a result, white collar crime and financial crimes are more common in India than elsewhere. No university offers forensic accounting as a part of their curriculum. Forensic accounting was found to be the most effective tool for detecting fraudulent transactions and assessing risk. External and internal auditing also benefit from forensic accounting. (Singh et al., 2015) An auditor is someone who works within an organization to improve the lives of all stakeholders. However, the forensic auditor also

works for the court as an expert opinion and consultant in litigation. (Yadav & Yadav, 2013) (Singleton et al., 2006) (Golden et al., 2006) (Upadhyay, 2018) (Peshori, 2015). The internal control system within an organization provides a foundation for detection and prevention of fraud. Auditors identify red flags and evaluate fraud possibilities. Audit procedures are used by auditors to reduce frauds. However, only 56 of the 218 audit procedures are effective. Auditors can only investigate as much as they are allowed. This indicates weaknesses in the internal control system. Forensic accounting is essential. The technology-assisted techniques can be used to help auditors identify frauds, but small businesses are reluctant to spend large amounts on activities that might not occur. Auditors can also play a significant role in fraud prevention if they are able to work on their own. (Ejoh & Ojong, 2017) (Gould, 2012) (O. R. Gray & Moussalli, 2014). A forensic accountant is a combination of an auditor and a private investigator, with more skills than the auditors. The court of law is the source for forensic accounting standards. Therefore, the expert witness in court is the forensic accountant. Auditors are not appointed to prevent fraud but to identify and prevent errors. The chances of fraud becoming a problem are reduced if errors can be identified and stopped promptly. Auditors cannot go through every transaction. Fraud can still occur if there is a material error. Frauds can still occur even after the audit of financial statements. SAS 99 states that auditors are only responsible for identifying fraud possibilities. Management and organizations are responsible for preventing or detecting fraudulent activity. (D. Gray, 2008). Effective auditing requires auditors to have communication skills, multidisciplinary skills, and strategic thinking. Financial frauds can be controlled by having a strong internal control system and good corporate governance. (Rathnasiri & Bandara, 2018). For the betterment and development of the economy, it is vital to be informed about the requirements and scope of forensic accountants. (Evans, 2020)

III. RESEARCH METHODOLOGY

This exploratory study uses both primary and secondary data. Secondary data was gathered from published Govt. reports, global survey reports such as Deloitte, Price water House and KPMG, which aid in identifying the problem. 105 external auditors and internal auditors were selected from the public, private, NPO's, and govt companies. A structured questionnaire is used to collect information. 14 questions were used to determine the auditors' knowledge of fraud. This questionnaire is designed to assess auditors' abilities to detect and prevent fraud. These hypotheses can be developed using descriptive analysis or chi square non parametric tests. Statements of Auditors awareness regarding fraudulent activities in organization

Table 1: Statements used for data analysis and interpretation

1. Gender:
1) Male
2) Female
3) Transgender
2. Age:
1) 21-35
2) 35- 50
3) 50- 65
3. What is your organizational position -
1) Internal Auditor
2) External Auditor
3) Both
4. Level of awareness of Forensic accounting.
1) Highly aware
2) Moderate aware
3) Low aware
5. What is your source of awareness of forensic accounting. (Can tick more than one)
1) Part of syllabus content
2) Any course/ Diploma/ Degree
3) govt. documentation
6. What is tenure of your service.
1) Below 10 years
2) 10-20
3) 20-30
4) 30 and above.
7. Which type of Organization you are working in.
1) Private
2) Public
3) Govt.
4) Non-profit org.
8. Nature of Industry you are serving.
1) Manufacturing
2) Service
3) Trading
9. What is the Turnover of your organization (per annum).
1) Below 5 crore
2) 5-50 crore
3) 50- 250 crore
4) 250 and above
10. In previous time, is any fraud identified in organization where you are serving now.
Yes () no ()
11. Which category is more closely related to fraud.
1) Employee
2) Managers
3) Owners/ executives
12. What do you think in which area risk of fraud is high.
1) Asset Misappropriation
2) Corruption
3) Financial statement fraud

Source: Author's own

Analysis and interpretation

Hypothesis 1

H0: There is no association between tenure of service and level of awareness of auditors.

H1: There is association between tenure of service and level of awareness of auditors.

Table 2: Association between tenure of service and level of awareness

			Level of awareness of forensic accounting		
			Highly aware	Moderate aware	low aware
Tenure of service	below 10 years	Observed	17	12	6
		Expected	10.3	19.0	5.7
	10-20	Observed	9	8	1
		Expected	5.3	9.8	2.9
	20-30	Observed	2	32	0
		Expected	10.0	18.5	5.5
	30 and above	Observed	3	5	10
		Expected	5.3	9.8	2.9

Source: SPSS 21

Table 2 (a)

Chi-Square Tests				
	Value	Df	Asymp. (2-sided)	Sig.
Pearson Chi-Square	53.479	6	.000	

Source: SPSS 21

Table 2 (b)

Symmetric Measures			
		Value	Approx. Sig.
Nominal by Nominal	Phi	.714	.000
	Cramer's V	.505	.000

Source: SPSS 21

Interpretation: Chi square test is significant as p value <0.05, so null hypothesis is not accepted (rejected) i.e. there is no significance association between age and level of awareness of auditors. Even Cramer's V (0.505) found more than moderately strong association between the variables. As shown in Table 2 auditors having below 10 years' experience, say newly appointed, are highly aware about forensic accounting. The auditors with tenure of 10-20 years are also highly aware but less than whom having below 10

years' experience. Auditors with 20-30 years' service are moderately aware and 30 above are also aware but at low level.

Hypothesis 2

H0: There is no association between source of awareness and level of awareness of forensic accounting.

H1: There is association between source of awareness and level of awareness of forensic accounting.

Table 3: Association between source of awareness and level of awareness of forensic accounting

			Level of awareness of forensic accounting		
			Highly aware	Moderate aware	low aware
Your source of awareness of forensic accounting	Part of syllabus content	Observed	0	3	1
		Expected	1.2	2.2	.6
	Any course/Diploma/Degree	Observed	1	2	0
		Expected	.9	1.6	.5
	Govt. Documentation	Observed	0	8	15
		Expected	6.8	12.5	3.7
	Any Course/Diploma/Degree+Govt. Documentation	Observed	1	20	0
		Expected	6.2	11.4	3.4
	Part of syllabus content+ govt documentation	Observed	0	20	1
		Expected	6.2	11.4	3.4
	Part of syllabus content+Any course+Govt documentation	Observed	29	4	0
		Expected	9.7	17.9	5.3

Source: SPSS 21

Table 3(a)

Chi-Square Tests				
	Value	Df	Asymp. (2-sided)	Sig.
Pearson Chi-Square	127.666	10	.000	

Source: SPSS 21

Table 3(b)

Symmetric Measures			
		Value	Approx. Sig.
Nominal by Nominal	Phi	1.103	.000
	Cramer's V	.780	.000

Source: SPSS 21

Interpretation: As $p < 0.05$ and Cramer's V value is .780 so, a highly strong significant association is found between the variables and null hypothesis i.e. there is no significant association between source of awareness and level of awareness of internal, external and both auditors; is not accepted.

Hypothesis 3

H0: There is no association between type of organization and category related to fraud.

H1: There is association between type of organization and category related to fraud.

Table 4: Association between type of organization and category related to fraud

			Category more closely related to fraud		
			Employee	Managers	Owners/Executives
Type of organization you are working in	Private	Observed	2	3	25
		Expected	16.3	6.0	7.7
	Public	Observed	20	1	0
		Expected	11.4	4.2	5.4
	Govt	Observed	28	6	2
		Expected	19.5	7.2	9.3
	Non profit org.	Observed	7	11	0
		Expected	9.8	3.6	4.6

Source: SPSS 21

Table 4 (a)

Chi-Square Tests				
	Value	Df	Asymp. (2-sided)	Sig.
Pearson Chi-Square	97.265	6	.000	

Source: SPSS 21

Table 4 (b)

Symmetric Measures			
		Value	Approx. Sig.
Nominal by Nominal	Phi	.962	.000
	Cramer's V	.681	.000

Source: SPSS 21

Interpretation: Table 4 (a), 4 (b) indicate that there is significant and strong association between the variables. Thus, null hypothesis is not accepted (rejected), that, there is no significant association between type of organization and category related to fraud. The table 4 represents that in private sector owners/ executives are most commonly related to the fraud and in public & Govt. sector the fraudsters are

employees. In the non-profit organization, managers are more indulged in fraudulent activities.

Hypothesis 4

H0: There is no association between Type of organization, nature of organization and Area of highest fraud risk.

H1: There is association between Type of organization, nature of organization and Area of highest fraud risk.

Table 5: Association between Type of organization, nature of organization and Area of highest fraud risk.

Nature of organization				Area in which risks of fraud is high		
				Asset Misappropriation	Corruption	Financial Statement Fraud
Manufacturing	Type of organization you are working in	Private	Observed	0	1	7
			Expected	5.6	1.1	1.3
		Public	Observed	13	0	0
			Expected	9.1	1.8	2.1
		Govt	Observed	17	5	0
			Expected	15.3	3.1	3.6
Service	Type of organization you are working in	Private	Observed	1	0	10
			Expected	2.8	5.3	3.0
		Public	Observed	2	0	1
			Expected	.8	1.4	.8
		Govt	Observed	6	5	1
			Expected	3.0	5.7	3.3
		Non profit org.	Observed	2	16	0
			Expected	4.5	8.6	4.9
Trading	Type of organization you are working in	Private	Observed	0		11
			Expected	3.7		7.3
		Public	Observed	5		0
			Expected	1.7		3.3
		Govt	Observed	1		1
			Expected	.7		1.3

Source: SPSS 21

Table 5 (a)

Chi-Square Tests				
Type of serving organization		Value	df	Asymp. Sig. (2-sided)
Manufacturing	Pearson Chi-Square	41.127	4	.000
Service	Pearson Chi-Square	43.611	6	.000
Trading	Pearson Chi-Square	129.163	6	.000

Source: SPSS 21

Table 5 (b)

Symmetric Measures					
Type of serving organization			Value	Approx. Sig.	
Manufacturing	Nominal	by	Phi	.978	.000
	Nominal		Cramer's V	.692	.000
Service	Nominal	by	Phi	.996	.000
	Nominal		Cramer's V	.704	.000
Trading	Nominal	by	Phi	.935	.000
	Nominal		Cramer's V	.935	.000

Source: SPSS 21

Interpretation: From the above table 5 (a) a significant association can be measure between the variables. The values of Cramer's V (.692, .996, .935, .784) indicates the association is highly strongly significant. Chi-square table represents that in private manufacturing company's financial statement frauds (as Observed-7, Expected 1.3), in public companies fraud of asset misappropriation (as Observed-13, Expected 9.1) and in govt. manufacturing companies' asset misappropriation and corruption (as Observed-17, Expected 15.3, 5 and 3.1) can be found. Similarly, in service providing

private companies financial statement frauds can be seen in govt. service sector asset misappropriation and non-profit organizations are high level of corruption. The trading private companies having financial statement frauds and public trading companies have asset misappropriation.

Hypothesis 5

H0: There is no association between turnover of organization (per annum) and identification of fraud.

H1: There is association between turnover of organization (per annum) and identification of fraud.

Table 6: Association between turnover of organization (per annum) and identification of fraud

			any fraud identified in organization where you are serving	
			Yes	No
Turnover of organization per annum	Below 5 Crore	Observed	4.5	12
		Expected	7.2	4.8
	5-50 crore	Observed	23	24
		Expected	28.2	18.8
	50-250 crore	Observed	12	4
		Expected	9.6	6.4
	250 and above	Observed	28	2
		Expected	18.0	12.0

Source: SPSS 21

Table 6 (a)

Chi-Square Tests				
	Value	Df	Asymp. (2-sided)	Sig.
Pearson Chi-Square	35.786 ^a	3	.000	

Source: SPSS 21

Table 6(b)

Symmetric Measures			
		Value	Approx. Sig.
Nominal by Nominal	Phi	.584	.000
	Cramer's V	.584	.000

Source: SPSS 21

Interpretation: The association between turnover of the company and identification of fraud is strongly significant (Cramer's value .584, more than .5), the null hypothesis is not accepted (rejected) i.e. There is no significant association between turnover of organization and fraud identified. As chi square table indicates companies with below 5 crore and 5-50 crore turnover facing less fraudulent activities but companies with higher turnover i.e. 50-250 & 250 and above are facing more frauds. Thus, higher the turnover of the company, higher will be the fraud risk.

IV. CONCLUSION AND SUGGESTIONS

Analysis and interpretation represent the relationship between variables. All hypotheses are accepted at p 0.05. Significant association is shown by Cramer's V value. The findings show that auditor's awareness is strongly associated with the length of time served by both internal and external auditors. Newly appointed auditors with less than 20 years' experience in forensic accounting are well-aware. The Table 3 shows that highly-aware auditors were aware of a variety of sources, including government papers, a course and a syllabus. Auditors are now taking forensic accounting courses to expand their knowledge. Forensic accounting is a hot topic. Based on their experiences, the auditors are asked about their perception of which type of organization is most closely linked to fraud. This includes their views of employees, managers and owners/executives. The auditors found that owners/executives in the private sector are more involved with fraudulent operations than employees in

government and public sectors. Managers are more involved in fraud in non-profit organizations. The Researcher also discovered an association between the nature of companies such as manufacturing, trading and service. This was in addition to the type of company and the area of fraud. Financial statement frauds in manufacturing, trading and service sectors are most closely linked to the private sector. Public companies mainly deal with asset misappropriation. Companies that are facing misappropriation of assets in the manufacturing or service sector, NPOs will adjust with corruption (Table-5). Table 6 shows that the risk of misappropriation is higher for companies with higher turnover.

Forensic accounting, a new area of accounting, is drawing the attention of both investors and auditors. A company with forensic accountants can quickly identify frauds. It also increases creativity and investigative skills. Institutes that offer chartered accountant courses understand the importance of forensic accounting awareness among auditors. The type and extent of fraud or loss can vary depending on the organization and the perpetrator. According to a report to the countries (Global study of occupational fraud and abuse 2020), asset misappropriation frauds are the most prevalent fraud in nations, but they are also the less costly. On the other hand, financial statements frauds are the least common, but are high-cost and corruption is the most widespread in world economies. Large organizations are most at risk for fraud. Despite only 20% of the fraud committed by their owners/executives, the risk of losing money is very high. Private companies that have a higher turnover often face more frauds than those with smaller turnover. Fraudsters

are a common threat to large business houses. They should appoint auditors who are familiar with forensic accounting. Auditors work within their boundaries. This is why they cannot deter, detect and prevent fraud from being committed by organizations. Although auditors may be aware of what is going on in an organization, they are not able to reveal the frauds due to lack of evidence and management support. Forensic accountants can be called when frauds have been committed. They also provide assistance in court when required. The literature shows that auditors cannot identify all frauds and only 30% to 40% of frauds can be solved by them. Auditors and organizations should accept forensic accounting and apply whenever they identify red flags. It will prevent organizations from huge risk of loss and get rid of from fraud at early stage.

REFERENCES

- [1] Akhidime, E., & Uagbale-Ekatah, R. E. (2014). The Growing Relevance of Forensic Accounting as a Tool For Combating Fraud and Corruption: Nigeria Experience. *Research Journal of Finance and Accounting*, 5(2), 2222–2847.
- [2] Asllani, A., & Naco, M. (2014). Using Benford's Law for Fraud Detection in Accounting Practices. *Journal of Social Science Studies*, 2(1), 129–143. <https://doi.org/10.5296/jsss.v2i1.6395>
- [3] Bhasin, M. (2007). Forensic Accounting: A New Paradigm For Niche Consulting. *The Chartered Accountant*, January, 1000–1010.
- [4] Biswas, M., Hiremath, K. G., & Ramaswamy, S. (2013). Forensic Accounting in Indian Perspective. The 5th International Conference on Financial Criminology (ICFC): Global Trends in Financial Crimes in the New Economies, 98–106.
- [5] Chakrabarti, M. (2014). Problems and Prospects of Forensic Accounting Profession in India. *International Journal for Informative and Futuristic Research*, 59(6), 1–9.
- [6] Dibia, N. O. (2017). An Overview of Forensic Accounting in Nigeria. *Journal of Finance and Economic Research*, 3(2), 104–109.
- [7] DUTTA, P. P. (2018). Forensic Accounting in India: A new vibrant approach to prevent white collar crimes: an empirical study. *International Journal of Basic and Applied Research*, 8(9), 1122–1137.
- [8] Ejoh, & Ojong, N. (2017). Forensic Accounting, Internal Controls and Fraudulent Practices in Nigeria. *Scholars Journal of Economics, Business and Management*, 4(8B), 555–562. <https://doi.org/10.21276/sjebm>
- [9] Enofe, A. O., Agbonkpolor, O. R., & Edebiri, O. J. (2015). Forensic Accounting and Financial Fraud. *International Journal of Multidisciplinary Research and Development*, 2(10), 305–312.
- [10] Evans, C. D. (2020). Forensic Accounting and Fraud Deterrence. *Corporate Fraud Exposed*, 261–278. <https://doi.org/10.1108/978-1-78973-417-120201017>
- [11] Evaz, H., & Ramazani, M. (2012). Accountant's Perception of Forensic Accounting (Case Study of Iran). *Global Journal of Management and Business Research*, 12(6).
- [12] Golden, T. w., Skalak, S. L., & Clayton, M. M. (2006). A Guide to Forensic Accounting Investigation.
- [13] Gould, M. (2012). Forensic Accounting. Institute of Certified Public Accountants of Pakistan, Module 6. <https://doi.org/10.4135/9781412964289.n407>
- [14] Gray, D. (2008). Forensic Accounting And Auditing: Compared And Contrasted To Traditional Accounting And Auditing. *American Journal of Business Education (AJBE)*, 1(2), 115–126. <https://doi.org/10.19030/ajbe.v1i2.4630>
- [15] Gray, O. R., & Moussalli, S. D. (2014). Forensic Accounting and Auditing United Again: A Historical Perspective. *Journal of Business Issues*, 2006(2), 15–25.
- [16] Konar, E. M., & Aiyar, S. (n.d.). A STUDY ON FORENSIC ACCOUNTING PROFESSION IN INDIA AND AROUND THE WORLD. *Tactful Management Research Journal*, 85–91, ISSN: 2319-7943.
- [17] Lama, M., & Chaudhuri, M. (n.d.). Forensic Accounting: a Study of Its Role in Investigating Corporate Frauds and Scams in India. 11th International Conference on Science, Technology and Management, Osmania University Centre for International Program, Osmania University Campus, Hyderabad (India), 72–84, www.conferenceworld.in, ISBN:978-93-86171-9. <http://data.conferenceworld.in/11ICSTM/11.pdf>
- [18] Mcgurrin, D., Jarrell, M., Jahn, A., & Cochrane, B. (2013). White Collar Crime Representation in the Criminology Literature Revisited, 2001-2010. *Journal of the Western Society of Criminology*, 14(2), 3–19.
- [19] Mishra, S., & Singh, G. (2017). Forensic Accounting: An Emerging Approach to Deal with Corporate Frauds in India. *Global Journal of Enterprise Information System*, 9(2), 104–109. <https://doi.org/10.18311/gjeis/2017/15922>
- [20] Moid, S. (2016). Application of Forensic Accounting to Investigate Scams in India. *MJBR - MITS International Journal of Business Research*, 3(1), 24–31. [http://www.mba.mits.ac.in/MJBR/Article 4 Sana - Forensic Accounting.pdf](http://www.mba.mits.ac.in/MJBR/Article%204%20Sana%20-%20Forensic%20Accounting.pdf)
- [21] Okoye, E.I. & Gbegi, D. O. (2013). Forensic Accounting : A Tool for Fraud Detection and Prevention in the public sector. *International Journal of Academic Research in Business and Social Sciences*, 3(3), 1–19. www.hrmas.com/journals
- [22] Olojede, P., Erin, O., Asiriwu, O., & Usman, M. (2020). Audit expectation gap: an empirical analysis. *Future Business Journal*, 6(1), 1–12. <https://doi.org/10.1186/s43093-020-00016-x>
- [23] Peshori, C. (2015). Forensic Accounting a Multidimensional Approach to Investigating Frauds and Scams. *International Journal of Multidisciplinary Approach & Studies*, 2(3), 26–36. <http://ijmas.com/upcomingissue/04.03.2015.pdf>
- [24] Rathnasiri, U. A. H. A., & Bandara, R. M. S. (2018). The Forensic Accounting in Sri Lanka "Perception of Professional Accountants." *Kelaniya Journal of Management*, 6(2), 68–82. <https://doi.org/10.4038/kjm.v6i2.7546>
- [25] Rezaee, Z., Lo, D., & Ha, M. (2014). International Emergence of Forensic Accounting Education and Practice. *Open Journal of Social Sciences*, 02(12), 1–3. <https://doi.org/10.4236/jss.2014.212001>
- [26] Shaheen, I., Pranathi, Sultana, A., & Noor, A. (2014). Forensic accounting and fraud examination in India. *International Journal of Innovative Research & Development*, 3(12), 171–177.
- [27] Sharma, A. (2014). Frauds in India and Forensic Accounting. *International Journal of Research & Development in Technology and Management Science -Kailash*, 21(5), 200–207. <http://journal.rtmonline.in/vol21iss5/053066.pdf>
- [28] Silverstone, H., & Sheetz, M. (2007). Forensic Auditing and Fraud Investigation for Non-Experts.
- [29] Singh, D., Grewal, M., & Jaspal, M. (2015). Forensic Accounting as Fraud and Corruption Detection Tool: An Empirical Study. *International Journal of Science Technology and Management (IJSTM)*, 486–495. <http://data.conferenceworld.in/ICSTM2/P486-495.pdf>
- [30] Singleton, T., Singleton, A., Bologna, J., & Lindquist, R. (2006). *Fraud auditing and Forensic Accounting*. <https://books.google.com/books?hl=en&lr=&id=HN4KzIG8q7wC&oi=fnd&pg=PR3&dq=related:mqVg4uVQ8SMJ:scholar.google.com/&ots=B-4xeYZu60&sig=2ZwyTEuNn4s8-NXOedidRaJ8Y>
- [31] Upadhyay, J. P. (2018). Application of Forensic Accounting in Nepal. *NCC Journal*, 3(1), 82–89. <https://doi.org/10.3126/nccj.v3i1.20250>
- [32] Yadav, S., & Yadav, S. (2013). Forensic accounting: A new dynamic approach to investigate fraud cases. *EXCEL International Journal of Multidisciplinary Management Studies*, 3(7), 1–9. <http://www.indianjournals.com/ijor.aspx?target=ijor:xijmms&volum=3&issue=7&article=001>

Websites

- [33] <https://fcpasyoungandlicensed.com/2016/04/04/the-difference-between-forensic-accounting-and-auditing/>
- [34] <https://www.ace.com/report-to-the-nations/2020/>
- [35] <https://www.pwc.com/gx/en/services/forensics/economic-crime-survey.html>
- [36] <https://www2.deloitte.com/in/en/pages/finance/topics/forensic/india-corporate-fraud-perception-survey-2020.html>

Arduino Based Patient Health Monitoring System using Internet of Things

^[1] Shadakshari, ^[2] Charutha M V, ^[3] Shyamala P Bhat

^[1] Assistant Professor, Raja Reddy Institute of Technology, Bangalore

^[2] Assistant Professor, Raja Reddy Institute of Technology, Bangalore

^[3] Assistant Professor, Raja Reddy Institute of Technology, Bangalore

Abstract— The main focus of this project is to implement a prototype model for the real time patient monitoring system. The proposed project is used to measure the physical parameters like body temperature, heart beat rate and ECG of the patient with wireless communication technology. In this system, the patient health will be monitored and the data which is collected is transmitted to Wifi wireless networks. Arduino Nano embedded processor supports for analysing the input from the patient and the results of all the parameters will be stored in the database. The proposed system uses ECG sensor, heart beat sensor and temperature sensor to measure the physical parameters of the patient. Arduino controller controls the complete operations of the proposed system. If the abnormality is sensed then an alert message will be sent to the concerned ward through GSM.

Keywords: Arduino Nano, ECG Sensor, Heartbeat sensor, Temperature Sensor.

I. INTRODUCTION

Nowadays Wireless Sensor Network (WSN) plays an important role in the field of research, which results in the development of various smart sensing systems. New research is focusing at improving the quality of human life in terms of health by designing and fabricating sensors which are in contact with the human body directly or indirectly. Health monitoring is an informal, non-statutory method of surveying our workforce for symptoms of ill health, including the back pain. This type of occupational health management system will enable us as an employer, awareness of health problems and its prevention is very much important. Another important role of health monitoring is to give feedback into a system that reviews the current control methods in a place. In addition, there are specific regulations dealing with manual handling and whole body vibration in the workplace. To ensure the duties under these regulations one should refer the HSE (health system engineering) guidance, if manual handling or whole body vibrations are at risks in their workplace.

The development of biomedical engineering is responsible for improving healthcare diagnosis, monitoring and therapy. The novel idea behind the proposed health line is to provide quality health service to everyone. This idea is driven by the vision of a cable free biomedical monitoring system. On-body sensors monitor the vital parameters (ECG, temperature and heart beat rate) and transmits the data to the doctor via wireless communication network. Periodic health

monitoring allows people to discover and treat health problems early, before they have consequences. Especially for risk patients and long term applications, such technology offers more freedom, comfort and opportunities in clinical monitoring.

II. LITERATURE SURVEY

[1] Microcontroller based system which sends the text message to the mobile phone. When the readings are not normal or increased beyond the threshold level, the device sends the report of patient's health condition along with the location to the caretaker's phone. [2] This system is designed to monitor health parameters. Data is collected from the sensors which are connected to the arduino and the data is uploaded to the web page through the internet. [3] Here, four layers namely, sensor layer, network layer, internet layer and service layer are used. Data is collected from the sensors and data communicated with the help of different protocols and stored in the cloud.[4] Credit card sized minicomputer is placed beside the patient's bed with power and results can be seen on the screen of computer which is in the same area network. It provides readings of body temperature and heartbeat. The detected values will be uploaded on the webpage.[5] System monitoring of ECG wave using panda board is proposed which is connected to the Ethernet for internet connection. Health parameters like body temperature, heart rate and ECG can be measured.

III. METHODOLOGY

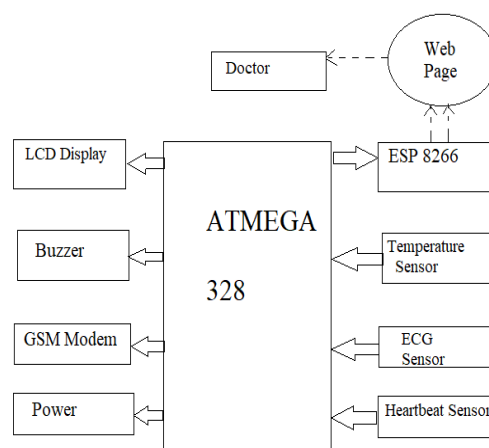


Fig.1 Block diagram of proposed system

The diagram is divided into two sections: Transmitter and receiver. In the transmitter section, the data is collected with the help of sensors that are connected to the Arduino ATMEGA 328. A threshold level is set considering the parameters of the healthy person, if it exceeds the threshold value then the data is sent to the server using ESP and

thereby the caretaker gets the message using GSM module. In the receiver section, a web page is built and data collected is displayed on the web page. Doctors can login to the webpage through the IP address and collect the required information. The data stored in a database can be accessed only by the authorized personnel.

IV. IV. EXPERIMENTAL RESULTS

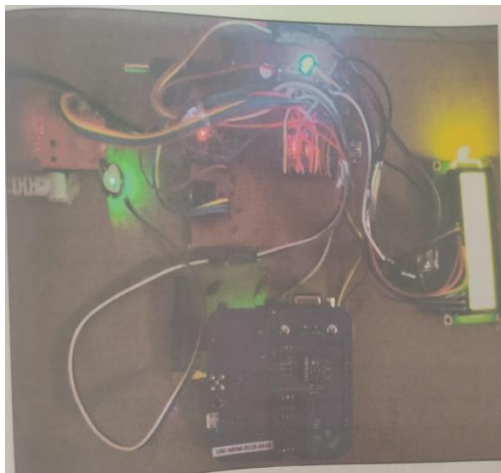


Fig.2 Prototype of the proposed system

Fig. shows the interfacing of all the sensors to the microcontroller and the connection with LCD display.

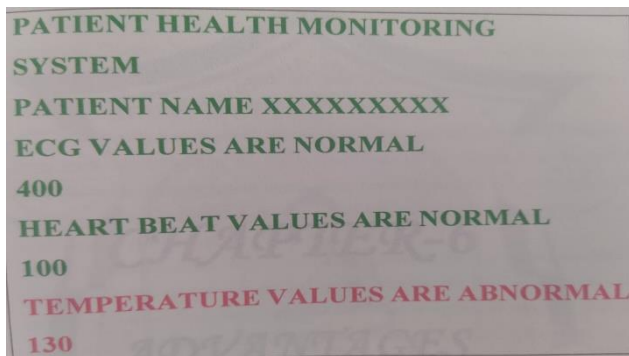


Fig.3 Data displayed on the webpage

Fig shows the health parameters of the person. Different values for heart beat, ECG, Temperature will be displayed. If the threshold value of the parameters is increased then it will be displayed in the colour red on the web page. The values which are normal will be displayed in the colour green.

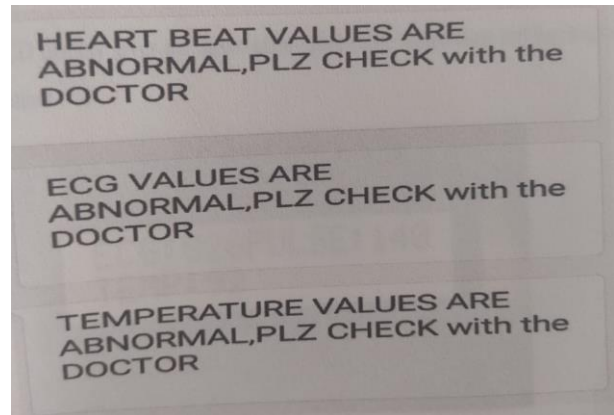


Fig.4 Message sent through GSM

Fig shows the message which will be sent to the caretaker when the health parameters exceed the threshold value. Message along with the particular abnormal health parameter will be sent to the caretaker so that they can monitor the patient's condition accordingly.



Fig.5 Values displayed on LCD

Fig. shows the health parameter values displayed on LCD. If the patient or doctor wishes to check the parameter values they can check it through this LCD.

V. CONCLUSION

The progress in bio medical engineering, science and technology paved way for new inventions and technologies. As the technology is moving towards miniaturization, handy electronic components are in great demand. New products and new technology are being invented. Arduino was found to be more compact, user friendly and less

complex, which could readily be used in order to perform several tedious and repetitive tasks. Simulation is performed using Proteus software by placing appropriate sensors like temperature and heart beat rate for sensing health condition and the results analysed under normal and abnormal conditions.

REFERENCES

- [1] Augustus E. Ibhaze, MNSE, Francis E. Idachaba, et al., “E-Health Monitoring System for the Aged IEEE International Conference on Emerging Technologies, 2016.
- [2] Punit Gupta, Deepika Agarwal et al., “IOT based Smart HealthCare Kit” Jaypee University of Information Technology. Himachal Pradesh, India, IEEE, 2015.
- [3] KaleemUllah, MunamAli, et al., “Effective Ways to Use Internet of Things in the Field of Medical and Smart Health Care”, IEEE International Conference on Identification, 2015.
- [4] AbhilashaIngole, ShrikantAmbatkar, Sandeep Kakde, et al., “Implementation of Health-care Monitoring System using Raspberry Pi”, IEEE ICCSP conference, 2015.
- [5] Amir-Mohammad Rahmani, Nanda Kumar Thanigaivelan et. al., “Smart e-Health Gateway: Bringing Intelligence to Internet of Things Based Ubiquitous Healthcare Systems”, IEEE consumer communications and networking, 2015.
- [6] M. Weislik, M. Pozoga, P. Smerdzynskiet al., “Wireless Health Monitoring System”, IFAC(International Federation of Automatic Control) Hosting by Elsevier Ltd, 2015.
- [7] VandanamilingRohokale, Li Da Xu et al., “Ubiquitous Data Accessing Method in IOT-Based Information system for emergency medical services” Federation of Automatic (International Federation of Automatic Control) Hosting by Elsevier Ltd, 2014.
- [8] Joao Martinhoa, LuisPratesa, Joao Costaa et al., “Design and Implementation of a Wireless Multi Parameter Patient Monitoring System”, Conference on Electronics, Telecommunications and Computers – CETC Hosting by Elsevier Ltd, 2014.
- [9] Hoi Yan Tung, Kim Fung Tsang et al., “The Design of Dual Radio Zigbee Homecare Gateway for Remote Patient Monitoring”, IEEE Transactions on Consumer Electronics, November 2013.
- [10] Luigi Atzoriet, “The Internet of Things: A survey”, Computer Networks, 2010.

BLDC Motor Based Solar Photovoltaic Array Fed Water Pumping System Using Interleaved Boost Converter

^[1] Shailesh Kumar, ^[2] Shashi Bhushan Singh

^[1] M.Tech Student, ^[2] Assistant Professor

^{[1][2]} Department of Electrical Engineering, National Institute of Technology Kurukshetra, Haryana-136119, India

Abstract— Renewable energy is a safe and environment friendly source of power. Solar power systems have a long history of research, cheap manufacturing costs, and great efficiency. As energy consumption rises, energy output will no longer be able to satisfy the full load need so in future for fulfillment of energy demand solar energy will be best option. This paper discussed the use of Brushless dc motor to satisfy a sustained water pumping frame (BLDC). Perturbation and observation (P&O) MPPT Controller used in the solar photovoltaic array to extract maximum power available. The system proposed includes an arrangement of solar panels, Interleaved boost converter, three phase voltage source inverter and Brushless dc motor. An appropriate control of Interleaved boost converter through the Perturb & Observe maximum power point tracking (P&O MPPT) algorithm offers good starting of the BLDC motor. Interleaved boost converter fed BLDC motor with PID controller is designed to examine and optimise Torque, speed performance and efficiency. This paper is going to investigate different operating conditions for solar photovoltaic array for different solar irradiance. Simulation results using MATLAB/SIMULINK 2018a show the suitability of suggested method under actual operating conditions.

Keywords: Photovoltaic systems, Interleaved Boost converter, P&O MPPT, VSI, and BLDC Motor.

I. INTRODUCTION

Nowadays Solar photovoltaic (SPV) energy has developed as a viable alternative to traditional electricity generating. With the growing depletion of fossil fuels, the cost of a solar PV array has dropped dramatically in the recent decade, making solar energy one of the most reliable non-renewable energy sources. Solar energy is an endless energy source that can be harvested using solar PV array systems and solar thermal systems. Due to the lower cost of solar PV material and pollution-free energy generation, academicians, researchers, scientists and industrialists are becoming more interested in solar PV systems.

The gradual decline in the cost of power Electronics equipment, as well as the imminent depletion of fossil fuels, promote the use of solar photovoltaic provided electrical energy for a variety of applications. Water pumping systems is used widely because of using as a standalone application of electricity generated by solar photovoltaics, is gaining popularity these days because of It can be used as

agriculture area, industrial applications and household applications. For the Standard Test Condition(STC) the temperature(T) should be 25° C, the air mass(AM) should be 1.5, and the light intensity(Insolation) deciduous on solar panels should be 1000 W/m². PV system efficiency and performance are affected by a variety of operating conditions [1]. Because of its suitability It is used in polluted and seclusion areas, minimum cost efficiency and low maintenance requirement, BLDC motors are commonly used in comparison to induction motors. BLDC motor solar array fed is used for water pumping for irrigation and domestic purposes [2-4]. Interleaved boost converter is used because of its internal behavior of low switching stress, maximum conversion efficiency due to reduced components, high switch usage, and the absence of an input ripple filter because input inductor functions as a ripple filter [5].

This thesis is focused on simulating BLDC motor using interleaved boost converter going to investigate different operating conditions for solar photovoltaic array for different solar irradiance. The suggested pumping system, which offers simple, compact and affordability efficiency, is designed to work even in 20 percent of the standard solar irradiance the MATLAB/SIMULINK systems, the system is developed, modelled, and its output is evaluated.

II. DESIGN OF PROPOSED SYSTEM

BLDC motor with multi-stages converter, solar Photovoltaic collection, and voltage source inverter are shown in Fig.1. Interleaved boost converter receives the output from the solar Photovoltaic array, and the inverter receives the output from interleaved boost-converter. The solar Photovoltaic arrays DC output is converted into AC power by this inverter. This inverter output is fed to a single BLDC motor. For PV array efficiency enhancement by interleaved boost converter operation, a P&O MPPT controller is used.

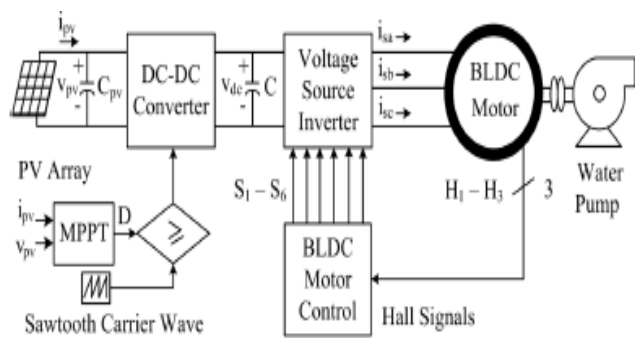


Fig.1 Conventional water-pumping BLDC motor, PV conversion system based on two stage for solar energy [6].

For enhancement efficiency of Solar PV array using Interleaved boost converter a Perturb and Observed (P&O) MPPT controller is used. Speed is controlled by PWM control of VSI and also electronic commutation. An integrated encoder installed on the BLDC motor provide the three Hall signals, which is convert into six pulses following the rotor position. The following sections elaborate on the design methods of the proposed system.

III. PROPOSED SYSTEM DESIGN

BLDC motor and pump selection are the basis of the design of the proposed water pumping system. A 2 HP (Horse Power) BLDC motor is chosen where, as shown in Table I, 1 HP = 746 Watts approximate and the remaining step of the panel is selected, such as the solar photovoltaic array, Interleaved boost converter and water pump [8]. In the following sections, the estimation of different parameters is developed.

A. Design of Solar photovoltaic Array

In order to avoid any loss of energy associated with various stages, a Solar photovoltaic array of 2.2 kW of peak power capacity is chosen that is a little more than necessary for the BLDC motor. At the irradiance level of 1000W/m², the parameters for SPV(solar photovoltaic) arrays are assessed. An SPV module is created by 60 cells series connected. One single module's current short circuit is 7.97A and the voltage of the open circuit is 36.6V. At 80.4% of the open circuit voltage and 91.61% for short circuit current, optimum module power is obtained [9]. Each module have maximum power capacity of 220watts [7]. The optimal capacity of the SPV array is determined by

$$P_m = (N_s \times V_m) \times (N_p \times I_m) \quad (1)$$

Where N_p and N_s are a number of parallel and series connected module and I_m and V_m are current and voltage at maximum power. N_p and N_s are calculated as for 2.2 KW solar PV array described below.

$$2200 = (N_s \times 29.3) \times (N_p \times 7.47) \quad (2)$$

$$I_{mpp} = 23.73 \text{ amp}, I_m = 7.47 \text{ amp}$$

$$\text{Parallel modules given as } \frac{I_{mpp}}{I_m} = \frac{23.73}{7.47} = 3.17 \sim 3$$

$$N_p = 3$$

Putting this value of N_p in equation (3)

$$2200 = 3 \times 28.7 \times N_s \times 7.47 \quad (3)$$

Which gives $N_s = 3.49$ which is taken $N_s = 4$

Thus, Solar PV array with 3 modules in parallel and 4 modules in series gives the maximum power capacity of 2.2 kW. Table II shows detailed design parameters.

Table I
SPECIFICATION OF BLDC MOTOR

Power, P	2HP
Speed, Nr	3000 rpm
DC Voltage, Vdc	310 V
Poles, P	4
Inertia, J	3.5 kg.cm ²
Current Is	5.64 A
Voltage Constant, Ke	78 V/Krpm
Torque constant, Kt	0.74 Nm/A
Phase Resistance, Rs	2.3 Ω
Phase Inductance, Ls	7.68 mH

Table II

DESIGN OF SPV ARRAY

Solar PV Module	
Cells	60
Module voltage	36.6 V
Module current	7.97 A
Module MPP voltage, V_m	29.3V
Module MPP current, I_m	7.47 A
Solar PV array	
MPP voltage, $V_{mpp} = v_{pv}$	90.25 V
Power at MPP, $P_{mpp} = p_{pv}$	2200 W
Current at MPP, $I_{mpp} = i_{pv}$	23.73A
Numbers of modules in series, N_s	4
Numbers of modules in parallel, N_p	3

B. Design of Interleaved Boost DC-DC Converter

As mention earlier about Interleaved boost converter have properties to reduce the stress on switch and its inductor reduces the ripple in the circuit. Now the designing of interleaved boost converter is discribed below in detail in Table III.

Where:

- ΔV_{dc} is the ripple voltage across the capacitor.
- V_{dc} is the output volatge of intealeaved boost converter.
- f_s is switching frequency of IGBT switch of Interleaved boost converter.
- ω = speed in rad/sec.
- N_r = Nominal speed of BLDC motor in rpm.
- P = Poles present in BLDC motor.
- f = Output voltage frequency of VSI in Hz.
- V_{dc} = Output voltage of Interleaved boost converter.
- V_{pv} = Solar PV array output voltage.
- $\Delta I_L = 10\%$ of I_L [8]
- $\Delta V_{dc} = 2\%$ of V_{dc} [8]

The converter parameters values are selected in such a way that, even in bad weather, the system is successful.

Table III
DESIGN OF INTERLEAVED BOOST DC-DC CONVERTER

PARAMETERS	EXPRESSION	DATA	VALUE	SELECTED VALUE
DUTY CYCLE D	$\frac{V_{dc} - V_{pv}}{V_{dc}}$	$V_{dc} = 310\text{ V}$ $V_{pv} = 90.12\text{ V}$	0.7	0.7
INDUCTOR L	$I_L = N_p \cdot I_M$ $L = \frac{D \cdot V_{pv}}{\Delta I_L \cdot f_{sw}}$	$D = 0.7$ $V_{pv} = 90.12\text{ V}$ $f_{sw} = 20\text{ kHz}$ $N_p = 3$ $I_M = 7.47\text{ A}$ $\Delta I_L = 10\%$ of I_L	1.41mH	2mH
CAPACITOR C	$\omega = \frac{2 \cdot \pi \cdot f}{2 \cdot \pi \cdot N_r \cdot P}$ $I_{dc} = P_{mpp} / V_{dc}$ $C = \frac{I_{dc}}{6 \cdot \omega \cdot \Delta V_{dc}}$	$P = 4$ $N_r = 3000\text{ rpm}$ $V_{dc} = 310\text{ V}$ $P_{mpp} = 2200\text{ W}$ $\Delta V_{dc} = 2\%$ of V_{dc}	309 μF	500 μF

C. Designing of the water Pump

Based on nominal speed and power, a BLDC motor designed for a water pump. Since the rated speed, and power are 3000rpm and 2.2KW respectively, the K_ω is estimated by power-speed characteristics [1,10-11].

$$k_\omega = \frac{P_m}{\omega_m^3} = \frac{2200}{\left(\frac{2 \cdot \pi \cdot 3000}{60}\right)^3} \quad (4)$$

$$= 7.095 \cdot 10^{-5} \text{ W}/(\text{rad}/\text{sec})^3$$

IV. SIMULATION AND RESULTS

The introduce water pump system is modelled in different Steady states, starting behaviour and dynamic conditions, with its performance simulated in MATLAB/Simulink. Simulated results show the value of the system.

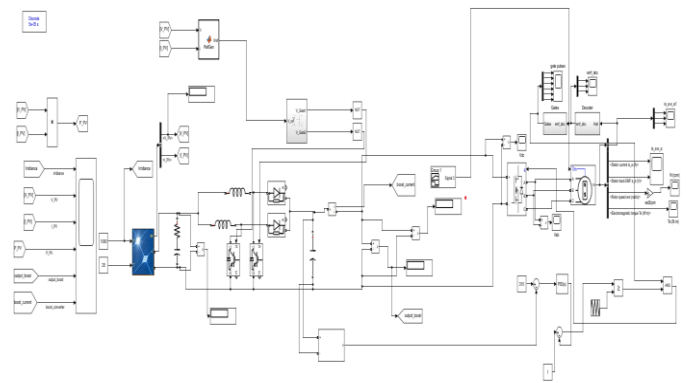


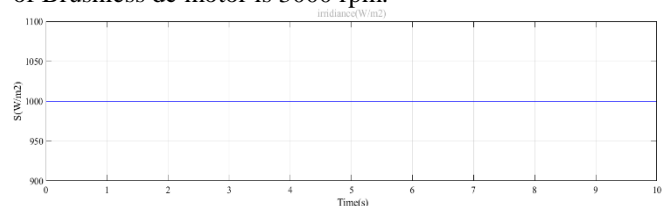
Fig.2 simulink model of the proposed system.

A. Starting and steady state performance at 1000 W/m²

The Steady states response of the solar photovoltaic array and BLDC motor pump has been shown in Fig.3 (1-2) and described by one by one.

1) *Solar PV Array Performances:* The current, I_{pv} , voltage, and power, P_{pv} of a solar PV array at 1000 W/m² are shown in Fig.3.1

2) *BLDC Motor-Pump Performances:* Fig.3.2 shows the various indices of a BLDC motor, for example winding current, i_{sa} ; back emf, e_a ; torque, T_e ; back emf, e_a ; and load (water pump) torque, T_L . The pump is run at maximum speed, and the motor produces a rated torque. Furthermore, i_{sa} response demonstrates that the motor starting current is controlled and that it starts smoothly. In this part load on the BLDC motor is maximum 4.5-NM which can draw maximum amount of water and the speed of BLDC motor is 2500 rpm. As described above in table I the nominal speed of Brushless dc motor is 3000 rpm.



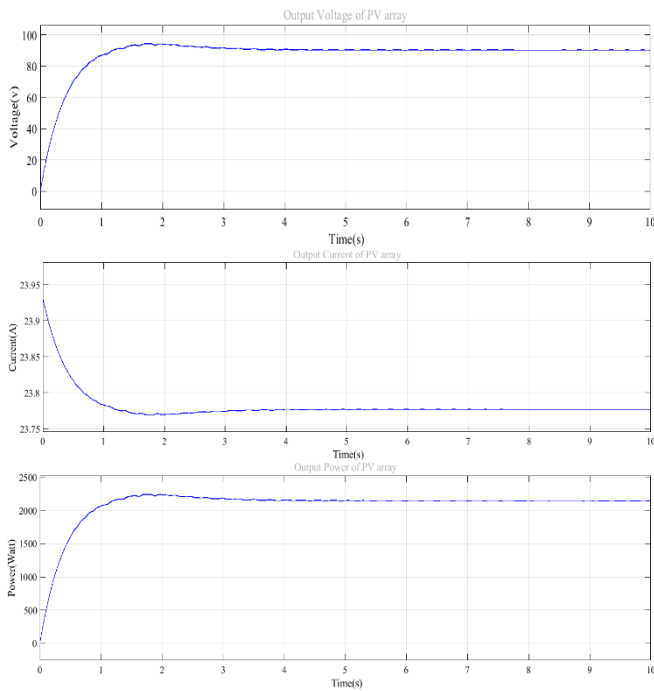


Fig.3.1 Starting and strady states performances of Solar PV array at 1000 W/m²

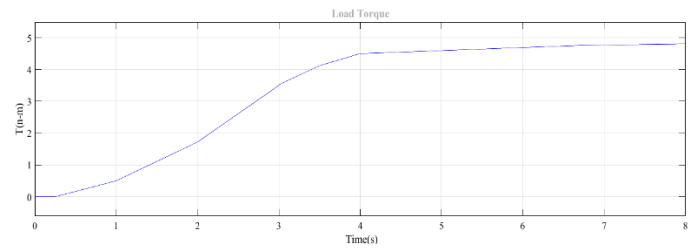
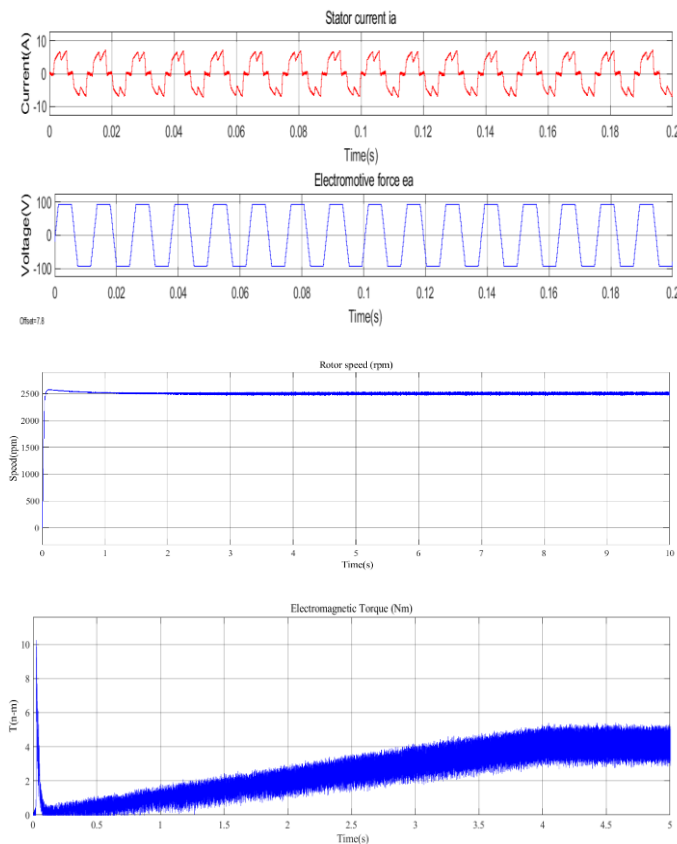


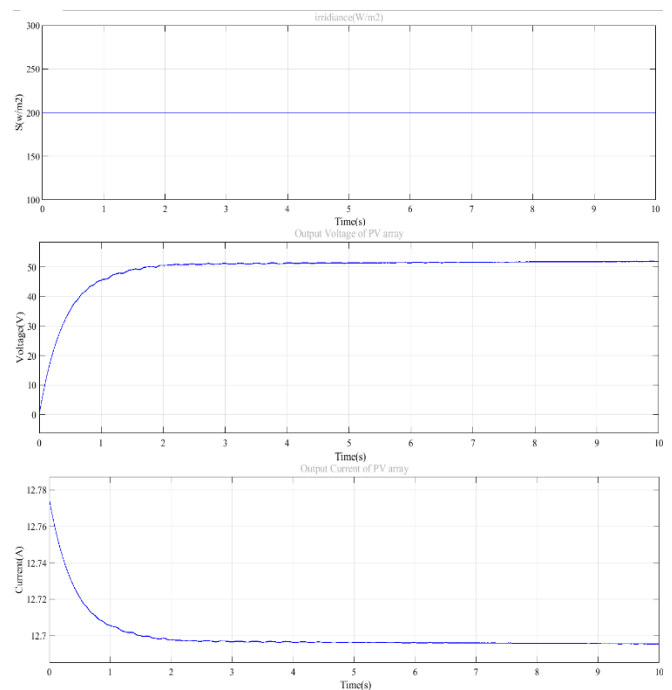
Fig.3.2 Starting and steady states performances of Motor Pump at 1000 W/m²

B. Starting and steady states performance at 200 w/m²

Even at 20% irradiance from standard one, a suggested water pumping system works in Fig.4 (1-2).The Starting and steady states behaviors are described in the following part.

1) *Solar PV Array Performances:* As shown in Fig. 4.1 the Maximum power point is able to tracked at 200 W/m². By modifying the duty ratio of VSI, an optimal duty ratio is obtained, which is then use to manage the motor pump speed.

2) *BLDC Motor-Pump Performances:* A motor must reach a speed of at least 1100 rpm in order to pump the water. As shown in Fig. 4.2, the motor-pump achieves a higher speed than 1200rpm, proving successful pumping at a 20% irradiance level.



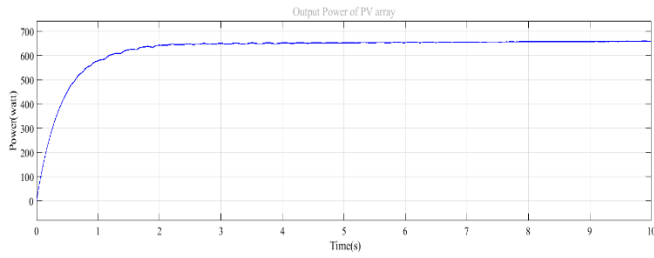


Fig.4.1 Starting and steady states performances of PV array at 200 W/m²

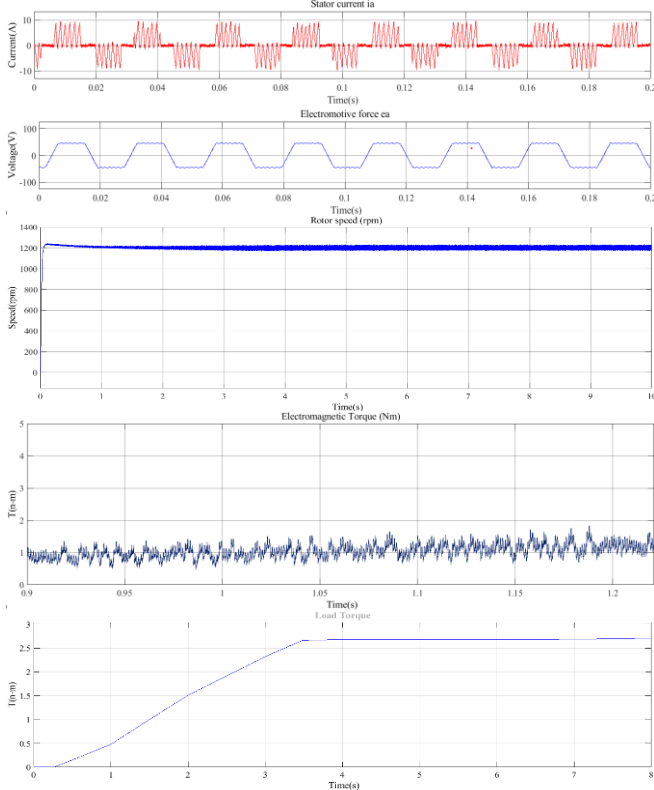


Fig.4.2 Starting and steady states performances of Motor pump at 200 W/m²

C. Dynamic Performances

The system exhibits good dynamic operation under various irradiance conditions, as shown in Fig.5 (1-2). The solar PV array and the motor-pump performance are demonstrated in the category that follow.

1) *Solar PV Array Performances:* The level of irradiation is reduced to 500 W/m² from 1000 W/m² and after that increased to 1000 W/m².as illustrated in Fig.5.1 Under the considered dynamics, the PV array power is successfully optimized. For each irradiance level that participates in the controlling of motor-pump speed, an optimal duty ratio is generated.

2) *BLDC Motor-Pump Performances:* The motor indices, as shown in Fig.5.2, are extremely sensitive to changes in atmospheric conditions. The motor maintains its smooth

dynamic performance. The PV array power controls the motor-pump speed, which are changed by regulating the motor input voltage to achieve the best duty ratio. Power from the PV array is available, the BLDC motor-pump responds correctly. Even at a low output power, BLDC motor provide good water because they are high-efficiency motor.

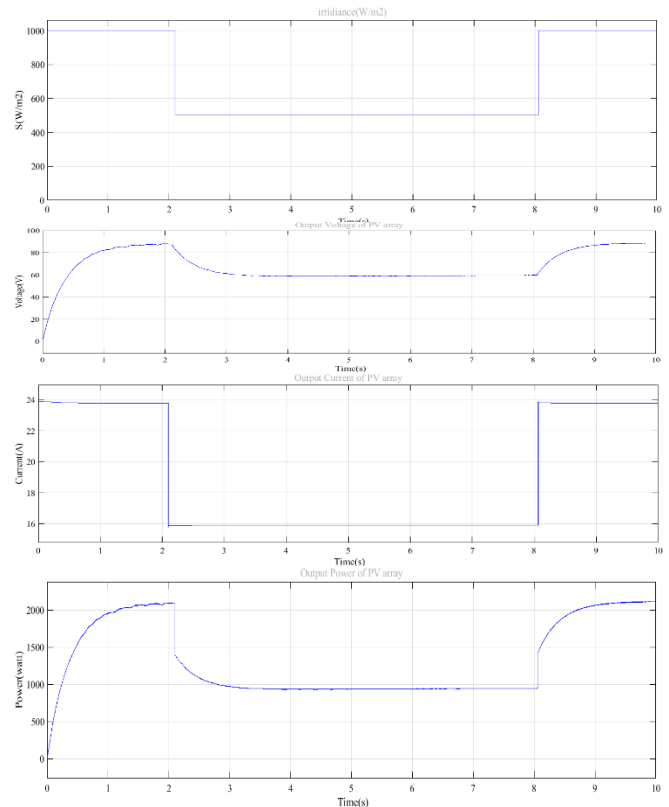
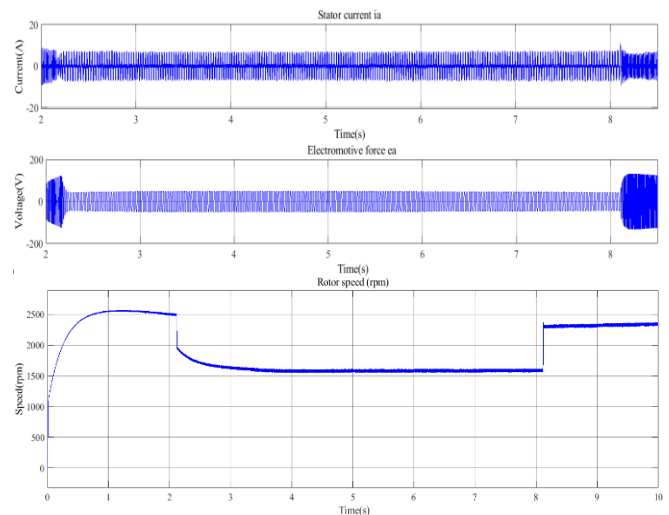


Fig.5.1 Dynamic performances of Solar PV array of the introduced water pumping.



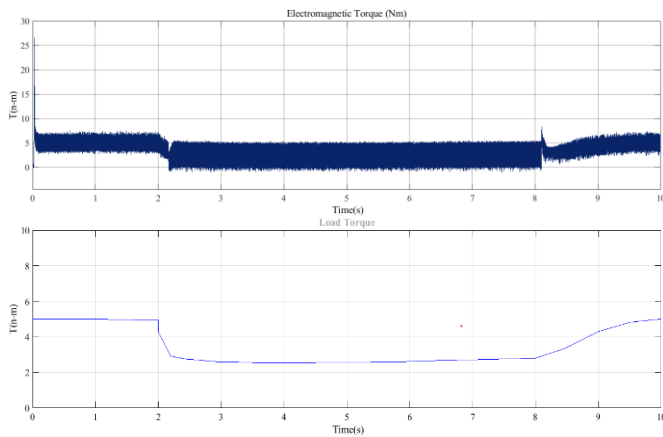


Fig.5.2 Dynamic performances of Motor-pump of the introduced water pumping.

V. CONCLUSIONS

The suggested BLDC motor used water pumping system, which is based on solar photovoltaic generation, validated through demonstrations of its starting, steady states and dynamic performance. MATLAB toolboxes are used to simulate the system, which was then implemented on an experimental prototype. A simple, reliable, and cost-effective method for control the speed of a BLDC motor has been proposed, which eliminates the need for current sensing elements entirely. The Interleaved boost converter can now monitor MPP regardless of weather conditions thanks to the proper range of SPV collection. A Interleaved boost converter with the best design has been presented. Brushless DC motors can now be started safely without the use of any external controls. At the same time 20% of normal solar irradiance, the introduced system works good has been demonstrated. Proper designing of solar photovoltaic array, Interleaved boost converter, water pump head are described.

REFERENCES

- [1] R. Kumar and B. Singh, "Solar PV array fed Cuk converter-VSI controlled BLDC motor drive for water pumping," 6th IEEE Power India Int. Conf. (PIICON), 5-7 Dec. 2014, pp. 1-7.
- [2] B. Singh and V. Bist, "A BL-CSC Converter-Fed BLDC Motor Drive With Power Factor Correction," IEEE Trans. Ind. Electron., vol. 62, no.1, pp. 172-183, Jan. 2015.
- [3] R. Kumar and B. Singh, "BLDC Motor Driven Solar PV Array Fed Water Pumping System Employing Zeta Converter," IEEE Trans. Ind. Appl., vol. 52, no. 3, pp. 2315-2322, May-June 2016.
- [4] B. Singh and V. Bist, "A Single Sensor Based PFC Zeta Converter Fed BLDC Motor Drive for Fan Applications," Fifth IEEE Power India Conference, pp.1-6, 19-22 Dec. 2012.
- [5] S. H. Elkelani Babaa, "High efficient interleaved boost converter with novel switch adaptive control in photovoltaic application," Ph.D. Thesis, Electronic and Computer Eng. Dept., Univ. of Newcastle, Newcastle, England, 2013.
- [6] R. Kumar and B. Singh, "Single Stage Solar PV Fed Brushless DC Motor Driven Water Pump" JESTPE-2016-12-0617.R2
- [7] Standard Solar PV Module Specifications [Online] Available: <http://www.hbl.in/brochures%20pdf/SOLAR%20MO DULEBroucher. Pdf>

- [8] R. Kumar and B. Singh, "Solar PV Array Fed Brushless DC Motor Driven Water Pump" JESTPE-2016-12-0617.R2
- [9] Trishan Eswam and Patrick L. Chapman, "Comparison of Photovoltaic Array Maximum Power Point Tracking Techniques," IEEE Trans. Energy Conversion, vol. 22, no. 2, pp. 439-449, June 2007.
- [10] W.V. Jones, "Motor Selection Made Easy: Choosing the Right Motor for Centrifugal Pump Applications," IEEE Ind. Appl. Mag., vol.19, no.6, pp.36-45, Nov.-Dec. 2013.
- [11] Bhim Singh and Rajan Kumar, "Solar PV Array Fed Water Pump Driven By BLDC Motor Using Landsman Converter," IET Ren Generation, Early Access.
- [12] Masoum, M. A., Badejani, S. M. M., & Fuchs, E. F. (2004). Microprocessor-controlled new class of optimal battery chargers for photovoltaic applications. IEEE Transactions on energy conversion, 19(3), 599–606.
- [13] Dabra, V., Paliwal, K. K., Sharma, P., & Kumar, N. (2017). Optimization of photovoltaic power system: A comparative study. Protection and Control of Modern Power Systems, 2(1), 3.
- [14] Kumari, J. S., Babu, D. C. S., & Babu, A. K. (2012). Design and analysis of P&O and IP&O MPPT techniques for photovoltaic system. International Journal of Modern Engineering Research, 2(4), 2174–2180.
- [15] A. Harrag and S. Messalt, "Variable step size modified p&o mppt algorithm using ga-based hybrid offline/online pid controller," Renewable and Sustainable Energy Reviews., vol. 49, p. 1247 – 1260, 2015.

Conversion of Waste Heat into Electricity Using Teg

^[1]Shifanaaz A, ^[2]Misbah Falak M, ^[3]Anil Kumar T, ^[4]Gowtham. G

^{[1][2][3]} Student, EEE Department, RRIT, Bangalore, VTU University.

^[4]Guide, Assistant professor, EEE Department, RRIT, Bangalore, VTU University

Abstract— Even the most efficient power plants convert only about 40% of energy they produce into electricity and the combustion engine used in most vehicles are even worse, yielding only about a third of their energy as usable power. Recent development of material science, nanotechnology have hinted at a new class of energy harvesting devices thermoelectric generators (TEG) small enough to trap waste heat from even the smallest household appliances and to turn that heat into electricity. Small thermoelectric generators could be placed around the exhaust system of the car and the exhaust waste heat is utilized to charge the battery of the car and these thermoelectric generators are attached to a stove so that while cooking the food the battery can be charged and can run the emergency lights. These small thermoelectric generators cannot be connected directly to the battery as the power generated is not constant, if the power generated from the TEG is low to charge the battery; a boost converter is required in between the TEG and the battery. The output of the boost converter is greater than the input hence enough power is boosted through the converter for the charging of battery. The research has been going on to improve the efficiency of TEG's. The main achievement until obtained from the TEG's is harvesting the power from the waste heat from exhaust pipe of a BMW car to charge its battery. This technology is fixing for some of its applications because of its cost. This project will be done to apply this technology for home appliances. The heat from the candle is taken as heat source for the TEG's to run the load. We all know that the efficiency of TEG's is so small; this project also explains how we can improve the efficiency

Keywords: Renewable energy sources, nanotechnology, TEG, boost converter.

I. INTRODUCTION

Many nations count on coal, oil & Natural gas to supply most of their needs, but these are all a finite resource. Eventually the world will run out of fossil fuels, or it will become too expensive to retrieve those that remain. Renewable energy resources such as wind, solar & hydro power offer clean alternatives to fossil fuels. They produce little or no pollution or greenhouse gases & they will never run out. Most renewable energy comes either directly or indirectly from the sun, sunlight or solar energy can be used directly for heating and lighting homes & other buildings, for generating electricity & for variety of commercial & industrial uses. The sun's heat also drives the wind, whose energy is captured with wind turbines. These wind & sun's energy causes water to evaporate which causes rain & this flowing kinetic energy is used as hydroelectric power. Biomass can be used to produce electricity, as a transportation fuel or chemicals, this is called bio energy. Ethanol is also used as a fuel with gasoline which is replacing gasoline now days. Geothermal

energy taps the earth's internal heat for a variety of uses including electric power production. In addition to tidal energy ocean energy which are driven by both the tides and the winds.

One disadvantage with renewable energy sources is that it is difficult to generate the quantities of electricity that are as large as those produced by traditional fossil fuel generators & its reliability of supply. Renewable energy often relies on weather for its source of power.

II. THERMOELECTRIC GENERATORS (TEG), DC-DC CONVERTERS

TEG is an acronym for 'thermoelectric generator'. A TEG is a device utilizing one or more thermoelectric modules as the primary component, followed by a cooling system that can be either passive or active. Such as an open air heat sink, fan cooled heat sink, or fluid cooled. These components are then fabricated into an assembly to function as one unit called a TEG.

A. Background of Thermoelectric generators

Metals are good conductors because electrons can move freely within them similar to a fluid full of water and you raise one end, what happens? The water will flow down the pipe from the high end to the low end. This is because when you raised the pipe you increased the potential energy and the water wants to flow downhill. In a thermoelectric material the same thing happens to the fluid like electrons when you heat it. Heating one end a thermoelectric material causes the electrons to move away from the hot end toward the cold end. When the electrons go from the hot side to the cold side this causes an electrical current. The larger the temperature difference the more electrical current is produced and therefore more power generated. Thermoelectric power is the conversion of a temperature differential directly into electrical power results primarily from two physical effects; the Seebeck effect & Peltier effect. The Seebeck effect named after Thomas. J. Seebeck, who first discovered the phenomenon in 1821. Seebeck noticed that when a loop comprised of two dissimilar materials was heated on one side an electromagnetic field (EM) was created. He actually discovered the EM field directly with a compass. He noted that the strength of the electromagnetic field and therefore the voltage is proportional to the temperature difference between the hot & cold sides of the material. The magnitude of the Seebeck coefficient (S) varies with material and temperature of operation. The Seebeck coefficient is thus defined as

$$S = -\Delta V / \Delta T \quad (1)$$

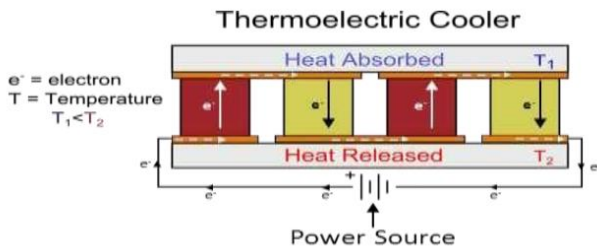


Fig .1 Thermo electric cooler.

B. DC-DC CONVERTER

In many industrial applications it is required to convert a fixed voltage dc source in to a variable voltage dc source. A dc-dc converter converts directly from dc to dc and is simply known as a dc converter. Dc converters are widely used for traction motor control in electric automobiles, trolley cars, marine hoists, forklift trucks, and mine haulers. They provide smooth acceleration control, high efficiency and fast dynamic response. Dc converters can be used in regenerative braking of dc motors to return energy back in to the supply, and this features results in energy savings for transportation systems with frequent stops. DC converters are used in dc voltage regulators.

There are four basic topologies of switching regulators

1. Buck regulator
2. Boost regulator
3. Buck-Boost regulator

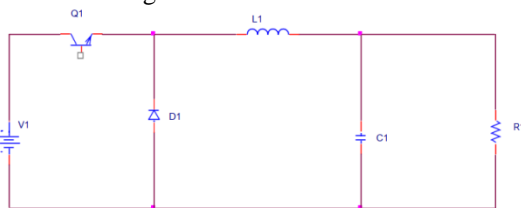


Fig 2. Buck Converter

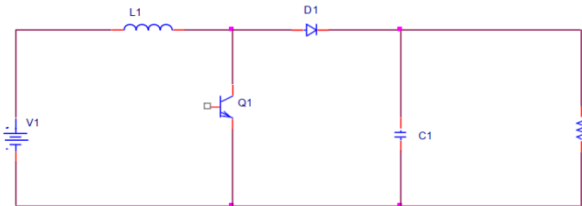


Fig 3. Boost Converters

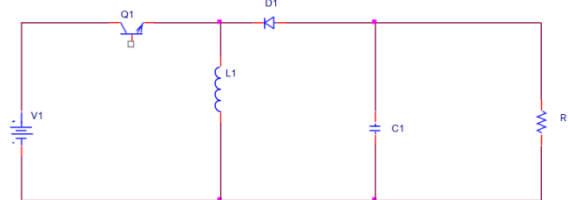


Fig 4. Buck-Boost converter

III. PROPOSED DESIGN

Any heat source will be taken as input to the TEG, when the heat is applied to the hot side plate of the TEG by maintain cold side on the cold plate, the temperature difference of two dissimilar metals leads to generation of electricity. Higher the temperature difference between the two metals higher will be the generation of electricity. The figure 5 shows the TEG module, Where the upper and lower part is covered by ceramic plates. The bismuth and telluride materials have been used to make P-type and N-type semiconductors. The designing of cold side includes the aluminium metal i.e. heat sink or circulation of fluids. The generated power is fed to the dc-dc buck boost converter, and it leads to charge a battery. The generated power will be boosted for the required voltage by proper designing of DC-DC converter. The TEG will generate the voltage from millivolts to some volts and small milliamperes of current. This small output power of TEG can be boosted to higher power which is enough to charge a small lead ion battery.

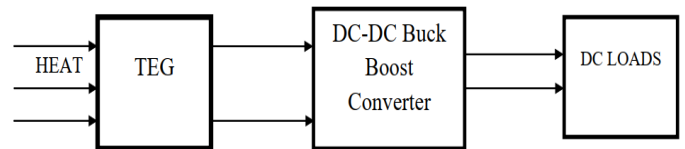


Fig 5. Block diagram of proposed circuit

IV. MODELING & SIMULATION

A. The simplified TEG module:

The modelling of TEG as shown in figure 6. The input to the model will be variable hot temperature by keeping cold side constant. The output will be resistance of TEG R_{teg} and the open circuit voltage V_{oc} . TEG module TEG1-12611-6.0 is used in the simulation.

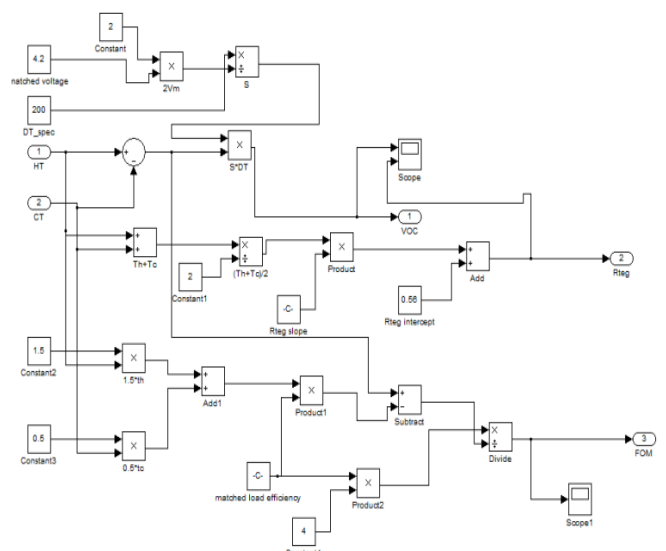


Fig 6. Simulation model of TEG module

V.V. RESULTS

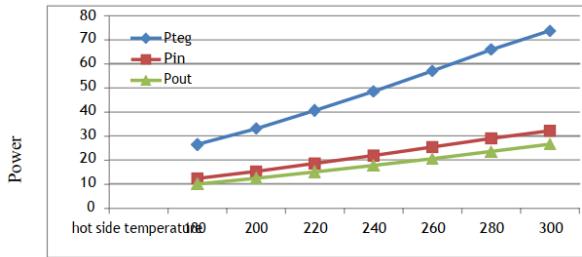


Fig 7. Power output for various temperatures

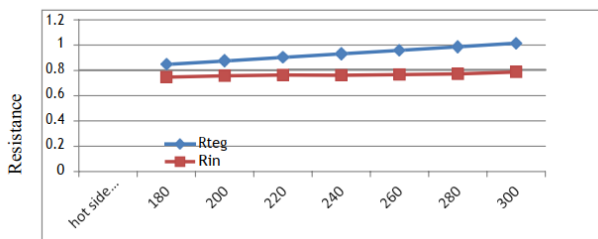


Fig 8. Resistance for various temperatures

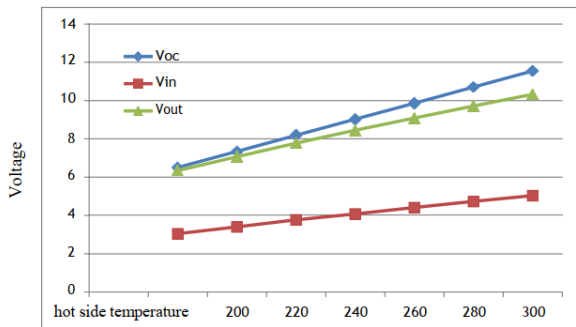


Fig 9. Voltages for various temperatures

VI. HARDWARE MODEL

The hardware model of the project includes designing of four main components.

This chapter clearly explains the complete hardware step-up.

- Thermoelectric Generator
- DC-DC Boost converter
- Programming of
- Load (LED light, Motor)

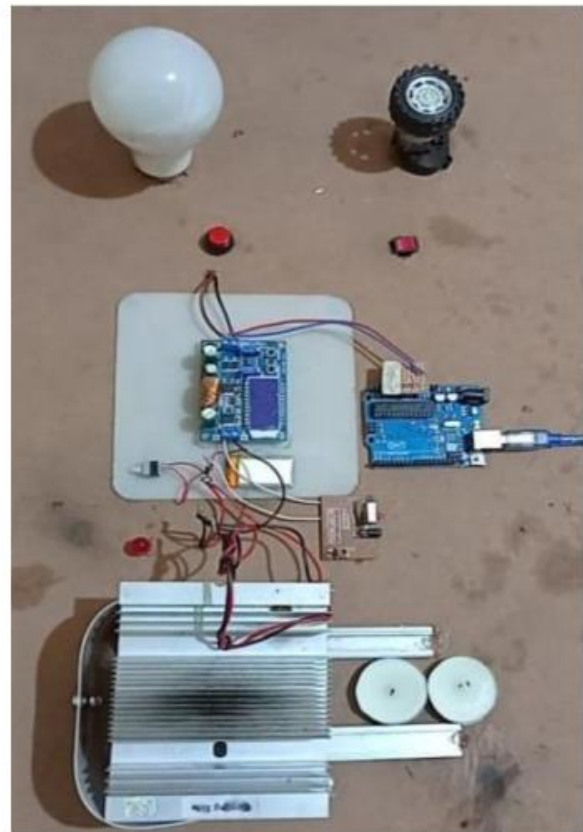


Fig 10. Hardware setup with heat sink at cold side

VII. VII. CONCLUSION

Thermoelectric Generators (TEG) are new era of generating power resources which are replacing the traditional power sources. In proposed project the simulation is carried out in MATLAB/SIMULINK for whole model and results are concluded by varying the hot side temperature of TEG to be from 1800- 3000 by keeping cold side for 250. While in the hardware TEG are designed to provide the power for two loads, as LED load and to run a motor. These two applications are common in every home. TEG's can generate small electricity which cannot be fed directly to the load; hence a DC-DC boost converter is combined to the TEG to boost the generated power which is sufficient for the load. The output of converter is also designed for different voltages of 4.35V for LED's and 5.13V for charging a mobile of current 800mA. The motor has been designed by keeping the certain conditions such as the temperature of heat near the TEG which should be small enough to generate a power which can be boosted to run the motor.

REFERENCES

- [1] www.renewableenergyworld.com the introduction to renewable energy sources.
- [2] Orsha gray Davidson published a paper companies which are producing 100% renewable energy sources in Forbes website.
- [3] Adam Jones special assistant for energy policy at American progress.

- [4] www.powerpot.com – peltier effect & see beck effect
- [5] Joseph.w.haepster a ralphstrohlreiner decher & standy published a paper on Thomson effect in escola.bsintanica.
- [6] www.tegpower.com thermoelectric coolers and thermoelectric generators
- [7] Molan Li, KTH information & communication Technology, published a paper on Thermoelectric Generator based DC-DC conversion network for automotive Applications”.
- [8] Dr. Jerry Hendricks & William T. Choate, engineering scoping study of “Thermoelectric generator system for industrial waste heat recovery”.
- [9] Muhammad H. Rashid a book on “Power Electronics, circuits devices and applications”
- [10] Li. Xuejun, A thesis in Department of electrical & computer engineering wrote a paper on “ an improved Perturbation & Observation Maximum Power Point Algorithm for PV panels”.

Model Reduction and Optimization of Interval System Using H-infinity Norm and Genetic Algorithm

^[1] Shubham, ^[2] A.N. Jha

^{[1][2]} Instrumentation and Control Division, NSUT, New Delhi, India

Abstract— *The paper is organised as follows: Section 1, introducing the system based on previous studies and introduces the problem statement. Section 2 gives impression about interval mathematics as well as modeling of the linear interval system. Section 3 describes the proposed method to reduce the system and to optimize the parameters of the system using genetic algorithm. In section 4, a numerical example is incorporated for the illustration of the suggested technique along with the MATLAB simulation and results. Last section, section 5 gives the comparison of various parameters and concludes the paper.*

Keywords: *Interval System, Model Reduction, Genetic Algorithm, H-inf Norm.*

I. INTRODUCTION

Estimation of models of high-order with models of reduced order is considered an area which is active of study in a lot of applications for engineering. Particularly, in the analysis of control system as well as designing for the reduction of the cost as well as the complexity. Numerous techniques have been planned to reduce the model order in which few of the conventional techniques have been Pade estimation (Smash, 1974); Routh estimation (Hutton et al, 1975); Hurwitz polynomial estimation (Appaih, 1978); Stability equation techniques (Chen et al, 1978); Mihailov criterion (Wan, 1981); Pole clustering techniques (Sinha et al, 1990) etc. To daze with demerit of the un-stability, few of the mixed techniques were even established for using the combination of the above-mentioned techniques. Report as well as strategy issues involve indecision to the variable degree.

Though, in a lot of systems coefficients are relentless but undefined within restricted limit. These systems have been classified into interval systems. Techniques for reducing a few of conventional order has been prolonged via interlude arithmetic to derive the estimate for the interval systems of the high-order like Routh-Padé approximation (Bandyopadhyay et al, 1994) to reduce the model of consecutive interval systems in which denominator has been retained with the use of truncation of Routh table which is direct as well as numerator has to be retained from matching of time moments of interval system of high-order the estimate.

Further, some of techniques have been established by Bandyopadhyay et al (1995, 1997a, 1997b). Also, Hwang et al (1999) proposed to improve the computation of the Routh

approximants, Dolgin et al (2003) established Routh-Pade approach as well as further a lot of approaches have been deliberated by Singh et al (2010, 2011) along with Kranthi et al (2011, 2012). In the following study, novel assorted technique to reduce the order of interval-systems has been proposed which is leeway of the Parmar et al's approach (2007) to combine Eigen spectrum analysis (Mukherjee, 1996) as well as the algorithm of the factor division (Lucas, 1983) across Kharitonov's Theorem (Kharitonov, 1978). The numerator as well as denominator of high order interval system have been reduced by the factor division as well as the Eigen spectrum analysis approach.

Model Reduction is an outlet of the systems as well as the theory for the control, that studies about the properties of the dynamical systems for the reducing of complexity, along with the preservation of the nature of their input-output. It is even vital for the filter design as well as the quality of model of the reduced order. The measure for the correctness of estimation should be considered with the difference between the nature between the original as well as the reduced order model.

Different Norms can be used for the formulation of the model reduction problem. Of-course, one has to be aware of the following facts (Bettayeb, 1981):

1. The use of different norms gives rise to different approximations. A good approximation in one norm is not necessarily good in another norm.
2. Close approximations based on time domain criteria do not necessarily translate into good frequency domain approximations.

The Model Reduction problem is a tradeoff between two conflicting desirable objectives (Bettayeb, 1981):

1. To derive from the high order system a model as simple (low order) as possible (complexity).
2. The low order model is reasonably close to the original system (accuracy).

Assume one has a device, and that (using finite-difference discretization or any other modeling technique) its description is obtained in the form of a differential equation, or a transfer function. Usually, this will result in a system of a very high order, evidently redundant for representing some properties of interest. Model Reduction is used to create the

smallest possible model while preserving the system's input-output behavior.

1.1 Model Reduction

Consider usual representation of the state space model of SISO time-invariant linear continuous time system:

$$\dot{x}(t) = Ax(t) + Bu(t) \quad (1)$$

$$y(t) = Cx(t) \quad (2)$$

In which the $x(t)$ being state, $u(t)$ being input, also $y(t)$ being output. The model of the state space could be shown by the transfer function of the n^{th} order:

$$G(s) = \frac{b_1s^{n-1} + b_2s^{n-2} + \dots + b_{n-1}s + b_n}{s^n + a_1s^{n-1} + \dots + a_{n-1}s + a_n} \quad (3)$$

The objective of the reduction in the optimal model is for obtaining a state space model of the reduced order presentation or the transfer function of the system which shows traditional system.

$$\dot{x}_r(t) = Ax_r(t) + Bu(t) \quad (3)$$

$$G_r(s) = \frac{d_1s^{r-1} + d_2s^{r-2} + \dots + d_{r-1}s + d_r}{s^r + c_1s^{r-1} + \dots + c_{r-1}s + c_r} \quad (5)$$

In this thesis, the reduction problems will be investigated with the H_∞ norm using Genetic Algorithm Optimization (GAO).

The H_∞ norm on the other hand is defined as:

$$\|e\|_\infty = \lim_{p \rightarrow \infty} \left[\int_0^\infty |e(t)|^p dt \right]^{\frac{1}{p}} \quad (4)$$

In which $e(t)$ is instinct reply difference in between original as well as the reduced system:

$$e(t) = g_{\text{original_system}}(t) - g_{\text{reduced_system}}(t) \quad (5)$$

The thesis is organised as follows: Chapter 2 gives the basic idea of the previous work that has been done and various research papers which have been studied during our work. Chapter 3 provides a detailed impression about interval mathematics as well as modeling of the linear interval system. Chapter 4 describes the proposed method to reduce the system and to optimize the parameters of the system. In chapter 5, a numerical example is incorporated for the illustration of the suggested technique along with the results and conclusion.

II. MODELING OF THE INTERVAL SYSTEM

A. INTRODUCTION

Let transfer function of the interval systems of the higher order be:

$$G_n(s) = \frac{N(s)}{D(s)} = \frac{\sum_{i=0}^{n-1} [n_{ii}, n_{ui}] s^i}{\sum_{j=0}^n [d_{ji}, d_{uj}] s^j} \quad (6)$$

Where, $[n_{ii}, n_{ui}]; 1 \leq i \leq n-1$ and $[d_{ji}, d_{uj}]; 1 \leq j \leq n$ are constants which are scalar.

The of transfer function reduced order model has been taken in consideration as

$$G_n(s) = \frac{N(s)}{D(s)} = \frac{\sum_{i=0}^{n-1} [n'_{ii}, n'_{ui}] s^i}{\sum_{j=0}^n [d'_{ji}, d'_{uj}] s^j} \quad (7)$$

Where $[n'_{ii}, n'_{ui}]; 1 \leq i \leq r-1$ and $[d'_{ji}, d'_{uj}]; 1 \leq j \leq r$ are constants which are scalar.

B. INTERVAL MATHEMATICS

Instructions of the interval arithmetic have been shown. Let $[l_1, u_1]$ and $[l_2, u_2]$ be two of the intervals, then

Addition:

$$[l_1, u_1] + [l_2, u_2] = [l_1 + l_2, u_1 + u_2] \quad (8)$$

Subtraction:

$$[l_1, u_1] - [l_2, u_2] = [l_1 - l_2, u_1 - u_2] \quad (9)$$

Multiplication:

$$[l_1, u_1] \times [l_2, u_2] = [[\text{Min}(x)], [\text{Max}(x)]] \quad (10)$$

Where $x = [l_1l_2, l_2u_1, l_1u_2, u_1u_2]$.

Division:

$$\frac{[l_1, u_1]}{[l_2, u_2]} = [l_1, u_1] \times \left[\frac{1}{l_2}, \frac{1}{u_2} \right] \quad (11)$$

Transfer Function of the Original Interval System:

$$G(s) = \frac{[2,3]s^2 + [17.5, 18.5]s + [15, 16]}{[2,3]s^3 + [17,18]s^2 + [35,36]s + [20.5, 21.5]} \quad (12)$$

Defining the range of the transfer function in equation 14,

(a) Transfer Function of Lower Bound Range is:

$$G(s) = \frac{2s^2 + 17.5s + 15}{2s^3 + 17s^2 + 35s + 20.5} \quad (13)$$

(b) Transfer Function of Upper Bound Range is:

$$G(s) = \frac{3s^2 + 18.5s + 16}{3s^3 + 18s^2 + 36s + 21.5} \quad (14)$$

III. OPTIMIZATION

A. GENETIC ALGORITHMS

GA has been established by John Holland, his students as well as colleagues at the University of Michigan in the 70s. Objective of the study is:

- a. Abstraction as explaining adaptive processes of the natural systems.
- b. Designing the systems software that is artificial for retaining prominent natural systems mechanisms.

GAs have been the search algorithms which help in mimicking the mechanism of the natural genetics as well as the selection. They syndicate that the fittest would be surviving with structures of the string that has a structured yet exchange of the information that is randomized for the formation of a search algorithm that has a few of innovative flair of the human search. Gas have been empirically as well as theoretically proved for giving the robust search in the complex spaces (Goldberg, 1989).

Gas have been made of three main operators:

1. Reproduction: individual strings are copied with respect to the value of the fitness function.
2. Crossover: members of strings that have been produce recently in mating pool, mated randomly.
3. Mutation: the random alteration in the value of position of the string.

Individuals in GAs population set are programmed as restricted measurement strings over the finite alphabet. Originally, the those have been shown in the binary as the strings of 0s and 1s, nonetheless other encodings are probable. Every string in the population is called chromosome. Distinctive chromosome looks like:
 10010101110101001010011101101110111111101

Development generally starts from population of the individuals that have been generated randomly. In every generation, the fitness of each persons in the population has been assessed with respect to the function of the fitness. The function for the fitness is issue reliable. It is measure of profit, use that requires to be maximized.

Many persons are selected in stochastic manner with use of a criteria of selection from the current population that is based on the fitness and has been modified for the formation of a new population. This results in the population development of the individuals which have been better suited with respect to the environment than individuals from which they have been made like in the natural selection. The novel population is further utilized in another iteration for the algorithm.

The Roulette Wheel has been a broadly used criteria of selection in the GA. It doesn't ensure that the member who is fittest goes through the next generation but makes it highly probable. Suppose that total fitness score of the population's is shown by the pie chart or the roulette wheel. Present day,

let's allot a wheel slice to every population member. The slice size is in the proportion with the score of the fitness of chromosome. i.e., the member who is fitter receives bigger pie slice. Now, we choosing a chromosome for spinning the ball as well as grabbing the chromosome at its stopping point.

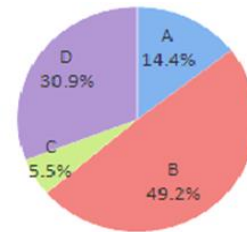


Fig 1. Roulette Wheel.

The GA eliminates when one of extreme generations have been formed or on reaching a satisfying level of fitness for the population. If algorithm has eliminated because of the extreme number of generations, then satisfying explanation can be may not be reached.

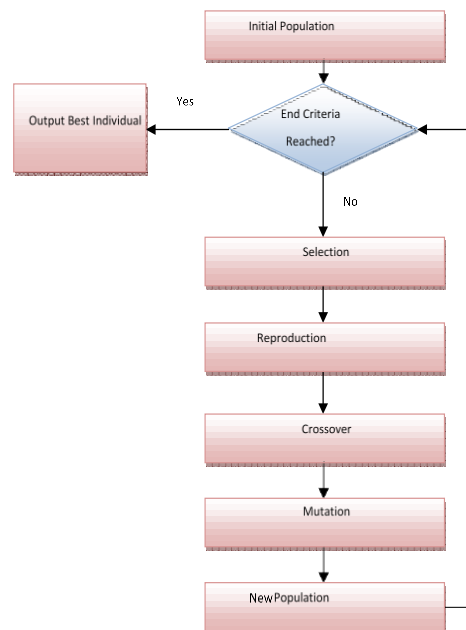


Fig 2: Genetic Algorithm Flowchart.

H_∞ Norm Model Reduction

The H_∞ norm on the other hand is defined as:

$$\|e\|_{\infty} = \lim_{p \rightarrow \infty} \left[\int_0^{\infty} |e(t)|^p dt \right]^{\frac{1}{p}} \quad (15)$$

In which e(t) is instinct response difference between original as well as the reduced system.

The H_∞ Norm fitness function of eq. (1.8) was executed in MATLAB with the help of trapezoidal numerical integration that computes an estimate integral of error in between step

response of traditional system as well as step response of the reduced order system with respect to time with the same stability constraint.

IV. SIMULATION AND RESULTS

The transfer function of the original system is shown in equation:

$$G(s) = \frac{[2,3]s^2 + [17.5, 18.5]s + [15, 16]}{[2,3]s^3 + [17,18]s^2 + [35,36]s + [20.5, 21.5]} \quad (16)$$

1. The step response of the lower bound transfer function is shown in figure:

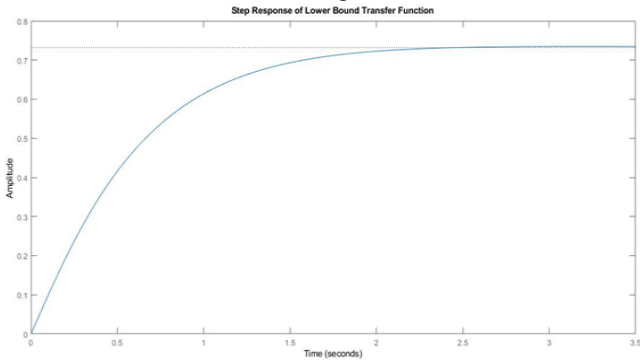


Fig 3: Step Response of Lower Bound Transfer Function (Original System)

2. The step response of the lower bound transfer function is shown in figure:

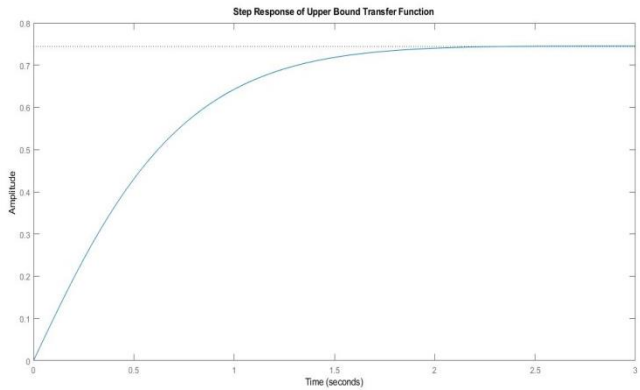


Fig 4: Step Response of Upper Bound Transfer Function (Original System)

After applying the H_∞ normalization along with the Genetic Algorithm to optimize the parameters of the transfer function.

1. The resultant reduced transfer function of the lower bound transfer function is:

$$Gr = \frac{0.9279 s + 19.55}{s^2 + 16 s + 26.28} \quad (17)$$

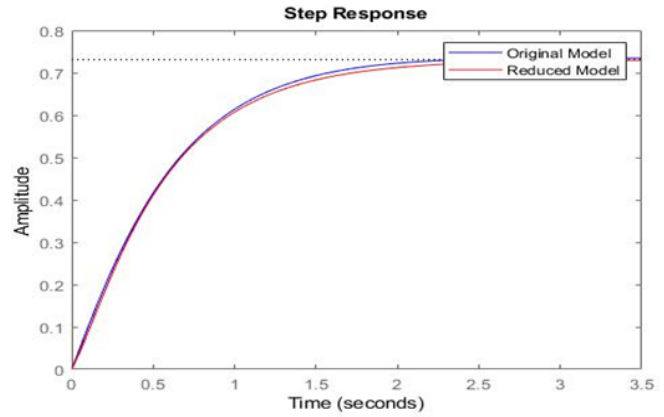


Fig 5: Step Response of Lower Bound Transfer Function (Original and Reduced System)

Table 1. Characteristics Comparison of Lower Bounded Transfer Function (Original and Reduced Order)

	Original System	Reduced System
Rise Time	1.1494	1.1623
Settling Time	1.8577	2.0898
Peak	0.7347	0.7218

2. The resultant reduced transfer function of the upper bound transfer function is

$$Gr = \frac{0.9454 s + 9.812}{s^2 + 8.5 s + 13.31} \quad (18)$$

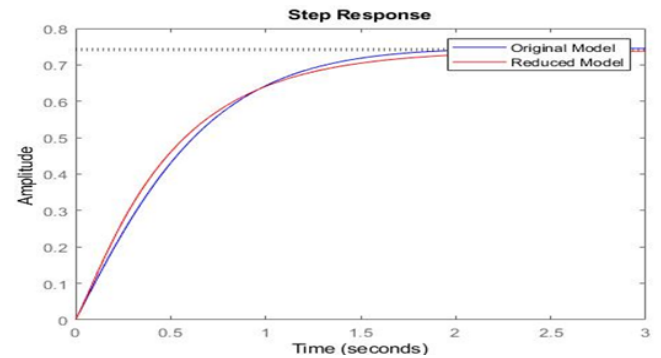


Fig 6: Step Response of Upper Bound Transfer Function (Original and Reduced System)

Table 2. Characteristics Comparison of Upper Bounded Transfer Function (Original and Reduced Order)

	Original System	Reduced System
Rise Time	1.0482	1.5734
Settling Time	1.6724	2.8060
Peak	0.7453	0.7602

V. CONCLUSION

1. On comparing the various time, parameters of the original system (Lower bound and the upper bound) with reduced order (lower bound and the upper bound) transfer function, it could be concluded that the system is practically possible to be used and is stable.

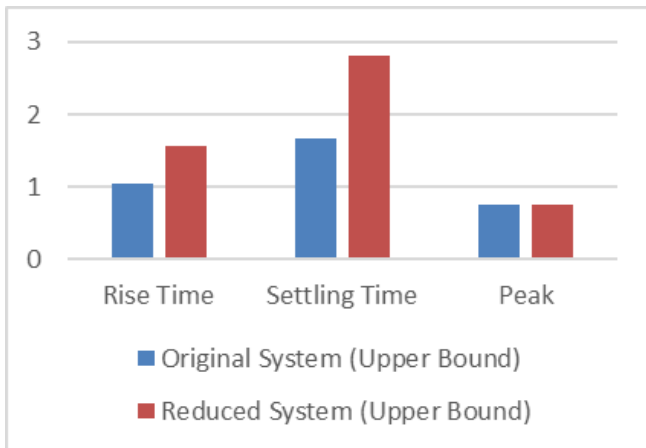


Fig 7. Graphical Representation of Comparison of Upper Bounded Transfer Function (Original and Reduced Order)

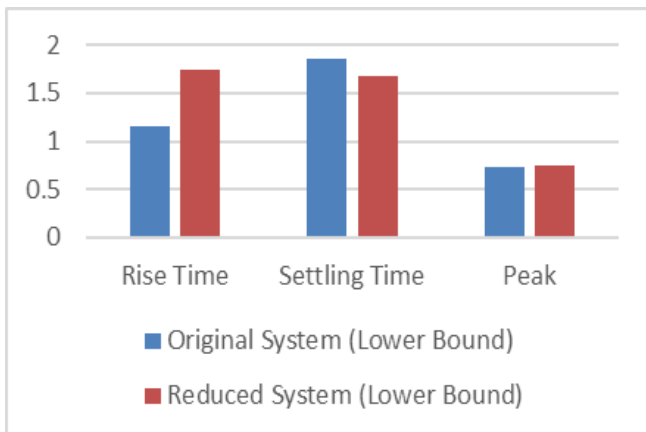


Fig 8. Graphical Representation of Comparison of Lower Bounded Transfer Function (Original and Reduced Order)

1. Frequency Response of the Lower Bound reduced system:

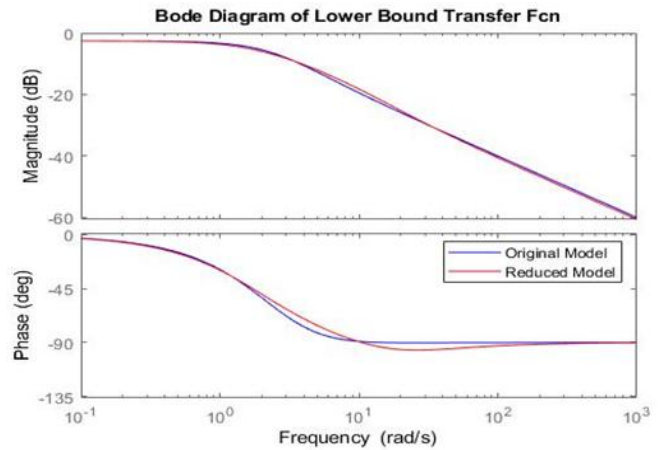


Fig 9. Bode Plot of Lower Bounded Transfer Function (Original and Reduced Order)

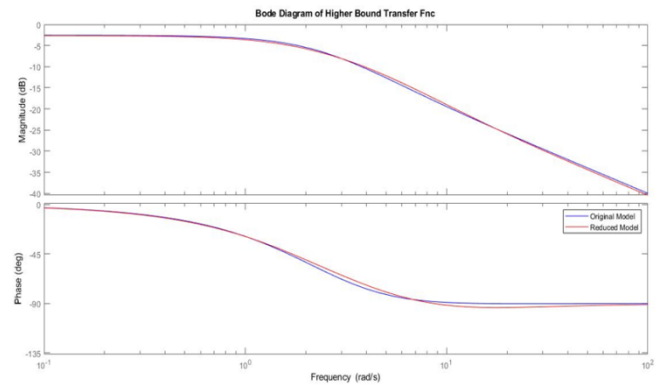


Fig 10. Bode Plot of Upper Bounded Transfer Function (Original and Reduced Order)

REFERENCES

- [1] Al-Amer, S.H.H. (1998). New Algorithms for H_{∞} -Norm Approximation and Applications. Ph. D. Thesis, King Fahad University of Petroleum & Minerals, Dharaan, KSA.
- [2] Al-Saggaf, U.M. and Bettayeb, M. (1993). Techniques in Optimized Model Reduction for High Dimensional Systems. Control and Dynamic Systems, Digital and Numeric Techniques and their Application in Control Systems, 55(1): 51-109.
- [3] Anic, B. (2008). An interpolation-based approach to the weighted H_2 model reduction problem.
- [4] Master Thesis, Virginia Polytechnic Institute and State University, USA.
- [5] Assunção, E. and Peres, P.L.D. (1999a). H_2 and/or H_{∞} -Norm Model Reduction of Uncertain Discrete-time Systems. Proceedings of the American Control Conference, San Diego, California, USA, pp. 4466-4470.
- [6] Assunção, E. and Peres, P.L.D. (1999b). A Global Optimization Approach for the H_2 -Norm Model Reduction Problem. Proceedings of the 38th Conference on Decision and Control, Phoenix, Arizona, USA, pp. 1857-1862.
- [7] Beattie, C.A. and Gugercin, S. (2007). Krylov-Based Minimization for Optimal H_2 Model Reduction. Proceedings of the 46th IEEE Conference on Decision and Control, New Orleans, LA, USA, pp. 4385-4390.
- [8] Bettayeb, M. (1981). Approximation of Linear Systems: New Approaches based on Singular Value Decomposition. Ph.D. Thesis, University of Southern California, Los Angeles.
- [9] Bettayeb, M. and Kavranoglu, D. (1993). Performance Evaluation of A New H_{∞} Norm of Large Dynamic Systems. Proceedings of the 1969 JACC, 669-674.

- [10] Clerc, M. and Kennedy, J. (2002). The Particle Swarm: Explosion, Stability, and Yang, Z.J., Hachino, T. and Tsuji, T. (1996). Model Reduction with Time Delay Combining the Least-Squares Method with the Genetic Algorithm. IEE Proceedings on Control Theory and Applications, 143(3): 247-254.
- [11] Zhang, L., Shi, P., Boukas, E.K. and Wang, C. (2008). H_∞ model reduction for uncertain switched linear discrete-time systems. Technical Communique, Elsevier Ltd..
- [12] Zhang, L., Boukas, E.K. and Shi, P. (2009). H_∞ model reduction for discrete-time Markov jump linear systems with partially known transition probabilities. International Journal of Control, 82(2): 343-351.
- [13] Zhao, G. and Sinha, N.K., (1983). Model selection in Aggregated Models. Large Scale Systems, pp. 209-216.
- [14] Zhou, K. (1995). Frequency-Weighted l_∞ Norm and Optimal Hankel norm Model Reduction. IEEE Transaction on Automatic Control, 40(10): 1687-1699

Cost-Efficient Solar Based Multipurpose Crop Cutting Machine

^[1]Shyamala P, ^[2] Amith M Y, ^[3]Bharath V, ^[4] Vishwas Gowda H R

^{[1][2][3][4]} Electronics And Communication Engineering, R.R Institute of Technology, Bangalore

Abstract— This project is aimed to develop crop cutter machine that works towards reducing manpower as well as saving electricity through the utilization of solar energy. In this project the conversion of solar energy to mechanical energy will be attempted. Extend the concept of solar technology on solar crop cutting as energy alternate device. In addition, a prototype of the proposed system is to be implemented. Finally, functionality of the prototype in terms of crop cutting effectiveness is to be tested.

I. INTRODUCTION

As today's world is in constant need for energy as well as the increasing in environmental concern, non-renewable alternatives use as well as polluting fossil fuels has to be carefully investigated. A good alternative would be renewable energies such as solar energy. Solar energy can be implemented in various fields, however for the purpose of this project the discussion would be only with regards to using it for crop cutter machines as it is the device being fabricated. Nevertheless, when utilizing solar energy instead of gasoline in powering crop cutters the gained advantage would be mainly ecological. It is rather inconvenient to operate crop cutters with a standard motor powered as it generates noise pollution because of the loud engine sound, and local air pollution because of the engine combustion. In addition, a motor powered engine needs recurrent maintenance like changing oil of the engine. Even though electric crop cutters carry less environmental pollution however they still carry some hazardous issues in addition to not being easy to utilize. Moreover, if the electric crop cutter is corded, cutting could be problematic and dangerous. To solve this issue a solar based crop cutting machine is to be fabricated with the ability of mowing a lawn by itself after getting programmed

II. PROPOSED SYSTEM

The solar crop cutter working principle is having panels fixed in a specific arrangement in such a way that it can obtain from the sun solar radiation with high intensity easily. These solar panels are used to convert solar energy to electrical energy. The resulting electrical energy is stored in batteries through utilizing solar charger. The solar charger main function is maximizing current from the panels while batteries are charging, and when batteries are fully charged it disconnects the solar panels and reconnects panels when batteries charging are low. The motor is linked to the batteries using connecting wires. Breaker switch is added between

these two mechanical circuits basically it starts and stops motor operations. The solar powered crop cutter designed contains DC motor, control switch, solar panel, a stainless steel blade and a rechargeable battery. Cutting is accomplished through utilizing DC motor which offers the needed torque to drive the stainless steel blade which is coupled directly to the D.C motor shaft. The solar powered crop cutter is operated using the switch on the board which switches the circuit off and permits the current flow to the motor which drive the moving blade. Using solar charging controller the battery recharges.

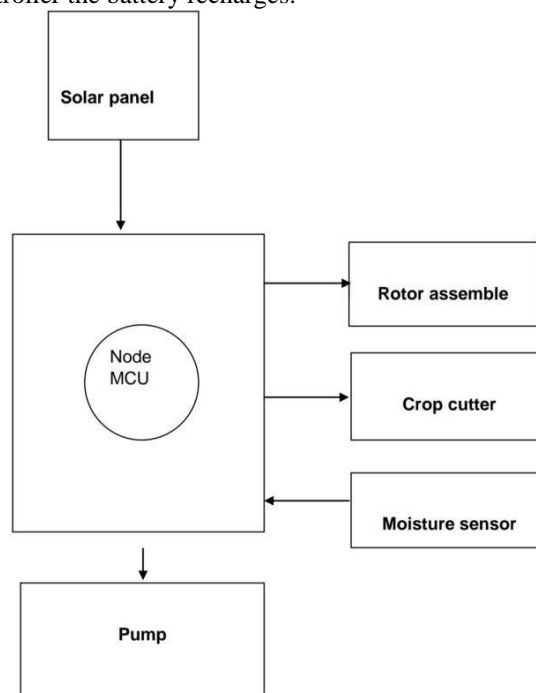


Fig 1. Block Diagram Of Proposed System

III. HARDWARE AND SOFTWARE REQUIREMENTS

Hardware:

- Node MCU
- Blades
- Moisture sensor
- Battery
- DC Motor
- Solar Panel
- Sprinkler

- Water Pump
- Software**
- Embedded C

Blynk app interface

Blynk app is a digital dashboard where one can build a graphical interface for their project. It is done by dragging and dropping the pre-available widgets. It is used to satisfy the requirement to reach the information to the cultivator. The sensor's data are stored in the cloud which can be utilized for the further future analysis whenever it is required.

First, go to Blynk App and sign in with your credentials. open a project (or create a new one -- use Project > Start New Project and give your project a name).

- Adding buttons and assigning functions.
- Terminal interface.

IV. IMPLEMENTATION

In this chapter we discuss about the methodology and working of our project.

V.METHODOLOGY

A brief description of the project is illustrated in figure 2 placed in the result section. The design basically includes ultrasonic sensors, Moisture sensor and Node MCU. When these elements are added together the result would be robotic crop cutter and sprinkler. The aim of the robot was to see the difference between concrete and crop while continuously monitoring its surroundings. Object detection ultrasonic sensor was used to detect if the robot was heading into an object. When designing a robot with blades, safety would be the main concern. For input inserting 16*2 matrixes Keypad was utilized. Proteus the programming was done in Node MCU. And solar pesticide sprayer can give less tariff or price in effective spraying. Solar energy is absorbed by the solar panel which contains photovoltaic cells. The conversion of the solar energy into electrical energy is done by these cells. This converted energy utilizes to store the voltage in the DC battery and that battery further used for driving the spray pump.

Figure 2 demonstrates the hard ware set up which comprises of seven sections being ultrasonic sensor, power supply unit, sprinkler, moisture sensor voltage regulator, and battery, relay and Node MCU module. Where there is plenty of sunshine but insufficient water to carry out farming activities, such as rubber plantation, strawberry plantation, or any plantation, that requires frequent watering. The system is powered by solar system as a renewable energy which uses solar panel module to convert Sunlight into electricity. In addition, the system is powered by an intelligent solar system in which solar panel targets the radiation from the Sun. Other than that, the solar system has reduced energy cost as well as pollution. The system is equipped with four input sensors; two soil moisture sensors, two level detection sensors. Soil moisture sensor measures the humidity of the soil, whereas

the level detection sensors detect the level of water in the tank. The output sides consist of two solenoid valves, which are controlled respectively by two moistures sensors.

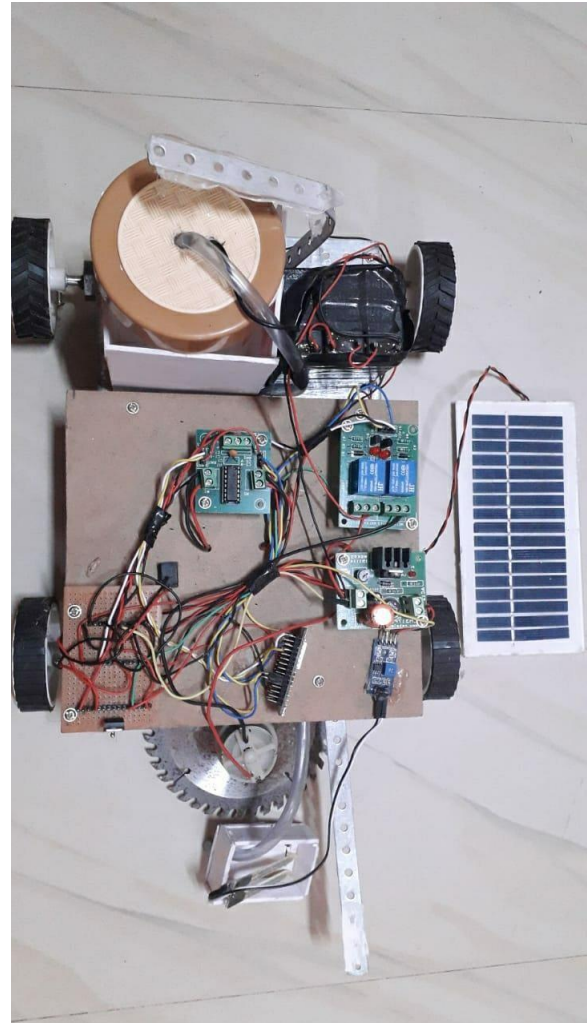


Fig 2. Overall Hardware Kit

ADVANTAGES

1. This is an inexhaustible source of energy and the best replacement to other non-renewable energies in India.
2. Solar energy is environment friendly. When in use, it does not release CO₂ and other gases which pollute the air.
3. Solar energy can be used for variety of purposes like as heating, cooking, drying, or electricity, which is suitable for the rural areas in India.
4. Solar power is inexhaustible. In an energy deficient country like India, where power generation is costly, solar energy is the best alternate means of power generation.

DISADVANTAGES

1. We cannot generate energy during the night time with solar energy.
2. Only the areas that receive good amount of sunlight are suitable for producing solar energy.
3. Solar panels also require storage batteries and invertors to convert direct electricity to alternating electricity so as to generate electricity. Installing a solar panel is quite cheap, installing other equipment's becomes more expensive.
4. Energy production is quite low compared to other forms of energy.

VI. CONCLUSION AND FUTURE SCOPE

The title of this paper and main aim is designing and fabrication of solar operating crop cutting machine. In this project the solar panel will be connected to charge the battery which will operate the crop cutter machine. When sun rises the solar panel will attract the solar energy available in the radiation of the sun then convert it to electrical energy, and when night time comes the machine will still operate by the electrical energy stored in the battery which was charging full morning through the solar panels. The system will be designed and fabricated using a set of components being blades, frame, solar panel, battery along with different electronic components do control the system and The system is equipped with four input sensors; two soil moisture sensors, two level detection sensors. Soil moisture sensor measures the humidity of the soil, whereas the level detection sensors detect the level of water in the tank. The output sides consist of two solenoid valves, which are controlled respectively by two moistures sensors.. This system would be helpful and economic as it consumes no fuel hence reducing environment pollution.

One of the main lessons learnt through this study is that success of PV programmers is significantly enhanced when an integrated strategy is followed. Solar photovoltaic systems, through their flexibility in use, offer unique chances for the energy sector to provide packages of energy services to remote rural areas.

With continuing price decreases of PV systems, other applications are becoming economically attractive and experience is gained with the use of PV in such areas as social and communal services, agriculture and other productive activities, which can have a significant impact on rural development.

To add a feature of charging the battery with electricity along with solar energy.

REFERENCES

- [1] Shubham, S., Vaibhav, S., Dipak, B., Sharad, B., Shrikant, A., 2016. Manufacturing of Solar Crop Cutter. International Journal of Research in Advent Technology. (E-ISSN: 2321- 9637) Special Issue, pp. 325355.
- [2] Sravan, K., Abdul, S., &Surya., 2017. Design and Fabrication of Automated Crop Cutting Machine by Using Solar Energy. International Journal & Magazine of Engineering, Technology, Management and Research. 4(4), pp. 153-159.
- [3] David, W., 2014. Energy definition. [ONLINE] Available at: <http://www.ftexploring.com/energy/definition.html>. [Accessed 03 December 2017].
- [4] Electronics Hub. 2015. 7805 IC Voltage Regulator Circuit Working and Applications. [ONLINE] Available at: <https://www.electronicshub.org/understanding-7805-ic-voltage-regulator/>. [Accessed 06 December 2017].
- [5] MagLab. 2017. Simple Electrical Cell. [ONLINE] Available at: <https://nationalmaglab.org/education/magnet-academy/watchplay/interactive/simple-electrical-cell>. [Accessed 06 December 2017].
- [6] Martin, D., 2017. What is Solar Energy and How Do Solar Panels Work. [ONLINE] Available at: <https://us.sunpower.com/blog/2017/10/25/how-does-solar-energy-work/>. [Accessed 06 December 2017].

Handwritten Character Recognition (HCR): A Literature Review

^[1] Siddanna S R, ^[2] Dr. Kiran Y C

^[1] Dept. of Information Science and Engineering, Sjbite

^[2] Dept. of Information Science and Engineering, GAT

Abstract— Hand Written Character Recognition (HCR) is major surprising and troublesome examination space nearby Image preparing. Recognition of Handwritten Kannada letter sets have been extensively concentrated in the earlier years. As of now different recognition systems are in notable used for recognition of transcribed Kannada letters in order (character). Application space of HCR is computerized record handling like mining data from information section, check, applications for advances, Visas, charge, medical coverage structures and so forth During this overview we present a blueprint of ebb and flow research work led for recognition of transcribed Kannada letters in order. In Handwritten original copy there is no limitation on the composing procedure. Hand written letter sets are muddled to perceive on account of random human penmanship procedure, contrast fit as a fiddle of letters, point. An assortment of recognition procedures for hand written Kannada letters in order are met here close by with their exhibition.

Keywords— Hand written Character Recognition (HCR), feature extraction, Optical Character Recognition (OCR), classifiers, Pre-Processing

I. INTRODUCTION

OCR is a popular technology for handwritten text or converting printed images to Digital, to enable more efficient and accurate electronic editing, storage and search. While there have been decades of studies and improvements in the region, but machines still do not have access to human analytical capabilities. The purpose of the OCR method is to preserve the manuscript in an elusive article.

In online text recognition, words and characters are perceived at run time as fast as they are composed, and thus, have fleeting data. Online techniques acquire the situation of the pen as an element of time directly from the interface. This is commonly done through pen-based interfaces some place the writer composes with an individual pen on an electronic tablet. Dynamic information, which is normally accessible for online content acknowledgments, is complete strokes, set of strokes, approach of stroke, and speed of composing inside each stroke. This valuable data helps in recognition of articles and regularly advisers for improve performing strategies differentiated to offline recognition. A few uses of online recognition are in PDAs, Tablet PCs and advanced cells. The advantage of online recognition techniques over offline strategies is intuitiveness, approval of creator to digitizer (or the other way around), accessible transient data and less inclined commotion. The downside is that the whole article

isn't reachable for handling and afterward, data needs to be prepared powerfully.

An Offline text recognition technique measures a static portrayal of an article. Recognition disconnected content is apportioned in two sub classifications of Typed and Handwritten articles. In both sub classes, a picture of the article acquired from a scanner or camera is handled. Obviously, because of the variety of styles in penmanship and un-benchmarked nature of penmanship styles, the issue of disconnected handwritten recognition is the principle urgent intricacy in OCR and it ordinarily requires language explicit strategies. On the another hand, OCR of composed articles are amazingly much popular for down to earth applications like chronicled article investigation, official note and article handling, and vehicle plate recognition. OCR of composed record for Kannada letter sets has gotten one of the major effective utilizations of innovation in pattern recognition (PR) and artificial intelligence (AI). Practically the entirety of the current exploration around there is to pledge with incredibly complex articles, boisterous and bent articles, as fine as improving recognition rates for messages. there difference. The ideal limit is choosen so that which has least interclass fluctuation.

Skeletonization : It's anything but a morphological activity which changes over the picture in to one pixel wide portrayal without influencing their availability. Diminishing needed to acquiring the skeleton of a picture by disposing of pixels that have multiple neighbors.

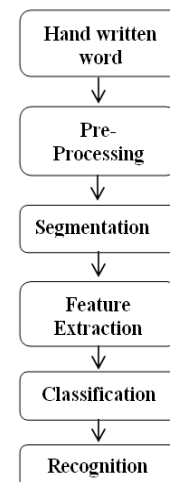


Fig 1: Flow diagram of image processing

Preprocessing is a significant advance in character acknowledgment, which incorporates removal of noise, binarization, skeletonization and standardization .

Removal of Noise is the undesirable power esteems in a picture that has no importance in the yield. Various kinds of noise, for example gaussian noise, impulse noise are added to the image during picture securing. Removing of noise is the strategy needed to dispense with this undesirable piece designs. Linear and non linear separating can be utilized for noise removal. Median channel is a non linear channel extremely compelling in eliminating salt and pepper noise, which is a motivation noise present in picture as little highly contrasting dabs. Median channel sort every one of the pixels in a specific region and supplant the middle pixel with the middle of arranged qualities.

Binarization : Cycle of changing over shading or dark scale picture into bilevel picture. Nearby and worldwide thresholding is the strategy utilized for binarizing a picture. In nearby thresholding distinctive edge esteems are picked however for worldwide thresholding a solitary worth is utilized. Otsu is the worldwide thresholding utilized which iteratively decide all conceivable edge esteems and discover

Normalization Interaction of changing over picture into some standard structure. Standardization incorporates size and slant standardization. Size standardization changes over picture in to fixed size. Bilinear and bicubic insertion can be utilized. Slant may present in the picture at the hour of filtering, which is the deviation of text from standard. To adjust this content slant discovery and rectifications are required.

Segmentation is the way toward changing over input picture in to singular characters. First line segmentation is done followed by word segmentation and followed character segmentation.

Feature extraction is the fundamental stage in character recognition. Which extricate most important features. Recognition exactness is principally relies upon separated features. Diverse element extraction strategies depicted are Contourlet change , Ridgelet change, Curvelet change, Gabor filter, Directional features.

Classification is the dynamic phase of character recognition. The extracted feature are utilized for perceiving characters. The classification of pertinent features are finished by utilizing diverse classifier.

II. BACKGROUND AND RELATED WORK

Manually written letter sets recognition framework's exactness of any picture hand-off upon the affectability of the selection of highlights and classification of classifier used. Subsequently, so many element evacuation and arrangement methods could be set up in the writing.

Following exploration work execute handwritten letter sets recognition of Kannada phrases

Acknowledgment of high exactnesses towards south Indian character recognition is one the really fascinating exploration challenge. Our examination is centered on recognition of quite possibly the most generally utilized south Indian content called Kannada. Specifically, analyze is subject towards the recognition of degraded character pictures which are removed from the antiquated Kannada verse archives and furthermore on the written by hand character pictures that are gathered from different unconstrained conditions. The character pictures in the degraded archives are somewhat foggy because of what character picture is forced by a sort of broken and untidy appearances, this specific viewpoint prompts different clashing practices of the performance calculation which thusly diminishes the exactness of recognition. The preparations of degraded examples of character picture tests are completed by utilizing one of the profound convolution neural networks known as Alex net. The exhibition assessment of this experimentation is subject towards the written by hand datasets accumulated artificially from clients old enough gatherings between 18-21, 22-25 and 26-30 and furthermore printed datasets which are extricated from old report pictures of Kannada verse/writing.[1]

Researchers have discovered the numerous advances to perceive hand written character into text. Handwriting recognition is the capacity of a computer to peruse handwriting as real content. To change handwriting over to text, this is undeniably the best program which can be utilized to defeat the numerous issues which are available in recognition. Focus is on centers around fundamental issue looked in recognition of stroke edges in the written by hand character with different example of recognition methods. In view of the overview taken for this issue, say that division of the character is low and forestalls high prominence exactness of unconstrained handwriting [2]

Digitization of machine printed or handwritten content records have gotten exceptionally famous with the progressions in figuring and innovation. People have attempted to automatized their work by supplanting themselves with machines. The change from manual to automatization offered ascend to a few exploration territories and text acknowledgment is one among them. Profound learning and AI methods have been end up being entirely appropriate for optical character acknowledgment. An exceptional outline of four AI and profound learning designs [3].

A Pre-preparing is the underlying and fundamental stage in optical character recognition is the Pre-processing. Segmentation manages the extraction of individual segment from a report picture. Number of procedures like projection profile, associated parts, gaps between characters/segments is

accounted for in the writing for segment extraction followed by feature extraction and recognition of the individual segment. These procedures gives great outcomes if segments are confined yet falls flat if parts are contacted, shadowed or slanted. An epic method is needed to deliver such issues to improve the acknowledgment rate. The issue of division for Roman content cursive handwriting is tended to by different creators yet insufficient tended to for Indian content particularly Devanagari content. An audit which is limited to disconnected written by hand content space. It endeavor to survey different methods for character division considering contacting characters for disconnected written by hand words in Devanagari content and contents having comparable attributes (like Bangla, Gurumukhi), information base utilized and their exactness detailed in the writing[4]

At the point when Handwritten Kannada report goes through text line segmentation, the interaction is alluded to as Text line segmentation and skew correction. This is very fundamental for the HCRS (Human Character Recognition System). The cycle of Text line segmentation and skew correction will in general hush up testing during report examination. The proposed framework presents extemporized text-line segmentation alongside skew correction for which the handwritten Kannada record shapes the dataset. Following are the three techniques for

completing preprocessing, specifically: (i) separating (ii) dim scale change and (iii) Binarization. The ESLD (Enhanced Supervised Learning Distance) calculation is being received for the appraisal of distance in the midst of text lines and G_Clustering helps in gathering of words or the Connected Components. Additionally, by registering slant point as for the hole, Skew assessment can be performed. It's explained from the yield that the proposed framework displays better.[5]

Optical character recognition framework is a need for the field of man-machine association. Handwritten character recognition is a subset of OCR method by which computer classifies the handwritten letter sets just as digits. In this work, four techniques utilizing a vanilla Autoencoder and a Convolutional Autoencoder. For classification reason KNN, SVM based classifiers, for example, cross breed KNN-SVM and m-SVM.[6]

A cross language stage to see characters and articulations of low resource substance for instance substance which don't have standard dataset and the datasets are not open for nothing. Indic substance come from ordinary source and a segment of the substance have an average 3 zonal plan. Affirmation of such substance ought to be conceivable with the help of various substance having tantamount development. To see these characters the model is set up with source language Kannada with zone-wise getting ready and testing is done with both Kannada and the target language Telugu. An accuracy of 88% for Kannada and 62% for

Telugu characters is refined by using Inception Model which is amassed using Convolution Neural Networks (CNN) picture classifier. The dataset contains 10700 Kannada characters. The model is moreover gone after for 100 articulations of Telugu and Kannada with an accuracy of 72% and 82% independently.[7]

In design acknowledgment, recognizing Kannada manually written numerals are a mind boggling tie. To achieve a most powerful Kannada Numerals acknowledgment measure. In this, handwritten Kannada characters are enthralled in report style and are exposed to Pre-processing and characteristic extraction measures. Pre-processing involves steps like noise removal, binarization, normalization, slant alteration, and thinning. Features are removed by misusing procedures like Drift Length Count, Direction related movement code, DWT and Curvelet Transfiguration Wrapping. For an amazing classification measure profound convolution neural network classifier is liked. Separation precision of Kannada numeral pointed here will rethink 96% of exactness[8]

Recognition of recorded printed degraded Kannada characters isn't tackled totally and stays as a test to the analysts still. A scale for estimating degraded of a character is proposed. Further, the debasement is portrayed to high, medium and low dependent on this scale, and use it to contemplate the effectiveness of the character rebuilding method planned. Another methodology, fit discriminant examination (FDA) for recognition is proposed and contrasts its recognition exactness and the current procedures support vector machines (SVM) and Fisher Linear discriminant (FLD) analysis. Through broad experimentation it is set up that revamping of characters improves the recognition exactness of learning-based methodologies SVM, FDA, and FLD altogether. Further, it is set up that the proposed approach FDA gives the best recognition precision for chronicled printed degraded reports. It is additionally demonstrated that preparation testing set applying the proposed degradation measure is needed for better acknowledgment precision.[9]

Word Spotting has been a developing field of exploration in the previous few decades. Getting going with the word spotting in printed text the advancement has now unfolded upon the spotting of words in manually written records. Recognition of handwritten words is a difficult issue due to changed styles of characters and similitude of their shape. Word Spotting makes archive ordering simpler and assists helps in interpreting the reports. Break down different technique by which word recognition should be possible in Kannada handwirten records. At the point when a client gives a question as a picture, the word is perceived showing its comparing special name. Different element extraction strategies alongside Deep Learning methods have been tested. We find that CNN with a spatial layer change beats different methods for Kannada Handwritten words.[10]

III. ONCLUSION

Detailed review of character recognition in kannada language using different algorithms for recognition, from this survey it can be observed that : Creation of large database of kannada handwritten word of different age group, reliable extraction/segmentation of touching handwritten character, adoption of efficient algorithm for separation and recognition of modifiers, analysis and understanding of numerals and ambiguous characters in handwritten word. The accuracy of recognition depends on the segmentation and classification methods used.

REFERENCES

- [1] Shobha Rani, N Et Al. Deformed Character Recognition Using Convolutional Neural Networks. *International Journal Of Engineering & Technology*, [S.L.], V. 7, N. 3, P. 1599-1604, July 2018. Issn 2227-524x. 2021.
- [2] Monisha G.S., Malathi S. (2021) Effective Survey On Handwriting Character Recognition. In: Singh V., Asari V.K., Kumar S., Patel R.B. (Eds) *Computational Methods And Data Engineering*. Advances In Intelligent Systems And Computing, Vol 1257. Springer, Singapore.
- [3] R. Sharma, B. Kaushik And N. Gondhi, "Character Recognition Using Machine Learning And Deep Learning - A Survey," 2020 International Conference On Emerging Smart Computing And Informatics (Esci), Pune, India, 2020, Pp. 341-345.
- [4] Monika Kohli; Satish Kumar. "Comparative Analysis Of Segmentation And Recognition Techniques For Offline Handwritten Words". *International Research Journal On Advanced Science Hub*, 2, 8, 2020, 41-48.
- [5] Shakunthala B S, Dr. C S Pillai Enhanced Text Line Segmentation And Skew Estimation For Handwritten Kannada Document. *Journal Of Theoretical And Applied Information Technology* 15th January 2021. Vol.99. No 1
- [6] Mahapatra D., Choudhury C., Karsh R.K. (2020) Handwritten Character Recognition Using Knn And Svm Based Classifier Over Feature Vector From Autoencoder. In: Bhattacharjee A., Borgohain S., Soni B., Verma G., Gao Xz. (Eds) *Machine Learning, Image Processing, Network Security And Data Sciences*. Mind 2020.
- [7] Communications In Computer And Information Science, Vol 1240. Springer, Singapore.
- [8] Hebba C., Mamatha H.R., Sahana Y.S., Dhage S., Somayaji S. (2020) A Convolution Neural Networks Based Character And Word Recognition System For Similar Script Languages Kannada And Telugu. In: Singh P., Panigrahi B., Suryadevara N., Sharma S., Singh A. (Eds) *Proceedings Of Iccit 2019. Lecture Notes In Electrical Engineering*, Vol 605. Springer, Cham.
- [9] Hallur, Vishweshwrayya & Hegadi, Ravindra. (2020). Handwritten Kannada Numerals Recognition Using Deep Learning Convolution Neural Network (Dcnn) Classifier. *Csi Transactions On Ict*. 8. 10.1007/S40012-020- 00273-9.
- [10] Sandhya, N. & Rangarajan, Krishnan & Babu, Ramesh & Rao, N.. (2019). An Efficient Approach For Handling Degradation In Character Recognition. *International Journal Of Advanced Intelligence Paradigms*. 14.14.10.1504/Ijaip.2019.102960.
- [11] T. Sureka, K. S. N. Swetha, I. Arora And H. R. Mamatha, "Word Recognition Techniques For Kannada Handwritten Documents," 2019 10th International Conference On Computing, Communication And Networking Technologies (Iccnt), Kanpur, India, 2019, Pp. 1-7.
- [12] R. Fernandes And A. P. Rodrigues, "Kannada Handwritten Script Recognition Using Machine Learning Techniques," 2019 Ieee International Conference On Distributed Computing, Vlsi, Electrical Circuits And Robotics (Discover), Manipal, India, 2019, Pp. 1-6.
- [13] K. G. Joe, M. Savit And K. Chandrasekaran, "Offline Character Recognition On Segmented Handwritten Kannada Characters," 2019 Global Conference For Advancement In Technology (Gcat), Bangalore, India, 2019, Pp. 1-5.
- [14] Bannigidad P., Gudada C. (2019) Age-Type Identification And Recognition Of Historical Kannada Handwritten Document Images Using Hog Feature Descriptors. In: Iyer B., Nalbalwar S., Pathak N. (Eds) *Computing, Communication And Signal Processing*. Advances In Intelligent Systems And Computing, Vol 810. Springer, Singapore.
- [15] Gudada, Chandrashekar & Bannigidad, Parashuram. (2018). Identification And Classification Of Historical Kannada Handwritten Document Images Using Lbp Features. *International Journal Of Intelligent Systems Design And Computing*. 2. 176.10.1504/Ijisd.2018.10017638.
- [16] N. S. Rani, A. C. Subramani, A. Kumar P. And B.R. Pushpa, "Deep Learning Network Architecture Based Kannada Handwritten Character Recognition," 2020 Second International Conference On Inventive Research In Computing Applications (Icirca), Coimbatore, India, 2020, Pp. 213-220.

Assessment of Surface properties of Benincasa hispida and Cucurbita peels for Chromium uptake

^[1] Soibam Sangeeta, ^[2] Thiyam Tamphasana Devi, ^[3] Potsangbam Albino Kumar
^{[1][2][3]} National Institute of Technology, Manipur

Abstract— This study investigates the chromium adsorption feasibility by agricultural waste based activated ash gourd (AGP) and activated pumpkin peels (APP) by employing Kinetic models (Intra – particle diffusion, Elovich, First order and Second order models) and non – linear isotherms (Langmuir and Freundlich) models. The surface morphology and pore size distribution of AGP and APP were measured using Scanning Electron Microscope (SEM), Energy Dispersive X-ray Measurements (EDAX), and Brunauer Emmett Teller (BET). The adsorption data reveals fixing on Elovich equation with correlation coefficient (R^2) of 0.97 and 0.94 respectively for AGP and APP as compared to 0.89 and 0.91 for diffusion model. These finding suggest the predominantly physical adsorption behaviour of total chromium by both the adsorbents. Freundlich's isotherm model showed a better fit than Langmuir's equation for AGP and APP with lesser Chi square (χ^2) error of 0.31 and 1.11 respectively against that of Langmuir with 8.11 and 11.14 indicates the heterogeneous surface of these agricultural based adsorbents.

Keywords— Bioadsorbents, Elovich, Intra-particle diffusion and Non-linear Regressions

I. INTRODUCTION

Heavy metals are known toxic environmental pollutants. Some of the most toxic heavy metals includes chromium, arsenic, cadmium, mercury, lead, nickel, and zinc [1]. Various natural and anthropogenic sources of heavy metals include soil erosion, natural weathering, mining, industrial effluents and many others [2]. The most commonly occurring forms of Chromium are Cr^{3+} and Cr^{6+} . Toxic Chromium are generated from welding on stainless steel, metal structures coated with chromate paints, sewage and fertilizers [3], electroplating (chrome plating), leather tanning, textile dyes, pigments in paints, inks and plastics etc. [4] leading to an adverse effects on both ecological and biological species. Ingestion of chromium causes cancer, haemorrhaging, irritation in the nose, lungs and throat and ulcers. Due to ample abundance of oxygen in the environment, lesser toxic Cr (III) gets reduced to highly toxic and soluble Cr (VI). Thus, becoming major concerns for its removal.

Many conventional and non - conventional methods were employed by several researchers for the removal and reduction of chromium ions from aqueous solutions. Some of the methods are chemical precipitation, reverse osmosis, ion exchange, electro - dialysis, adsorption and bio – sorption [4]. Among these methods, bio – adsorption is most commonly used in the past decade due to its cost effectiveness, technical

feasibility, eco - friendly, easy handling and abundant availability of low cost bio – adsorbents.

In this study, activated carbon derived from Ash Gourd (AGP) and Pumpkin peels (APP) used for chromium removal were analysed by intra - particle diffusion model. Batch experiments were conducted at different pH, concentration and contact time. The parameters were analysed using different non – linear kinetic models and Isotherms.

II. MATERIALS AND METHODS

A. Preparation and Characterization

Ash Gourd and Pumpkin used as adsorbents were procured from local market. They were peeled, washed and oven dried at 80 °C for 12 hours. The Ash gourd and pumpkin peels were crushed into fine powders and were further impregnated with H_3PO_4 acid and activated in the muffle furnace at 300 °C and 250 °C respectively. The activated carbons were washed thoroughly and oven dried at 100 °C and allowed to pass through 125 mesh size screen. The dried and activated carbon were then stored in the desiccator for further use.

To understand the surface morphologies and textures of the activated carbons, Scanning Electron Microscopy (SEM) (Sigma 300) was operated at 5.00 kV, magnification 100.00 KX coupled with Energy dispersive X-ray analysis (EDAX) (Zeiss Gemini) to give the confirmation for total chromium removal after the adsorption processes. Brunauer-Emmett-Teller (BET) analyser was also used to determine the size distribution and mean particle sizes of both the adsorbents [5].

B. Batch Experiments

The stock solution (1000 mg/L) was prepared by dissolving required amount of $K_2Cr_2O_7$ in double distilled water. A series of sample solution were further diluted from the stock solution and appropriate amounts of both the adsorbents were added onto the series of 500 mL Tarson beakers at various initial chromium concentrations. The solution were operated in the orbital shaker at 250 rpm (Phipps and Bird Jar Test Apparatus, (PB-600) for 150 min. All the experiment tests were conducted in triplicates and if the average value has more than a standard deviation of 5, the values are discarded and the experiments are repeated again to avoid any experimental errors. The samples were then diluted and filtered using Whatman No. 47 filter paper. Finally, the filtered solution were determined by Atomic Absorption Spectroscopy (AAS, Perkin Elmer, USA) and UV Visible Spectrometer (Evolution 201, Thermo Fischer Scientific) at a wavelength of 540nm. Cr (III) reduced is calculated from the

difference between the total chromium and Cr (VI) adsorbed. The adsorption capacity is given by:

$$q = \frac{C_o - C_t}{m} V \dots \dots \dots (1)$$

Where, q is the amount of adsorbed in mg/g, C_o and C_t are the initial and final concentrations, m is the mass of the adsorbent used and V is volume of the solution in litres.

C. Kinetics, Isotherms and Error analysis

In order to stimulate the adsorption kinetics, intra – particle diffusion model (IDP), Elovich model, Pseudo 1st order and 2nd order equations were applied for chromium – AGP and APP interactions. After the attainment of equilibrium conditions, Langmuir and Freundlich Isotherm models were applied to better understand the monolayer adsorption by identical sites and/or surface heterogeneity of the adsorbents respectively [5]. The non – linear regression involves the error distributions between the calculated and predicted values based on the convergence data and were used for analysing the adsorption processes. Lower values of χ^2 indicated the similarities of the experimental data.

$$\chi^2 = \sum_{i=1}^n \frac{(q_{e,cal.} - q_{e,pred.})^2}{q_{e,pred.}} \dots \dots \dots (2)$$

III. RESULTS AND DISCUSSIONS

A. Characterization

The SEM analysis of AGP and APP before and after total chromium adsorption indicates the presence of large sizes pores on their surfaces, which were responsible for the enhancement of the adsorption of chromium ions. The SEM images are shown in Fig 1. The hollow and porous portions available on the surfaces binds the adsorbate with the adsorbents [6]. The chemical nature of the adsorbents before and after the adsorption were obtained from the EDAX analysis. It focuses on the different areas and the peaks are shown in Fig 2 (1B and 2B), confirming the presence of chromium after the adsorption processes. The specific surface area, pore sizes and volume distributions were studied using BET method. The particulate properties are listed in Table 1.

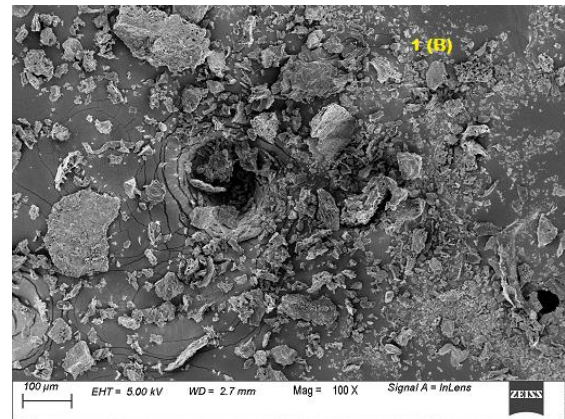
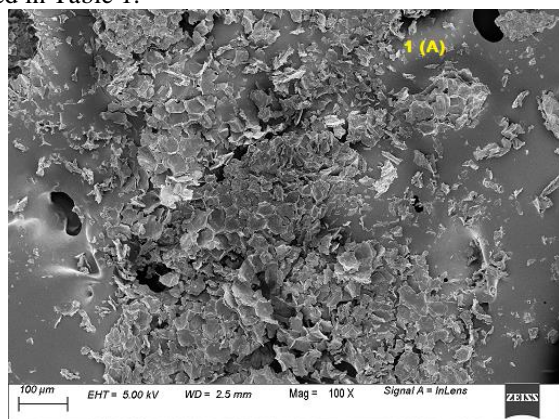


Fig. 1: SEM images (A) before and (B) after adsorption of total chromium by AGP

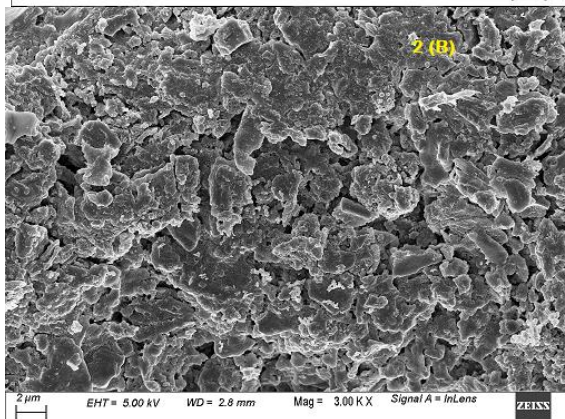
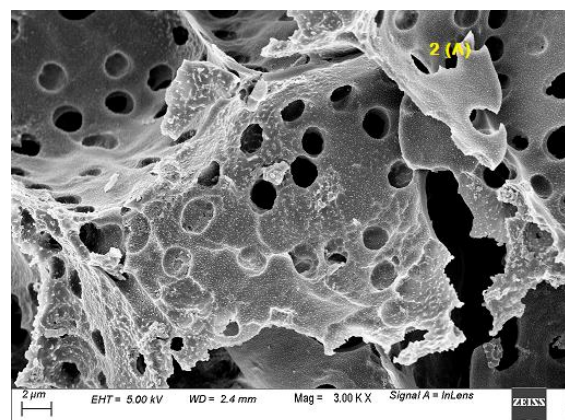


Fig. 2: SEM images (A) before and (B) after adsorption of total chromium by APP

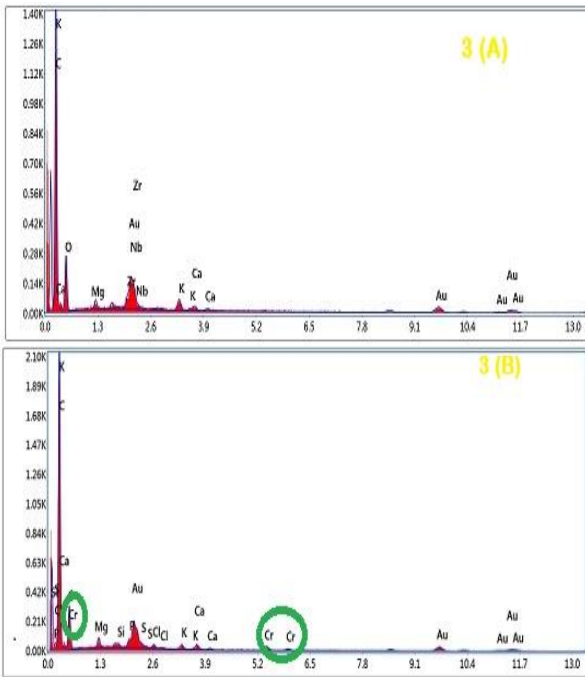


Fig. 3: EDAX images (A) before and (B) after adsorption of AGP

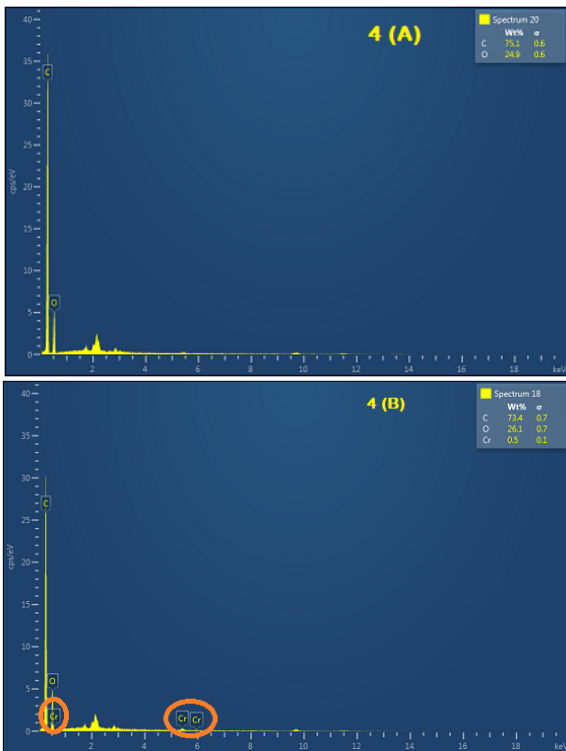


Fig. 4: EDAX images (A) before and (B) after adsorption of total chromium by AGP

Table 1: BET analysis data for AGP and APP adsorbents

Adsorbents	Surface Area (m ² /g)	Average pore diameter (nm)	Pore volume (cm ³ /g)
AGP	36.036	7.612	0.153
APP	33.979	4.102	0.175

A. Adsorption kinetics

For any adsorption system design, prediction of kinetic models is most important [7]. The initial adsorption was analysed by Intra – particle Diffusion model. It is a 3 step process, external diffusion, diffusion inside the pores and diffusion on the surface phase. This step determines the rate of the reaction. It is given by:

$$q_t = K_{IPD}t^{1/2} + C \dots \dots \dots (3)$$

Where, q_t is the adsorption capacity in mg/g, K_{IPD} is the rate constant in mg/g min^{1/2} and C is the boundary thickness in mg/g.

The intra – particle diffusion model fit and data for chromium adsorption onto the adsorbents AGP and APP is shown in the Fig. 5 and Table 2. The first phase ranges from 5 to 20 min of contact time with rapid removal from 26% to 72% and the second phase from 20 to 120 min with removal from 72% to 86%. The initial stage indicates rapid fast adsorption, where rates (K_{IPD}) and boundary thickness (C) increases with the increase in concentration. But the second stage indicates slower rates.

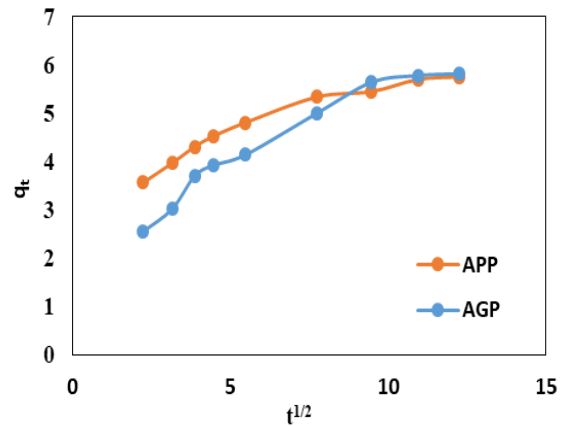


Fig. 5: Intra – particle diffusion model plot for chromium adsorption by AGP

The Non – linear kinetic models of Elovich, first order and second order kinetic equations are given by:

$$q_t = \frac{1}{\beta} \ln(1 + \alpha\beta t) \dots \dots \dots (4)$$

$$q_t = q_e - e^{-K_1 t} \dots \dots \dots (5)$$

$$q_t = \frac{K_2 q_e^2 t}{1 + K_2 q_e t} \dots \dots \dots (6)$$

Where, q_t is the adsorption capacity in mg/g, α and β are Elovich constants in mg/g min and g/mg respectively, t is the time in min, q_e is the amount adsorbed at equilibrium in mg/g,

K_1 and K_2 are the first order and second order constants in /min and mg/g min respectively.

The plots for all the three models (Elovich, First order and Second order) are shown in Fig. 6 and 7 for both the adsorbents AGP and APP. The Elovich coefficients (α and β), rate constants (K_1 and K_2), adsorption capacities (q_e), correlation coefficients (R^2) and χ^2 for both the adsorbents for all kinetic models are given in Table 2. The evaluated data of R^2 clearly indicates that Elovich model have performed better for both the adsorbents. The first and second order kinetics are discarded due to higher χ^2 values (5.33 and 1.74) and lesser R^2 (0.84 and 0.66) values. Considering all the evaluated values, the kinetics of adsorbents (AGP and APP) adsorption can be described in the order of fitting: Elovich, Pseudo second order and Pseudo first order equations.

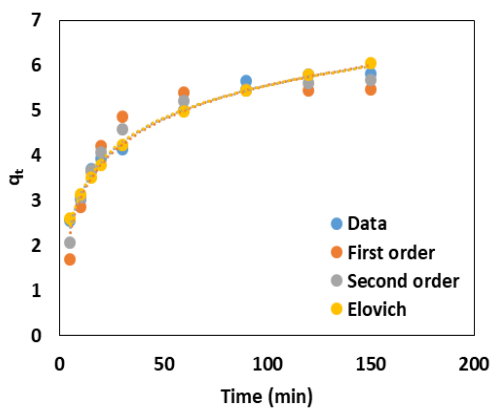


Fig. 6: Non – linear fit of kinetic models for chromium adsorption by AGP

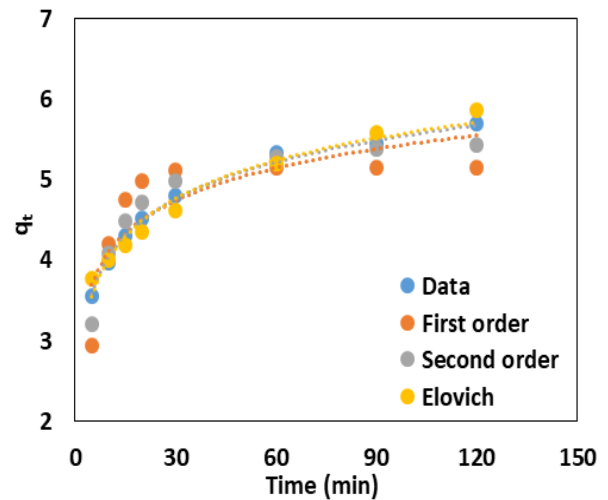


Fig. 7: Non – linear fit of kinetic models for chromium adsorption by APP

Table 2: Parameters of different Kinetic models

Kinetics							
Intra – particle diffusion model				Pseudo first order			
	K_{IPD} (mg/g min ^{1/2})	C	R^2	χ^2	K_1	R^2	χ^2
AGP	1.86	0.24	0.89	2.56	5.45	0.84	5.33
APP	2.89	0.14	0.91	1.562	5.15	0.66	1.74
Elovich model				Pseudo second order			
	α (mg/g min)	β (g/mg)	R^2	χ^2	K_2	R^2	χ^2
AGP	1.20	3.62	0.97	0.132	0.62	0.93	6.13
APP	1.19	1.95	0.94	1.254	1.51	0.91	3.21

B. Adsorption Isotherm

The adsorption isotherm indicates the molecular distribution phenomena of adsorbate adsorbent interaction phase on reaching the equilibrium [7]. Langmuir and Freundlich isotherm models are analysed for the theoretical evaluation and interpretation of all the predicted data for equilibrium adsorption capacity of chromium on both the adsorbents (AGP and APP). The equations are given by:

$$q_e = \frac{K_L C_o}{1 + a_L C_o} \dots \dots \dots (7)$$

$$q_e = K_F C_e^{1/n} \dots \dots \dots (8)$$

Where, q_e is the amount adsorbed at equilibrium in mg/g, K_L and K_F is the Langmuir and Freundlich constant in L/g, C_o and C_e are the initial and equilibrium concentrations in mg/L.

The parameters of both the Langmuir and Freundlich equations were evaluated by using non – linear regression analysis and are summarized in Table 3. The experimental data and plots for both the adsorbents are shown in Fig. 8 and 9 for both the adsorbents AGP and APP. The values of χ^2 and R^2 suggest that Freundlich isotherm is the better fit

isotherm for both the adsorbents (AGP and APP). The Freundlich isotherm exponents indicates the surface heterogeneity and formation multiple layer physisorptions. The maximum adsorption capacity obtained were 8.429 mg/g

and 6.214 mg/g for the adsorbents AGP and APP respectively.

Table 3: Parameters of Langmuir and Freundlich Isotherm non – linear models

Langmuir Isotherm						Freundlich Isotherm				
Adsorbents	K_L	a_L	R^2	SD	$\sum \square^2$	K_f	b_f	R^2	SD	$\sum \square^2$
AGP	1.11	0.48	0.91	0.03	8.114	1.09	1.93	0.99	0.08	0.31
APP	0.62	-0.3	0.90	0.32	11.241	9.86	1.14	0.96	0.4	1.115

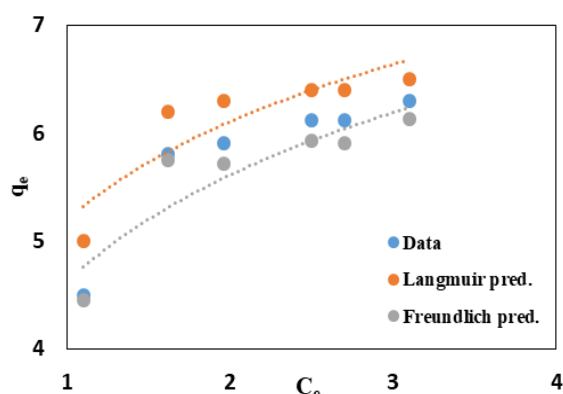


Fig. 8: Langmuir and Freundlich isotherm for total chromium adsorption by AGP

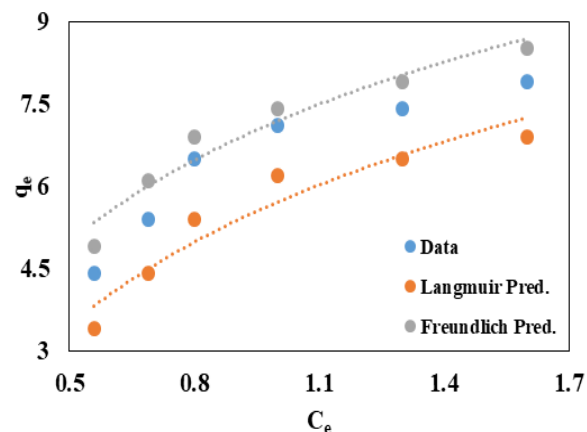


Fig. 9: Langmuir and Freundlich isotherm for total chromium adsorption by APP

IV. CONCLUSION

The experimental data were tested against the different models. The data evaluated in the previous findings for the linear regression fitted better with pseudo second order kinetics with a correlation coefficient R^2 of 0.99 and \square^2 of 0.012 [8]. But for the non – linear regression, the adsorption process follows Elovich kinetic model with R^2 of 0.97 and 0.94 for AGP and APP respectively. The adsorption follows Freundlich isotherm model with a maximum adsorption capacity of 8.429 mg/g and 6.214 mg/g and R^2 value of 0.99

and 0.96 for AGP and APP respectively. This study proves that both the bio – adsorbents AGP and APP are suitable for the removal of total chromium from aqueous solutions containing chromium ions.

REFERENCES

- [1] M. Mohanty and H. K. Kumar, "Effect of ionic and chelate assisted hexavalent chromium on mung bean seedlings during seedling growth", *Journal of Stress physiology and Biochemistry*, vol. 9 (2), pp. 230-241, Feb. 2016.
- [2] A. Ghani, "Effect of chromium toxicity on growth, chlorophyll and some mineral nutrients of Brassica juncea L", *Egyptian Acad J Biol Sci.*, vol. 2(1), pp. 9-15, August 2011.
- [3] R. Gürkan, H. I. Ulusoy and M. Akçay, "Simultaneous determination of dissolved inorganic chromium species in wastewater/natural waters by surfactant sensitized catalytic kinetic spectrophotometry", *Arabian J Chem.* Vol. 5(2), pp. 12-16, June 2017.
- [4] L. Largitte and R. Pasquier, "A review of the kinetics adsorption models and their application to the adsorption of lead by an activated carbon", *Chemical Engineering Research and Design*, vol. 109, pp. 495-504, Feb. 2016
- [5] F. Batool and J. Akbar, "Study of Isothermal, Kinetic, and Thermodynamic Parameters for Adsorption of Cadmium: An Overview of Linear and Nonlinear Approach and Error Analysis", vol. 11, pp. 15-21, July 2018.
- [6] C. Nagy and C. Manzatu, "Linear and nonlinear regression analysis for heavy metals removal using Agaricus bisporus macrofungus", *Arabian Journal of Chemistry*, vol. 10, pp. 569-579, March 2014.
- [7] S. Sangeeta and P. A. Kumar, "Efficacy of bio-carbon mediated chromium adsorption from contaminated groundwater: A kinetic approach", *Journal of Indian Chemical Society*, vol. 10(b), pp. 1-4, October, 2020.

Indoor Navigation Using Beacons

^[1]Spandana, ^[2]Veena.S

^[1] Student, Dept. of ECE, PES University, Bengaluru, India

^[2] Assistant Professor, Dept. of ECE, PES University, Bengaluru, India

Abstract— *Invention of Indoor Navigation system (INS) is widely adapted in past few years. Due to the inefficiency of Global Positioning System (GPS) signals in the indoor environment, several other technologies such as Wi-Fi, Digital Compass Technologies, QR Code, RFID etc. are used. This paper presents the use Bluetooth Low Energy (BLE) Beacon for INS as it is most prominent in terms of accuracy, range, and privacy. BLE is a wireless technology designed and marketed by Special Interest Group (SIG). Beacons emit radio frequency signals that can be used for distance calculation and in turn the user's location is estimated. For this purpose, a mobile application is developed that helps to track the user's current location with the help of BLE Beacon signals as reference points. It also provides the shortest path using Dijkstra's algorithm and navigates the user from one location to their desired location based on these signals.*

Keywords— *Beacon, Dijkstra Algorithm, Indoor Navigation, Trilateration.*

I. INTRODUCTION

and controlling the movement of a person or an object from one place to another. GPS is the most common system used for this purpose since it provides high precision location information in open environment [1]. However, GPS has its own limitations. In indoors spaces, GPS signals gets blocked by the walls and cannot enter the room making it impossible to calculate the exact location. Also the cost of GPS implementation for indoor navigation is very huge. Due to these reasons, methods like Position Dead Reckoning (PDR), Computer vision, Radio Frequency (RF) signals can be utilized for this purpose.

In this paper, the use of BLE is demonstrated which allows the incorporation of Bluetooth transmitters into small physical systems, that are power efficient. Beacon technology is the perfect platform for attracting supporters and providing relevant and useful information. In addition, the increasing penetration of the Internet of Things (IoT) across the world is also projected to drive the growth of the beacon technology market. Furthermore, it has high significance in the retail and marketing sector since they are cost-effective and easy to deploy.

This paper aims in providing accurate real time location of the user by developing an application that provides navigation services by first creating the blueprint of a given building, where there is no layout information and also to navigate the user within the building. The Received Strength Signal Indicator (RSSI) values obtained from BLE beacons play a very important role for this purpose. It also aims in

providing the shortest path for the user to reach the destination.

Section II in this paper represents previous works on INS which describes the inefficiency of other technologies in comparison. Section III explains the methods considered in implementing this system. Section IV demonstrates the project implementation and the project results are explained in section V. Section VI concludes the paper.

II. RELATED WORK

Various technologies like Wi-Fi, Bluetooth, RFID, VLC, UWB etc., were considered in implementing the INS [2]. Each technology has certain advantages as well as few disadvantages. Infrared and Ultrasound are low in cost and has high accuracy but is affected by interference of obstacles and used only in small areas. RFID provides limited range, less than 1m. It is not suitable for exhaustive localization. Wi-Fi do not require additional infrastructure. But it offers low power accuracy of 5 – 15m which is less than BLE. Wireless network has greater coverage but its performance can be affected by the obstacles. Therefore, beacons are used.

The system can also be implemented using a web application that would provide same functionalities where, the user is alerted with a URL notification. Attached messages can be added to beacons using an attachment and it can be accessed with any desired application. These notification along with a location service helps in analysing the environment effectively. "Mapbox GL JS" tool is used to develop custom map styles since it is compatible with android, iOS and also for web application for designing the suitable indoor maps [6].

III. METHODOLOGY

A. BLE BEACONS

Beacons are small and wireless radio transmitters that uses BLE to transmit signals to other devices nearby by broadcasting small data packets at every regular intervals of time within a short range of 100ms to few seconds and operate on coin-cell batteries without any internet connection. It is feasible to carry and install due to its small size, highly cost-effective and low maintenance. These data packets are received by the compatible devices via radio waves.

1) Beacon Protocol

Beacon protocols are the standards of BLE communication. Each protocol describes the data packet structure broadcasted by the beacons which are divided into small segments. It contains beacon data like output power, signal strength, unique id etc. These data are interpreted using

the code or by the tool provided by the protocol developer. Some of the beacon protocols are iBeacon, Eddystone, AltBeacon, Geo-Beacon, URI Beacon etc. Among these, iBeacon and Eddystone are the popular ones.

i) iBeacon: iBeacon is a name of Apple's technology standard and the first developed BLE technology that allow the applications running on both iOS and Android devices to detect Bluetooth signals. Under iBeacon format, the advertising packets has four piece of information as in Fig.1, UUID, Major, Minor, Tx power- It is the signal strength measured 1m from the device and is hardcoded in advance.

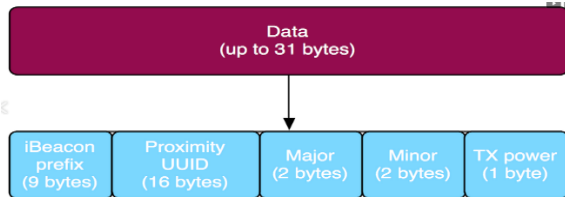


Fig.1. iBeacon data field.

iBeacons are widely used protocol but while implementing, certain measures must be considered. The data signal has to be transmitted at every 100ms, assuring its availability but it reduces the battery life by consuming more power. Its private distribution is also a drawback i.e., to use iBeacon protocol and its related APIs, a paid Apple developer account must be created and register to their MFi program. Even though it provides a platform for both iOS and Android, iBeacon mobile applications is somehow feasible to Apple products only.

ii) Eddystone: Eddystone is a BLE beacon format developed by Google with transparency and robustness. It is an open source and can be detected by both Android and iOS devices and provides numerous advantages over iBeacon. The Eddystone data field contains information same as in iBeacon, formatted in different way shown in Fig.2. Here, the Tx power is measured at a distance of 0m.

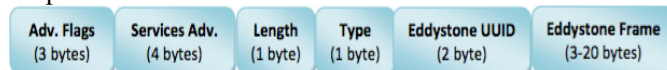


Fig.2. Eddystone data field

Depending on the beacon purpose, several frame types are available-

- Eddystone-UUID: It broadcasts an identifying code enabling the application to retrieve data from their servers. It is a unique, static ID with a 10B Namespace part and a 6B Instance part [6].
- Eddystone-URL: It broadcasts URL of at most 18 characters directly used by the client.
- Eddystone-TLM: It provides beacon data such as battery level, sensor data, beacon temperature, advertisement count etc., to the beacon administrators. Since it does not contain any ID it has to be accompanied by other frame (either UID or URL).
- Eddystone-EID: It is similar to the UID frame but to increase the protocol security, it broadcasts encrypted rotating identifier.

B. RF Signals

RF signal refers to wireless electromagnetic signal, mainly used for communication and is measured using the parameter known as RSSI. It defined as the power measured in the received radio signal, expressed in dBm. This value varies due to multiple external factors influencing the radio waves. Value less than -100dBm is considered as poor signal and value above -50dBm is a strong value. The RSSI value can be converted into distance and stored in any database. Between the transmitter and receiver, the signal strength does not require any time synchronization. Hence, it is a good choice for INS.

C. Distance Calculation

Different models have been proposed for understanding the signal propagation which accounts for estimating the distance based on the RSSI values. Some of them are discussed in this section.

1) Path loss Model: INS can be modelled using parametric model like log-normal shadowing model. The distance estimation equation based on this model can be expressed using the equation below.

$$RSSI = Tx\ power - 10n\log\left(\frac{d}{d_0}\right) + X \quad (1)$$

Here, the distance between the transmitter and receiver is denoted as d ; d_0 is reference distance; RSSI is signal strength of the beacon as observed on the receiving device; Tx power is the calibrated power measured in dBm; 'n' is the environmental constant, varies between 2 to 4; X represents normally distributed random variable and its average is 0. The above equation can be simplified to the equation given below.

$$d = 10^{\left(\frac{Tx\ power - RSSI}{10n}\right)} \quad (2)$$

Log shadowing is one of the easiest model to calculate the distance since it only requires measuring the signal strength.

2) Android Beacon Library Model: Similar to log shadowing model, this model is also a parametric model that estimates the distance by making use of the RSSI values and empirical measurements to calculate the logarithmic equation constants [7] [8]. Android library model uses the formula given below.

$$d = A \times \left(\frac{RSSI}{Tx\ power}\right)^B + C \quad (3)$$

Here, A, B and C are constants. Researches have been conducted to estimate these coefficients. Based on the values of the coefficients, there are two versions of the above mentioned equation. The old version uses the equation given below to estimates the distance.

$$d = 0.89976 \times \left(\frac{RSSI}{Tx\ power}\right)^{7.7095} + 0.111 \quad (4)$$

Whereas the new version uses the below mentioned equation.

$$d = 0.42093 \times \left(\frac{RSSI}{Tx\ power}\right)^{6.9476} + 0.54992 \quad (5)$$

D. Fingerprinting

Fingerprinting is RSSI based technique that records the signal strength of wireless access point (BLE beacon). This data along with the location coordinates of the known client device are stored in the database in an offline phase. In the online phase, continuous scans are performed to estimate the

user's location by comparing the current RSSI value at an unknown location with the database information and closest value is returned [5]. Such technologies offer high accuracy, precision and reliability with 1.3m tail accuracy and median accuracy of 0.6m. It has some drawbacks as well. The data collection is time consuming and if there is any changes in the building, again the data should be collected, modelled and updated. In case of complex indoor space, signal intensity might get affected due to multipath fading.

E. Trilateration

Trilateration is a technique to calculate the position of a point in 3D space by measuring its distance from at least three reference points (BLE beacons). The beacons are placed such that they cover an entire area and also its signals must intercept. Since, the location coordinates of each beacon is already known, an imaginary circle around them can be drawn. The radii of these circles are obtained from each beacon's RSSI readings i.e., converted into distance. Once the circles overlap, the intersection point represents the user's current location [10]. Fig.3 shows the representation of this method where, A, B, C represents the beacon position with coordinates (x_A, y_A) , (x_B, y_B) , (x_C, y_C) and distance d_A , d_B and d_C . The exact position of the user, D can be calculated using the equations given below.

$$\begin{aligned} (x - x_A)^2 + (y - y_A)^2 &= d_A^2 \\ (x - x_B)^2 + (y - y_B)^2 &= d_B^2 \\ (x - x_C)^2 + (y - y_C)^2 &= d_C^2 \end{aligned} \quad (6)$$

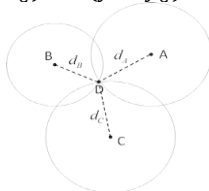


Fig.3. Trilateration representation

The trilateration method can be time consuming and it also requires a very good plan for organizing the collected data. In case of positioning multiple user location, algorithm complexity might increase and also the accuracy decreases in the presence of obstacles.

F. Dijkstra Algorithm

Dijkstra Algorithm is a classical approach to find the shortest path from source to destination. Input to this algorithm is a non-negative weighted graph that can be either directed or undirected and each edge has a numerical value. It is based on 'Principle of Greedy', where the optimal path is found in each step and continues to find the overall optimal route [9]. Once the minimal path from single source to single destination is obtained, the computation can be brought to halt. Hence, the algorithm can also be called as single source shortest path problem.

The Dijkstra algorithm has the following steps-

- Set the distance of the source node to 0 and the distance of all other vertices from the source node is set to infinity.
- The source vertex is pushed to minimum priority queue.
- The vertex with minimum distance is popped.

- The popped vertex is updated with the distance of the connected vertices if $(\text{source distance} + \text{edge weight}) < \text{next vertex distance}$, and push the new vertex distance into the priority queue.
- The queue is not updated, if the popped vertex is already visited.
- The above steps are repeated till the priority queue is empty [10].

This algorithm is only applicable for positive values and does blind search thereby consuming more time and waste of necessary resource.

IV. IMPLEMENTATION

In the proposed system as shown in Fig.4, as the user enters the region where BLE beacons are placed with a mobile device and activated Bluetooth protocol, the mobile device continuously scans for beacons signals and gathers necessary information based on the configured protocol. In this system, iBeacon protocol is used to record the values. This data is applied to the trilateration algorithm to locate the real time user location. Further, the shortest path is obtained from user's current location to the destination using Dijkstra algorithm.

The proposed INS consists of three main components-

- Data Acquisition model- records the real world physical signals and convert them into digital numerical form that can be manipulated by computer. The application developed for the purpose of navigation collects the data from the beacon devices such MAC value, beacon identifier, Tx power, RSSI value that helps in determining the location of the user.

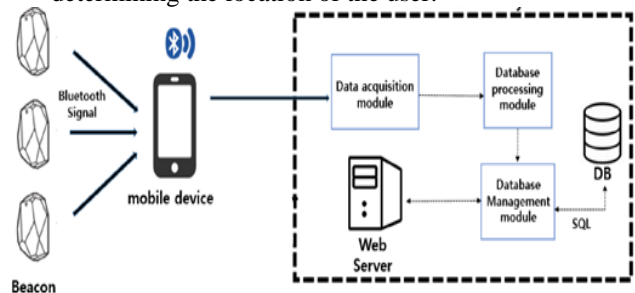


Fig.4. Block diagram of Indoor Navigation System.

- Data pre-processing model- removes the unwanted data such as noise signals from the raw data using the filter algorithm such as Kalman filter or Gaussian filter to obtain efficient data. This model uses the RSSI and Tx power data to calculate the distance between each beacon to the mobile device.
- The location of the user is specified in Database Management Model. It also manages the various data collected from the other two model. The Database is used to store the computed location and also to store the location information of each beacon [3].

Fig.5 shows the software implementation flowchart.

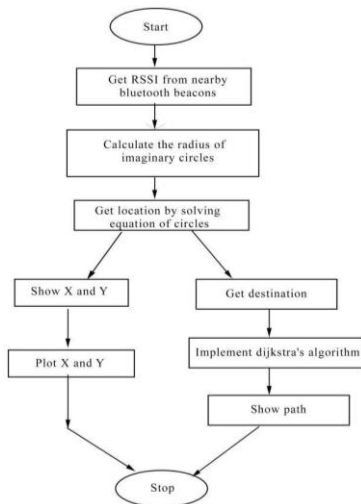


Fig.5. Implementation flowchart

A. Hardware

1) Android OS is used in this project to develop the application prototype. Since BLE is made available on Android devices with version starting from 4.3, it is now possible for them to interact with the iOS protocol as well. For BLE technology to get activated in the application, BLUETOOTH and BLUETOOTH_ADMIN option must granted. The application can then discover BLE beacons, read iBeacon data and measure RSSI values. With the help of the built in API, the application scans for beacons automatically using the function startLeScan() and stops the scan using stopLeScan() function based on the predefined amount of time.

2) For this project, we have considered the beacons that are manufactured by the Techolabz Company. Broadcasting format can be configured to either Eddystone URL, Eddystone UID or iBeacon UUID using the configuration app. Broadcasting Power and Advertising Interval can also be configured through the application provided by the beacon manufacturer.

B. Software

Android Studio is an official Integrated Development Environment (IDE) for developing applications that is built on [JetBrains' IntelliJ IDEA](#) software for Android OS [4]. It is a Java IDE that provides code editing and developing tools. It supports IntelliJ, Java, C++, Kotlin programming languages. Once application is developed and compiled with the Android Studio, it can be published in the Google Play Store.

In this project, the application for android is developed using Java and Android Studio. An application named “BLEIndoorApp” is developed and implemented on OnePlus 7 android phone with an android version 10 to host the application

V. RESULT

This section explains about the application result and the simulation results of RSSI distance calculation and the user’s current position.

The experiment was conducted in the ground floor building with an area of 1200 sq.ft. The Fig.6 represents the blueprint of the house with label A, B, C represents the spot

where beacons are placed. The Fig.7 represents the graph of RSSI (dBm) vs time (sec). The fluctuation seen in the graph is due to the obstacles.

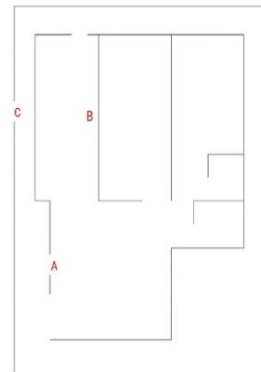


Fig.6.

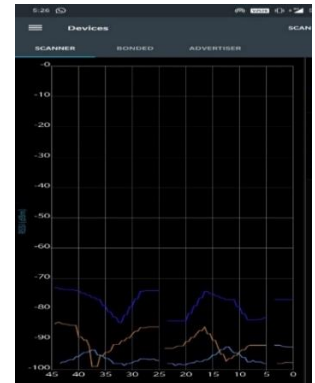


Fig.7.

Fig.6. House blueprint with beacon placement marking.

Fig.7. Graph of RSSI (dBm) vs time (sec).

On placing the beacons in the indoor environment, they start emitting the signals at specified advertising interval. The application starts performing first by requesting for the Bluetooth permission as shown in Fig.8. Once it is granted it scans for all the BLE beacon signals and records all the necessary required details such as MAC address, UUID, Minor, Major, RSSI value and Tx power. Based on all these information, the distance from each beacon to the mobile device will be calculated, which in turn displays the user’s current location as in Fig.9. The distance calculation results can be seen in the logcat file shown in Fig.10 and is interpreted in Table I .



Fig.8.



Fig.9.

Fig.8. Application requesting Bluetooth permission.

Fig.9. User’s current dot location.


```

00:00:00.000: D/BluetoothGatt: Advertising packet received: 00:00:00:00:00:00 (RSSI: -48)
00:00:00.000: D/BluetoothGatt: Advertising packet received: 00:00:00:00:00:00 (RSSI: -55)
00:00:00.000: D/BluetoothGatt: Advertising packet received: 00:00:00:00:00:00 (RSSI: -74)
00:00:00.000: D/BluetoothGatt: Advertising packet received: 00:00:00:00:00:00 (RSSI: -80)
00:00:00.000: D/BluetoothGatt: Advertising packet received: 00:00:00:00:00:00 (RSSI: -86)
00:00:00.000: D/BluetoothGatt: Advertising packet received: 00:00:00:00:00:00 (RSSI: -94)
00:00:00.000: D/BluetoothGatt: Advertising packet received: 00:00:00:00:00:00 (RSSI: -101)
    
```

Fig.10 Simulation results of distance.

The explanation of the logcat file is given below

- The function `getBluetoothAddress()` returns the Bluetooth mac address.
- The function `getBluetoothName()` returns the name of the Bluetooth device, transmitted by the remote beacon device.
- The function `getIdentifiers()` returns the list of identifiers transmitted with the advertisement.
- The function `getRSSI()` returns the number of packets detected in the last ranging cycle.
- The function `getTxPower()` returns the measured Tx power of the Beacon in dBm that is calibrated during manufacturing.
- The function `getDistance()` returns the estimated distance to the beacon based on average RSSI and calibrated Tx power[11].

TABLE I . AVERAGE RSSI MEASUREMENTS AND THEIR DISTANCE.

RSSI(dBm)	Distance(meters)
-48	0.12
-55	1.28
-74	3.108
-80	3.89
-86	5.869
-94	9.427
-101	17.451

From the above table, we can infer that as the RSSI value i.e., the strength of the beacon signal between the transmitter and the receiver decreases, distance increases.

```

00:00:00.000: D/BluetoothGatt: Advertising packet received: 00:00:00:00:00:00 (RSSI: -48)
00:00:00.000: D/BluetoothGatt: Advertising packet received: 00:00:00:00:00:00 (RSSI: -55)
00:00:00.000: D/BluetoothGatt: Advertising packet received: 00:00:00:00:00:00 (RSSI: -74)
00:00:00.000: D/BluetoothGatt: Advertising packet received: 00:00:00:00:00:00 (RSSI: -80)
00:00:00.000: D/BluetoothGatt: Advertising packet received: 00:00:00:00:00:00 (RSSI: -86)
00:00:00.000: D/BluetoothGatt: Advertising packet received: 00:00:00:00:00:00 (RSSI: -94)
00:00:00.000: D/BluetoothGatt: Advertising packet received: 00:00:00:00:00:00 (RSSI: -101)
    
```

Fig.11. Simulation results of location

The logcat file shown in the above Fig.11 displays the latitude and longitude value of the user's current position. The lat = 13.039082425460548 and longitude = 77.5021354627045 is obtained from one of the beacon with MAC address 00:A0:50:06:84:4A; RSSI value of -71dBm at a distance of 2.04037308972865 meters. At this coordinate, the user position is displayed in the application. As the user travels within the region, the above mentioned values gets updated automatically, and the result can be viewed in the application.

```

C:\Users\ADMIN\Desktop\Dijkstra-Algo>java LocationGraph -shortdist .../data/cy-locations.csv
Creating graph...
Graph is ready! You can view the graph in the file /data/graph.csv.
Give the first location:
a
Give the second location:
i
The shortest between a and i distance is : 0.03 km
C:\Users\ADMIN\Desktop\Dijkstra-Algo>java LocationGraph -shortdist .../data/cy-locations.csv
Creating graph...
Graph is ready! You can view the graph in the file /data/graph.csv.
Give the first location:
g
Give the second location:
i
The shortest between g and i distance is : 0.01 km
    
```

Fig.12. Simulation results of Dijkstra Algorithm.

The Fig.12 shows the simulation results of the algorithm that gives the shortest path between two nodes. Once the class is initiated, graph is created based on the values stored in the memory. The two inputs are first (source) and second (destination) location i.e., a and i. As explained in section 3.9, the distance obtained between these two nodes is 0.03km (30m).

V.CONCLUSION

In this paper, INS using Bluetooth technology is discussed, and the various technologies considered for this purpose is also explained. Ibeacon protocol is used to obtain the necessary data for determine the distance between beacon and the mobile device and to coordinate the position of the user. Certain fluctuations exists in locating the user position. Under ideal conditions, this method has a positioning error of 1 to 3m. Later, it provides the shortest path for navigation. Though the beacons transmit signals at different intensity at

every different interval, the proposed system works in almost every conditions. For future work, IMU sensor can be used to obtain more information like angle, acceleration etc. of the destination location. To overcome the accuracy problems of the system, audio or visuals could be installed on the lost assets.

REFERENCES

- [1] An Zhen-peng, Sui Hu-lin, Wang Jun, "Classify and prospect of indoor positioning and indoor navigation", 2015 Fifth International Conference on Instrumentation and Measurement, Computer, Communication and Control, China, 2015.
- [2] Kunhoth. J, Karkar. A, Al-Maadeed. S, Abdulla Al-Ali, "Indoor positioning and wayfinding systems: a survey", Human-centric Computing and Information sciences 10: 18, 2020.
- [3] Jinsu Kang, Jeonghoon Seo and Yoojae Won, "Ephemeral ID Beacon-Based Improved Indoor Positioning System", November 2018, Symmetry 10(11):622.
- [4] R. Jyothis, Aathira, S. Ashiq, Gouri Ramesh, "Indoor Navigation Based on Bluetooth Beacons", AIP Conference Proceedings 2222,040018, 2000.
- [5] Santosh Subedi, Jae-Young Pyun, "Practical Fingerprinting Localization for Indoor Positioning System by using Beacons", Journal of Sensors, Article ID 9742170, 2017.
- [6] Akshay Bhosale, Gloria Benny, Robin Jaison, Adil Khot4, Sandhya Pati, "Indoor Navigation System using BLE Beacons," 2019 International Conference on Nascent Technologies in Engineering (ICNTE), India, 2019.
- [7] Qathradly Mimonah, Helmy Ahmed. "Improving BLE Distance Estimation and Classification Using TX Power and Machine Learning: A Comparative Analysis", 20th ACM International Conference on Modelling, Analysis and Simulation of Wireless and Mobile Systems, November 2017, pp. 79-83.
- [8] Camellia S. Mouhammad, Ahmed Allam, Mohamed Abdel-Raouf, Ehab Shenouda, Maha Elsabrou, "BLE Indoor Localization Based on Improved RSSI and Trilateration", 2019 7th International Japan-Africa Conference on Electronics, Communications, and Computations, (JAC-ECC), 2019.
- [9] Risald, Antonio. E. Mirino, Suyoto, "Best Route Selection Using Dijkstra and Floyd – Warshall Algorithm," 2017 International Conference on Information & Communication Technology and System (ICTS), Surabhaya, 2017, pp. 155-158.
- [10] N. Jasika, N. Alispahic, A. Elma, K. Ilvana, L. Elma and N. Nosovic, "Dijkstra's shortest path algorithm serial and parallel execution performance analysis," 2012 Proceedings of the 35th International Convention MIPRO, Opatija, 2012, pp. 1811-1815.
- [11] Beacon Library Available from: <https://altbeacon.github.io/android-beacon-library/javadoc/reference/org/altbeacon/beacon/Beacon.html>

MPPT based Solar PV system simulation and analysis using Matlab/simulink

^[1] SriLakshmi R, ^[2] Dr.Chayapathy V, ^[3] Dr.Anitha G S

^[1] Jyothy Institute of technology, ^{[2][3]} R V college of engineering

Abstract— Distributed Energy resources (Solar PV systems) plays an eminent role in the economic evolution of a country and India being a developing country has got a notable power sector with sources of power generation from conventional resources to non-conventional energy resources. With the known fact of rising daily demand in power sector, integration of distributed energy resources to grid has gained interest in the field of research. Nevertheless, as a consequence of the grid integration of distributed energy resources (Solar PV systems) and usage of non-linear loads results in power quality issues, which in turn affects most of the client's load and their electricity bills too. Former to the grid integration one should be familiar with the basic Solar PV system structure and its analysis. Since another issue of worry is to maintain the maximum power extraction of a solar PV system, which is dependent on the MPPT technique used in grid integration. As per literature, many MPPT techniques are available from conventional mechanical tracking to electrical tracking. To start with, an effort should be made to firstly to understand the basics of PV system like the converter topologies available with its pros and cons and secondly with MPPT techniques. The frequently used MPPT technique is Perturb and Observe method due to its simplicity. In this paper an effort is made to emphasize the basic Solar PV structure with different converter methods and comparative analysis of P and O method with incremental conductance method of MPPT. Simulation is done using MATLAB Simulink and an analysis will be done for various conditions like change in irradiance and temperature etc., giving the information of Basic PV system analysis and modelling before integrating it to the grid.

Keywords— DER, PV, Converter topology, MPPT, P and O, Incremental conductance.

I. INTRODUCTION

With the fact of non-renewable nature of conventional power grids and its environmental impacts, the power industry is now drifting towards green energy comprising of solar PV systems, wind mills etc., Solar PV systems are encouraged more in domestic customer side as it makes much more sense for residential electricity customers looking for savings. While using solar PV systems, we can choose it to be on grid or Off grid. For both we need to be familiar with the basic structure of PV system. Solar energy being intermittent in nature, the output of PV system cannot be directly connected to grid. Doing so would result in circulating current between grid and PV system which will damage other power system components. A converter must be used to match the voltage of PV system to grid voltage. Also, for having maximum power transfer to the grid, the current that is to be fed into the

grid must be in phase with the grid voltage. To make sure of the grid current to be in phase with grid voltage, we need to compare it with the current of the PV system. MPPT method makes sure that this current of PV system is such that PV system is operating at its Maximum power point. In the following section the simulation and comparative analysis of a PV system is described in detail.

II. METHODOLOGY

This section gives a brief idea of the procedure followed throughout this work.

1. Firstly, the raw data of a Roof top solar PV system is taken and analyzed.
2. According to the data collected in step1 a PV Simulink model is configured.
3. The system is analyzed for two MPPT techniques along with the variations in parameters such as temperature and irradiance.

III. DESCRIPTION

A. PV System

Photo voltaic system comprises of solar cells that convert solar irradiation into electricity. The output of a PV system is in the form of DC. The output of PV system cannot be directly utilized as it will be intermittent in nature. The output of PV system depends many factors like temperature, irradiance, the mounting of PV panels and others. To stabilize the output of a PV system and to match it with grid voltage is a serious issue that still can be worked out. PV block is available in Simulink with different configurations and also can be configured by the users. The output of a PV system is connected to the converter to step-up or step-down the PV voltage and the control signal to the converter is from PWM who's input is in turn controlled by MPPT block. MPPT block makes sure the PV cells operate at their maximum power point. The output of the converter now is fed Inverter circuit where the DC is converted into AC signal. Finally, it will be connected to grid through a transformer as shown in fig (a).

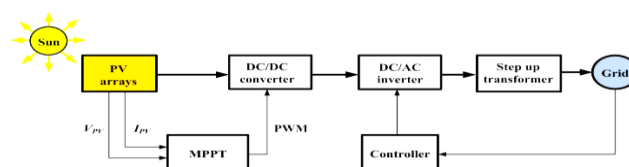


Fig (a) Grid connected PV system

B. Converters

The basic structure of a PV system with a converter is as shown below in Fig(b). converters are used in PV systems to make sure the voltage of PV system matches with the grid voltage. Many converters are in use like boost converter, buck converter, buck boost converter etc.

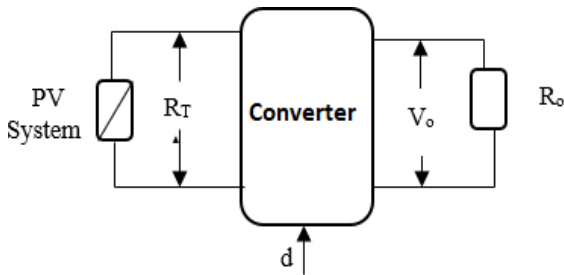


Fig (b) PV system with converter

$RT = VT / IT$, PV output voltage/ PV output current

$Ro = V0 / IO$, output voltage/ output current on load side d = Control signal from PWM block

Converter selection depends on whether the output of PV system is greater than or lesser than or equal to the grid voltage. For any converter the peak point should be in the zone of operation so that it is reachable by converter.

C. MPPT

The efficiency of a PV cell can be assessed from its I-V characteristics. Maximum power that a PV cell can have can be determined by its I-V characteristics as shown below in Fig(c), as the power is the product of voltage and current.

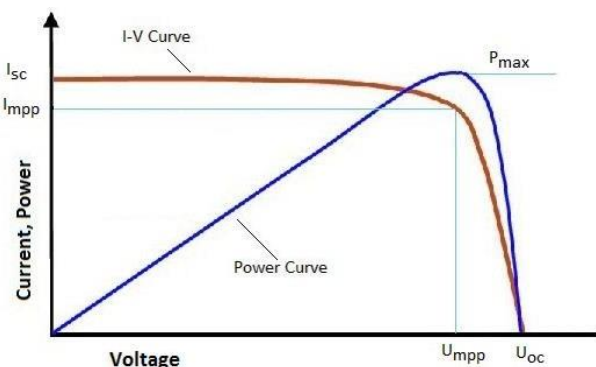


Fig (c) I-V and P-V characteristics

Various MPPT algorithms are reported in literature with their pros and cons. The most popular and frequently used are Perturb and observe algorithms and Incremental conductance algorithm owing to their simplicity.

Main aim of MPPT is to control $RT = \Delta VT / \Delta IT$. That is by controlling V and I values we can fix the maximum power point on PV curve. The output of MPPT then is applied as a reference to controller and an error signal is generated by comparing it with grid values. This error signal will be given to controllers like PI or PR controllers.

D. Perturb and observe algorithm

The perturb and observe (P&O) algorithm is mostly the frequently applied algorithm for the PV systems. It has many advantages like its simple structure, less costly, easy implementation, reduced number of sensors to be used etc. But the main issue is the maximum power point is always unsettled in nature. P and O algorithm depends on the relation between output power of PV module and its voltage.

This algorithm keeps on tracking the value of $\Delta P / \Delta V$ as is shown in Fig(d). Depending on whether the value is positive, negative or zero, the operating region is decided. When the $\Delta P / \Delta V$ is positive, the operating point of the PV module is on the left side of the curve, which means the PV voltage must be increased in order to reach the actual maximum power point. Similarly, if $\Delta P / \Delta V$ is negative, the operating point of the module is on the right side of the curve, then the perturbation of the PV module voltage should be reduced to reach maximum power point.

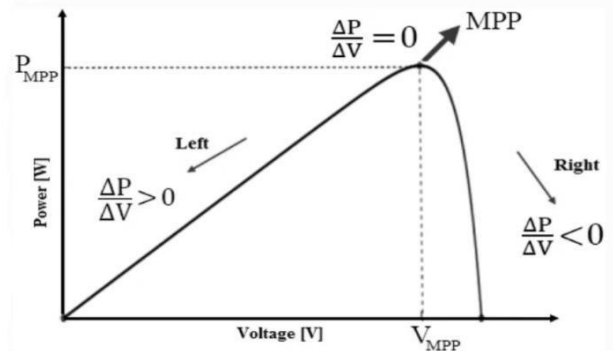


Fig (d) P-V characteristics curve (P and O MPPT)

E. Incremental conductance algorithm

In this algorithm, the controller measures incremental changes in the ratio of current and voltage, which we term it as conductance. Hence it is named as Incremental conductance algorithm. This algorithm needs two sensors for measuring PV voltage and current. Also, this algorithm requires additional computation in the controller, but it is able to track fluctuating conditions more quickly than the P&O algorithm. This technique uses the conductance ($\Delta I / \Delta V$) of the PV array to determine the sign of the changes in power w.r.t. voltage ($\Delta P / \Delta V$). This algorithm measures the difference between the incremental conductance ($\Delta I / \Delta V$) with the actual array conductance (I / V). If there is a zero difference, then it is concluded that the PV system is operating at its MPP. Then the controller maintains this voltage until there is a change in irradianations or other parameters. Below mentioned table are used while and tracking and refixing the operating points.

Condition	Operating point
$\Delta I / \Delta V = -I / V$	Operating point is at MPP

$\Delta I/\Delta V \geq -I/V$	Operating point is on left side of MPP
$\Delta I/\Delta V \leq -I/V$	Operating point is on right side of MPP

The output voltage now will be set so that to get zero difference between measured incremental conductance and actual conductance.

F. Simulation Details

A 100KW PV system is considered with a boost converter for simulation. In the Case1 Fig(e), the system is simulated using P and O algorithm then followed by analyzing the system by incremental conductance method Fig(f). Then finally a comparative analysis is made to authenticate a suitable algorithm for PV system. The values of L and C of boost converter is obtained by using equations as shown below.

Solar PV system with perturb and Observe algorithm

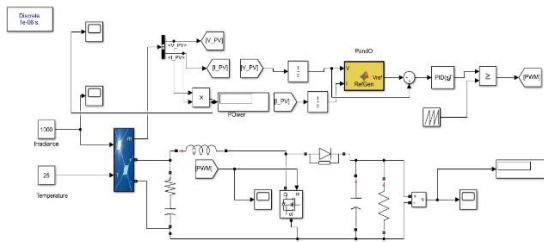


Fig (e) Simulink model with P and O MPPT

$$D = \frac{V_{in}(V_{out}-V_{in})}{f_{sw} \cdot \Delta I \cdot V_{out}} \longrightarrow ()$$

$$D = \frac{I_{out}(V_{out}-V_{in})}{f_{sw} \cdot \Delta V \cdot V_{out}} \longrightarrow ()$$

Where, V_{in} is the input voltage
 V_{out} is the desired output voltage
 f_{sw} is the switching frequency, ΔI and ΔV are ripple current and ripple voltage.

IV. RESULTS AND DISCUSSION

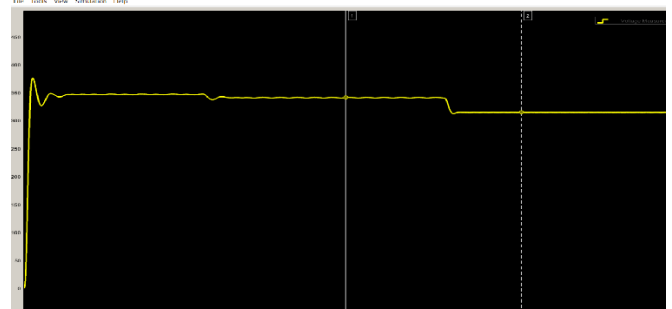
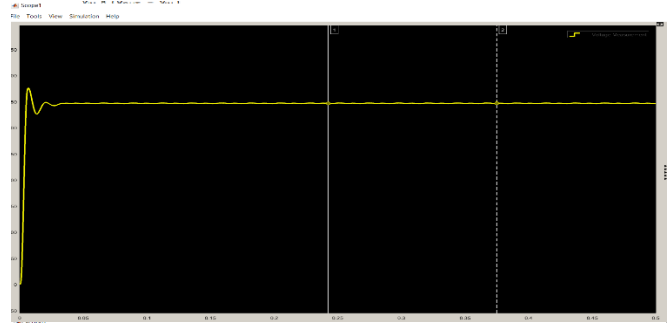


Fig (g) Output voltage and variation of voltage with change in irradiation

Solar PV system with Incremental conductance algorithm

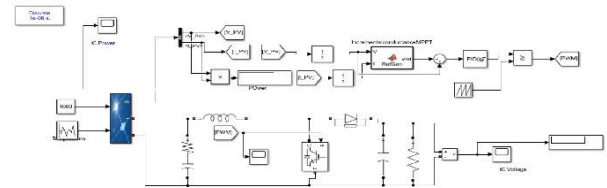


fig (g) Simulink model



Fig (h) Output voltage and variation of voltage with change in irradiation

As seen from the results, the following observations were made.

MPPT method	Time required in Sec	Output voltage
Perturb & observe	0.248	439 volts
Incremental conductance	0.042	472 volts

Vrms voltage = 421.11 volts

MPPT method	Time required in Sec	Output Power
Perturb & observe	0.125	969.9 watts
Incremental conductance	0.125	999.5 volts

Vrms voltage = 435 volts

As seen from results it is clear that incremental conductance method is faster and is having better output voltage and power compared to perturb and observe method. Also, the variation in output voltage with change in irradiance is also shown in fig (g) and (h).

V.CONCLUSION

In this paper an effort is made to shed light on the part of obtaining the suitable PV output, which plays an important role in maintaining grid synchronization. Hence a small effort is made in simulation and comparative analysis of a PV structure for two MPPT algorithms viz perturb and observe MPPT method and Incremental conductance method. Also, the variation of output voltage with change in irradiance.

REFERENCES

- [1] ShraddhaUdgir, SarikaVarshney,Laxmi Srivastava“Optimal Placement and Sizing of SVC for Voltage Security Enhancement”, International Journal of Power System Operation and Energy Management, Volume- 1, Issue-2, pp: 54-58, 2011.
- [2] Ranjit Kumar Bindal: “A Review of Benefits of FACTS Devices in Power System”, International Journal of Engineering and Advanced Technology (IJEAT), Volume-3, Issue-4, pp. 105-108, April 2014
- [3] R. Mohan mathur, Rajiv k. Varma “Thyristor-based facts controllersFor electrical transmission systems”, A John Wiley & Sons, Inc. Publication
- [4] Sandesh Jain, Shivendra Singh Thakur: “Voltage Control of Transmission System Using Static Var Compensator”, International Journal of Science and Engineering Applications (IJSEA) Volume 1, Issue 2, pp. 107-109, 201
- [5] Claudia Reis, F.P. Maciel Barbosa: “A Comparison of Voltage Stability Indices”, IEEE Melecon 2006, May 16-19, pp. 1007-1010.
- [6] H. Iyer, Student Member, S. Ray: “Voltage Profile Improvement with Distributed Generation”, IEEE 2005, pp. 1-8.
- [7] A.A. Alabduljabbar, J.V. Milanovic: “Assessment of techno-economic contribution of FACTS devices to power system operation”, Electric power Systems Research 80, Elsevier, pp.1247–1255, 23 May 2010.
- [8] J.M. Enrique a, E. Dura' n a, M. Sidrach-de-Cardona b,1, J.M. Andu' jar a “Theoretical assessment of the maximum power point tracking efficiency of photovoltaic facilitieswith different converter topologies” Available online at www.sciencedirect.com Solar Energy 81 (2007) 31– 38.
- [9] S.Daison Stallon, K.Vinoth Kumar, S. Suresh Kumar” High Efficient Module Of Boost Converter In PV Module” International Journal of Electrical and Computer Engineering (IJECE) Vol.2, No.6, December 2012, pp. 758~781 ISSN: 2088-8708.

Design and Implementation of a Vehicle To Vehicle Communication System Using Li-Fi Technology

^[1] Sugnyani Patil, ^[2] Mohan Kumar B N, ^[3] Vani K

^{[1][2]} Assistant Professor, RRIT, Bengaluru

^[3] Student, RRIT, Bengaluru

Abstract— Vehicle to vehicle communication are advanced applications which provide various services to facilitate road safety and traffic management. This system uses wireless communication system which provides warning signals In order to reduce road accidents and congestions. This system improves the efficiency of driving by enabling the vehicles to communicate accident related messages. This also assists the driver to take the proper decision and avoid collision. This paper deals with the vehicle to vehicle communication using Li-Fi (light fidelity). The proposed system uses Li-Fi technology comprising mainly light-emitting diode (LED) bulbs as means of connectivity by sending data through light spectrum as an optical wireless medium for signal propagation. The usage of LED eliminates the need of complex wireless networks and protocols. Vehicle's speed can be controlled by the switch using PWM concept. Hence multiple information can be communicated with the other vehicle efficiently.

Keywords— LI-FI, LED, visible light communication (VLC)

I. INTRODUCTION

Nowadays since the number of vehicles is increasing, the deaths/disabilities are also increasing due to tremendous number of accidents. This system reduces the above complications by providing a warning messages to driver so that the driver can take alternative precautions. This is achieved using LI-FI technology.

Li-Fi

Light Fidelity (Li-Fi) is a bidirectional, high-speed and fully networked wireless communication technology similar to Wi-Fi. The term was coined by Herald Haas and is a form of visible light communication and a subset of optical wireless communications (OWC) And could be a complement to RF communication (Wi-Fi or cellular networks), or even a replacement in contexts of data broadcasting. It is wire and UV visible-light communication or infrared and near-ultraviolet instead of radio-frequency spectrum, part of optical wireless communications technology, which carries much more information

and has been proposed as a solution to the RF-bandwidth limitations. Transfer of data from one place to another is one of the most important day-to-day activities. The current wireless networks that connect us to the internet are very slow when multiple devices are connected. As the number of devices that access the internet increases, the fixed bandwidth available makes it more and more difficult to enjoy high data transfer rates and connect to a secure network.

But, radio waves are just a small part of the spectrum available for data transfer. A solution to this problem is by the use of Li-Fi. Li-Fi stands for Light-Fidelity. Li-Fi is transmission of data through illumination by taking the fibre out of fibre optics by sending data through an LED light bulb that varies in intensity faster than the human eye can follow.

Li-Fi is the term some have used to label the fast and cheap wireless communication system, which is the optical version of Wi-Fi. Li-Fi uses visible light between 400 THz (780 nm) and 800 THz (375 nm) as optical carrier for data transmission and illumination instead of Gigahertz radio waves for data transfer. It uses fast pulses of light to transmit information wirelessly.

The data can be encoded in the light by varying the flickering rate at which the LEDs flicker on and off to generate different strings of 1s and 0s. The LED intensity is modulated so rapidly that human eye cannot notice, so the light of the LED appears constant to humans.

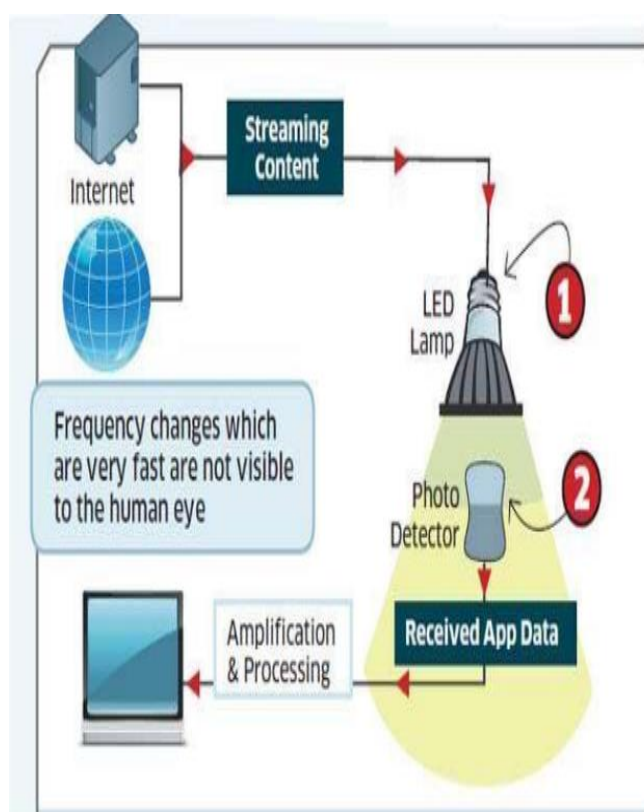


Figure 1: General Block Diagram of Li-Fi[3]

Light-emitting diodes (commonly referred to as LEDs and found in traffic and street lights, car brake lights, remote control units and countless other applications) can be switched on and off faster than the human eye can detect, causing the light source to appear to be on continuously, even though it is in fact 'flickering'.

The on-off activity of the bulb which seems to be invisible enables data transmission using binary codes: switching on an LED is a logical '1', switching it off is a logical '0'. By varying the rate at which the LEDs flicker on and off, information can be encoded in the light to different combinations of 1s and 0s. This method of using rapid pulses of light to transmit information wirelessly is technically referred to as Visible Light Communication (VLC), though it is popularly called as Li-Fi because it can compete with its radio-based rival Wi-Fi.

II. SYSTEM DESIGN

The proposed system is designed such that two vehicle can communicate with each other by sending & receiving the warning messages.



Figure 2: vehicle to vehicle communication using VLC

The proposed system consist of sensors, controller, Light emitting diode and LCD to display the warning messages .This system has many features such as high performance, cost sensitivity, Low power consumption etc.

This system consist of two major units,they are Transmitter unit and Receiver unit

Transmitter unit is responsible for transmitting data between vehicles & receiving unit helps in displaying warning messages. The Ultrasonic sensor consists of an ultrasonic transmitter and receiver. It works on the Doppler Effect. The transmitter transmits the signal in one direction then signal is reflected back and received by the receiver. The distance between the object is measured by the total time taken by the signal to transmit and receive back.

The transmitter block is consisting of DC motor, braking system, switched and Li-Fi transmitter module. Separate switch is used to transfer the data to the vehicle through LiFi module.

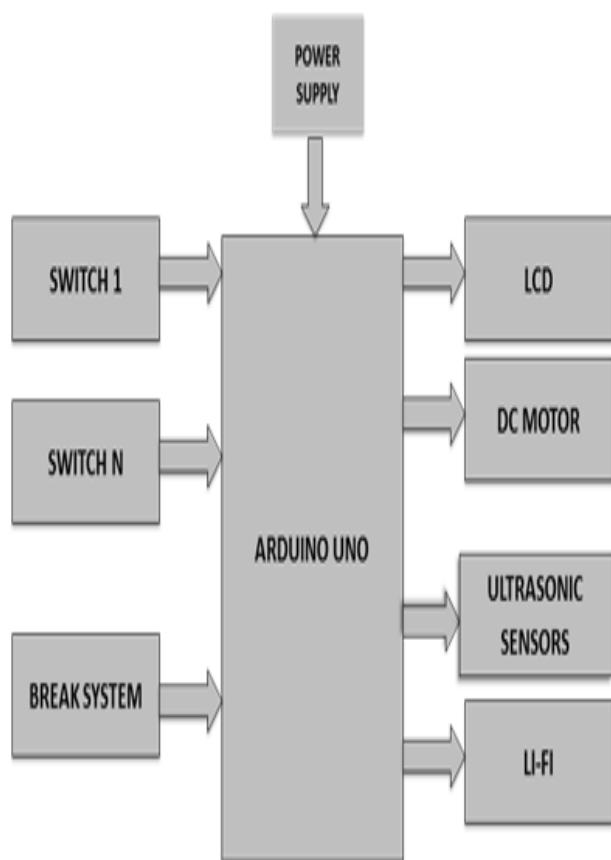


Figure 3: Transmitter block diagram

If the braking system in vehicle is not working properly then the DC motor couldn't run. All the information about the transmitting status has been showed on the LCD. Thus the LCD has been interfaced with the controller. Li-Fi module is consisting of transmitter driver with the LED circuit. It transmits the data into the light signal.

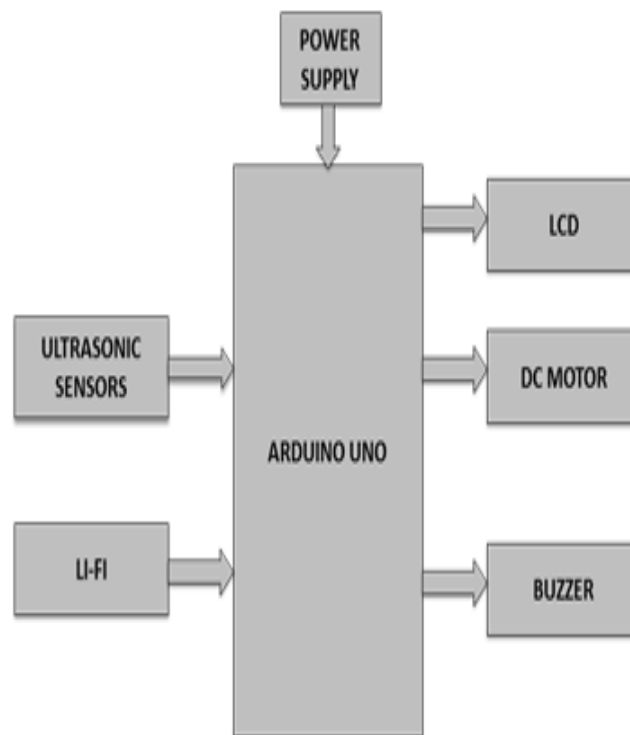


Figure 4: Receiving block diagram

Receiver block is consisting of controller, LCD, DC motor, buzzer with Li-Fi receiver module. All the instruction from the transmitter is received by the Li-Fi module. IR sensor has been interfaced with the controller to detect the obstacle nearer to the vehicle.

Li-Fi module consists of photo detector and amplifier. It receives the light signal and converts into the data signal. Then it translates into the understandable data information.

Ultrasonic Sensor attached in the bonnet using Doppler-effect is made to sense continuously. When the distance between the two vehicles decreases a warning message is transferred to back vehicle using the transmitter attached in the front vehicle it is received by the photo-detector attached to the back vehicle so he can take necessary steps to ensure that collision is avoided.

In this proposed system, power consumption is very low when compared to the existing system. The light quality of LEDs used for LiFi, the

modulating signal is DC balanced based on the user expectation.

The propose plan of action for our project is to initiate on optical wireless communication model that gives high data rates (in the range of MHz to GHz) and transmission distances is near about 1m. In this system at the transmitter section input data give to the switching control system. Based on the data, the switching control generates a stream of 1s and 0s thereby encoding the data in binary. The output of this control is given to the array of LEDs which turn OFF and ON at extremely high speeds

The output of this control is given to the array of LEDs which turn OFF and ON at extremely high speeds

The demodulated signal is then sent to a filter destroy unwanted noise. This filter signal is then amplify using signal amplification mechanism. The filter and amplify signal is then given to an output device such as an LCD display. Another vehicle can able to control from our vehicle by sensing distance. For sensing the object and speed can be controlled by PWM concept. These whole operations are controlled by the Arduino microcontroller.

III. SIMULATION RESULTS

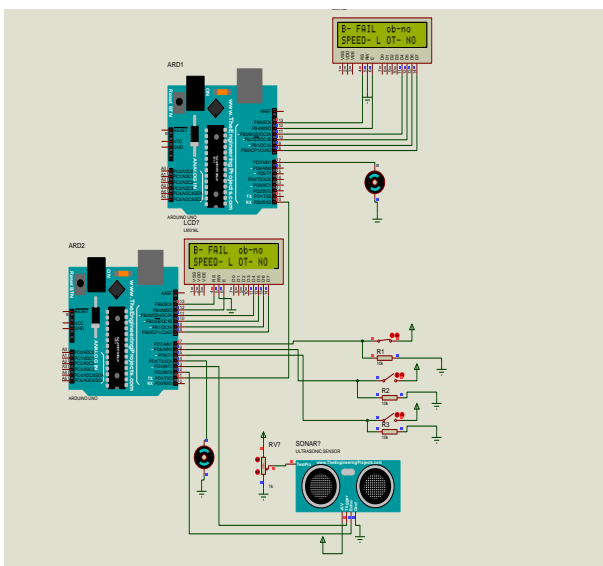


Figure 5: Break fail condition

As shown in figure 5, on LCD it will display break condition as fail and speed of vehicle low

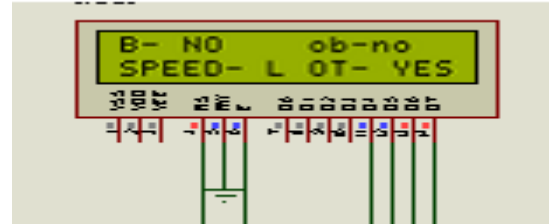


Figure 6: overtake condition

As shown in figure6, it show the status of vehicle and if other vehicle's speed is low then OT flag is raised , then our vehicle can overtake

IV. CONCLUSION

The concept of Li-Fi will introduce along with existing techniques used for vehicle to vehicle communication. The hardware aspects for the development of visible light communication consist of LED for both transmitting & receiving messages In this work, the concept of Li-Fi had been introduced along with existing techniques and classical trends used for vehicle to vehicle communications. The proposed system has a cost effective solution to reduce accidents. The design guidelines and details of system components were thoroughly explained in this paper. The proof of concept has been illustrated in this paper by sending data through Li-Fi small-scale prototype model. Finally the result has been measured between the vehicles to vehicle.

V. FUTURE SCOPE

At present, development of first generation of vehicle to vehicle systems is underway. Function of these systems is limited only up to giving warning to the driver.

The second generation of vehicle to vehicle systems would be able to take control of the vehicle in danger and provide the corrective action. These systems would ultimately merge with the autonomous driving technology.

REFERENCES

- [1] W.-L. Jin, "SPIVC: A Smartphone-based inter-vehicle communication system," Proceedings of Transportation Research Board Annual Meeting, 2012.
- [2] Ariel Gomez, Kai Shi, "Beyond 100-Gb/s Indoor Wide Field-of-View Optical Wireless Communications", 2015.

- [3] T. H. M. A. Y. K. K. Isamu Takai, "Optical Vehicle-to-Vehicle Communication System Using LED Transmitter and Camera Receiver," IEEE Photonics Journal, Vol. 6, No. 5, pp. 7902513-7902513; October 2014.
- [4] Paul Anthony Haigh, Francesco Bausi, "Wavelength-multiplexed Polymer LEDs: Towards 55MB/s Organic visible light communications",2015.
- [5] Jonathan, J.D.McKendry, David Massoubre,"Visible –Light Communications Using a CMOS-Controlled Micro-Light-Emitting –Diode Array", 2012.
- [6] Jonathan J.D.McKendry, Richard P.Green,"High Speed Visible Light Communications Using Individual Pixels in a Micro Light-Emitting –Diode Array", 2010.
- [7] W. Jia-yuan, Z. Nian-yu, W. Dong, I. Kentaro, I. Zensei and N. Yoshinori, "Experimental study on visible light Communication based on LED," The Journal of China Universities of Posts and Telecommunications, Vol.19, No. 2, pp. 197-200, October 2012.
- [8] H. Elgala, R. Mesleh, H. Haas and B. Pricope, "OFDM Visible Light Wireless Communication Based on White LEDs," In the Vehicular Technology Conference Proceeding, pp. 2185-2189, 22-25, April, 2007.
- [9] W.-L. Jin, "SPIVC: A Smartphone-based inter-vehicle communication system," Proceedings of Transportation Research Board Annual Meeting, 2012.

Radar System Using Arduino and Ultrasonic Sensor

^[1]Sunanda C V, ^[2]Varun K, ^[3]Bharath KL, ^[4]Tashi Wangyal B, ^[5]Prarthan SB

^[1]Assistant Professor, RRIT

^[2]^[3]^[4] Student, RRIT

Abstract— This paper is about Radar System controlled via Arduino. This RADAR system consists of an ultra-sonic sensor and servo motor; these are the major components of the system. Basic working of the system is that it has to detect objects in its defined range. Ultra-sonic sensor is attached to the servo motor it rotates about 180 degrees and gives visual representation on the software called processing IDE. Processing IDE gives graphical representation and it also gives angle or position of the object and distance of the object. This system is controlled through Arduino. Arduino UNO board is sufficed to control ultrasonic sensor and also to interface the sensor and display device. On our research, we learned about existing navigation and obstacle detection innovations and different systems where ultrasonic sensors are used efficiently. Main application of this RADAR system comes into different field of navigation, positioning, object identification, mapping, spying or tracking and different applications. These less investment system are also suitable for indoor applications.

Keywords— Arduino, ultra-sonic, radar, positioning, surveillance, obstacle detection.

I. INTRODUCTION

RADAR system is an object detection or tracking system which uses radio waves to decide or get the range, height, heading, or speed of items or objects. Radar frameworks or system arrive in an assortment of sizes and have distinctive performance particulars. Some radars are utilized for aviation authority at air terminals and others are utilized for long range observation and early cautioning frameworks [1]. There are some ways to show radar working data. There are also some modified radar systems which have advance technology of handling the systems. These modified systems are used at higher levels to get or extract the helpful or important data [2]. Our proposed system's working principle is linked by the following components which are is ultra-sonic sensor connected to the microcontroller (we have chosen Arduino) digital input and output pins. Then we have servo motor which is also connected to digital output and input pins. Our both main components ultra-sonic sensor and servo motor are connected simultaneously so that when our servo motor rotates from 0 degree to 180 degree from extreme right to extreme left the motor will rotate nearby its axis [3]. We utilize Computer screen to demonstrate the data (distance and angle) through software called "Processing development Environment".

II. LITERATURE SURVEY

Subsequent to experiencing a portion of the papers with respect to usage utilizing ultrasonic sensors and ARDUINO, it was found that this idea is searched a lot and is a mainstream idea which is still in advance. The advances utilized were not just productive and solid yet in addition financially achievable [5]. Not only this, here other very useful applications of ultrasonic sensors were observed too. This paper discusses about a monitoring system which is designed measure to volume of water, then all the water will submerge with land and this phenomenon is called as flood or surge. We can overcome this flood problem by earlier identification in height of water and observing speed. If we identify problem earlier we can overcome this problem before it become crisis. By accuracy of 96.6%. But when it is implemented in the rivers there are many errors because of different type of water levels due to heavy waves and speed of water and also due to floating of heavy objects. Unlike Previous testing results, author directed this analysis on tracking of speed of water improvement or modification and level of water in flooding. The test was completed when the Arduino used as controller of application. For more research, information of depth level and speed of water of this system will be sent to database server website to be checked regularly [8].

An intelligent driver monitoring and vehicle control system is introduced in this research. This technology is creating to avoid accidents by monitoring the driver's activities. The writer states some of the main reasons of accidents today. These are alcohol consumption by the driver, carelessness, drowsiness or medical illness. The various units in the framework, including motors, relays, power unit and ESP8299 module are tried and are observed to be in working condition. Ultrasonic sensor is utilized to alarm the driver if any vehicle draws close to his vehicle. The status of the driver can be observed by the assistance of sensors executed in the vehicle and the subtle elements are refreshed to the proprietor. This system overcomes all the different aspects due to which other technologies designed for this purpose have failed, making the system more useful, efficient and less costly and less time consuming [7]. In this research paper authors have given information about the detection of radio waves and tracking or ranging through radar set which is built from components like an ultra-sonic sensor, a servo motor and an Arduino. The author discuss about the linear measurement problem because of which distance

measurement was not possible between some objects, was resolved with the introduction of Ultrasonic distance measurer. It allows to take non-contact measurements. This radar system can drastically reduce power consumption. The author says, that this system is an extremely handy radar system, it can read or track the distance and angle of an obstacle and shown it up on the monitor screen. The ultra-sonic was attached on top of the servo motor to detect obstacles at 0 degree to 180 degree from right to left. Both the ultra-sonic sensor and the servo were fueled and controlled by the Arduino controller. The GUI was built using the JAVA programming language to show the result on the monitor [3].

This paper represents a system for obstacle detection in a known environment. This system works through an android based mobile camera. People who are visually impaired, face difficulties in detecting obstacles and navigation while they walk. They use sticks for this problem nonetheless this manner or technique is not right way of doing it. Object indicator or detector can overcome accidents or collision problems of people or the other way is they can to accurate map reading. The algorithm which is proposed in this paper is made for indoor mapping. In indoor surrounding all distinctive floors are taken in consideration and single image is kept or stored for distinctive floors. These images of floor are taken as reference image. The author mentions that this algorithm is 96% accurate and works in real time. There are different techniques discussed in this paper for obstacle detection. For these types of problems we can use the approach of SONAR sensor and also laser camera. In this paper introduced a calculation for identifying hindrance in known condition with an android based versatile camera which scans chosen territory before the camera for impediment location [9]. This research is about a blind walking stick made for blind people through which they can avoid obstacles while they walk and recognize currency. With the thought of visually impaired individuals, it is to some degree troublesome job to distinguish the cash or any unexpected obstacle. Despite the fact that currency dependent on size could possibly be recognized however it is relatively hard to distinguish that whether the note is unique or phony. So to overcome this issue the authors have designed the Currency Recognition Blind Walking Stick. A lot of work is done on currency recognition and obstacle detection using advanced technologies like optical character recognition, SURF and pattern extraction through colors. But none of these systems had the feature for obstacle detection for blind people. Therefore this framework is efficient as the other ones having an extra feature for helping the visually impaired [10].

III. BLOCK DIAGRAM

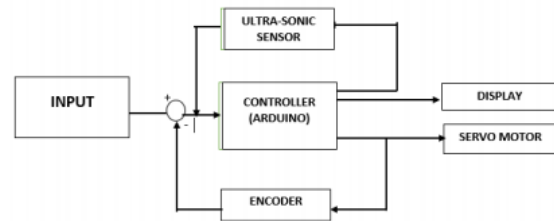


Figure 1 Block Diagram of Radar System

Figure 1 represents the system's block diagram. Here, it can be seen how the work flow in this radar system. The sensor is going to sense the obstacle and determine the angle of incident and its distance from the radar. The servo motor is constantly rotating to and fro, hence making the sensor move. The data obtained is encoded and fed to the processing IDE which represents it on the screen. The results are displayed further in this paper. All these operation are done by Arduino microcontroller from the rotation of the servo, data collection from the sensor, feeding the data to encoder to transferring it to the display.

IV. METHODOLOGY

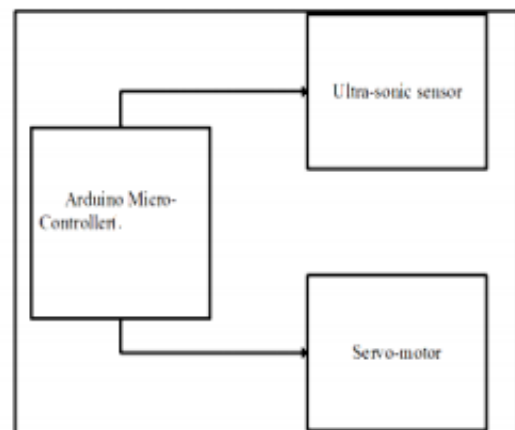


Figure 2.Overview

The above figure represents a brief overview of this radar system. Here, as it is shown the controller we are using is Arduino, with the input Ultrasonic sensor and the output is the servo motor which rotates 180 degrees. The microcontroller controls all the operations of this system, from rotation of the motors to the obstacle detection of the ultrasonic and representation of the result on the screen.

In this research paper we have mentioned that our system is designed consisting following components such as, a servo-

motor, an ultra-sonic sensor and a micro-controller (Arduino). System's objective is to track the distance and angle of the object and to represent this information graphically, means its output should be in graphical form which will be represented through processing software. We can have an idea of an efficiency of this radar by testing objects at different levels and observe how faster or smoothly it detects an object that it finds in a way and gives us an expected range of the obstacle [3].

Following figure show the results of the monitor screen of our design when the sensor rotates through the area and detects obstacle in the way. The red area indicates the presence of obstacle and below the angle of incident and distance is being displayed.

Testing of the system

a) Object 1 is placed 30.5 far from the radar, radar gives the distance 32

cm, so:

$$* \text{error} = (32-30.5)/30.5 * 100 = 4.918\%$$

$$* \text{efficiency} = 100 - \text{error} = 95.08\%$$

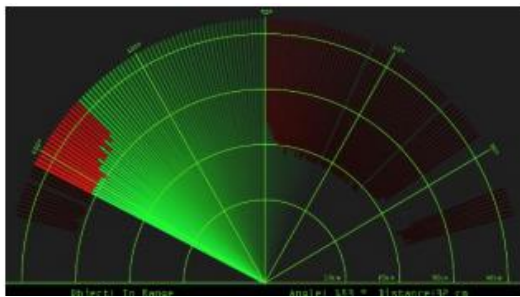
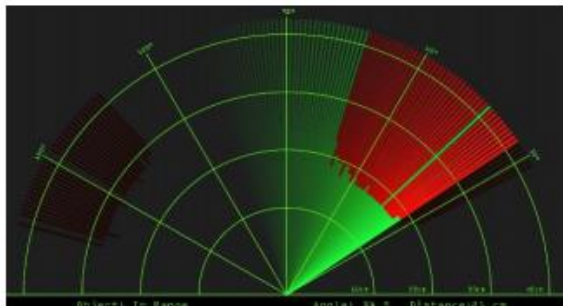


Figure 3 . Processing IDE output of the system when tested by placing object

b) object 2 placed at a distance of 20.3 cm, radar gives the distance 21 cm so,

$$* \text{error} = ((21-20.3)/20.3) * 100 = 3.44\%$$

$$* \text{efficiency} = 100 - \text{error} = 96.55\%$$



. Figure 4. Processing IDE output of the system when tested by placing object.

After the observations and calculations, we can conclude that this system is 95.815% efficient.

This Radar System has various applications for security purposes and it is mainly used for mapping.

* APPLICATION IN AIR FORCE:

It is used in airplanes or aircraft machines which have implemented radar system in it to detect the objects that comes in a way. It is also used to calculate height.

* APPLICATION IN MARINE:

This radar system can be used in ships or marine. It can be implemented on big ships to calculate the distance of other boats or any sea vehicles. This can also reduce sea accidents.

*APPLICATION IN METEROLOGY:

For weather forecast.

V.CONCLUSION

This project is based on the operation of remote controllable and operated servo motor has been used as an actuator called electrical actuator. These electrical actuator is more reliable, less expensive, fast response, less weight, and appearance is good. This results shows high speed applications and higher efficiency is achieved mapping method of whole system is assessed on small principles or scale [11]. The field that we have chosen for our design "Radar System" is a very vast field and future scope of this technology is very high. We have tremendous applications in which radar system have been implemented. As we have designed a short range radar therefore our research was specified and limited. This system can only detect objects from 0 to 180 degrees only because the servo motor that we have used can rotate only to this range. So, due to this limitation our design cannot be applied to places or areas for obstacle detection on a larger scale. Usage of a 360 degrees rotating servo motor can make the system more efficient. We look forward to modify this system and enhance our research work by using a fully 360 degrees rotating servo and a higher ranged ultrasonic sensor. We can further add features to this system i.e. making it mobile, mounting an alarm system to it which turns on when obstacle is detected. Further modifications could be an obstacle avoiding robot with surveillance system.

REFERENCES

- [1] Ahman Emmanuel Onoja, Abdusalaam Maryam Oluwadamilola, Lukman Adewale AJAO-"Embedded System Based Radio Detection and Ranging (RADAR) System Using Arduino and Ultra-Sonic Sensor"
- [2] Shreyes Mehta, Shashank Tiwari-"RADAR SYSTEM USING ARDUINO AND ULTRASONIC SENSOR" IJNRD, Volume 3, Issue 4 April 2018
- [3] Antonio Tedeschi ; Stefano Calcaterra , Francesco Benedetto-"Ultrasonic RADar System (URAS): Arduino and Virtual Reality for a Light-Free Mapping of Indoor Environments" IEEE Sensors Journal Volume: 17 , Issue: 14 , July 15, 15 2017
- [4] Kiruthikamani.G, Saranya.B, Pandiyan.P-"Intelligent Driver Monitoring and Vehicle Control System" IJSRD - International Journal for Scientific Research & Development| Vol. 5, Issue 09, 2017.
- [5] Mohanad Mahdi Abdulkareem,Qusay Adil Mohammed ,Muhanned Mahmood Shakir-"A Short Range Radar System"Rangefinder". Mahmood Shakir-"A Short Range Radar System"Rangefinder"

Bearing Fault Detection based on Support Vector Machine classifier using CWRU data

^[1]Tushar Anand ^[2]Bhavnesk Kumar

^{[1][2]} Netaji Subhas University of Technology, New Delhi-110078, India

Abstract— *Three-phase induction motors (IM) Induction motors (IM) are widely used in industry due to their numerous advantages, including low cost, minimal maintenance, simple and strong construction, self-reliable operation, and higher efficiency than other motors. If a failure in an induction motor is not detected early on, it can result in unforeseen malfunctions, economic loss, and even devastating consequences for the industry. Keeping all this in mind, this paper presents a bearing fault detection scheme of three-phase induction motor. Various methods based on machine learning (ML) algorithms have been developed in recent decades to detect bearing faults. This paper presents a fault detection system for induction motors using the SVM (Support Vector Machine) approach. In the presented method, vibration signal dataset is used and a comparative study with various kernels of SVM as Linear, Sigmoid, Polynomial and Rbf is presented and the following Classification report is observed. The proposed approach outperforms the traditional data-based models/techniques in the accuracy under all working conditions.*

Keywords— *induction motor, bearing fault, Support Vector Machine, fault detection system;*

I. INTRODUCTION

Condition monitoring of induction motors for electrical equipment maintenance is a rapidly growing technology [1], and because it can reduce the frequency of unexpected failures of a critical system, it has gotten a lot of attention throughout the world.

The three primary types of bearing defect detection systems are model-based, signal-based, and data-driven. In model-based techniques, the projected or estimated signal is compared to the measured signal [2]. Model-based approaches have the major drawback of being unable to identify faults unless a one-to-one mapping between model parameter and physical coefficients is developed. Signal-based techniques involve time domain or spectrum analysis of time-domain signals. Signal-based approaches take a long time to compute, and spectrum analysis is very sensitive to noise [3]. Data driven techniques recognise the healthy and defective states from a large volume of data without any previously set models or parameters.

Vibration signals analysis is the most effective method for detecting and categorizing bearing defects in induction motors, according to the literature [4],[5]. It has been claimed that bearing fault detection may be done using feature

extraction from vibration signals in the time domain [4] and frequency domain [5].

Within various Induction motor faults (Bearing fault - 44 % ,Stator fault - 22 % ,Rotor fault - 8 % ,Other fault - 26 %), The suggested inquiry has been limited to bearing problems exclusively since motor dependability research studies demonstrate that bearing faults account for 44% of induction motor errors, as illustrated in Fig.1.[1].

Machine learning algorithms are used extensively in speech or text recognition, industrial applications, medical diagnostics, and social networking sites [6]. The use of these machine learning approaches in the building of a knowledge base system has been shown to be effective in detecting flaws early, preventing catastrophic failure, and minimising running costs [7]

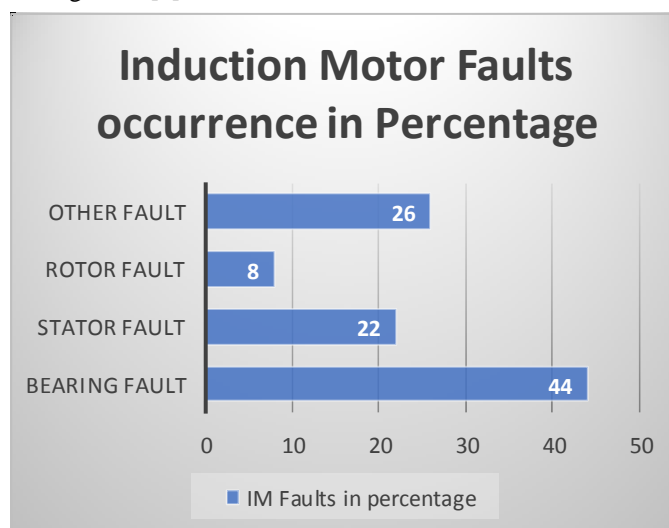


Fig 1. Induction Motor Faults occurrence in Percentage [1]

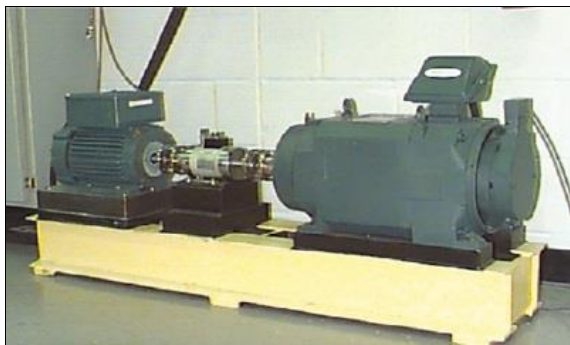
Artificial neural networks (ANN)[8], principal component analysis (PCA)[9], support vector machines (SVM)[10],[11], k-Nearest Neighbours (k-NN)[12], singular value decomposition (SVD)[13] are some of the widely used ML algorithms in bearing fault identification. These algorithms thoroughly assess data, learn from it, and then apply what they've learned to make informed decisions concerning the occurrence of bearing failures. Furthermore, these machine learning techniques have shown to be effective in this field.

SVM has been shown to have a solid theoretical foundation and intuitive geometrical interpretation. It's widely used, and

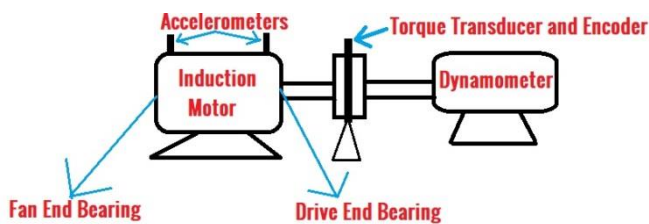
it's even been used as the foundation for computer vision, pattern recognition, information retrieval, and data mining [14]. The goal of our approach is to show that using SVM as a classification tool for bearing defects diagnosis is a wise decision.

II. EXPERIMENTAL SETUP

The proposed approach was tested using data from CWRU-supplied motor bearings in this study (Case Western Reserve University). Fig.2.depicts the experimental apparatus and its schematic diagram, which were used in the investigation. A 2-horsepower (hp) motor with a torque transducer/encoder and a dynamometer make up the bearing experimental setup. The electric motor was subjected to various loads using the dynamometer. A 2 hp motor (left), a torque transducer/encoder (centre), a dynamometer (right), and control electronics make up the test stand depicted in Fig.2. The motor shaft is supported by the test bearings. A dynamometer and an electronic control system provide torque to the shaft.



(a)



(b)

Fig 2. (a) CWRU Bearing Experimental test and (b) Schematic Diagram of test rig

Electro-discharge machining was used to induce single point defects to the test bearings with fault dimensions of 7 mils, 14 mils, 21 mils, 28 mils, and 40 mils (1 mil=0.001 inches). Accelerometers with magnetic bases attached to the housing were used to capture vibration data. At both the driving and fan ends of the motor casing, accelerometers were mounted at 12 o'clock. Matlab (*.mat) format is used for all data files. Digital data was captured at a rate of 12,000 samples per

second, with 48,000 samples per second collected for drive end bearing failures.

The torque transducer/encoder was used to acquire speed and horsepower data, which was then manually recorded. Because outer raceway faults are immovable, their location in relation to the bearing's load zone has a direct impact on the motor/bearing system's vibration response. Experiments were carried out on both fan and drive end bearings with outer raceway defects positioned at 3 o'clock (immediately in the load zone), 6 o'clock (orthogonal to the load zone), and 12 o'clock to quantify this effect. Electro-discharge machining was used to seed defects in motor bearings (EDM). Faults with diameters ranging from 0.007 inches to 0.040 inches were introduced at the inner raceway, outer raceway, and rolling element independently (i.e. ball). The test motor's faulty bearings were reinstalled, and vibration data was taken for motor loads ranging from 0 to 3 horsepower (motor speeds of 1797 to 1720 RPM).

III. DATA DESCRIPTION

We look at the CWRU data set in this research, which contains bearing data such ball faults, inner race faults, and outer race faults. It is also considered to have a baseline (normal) bearing data with null defects. Some data is gathered at a sample frequency of 12 kHz, while others are recorded at a sampling frequency of 48 kHz. We will only analyse data recorded at a sample frequency of 48 kHz [23] with faults of varied depths (0.007-inch, 0.014-inch, 0.021-inch) and a 1 hp external load in this investigation. Bearing fault situations are divided into ten types: T1, T2, T3, T4, T5, T6, T7, T8, T9, and T10, with varied fault depths (0.007-inch, 0.014-inch, 0.021-inch) diameter at an external motor load of 1 hp and Motor Shaft Speed of 1772 rpm is shown in Table I.

Table I. Description of various Bearing fault type and Fault Diameter

Bearing Fault Category	Bearing Fault type	Fault Diameter (in inch)
T1	Ball fault	0.007
T2	Ball fault	0.014
T3	Ball fault	0.021
T4	Inner race fault	0.007
T4	Inner race fault	0.014
T6	Inner race fault	0.021
T7	Normal (No fault)	0.000
T8	Outer race fault (6 O'clock position)	0.007

T9	Outer race fault (6 O'clock position)	0.014
T10	Outer race fault (6 O'clock position)	0.021

IV. PROPOSED METHODOLOGY

The methodology is divided into four primary sections, as follows: (i) Vibration Data Collection Process, (ii) data acquisition, (iii) Feature Extraction or pre-processing and (iv) Post-Processing using SVM Classifier. Motor vibration signals during start-up are analyzed and examined to identify faults. An accelerometer probe was used to capture data related to a motor condition, which was then recorded and saved onto the database.

A. Data Preparation

Data for each bearing fault type is gathered and split into multiple segments for each fault type in our study, with each segment containing approximately 2048 data points. To compute the feature matrix, we had to first segment our data into 2048-segment segments. The time domain features extracted for each individual segment, such as maximum level of vibration, minimum level of vibration, mean value, standard deviation, root mean square value (RMS), skewness, kurtosis, crest factor, and form factor, are calculated using the information in Table II and compiled into a feature matrix. For each fault considered, the reshaped matrix data now contains exactly 230 (total: 230x10=2300) data samples, which are applied with 9 derived time domain features as an input. As a result, the created feature matrix is 2300x9. The final feature matrix has a size of 2300x10 after adding fault type as an Output to the feature matrix.

B. Statistical feature extraction

Statistical Feature extraction is required for processing raw current data to reduce the training set size while keeping features that correspond to the state of the IM faults. Table II gives a summary of the retrieved features (k 1 through k 8) used.

Table II. Description of Extracted Statistical Time Domain Features

Statistical Time Domain Features	Description
k_1 : Maximum	$\max(X_i)$
k_2 : Minimum	$\min(X_i)$
k_3 : Mean Value	$\frac{1}{2N + 1} \sum_{i=-N}^N X_i$

k_4 : Standard deviation	$\sqrt{\frac{\sum_{i=-N}^N (X_i - k_3)^2}{2N + 1}}$
k_5 : Root mean Square Value (RMS)	$\sqrt{\frac{\sum_{i=-N}^N X_i^2}{2N + 1}}$
k_6 : Skewness	$\frac{\sum_{i=-N}^N (X_i - k_3)^3}{2N \times k_4^3}$
k_7 : Kurtosis Value	$\frac{\sum_{i=-N}^N (X_i - k_3)^4}{2N \times k_4^4}$
k_8 : Crest factor	$\frac{\max(X_i)}{k_5}$
k_9 : Form factor	$\left(\frac{k_5}{k_2}\right)$

C. SVM Classifier

Use Support vector machines (SVMs) are supervised learning methods for classification that use a subset of training points (called support vectors) in the decision function, making it memory efficient and allowing for outlier detection, as well as Versatility, with various Kernel functions that can be specified for the decision function[24].

Fig 3 depicts the classification of a sequence of data points into two classes: Class I (aqua circle dots) and Class II (dark orange circular dots). The SVM attempts to place a Hyperplane between the two classes, which is a linear boundary represented by a bold line, and orients it in such a way that the margin is maximised, i.e. the distance between the border and the nearest data point in each class is maximal.

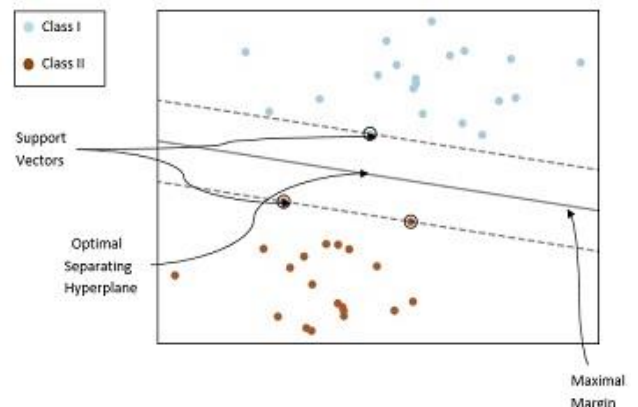


Fig 3. Classification of 2 different classes of Data

Support Vectors are the closest data points that are utilised to depict the margin. The various parameters for SVM classifier is depicted in Table III.

Table III. SVM Parameters description

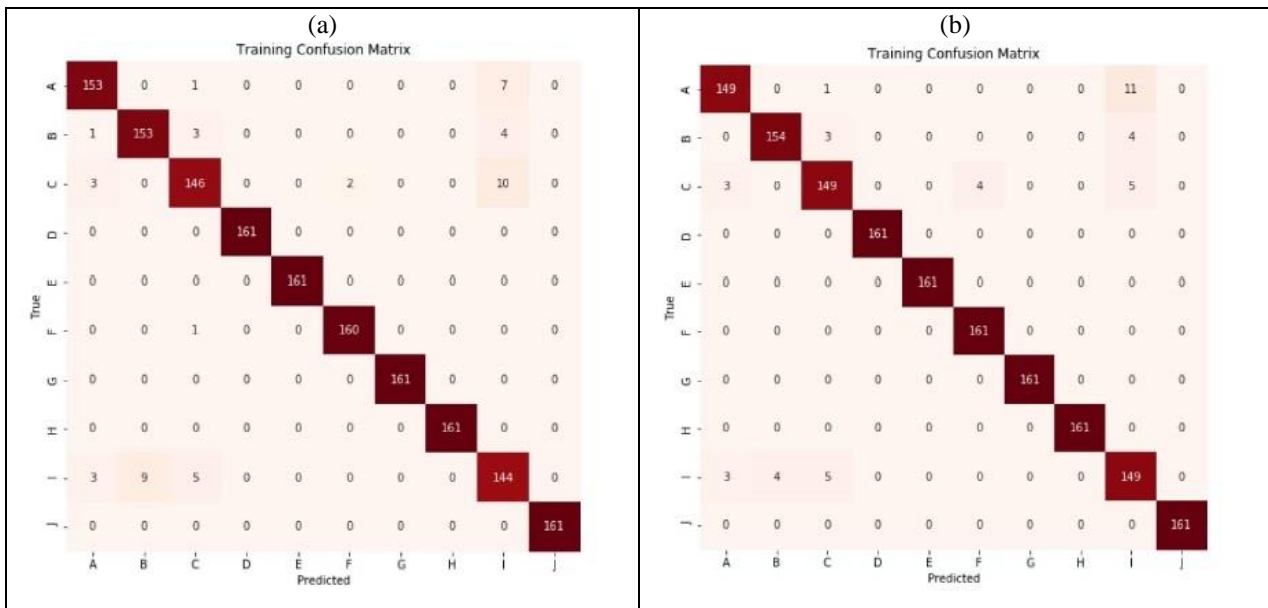
C	50
gamma	0.05
max_iter	-1
probability	False
Random_state	None
Degree	3
Shrinking	True
Tol	0.001
Verbose	False
Break_ties	False
Cache_size	200
Class_weight	None

Decision_function	ovr
Coef0	0.0

The non-linearly separable data to be classified is translated onto a high-dimensional feature space via a transformation $\varphi(x)$, where the data can be linearly classified or separated. onto a high-dimensional feature space, where the data can be linearly classified or separated [25].

D. Training Data

The SVM model was trained with vibration data sets with the help of the Jupyter Notebook software. In SVM classification, various kernel functions such as Radial Basis kernel Functions (RBFs), Linear, Polynomial and Sigmoid were considered. The optimised model with the fewest Support Vectors was selected, because the fewer the Support Vectors, the greater the generalisation [27]. The confusion matrix plot was obtained using Python code and implemented in Jupyter Notebook. Fig 4 shows the Training Confusion Matrix plot for Train-Test split as 70:30 with varying Kernel as (a)Linear, (b)Poly, (c)Sigmoid and (d)Rbf .The changes in true and predicted values is observed in each case.



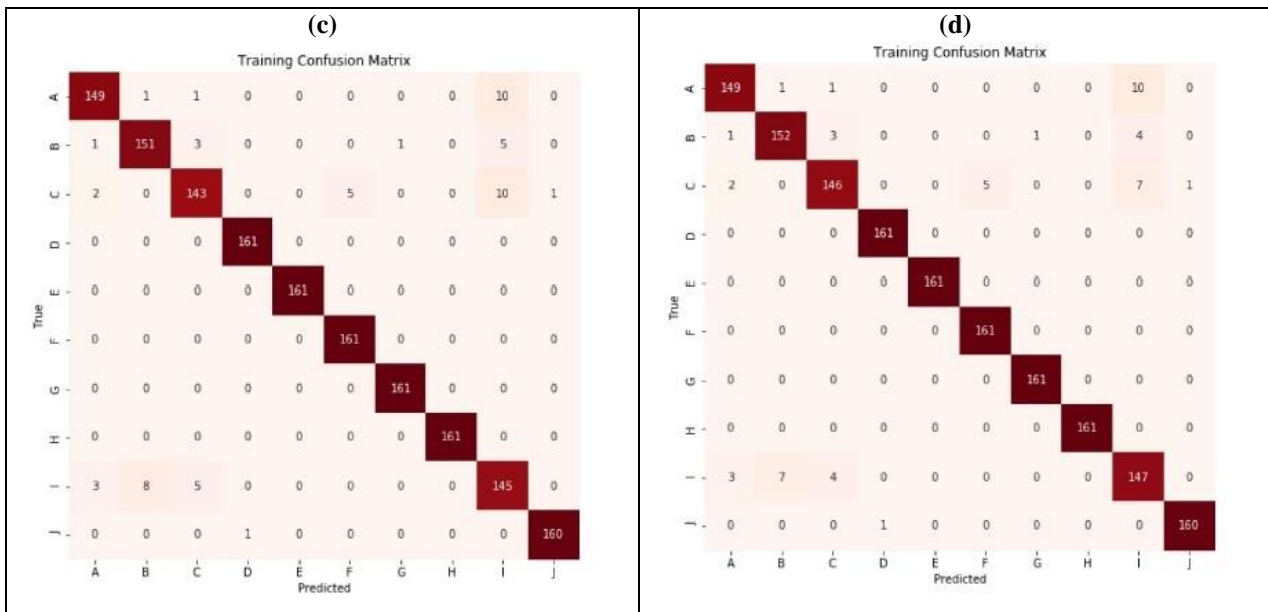
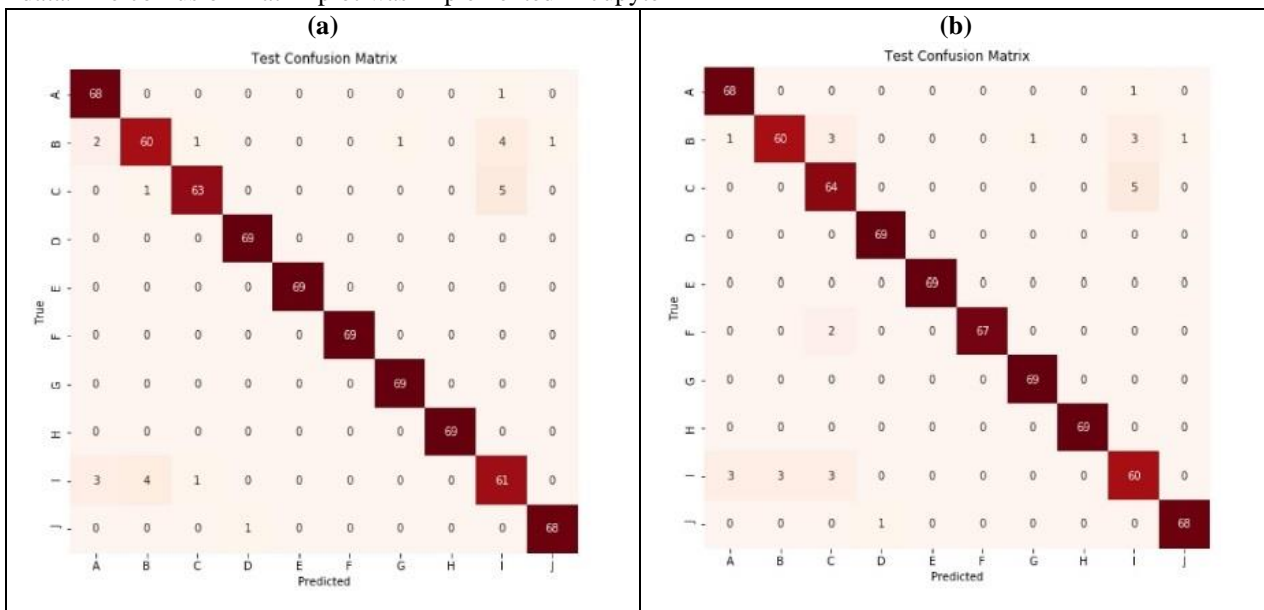


Fig 4. Training Confusion Matrix plot for various Kernel as (a)Linear, (b)Poly, (c)Sigmoid and (d)Rbf

E. Testing Data

The SVM model created after successful training was utilised to evaluate the testing file in order to determine the classifier's generalisation ability. The confusion matrix gives the relation between true and predicted values for testing data. The confusion matrix plot was implemented in Jupyter

Notebook using Python code. Fig.5. shows the Testing Confusion Matrix plot for Train-Test split as 70:30 with varying Kernel as (a)Linear, (b)Poly, (c)Sigmoid and (d)Rbf. The minute change in true and predicted values is observed in each case.



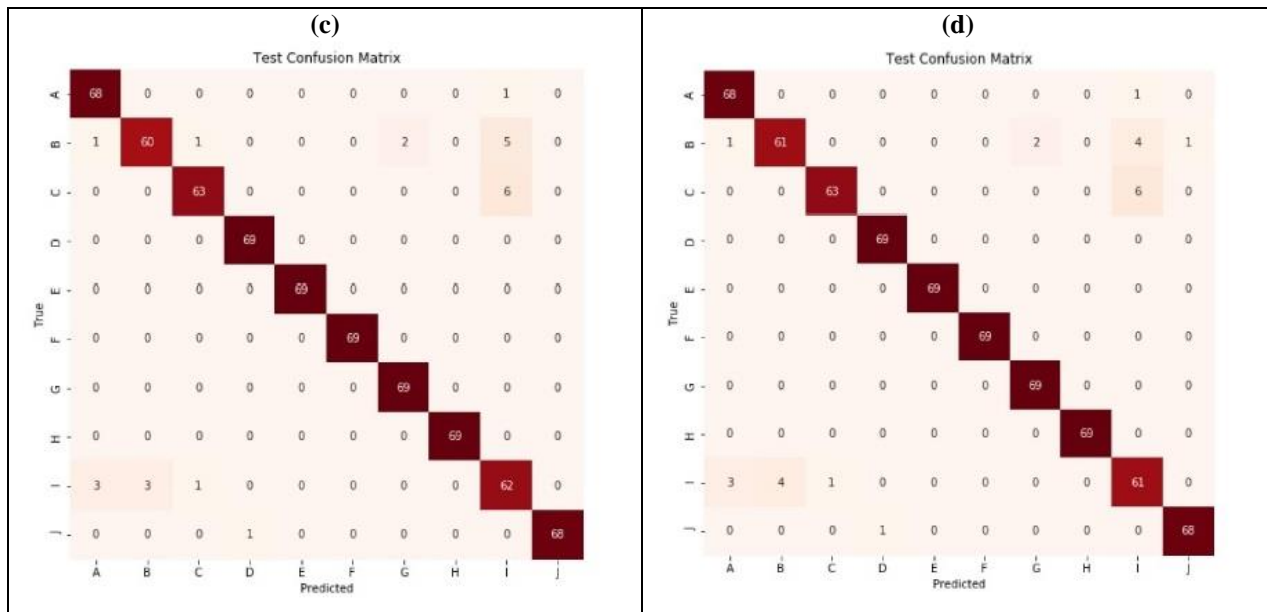


Fig 5. Testing Confusion Matrix plot for various Kernel as (a)Linear, (b)Poly, (c)Sigmoid and (d)Rbf

V.RESULTS AND DISCUSSION

After applying the SVM Classifier to the Dataset collected for considered 10 Bearing fault type, the corresponding Precision, Recall, F1 score and Overall Accuracy as Classification result is obtained for each varying kernel. The Kernel parameters were varied for various train-test split in determining the optimized model. The SVM Classification result with different train-test split ratio with various Kernel is shown in Table IV.

In Table IV, For training sample considered as 161 and corresponding test sample as 69 thereby making the train-test split ratio as 70:30, it is found that the overall Accuracy (96.522%) obtained for both Sigmoid and Rbf kernel is approx. same and higher than another kernel. Simultaneously, if the training and test ratio is varied further it is observed that the maximum accuracy is obtained for Rbf kernel and concluded as the best considered kernel in predicting the accuracy. The Accuracy percentage for each kernel is also depicted in Fig.6

Table IV. SVM Classification report of Bearing Fault type with various Kernels

Kernel	Bearing Fault Category	Precision	Recall	F1 Score	Overall Accuracy
Linear	T1	0.93	0.99	0.96	0.96377
	T2	0.92	0.87	0.90	
	T3	0.97	0.91	0.94	
	T4	0.99	1.00	0.99	
	T5	1.00	1.00	1.00	
	T6	1.00	1.00	1.00	
	T7	0.99	1.00	0.99	
	T8	1.00	1.00	1.00	
	T9	0.86	0.88	0.87	

Poly	T10	0.99	0.99	0.99	0.96087
	T1	0.94	0.99	0.96	
	T2	0.95	0.87	0.91	
	T3	0.89	0.93	0.91	
	T4	0.99	1.00	0.99	
	T5	1.00	1.00	1.00	
	T6	1.00	0.97	0.99	
	T7	0.99	1.00	0.99	
	T8	1.00	1.00	1.00	
	T9	0.87	0.87	0.87	
Sigmoid	T10	0.99	0.99	0.99	0.96522
	T1	0.94	0.99	0.96	
	T2	0.95	0.87	0.91	
	T3	0.97	0.91	0.94	
	T4	0.99	1.00	0.99	
	T5	1.00	1.00	1.00	
	T6	1.00	1.00	1.00	
	T7	0.97	1.00	0.99	
	T8	1.00	1.00	1.00	
	T9	0.84	0.90	0.87	
Rbf	T10	1.00	0.99	0.99	0.96522
	T1	0.94	0.99	0.96	
	T2	0.94	0.88	0.91	
	T3	0.98	0.91	0.95	
	T4	0.99	1.00	0.99	
	T5	1.00	1.00	1.00	
	T6	1.00	1.00	1.00	
	T7	0.97	1.00	0.99	
	T8	1.00	1.00	1.00	
	T9	0.85	0.88	0.87	
T10	0.99	0.99	0.99		

Fig.6. represents the impact of SVM Classification through the results predicted in the detection of various fault type.

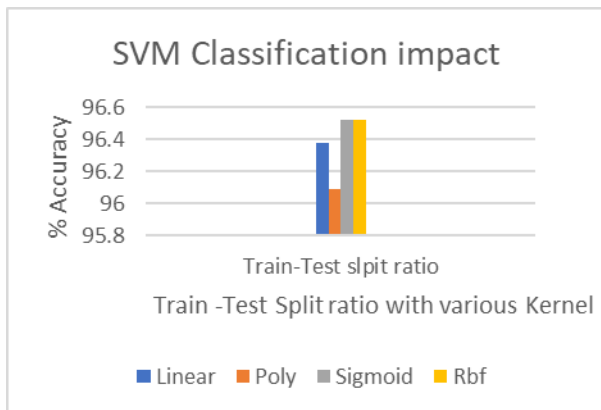


Fig 6. The impact of SVM Classification technique selection in faulty motor detection

Here, Train-test Split ratio represents the train-test split ratio 70:30 i.e. 161 data samples in the training set and 69 data samples in the test set from an overall 230 dataset of each 10 bearing faults taken into consideration. It is very clear from the graph that the maximum Accuracy of 96.522 % is obtained for Sigmoid and Rbf kernel. And if the case to choose then Rbf gives the best performance for other data samples.

VI. CONCLUSION

This research proposes an SVM-based induction motor failure detection system. By inputting statistical time domain features extracted from vibration data collected through the CWRU open source dataset, an induction motor fault is detected using the proposed method for bearing fault (ball, inner raceway, and outer raceway with fault diameters of 0.007inch, 0.014inch, and 0.021inch, respectively). Before using SVM, these features for various failure kinds are trained and tested. With a variable kernel, parameter $C=50$, $\gamma=0.05$, and most other parameters set to default, the SVM Classifier now classifies the fault type.

With an overall accuracy of 96.522 percent, the SVM Classifier's outcome in this comparison analysis is extremely excellent. The proposed induction motor fault detection system is expected to help to facility maintenance and cost reduction by predicting the occurrence of a fault in advance.

REFERENCES

[1] Konar, P. and Chattopadhyay, P. (2011) Bearing Fault Detection of Induction Motor Using Wavelet and Support Vector Machines (SVMs). *Applied Soft Computing*, 11, 4203-4211. <https://doi.org/10.1016/j.asoc.2011.03.014>

[2] T. Ince, S. Kiranyaz, L. Eren, M. Askar and M. Gabbouj, "Real-Time Motor Fault Detection by 1-D Convolutional Neural Networks," in *IEEE Transactions on Industrial Electronics*, vol. 63, no. 11, pp. 7067-7075, Nov. 2016, doi: 10.1109/TIE.2016.2582729.

[3] X. Dai and Z. Gao, "From Model, Signal to Knowledge: A Data-Driven Perspective of Fault Detection and Diagnosis," in *IEEE Transactions on Industrial Informatics*, vol. 9, no. 4, pp. 2226-2238, Nov. 2013, doi: 10.1109/TII.2013.2243743.

[4] B. R. Nayana and P. Geethanjali, "Analysis of statistical time-domain features effectiveness in identification of bearing faults from vibration signal," *IEEE Sensors J.*, vol. 17, no. 17, pp. 5618-5625, Sep. 2017.

[5] J. Tian, C. Morillo, M. H. Azarian, and M. Pecht, "Motor bearing fault detection using spectral kurtosis-based feature extraction coupled with K-Nearest neighbor distance analysis," *IEEE Trans. Ind. Electron.*, vol. 63, no. 3, pp. 1793-1803, Mar. 2016.

[6] A. Dey, "Machine learning algorithms: A review," *Int. J. Comput. Sci. Inf. Technol.*, vol. 7, no. 3, pp. 1174-1179, 2016

[7] P. K. Kankar, S. C. Sharma, and S. P. Harsha, "Fault diagnosis of ball bearings using machine learning methods," *Expert Syst. Appl.*, vol. 38, no. 3, pp. 1876-1886, Mar. 2011.

[8] M.-Y. Chow, P. M. Mangum, and S. O. Yee, "A neural network approach to real-time condition monitoring of induction motors," *IEEE Trans. Ind. Electron.*, vol. 38, no. 6, pp. 4484-4491, 1991.

[9] Tian, J.; Morillo, C.; Azarian, M.H.; Pecht, M. Motor Bearing Fault Detection Using Spectral Kurtosis-Based Feature Extraction Coupled with K-Nearest Neighbor Distance Analysis. *IEEE Trans. Ind. Electron.* 2016, 63, 1793-1803.

[10] D. Neupane and J. Seok, "Bearing Fault Detection and Diagnosis Using Case Western Reserve University Dataset With Deep Learning Approaches: A Review," in *IEEE Access*, vol. 8, pp. 93155-93178, 2020, doi: 10.1109/ACCESS.2020.2990528.

[11] S. Bhandari, H. P. Zhao, H. Kim, P. Khan, and S. Ullah, "Packet scheduling using SVM models in wireless communication networks," *J. Internet Technol.*, vol. 20, no. 5, pp. 1505-1512, 2019.

[12] D. H. Pandya, S. H. Upadhyay, and S. P. Harsha, "Fault diagnosis of rolling element bearing with intrinsic mode function of acoustic emission data using APF-KNN," *Expert Syst. Appl.*, vol. 40, no. 10, pp. 41374-4145, Aug. 2013.

[13] F. Shen, C. Chen, R. Yan, and R. X. Gao, "Bearing fault diagnosis based on SVD feature extraction and transfer learning classification," in *Proc. Prognostics Syst. Health Manage. Conf. (PHM)*, Oct. 2015, pp. 1-6.

[14] WU, Shuen-De, WU, Po-Hung, WU, Chiu-Wen, et al. Bearing fault diagnosis based on multiscale permutation entropy and support vector machine. *Entropy*, 2012, vol. 14, no 8, p. 1343-1356.

[15] Case Western Reserve University Bearing Data Center. Case Western Reserve University Bearing Data Center Website. Available online: <https://csegroups.case.edu/bearingdatacenter/pages/welcome-case-western-reserve-university-bearing-data-center-website>

[16] Lou, X.; Loparo, K.A. Bearing fault diagnosis based on wavelet transform and fuzzy inference. *Mech. Syst.Signal Process.* 2004, 18, 1077-1095.

[17] Smith, W.A.; Randall, R.B. Rolling element bearing diagnostics using the Case Western Reserve University data: A benchmark study. *Mech. Syst. Signal Process.* 2015, 64-65, 100-131.

[18] Yuwono, M.; Qin, Y.; Zhou, J.; Guo, Y.; Celler, B.G.; Su, S.W. Automatic bearing fault diagnosis using particle swarm clustering and Hidden Markov Model. *Eng. Appl. Artif. Intell.* 2016, 47, 88-100.

[19] Nayana, B.R.; Geethanjali, P. Analysis of statistical time-domain feature effectiveness in identification of bearing faults from vibration signal. *IEEE Sens. J.* 2017, 17, 5618-5625.

[20] Zhuang, Z.; Lv, H.; Xu, J.; Huang, Z.; Qin, W. A Deep Learning Method for Bearing Fault Diagnosis through Stacked Residual Dilated Convolutions. *Appl. Sci.* 2019, 9, 1823.

[21] Zhang, W.; Peng, G.; Li, C.; Chen, Y.; Zhang, Z. A New Deep Learning Model for Fault Diagnosis with Good Anti-Noise and Domain Adaptation Ability on Raw Vibration Signals. *Sensors* 2017, 17, 425

[22] Y. S. Wang, Q. H. Ma, Q. Zhu, X. T. Liu, and L. H. Zhao, "An intelligent approach for engine fault diagnosis based on

- HilbertHuang transform and support vector machine," Appl. Acoust., vol. 75, pp. 1-9, Jan. 2014.
- [23] 48k Drive End Bearing Fault Data Bearing Data Center. Available from: <https://csegroups.case.edu/bearingdatacenter/pages/48k-drive-end-bearing-fault-data>
- [24] Support Vector Machines—scikit-learn 0.24.2 documentation. Available from: <https://scikit-learn.org/stable/modules/svm.html#id15>
- [25] V.N. Vapnik, The Nature of Statistical Learning Theory, Springer-Verlag, New York, 2000.
- [26] Support Vector Machines—scikit-learn 0.24.2 documentation. Available from: <https://scikit-learn.org/stable/modules/svm.html#id15>
- [27] V.N. Twknillinen Korkeakoulu, Telniska Hogskola, Support Vector Machine Based Classification in Condition Monitoring of Induction Motors, Helsinki University of Technology Control Engg. Lab, ESPOO, June, 2004.

Electronic Voting Machine using Face and Fingerprint Recognition

^[1] Vani, ^[2] Sugnyani Patil, ^[3] Asha L, ^[4] Sowmya, ^[5] Mohit kumar singh

^{[1][3][4][5]} Students, ECE Department, R.R Institution of Technology, Bengaluru

^[2] Assistant Professor, ECE Department, R.R institution of Technology, Bengaluru

Abstract— *The primary right of voting in the election is the fundamental yardstick of a democratic citizen. During the modern era, Electronic Voting Machine has been introduced which has marked a significant change in the conventional voting system in India replacing ballot papers and boxes which are used earlier. We all know that, fake voting is still a major drawbacks in the Elections. In order to overcome this we are designing a Smart Voting machine based on face and fingerprint recognition.*

Keywords— *Electronic Voting Machine, Face Recognition, Fingerprint Recognition, Arduino uno.*

I. INTRODUCTION

Election is the act of party casting votes to elect on individual for some type of position. election may involve a public or private vote depending on the position. most position in the local, state, and federal governments are voting on in some type of election. in paper-based elections, voters cast their votes by simply depositing their ballots in sealed boxes distributed across the electoral circuits around a given country. When the election period ends, all these boxes are opened and votes are counted manually in presence of the certified officials. in this process, there can be error in counting of votes or in some cases voters find ways to vote more than once some times votes are even manipulated to distort the results of an election in favor of certain candidates. in order to avoid these shortcomings, the government of India came up with direct-recording electronic (DRE) voting system which are usually electronic voting machine (EVM). These devices have been praised for their simple design, ease of use and reliability. however, it has been found that EVM's are not tamper proof and are easily hacked. moreover this attacks, hardware as well as software, go without any detection but are quite simple to implement. This made us to bring forth a system that is secure, transparent, reliable as well as easy to use for the citizens. Smart EVM systems are not a phenomenon anymore they are being actively used in many developing nations. In this project, we propose an idea to avoid fraudulence in mechanism to make e-voting in India a reality. It improves the security

performance and avoid forgery vote because naturally one human finger print is different from other human.

II. PROPOSED SYSTEM

In the proposed method, the details of the voter will get from the registered Voter ID and AADHAR card database. It was already developed a database which is having all the information about the people,. By using this data base we took the voter's information will be stored in the excel sheet. Face and Finger print recognition refers to the automated method of verifying a voter. Web camera capture the face image and compare or match to the database, capture face and database face matched means this person will be asked to place his face on the biometric fingerprint device which compare the finger print and database fingerprint if it is matched means this person will be valid for casting his vote otherwise it will display a message in the LCD and also through voice saying that unknown voter. If the person try to fake his vote which means if he try to vote for second time then the warning message will be displayed saying that already voted. It uses a advanced microcontroller arduino uno.

III. BLOCK DIAGRAM

The System uses a Arduino uno controller for fingerprint recognition and all the details are displayed in LCD as shown in the block diagram in figure 1.

Hardware Arduino uno

Arduino is an open source prototype platform based on an easy-to-use hardware and software. Arduino Uno is a microcontroller board based on the ATmega328 (datasheet). It has 14 digital input/output pins [12] (of which 6 can be used as PWM outputs), 6 analog inputs, a 16 MHz crystal oscillator, a USB connection, a power jack, an ICSP header, and a reset button. Microcontroller: ATmega328, Operating Voltage: 5V, Input Voltage (recommended): 7-12V, Input Voltage (limits): 6-20V, Digital I/O Pins: 14 (of which 6 provide PWM output), Analog Input Pins: 6, SRAM: 2 KB (ATmega328), DC

Current per I/O Pin: 40 mA, DC Current for 3.3V Pin: 50 mA, Flash Memory:

32 KB of which 0.5 KB used by boot loader, EEPROM: 1 KB (ATmega328), Clock Speed: 16 MHz.

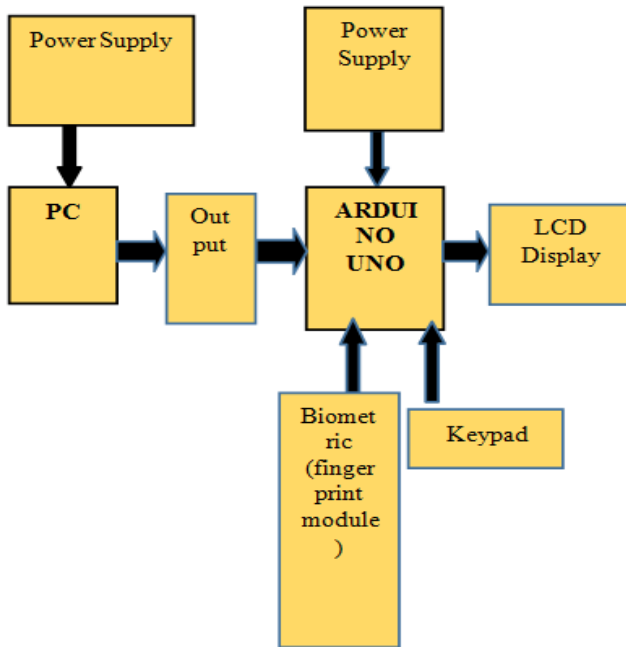


Figure 1. Block diagram

Power source module:

The major blocks of power supply are given below Transformer, Rectifier, Filter, 7805 voltage regulator

.These will provide the regulated power supply to the unit which is first converted into 12V AC .12V AC is converted into DC using rectifier circuit .Finally the 7805 voltage regulator provides constant 5V DC supply which will be given to circuit.

Keypad:

Push buttons are used in keypad. A push-button or simply button is a simple switch mechanism for controlling some aspect of a machine or a process. Buttons are typically made out of hard material, usually plastic or metal.

Voice IC:

MP3 mode, one to one key mode, Up to 7 kinds of operating modes : parallel mode, one record one play key mode , Audio-book mode, two-wire serial mode and three - wire serial mode , Support MIC and LINE -IN recording, Support plug-in 64M bit SPI-FLASH, recording time up to 1600 seconds, Support upload and download voice via USB.

Web camera:

A webcam is a video camera that feeds or streams its image in real time to or through a computer to a computer network. When "captured" by the computer, the video stream may be saved, viewed or sent on to other networks via systems such as the internet.

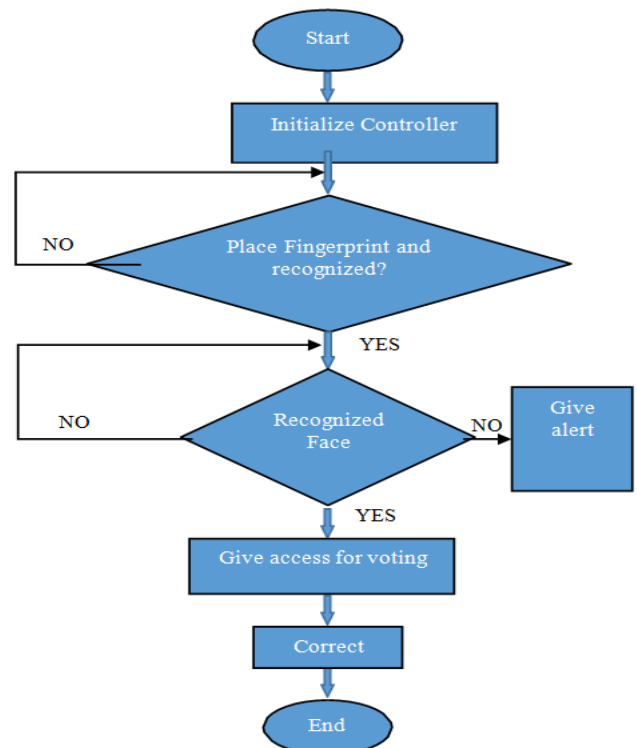
Fingerprint module:

The device is the most popular among all the identification devices because of its ease in acquisition, and also the number of sources that are available for its data collection. It has found its vast use in law enforcement and immigration purposes .The module used here is R252. The basics of this identification process comes from “Galton points” – a certain characteristics defined by Sir Francis Galton, through which the fingerprints can be identified. In this module the scanned image are compared with an earlier existing finger print of yours to get the correct identity. The comparison is carried out by the processor and the comparison is made between the valleys and ridges

Software

In this Voting Machine, we use Embedded C for Finger print recognition and python for Face recognition.

IV. FLOW CHART



V. ADVANTAGES AND DISADVANTAGES

Advantages

- Cost effective
- This system allows only authenticated voting than the existing equipment as the person is identified based on his fingerprint and Face Recognition.
- Low power consumption.
- It is economical.
- Less manpower required.
- Time conscious, less time required for voting and counting.
- Avoids invalid voting as it prevents unregistered voters from voting.

Disadvantages

Sometimes Face Recognition may go wrong due to some major changes in the facial aspects.

- Before voting the user has to enroll first.
- Sensitivity of finger print module causes sometimes Combine character error.

Applications

This project can be used as a voting machine to prevent rigging, during the elections in the polling booth.

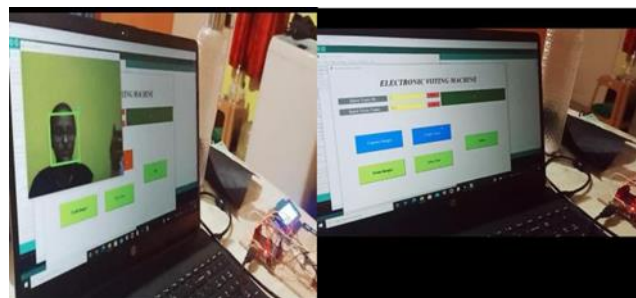
Fast track voting which could be used in small scale elections, like resident welfare association, “Panchayat” level election and other society level elections, where results can be instantaneous.

It could be used to conduct option polls during annual shareholders meeting.

It could also be used to conduct general assembly elections where number of candidates are less than or equal to eight in the current situation, on a small scale basis.

VI. RESULT ANALYSIS

In this figure, as you can see that the web camera and fingerprint scanner are attached with the Arduino uno microcontroller and LCD. We used LCD for the display purpose and j-tag for voting and fingerprint registration purpose.



The final experimental result in which person is giving his/her vote using biometric system and that templates match the previously stored templates and the person can vote. And second time if that person trying to give vote with the wrong finger print and face identification that indicates the fake voting. And we will get the warning message from the speaker, and we can now completely overcome the problems of fake voting.

VII. CONCLUSION

The project “ELECTRONIC VOTING MACHINE USING FACE AND FINGERPRINT RECOGNITION” was

manually intended to avoid fake voting and to develop a face and fingerprint recognition based advanced ELECTRONIC VOTING MACHINE (EVM) which helps in free and fair way of conducting elections which are basis for democratic country like India.

REFERENCES

- [1] Umang Shah, Trupt Shah, Marteen Kansagara, Saagar Daxini, „Biometric Secured Voting Machine to Avoid Bogus Voting Based on AADHAR CARD” , International Journal of Innovative Research in Computer and Communication Engineering , Vol. 3, Issue 3, March 2015
- [2] Rudrappa B. Gujanatti, Shivaram N. Tolanur, Murughendra S. Nemaoud, Shanta S. Reddy, Sangameshwar Neelagund, “ A Finger Print based Voting System” , International Journal of Engineering Research & Technology (IJERT), ISSN: 2278-0181. Vol. 4 Issue 05, May-2015
- [3] “Smart voting machine based on fingerprint and face recognition” by Nadar Rajkani Paulraj, G.Rajagopalan, M. Rajesh, S. V. Kirurthika, I. Jasmine A/P Dept. of ECE Fatima

Michael college of Engg & Tech, Madurai IJERT,
NCIECC-201 Conference

- [4] M.Sudhakar, B.Divya Soundarya Sai,“ Biometric System Based Electronic Voting Machine Using Arm9 Microcontroller,, IOSR Journal of Electronics and Communication Engineering (IOSR-JECE) e-ISSN: 22782834,p- ISSN: 2278-8735.Volume 10, Issue 1, Ver. II (Jan- Feb. 2015)

Case study on the effect of chilling to reduce shrinkage defect on cast-iron castings

^[1] Veeresh Gurav, ^[2] Veeranna, ^[3] Mahesh Kori

^[1] M. tech in Machine design (Mechanical Engineering), Gogte Institute of technology, Belagavi, India

^[2] M. tech in Machine design (Mechanical Engineering), Gogte Institute of technology, Belagavi, India

^[3] Assistant professor, Department of mechanical engineering, Gogte Institute of technology, Belagavi, India

Abstract— Casting is one of basic/primary manufacturing process to shape the material into desired shape and size. There are too many imperfections to be discovered during casting, some deformities are actually found here and some deformities are difficult to track down. These deformities are a consequence of some assembly factors, distinguishing the elements that cause the imperfections is the problematic task. Part of the normal projection imperfections found in casting during projection deformity investigation are gaps, shrinkage, cold close, slag consideration, hot tears, and more. To solve these projection problems and create flawless castings, foundries face a number of problems. The cementation cycle is of a bewildering nature and some of the deformities occur during the hardening measure, so to speak. In foundries, the expectation of shrinkage deformity has become the fundamental part of the projection. In this article we mainly think about addressing the shrinkage imperfection in the articles by giving shivers to the projected shape of the sand, gives a significant effect on the nature of the projection, and can also expand the projection performance.

Keywords— casting; deformities; shrinkage; projection

I. INTRODUCTION

At the beginning of civilization, stone and metal molds were used for projection interaction. To provide metal parts, there is only one better and more effective interaction that occurs in different mature ages, which is called projection. The spray cycle is the fundamental measure of assembly in the foundry. This interaction is basically used to create basic and intricate segments. Huge objects are produced simply by the interaction projected onto a solitary piece by emptying the liquid metal into the cavity of the sand shape and allowing the liquid metal to harden in the hole of the shape into a vacuum shape. In this interaction, only the majority of imperfections will occur in the segment. Using certain cycles or strategies, small deformities can be addressed but significant imperfections in the firing of the projection indications can be faced and this high rate of firing causes a considerable waste of the article, therefore, the bites of the dust launcher must take into account a wide range of deformity and must have information to distinguish the main drivers and their treatments. The deformity projection generates a high-cost risk due to the expected dismissal.

Casting imperfections can be called:

- (i) Rapid hardening in the sprinter.
- (ii) Rapid hardening before the complete filling of the mold.
- (iii) Gaseous entrapments.
- (iv) Lack of riser structure and moderate cementation rate.
- (v) Local hardening shrinkage.
- (vi) Delayed cooling compression.

Shrinkage deformity is the significant imperfection that happen in the metal projecting cycle. This occurs in the foundry a large portion of the occasions during hardening cycle of the liquid metal. Shrinkage imperfection starts with the liquid metal beginnings filling the form hole and closures when all aspects of the metal got cemented totally. The reason for this deformity is material psychologist and this shrinkage imperfection prompts part disappointment, spillage and these are foundations for projecting dismissal. A few times this deformity is showed up on the outside of the projected part and this can be effectively distinguished outwardly or from color penetrant or from some non-ruinous systems. Now and again, the deformities are happened inside and these can found by some ruinous tests to uncover the imperfection. Casting defects result in increased unit cost and lower morale of shop floor personnel. Casting

defects can be classified as:

- (i) Misruns (due to rapid solidification in the runner),
- (ii) Cold shuts (due to rapid solidification before complete filling of the mold),
- (iii) Blow holes (due to gaseous entrapments),
- (iv) Shrinkage cavity (due to lack of riser system),
- (v) Micro-porosity (due to localized solidification shrinkage),
- (vi) Hot tearing (due to the delayed cooling contraction).

Casting defects result in increased unit cost and lower morale of shop floor personnel. Casting

defects can be classified as:

- (i) Misruns (due to rapid solidification in the runner),
- (ii) Cold shuts (due to rapid solidification before complete filling of the mold),
- (iii) Blow holes (due to gaseous entrapments),
- (iv) Shrinkage cavity (due to lack of riser system),
- (v) Micro-porosity (due to localized solidification shrinkage),
- (vi) Hot tearing (due to the delayed cooling contraction).

Shrinkage deformity is the significant imperfection that occurs in the metal projection cycle. This occurs in the foundry most of the time during the liquid metal quenching cycle. Shrinkage imperfection begins with the onset of liquid metal filling the hole in the mold and closing when all aspects of the metal are fully cemented. The reason for this deformity is the materials psychologist and this shrinking imperfection partly causes disappointment, leakage and these are reasons to project dismissal. This deformity rarely occurs on the outside of the projected part and can be effectively distinguished from the outside or by the penetrating color or some non-ruinous systems. Deformities develop inside from time to time and these can be found with some ruinous tests to discover the imperfection.

II. LITERATURE REVIEW

Rahul T Patil, Veena S Metri, Shubhangi S Tambore(2015) these three individuals from Pune University showed distinctive shrinkage deformities, their causes, and solutions for those imperfections. These will help to quality control branch of casting businesses for examination of casting deformity. This investigation will be useful in improving the efficiency and yield of the projecting and they showed dismissals of the casting based on the giving imperfection ought to be a role as limited.

Rahul T Patil, Veena S Metri, Shubhangi S Tambore(2015) these three people from Pune University showed unmistakable projecting disfigurements, their causes, and answers for those blemishes. These will help to quality control part of extending organizations for assessment of projecting disfigurement. This examination will be helpful in improving the productivity and yield of the anticipating and they showed excusals of the projecting dependent on the giving blemish should be a job as restricted.

Vaibhav Ingle, Madhukar Sorte(2017) thought of another grouping of deformities and flaws or Al compound castings has been introduced. three classes of projecting imperfection have been distinguished: filling-related deformities, shrinkage abandons, shape related imperfections, warm

related deformities, Briefly, Filling-related deformities, warm related imperfections result from the connection between liquefy streams at various temperature, while undesired stages are non-metallic stages, like oxides, bits of hard-headed and dross, which come from the association among soften and climate. At long last, warm compression absconds are breaks because of the projecting constriction obliged by the kick the bucket or effectively set material. In this examination work distinctive projecting imperfections are considered. By alluding diverse examination papers causes and their cures are recorded. These will assist with improving the quality in enterprises for investigation of projecting deformity. This investigation will be useful in improving the profitability. Dismissals of the giving ought to be a role as limited and get better calibre.

Hardik Rathod (2017) from V. V. P Engineering school thought of a paper named "Expectation of Shrinkage Porosity Defect in Sand Casting Process of LM25" in this paper It is reflected from test results that there are more odds of shrinkage porosity event close to the focal point of calculation for Y intersection. It can likewise be seen that huge measure of shrinkage porosity was shaped close to the middle as found in recreation. In any case, the area of shrinkage porosity can differ as indicated by mathematical and warm boundary change. In the current exploration work, 'Y' intersection is utilized for forecast of shrinkage porosity, which might be stretched out for different intersections moreover.

Pradeep Kumar Ganguly, &Rajesh Rana (2018) accomplished a work on "A survey on diminishing projecting deformities and improving efficiency in a limited scale foundry utilizing DMAIC approach". Here this contextual analysis essentially centers around steel foundry, present china furnishes projecting item great quality with less time. different kinds of projecting interaction like softening, shaping, center making, dissolving, pouring, shake out. Learn about different projecting deformities happen in foundry industry like shrinkage, blow opening, porosity, pinhole, sand incorporation, cold shut, miss run, surface intermittence, form break, streak and so forth Give thought regarding how deformities happens and which kinds of safeguard taken in future. measure planning implies stream measure outline material sorts in which shows all movement from crude material to complete products with time, find non worth added action and eliminate it. Numerous analysts have led trials to discover the sand interaction boundaries to improve quality castings. They have effectively decreased the projecting deformities impressively up to 6% by appropriate choosing sand boundaries. DoE is the method which can be carried out in any preparing industry. In India there are number of limited scope ventures which can execute such strategies to improve the yield, give standard interaction

boundary and increment the compelling limit of the unit. It can likewise be reasoned that DMAIC technique is for the most part utilized by the enterprises for their exhibition improvement. This investigation will assist limited scope foundry with starting Six Sigma projects in their associations and improve their exhibition regarding consumer loyalty just as monetary advantages with expansion in intensity in overall market of foundry.

Olakunle F. ISAMOTU, Kabiru M. RAJI (2019) introduced research work on execution assessment of various materials as chills in sand projecting of aluminium composite. This investigation has assessed the viability of metallic materials as chill in sand projecting of aluminium amalgam. Experimentation included testing of mechanical properties and metallographic investigation of cast tests. The outcomes got uncovered that the example chilled with copper has the most elevated mechanical properties and the cast test embedded with metal chill additionally shows higher qualities in mechanical properties than test with steel chill and unchilled test. The cast test embedded with copper chill set quicker than some other cast test with chill. The cast test embedded with metal chill cemented quicker than the cast test with steel chill.

III. SHRINKAGE

Shrinkage is nothing but the cavities which are formed during solidification of the molten metal. They mainly appear in irregular shapes and have improper rough walls. They usually appear in the bottom wide portions of the component or top big portion of the component and it also appear inside the walls of the product. Sometimes shrinkage effect takes place inside the product which will not appear on the surface of the product so to find out this we have to go through the cut section of the component.

a. The causes behind the of shrinkage defects are:

- Improper casting methods.
- Improperly designed part which has to be casted.
- Rate of solidification is mainly considered between semi solid state and final solidification. Lower the rate of solidification chances of shrinkage occurrence is low.
- Shrinkage can appear if we use extremely high casting temperature.
- Improperly designed runners and risers leads to shrinkage defects.
- By using excessive graphite during casting can cause swelling inside the molds.

b. About chill

A chill is an article used to advance hardening in a particular segment of a metal projecting mold. Regularly the

metal in the form cools at a specific rate comparative with thickness of the projecting. At the point when the calculation of the embellishment pit keeps directional hardening from happening normally, a chill can be deliberately positioned to help advance it.

IV. EXPERIMENTATION

In this paper we mainly concentrated on shrinkage defects with the help of industry. we conducted two case studies on casting parts which are currently manufacturing in industry.

A. Case study 1

Here we selected a part Hydraulic cylinder which is used in construction which was facing the major shrinkage defect during casting.

Shrinkage occurs because of molten metal solidifies at a higher rate due to liquid metal is denser compared to solid metal. During solidification due to slow cooling of the molten metal the final solidified metal will have some irregularities. In the foundry, when molten meatal was poured in the casting, the metal was solidifying at a slower rate in the bottom portion of the casting. Most of the shrinkage holes are generated in the upper part of the hot joint of the casting. In this cylinder the shrinkage occurs mainly in cylinder head.

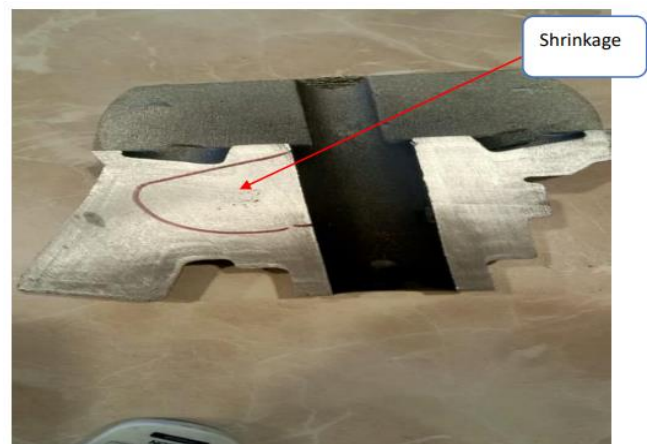


Fig 1: - Cut section of cylinder head which shows the shrinkage

Because of shrinkage defect lot of casting rejections are happening in the industry. To solve this defect, we provided a chill at the head portion of the cylinder.

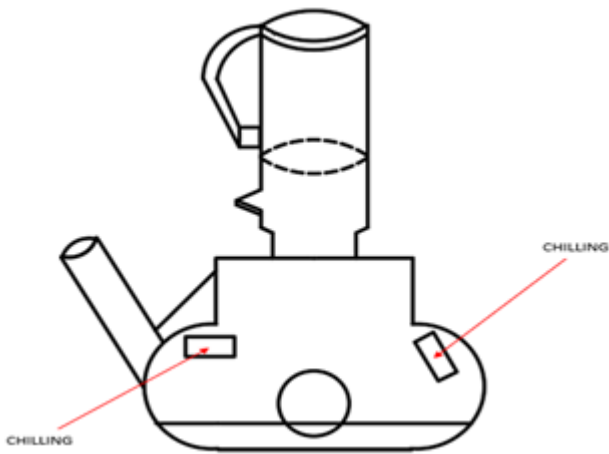


Fig 2: - 2-D diagram of cylinder which shows chilling at cylinder head



Fig 3: -Chills provided in sand mould of cylinder before molten metal pouring.

Here we gave the interior chills implies these are bits of metal that are set inside the embellishment hole. At the point when

the depression is filled, some portion of the chill will liquefy and eventually become part of the projecting, accordingly the chill should be a similar material as the projecting. Note that inside chills will assimilate both warmth limit and warmth of combination energy. By this way the shrinkage issue got diminished.

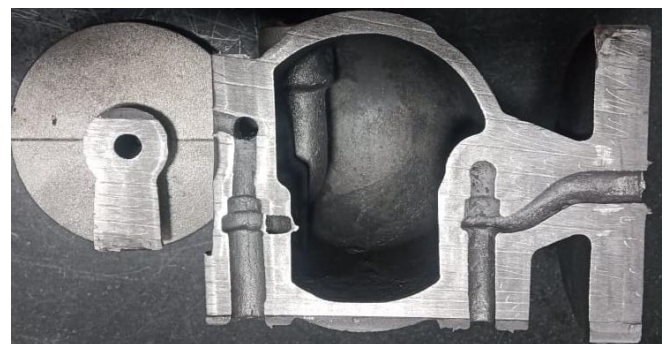
Case study 2

Here we selected a part Compact Module Two Orifice Float Trap (CMTOFT) cover which is used in boilers which was facing the major shrinkage defect during casting.



Fig 4: - Shows shrinkage defect in CMTOFT over

As shown in above figure the shrinkage defect was formed inside the valve of CMTOFT cover Here in CMTOFT cover the shrinkage problem was taking place in the core cavities and inside wall. To solve this shrinkage problem, we applied chilling here also.



The above figure shows the cut section of CMTOFT cover it has done to check the shrinkage, which occurs inside the part which is not appear on outside of the body of the cover. As we saw in previous figure the shrinkage is appear only in the inside wall of valve.

Here in CMTOFT cover the shrinkage problem was taking place in the core cavities and inside wall. To solve this shrinkage problem, we applied chilling here also.

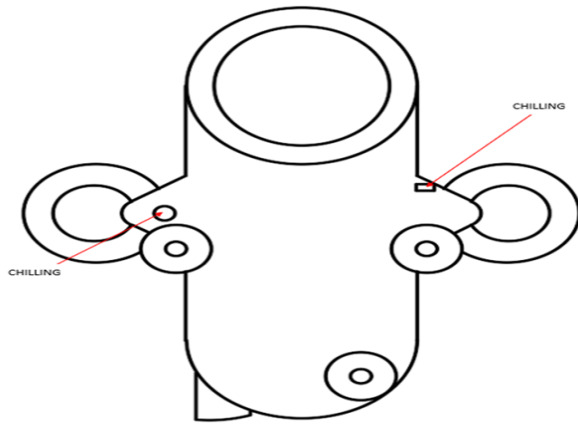


Fig 6: -2-D outline diagram of CMTOFT cover which represents chilling



Fig 7: -view of sand mould which shows chill



Fig 8: -CMTOFT cover after solidification

By applying chilling on this part, we got great outcomes. At the point when Liquid metal enters the shape through gravity

or low pressing factor. Pouring of the metal and development of the form are facilitated to maintain a strategic distance from choppiness when the metal enters the shape.

Since liquid metal streams into all pieces of the shape by gravity pressure, each projecting is dimensionally precise and liberated from porosity. As the metal is poured, the shape is tenderly vibrated to guarantee the total filling important to create sharp corners and fine detail in the castings. By this chilling cycle projecting item currently have irrelevant shrinkage deformity.

General rules and observations regarding the use of chills: -

Their surface should be clean and accurately contoured to fit the area to be chilled.

The ends and sides of large chills should be tapered or moulded using mouldable sands to reduce the potential for drastic cooling that may occur. The failure to recognize this fact can increase the incidence of localized stress cracks.

Chills should be adequately sized so that they don't fuse to the casting. Excessively thick chills have no beneficial effect.

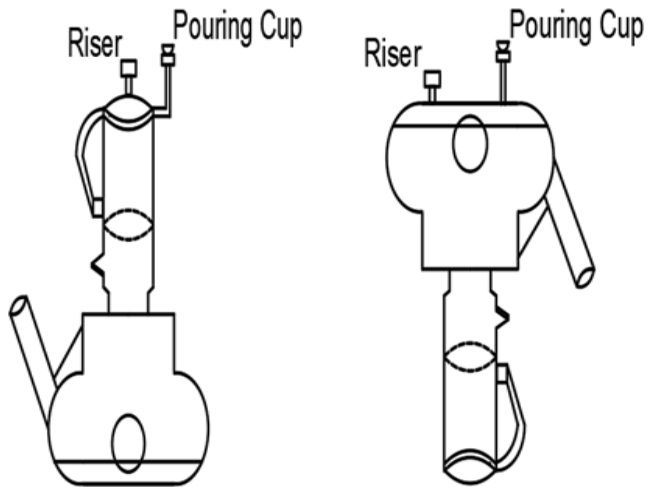
Chills should not be positioned close to ingates, as the volume of metal passing across the chill surface will saturate the chill with heat, losing their effectiveness.

To ensure the maximum chilling efficiency of a metal chill it must lie against the surface of the casting.

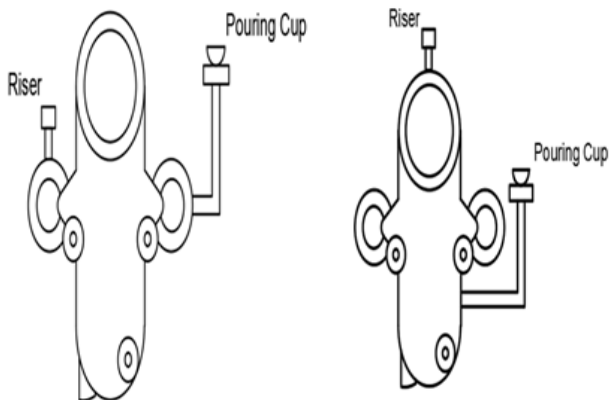
V.RESULTS AND DISCUSSION

Generally projecting imperfections are worried about measure boundaries. Subsequently one needs to control the interaction boundary to accomplish zero deformity parts. So first we attempted to tackle this shrinkage issue by changing the places of sprinter and riser. This can be refined by utilizing a sprinter and entryway framework with risers to supply the liquid metal, which includes channels for the metal to move through into the form and supplies of fluid metal on top of the shape to fill in where the metal psychologists.

A. Variations in position of runner and riser of cylinder as shown below



B. Variation in position of runner and riser of CMTOFT cover are shown below



Here to get a freed of from shrinkage deformity we utilized sprinter to take care of liquid metal and riser, otherwise called a feeder, is a supply incorporated into a metal projecting mold to forestall holes because of shrinkage. By utilizing these sprinter and riser we got 40% - 45% decrease in shrinkage however it isn't sufficient and furthermore have a few burdens as referenced underneath.

- It is time consuming.
- Need extra energy investment.
- Need more time for solidification.
- We have to remove runner and riser from casting product after solidification this needs to reuse of runner and riser this leads to waste of time and energy.

- While removing runner and riser there may be chance of main product failure.
- Part dimension variation may occur.

considering above points chilling process have more benefits than using runner and riser. We got good results by using chilling in casting and shrinkage got 75% -80% reduction in shrinkage. The finished parts are shown below.



Fig 9: View of Finished Cylinder with Negligible Defect



Fig 10: View of Finished CMTOFT Cover with Negligible defect

We came up with several benefits by using chilling as mentioned below.

- Good for high volume production.
- Uniform material properties throughout the casting part.

- Superior surface finish.
- Close tolerances.
- Dimensional accuracy
- Smaller cast holes.
- Time consumption is less.
- Minimized part variation.
- Superior mechanical properties

By considering above outcomes chilling is better and effective approach to decrease shrinkage imperfection. An appropriately planned projecting, an appropriately arranged shape and accurately softened metal should bring about an imperfection free projecting. Be that as it may, if legitimate control isn't practiced in the foundry-once in a while it is excessively costly.

The synthetic synthesis of the end results are as referenced underneath

Table 1: For cylinder

CHEMICAL COMPOSITION		
S.NO	CHARACTERISTICS	SPECIFICATIONS
01	C.E-Carbon equivalent	
02	T.C.-Tungsten carbide	3.40-3.60
03	Si-Silicon	2.10-2.50
04	Mn- Manganese	0.20-0.50
05	P-Phosphorous	0.10% max
06	S-Sulphur	0.02% max
07	Mg-Magnesium	0.030-0.060
08	Ni-Nickel	0.1max
09	Mo-Molybdenum	0.20-0.35
10	Cr-Chromium	0.07max
11	Cu-Copper	0.70-0.95

Table 2: For CMTOFT cover

CHEMICAL COMPOSITION		
S.NO	CHARACTERISTICS	SPECIFICATIONS
01	C.E -Carbon equivalent	
02	T.C. -Tungsten carbide	3.40-3.85
03	Si -Silicon	2.30-2.90
04	Mn -Manganese	0.40% max
05	P -Phosphorous	0.05% max
06	S -Sulphur	0.02% max
07	Mg -Magnesium	0.030-0.060
08	Ni -Nickel	-
09	Mo -Molybdenum	-
10	Cr -Chromium	-
11	Cu -Copper	-

For CMTOFT cover the tensile strength test is as given below

INFO DATA: -

Sample shape : Solid Round

Sample type : S G Iron

Sample Diameter : 14 mm

Introductory G I For % stretching : 70 mm

Pre burden esteem : 0 KN

Max Load : 400 kN

Max Elongation : 200 mm

Example cross segment territory : 153.938 mm²

Last Sp Diameter : 12.3 mm

Last Gauge Length : 87 mm

Last Area : 118.82 mm²

Yield DATA: -

Burden at Yield : 43.016 kN

Extension At Yield : 4.370 mm

Yield Stress : 279.437 N/mm²

Burden at Peak : 65.696 kN

Extension At Peak : 18.500 mm

Elasticity : 426.769 N/mm²

Burden At Break : 62.376 kN

Prolongation At Break : 23.740 mm

% Reduction territory : 22.81 %

% Elongation : 24.29 %

VI. CONCLUSION

By investing man, machine and material in huge amount the casting manufacturing in the foundry will be able to run. Dismissal of projecting prompts substantial misfortunes to projecting producers. In current foundries till date the issues are settled by experimentation strategies. In this paper shrinkage abandons prompting dismissal of Casting are talked about alongside their causes and cures which will be useful to every single one who are engaged with assembling of shape Casting and will be massively gainful to diminish the dismissal of Casting prompting counteraction of colossal monetary misfortunes looked by Manufacturers. It is reflected from test results that there are more odds of shrinkage imperfection event when we use sprinter and riser to settle shrinkage deformity where just 40%-45% of shrinkage decreases. While if we use chilling to solve problem there will be 75% to 80% reduction in shrinkage. So finally, we conclude that chilling is the most efficient and better way to solve shrinkage than using runner and riser.

REFERENCES

- [1] A.P.More, Dr.R.N.Baxi, Dr.S.B.Jaju "Review of casting defect analysis to initiate the improvement process" International Journal of Engineering Technology and sci Vol 2(4),292-295, 2011
- [2] Vaibhav Ingle, Madhukar Sorte "Defects, root causes in casting process and their remedies review" International Journal of Engineering Research and Application Vol. 7, Issue 3, (Part -3), pp.47-54, March 2017
- [3] Beeresh chatrad, Nithin Kammar, Prasanna P Kulkarni, Srinivas patil. "A study on minimization of critical defects in casting process considering various parameters" International Journal of Innovative Research in Science, Engineering and Technology, Vol. 5, Issue 5, May 2016
- [4] Hardik Rathod "Prediction of shrinkage porosity defect in sand casting process of Im25" IOP Conf. Series: Materials Science and Engineering 225, 2017

- [5] M. Copur, A. Turan, M. N. Eruslu. "Effects of chills on the solidification pattern of an axial steel cast impeller" METALURGIJA 54, Vol. 3, 515-518, (2015)
- [6] Wossenu Ali, Wollo "Defect analysis for sand casting process (case study in foundry of kombolcha textile share company)" International Research Journal of Engineering and Technology, Volume: 07 Issue: 01 | Jan 2020
- [7] Avinash Juriani "Casting defects analysis in foundry and their remedial measures with industrial case studies" IOSR Journal of Mechanical and Civil Engineering, Volume 12, Issue 6 Ver. I (Nov. - Dec. 2015)
- [8] Rahul T Patil, Veena S Metri, Shubhangi S Tambore "Causes of casting defects with remedies" International Journal of Engineering Research & Technology (IJERT), Vol. 4 Issue 11, November-2015
- [9] Olakunle F. Isamotu, Kabiru M. Raji "Performance evaluation of different materials as chills in sand casting of aluminum alloy", Research Gate, vol.3, December 2019
- [10] A.G.Thakare , Dr.D.J.Tidke Research Scholar. "Root cause analysis of defects in duplex mould casting", International Journal of Innovations in Engineering and Science, Vol. 1, No.3, 2016
- [11] E. Fraś, M. Górny, H. F. Lopez "Mechanism of the silicon influence on absolute chilling tendency and chill of cast iron" Archives of metallurgy and materials, Volume 54, Issue 1, 2009
- [12] Ganguly, P., & Rana, R. "A review on reducing casting defects and improving productivity in a small-scale foundry using dmaic approach". international journal of engineering sciences & research technology, 7(7), 115-122. 2018
- [13] Bhushan Shankar Kamble. "Analysis of different sand-casting defects in a medium scale foundry industry" International Journal of Innovative Research in Science, Engineering and Technology, Vol. 5, Issue 2, February 2016
- [14] Abhijeet B. Vante, G.R.Naik "Quality improvement for dimensional variations in sand casting using quality control tools" International Journal of Innovative Research in Science, Engineering and Technology , Vol. 4, Issue 8, August 2015
- [15] Dr D.N. Shivappa, Mr Rohit, Mr. Abhijit Bhattacharya "Analysis of casting defects and identification of remedial measures- a diagnostic study" International Journal of Engineering Inventions, Volume 1, Issue 6, PP: 01-05 (October 2012)

Experimental Investigation and Vibration Analysis of Laminated Composite Beams with Multiple Edge Cracks

^[1] Vishal Omprakash Jadhav, ^[2] Prof. Dr. Harshal Ashok Chavan

^[1] Dept. of Mechanical Engineering, MET' s I.O.E. BKC, Nashik

^[2] Asst. Professor- Dept. of Mechanical Engineering, MET' s I.O.E. BKC, Nashik

Abstract— *Crack developed suddenly in the vibrating component may cause disastrous failures. The occurrence of splits changes the physical features of a structure that changes its dynamic response. So the effects of broken structures must be understood. The essential parameters are the number of crack, the depth and placement of crack. Therefore, changes in structure response parameters are important for structural completeness, performance and security to be monitored. The finite element model is presented with the vibrational Composite laminated beam analysis, including open transverse cracks. Experimental validation under six damage scenarios for a laminated cantilever beam is also accomplished through ambient vibration tests. The three-dimensional model of a split beam was designed using CATIA V5. FFT analyzer was performed for the experimental testing. The analysis was conducted using the program ANSYS 19. New results were analyzed in comparison. The results and conclusion of the comparative analysis were drawn.*

Keywords— *Cutting tool, modal analysis, vibration test, FFT.*

I. INTRODUCTION

Structures need to work safely during their lifetime. However, damage causes the structures to collapse. Cracks in structures are one of the most common types of damage. The structural cracks may be dangerous because of the static or dynamic loads, which mean that crack detection plays a significant role in the monitoring of structural health. Beam type structures are popular in the manufacturing of steel and machinery. The Beam structural safety, particularly detection of fractures via structural health surveillance, is covered in various researches in the literature. Structural health surveillance studies for fracture identification address changes in natural and beam mode frequencies.

The structural flaw most typical is that a crack exists. Because of many reasons, cracks are prevalent in structures. Not only may the presence of a fracture create a local difference in rigidity, but it could significantly impact the mechanical behavior of the whole structure. Due to the reduced fatigue strength, cracks may be generated by fatigue under operational conditions. Mechanical faults can also lead to them. During manufacturing procedures, another group of fractures are initiated. They are usually small in sizes. Due to shifting stress conditions, such little cracks are known to spread. If these propagating fissures remain undiscovered

and reach critical dimensions, there may be a rapid structural breakdown. Natural frequency measurements can therefore be used to detect breakages.

A variety of publications have been examined, examined and analyzed in the present study. The influence of single fracture on the structural dynamics has been explored by most scholars. In actuality, however, structural components For example, fatigue beams are more likely to result in cross-sectional fractures. The dynamic behavior of basic structures has thus been extensively examined by crack. The goal is to do vibration analysis with and without a crack on a cantilever beam. The analytically achieved results are checked with the results of the simulation. In the initial phase of work, the analysis expressions in the dynamic properties of structures contain two cross-surface fractures. These cracks impose new limits on the structures at the crack places. The limits result from the strain energy equation using the theorem of castiglian. Crack also affects the rigidity of the structures formed from the rigidity matrix. In later parts, full analyzes of break modeling and rigidity matrices are shown. For dynamic features of transverse cracked beams the beam theory of Euler-Bernoulli is used. Natural frequencies theoretical formulae and the mode for beams have been employed to identify modified boundary conditions because of the crack presence. Due to its capacity to deal with examination of neural networks have been utilized to destroy structures without the need for expensive calculations identify harm for several years. The need for intense calculation is predicted to be recent neural networks. Neural networks have recently been anticipated as a possible solution for detecting structural degradation. In that study the input (situation and Crunch depth (structural frequencies of the system) output relationship is utilized to build multi-layered, back- propagating neural networks. A neural structure network is trained for the cracked structure using a dataset for various crack sizes and locations structure's response.

Beams are frequently utilized in civil, mechanical, marine and aeronautical engineering as a structural element. Damage is one of the important topics of engineering and structural analysis. Damage analysis will improve both the safety and economic development of the business. All structures undergo degenerative effects during operation which can lead

to structural faults such as cracking, resulting in a catastrophic failure or disintegration of the structure as the time proceeds. Earlier crack identification is vital to avoid the unexpected or sudden failure. One of the most crucial areas for many studies is that of taking this ideology into account crack detection. Many researchers are developing different approaches to detect the Place, depth, magnitude and structural pattern of damage at an early stage. Worldwide, many unstructured approaches have been used for crack detection. However, for the identification of crack/damage the vibrational method is fast and cheap.

The principle VIBRATION is intrinsic to any structure subject to static or dynamic loads in the physical sciences. All constructions generate certain anomalies throughout their life cycle due to their rigidity, which lead to fracture development. The problem with crack is the fundamental problem of material science. Taking into account crack as an essential kind of Modeling of such damage is a key step in monitoring the behavior of damaged structures on structural health. SHM is commonly used to detect and locate the existence of damage to the structure in different infrastructure forms. Beam or shaft may be designed to understand the effect of fracture on steepness, using Euler-Bernoulli or Timoshenko theories. Beam border conditions are used along with crack compatibility relations to establish the natural frequency, crack depth and location of the others beam characteristics. Beam border conditions are used. Crack detection study on structural health monitors variations in natural frequencies and beam mode.

II. LITURATURE REVIEW

MarjanDjidrov etal. [1] Mechanical structures may be susceptible to damage throughout their functional operations, and as a result, it is not possible to guarantee a certain operating mode devoid of defects and successful functioning. This research analyzes the vibration and frequenz response of a cantilever aluminum beam using a connected piezoelectric transducer using the finite-element method. In the Finite Element Analysis Program ANSYS the findings are given. It investigates the vibration response of a cantilever beam; the numerical results of a beam modell are compared with various structural damage scenarios based on the position and depth of a single transverse beam fracture. The method is based on the idea that when a fracture develops in a mechanical structure changes in the structure's physical qualities, which produces changes in structural modal properties.

Techniques for detecting damage in mechanical structures, as well as their application, have risen in importance in recent years across practically all industries in the mechanical, aerospace, and civil engineering fields, according to the American Society of Mechanical Engineers. It is possible to increase the future reliability of mechanical systems and minimize their life-cycle costs by incorporating the ability to detect and understand undesirable changes in a structure. The

primary goal of Structural health surveillance is the identification and characterisation of damage that may affect the structural integrity and functionality of mechanical component structures. Conventional inspection procedures and processes in a professional setting may be costly and time-consuming. Important progress may be achieved in the solution of these problems via the development and use of equipment-driven techniques and processes capable of efficiently detecting damage and providing information on the location and degree of damage inside a building. This often makes the piezoelectric transducers, which may serve as sensors and actuators, use in systems that monitor the structural sant  of buildings for damage detection.

Prathamesh M. Jagdaleetal. [2] Cracks contribute to changes to the physical characteristics of a structure, adding flexibility to the structure and therefore reducing its rigidity, resulting in a related decrease of modal natural frequencies. As a consequence the beam's dynamic reaction varies. In this study, we propose a model for free vibration analysis of an open edge fracture beam which may be utilized to study beam vibration. In this study, fluctuations in natural frequencies produced by fractures at various locations and with different break depths have been examined. In this instance, a parametric investigation was carried out. The broken beams have been examined in detail under various boundary circumstances. The findings gained from previous experiments must be compared with those achieved in the analysis of finite elements in this study. With the aid of the ABAQUS software the analysis has been carried out. If most components of the engineering structures are loaded, damage or cracking in overstrained regions may occur. A structural component with cracks such as a beam is subject to local rigidity variations, which are mainly influenced by its position and depth. In the presence of fractures, the physical properties of a structure change and the dynamic reaction characteristics of a structure change. Monitoring changes in the structural response characteristics of a structure have been extensively used for many years in structural integrity, performance and security assessment. Irregular variations in recorded vibration response characteristics were observed depending on whether the fracture was closed, open or breathable during the vibration.

Ahmed Khnajar et al. [3] It is presented in this study that To solve the issue of fractured beam vibrations, a new discrete physical model is created. The model consists of a beam made of many tiny, evenly spaced bars. Spiral spring, also a crack model, is used to mimic the beam's bending rigidity. The inertia of the beam is represented by concentrated masses at the ends of the bar. Because of its discrete form, this model offers the advantage of simplifying parametric investigations while also allowing for easy change of the fracture position and amplitude, among other things. Since the model has been built, many practical applications can be carried out without the need to repeat the entire process of developing the formulations again. A parametric analysis can then be carried

out using this model, with the goal of easing the diagnostics procedure, which includes both fracture location and depth estimation.

Geethu Lal et al. [4] Cracks are frequently found in structural elements, and cracking can result in major durability difficulties as well as structural damage in some cases. It has been found that cracks have an impact on the structural components' dynamic properties, and this was the subject of many studies. This study provides a numerical analysis of a fractured isotropic cantilever beam's transverse free vibration response using the Finite Element technique and the ANSYS software. A parametric analysis has also been done to evaluate the effect of the ratio of crack depth, the position of the cracks and the number of breakages of the first three natural frequencies of the beams on the natural frequencies. In addition, research is being out on vibration control. In real time, environmental vibration data may be monitored to locate cracks and cracking severity inside a distant or huge structure, and the results can be used to determine the location of cracks and cracking intensity.

In civil engineering constructions cracking is inevitable, and if it develops above a specific threshold, structural damage and the structure's serviceability and long-term sustainability may be affected adversely. Cracks may have a significant effect in the dynamic characteristics of a structural component in structural components. In the engineering practice, the early identification of cracking in structural components is important, and changes to structural elements' dynamics may be seen in the course of time. Vibration controls are described as a method that reduces or controls the vibration of a building by giving an adverse force to a properly decayed structure with the initial vibration but equal in amplitude with it.

Dr. K. B. Waghuldeet al. [5] Beams are frequently employed as structural elements in a variety of engineering disciplines, including Civil engineering, mechanical engineering and aeronautics. Damage in structural engineering and analysis is one of the most important factors. Damage analyzes are carried out to guarantee employees' safety and business economic development. All structures have degenerative effects during regular functioning, which can result in the development of structural flaws such as fractures that, as time proceeds, can result in the catastrophic collapse or breakdown of the structure. Early crack identification is critical in order to avoid unexpected or sudden failure. Many researchers believe crack detection to be one of the most significant sectors in which to work, taking this ideology into consideration. Many research have focused on developing many methods to early detection of the location, depth, size and pattern of damage inside a building. Many techniques have been developed and are used throughout the globe to identify non-destructive fractures. On the other hand, the vibratory technique is both fast and cost efficient for the detection of crack/damage. Several cost-effective and trusted analytical numerical and experimental methods have been

attempted by different scholars to analyze the vibrations of cracked beams described in this work. In this research, the impact on the modal parameters susceptible to vibration of the damaged beam of various factors, including fracture size, crack position and the length of the beam are also addressed in detail.

Ashish S. Apate et al [6] it is needed that the structure functions in a safe manner over its lifetime of service. As structural fractures may be hazardous as a result of static and dynamic stresses, the identification of cracks is important for applications of structural health monitoring, among others. Non-destructive methods for early recognition of crack, crack profile and crack size are being used by many studies. Many researchers a number of techniques, including computational, analytical and experimental procedures, are available to investigate the issue of a fractured beam. A method called FEM is used to get the stiffness matrix of the cracked beam element (Finite Element Method). The objective of this study is to examine a large number of reliable and experimental mathematical methods for the analysis of vibrations of fractured beams developed by different researchers.

F. Bakhtiari-Nejadr et al [7] It is demonstrated in this study that A beam with one or two cracks may be used to identify natural frequencies as well as mode shapes to overcome the difficulties in addressing the issue of its own value by providing the analytical assessment based on Rayleigh's method. The first thing needed to find an algebraic equation is to numerically calculate precise natural frequencies and mode forms by utilizing matrices generated from compatibility requirements at each crack and limit point of trigonometric and hyperbolic terms in modes. This technique thus does not explicitly show the effects of the size of the fracture and its placement.

Kaushar H. et al [8] Intensive research has been conducted over the Researchers have been designing a number of methods to achieve this objective over the last several decades on the detection of fractures by utilizing vibration-based techniques. The present paper reports on the detection of a fracture that occurs on the surface of a structural element of a beam type using natural frequency. In the case of split beam, the first two natural frequencies were experimentally measured and used to estimate the location and size of the split. The locations and sizes of the cracks that have been identified are compared to the real findings and are well agreed. This section also discusses the impact of fracture location and depth on the natural frequency.

III. PROBLEM STATEMENT

When designing Beams are one of the main charging components to consider as the engineering structure Fractures in beams occur often and cracks also develop in other sections of the structure. A wide range of study works, including one- and multiple cracks, has been published in scientific publications to address a range of problems

connected to elastic beams. Damaged beamed studies may be classified into structural and nonstructural categories. In case of damage, one group is charged with examining the structure's dynamic behavior, while another is tasked with identifying damage inside the structure, which is critical for the monitoring of structural health.

IV. OBJECTIVES

- ❖ Vibration Analysis of Cracked cantilever laminated composite beam.
- ❖ Natural Frequency of cantilever laminated composite beam according to various parameters.
- ❖ Experimental Cracked cantilever laminated beam with and without crack estimation of the natural frequency.
- ❖ Natural Cracked Beam Determination with and without Cracking using FEA.
- ❖ Natural frequency determination of effect cracks of cracked beam.

V. METHODOLOGY

- Step 1: - Going through lots of literature I have figure out what things are needed.
- Step2: - Components which are required for project is decided based on literature survey.
- Step 3: - After finalization of components, 3D model is drafted using CATIA software.
- Step 4: - Using the ANSYS software of FEA analysis of component is done.
- Step 5: - The Experimental Testing will be carried out at Lab.
- Step 6: - Comparative analysis between the experimental & analysis result & then the result & conclusion will be drawn.

VI. FEA ANALYSIS OF SPECIMEN

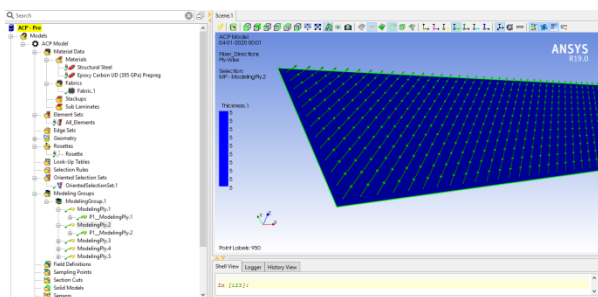


Fig.1 ACP environment

CAD MODEL

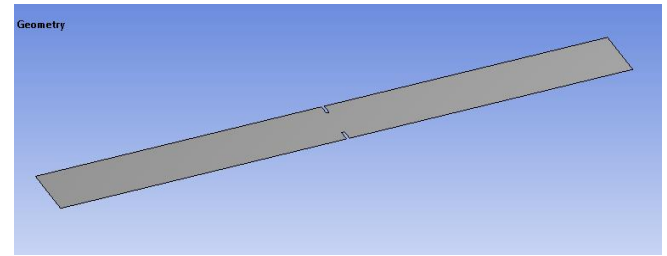


Fig.2 CAD Model of laminated composite beams with multiple edge cracks

FEA ANALYSIS OF UNCRACKED BEAM

Material Selection – EPOXY CARBON

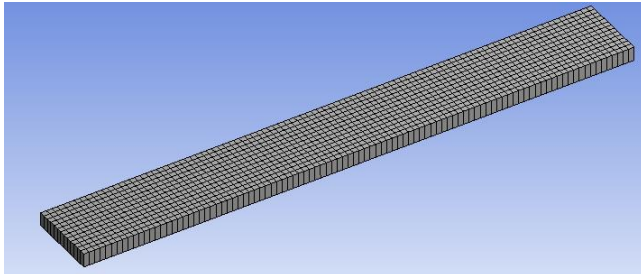
Table 1 Material Properties

A	B	C
Property	Value	Unit
Density	1.54E-09	mm ³ -3t
Orthotropic secant coefficient of thermal expansion		
Orthotropic elasticity		
Young' s modulus X direction	2.09E+05	MPa
Young' s modulus Y direction	9450	MPa
Young' s modulus Z direction	9450	MPa
Poisson' s ratio XY	0.27	
Poisson' s ratio YZ	0.4	
Poisson' s ratio XZ	0.27	
Shear modulus XY	5500	MPa
Shear modulus YZ	3900	MPa
Shear modulus XZ	5500	MPa

MESH

The basis for the most appropriate mesh is to be made for engineering simulations. ANSYS Meshing understands what solutions this project may use and provides the necessary criteria to create the most appropriate mesh. ANSYS Meshing will be integrated with every solver in the ANSYS workbench environment. For quick inspection or for new and unique users, a helpful mesh may be created with a mouse click. Based on the model analysis and geometry, ANSYS

Meshing selects the best choices. Particularly helpful is ANSYS Meshing's ability to utilize parallel processing automatically with the available cores on the computer and therefore minimize the time needed to generate a mesh. Parallel meshing without extra costs or licensing needs is provided.



Statistics	
<input type="checkbox"/> Nodes	1414
<input type="checkbox"/> Elements	1300

Fig. 3 meshing of uncracked beam

After meshing of cutting tool nodes are 1414 and elements 1300.

BOUNDARY CONDITION

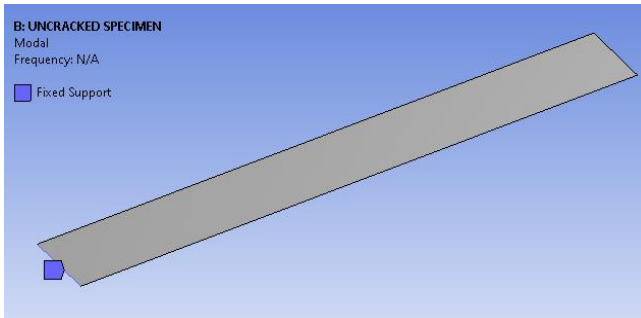


Fig. 4: Details of boundary conditions for Uncracked Beam

MODE SHAPES RESULTS (UNCRAKED BEAM)

MODE SHAPE 1

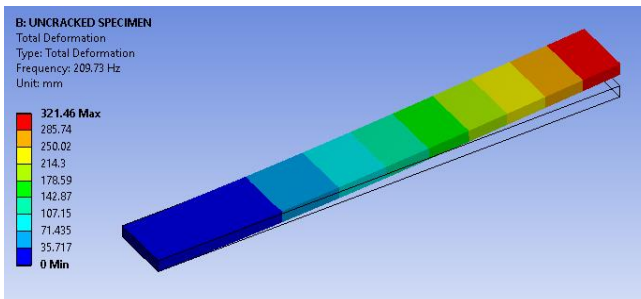


Fig.5 Natural frequency of lathe cutting tool at mode shape 209.73Hz

MODE SHAPE 2

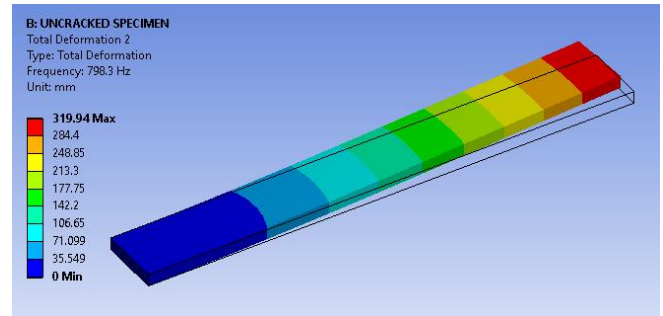


Fig.6 Natural frequency of lathe cutting tool at mode shape 2 was 798.3Hz

MODE SHAPE 3

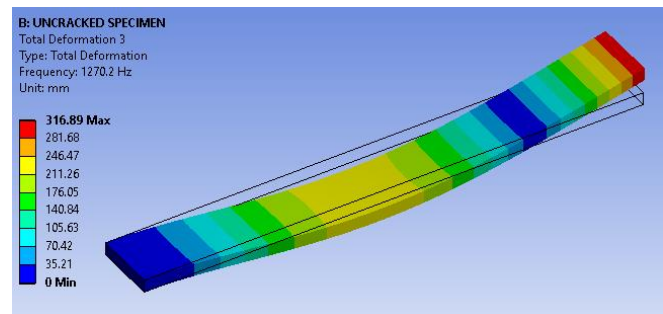


Fig. 7 Natural frequency of lathe cutting tool at mode shape 3 was 1270.2

MODE SHAPE 4

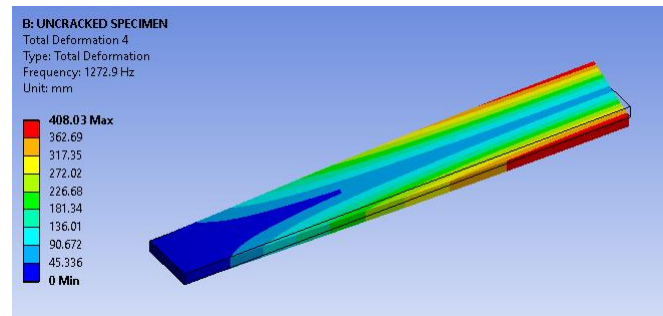


Fig. 8. Natural frequency of lathe cutting tool at mode shape 4 was 1272.9Hz

MODE SHAPE 5

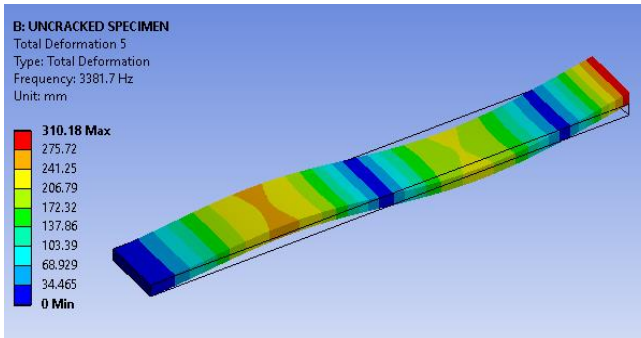


Fig. 9 Natural frequency of lathe cutting tool at mode shape 5 was 3381.7Hz

MODE SHAPE RESULTS (CRACKED BEAM)

MODE SHAPE 1

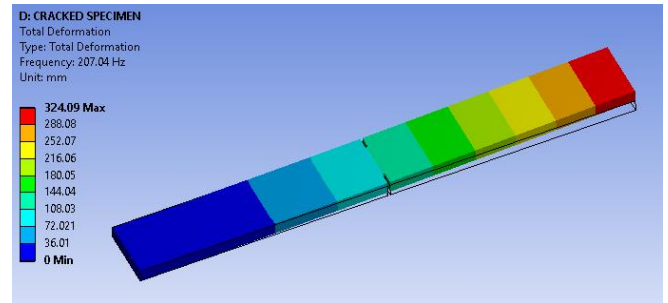


Fig. 12 Natural frequency of Cracked Beam at mode shape 1 Was 207.04Hz

MODAL ANALYSIS OF CRACKED BEAM

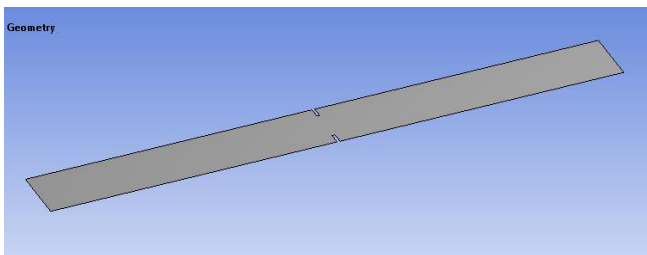
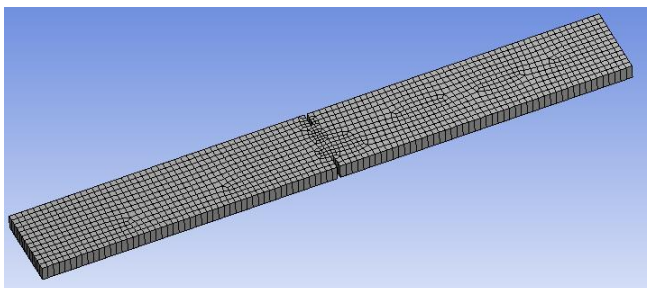


Fig. 10 Geometry of Cracked Beam

MESH



Statistics	
<input type="checkbox"/> Nodes	1459
<input type="checkbox"/> Elements	1336

Fig. 11 meshing of cracked beam

MODE SHAPE 2

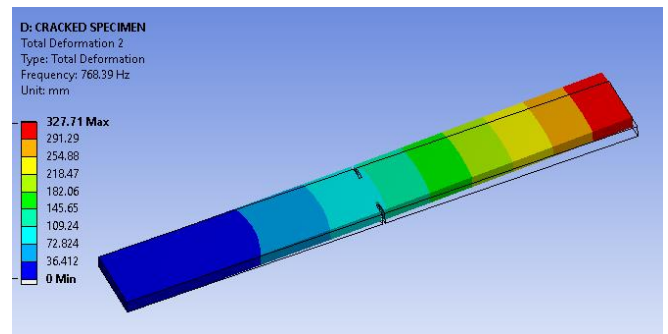


Fig. 13 Natural frequency of Cracked Beam at mode shape 2 Was 768.39Hz

MODE SHAPE 3

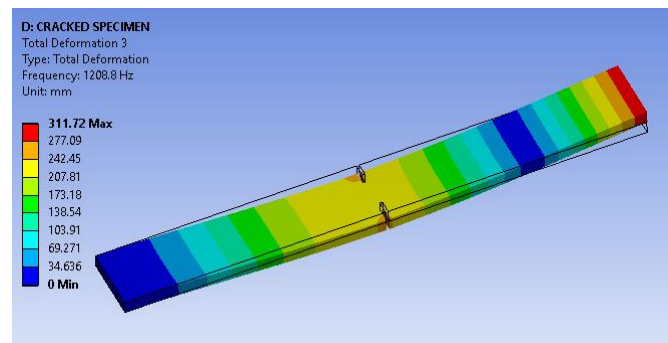


Fig. 14 Natural frequency of Cracked Beam at mode shape 3 Was 1208.8Hz

MODE SHAPE 4

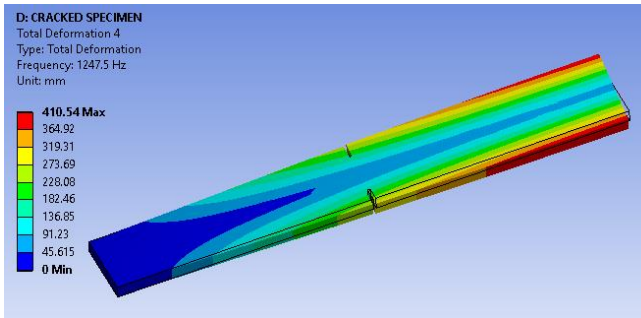


Fig. 15 Natural frequency of Cracked Beam at mode shape 4 Was 1247.5 Hz

MODE SHAPE 5

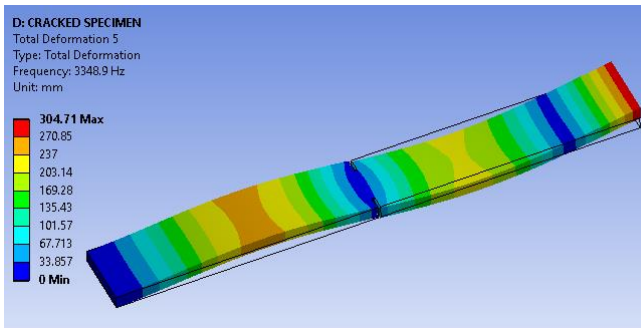


Fig. 16 Natural frequency of Cracked Beam at mode shape 5 Was 3348.9 Hz

FFT quickly calculates transformations such as these by making the DFT matrix a sparse (mainly zero) product. As a consequence, the $O(n^2)$ computational complexity, that emerges if the definition of DFT is used, may be reduced to $O(n \log n)$, where n is the data size. The performance difference may be huge, in particular for large data sets where N might be hundreds or millions. Many FFT methods are considerably more accurate in the presence of round-off errors than direct evaluation of the DFT specification. The FFT algorithms are based on various published theories, from basic arithmetic for complex numbers through group theory and count theory



Fig.17 Experimental setup for FFT analysis

FFT Analysis

In every sequence FFT is one of the most common properties. Many transformations are performed to determine this FFT characteristic for any given sequence. The time and memory management are the main problems to be noted in discovering this attribute. To calculate the FFT and autocorrelation of any given sequence, two alternative methods have been developed. The two methods for memory and time management are compared, and the superior one is pointed out. The comparison of time and memory is written between two algorithms, taking the only principal restrictions into account. Time to determine the fundamental frequency is occupied by both transformations. At the same time, both methods also verify the memory used. On this basis, the algorithm to be utilized for improved outcomes is chosen.

A **fast Fourier transform (FFT)** is a calculation method for the discrete or inverse Fourier transformation (DFT) of a series (IDFT). Fourier analyzes transform a signal in the Frequency Domain from its original domain (typically time or space) and vice versa. The DFT is produced by breaking down a series of numbers into several frequency components. In many areas, this procedure is helpful, but it is frequently too slow to be useful to compute straight from the definition.

EXPERIMENTAL FFT ANALYSIS OF LAMINATED UNCRACKED COMPOSITE BEAMS

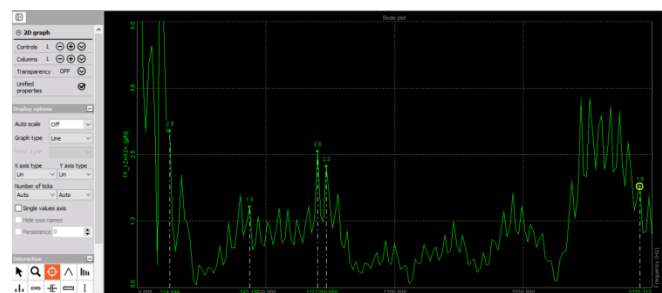


Fig. 18 FFT plot of uncracked beam

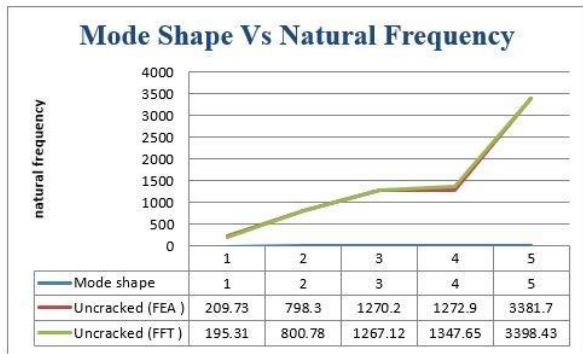
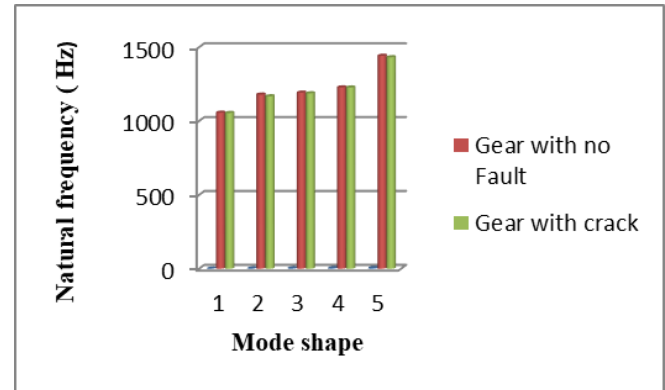


Fig 19 . Chart. Comparison between FEA and experimental result

FEA Result of Cracked and Uncracked Beam



EXPERIMENTAL FFT ANALYSIS OF LAMINATED CRACKED COMPOSITE BEAMS

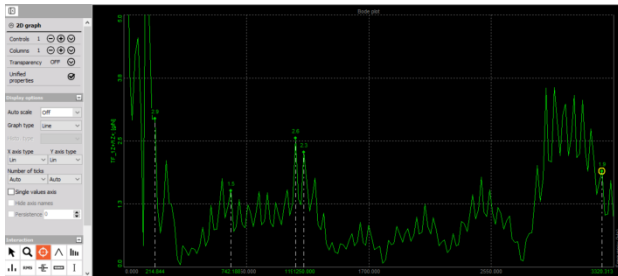


Fig. 20 FFT plot of cracked beam

Table 3 FEA and FFT result of uncracked beam

Mode shape	Uncracked (FEA)	Uncracked (FFT)
1	209.73	195.31
2	798.3	800.78
3	1270.2	1267.12
4	1272.9	1347.65
5	3381.7	3398.43

Table 4 FEA and FFT result of cracked beam

Mode shape	cracked (FEA)	cracked (FFT)
1	207.04	214.84
2	768.39	742.18
3	1208.8	1198.35
4	1247.5	1250
5	3348.9	3320.31

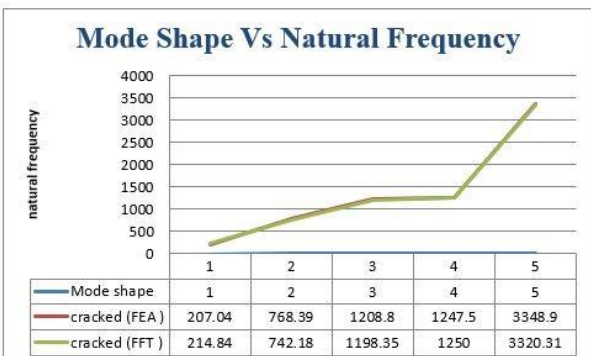


Fig. 21 Chart. Comparison between FEA and experimental result

VII. RESULTS

Table 2 Details of Mode Shape with Cracked and Uncracked Beam

Mode shape	Uncracked	Cracked	% Decrease
1	209.73	207.04	1.286
2	798.3	768.39	3.746
3	1270.2	1208.8	4.833
4	1272.9	1247.5	1.995
5	3381.7	3348.9	0.969

VIII. CONCLUSION

- Current study has carried out modal beam analysis with and without fracture.
- The beam with crack is found to have fewer frequencies than without crunchy beam, as it forecasts that if the beam is crashed it would reduce its rigidity.
- Carbon fibre beam production was performed by means of a hand layout technique.
- If Natural frequencies derived from the findings of analysis and testing are nearly the same, the result is validated.
- Both beam and non-crack frequency vary by 2.58% from each other.

REFERENCES

- [1] Ranjan K. Behera, Anish Pandey, Dayal R. Parhi, “ Numerical and Experimental Verification of a Method for Prognosis of Inclined Edge Crack in Cantilever Beam Based on Synthesis of Mode Shapes” , International Conference on Innovations in automation and mechatronics engineering, ICIAME, pp.67-74, 2014.
- [2] Aniket S. Kamble, D. S. Chavan, “ Identification of crack parameters in a cantilever beam using experimental and wavelet analysis” , International Journal on Mechanical Engineering and Robotics (IJMER), pp.23-27, 2014.
- [3] Marco A. Perez, Lluís Gil, Sergio Oller, “ Impact damage identification in composite laminates using vibration testing” , Composite Structures 108, pp.267– 276, 2014.
- [4] Missoum Lakhdar , Djermame Mohammed, Labbaci Boudjemâa, Abdeldjebar Rabiâa, Moudden Bachir, “ Damages detection in a composite structure by vibration analysis” , TerraGreen 13 International Conference 2013 - Advancements in Renewable Energy and Clean environment, pp.888-897, 2013.
- [5] P. K. Jena, D. N. Thatoi, J. Nanda, D. R. K. Parhi, “ Effect of damage parameters on vibration signatures of a cantilever beam” , International Conference on Modelling, Optimisation and Computing (ICMOC 2012), pp.3318-3330, 2012.
- [6] Kaushar H. Barad, D. S. Sharma, Vishal Vyas, “ Crack detection in cantilever beam by frequency based method” , Nirma University International Conference on Engineering (NUiCONE), pp.770-775, 2013.
- [7] Amit Banerjee, G Pohit, “ Crack Investigation of Rotating Cantilever Beam by Fractal Dimension Analysis” , International Conference on Innovations in Automation and Mechatronics Engineering, ICIAME, pp.88-195, 2014.
- [8] Prasad Ramchandra Baviskar, Vinod B. Tungikar, “ Multiple Cracks Assessment using Natural Frequency Measurement and Prediction of Crack Properties by Artificial Neural Network” , International Journal of Advanced Science and Technology, pp.23-38, 2013

Assessment of Land Suitability for Solid Waste Disposal and Leachate Treatment by waste derived *Parkia Speciosa* (Petai) pods Activated Carbon

^[1]Vivek Laishram, ^[2]Oinam Bakimchandra, ^[3]Potsangbam Albino Kumar
^{[1][2][3]}Department of Civil Engineering, National Institute of Technology Manipur

Abstract— Assessment of solid waste disposal site selection in and around Imphal East district, Manipur was carried out using Geographic Information System (GIS), the Analytical Hierarchy Process (AHP) and the Remote sensing method. A waste derived *Parkia Speciosa* (Petai) pods activated carbon (PPAC) synthesized with 30% H3P04 at an impregnation ratio of 1:1 was employed for organic ions (COD) uptake from landfill leachate collected from Lamdeng Solid Waste Management Plant, Imphal, Manipur which was pretreated in the previous part of this study. To study the sorption mechanism and rate controlling steps, intra-particle diffusion, Elovich model and non-linear Langmuir and Freundlich isotherm models were used to test the adsorption data. The adsorption equilibrium was practically reached at 90 min contact time yielding 93% COD removal at an optimum dose of 11g/L PPAC in the previous part of the study. The adsorption kinetic studies revealed that the correlation coefficients (R²) for Elovich model was 0.953 as compared to 0.847 for diffusion model signifying the better fit of the adsorption kinetics data on Elovich model. In the previous part of this study, the linearized Langmuir model fitted better yielding a higher R² value of 0.998 as compared to 0.497 for the linearized Freundlich isotherm model with lesser Chi-square (χ^2) of 0.56 for Langmuir's isotherm against that of 13.87 for Freundlich. However, in this part of the study also, the modeling results revealed that the non-linearized Langmuir model (R²=0.971) even fitted the data better than non-linearized Freundlich model (R²=0.891) with χ^2 value of 0.94 and 4.65 for Langmuir and Freundlich isotherm respectively. From the observations, the organic ions mainly COD is adsorbed on PPAC (q_{max}=180.65mg/g), the surface of which is mostly homogenous. Monolayer adsorption occurs without lateral interactions between the adsorbed molecules suggesting the nature of adsorption to be predominantly chemical adsorption.

Keywords— Activated Carbon, Adsorption, COD, Landfill leachate, *Parkia Speciosa*.

I. INTRODUCTION

The major environmental issues faced by people with the process of urbanization and industrialization are the rapid generation of solid waste. In Imphal city, the disposal of solid waste is a serious issue. Due to the rapid growth in population, the quantity of solid waste has come in abundance. The municipal solid waste (MSW) generates leachate which contains biodegradable organic matter, heavy metals and inorganic salts in enormous quantities. Leachate affects living organisms and ecosystems by causing soil, air, surface water and groundwater pollution [1] [2]. The

treatment methods used for leachate generally involves a combination of appropriate techniques because it cannot be treated efficiently by using only a single technique due to its refractory nature. The coupling of the biological and physico-chemical processes leads to more efficient treatment and have been reported as an effective treatment for leachate [3]. The pre-treatment of stabilized leachate from Imphal city, India by coagulation-flocculation has been presented in our previous part of this study [4]. Low cost waste derived activated carbon (AC) has gained interest in the last decades due to its efficiency in treating wastewater and potential for the minimum generation of agro-residues [5]. Owing to these issues and search for sustainable alternatives for leachate treatment, the pre-treated stabilized leachate obtained after coagulation-flocculation in the previous part of this study [4] is further explored by adsorption on PPAC, the kinetics and isotherm analysis of which is mainly discussed in the part of this study. This study also involves the assessment of solid waste disposal site selection using Geographic Information System (GIS), the Analytical Hierarchy Process (AHP) and the Remote sensing method in and around Imphal East district, Manipur.

II. MATERIAL AND METHODS

A. Methodology for selection of solid waste disposal site

Eight different parameters were considered in this study namely euclidean distance from roads, euclidean distance from rivers, euclidean distance from settlement, lithology, slope, aspect, elevation and land use. Later these parameters were lumped into four major criteria i.e., topography suitability, environmental suitability, land availability and transportation feasibility to examine the feasibility in relation to solid waste dumping site selection in Imphal East district of Manipur.

B. Synthesis and characterization of pretreated leachate and adsorbent

The waste derived PPAC was synthesized by impregnating 100 g of crushed petai pods with 167 ml of 30% phosphoric acid solution (activating agent) at a mass impregnation ratio of 1:1 for 24 hours and then carbonizing the impregnated petai pods at 400°C for a duration of 30 minutes in a muffle furnace. The activated PPAC was then rinsed repeatedly for residue removal and oven dried at 100°C. The final PPAC

was then sieved using a 125 μ sieve and stored in desiccators for further use in adsorption experiments. The effluent COD concentration was as high as 1280 mg/L after pretreatment with alum in our previous study [4]. Similar studies were also reported with pretreated stabilized leachate yielding 1560 mg/L using alum as coagulant [6]. Surface analysis using Scanning Electron Microscopy (SEM) and Energy Dispersive X-Ray Analysis (EDAX) were investigated using Zeiss Sigma-300 Model. Surface area, pore volume of adsorbent were evaluated using Quantachrome operated Nova Station–A-BET analyzer and pore dimensions was determined using the Brunauer-Emmett-Teller (BET) method [7].

C. Adsorption experiments

For the equilibrium study, the batch experiments were conducted by the addition of appropriate amount of PPAC to a series of 1L pretreated leachate samples using a Phipps and Bird Jar Test Apparatus (PB – 600). After being agitated for 3 hours at 300 rpm, 30 min settling time was given and the supernatant was filtered using Whatman No.47 filter paper and the equilibrium COD concentrations (C_e , mg COD/L) in the filtrates were analyzed by closed reflux method. Adsorbate (COD) uptake at equilibrium (q_e , mg COD/g) was calculated from Eqn. (1):

$$q_e = \frac{C_o - C_e}{m} V \quad (1)$$

where, C_o = initial concentration, V = volume of pretreated leachate sample in L and m = mass of PPAC in g.

D. Adsorption kinetics and isotherms

The adsorption data was studied by the application of two adsorption kinetics models namely Elovich model [8] and diffusion model [9]. After attainment of equilibrium conditions, non linearized form of Langmuir [10] and Freundlich [11] isotherms were employed to understand the adsorbate molecules distribution. The non-linear regression involves the error distributions between the calculated and predicted values based on the convergence data and were used for analyzing the adsorption processes [12].

III. RESULTS AND DISCUSSION

A. Selection of solid waste disposal site

The four major criteria considered for the identification of solid waste dumping site are topography suitability, environmental suitability, land availability and transportation. These criteria was identified and weights are developed by AHP score (Table I). Mapping is done using GIS and final map was produced by weighted overlay analysis (Fig.1). In this study, 12 main potential sites for solid waste dumping were identified and illustrated in Fig.1 with legends. Only 3 sites were found to have some errors in model predictions.

Table I: Weights for the main criteria

Sl. no.	Main Criteria	Weight
1.	Topography Suitability	0.172
2.	Environmental Suitability	0.082
3.	Transportation feasibility	0.147
4.	Land Availability	0.599

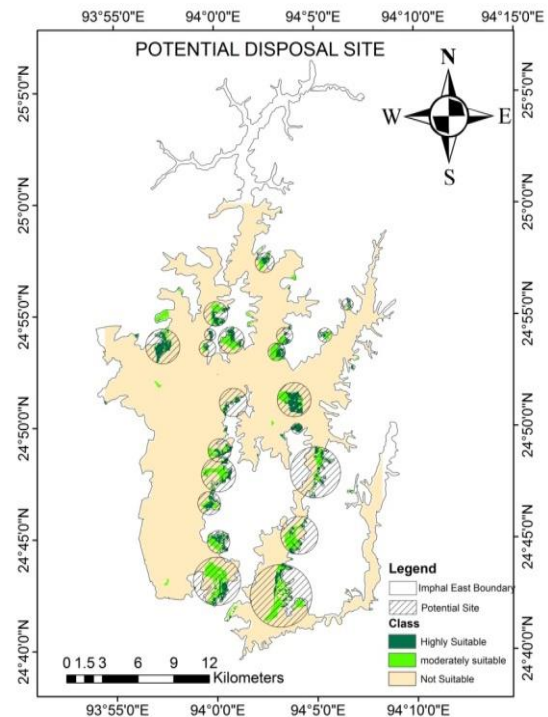


Fig.1: Potential site for solid waste disposal in Imphal East District, Manipur, India

B. Characterization of PPAC

PPAC when activated at 400 °C gives BET surface area of 239.13 m²/g corresponding to 3.218 nm pore diameter and 0.072 cc/g pore volume (Table II). Similar studies were also reported with BET surface areas of 188-300 m²/g at 350-400°C activating temperatures [6]. SEM image before PPAC adsorption (Fig.2) have a smooth and uniform micro porous structure favourable for the uptake of organic ions from leachate whereas after adsorption (Fig.3) most of the available pores are filled with the ions in leachate leading to the saturation of PPAC. EDAX analysis gives the elemental compositions of PPAC before and after adsorption which corresponds to the peak on the EDAX image (Fig.4a, b) confirming the adsorption of ions onto PPAC which was in the range of 0.20 – 4.12 keV in the EDAX spectra.

C. Adsorption kinetics

The study of adsorption kinetics on COD removal by PPAC was conducted with pretreated leachate COD of 1280 mg/L using 8 g/L adsorbent dose at optimum pH 2. Kinetics of adsorption gives the rate of uptake amount of ions or adsorbed from the solution [12]. The kinetics data was analyzed first by Elovich model which is represented by Eqn. (2):

$$q_t = \frac{1}{\beta} \ln(\alpha \beta) + \beta \ln(t) \quad (2)$$

where, q_t (mg/g) is the adsorbed amount at time t , α (mg/g min) is the initial sorption rate and β (g/mg) is the desorption constant. From Fig.5, it can be observed that the correlation coefficient (R^2) value is above 0.95 suggesting that the adsorption kinetics data obeys the Elovich model. The evaluated value of α and β for Elovich model are shown in Table III for comparison with that of the Diffusion model coefficients.

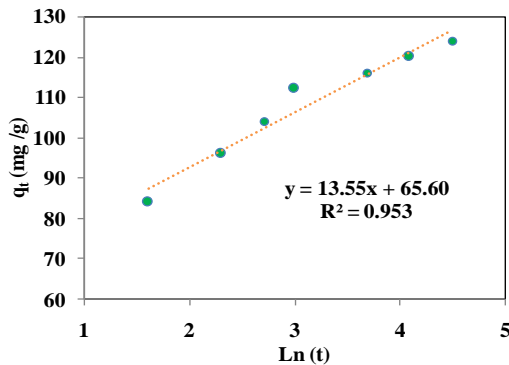


Fig.5: Elovich kinetics model for COD adsorption on PPAC

To analyze the rate-controlling factors of adsorption, the kinetic data was also treated with diffusion model given by Eqn. (3):

$$q_t = K_d t^{1/2} + C \quad (3)$$

where q_t (mg/g) is the amount of adsorbed ions at time t , K_d (mg/g min^{1/2}) is the diffusion rate constant and C (mg/g) is the diffusion constant [9]. The value of K_d and C were given by slope and the intercept of the linear plot of $t^{1/2}$ vs. q_t respectively. From Fig.6, it was observed that the kinetics data did not obey diffusion model as the R^2 value was less than 0.95. The evaluated coefficients of diffusion model K_d and C are shown in Table III.

For comparison between Elovich and Diffusion model, the predicted q_t values are plotted against the experimental q_t values. In Fig.7, the predicted q_t values of Elovich model are observed to be much closer to the experimental q_t values than that of Diffusion suggesting a better fit on Elovich model.

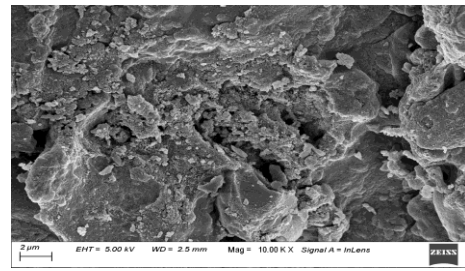


Fig.2: PPAC before adsorption

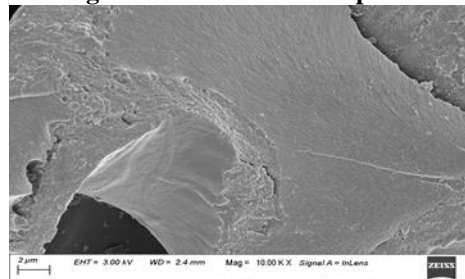


Fig.3: PPAC after adsorption

Table II: Porosity structures of PPAC

Properties	Activation (400 °C)
BET Surface Area (m ² /g)	239.13
Pore Diameter (nm)	3.218
Pore Volume (cc/g)	0.072
Pores Surface Area (m ² /g)	79.32
Micropore Volume (cc/g)	0.035
Micropore Area (m ² /g)	101.18
External Surface Area (m ² /g)	136.62

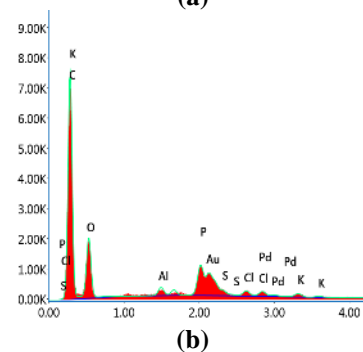
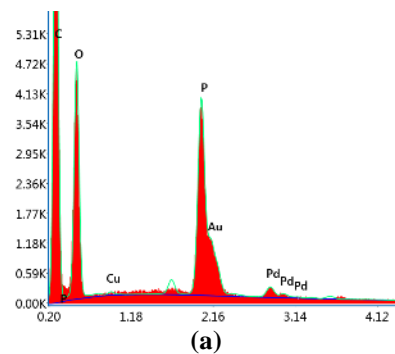


Fig.4: EDAX spectra of PPAC (a) before and (b) after adsorption

The experimental and predicted q_t values were also compared through evaluated errors using the Chi-square equation given by Eqn. (4):

$$\chi^2 = \sum \frac{(q_t(\text{exp.}) - q_t(\text{pred.}))^2}{q_t(\text{exp.})} \quad (4)$$

where, q_t (exp.) and q_t (pred.) are the experimental and the predicted amount of ions adsorbed per gram of adsorbent at time t . The evaluated χ^2 values for both Elovich and Diffusion were shown in Table III. The χ^2 value for Elovich is 0.75 against very high value of 6.63 for Diffusion model indicating insignificant error for Elovich model. The kinetics data of COD adsorption on PPAC can thus be well explained by Elovich model.

Table III: Elovich and Diffusion parameters

ELOVICH			
R ²	α (mg/g min)	β (g/mg)	χ^2
0.953	9.35	13.55	0.75
DIFFUSION			
R ²	k_d (mg/g min ^{1/2})	C (mg/g)	χ^2
0.847	4.99	81.36	6.63

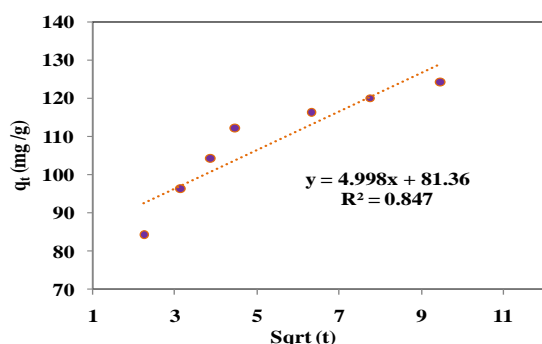


Fig.6: Diffusion model for COD adsorption on PPAC

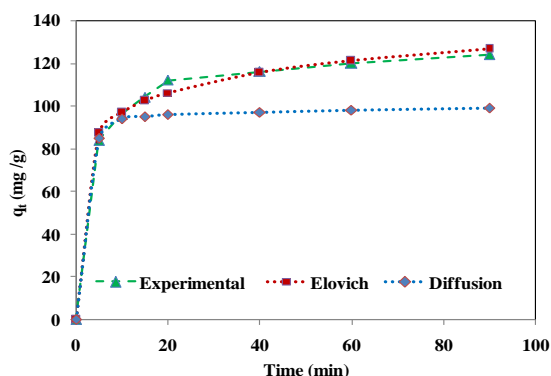


Fig.7: Experimental Vs. Predicted qt for Elovich and Diffusion models

D. Adsorption isotherm studies

The non-linear form of Langmuir (Eqn.5) and Freundlich (Eqn.6) isotherms were applied to the adsorption data after the kinetics study which are given by:

$$q_e = \frac{q_{max}bC_e}{1+bC_e} \quad (5)$$

$$q_e = K_f C_e^{1/n} \quad (6)$$

where, q_{max} is the maximum adsorptive capacity (mg/g), b is the Langmuir adsorption constant (L/mg), Freundlich coefficient K_f represents an indicator of adsorption capacity, $1/n$ indicates the adsorption intensity, while its reciprocal n represents the affinity factor for the Freundlich model [13]. As shown in Table IV, the non-linear Langmuir isotherm model correlates to the activated carbon adsorption yielding R^2 of 0.971 as compared to R^2 of 0.891 for non-linear Freundlich isotherm. Also for better comparison between the two isotherm models, the predicted q_e values are plotted against the experimental q_e values. From Fig.8, it can be observed that the predicted q_e values of non-linear Langmuir isotherm are closer to the experimental q_e values than that of the predicted q_e values of non-linear Freundlich isotherm. Also, when the experimental and predicted q_e values were compared using Chi-square and standard error (SE), lesser χ^2 and standard error of 0.94 and 5.99 respectively were observed for Langmuir isotherm against that of 4.65 and 11.58 respectively for Freundlich isotherm suggesting the better fit of COD adsorption onto PPAC by Langmuir's isotherm model. This finding indicated the homogenous surface of PPAC with adsorption of organic ions (COD) occurring through monolayer adsorption on the surface of PPAC with no interaction of adsorbed neighboring ions with each other.

Table IV: Regression data of Non-linear Langmuir and Freundlich isotherm models

Non-linear Langmuir isotherm	q_{max} (mg/g)	b (L/mg)	R^2	χ^2	SE
	180.65	0.0108	0.971	0.94	5.99
Non-linear Freundlich isotherm	K_f (L/g)	$1/n$	R^2	χ^2	SE
	25.36	3.17	0.891	4.65	11.58

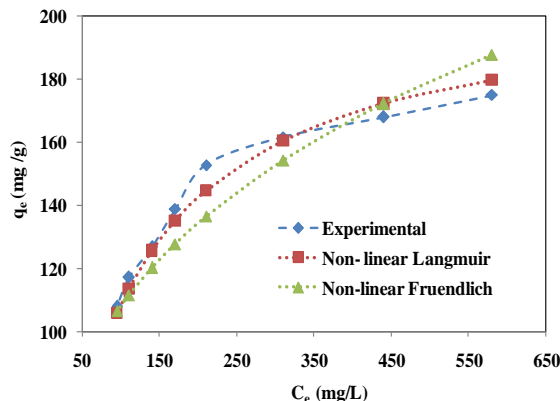


Fig.8: Experimental Vs. Predicted q_e for non-linear Langmuir and Freundlich isotherm models

IV. CONCLUSION

From the GIS based suitability study, most of the potential solid waste dumping sites in Imphal East District of Manipur, India were predicted far from the settlement zones, in the foothills. This part of the study also revealed that the kinetics data of the adsorption of organic ions (mainly COD) by PPAC from pretreated landfill leachate can be described by Elovich model ($R^2 = 0.953$) with predicted amounts of ions adsorbed much closer to experimental values and also with insignificant χ^2 error of 0.75. After the attainment of equilibrium conditions, the isotherm data fitted well to the non linearized Langmuir model ($R^2 = 0.971$) with χ^2 error of 0.94 yielding a maximum adsorption capacity of 180.65 mg COD/g. Both the kinetics and isotherm study revealed that, the adsorption of organic ions (COD) on PPAC was predominantly due to chemical adsorption with almost insignificant amount of physical adsorption or diffusion.

REFERENCES

- [1] A. A. Tatsi, A. I. Zouboulis, K. A. Matis, "Coagulation-flocculation pretreatment of sanitary landfill leachates", *Chemosphere*, vol. 53, pp.737-744, April 2003.
- [2] Z. Zhang, Z.P. Wang, Y.J. Lin, N.S. Deng, T. Tao, K. Zhuo, "Landfill leachate treatment by a coagulation-photooxidation process", *J. Hazard. Mater.*, vol. B95, pp.153-159, 2002.
- [3] X. Wang, S. Chen, X. Gu and K. Wang, "Pilot study on the advanced treatment of landfill leachate using a combined coagulation, fenton oxidation and biological aerated filter process", *Waste Management*, vol.29, no.4, pp.1354-1358, Dec. 2008.
- [4] V. Laishram and P. A. Kumar, "Reduction of COD and turbidity in leachates through coagulation-adsorption" *J. Indian Chem. Soc.*, vol. 97,no.10b, pp.1-10, 2020.
- [5] Y. Guo, D. A. Rockstraw, "Activated carbons prepared from rice hull by one-step phosphoric acid activation", *Microporous and Mesoporous Materials*, vol 100, no.1, pp.12-19, Nov 2006.
- [6] R. Gandhimathi, N. J. Durai, P. V. Nidheesh, S. T. Ramesh and S. Kanmani, "Use of combined coagulation-adsorption process as pretreatment of landfill leachate", *Iranian J. of Environ. Health Sci. & Engg.*, pp.10-24, 2013.
- [7] A. Reffas, V. Bernardet, B. David, L. Reinert, M. B. Lehocine, M. Dubois, N. Batisse and L. Duclaux, "Carbons prepared from coffee grounds by H₃PO₄ activation: Characterization and adsorption of methylene blue and Nylosan Red N-2RBL", *J. Hazard. Mater.* vol. 175, pp. 779-788, Oct. 2009.
- [8] D. L. Sparks, "Kinetics of reaction in pure and mixed systems, in *Soil Physical Chemistry*", Edited by Sparks, CRC Press, Boca Raton, Florida, 1986.
- [9] T. E. Hristova, "Comparison of different kinetic models for adsorption of heavy metals onto activated carbon from apricot stones", *Bulgarian Chemical Communications*, vol. 43, no. 3, pp. 370 - 377, 2011.
- [10] S. Jiang, T. Yu, R. Xia, X. Wang and M. Gao, "Realization of super high adsorption capability of 2D δ -MnO₂ /GO through intra-particle diffusion", *Materials Chem. and Phy.*, vol. 232, pp. 374-381, May 2019.
- [11] K. Pirzadeh and A. A. Ghoreyshi, "Phenol removal from aqueous phase by adsorption on activated carbon prepared from paper mill sludge", *Desalin. Water Treat.*, vol.52, pp.6505-6518, Oct. 2014.
- [12] J. Luna, L. Montes, S. M. Vargas, "Linear and nonlinear kinetic and isotherm adsorption models for arsenic removal by manganese ferrite nanoparticles", *SN Applied Sciences*, vol.1, pp. 950, July 2019.
- [13] S. Elabbas, L. Mandi, F. Berrekhis, M. N. Pons, J. P. Leclerc and N. Ouazzani, "Removal of Cr(III) from chrome tanning wastewater by adsorption using two natural carbonaceous materials: Eggshell and powdered marble", *J. of Environ. Manage.*, vol.166, pp. 589-595.

A New Cascaded Two Level Inverter based Multilevel STATCOM for High Power Applications

^[1] Vyshnav B, ^[2] Akshatha R Hegde, ^[3] Pradeesha J

^{[1][2][3]} Assistant Professor, Dept. of Electrical and Electronic Engineering, RR Institute of Technology

Abstract— A uncomplicated and reliable STATCOM project for static var compensation and refinement of power quality are debated in this paper. The analysis situs consist of combination of two level voltage source inverters. Cascaded inverter is attached to low tension side of three phase coupling transformer. The system is operated as four-level inverter by maintaining dc link voltages of two inverters at a determined proportion. Balancing od dc link voltage is primary challenge For cascaded inverters. MATLAB/SIMULINK is used to look over the system and for balanced and unbalanced conditions results are substantiated.

I. INTRODUCTION

Generation and transmission of power is complex process, it requires working of many components to produce maximum output. The reactive power is one of the main component. Voltage to be maintained to deliver the required active power through transmission lines. Reactive power is needed for the operation of loads like motor loads and other inductive load [2]. Nowadays a wide range of very flexible controllers, which capitalize on newly available power electronics components, are emerging for custom power applications. STATCOM is widely accepted as a reliable reactive power controller replacing conventional var compensators, such as the thyristor-switched capacitor (TSC) and thyristor-controlled reactor (TCR). This device yields reactive power compensation, active power oscillation damping, flicker attenuation, voltage regulation, etc.[3][4][5]. The VSC connected in shunt with the ac system put up a multifunctional topology which can be used for up to three quite distinct purposes [6][7].

Generally in high-power applications, Var compensation is acquired using multilevel inverters [8]. These inverters comprise of a large number of dc sources which are usually realized by capacitors. The converters draw a small amount of active power to maintain dc voltage of capacitors and to compensate the losses in the converter. The capacitors voltages are unbalanced due to mismatch in conduction and switching losses of the switching devices . Balancing these voltages is a major research challenge in multilevel inverters. Various control schemes using different topologies are reported in [9]–[10].

Static Var compensation by cascading conventional multi-level/two level inverters is an enticing solution for high power applications. It comprise of standard multilevel/two-level inverters connected in cascade through open-end windings of a three-phase transformer. These topologies are popular in high-power drives [11]. The number of levels in

the output voltage waveform can be increased by maintaining asymmetric voltages at the dc links of the inverter. This boosts PQ [12]. Since the overall control is simple compared to conventional multilevel inverters. Various var compensation schemes based on this topology are reported in [13]–[14]. In [12], a three-level inverter and two level inverter are connected on either side of the transformer low-voltage winding. The dc-link voltages are maintained by separate converters. In [15], three-level operation is achieved by using standard two-level inverters. The dc-link voltage balance between the inverters is affected by the reactive power supplied to the grid.

The topology, mentioning here, uses standard two-level inverters to achieve multilevel operation [1]. Four-level operation is obtained by regulating the dc-link voltages of the inverters at asymmetrical levels. Simulation study is carried out for balanced and unbalanced supply-voltage conditions to verify the efficiency of the proposed system. Whenever there is a sudden change in reference current, the inverter dc-link voltages collapse. In order to look over the behavior of the converter, the entire dynamic model of the system is developed from the equivalent circuit.

II. SINGLE TWO-LEVEL INVERTER-BASED STATCOM

The image-1 below exhibits the power system model contemplated in this journal [3]. Image-2 shows the circuit implementation of the single two level inverter based static compensator. The high tension side of transformer is associated to grid and low tension side to inverter.

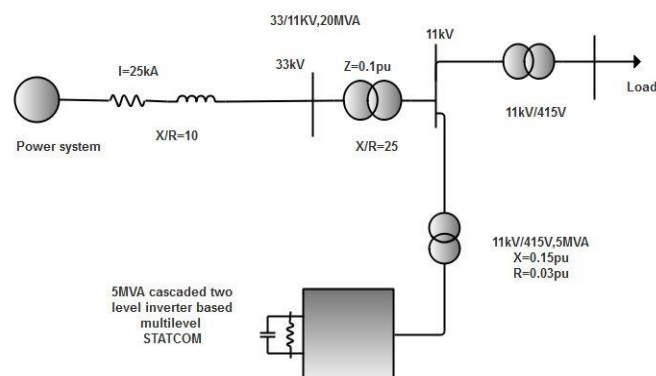


Image-1- Power system and the STATCOM model

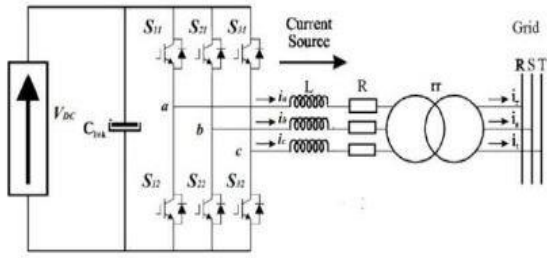


Image - 2- Two-level inverter based STATCOM topology

A battery or usually from a rectifier is used to supply direct current for three phase inverters. By using six switches, a six steps bridge is used for three phase inverter. Each step is elucidated as a change in the time performance for each transistor to the next transistor in kosher order. For a six step inverter each step would be of 60° interval, for one cycle. Large capacitors are connected at the supply side to make constant DC supply and also vanquish the harmonics fed back to the source.

III. CASCADED TWO-LEVEL INVERTER-BASED MULTILEVEL STATCOM

Image-3 conveys the circuit topology of the cascaded two level inverter based multilevel static compensator using standard inverters with two levels. The dc-link voltages of the inverters are kept constant and modulation indices are managed to accomplish the needed goal. Image-4 shows the equivalent circuit and the proposed control plan is derived from the ac side of it.

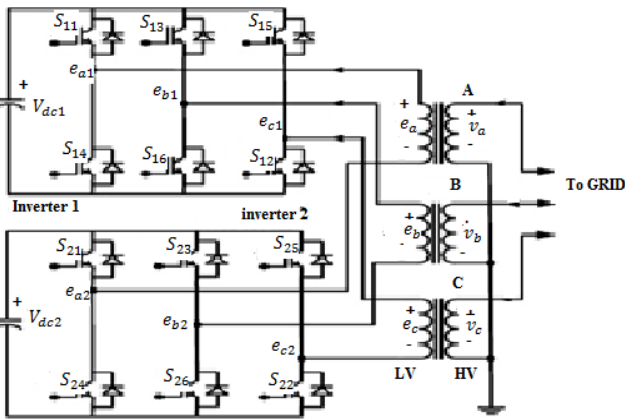


Image-3- Cascaded two level inverter based multilevel STATCOM

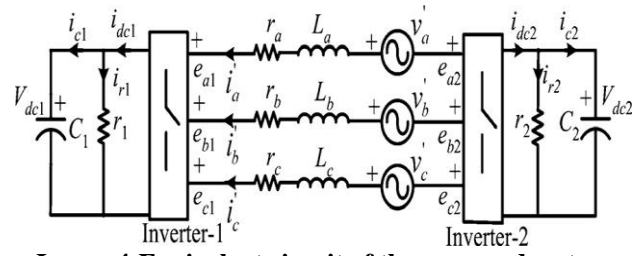


Image-4-Equivalent circuit of the proposed system

From the image-4, the three phase RMS source voltages V_a' , V_b' and V_c' referred to the low-voltage side of the transformer. L_a , L_b and L_c are the leakage inductances of low tension side of the transformer. r_a , r_b and r_c are the transformer losses are represented in terms of resistances. The voltage output of inverter1 and inverter2 are e_{a1} , e_{b1} , e_{c1} and e_{a2} , e_{b2} , e_{c2} . Finally leakage resistances of dc-link capacitors C_1 and C_2 are r_1 and r_2 respectively.

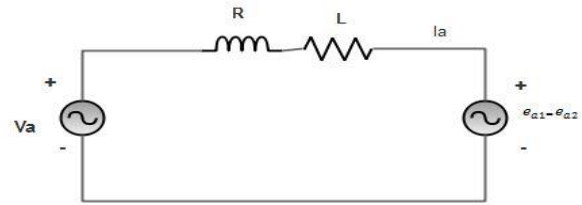


Image-4. Phase a-Equivalent circuit of

In the image-4, the RMS source voltage is represented as V_a' , R act for total loss in the system, L represents the transformer winding leakage inductance, e_{a1} and e_{a2} are primary side voltages of the transformer of inverter1 and inverter2.

Applying Kirchhoff's Voltage Law in loop,

$$-v'_a + R_a I'_a + L_a \frac{di'_a}{dt} + (e_{a1} - e_{a2}) = 0 \quad (1)$$

Likewise in phase b and c,

$$-v'_b + R_b I'_b + L_b \frac{di'_b}{dt} + (e_{b1} - e_{b2}) = 0 \quad (2)$$

$$-v'_c + R_c I'_c + L_c \frac{di'_c}{dt} + (e_{c1} - e_{c2}) = 0 \quad (3)$$

By taking resistances $R_a = R_b = R_c = R$ and inductances $L_a = L_b = L_c = L$, the equation can be rescript as,

$$\begin{pmatrix} \frac{di'_a}{dt} \\ \frac{di'_b}{dt} \\ \frac{di'_c}{dt} \end{pmatrix} = \begin{pmatrix} \frac{-r}{L} & 0 & 0 \\ 0 & \frac{-r}{L} & 0 \\ 0 & 0 & \frac{-r}{L} \end{pmatrix} \begin{pmatrix} i'_a \\ i'_b \\ i'_c \end{pmatrix} + \frac{1}{L} \begin{pmatrix} v'_a - (e_{a1} - e_{a2}) \\ v'_b - (e_{b1} - e_{b2}) \\ v'_c - (e_{c1} - e_{c2}) \end{pmatrix} \quad (4)$$

The mathematical model in the stationary reference form of cascaded two level inverter based static compensator is mentioned in above equation. To control active and reactive current separately, stationary reference frame relation is transformed into rotating reference frame. To align the source voltage of d-component with the synchronously rotating reference frame, the source voltage of q-component is set to zero.

The dynamic model in the synchronously rotating reference frame is,

$$5) \begin{pmatrix} \frac{d i'_d}{dt} \\ \frac{d i'_q}{dt} \end{pmatrix} = \begin{pmatrix} \frac{-r}{L} & \omega \\ -\omega & \frac{-r}{L} \end{pmatrix} \begin{pmatrix} i'_d \\ i'_q \end{pmatrix} + \frac{1}{L} \begin{pmatrix} v'_d - (e_{d1} - e_{d2}) \\ -(e_{q1} - e_{q2}) \end{pmatrix}$$

Here direct axis voltage component of ac source is v'_d and i'_d , i'_q are d-axis and q-axis current components of cascaded two-level inverter.

o Control Strategy

Image-5 shows the block diagram of controller of the entire system. The voltages of d-axis and q-axis can be managed as,

$$e_{d1}^* = -x_1 + \omega L i'_q + v'_d \quad (6)$$

$$e_{q1}^* = -x_2 - \omega L i'_d + v'_d \quad (7)$$

Where e_{d1}^* and e_{q1}^* are d-axis and q- axis reference voltage components of the cascaded inverter. The control parameters x_1 and x_2 are controlled as,

$$x_1 = k_{p1} + \frac{k_{i1}}{s} (i_{d1}^* - i'_d) \quad (8)$$

$$x_2 = k_{p2} + \frac{k_{i2}}{s} (i_{q1}^* - i'_q) \quad (9)$$

Direct (d)-axis reference current i_{d1}^* is given by,

$$i_{d1}^* = (k_{p3} + \frac{k_{i3}}{s}) [(V_{dc1}^* + V_{dc2}^*) - (V_{dc1} + V_{dc2})] \quad (10)$$

V_{dc1}^* and V_{dc2}^* are reference voltages of dc-link capacitors of inverter-1 and inverter-2. The reference reactive current component, i_{q1}^* , can be acquire either from load or from voltage regulation loop.

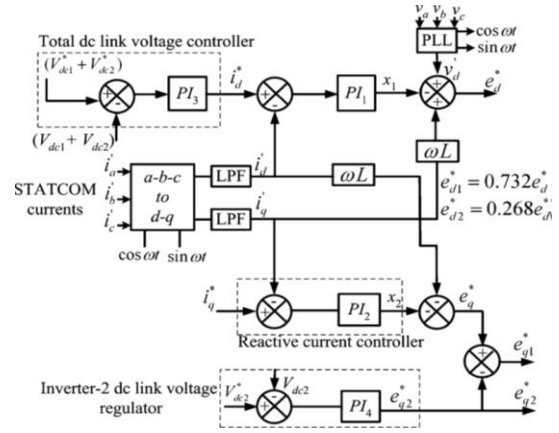


Image-5. Control block diagram.

The three phase voltages V_a, V_b, V_c are supplied to phase-locked loop and unit signals $\cos \omega t$ and $\sin \omega t$ are generated. To produce output signal to match the phase of input signal, Phase locked loop is used. These unit signals converts the converter currents i'_a, i'_b, i'_c into synchronously rotating reference frame currents. So control of reactive and active current components became uncomplicated. Low-pass filters are used to eliminate switching frequency ripples. The reference voltages to the converter are (e_{d1}^*, e_{q1}^*) are generated from controller using $(V_{dc1}^* + V_{dc2}^*)$ and reference reactive current. The inverter supplies desired reactive current component and draws active component of current. Which is used to control total inverter dc-link voltage.

o DC-Link Balance Controller

To provide magnitude and phase of resultant voltage supplied by the cascaded inverter, the total dc-link balance controller is used. The active power sharing between the inverter and grid is depends on angle δ . From the diagram, the q-axis reference voltage components of the two inverters e_{q1}^*, e_{q2}^* are,

$$e_{q1}^* = e_{q1}^* - e_{q2}^* \quad (11)$$

$$e_{q2}^* = (k_{p4} + \frac{k_{i4}}{s}) + (V_{dc2}^* - V_{dc2}) \quad (12)$$

Where e_{q1}^* and e_{q2}^* controls the dc-link voltage of inverter1 and inverter2. Four level operations is obtained and output voltage harmonic spectrum is improved, since the dc-link voltage of inverter 2 is controlled at 0.366 times of that of inverter 1. So the dc link voltage of inverter1 and inverter2 is communicated in terms of total dc-link (V_{dc}) voltage.

$$V_{dc1} = 0.732 V_{dc} \quad (13)$$

$$V_{dc2} = 0.268 V_{dc} \quad (14)$$

The power transfer is indirectly controlled to inverter1 and directly controlled for inverter2. So, when compared to inverter1, The inverter2 attain its reference value swiftly. To generate gate signals from the obtained reference voltages, The control circuit uses the sinusoidal pulse width modulation technique

○ *Unbalanced Conditions*

Supply frequency component in the dc-link voltage of the inverter doubled due to fault in the system. Because the unbalance causes the negative-sequence voltage in the supply voltage. There by third harmonic component in the ac side due to double frequency element. High negative sequence current passes through the inverter due to negative-sequence voltage, which cause the static compensator to fall down. In the course of fault, The inverter voltages are managed in such a way that either negative-sequence current to the inverter is stamp outed or minimizes the grid voltage unbalance.

IV. SIMULATION RESULTS

For simulation, the system configuration in Image-1 is considered. MATLAB/SIMULINK is used for simulation analysis.

The system parameters are given in Table-1

**TABLE-1
 SIMULATION SYSTEM PARAMETERS**

Rated power	5 MVA
Voltage rating of transformer	11kv/400
Supply frequency	50 Hz
DC link voltage of Inverter-1	659 V
DC link voltage of Inverter-2	241 V
Leakage reactance of Transformer	15%
Resistance of Transformer	3%
Capacitance	50mF
Switching frequency	1200Hz

**TABLE-2
 SIMULATION RESULT OF EXISTING SYSTEM**

N o.	Reactive power	Real power
1	5.85MVar	8.12MW

A. Simulation and analysis of complete system with cascaded two level STATCOM

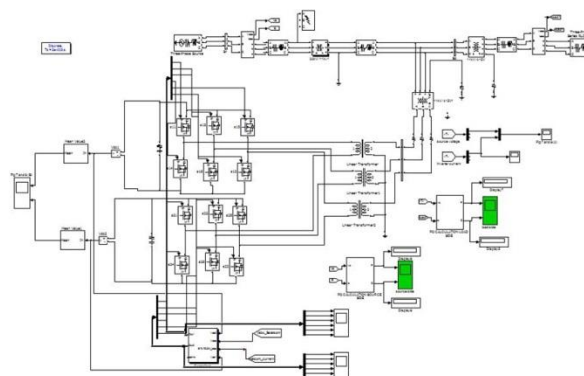


Image-6. Simulink model of system with cascaded two level STATCOM

a. *Reactive Power Control*

In this case, by keeping the reference reactive current component at a certain value, reactive power is directly applied into the grid. At first, i_q^* is kept at 0.5p.u. At $t=2.0$ s, i_q^* is changed to 0.5p.u. Image-13 indicates the dc-link voltages of two inverters. From that, it is seen that when the STATCOM mode is changed from capacitive to inductive, the dc-link voltages of the inverters are regulated at their respective reference values. By comparing the dc-link voltage two inverters, inverter 2 attains its reference value speedily.

b. *Load Compensation*

In this case, the STATCOM compensates the reactive power of the load. Initially, STATCOM is supplying a current of 0.5p.u. At $t= 2.0$ s, the load current is increased so that STATCOM supplies its rated current of 1 p.u. Fig.14 shows the dc-link voltages of two inverters. The dc-link voltages are maintained at their respective reference values when the operating conditions are changed.

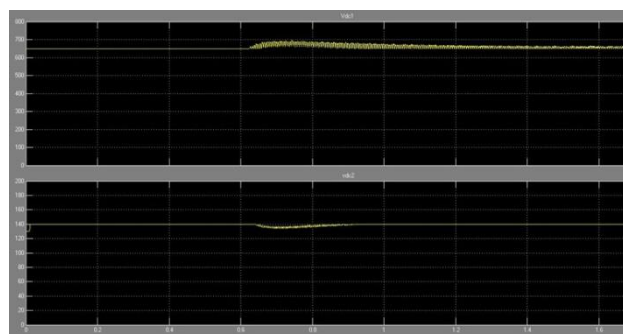


Image-7. Reactive power compensation-DC link voltages of two inverters

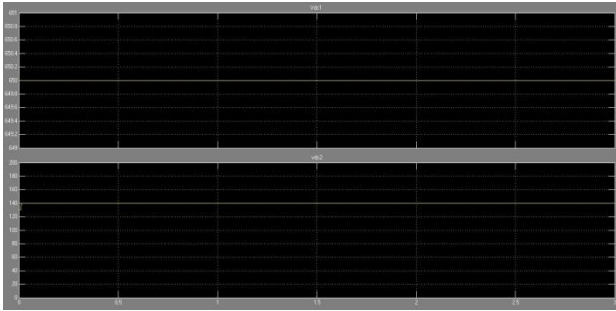


Image-8. Load compensation-DC link voltages of two inverters

c. Operation During the Fault Condition

To check for operation when a fault occurs, a single-phase-to-ground fault is made at $t = 1.2$ s, on the phase of the high tension side of the 33/11-kV transformer. The fault is cleared after 200 milliseconds. Image-9(a) conveys voltages across the low tension side and image-9(b) exhibits the d- axes components of negative-sequence current of the converter. During the fault condition, these currents are maintained at zero.

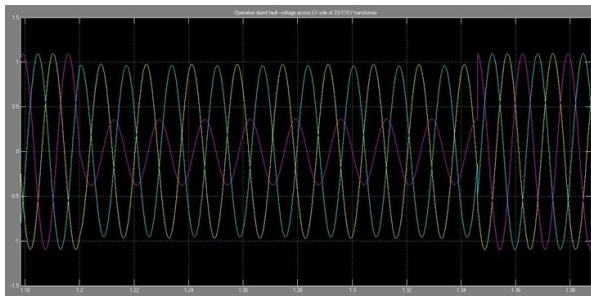


Image-9(a) Grid voltages on the low tension side of the transformer, during fault

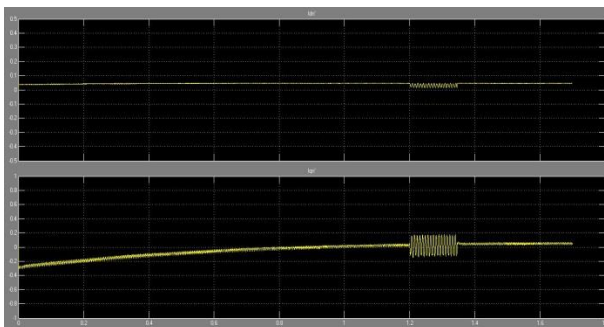


Image-9 (b) d-axis and q-axis negative-sequence current component, during fault

**TABLE-3
 SIMULATION RESULT OF PROPOSED SYSTEM**

No.	Reactive power	Real power
1	0.885MW	9.25MW

V.CONCLUSION

DC-link voltage balance is the paramount issue in a cascaded inverter based STATCOM. The proposed system introduces a cascaded H-bridge inverter based multi-level static compensator (STATCOM). The principal target is to compensate the reactive power with the better power quality. In this proposed system, a unadorned reactive power compensation scheme by a cascaded two-level inverter-based multilevel inverter are described. The dc-link voltage regulation of inverters at asymmetrical levels and reactive power compensation is guaranteed by the new strategy. The execution of the scheme is verified by simulating the system.

REFERENCES

- [1] N. N. V. Surendra Babu,, and B. G. Fernandes, "Cascaded Two-Level Inverter-Based Multilevel STATCOM for High-Power Applications," IEEE Transactions On Power Delivery, Vol. 29, No. 3, June 2014
- [2] Shukla, A. Ghosh, and A. Joshi, "Hysteresis current control operation of flying capacitor multilevel inverter and its application in shunt compensation of distribution systems," IEEE Trans. Power Del., vol. 22, no. 1, pp. 396–405, Jan. 2007.
- [3] Blazic and I. Papic, "Improved D-statcom control for operation with unbalanced currents and voltages," IEEE Trans. Power Del., vol. 21, no. 1, pp. 225–233, Jan. 2006.
- [4] Singh, R. Saha, A. Chandra, and K. Al-Haddad, "Static synchronous compensators (STATCOM): A review," IET Power Electron., vol. 2, no. 4, pp. 297–324, 2009.
- [5] based control strategy for balancing individual dc capacitor voltages in cascade multilevel inverter-based STATCOM," IEEE Trans. Ind. Electron., vol. 56, no. 6, pp. 2259–2269, Jun. 2009.
- [6] Schauder and H. Mehta, "Vector analysis and control of advanced static Var compensators," in Proc. Inst. Elect. Eng. C., Jul. 1993, vol. 140, no. 4, pp. 299–305.
- [7] H. Akagi, H. Fujita, S. Yonetani, and Y. Kondo, "A 6.6-kV transformerless STATCOM based on a five-level diode-clamped PWM converter: System design and experimentation of a 200-V 10-kVA laboratory model," IEEE Trans. Ind. Appl., vol. 44, no. 2, pp. 672–680, Mar./Apr. 2008.
- [8] H. Akagi, S. Inoue, and T. Yoshii, "Control and performance of a transformerless cascaded PWM STATCOM with star configuration," IEEE Trans. Ind. Appl., vol. 43, no. 4, pp. 1041–1049, Jul./Aug. 2007.
- [9] H.P.Mohammadi and M.T.Bina, "A transformerless medium-voltage STATCOM topology based on extended modular multilevel converters," IEEE Trans. Power Electron., vol. 26, no. 5, pp. 1534–1545, May 2011.
- [10] K. K. Mohaptra, K. Gopakumar, and V. T. Somasekhar, "A harmonic elimination and suppression scheme for an open-end winding induction motor drive," IEEE Trans. Ind. Electron., vol. 50, no. 6, pp. 1187–1198, Dec. 2003.
- [11] K. R. Padiyar and A. M. Kulkarni, "Design of reactive current and voltage controller of static condenser," Elect. Power Energy Syst., vol. 19, no. 6, pp. 397–410, 1997.

- [12] M. K. Mishra, A. Ghosh, and A. Joshi, "Operation of a DSTATCOM in voltage control mode," *IEEE Trans. Power Del.*, vol. 18, no. 1, pp. 258–264, Jan. 2003.
- [13] N. N. V. SurendraBabu, D. Apparao, and B. G. Fernandes, "Asymmetrical dc link voltage balance of a cascaded two level inverter based STATCOM," in *Proc., IEEE TENCON*, 2010, pp. 483–488.
- [14] R. Gupta and A. Ghosh, "Frequency-domain characterization of sliding mode control of an inverter used in DSTATCOM application," *IEEE Trans. Circuits Syst. I, Reg. Papers*, vol. 53, no. 3, pp. 662–676, Mar. 2006.
- [15] R. Gupta, A. Ghosh, and A. Joshi, "Switching characterization of cascaded multilevel inverter controlled systems," *IEEE Trans. Ind. Electron.*, vol. 55, no. 3, pp. 1047–1058, Mar. 2008.
- [16] X. Kou, K. A. Corzine, and M. W. Wielebski, "Over distention operation of cascaded multilevel inverters," *IEEE Trans. Ind. Appl.*, vol. 42, no. 3, pp. 817–824, May/Jun. 2006.
- [17] Kawabata, N. Yahata, M. Horii, E. Egiogu, and T. Kawabata, "SVG using open winding transformer and two inverters," in *Proc., 35th Annual IEEE Power Electron. Specialists Conf.*, 2004, pp. 3039–3044.
- [18] Y. Suh, Y. Go, and D. Rho, "A comparative study on control algorithm for active front-end rectifier of large motor drives under unbalanced input," *IEEE Trans. Ind. Appl.*, vol. 47, no. 3, pp. 825–835, May/Jun. 2011.

Camouflage based Emergency Vehicle priority with Intelligent Traffic Controller using Movable Road Dividers

^[1]Greeshma V., ^[2]Shruthi A S., ^[3]Yashaswini G., ^[4]Ramya B, ^[5]Anshu Deepak

^{[1][2][3]} Student of RRIT, Department of ECE

Assistant professor, Raja Reddy Institute of Technology, VTU

Abstract— *The main aim of this project is reducing the traffic congestion in our daily life. Road Divider is generically used for dividing the Road for on-going and incoming traffic. This helps keeping the flow of traffic; generally, there is equal width of lanes for both on-going and incoming traffic. The problem with Static Road Dividers is that the number of lanes on either side of the road is fixed. Since the resources are limited and population as well as number of cars per family is increasing, there is significant increase in number of cars on roads. This calls for better utilization of existing resources like number of lanes available. It is seen that terrible road congestion problems in cities. Moreover, the situation is getting worse when emergency vehicles have to wait for other vehicles to give way at intersections with traffic lights. This causes a delay of time and may affect the emergency case. Besides, the collisions with other vehicles from other direction might occur at intersections when emergency vehicles had to override the red traffic lights. All these difficulties faced by emergency vehicles can be avoided using this traffic light control system based on radio frequency transmission. The system will reduce accidents which often happen at the traffic light intersections because of another vehicle had to huddle for given a special route to emergency vehicle. As the result, this project successful analyzing and implementing the traffic assistance system for emergency vehicles. In the new evolving world, traffic rule violations have become a central issue for majority of the developing countries. People may violate the traffic rules, they may jump signal to avoid this our project presents Automatic Number Plate Recognition techniques. It recognizes Plate localization and Character recognition which makes it easier and faster to identify the number plate. Message is sent to vehicle owner for violating his rules and simultaneously it is sent to near by police station.*

Index Terms—Traffic management; Emergency vehicle Priority; Number plate Recognition

I. INTRODUCTION

Existing System

Commuters daily face extreme traffic during peak hours resulting in a delay to reach their destination. In the morning, during peak hours the traffic on one side of the road is more compared to opposite side of the road, same is the situation in evening. To tackle this problem Abdulreidha Abdulrasoul Alsaffar, had published an idea in US in 2013, which included a technique to solve the problem by moving road barriers using heavy vehicles before the accumulation of traffic in peak hours. The approach used to move the road barrier

transfer machine are, Barrier transfer machines, also known as zipper machines, are heavy vehicles used to transfer concrete lane barriers. It contains an S-shaped channel in its under-carriage which lifts the barrier segments off the road surface and transfers them over to the other side of the lane. This reallocates the traffic lanes to accommodate increased traffic for the currently dominant direction. These barriers are linked together with steel connectors to create a sturdy but flexible safety barrier. Moveable barriers are in permanent use in cities like Auckland, Montreal, Canada, Philadelphia, Pennsylvania, New York etc.

II. PROPOSED SYSTEM

In this proposed system, a module has been developed based on microcontroller that consists of an ultrasonic sensor which is used for measuring the traffic density in this case and two dividers normal and extended. When the signal turns red, the traffic density is measured and the action should take place before the signals turns into green. If the traffic density is high then the extended divider comes up and the normal divider goes to ground position. Since the traffic density is high a message is delivered stating that 'Alert PLS traffic density is high, extended divider is up' to the nearest traffic control room. If the traffic density is normal then no type of action is taken and the normal divider is up and the extended divider is to ground level. In this case the traffic density is normal then a message is delivered stating that 'Traffic density is normal. Normal divider is up and the extended divider is to ground level to the nearest traffic control room. Since it is a demo module, we are just showing for the one way of traffic flow.

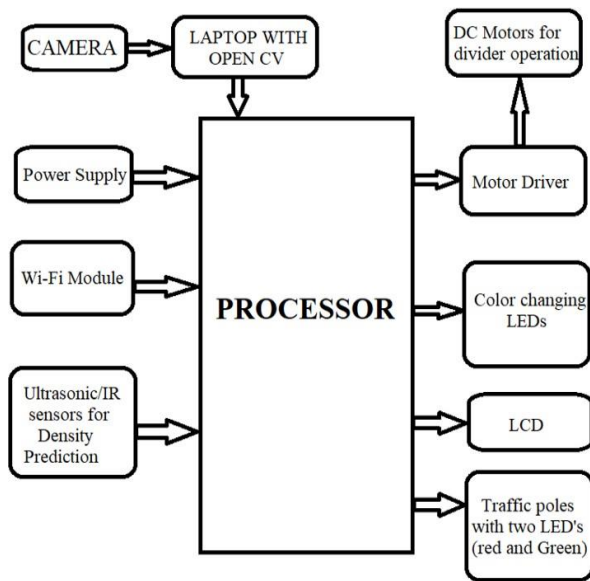


Figure 1: Block diagram

III. WORKING PRINCIPLE:

- Let us consider two roads as road A and road B, 2 IR sensors will be placed at the each road both at the entry point and exit point. Let's assume, road A IR2 sensor as entry point, IR1 sensor as exit point and in road B IR4 as entry point, IR3 as exit point.
- Threshold will be given as 30 vehicles and initially signal will be red. IR2 sensors counts till the 30 vehicles and enters the road A. when the threshold limit exceeds more than thirty the signal is sent and the road dividers start to move towards road B, making that side of the line as red signal.
- To avoid any accidents during the movement of divider on either sides, ultrasonic sensors are attached, this sensor senses if any object is present, once the divider is moved completely the signal on the road A turns green.
- The main aim of this principle is to reduce the traffic.

AMBULANCE DETECTION:

- RGB LED's deployed on two sides of the road.
- Whenever divider receives signal from ambulance RGB LED's connected on road side will start glowing.
- Divider creates shortest path and complete free path for ambulance. In order to create the path divider moves to one side according to the ambulance destination in such way that ambulance gets less passage free path compare to normal vehicles.
- Ex: If ambulance is going right divider also moves to right side so wide passage is created in left so that normal vehicles gets more pass.



Figure 2: Selection of road by using UDP/TCP app

LICENSE PLATE RECOGNITION:

- License plate recognition (LPR) is one form of ITS (Intelligent Transport System) technology that not only recognizes and counts the number of vehicles but also differentiates them.
- For some applications, such as electronic toll collection and red-light violation enforcement, LPR records license plate alphanumerically so the vehicle owner can be assessed the appropriate amount of fine.
- In other cases, like commercial vehicle operations or secure-access control, a vehicle's license plate is compared against a database of acceptable ones to determine whether a truck can bypass a weigh station or a car can enter a gated community or parking lot. A license plate is the unique identification of a vehicle.
- The basic issues in real-time license plate recognition are the accuracy and the recognition speed.
- A video is taken from a camera, and then each frame of the video is processed as the image. In this stage the license plate region from the given image is located and isolated.
- Quality of the image plays an important part hence prior to this stage pre-processing of the image is necessary. So first each frame pre-processed by binarization, noise reduction and edge detection. Then, the license plate is located by different image processing technique.



Figure 3: license plate detection

COMPONENTS REQUIRED

HARDWARE COMPONENTS:

ARDUINO MEGA



Figure 4: Arduino mega

The Arduino mega 2560 is a microcontroller board based on the ATmega 2560 (datasheet). It has 54 digital input/output pins, 16 analog inputs, 4 UARTs, a 16 MHz crystal oscillator, a USB connection, a power jack, an ICSP header and a reset button.

16 X 2 LCD



Figure 5: 16x2 LCD

An LCD is easy to interface with a micro-controller because of an embedded controller.

This controller is standard across many displays which means many micro-controllers have libraries that make displaying message as easy as a single line of code. It offers high flexibility to users.

H-BRIDGE

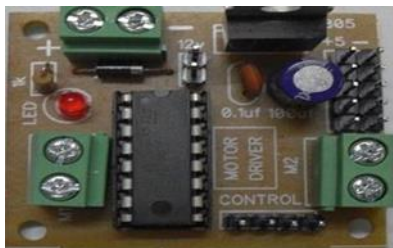


Figure 6: H-bridge L293d

L293D is a dual H-bridge motor driver integrated circuit (IC). So, two DC motors can be driven simultaneously, both in forward and reverse direction. Motor drivers act as current amplifiers since they take a low-current control signal and provide a higher-current signal. This higher current signal is used to drive the motors.

DC MOTOR



Figure 7: DC motor

An electric motor operated by DC is known as a DC motor. An DC motor converts DC electrical energy into mechanical energy. When a magnetic field and a electric field interact, a mechanical force is produced. The DC motor or direct current motor works on that principle. This is known as motoring action.

POWER SUPPLY



Figure 8: power supply

The most commonly used regulator IC;s, the 7805 voltage Regulator IC. A regulated power supply is very much essential for several electronic devices due to the semiconductor material employed in them have a fixed rate of current as well as voltage. Here comes the 7805 Voltage Regulator IC to the rescue. It is an IC in the 78XX family of linear voltage regulators that produce a regulated 5V as output.

ULTRA SONIC SENSOR



Figure 9: Ultrasonic sensor

An ultrasonic sensor is an electronic device that measures the distance of a target object by emitting ultrasonic sound

waves, and converts the reflected sound into an electrical signal. Ultrasonic sensors are also used as level sensors to detect, monitor and regulate liquid levels in closed containers.

**SOFTWARE COMPONENTS:
 ARDUINO SUITE**



Figure 10: Arduino logo

The Arduino is a single-board microcontroller solution for many DIY projects, we will look at the Integrated Development Environment, or IDE, that is used to program it. Once the installer has downloaded, go ahead and install the IDE. Arduino IDE is an open source software that is mainly used for writing and compiling the code into the Arduino Module.

TCP/UDP

TCP is a connection-oriented communication protocol. TCP rearranges data packets to be received in their intended order here the ambulance driver needs to select on which road he needs to drive after the selection of road. TCP provides apps a way to deliver (and receive) an ordered and error-checked stream of information packets over the network. The User Datagram Protocol (UDP) is used by apps to deliver a faster stream of information by doing away with error-checking.

TCP (Transmission Control Protocol)	UDP (User Datagram Protocol)
TCP is a connection-oriented communication protocol.	UDP is a connectionless communication protocol.
TCP rearranges data packets to be received in their intended order.	UDP sends datagrams independently, meaning that they may arrive in a different order.
TCP confirms data delivery receipts.	UDP doesn't use delivery receipts.
TCP results in higher latency.	UDP is designed for faster data transmission.
TCP guarantees data delivery by prioritizing data integrity, completeness, and reliability.	UDP prioritizes speed and often result in data loss.
TCP is ideal for reliable data transmissions.	UDP is ideal for real-time data transfer and streaming to avoid delay.

Figure 11: TCP/UDP difference

IV. CONCLUSION

The proposed structure helps to reduce the chances of traffic jams and to provide clearance of road for the emergency vehicles to an extent. In these proposed work we are aimed to clear the traffic in accordance to priority.

It will help in to reduce the traffic highway. Also it is helpful for the government to apply traffic rules. And people will follow the rules of traffic. It's applicable in almost all areas in the Pune city. It will be applicable in the cross road and traffic zone.

The main aim of this project is to automate change road divider & announce the status of the changes for users. In this system is also used to avoid accident problems. This project identifies the status of each car using IR transceivers and informs it to microcontroller.

This project is used to avoid the car collision, thus we save the valuable human lives and losses. So this project is useful for road transport departments. The recent survey from the social analytics was said that the most disadvantages in Indian road traffic.

REFERENCES

- [1] Rajeshwari Sundar, Santhosh Hebbar, and Varaprasad Golla, "Implementing intelligent Traffic Control System for Congestion Control, Ambulance Clearance, and Stolen Vehicle Detection" *IEEE Sensors Journal*, Vol. 15, No. 2, February 2015
- [2] Soufiene Djahel, "Reducing Emergency Services Response Time in Smart Cities: An Advanced Adaptive and Fuzzy Approach", *IEEE* 2015, pp 978- 986
- [3] George Kiokos, "Development of an Integrated Wireless Communication System for Connecting Electric Vehicles to the Power Grid", *IEEE conf.* 2015, pp 296-301.
- [4] Movable Traffic Divider: A Congestion Release Strategy (2017), vol-5,issue 1.
- [5] On road vehicle detection: A review Z Sun,G Bebis,R Miller -*IEEE transactions on pattern analysis* 2006
- [6] Rohini Temkar, Vishal Asrani, Pavitra Kannan, "IOT:Smart Vehicle Management System for Effective Traffic Control and Collision Avoidance" *International Journal of Science and Research (IJSR)*, 2015
- [7] *International Journal of Advanced Computer Science and Applications*, Vol 6, No.2, 2015 "Intelligent Traffic Information System Based on Integration of Internet of Things and Agent Technology
- [8] M.Collotta,G.Patu,G.Scatt.T. Campisi, "A Dynamic Traffic Light Management System Based on Wireless Sensor Networks for the Reduction of the Red-Light Running Phenomenon", *Transport and Telecommunication*, Vol.15, No.1, pp 1-11, 2014

Design of Hybrid Electric Vehicle with Solar Energy and Wireless Charging

^[1] Sunanda C V., ^[2] Ramachandra C, ^[3] G Gowtham, ^[4] Bidhya chhetri

^{[1][2][3]} Assistant Professor, RRIT

^[4] Student, RRIT

Abstract— With the advancement in 21st Century, there has been increase in usage of Oil and Gas leading to problems like Global Warming, climate change, shortage of crude oil, etc. Due to these reasons Automobile Companies have started doing research for making Hybrid Technology usable into the daily life. The technologies used in the making of Hybrid Cars such as “Hybrid Solar Vehicle”, “Hybrid Electric Vehicle” and “Plug In hybrid electric vehicles”. On this bases the explanation of such technologies, their function, drawback of this technology, efficiency of Hybrid Cars, and Case studies on the present commercial hybrid cars and the fuels and raw materials used in the Hybrid Cars. The advantages and disadvantages of Hybrid Electric Cars and technologies which will take over the world in future and would become the alternative of Petrol and Diesel Cars. Electric vehicles (EVs) as the next generation of vehicles are becoming more reliable. Battery charging system is an important challenge to make the EVs popular. Wireless charging are user friendly and safe systems. It proposed to overcome consumer’s concerns regarding charging battery and driving range. The wireless power transfer (WPT) circuit topology for EV charging applications are presented. The coil and ferrite shapes have been discussed. The health and safety issues as the highest priority for electrical, coupling fields and fire hazards are also discussed addressing related standards for WPT.

Index Terms— MPPT-Maximum Power Point Tracking, HEV-Hybrid Electric Vehicles, SPI-Serial Peripheral Interface, TWI-Two Wire Interface.

I. INTRODUCTION

Electric vehicles are the future of transportation since it reduces the use of fossil fuels to a larger extent. Developed and developing countries are encouraging use of electric vehicles due to its efficiency and supposed green technology. Though charging of electric vehicles is supposed to be eco-friendly, reports deny it. As charging the electric vehicle battery is again from grid which is energized by the use of fossil fuels, it can't be eco-friendly any more. Harnessing the solar power to charge an electric vehicle battery is the eco-friendliest alternative to charge an electric vehicle. To optimize the power output from solar panel, Maximum Power Point Tracking (MPPT) is implemented. MPPT maintains the operation of the panel at maximum power point so that the efficiency of the panel is increased.

The technologies for global transportation are dominated by internal combustion Engine powered vehicle that leads to major threat to Green gas emission. Even though the global

transportation technology partially moved to Hybrid fuels and battery electric vehicle. These technology improvements are not attracted the global customer because of its cost and its compatibility. Our aim is to build a low cost Solar Powered Electric Vehicle that would meet the requirements of the global customer. SPEV comprises of inbuilt solar panels to charge the vehicle, tachometer for measuring rotation speed, Motor controller and 15v DC motor used in SPEV. The vehicle has user interface supported with Android OS. The automated solar powered electric vehicles is added advantage that can be implemented for limited area with help of Ultrasonic array for obstacle avoidance, Lora, GPS Maps API and intelligence algorithm

II. LITERATURE SURVEY

1. A solar vehicle is an electric vehicle powered completely or significantly by direct solar energy. Usually, photovoltaic (PV) cells contained in solar panels convert the sun's energy directly into electric energy. The term "solar vehicle" usually implies that solar energy is used to power all or part of a vehicle's propulsion. Solar power may be also used to provide power for communications or controls or other auxiliary functions.

2. The technologies which will change the face of Automobile Sector would be “Hybrid Electric Vehicle”, “Hybrid Solar Vehicle”, “Hydrogen Fuel Cell”, etc. From all this Hybrid Electric Vehicle is considered as the most industrially matured technology and has efficiency more than cars running on Petrol/Diesel/CNG while Hybrid Solar Vehicle has lower efficiency than vehicle running on Petrol/Diesel/CNG. So, this technology is for drivers who want to cover less distance. To overcome this constraint, “Plug-In Hybrid Electric Vehicle” came into existence.

3. Regenerative braking is an energy recovery mechanism which slows down a vehicle by converting its kinetic energy into another form, normally into electrical energy, which can be used immediately or stored until needed in high voltage batteries. The electric motor is operated in reverse during braking or coasting, acting as generator. The rotors of electric traction motor are coupled with wheels; they experience opposing torque as current is induced in the motor coils. The wheels transfer kinetic energy via drivetrain to generator.

III. PROPOSED SYSTEMS

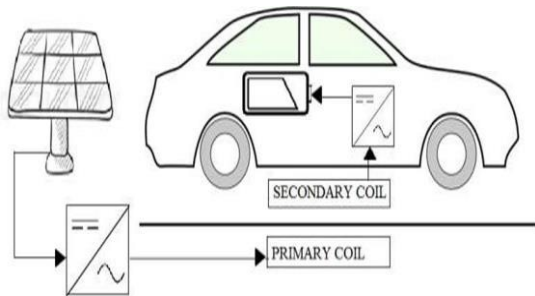


Figure 3.1. Prototype model of WPT for electric vehicle

In current scenario fossil fuel, based vehicles are used for transportation, which causes huge amount of greenhouse gases emission, and the fossil fuels are in a verge of extinction. To avoid this electric vehicle were introduced, but the major issues with electric vehicles is its charging related issues, such as long charging time, charging one vehicle at a time, insulation requirement in charging cable.

IV. BLOCK DIAGRAM

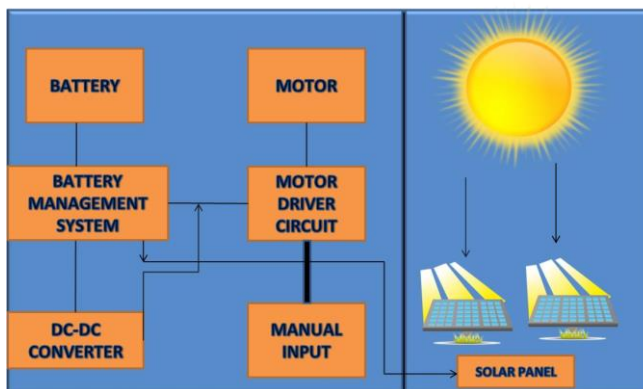


Figure 4.1. Solar Hybrid Vehicle Main Block Diagram

This project is completely based on solar energy usage and this technology is an integration of Vehicle and Photovoltaic Panels. The photovoltaic panels are mounted on the roof-tops of the vehicles. It is also classified into four types: - Series Hybrid, Parallel Hybrid, and Series-Parallel Hybrid and Complex Hybrid. Series Hybrid technology is very efficient and more compatible type and the block diagram is shown in figure 3.1. The track consists of aluminum shielding which concentrates the flux to the receiver. The receiver is basically a secondary coil placed at the bottom of electric vehicles. Due to the electromagnetic induction principle, EMF is induced in the secondary coil. A compensator is connected in parallel to the secondary coil, which forms a resonating tank circuit in order to remove the harmonics and the ripple contents. The secondary is connected to the full bridge rectifier which converts AC to DC. A regulator circuit is used to get a constant DC supply,

which charges the battery of the electric vehicle.

V. METHODOLOGY

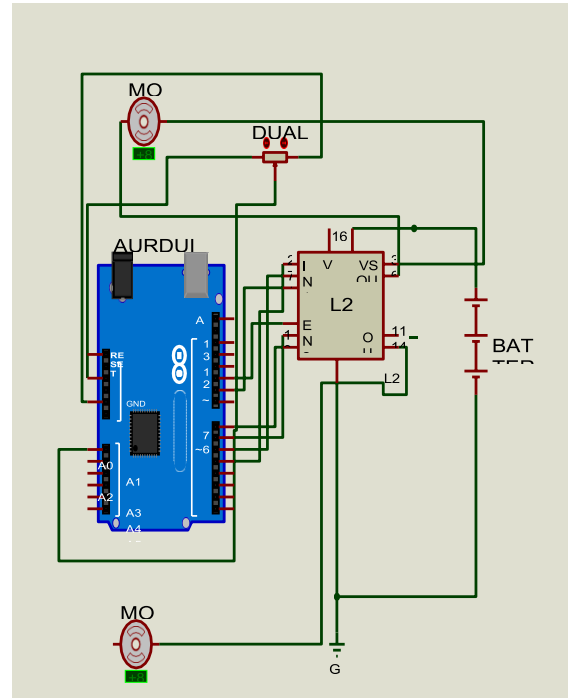


Figure.4.1. Circuit Diagram for the Motor Driver circuit

The follow circuit diagram is the driver circuit which uses an Arduino UNO board as the controller of the whole motor and a L239D motor controller for the 15v DC motor. The solar panel input is directly given to the Arduino to power the board and acts as a voltage regulator and the charging circuit is connected to the battery to charge the battery. The Arduino is then programmed to drive the two motors using a joystick or a Dual Axis XY module which assigns the direction of the vehicle as a controller of direction only in the prototype as this implies as a steering wheel in a real vehicle. The L239D motor is motor driver which uses a IC 1239 driver IC is connected to battery which consists of three lithium polymer cells each rated for 3.3v which makes it a total of 11.1V typical (12v Nominal).

The wireless power transfer is done using a transistor TTC 5200 which connected to a power supply which then the transistor is connected to a coil of copper with a Centre tap and the other side of the receiving coil is connected to the charging circuit after being rectified as the transferred energy is AC and is converted using a rectifier or a single diode to DC.

The Arduino UNO is an open-source microcontroller board based on the Microchip ATmega328P microcontroller and developed by Arduino.cc. The board is equipped with sets of digital and analog input/output (I/O) pins that may be

interfaced to various expansion boards (shields) and other circuits. The board has 14 Digital pins, 6 Analog pins, and programmable with the Arduino IDE (Integrated Development Environment) via a type B USB cable. It can be powered by a USB cable or by an external 9-volt battery, though it accepts voltages between 7 and 20 volts. It is also similar to the Arduino Nano and Leonardo. The hardware reference design is distributed under a Creative Commons Attribution Share-Alike 2.5 license and is available on the Arduino website. Layout and production files for some versions of the hardware are also available. "Uno" means one in Italian and was chosen to mark the release of Arduino Software (IDE) 1.0. The Uno board and version 1.0 of Arduino Software (IDE) were the reference versions of Arduino, now evolved to newer releases. The Uno board is the first in a series of USB Arduino boards, and the reference model for the Arduino platform. The ATmega328 on the Arduino Uno comes preprogrammed with a boot loader that allows uploading new code to it without the use of an external hardware programmer. It communicates using the original STK500 protocol. The Uno also differs from all preceding boards in that it does not use the FTDI USB-to-serial driver chip. Instead, it uses the Atmega16U2 (Atmega8U2 up to version R2) programmed as a USB-to-serial converter.

V. WORKING MODEL/PROTOTYPE



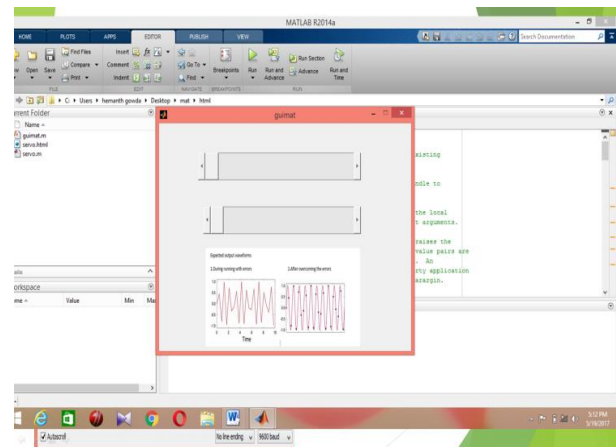
Fig.6.1 Assembled Prototype

There are many applications of photovoltaic in transport either for motive power or as auxiliary power units, particularly where fuel, maintenance, emissions or noise requirements preclude internal combustion engines or fuel cells.

WPT can use in moving targets like fuel-free-electric vehicles, fuel-free airplanes, fuel-free rockets, and moving robots. In addition, the other applications of WPT are Wireless power source or Ubiquitous Power Source, RF Power Adaptive Rectifying Circuits and Wireless sensors.

Many of the products that are being commercialized and developed on wireless power transmission technology come into life in the following areas. Some of them seem to enter our life in the near future.

VI. RESULT



VII. SCOPE OF FUTURE WORK

Smart Charging Station- Smart EV charging is worked on the basis of the back-end solution. If the charging stations are connected to the cloud, then they can manage based on the different signals such as local energy consumption. By using smart charging stations, we can easily find available charging points also we get fast charging, charge safer, save money and the environment and also avoid arguments with neighbors.

Renewable energy based charging station- Renewable energy based charging stations consist of the both solar and wind energy. Charging stations based on the solar or wind energy it is useful to prevent the environment from the pollution. By using solar energy based charging station we can produced power during the day and it can be used at night to charge EVs.

VIII. CONCLUSION

SPEV provides pollution less transportation and utilization of non-conventional energy. The SPEV would benefit by the end users like Industries, university campus, amusement parks. Physically challenged people would be benefited with automated driving mode concept. The technology used in SPEV contributes its supports to Green transportation. The complete solar charger circuit is simulated and the battery is seen to charge as required. Hence, solar power is used as the power source to charge the battery. By implementing solar power as a source to charge the batteries Such a system would also help to expand the grid since the of electric vehicles, non-renewable resources like fossil fuels, which are used in conventional vehicles can be con- served. Vehicles have their own sustainable method of charging, which frees up existing power plants for other loads.

It is seen that the distance between primary coil and secondary coil is decreases. When it comes to voltage generated on secondary side as the distance between two coils increases the induced voltage decreases. Hence for

wireless charging, the tradeoff is maintaining the distance between primary and secondary coil for smooth voltage characteristics. A voltage regulator is useful at receiver side for obtaining fixed voltage.

REFERENCES

- [1] P. Denholm, M. Kuss, and R. M. Margolis, "Co-benefits of large scale plug-in hybrid electric vehicle and solar PV deployment," *Journal of Power Sources*.
- [2] An Shi-qi, Qi An-ning, Zhu Yu-wei. Design and Realization of SPI Interface in Lithium-ion Battery Voltage Measuring System. The 6th International Conference on Computer Science & Education (ICCSE).
- [3] N. Uthaya Banu, U. Arunkumar, A. Gokulakannan, M. K. Hari Prasad and A. B. Shathish Sharma "Wireless Power Transfer in Electric Vehicle by Using Solar Energy" *Asian Journal of Electrical Sciences* ISSN:2249-6297, Vol.7, No.1, 2018, pp.6-9.
- [4] Erhuvwu Ayisire "Magnetic Resonance Coupling Modelling For Electric Vehicles Wireless Charging". IEEE 2018
- [5] Shubhangi Das, Kajal Pal, Prema Goswami, M. A. Kerawalla "Wireless power transfer in electric vehicles". *International Journal of Applied Environmental Sciences*, ISSN 0973- 6077 Vol 13, Number 7(2018), pp.643-659
- [6] Rajbansi Devmani Kamalbahadur, S Prabhu Ram, Kohar S. Suresh, M.R. Venugopitan, R. Karthikayan "Wireless Charging of Electric Vehicles by Solar Power Charging Station". *International Journal of ChemTech Research*, CODEN (USA): IJCRGG ISSN: 0974- 4290, Vol.10.No.14, pp 198-206, 2017
- [7] Miss Shital R. Khutwad. "Wireless Charging Systems For Electrical Vehicle" *International Conference on Signal Processing*.

Longitudinal Stability Analysis of an Aircraft using RBFANN

^[1] G Parimala Gandhi, ^[2] Dr Nagaraj

^{[1][2]} Associate Professor, RR Institute of Technology, Bangalore

Abstract— *The emergence of neural network is a promising tool for complex system for verifying nonlinear dynamic and stability analysis. One research area that is tremendously benefitted is intelligent control and performance analysis of aircraft this paper presents analysis of longitudinal stability and Develop and on-line control scheme that utilizes a dynamically structured Radial Basis Function Network (RBFN) for aircraft control. By using synthesis approach, the tuning rule for updating all the parameters of the dynamic RBFN which guarantees the stability of the overall system to be derived and Analysed. The robustness of the proposed tuning rule, Perform Simulation studies using the aircraft longitudinal model which demonstrates the efficiency of the method and also show that with a dynamically structured RBFN, a more compact network structure can be implemented for stability analysis of an aircraft.*

Keyword: Radial Basis Function , Gaussian Function, Longitudinal stability

I. INTRODUCTION

Neural networks have been used to tackle problems for which conventional approaches have been proven to be ineffective. However, the use of neural networks for on-line control schemes is sparse, especially in areas such as flight control because a large computation time is required for the learning process. Radial Basis Function (RBF) neural networks, have good global generalization ability and a simple network structure that avoids lengthy calculations. Number of algorithms have been proposed for training the RBF network, The classical approach to RBF implementation is to fix the number of hidden neurons a priori along with its centers and widths, based on some properties of the input data, and then estimate the weights connecting the hidden and output neurons. Two methods have been proposed to find the proper number of hidden neurons for a given problem. I.e build the hidden neurons from zero to the required number with the update of the RBF parameters being done by a gradient descent algorithm, other one is start with as many as hidden units as the number of inputs and reduce using clustering algorithm. However, in the main learning scheme is of batch type, which is not suitable for on-line learning Advent of engineering, simulation and predict of system behaviour play an important role in aircraft design. The Modern fighter aircraft involves a nonlinear system complex and design with adequate performance over its entire flight regime is a challenging problem. Hence incorporate Neural network with online learning can adapt and provide good fault tolerant capabilities[2]. Among various method the

RBFN has proven suitable with fixed number of neuron with center and width of the Gaussian function. In[3], Simon Fabri and Kadirkamanathan use a dynamically structured RBFN that grows according to system state. The RBFN are updated according to the tuning law derived from Lyapunov stability theory when there is no growth in the network, hence the changes in the system dynamics can be captured quickly. In flight dynamics 3 degrees-of-freedom longitudinal flight simulation model will have a capability to solve longitudinal equations of motion for any given aircraft geometry. The longitudinal dynamic stability characteristics of an aircraft are derived from longitudinal equations of motions and will be trimmed to determine whether an aircraft is statically and dynamically stable at be trimmed at reference flight condition. In Fabri's scheme, two neural networks are utilized to approximate the dynamics $f(z)$ and $g(z)$ of the affine system, while in this paper, the well known "feedback-error-learning" scheme is used since it has the advantage of learning the true inverse dynamics without requiring that the network be trained offline[5]. In this paper, a stable tuning rule for updating all the parameters of a RBFN controller is derived which will guarantee the stability of the overall system.

II. RADIAL BASIS FUNCTION NEURAL NETWORK

The radial basis function (RBF) neural network is a feed-forward neural network, which has good performance of best approximation and global optimum. The broad use of RBF is in function approximation, prediction and regressions problems. The RBF neural network architecture consist of three layers composed such as input layer, hidden layer, and output layer. The input layer accepts the input vectors to the network, perform data processing normalization processing. The hidden layer has number of hidden neurons and described based on issues described., Each hidden neuron has a radial basis function which is a center position and symmetric nonlinear function with local distribution. Upon the calculation of center, width, the input vectors are mapped to the hidden has radial basis function

$$y_i = f_i(x) = \sum_{k=1}^N W_{ik} \varphi_k(x, c_k) \\ = \sum_{k=1}^N W_{ik} \varphi_k(\|x - c_k\|_2), \\ \forall i = 1, 2, \dots, m \text{ -----} 1$$

Where $x \in \mathcal{R}^{n \times 1}$ is an input vector, $\phi_k(\cdot)$ is a function from \mathcal{R}^+ to \mathcal{R} , $\|\cdot\|_2$, indicates the Euclidean standard, W_{ik} are the weights in the output layer. N is the quantity of neurons in the hidden layer, and $c_k \in \mathcal{R}^{n \times 1}$ is the RBF focuses in the output space. The Euclidean distance between its related centers and the contribution to the system is registered for every hidden layer. The output of the hidden layer is a nonlinear capacity of the distance. At last, the output of the system is processed as a weighted whole of the hidden layer outputs. The functional type of $\phi_k(\cdot)$ is thought to be given and is generally Gaussian function as given by Eq. 2

$$\phi(x) = \exp\left(-x^2/\sigma^2\right) \quad \text{-----2}$$

Where σ parameter controls the "width" of RBF and is referred as spread parameter. The centers characterize the points and are expected for a sufficient sampling of the input vector space. They are typically picked as a subset of the input data. On account of the Gaussian RBF, the spread parameter σ is normally set by the accompanying heuristic relationship

$$\sigma = \frac{d_{\max}}{\sqrt{k}} \quad \text{-----3}$$

Where d_{\max} is the max Euclidean distance between the chosen centers and K is the No of centers. Considering Eq.4 the RBF of a neuron in the hidden layer of the N/W is given by

$$\phi(x, c_k) = \exp\left(-\frac{k}{d_{\max}^2} \|x - c_k\|^2\right) \quad \text{---4}$$

III. AIRCRAFT DYNAMICS

The aircraft dynamic is represented by the linearized equations about the equilibrium point. In particular, the linear time invariant system represent the stability and control of the aircraft. Linear systems are more amenable to analysis and control system design. At the steady-state conditions nonlinear aircraft equations are linearized by linearized equations of motion derived from small perturbation theory. The straight and level flight condition consists of the following equilibrium values of the state variables computed as $u = 81.31$ m/s $w = 16.08$ m/s $q = 0$ rad $\theta = 11.19$ deg $h = 600$ m $v = 0$ m/s $p = 0$ rad $r = 0$ rad $\Phi = 0$ rad

$$\text{Where, } \Delta x = [\Delta u \ \Delta w \ q \ \Delta \theta \ \Delta h \ v \ p \ r \ \phi \ \psi \ y]^T \quad \text{..... (5)}$$

$$\Delta u = [\Delta \delta e \ \delta a \ \delta r \ \Delta \delta \text{thr}]^T \quad \text{..... (6)}$$

$$\Delta y = [\gamma \ q \ \Delta \theta \ \Delta h \ \Delta Vt \ p \ r \ \phi \ ay \ \Delta \chi]^T \quad \text{..... (7)}$$

The Δ symbol indicates the deviation of the particular quantity above trim value. This is only applicable for those quantities, which $\Psi = 0$ rad $y = 0$ m.

The linearized F16 model at the straight level flight condition can be described using the following equations:

$$\Delta(\dot{x}) = A\Delta x + B\Delta u$$

$$\Delta y = C\Delta x + D\Delta u$$

The control design is further simplified if the longitudinal dynamics of the aircraft decoupled from the lateral dynamics. Accordingly, the system of equations given by the above set is separated into the longitudinal and lateral-directional set. The primary reason to solve the equations of motion is to obtain a mathematical description of all the motion variables in response to a control input. This enables an assessment of stability to be made. The trimming and linearization script described finds the longitudinal response to the input about a trim state. The longitudinal system matrices for the longitudinal state equation can be written as :

	-0.01831	0.1023	-15.3342	-9.6192	-0.00019	0
	-0.10604	-0.64851	73.62021	-1.90244	0.000932	0
Alon=	-0.00254	0.009827	-0.64908	0	-1.02E-20	0
	0	0	1	0	0	0
	0.194017	-0.981	0	82.84214	0	0

	0.00486	7.152217	0.018313	-0.09951	
	-0.13589	0	0.106034	0.653112	
B Long	-0.05981	0	0.002537	-0.01105	
	0	0	0	0	0
	0	0	0	0	0

	1	0	0	0	0	0
	0	1	0	0	0	0
	0	0	1	0	0	0
	0	0	0	1	0	0
Clong =	0	0	0	0	1	0
	0	0	0	0	0	1
	-0.1342	0.677727	0	0	0	0
	0.980987	0.1938	0	0	0	0
	0.1342	-0.67773	0	57.29578	0	0
	-0.00187	0.010428	0.076032	0	-1.92E-05	0

It is clearly seen that the longitudinal trimming and linearization script does an excellent job in producing the longitudinal state equation

IV. ANALYSIS

A basic longitudinal flight simulation model has been built and can determine both the static and dynamic stability of an aircraft.. The simulation model consisted of aerodynamic, Thrust and Equations of Motion and are linked together to form an integrated longitudinal flight simulation model. The results were generated in the form of a report that consisted of trimmed inputs, longitudinal equations of motion (A and B matrix), static stability in the form of $Cm\alpha$ and the dynamic stability fig 1 & Fig 2 in the form of roots for short-period modes. It was observed that the model was successful in accurately predicting the aircraft behavior as either the geometric data or flight condition varied since the flight dynamics principles were not violated. In essence, the flight

simulation model developed can be used as a solid foundation for longitudinal stability simulation study

- [3] Robert C. Nelson, Flight Stability and Automatic Control, McGraw-Hill, 1998, pp. 124
- [4] Ahmed, Umair, "3-DOF Longitudinal Flight simulation Modeling And Design Using MATLAB/SIMULINK" (2012).

V. CONCLUSION

This paper presents a performance analysis of the Radial basis function neural network for stability analysis. The results indicate that network realizes with better approximation accuracy.

Fig 1

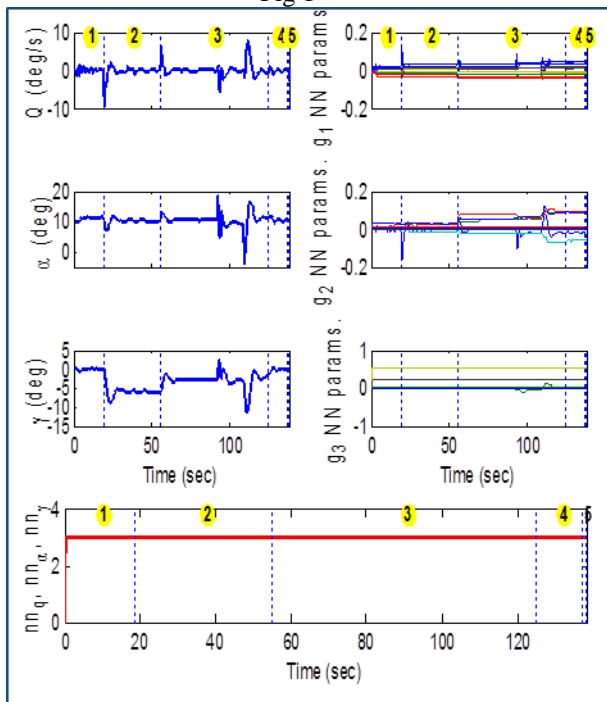
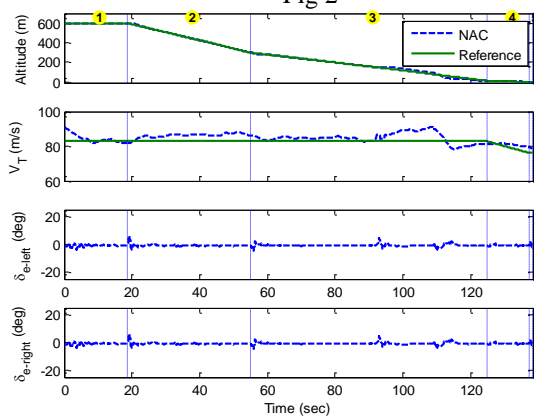


Fig 2



REFERENCE

- [1] Performance Evaluation of a Sequential Minimal Radial Basis Function (RBF) Neural Network Learning Algorithm - Lu Yingwei, Narashiman Sundararajan - EEE TRANSACTIONS ON NEURAL NETWORKS, VOL. 9, NO. 2, MARCH 1998
- [2] Arkadiy Turevskiy, Stacey Gage, and Craig Buhr, Model-Based Design of a New Lightweight Aircraft, 2008

Disk-Based Real-Time Applications for Power Consumption

^[1]B N Mohan Kumar, ^[2]Divya T M, ^[3]Sai Prashanth S

^{[1][2]} Assistant Professor, Department of ECE, RRIT, Bengaluru

^[3] Student, Department of ECE, RRIT, Bengaluru

Abstract— While several power optimization techniques have been proposed at all levels of design process abstractions for electronic equipment, until now, power consumption in mixed mechanical-electronic subsystems, such as disks, has not been addressed. We intend a conceptually simple, but realistic power consumption model for disk drives. The core of the paper are heuristics for optimization of power consumption in several common hard real-time disk-based design systems. We show how to coordinate tasks scheduling and their disk data assignment, in order to minimize power consumption in both electronic and mechanical components of used disks. Extensive experimental results indicate significant power reduction.

I. INTRODUCTION

Magnetic disks are the de-facto standard for providing non-volatile high volume memory capacity in modern computer systems. Disks provide superior trade-off with respect to common design metric such as cost, memory capacity, latency, data input-output bandwidth and reliability in comparison with all other alternatives. Until recently, disks have been used mainly in general purpose computing systems. However, convergence of several application and technological trends resulted in the rapidly increasing importance of massive storage in application specific systems. There is rapid growth in applications such as internet-based servers (e.g. world wide web), video-on-demand, interactive television, and video conferencing, all of which have as dominating components large volume data management. At the same time technological trends indicate that key design metrics of modern and future application specific designs, such as speed, power, and weight, are dominated by massive storage elements. Most often, magnetic disk is already a bottleneck in current application specific computer and communication systems.

Another equally pronounced consequence of the current application and technological trends is increasing importance of power minimization. Our main strategic objective is to give impetus for research and development of synthesis and compilation techniques for design of massive storage-based application specific systems. We have three main technical goals in this paper:

1. To establish an accurate, but computationally efficient, performance and power consumption models for disk-based systems.
2. To identify most effective ways to reduce power in disk-based application specific systems.

3. To develop a practical approach and optimization synthesis algorithms for a scheduling and assignment of disk-based real-time systems.

The detailed description of the synthesis approach for optimization of disk-based application specific systems can be found in [5].

II. BACKGROUND MATERIAL

In this section we first provide an overview of power consumption sources in a disk and briefly discuss the most popular timing models of a magnetic disk. We conclude the section, by explaining the selected hardware and computational models. The detailed description of disk technology is available in [5].

Power required by a hard disk drive is consumed by its many different components. To complicate matters even further, the power requirements of each component will vary with the current operational mode of the disk. Common operational modes with different power requirements are: Start-up, Seek, Read/Write: Idle, Standby and Sleep. In each of the distinct operational modes available, a different amount of strain is placed upon each of the individual disk components, varying the amount of power consumed [5]. A seek moves the disk

Table 1 Typical seek time for an IBM disk.

seek distance range [tracks]	seek time
1 - 50	$1.9 + \sqrt{\text{distance} - \text{distance}/50}$
51 - 100	$8.1 + 0.044 * (\text{distance} - 50)$
101 - 500	$10.3 + 0.025 * (\text{distance} - 100)$
501 - 884	$20.4 + 0.017 * (\text{distance} - 500)$

head (arm) from track to track. Several techniques have been proposed for analytic and empirical modeling of access data [13, 18]. The common denominator in all of them is that longer distance which arm has to travel corresponds to larger time overhead. Typical seek times for an IBM disk are given in Table 1 [11].

Our selection process of computational and hardware models was mainly guided by the goal to cover as large as possible set of modern and future disk-based application specific systems. The system has three components: disk, main memory, and processor. Processor by itself can have multiple processors and/or ASICs. Since for power minimization in both memory and processor (and ASIC) several approaches are readily available [12], we focus our attention on disk's

power optimization. We assume that a disk is a separate unit, as it is almost always the case in industrial practice.

We assume that each of tasks follows homogeneous synchronous data flow semantics and syntax individually [9]. We assume, with no loss of generality that all tasks have identical periods. When this is not the case, a simple preprocessing step and application of the least common multiple (LCM) theorem [8], in polynomial time transforms an arbitrary set of periods to this design scenario. We assume no task preemption. Note that this preemption restriction, actually does not impact any of the proposed methods, since in all discussed design cases non-preemptive policies yield superior results in comparison with preemptive policies. Furthermore, each task has a need to read or read and write data to the disk. We assume that for each task a sequence of disk blocks to be accessed for its execution is given. Time to serve one read or write request is the sum of seek time and data transfer time. Seek time is proportional to distance which disk's head has to travel, and read and write time is proportional to amount of data which has to be transferred. The typical seek times for an IBM disk in Table 1 have been used for experiments. The goal is to properly schedule all tasks and their required data transfers, so that all timing constraints are satisfied and disk's power consumption is minimized.

III. RELATED WORK

Although there have been constant stream of proposed alternative massive storage technologies, magnetic disks have dominated secondary storage since the mid sixties. Detailed description of magnetic disks can be found in many books [6]. Another brief, but excellent exposition are papers [13] and [4]. An introductory exposition of basic disk principles is also given in modern architecture and operating systems textbooks [11]. Wood and Hodges [17] survey state-of-the-art and technology trends in direct access storage devices, mainly magnetic disks. Disk modeling recently attracted a great deal of interests [4,11,13,18].

The early disk-related research in operating systems has been focused on development of scheduling algorithms for efficient use of high-volume storage in time-shared mainframes [16]. Later, operating systems researchers developed new disk scheduling algorithms for new general-purpose computing platforms assuming increasingly more realistic and complex disk models [14]. Grossman and Silverman discussed placement of records on a secondary storage device to minimize access time [3]. Recently a number of synthesis and compilation techniques for power optimization at all levels of abstractions during design process have been proposed [1, 15]. Although, power optimization is most effective at the higher levels of abstractions, until recently majority of power minimization techniques were proposed at logic synthesis and physical design phases of design [1, 12, 15]. A good survey of low power storage alternatives for general purpose mobile computing is given in [2].

IV. DISK POWER MODEL

Our model separately considers two subparts: mechanical and electronic subsystems. Those two parts have two sharply different power dependencies [4,5].

The electronic part follows standard power trade-offs of CMOS-based designs. The sources of power consumption in a CMOS integrated circuit are due to four types of currents: leakage, standby, short-circuit, and capacitive. All the currents except capacitive can be reduced to a relatively low percentage of the total design power by a combination of proper design techniques [12, 15] and are mainly independent from the synthesis tasks related to architectural and application design of disks electronic subsystems. Therefore, the power consumption can be quantified using the following widely quoted equation:

$P_{elect} = \alpha * C * V_{dd}^2 * f$ where α is the activity factor, C is average capacitance switched per cycle, V_{dd} is the supply voltage, and f is the cycle frequency, assuming that V_{sw} the switched voltage is equal to the supply voltage. For power-delay dependency, we use the 6th order Nevin's rational polynomial approximation proposed and experimentally verified by Chandrakasan et al. [1]. Elaborate measurements [4] show linear dependency between rotational spindle motor speed and power. In *disk* particular, we use the following formula, derived from [4]:

$= P_{fs} - \gamma * (nrs - ors)$, where P_{disk} is power consumption of the disk which operates on operating rotations speed, denoted *ors*, γ is constant scaling coefficient, P_{fs} is power consumption at nominal rotational operating speed, denoted by *nrs*.

We selected parameters in this formula, to follow our conservative estimation of improvements in power consumption. We used the following values in our experimentations: $P_{fs} = 700 \text{ mW}$; $\gamma = 110 \text{ mW}/1000 \text{ rpm}$; and $nrs = 5000 \text{ rpm}$.

V. OPTIMIZATION: APPROACH, PROBLEM FORMULATION, AND OPTIMIZATION STRATEGY

We now summarize our approach to power minimization. The key idea is to minimize seek time using proper scheduling and data assignment algorithms so that disk read/write time can be slowed down to result in the opportunities of exploiting power optimization degrees of freedom; the voltage of the electronic components can be reduced and the spindle motor speed of the mechanical component can be slowed down.

The most general version of the targeted problem can be formulated in the following way:

Problem: The Power Optimization Under Throughput Requirement Using Disk Seek Time Minimization, Spindle Motor Speed Scaling and Supply Voltage Scaling.

Instance: Given a set of M tasks described by the disk block access sequence, an initial voltage V , an initial spindle motor speed S and positive constants D and P .

Question: Are there a disk block assignment, a static periodic schedule of the tasks, a new spindle motor speed S' and a new voltage V' such that the disk seek time + read/write time is at most D and the power consumption is at most P' ? We proved that our problem is NP-complete [5]. We solve the power optimization problems in two steps. First, we find a task schedule and a disk assignment such that the disk seek time is minimized. Next, a voltage scaling and a spindle motor speed scaling are performed such that the throughput requirement is met.

Since the computational complexity of the disk head movement minimization problem forbids an exact or optimal solution, effective heuristic methods have been developed for the problem. The task scheduling problem is transformed into a TSP problem and an efficient and effective TSP heuristic [10] is applied to the transformed problem. For the disk assignment problem, the simulated annealing (SA) algorithm [7] has been used. The detailed description of the TSP and SA heuristics uses is given in [5]. The task scheduling and disk assignment problem

Number of Tasks	Task Scheduling Problem				Disk Assignment Problem				Task Scheduling and Disk Assignment Problem			
	Random		Optimized		Random		Optimized		Random		Optimized	
	Average	Best	Average	Best	Average	Best	Average	Best	Average	Best	Average	Best
50	529.69	521.16	355.81	355.81	543.24	516.57	420.54	419.44	539.73	521.49	311.83	308.80
100	1345.15	1328.51	865.25	865.25	1355.70	1308.31	980.69	977.22	1367.57	1330.07	693.07	679.21
150	2188.40	2133.48	1384.35	1384.29	2170.07	2112.88	1481.71	1465.89	2171.83	2116.32	1004.37	985.16
200	3165.81	3125.58	1896.31	1895.76	3217.62	3141.43	2136.19	2112.71	3242.36	3189.99	1373.38	1358.98
250	3877.75	3850.98	2182.20	2181.90	3934.39	3866.63	2488.37	2429.78	3944.79	3902.58	1555.03	1536.65

Table 2 The results for the disk seek time and read/write time minimization.

Number of Task	Task Scheduling Problem	Disk Assignment Problem	Task Scheduling and Disk Assignment Problem
50	0.65	48.04	19.26
100	2.96	144.12	50.68
150	9.10	293.90	102.27
200	9.59	578.42	198.13
250	16.03	1063.90	388.49

Table 3 Running Time for example from Table 2 (seconds on SUN SPARCstation 4)

Number of Task	Task Scheduling Problem			Disk Assignment Problem			Task Scheduling and Disk Assignment Problem		
	Optimized PD			Optimized PD			Optimized PD		
	Electronic	Spindle	Total	Electronic	Spindle	Total	Electronic	Spindle	Total
50	227.54	409.77	637.31	323.20	482.07	805.27	187.38	375.68	563.06
100	185.33	373.87	559.20	239.67	419.45	659.12	143.03	330.52	473.55
150	169.42	358.67	528.09	189.94	377.97	567.91	125.27	308.51	433.78
200	148.09	336.31	484.40	169.65	358.90	528.55	112.67	290.80	403.47
250	130.87	315.75	446.62	145.73	333.60	479.33	104.58	278.32	382.90

Table 4 The results for the power minimization using voltage scaling and spindle motor speed scaling.

employs a reiterative heuristic which repeatedly solves the task scheduling problem and the disk assignment problem separately using their TSP and SA heuristics until no improvement is achieved. The heuristic is described using the following pseudo-code:

Generate a random disk assignment. Apply the TSP heuristic to find a task schedule given the random disk assignment. Set the current schedule and assignment to the best-so-far solution. Repeat

Apply the SA algorithm to find a disk assignment given the current task schedule. If the new assignment does not improve upon the best-so-far, stops the loop and return the

best-so-far. Apply the TSP heuristic to find a task schedule given the current disk assignment. If the new schedule does not improve upon the best-so-far, stops the loop and return the best-so-far.

VI. EXPERIMENTAL RESULTS

We have generated random examples by varying the number of tasks. The number of blocks and the schedule period are chosen to be the same as the number of tasks. We have tried the examples of 50, 100, 150, 200, and 250 tasks. Each task accesses either one or two blocks. Each disk block access

involves a disk read and write. The disk seek time read/write time of the best random solution is used as a deadline. The initial power dissipation (PD), the initial PD by the spindle system, the initial PD by the electronic part, the initial supply voltage, the initial spindle motor speed and the initial disk read/write time has been set to 1.51 W, 700 mW, 810 mW, 5.0 V, 5,000 RPM and 1.0 ms, respectively. The Tables 2 and 4 illustrate the effectiveness of the power optimization using disk seek time minimization, voltage scaling, and spindle motor speed scaling. The power consumption reductions by factors of 3.13, 2.86, and 3.66 are achieved for the task scheduling problem, the disk assignment problem and the task scheduling and disk assignment problem, respectively. Table 3 illustrates the efficiency of the proposed heuristics and running times are on SUN SPARCstation 4 with 32 MB of main memory. Even on this relatively modest platform, the large instances of the problem has been solved in relatively short run-times.

VII. CONCLUSION

We studied a new problem of power optimization in disk-based application specific systems. We proposed a conceptually simple, but realistic power consumption model for disk drives. Simulated annealing and traveling salesman problem heuristics are used as optimization mechanisms for power minimization in several common hard real-time disk-based systems design scenarios. We demonstrated how to coordinate tasks scheduling and their disk data pattern access and assignment, so to minimize power consumption in both electronic and mechanical components of used disks. Extensive experimental results indicate significant power reduction ability of the proposed techniques and algorithms.

REFERENCES

- [1] A.P. Chandrakasan, et al. "Optimizing Power Using Transformations", IEEE Transactions on CAD, Vol. 14, No. 1, pp. 13-32, January 1995.
- [2] F. Douglis, et al, "Storage alternatives for mobile computers", USENIX Symposium on Operating Systems Design and Implementation (OSDI), pp. 25-37, 1994.
- [3] D. D. Grossman, H. F. Silverman, "Placement of records on a secondary storage device to minimize access time", Journal of the ACM, Vol. 20, No. 3, pp. 429-438, 1973.
- [4] E.P. Harris, et al, "Technology Directions for Portable Computers", Proc. of the IEEE, Vol. 83, No. 4, pp. 636- 658, 1995.
- [5] I. Hong, M. Potkonjak, "Power Optimization in Disk-Based Real-Time Application Specific Systems", UCLA, CS Dept. Technical Report 960025, 1996.
- [6] F. Jorgensen. "The complete handbook of magnetic recording", TAB Books, New York, NY, 1996.
- [7] S. Kirkpatrick, C. Gelatt, M. Vecchi, "Optimization by Simulated Annealing", Science, Vol. 220, No. 4598, pp. 671-680, 1983.
- [8] E. L. Lawler, C.U. Martel, "Scheduling periodically occurring tasks on multiple processors", Information Processing Letters, Vol. 12, No. 1, pp. 9-12, 1981.
- [9] E.A. Lee, T.M. Parks, "Dataflow Process Networks", Proc. of the IEEE, Vol. 83, No. 5, pp. 773-799, 1995.
- [10] O. Martin, S. W. Otto, E. W. Felten, "Large-Step Markov Chains for the TSP Incorporating Local Search Heuristics", Operations Research Letters, Vol. 11, No. 4, pp. 219-224, 1992.
- [11] D.A. Patterson, J.L. Hennessy, "Computer Architecture: A Quantitative Approach", Morgan Kaufmann, San Mateo, CA, 1990.
- [12] J. Rabaey, M. Pedram, ed., "Low power design methodologies". Kluwer, Boston, MA, 1995.
- [13] C. Ruemmler, J. Wilkes, "An introduction to disk drive modeling", IEEE Computer Magazine, Vol. 27, No. 3, pp. 17-28, 1994.
- [14] M. Seltzer, P. Chen, J. Ousterhout, "Disk Scheduling Revisited", Proc. of USENIX, pp. 313-323, 1990.
- [15] D. Singh et al., "Power Conscious CAD Tools and Methodologies", Proc. of the IEEE, Vol. 83, No. 4, pp. 570-594, 1995.
- [16] T.J.Teorey, T.B. Tinkerton, A comparative Analysis of Disk Scheduling Policies, Communications of the ACM, Vol. 15, No. 3, pp. 177-184, 1972.
- [17] C. Woods, P. Hodges, "DASD Trends: Cost, Performance, and Form Factor", Proc. of the IEEE, Vol. 81, No. 4, pp. 573-585, 1993.
- [18] B.L. Worthington, G.R. Ganger, Y.N. Patt, J. Wilkes, "On- line extraction of SCSI disk drive parameters", Performance Evaluation Review, Vol.23, No. 1, pp.:146- 56, 1995.

Cyber Crime

Anshu Deepak, Assistant Professor, ECE, RRIT
Greeshma V, ECE, RRIT

Abstract:-

Cybercrime can be defined as an "illegal act in which a computer is a tool or a goal or both". The use of computers has become extremely common and popular. However, the misuse of technology in cyberspace has led to cybercrime both nationally and internationally. With the intention of regulating criminal activities in the cyber world and protecting the technological advancement system, the Indian parliament approved the law on technological information, 2000. It was the first global law of India to deal with technology in the field of e-commerce, e- governance, electronic banking services, as well as penalties and punishments regarding computer crimes.

Law that regulates the internet must be considered in the context of the geographical in context of the internet and political borders, which are crossed in the process of sending data or exchanging information around the globe. The unique globe structure of the internet raises not only jurisdictional issues, that is, the authority to make and enforce laws affecting the internet , but also questions concerning the nature of the laws themselves.

This document will discuss the common types of cyber-crime and measures to prevent cybercrime.

Index Terms

Cyber bullying & stalking, Vishing, Pharming, Phreaking, Bots, phishing, spoofing attacks, malwares, email bombing, Data diddling.

Smart Notice Board Using IoT (Internet of Thing)

Ashok K N, Assistant Professor, ECE, RRIT

Anil Kumar K, Assistant Professor, ECE, RRIT

Abstract:--

Notice boards are playing very important role in our day to day life. By replacing conventional type notice board with IoT based smart notice board we can make information dissemination much easier in a paperless community. Here the admin can control notice board through internet. So information can be send from anywhere across the world and can be displayed within seconds in form of scrolling manner. Smart phone or PC is used for sending information and an IOT development board i.e., Node MCU is connected to internet at the receiving side. In addition to this an application which is installed on the admin's mobile phone can serve the same purpose.

Wireless Charging of Electric Vehicle in Smart Cities

Bidhya Chhetri, Student, Electrical and Electronics Engineering, RRIT/VTU

Hemanjali R, Student, Electrical and Electronics Engineering, RRIT/VTU

Ruchitha S, Student, Electrical and Electronics Engineering, RRIT/VTU

Rishi GN, Student, Electrical and Electronics Engineering, RRIT/VTU

Sunanda C V, Assistant professor, Electrical and Electronics Engineering, RRIT/VTU

Abstract:--

Currently, we are facing issues related to lack of fuel. So, we are moving towards electrical vehicle. But still people are not ready to prefer electrical vehicle over present ones. It is because of price as well as lack of available charging stations. Even if few charging stations are available, it is necessary to spend extra time for charging the vehicle. The vehicle battery charger station using renewable power system developed in this work provides a unique service to the traveler. It can be quickly and easily installed outside any business premises.

The application of Internet of Things (IoT) has been emerging as a new platform in wireless technologies primarily in the field of designing electric vehicles. To overcome all issues in existing vehicles and for protecting the environment, electric vehicles should be introduced by integrating an intellectual device called sensor all over the body of electric vehicle with less cost. Therefore, this article confers the need and importance of introducing electric vehicles with IoT based technology which monitors the battery life of electric vehicles. Since the electric vehicles are implemented with internet, an online monitoring system which is called Things Speak has been used for monitoring all the vehicles in a continuous manner (day-by-day).

Image segmentation of White Blood Cells using K-means and Gram-schmidth orthogonalisation algorithm

Chitharanjan das V, Assistant professor, R R Institute of Technology

Dr. Puttamade Gowda J, Associate professor, R R Institute of Technology

Abstract:--

A Blood cell is a liquid organ of the body produced through haematopoecisis in mammals, provides necessary ingredients like nutrients and oxygen to the cells. RBC, WBC and platelets are the general categories. RBC Carries oxygen to all parts of the body, WBC forms immune system of the body and fight against virus and bacteria in the body. WBC count plays a major role in disease diagnosis. Based on the data from blood test doctors treat the patients accordingly. There are many method like manual, clinical are available to diagnose the WBC which are in accurate and facing lot of issues in testing of blood Evaluation of WBC. In Image processing has given a strong foundation in medical diagnosis. The proposed method of WBC segmentation includes Gram -Schmidt with K means algorithm. By this method we can easily separate RBC, WBC and platelets from the microscopic image. So it is easy to analyze blood Components.

A wireless sensor networks for early Forest Fire detection and Monitoring

Deepti Thapa, Department of Electrical and Electronics Engineering, R R Institute of Technology, Bangalore, Karnataka, India

Sandeep Pandey, Department of Electrical and Electronics Engineering, R R Institute of Technology, Bangalore, Karnataka, India

Ramachandra C, Department of Electrical and Electronics Engineering, R R Institute of Technology, Bangalore, Karnataka, India

Abstract:--

The fire occurs in wild area due to carelessness and change in an environment the main focus of this project is to minimize the forest fire which may be caused by anything. There is existing system like satellite, cameras and other wired/wireless technologies but those systems have some limitations like satellites provides image of the earth after a long period of time so these systems are not accurate because it doesn't provide the real time data. This IoT based detection is real time, it detects fire at the very early stage and forest fire can be prevented. It has been found in a survey that 80% losses caused due to fire would have been kept away from if the fire was identified promptly. Node Mcu based IoT empowered fire indicator and observing framework is the answer for this issue. In this task, we have assembled fire finder utilizing Node Mcu which is interfaced with a temperature sensor, a smoke sensor and signal. The temperature sensor detects the warmth and smoke sensor detects any smoke produced because of consuming or fire. Buzzer associated with Arduino gives us an alert sign. At whatever point fire activated, it consumes protests adjacent and produces smoke. A fire caution can likewise be activated because of little smoke from candlelight or oil lights utilized as a part of a family. Likewise, at whatever point warm force is high then additionally the alert goes on. Bell or alert is killed at whatever point the temperature goes to ordinary room temperature and smoke level decreases. We have additionally interfaced LCD show to the Node Mcu board. With the assistance of IoT innovation. Node MCU fire checking serves for mechanical need and also for family unit reason. At whatever point it recognizes fire or smoke then it immediately alarms the client about the fire through the ethernet module.

Leak Localization on Gas Pipeline using Acoustic Sensors and the MUSIC algorithm

Ghassan Alnwaimi, Department of Electrical and Computer Engineering, King Abdulaziz University, Jeddah 21589, Saudi Arabia.

Hatem Boujemaa, SUPCOM-COSIM Lab., Ariana, 2083 Tunisia.

Feras Alfosail, Consulting Services Department, Saudi Aramco, Dhahran 31311, Saudi Arabia.

Nebras Sobahi, SUPCOM-COSIM Lab., Ariana, 2083 Tunisia.

Abstract:--

In this paper, we propose the use of the Multiple Signal Classification algorithm (MUSIC) to locate a leak on a gas pipeline using acoustic sensors. We compare the Root Mean Square Error (RMSE) of the leak position estimate to the intercorrelation method using two acoustic sensors and a pipeline of length 100m. At average Signal to Noise Ratio equal to 0 dB, the RMSE of the leak position estimate is equal 1.6m for the MUSIC algorithm while the RMSE is 7.4 m for the intercorrelation method. The MUSIC algorithm and intercorrelation method are unbiased as the RMSE converges to zero at high SNR.

Index Terms

Leak localization, Gas pipeline, Acoustic Sen- sors, MUSIC algorithm, Intercorrelation method.

Optimisation of Energy Demand Based on Thermal Comfort Criteria for an Office Building in the Tropical Warm Humid Climate

Poornima Kurup, Assistant Professor, Department of Architecture, TKM College of Engineering, Kollam

Abstract:--

Energy for comfort application is the single most contributor to the total energy used in building operation. Building sector contributes to a large part of global energy. The energy use in buildings makes the build infrastructure a significant contributor to the global carbon footprint. Building design could be optimized in the design stage by considering the factors that contribute to this energy load. Building envelopes should be designed taking into consideration the climatic parameter of the geographical location and elements in the building envelope could be optimized in ways that reduce the energy demand used for comfort applications in building occupancies. The current work uses a full factorial design to derive the significant factors for rooms in different orientations that contribute to energy load in buildings. The significance of factors and their interations have been iterated through an energy simulation software. Window to wall ratio is the most significant contributing factor for rooms in all directions along with the thermal transmittance of the roof.

Intelligent Accident Detection and Ambulance Rescue System

Rakesh S, Student of RRIT, Department of ECE

Pradeep B M, Student of RRIT, Department of ECE.

Shiva Kumar N, Student of RRIT, Department of ECE

Umesh Gouda V Patil, Student of RRIT, Department of ECE

Divya.T.M, Assistant professor, RRIT, Bangalore

Abstract:--

Road accidents and traffic congestion are the major problems in urban areas. Currently there is no technology for accident detection. Also due to the delay in reaching of the ambulance to the accident location and the traffic congestion in between accident location and hospital increases the chances of the death of victim. There is a need of introducing a system to reduce the loss of life due to accidents and the time taken by the ambulance to reach the hospital. To overcome the drawback of existing system we will implement the new system in which there is an automatic detection of accident through sensors provided in the vehicle. A main server unit houses the database of all hospitals in the city. A GPS module in the concerned vehicle will send the location of the accident to the main server which will rush an ambulance from a nearest hospital to the accident spot. Along with this there would be control of traffic light signals in the path of the ambulance.

This will minimize the time of ambulance to reach the hospital. A patient monitoring system in the ambulance will send the vital parameters of the patient to the concerned hospital. This system is fully automated, thus it finds the accident spot, controls the traffic lights, helping to reach the hospital in time.

Optimization of Physical Parameters for Production of Antimicrobial Compound by *Aspergillus Flavus* Mtcc 13062 Using Response Surface Methodology

Shruti Dudeja, Department of Bio & Nano Technology, Guru Jambheshwar University of Science & Technology, Hisar, Haryana, India.

Anil Kumar, Department of Bio & Nano Technology, Guru Jambheshwar University of Science & Technology, Hisar, Haryana, India.

Abstract:--

Multidrug-resistance amongst the pathogenic microorganisms is a serious problem all over the world. The development of new drugs with different mode of actions by using potent microorganisms to combat multidrug resistance is the most important concern nowadays. The present study was carried out with the aim of optimizing potent fungal strain *Aspergillus flavus* **MTCC 13062** exhibiting significant antimicrobial activity against bacteria *Streptococcus gordonii*, *Bacillus subtilis*, *Staphylococcus aureus*, *Escherichia coli*, *Salmonella enterica*, *Pseudomonas aeruginosa* and *Pseudomonas fluorescens* and fungus *Candida albicans*. The Box-behnken design (BBD) model of RSM used to optimize physical parameters of strain *A. flavus* and was found to be fit with regression (R^2) 0.8416 (*E. coli*), 0.8746 (*S. aureus*) and 0.9143 (*C. albicans*) with insignificant lack of fit. The maximum antimicrobial activity recorded with zone of inhibition 27 mm (*E. coli*) and 28 mm (*S. aureus*) and 30 mm (*C. albicans*) at the selected optimum conditions, which was 22 mm (*E. coli*), 16 mm (*S. aureus*) and 20 mm (*C. albicans*) before optimization. The antimicrobial activity found to be increased by 22% (*E. coli*), 75% (*S. aureus*) and 50% (*C. albicans*) at pH 7.5, 28 °C temperature, and incubation period of 7 days.

Keywords:

Antimicrobial, RSM, BBD, Fungi, Multidrug-resistance

Trash Can Monitoring System in the Smart Cities

Shyamala P, Assistant Professor, ECE dept R.R.Institute of Technology Bangalore, India

Charutha .M.V, Assistant Professor, ECE dept R.R.Institute of Technology Bangalore, India

Abstract:--

In today's world, the trash cans placed in the cities are jam-packed due to the increase in the waste. A lot of stinking and sewage problems causes bad hygienic conditions and leads to deadly diseases & human illness. To avoid these, we have designed a "Smart Trash Can Monitoring System" where it can overcome this in an innovative and efficient way. This idea can be implemented for Smart Buildings, Cities, Colleges, Hospitals, Public spots and Bus stands. Each trash can contain a smart device for level detection of the trash can which transmits the garbage/trash level with its token ID, accessed by the concerned municipal/regional authorities through the mobile app, so that they can take immediate actions to clean the trash can once it gets filled.

A Design Pattern Ranking and Optimization Method Based on Intent

Marwan Al-Akaidi, IEEE Chair SPC – UK & Ireland

Hui Guan, Shenyang University of Chemical Technology, Shenyang, China

Tianyu Ma, Shenyang University of Chemical Technology, Shenyang, China

Hongji Yang, Leicester University, Leicester, UK

Abstract:--

Design patterns are proven solutions to specific software design problems. They are often used to acquire the software knowledge needed to solve software design problems. However, choosing the appropriate design patterns is not an easy task. Design pattern intent is the shortest path to understand design patterns, so sorting design patterns by analyzing design pattern intent is more beneficial for users to obtain the required design patterns. This paper proposes an Intent-based Ranking method, to facilitate the choice of design patterns, defines the relevant similarity calculation method and the corresponding proof is given in the paper, and then through the genetic algorithm in this article, as defined by the parameters for the adjustment and optimization, the final actual problems in the actual development data set with software and design patterns, in the proposed method is verified and analyzed, and the experimental results show that the proposed method compared with other methods in a certain matching rate increased, and sorted the more correct results appear in the front of the plane.

Index Terms

WordNet ; Stanford Parser ; Genetic Algorithm ; Design pattern ; Ranking

Consumer Behaviour in Rural Market of Hanumangarh

Dr. Arun Aggarwal, Faculty of Commerce & Management, Shri Khushal Das University, Pilibanga, Hanumangarh

Anjali Chopra, Shri Khushal Das University, Pilibanga, Hanumangarh

Abstract:--

Consumer behaviour tells us how why and what people do when they buy products or avail of some services. It attempts to understand the buyer's decision-making process, both individually and in groups. (definition given by C.L Narayana and R.J Markin)

Consumer behaviour is the totality of a consumer's decisions and dynamic process which is influenced by multiple factors, it is the study of how individual customers, groups or organizations select, buy, use & dispose ideas, goods & services to satisfy their needs & wants. It refers to actions of consumers in the market place and the underlying motives for those actions. It defines how a consumer's emotions; attitude & preferences affect buying behaviour .

Consumer's behaviour emerged in 1940's & 50's as a distinct sub discipline of marketing. It studies all the consumer actions during searching, purchasing, using evaluating and disposing of products and services that they expect will satisfy their needs. The core of marketing identifying unfilled needs and delivering products and services that satisfy

International Virtual Conference on

Research Trends in Engineering & Management

Bangalore, India, 20th – 21st, August 2021

IFERP International Conference

IFERP Explore

<https://www.icrtem.net/> | info@icrtem.net

UPCOMING CONFERENCES



Technoarete[®] Group

Integrating Researchers to Incubate Innovation

SUPPORTED BY

